ЖУРНАЛ
ЭКСПЕРИМЕНТАЛЬНОЙ И ТЕОРЕТИЧЕСКОЙ
ФИЗИКИ
АКАДЕМИЯ НАУК СССР

SOVIET PHYSICS

JETP

VOLUME 1 NUMBER 1

A Translation

of the

Journal of Experimental and Theoretical Physics

of the

Academy of Sciences of the USSR

JULY, 1955

Published by the

AMERICAN INSTITUTE OF PHYSICS
INCORPORATED

SOVIET PHYSICS
JETP

A translation of the Journal of Experimental and Theoretical Physics of the USSR.

SOVIET PHYSICS is a bi-monthly journal published by the American Institute of Physics for the purpose of making available in English reports of current Soviet research in physics as contained in the Journal of Experimental and Theoretical Physics of the Academy of Sciences of the USSR. All issues of the Soviet journal after January 1, 1955, will be translated. The page size of SOVIET PHYSICS will be 7⅞" x 10½", the same as other Institute journals.

Transliteration of the names of Russian authors follows the system employed by the Library of Congress.

This translating and publishing project was undertaken by the Institute in the conviction that dissemination of the results of researches everywhere in the world is invaluable to the advancement of science. The National Science Foundation of the United States encouraged the project initially and is supporting it in large part by a grant.

One volume is published annually. Volume 1 (1955) will contain three issues. Subsequent volumes, beginning with January 1956, will contain six issues.

Subscription Prices:

Per year (6 issues)
United States and Canada.....$30.00
Elsewhere 32.00

1st Volume (3 issues)
United States and Canada.....$15.00
Elsewhere 16.00

Back Numbers
Single copies .....$ 6.00

Subscriptions should be addressed to the American Institute of Physics, 57 East 55 Street, New York 22, New York.

SOVIET PHYSICS
JETP

A translation of the Journal of Experimental and Theoretical Physics of the USSR.

VOL. 1, NO. 1, PP. 1-196 JULY, 1955

Editorial

THE American Institute of Physics is establishing *Soviet Physics JETP* as a translation journal with the purpose of bringing before American physicists the chief record of the scientific activities of Soviet physicists. It is hoped that this journal will provide an accurate basis of judgement of the caliber of the work done in the Soviet Union, as well as further insight into the problems of physics.

Prior to the creation of this journal there has been widespread discussion on the part of The Institute, the Committee on Russian Translations of the American Physical Society, and officials of the National Science Foundation, as to what scheme of translation would be most advantageous. A single journal was chosen, in preference to selected translations from all Soviet journals, because of the greater speed and economy with which a single journal could be prepared. A selection journal would have required the advance consideration of an editorial board, and several months delay would have been introduced. In addition, one man's treasure is often another man's junk, so that considerable disagreement over the relative merits of the selections would have been almost inevitable.

Once having decided on a single journal, The Institute selected the *Journal of Experimental and Theoretical Physics of the Academy of Sciences of the USSR* because it most nearly qualified as the Soviet equivalent of the *Physical Review.* The question of further translation journals has been left unanswered.

Soviet Physics JETP will carry, in translation, all scientific articles and letters appearing in the *Journal of Experimental and Theoretical Physics,* commencing with the January, 1955, issue, The articles will not necessarily appear in the same order as in the Russian journal, but all articles will eventually appear. Publication of the translated version in *Soviet Physics* can be expected within nine months of the appearance of the Russian original.

It will also be the policy of *Soviet Physics* to print translations of the Tables of Contents of the *Journal of Technical Physics (Zh. Tekhn. Fiz.)* and of the physics and related portions of the Tables of Contents of the *Proceedings of the Academy of Sciences of the USSR (Doklady Akad. Nauk SSSR).*

Soviet Physics represents a new departure in the publications of The Institute, and the editor and his associates ask for patience and understanding on the part of its readers regarding the imperfections and false steps that will almost certainly accompany the development of the publication.

Comments, criticisms and suggestions for improvement will be welcomed by the editor.

The Theory of Nuclear Reactions with Production of Slow Particles*

A. B. MIGDAL

(Submitted to JETP editor February 23, 1954)
J. Exper.. Theoret. Phys. USSR 28, 3-9 (January, 1955)

Energy and angular distribution of slow nucleons which result from nuclear reactions are obtained. An estimate is given of the probability of production of nucleons in a bound state.

---

1. IF as a result of nuclear reactions particles with low kinetic energy are produced, the mutual interaction of these particles may substantially influence their distribution in energy. The case will be considered in which two or more nucleons are obtained as reaction products, each with kinetic energy which is small compared to the interaction energy.

In this paper we obtain the distribution in energy of the nucleons which result from collisions of a nucleon with a deuteron and a deuteron with nuclei. In order to obtain the distribution in energy of the slow nucleons which are produced, it is sufficient to make use of quite general properties of their ψ-functions, and hence it is also possible to make some inferences concerning the distribution in energy for more complicated nuclear reactions. Below we give an estimate of the ratio of the cross-section for deuteron formation (or the di-neutron, if it exists) to the cross-section for production of free nucleons. We also obtain the angular correlation between exit directions of the two nucleons which results from their interaction.

2. Let a nucleon be incident on a deuteron, and let the velocity of the nucleon be much greater than the velocities of the neutron and proton in the deuteron. In order to obtain the cross-section for this process we shall use a method analogous to the one used in molecular theory, where one makes use of the smallness of the velocities of the nuclei as compared with the velocities of the electrons. In analogy with the molecular case, it is necessary, in order to find zero order functions, to solve first the problem of the scattering of the incident particle by the fixed nucleons of the deuteron. The zero order functions will have the form

$$\Psi = \psi(\mathbf{r}_3;\ \mathbf{r}_1, \mathbf{r}_2)\,\varphi(\mathbf{r}_1, \mathbf{r}_2),$$

where ψ is the function of the incident particle in the field of fixed particles of the deuteron, ϕ is a function of the slow nucleons.

If the scattering function of the incident particle with neutron and proton as scatterers is known, then neglecting the influence of the neutron on the function describing the scattering on the proton, and vice versa (this is legitimate for high energies of the incident particle, when $\sqrt{\sigma} \ll \mathbf{r}_d$, where σ is the scattering cross-section and $\mathbf{r}_d$ is the radius of the deuteron), we obtain the asymptotic form of the function ψ

$$(\psi)_{r_3\to\infty} \sim e^{i\mathbf{k}_0\mathbf{r}_3} + f_1\,(e^{ik_0 r_1}/r_3)\,e^{ik\,|\mathbf{r}_3-\mathbf{r}_1|}$$

$$+ f_2\,(e^{i\mathbf{k}_0\mathbf{r}_2}/r_3)\,e^{ik\,|\mathbf{r}_3-\mathbf{r}_2}$$

$$= e^{i\mathbf{k}_0\mathbf{r}_3} + (f_1 e^{i\mathbf{q}\mathbf{r}_1} + f_2 e^{i\mathbf{q}\mathbf{r}_2})\,(e^{ikr_3}/r_3)$$

where $\mathbf{q} = \mathbf{k}_0 - \mathbf{k}$, $\mathbf{k} = k\mathbf{r}_3/r$, and f_3 and f_2 are scattering amplitudes of the incident particle on the nucleons 1 and 2.

The wave function of the system of all three-particles will be determined by the condition that when $\mathbf{k}_0\mathbf{r}_3 \to -\infty$, the wave function must have the form $e^{i\mathbf{k}_0\mathbf{r}_3}\phi_0(\mathbf{r}_1, \mathbf{r}_2)$ where $\phi_0(\mathbf{r}_1, \mathbf{r}_2)$ is the wave function of the deuteron. The asymptotic form of the wave function of the entire system in zero approximation is given by the expression

---

* Read before the theoretical seminar at the Institute for Physical Problems in October of 1950.

Note added in proof: Since completion of this work several papers dealing with this problem have appeared [see, e.g., K. M. Watson, Phys. Rev. 88, 1163 (1952)].

$$\Psi_{r_3\to\infty} \sim e^{ik_0 r_3}\varphi_0(\mathbf{r}_1,\mathbf{r}_2) + (f_1 e^{i\mathbf{qr}_1} + f_2 e^{i\mathbf{qr}_2})\varphi_0(\mathbf{r}_1,\mathbf{r}_2)(e^{ikr_3}/r_3).$$

Expanding the expression

$$(f_1 e^{i\mathbf{qr}_1} + f_2 e^{i\mathbf{qr}_2})\varphi_0(\mathbf{r}_1,\mathbf{r}_2)$$

in terms of the eigenfunctions of the two slow nucleons produced as a result of the collision, and squaring the expansion coefficients, we obtain the cross-section for scattering with production of nucleons in various states. Introducing coordinates $\mathbf{r} = \mathbf{r}_1 - \mathbf{r}_2$; $\mathbf{R} = (\mathbf{r}_1 + \mathbf{r}_2)/2$, we obtain, after integration with respect to $\mathbf{R}$

$$d\sigma = \left|\int \sum \varphi_P^*(\mathbf{r})\chi_1 \{f_1 e^{i\mathbf{qr}/2} + f_2 e^{-i\mathbf{qr}/2}\}\varphi_0(\mathbf{r})\chi_0 d\mathbf{r}\right|^2 d\omega_k\, d\mathbf{P}/(2\pi\hbar)^3, \quad (1)$$

where $d\omega_k$ is the element of solid angle containing the vector $\mathbf{k}$; χ_0 and χ_1 are functions of the charge and spin coordinates of the two nucleons. The functions $\phi_p(\mathbf{r})$ are normalized to unit volume, function ϕ_0 to unity. The summation is with respect to the spin and charge variables of the two nucleons; P is the momentum of particles 1 and 2 in their center of mass system.

The cross-section for production of two nucleons in a bound state has the form

$$d\sigma_0 = \left|\int \sum \varphi_1^*\chi_1 \{f_1 e^{i\mathbf{qr}/2} + f_2 e^{-i\mathbf{qr}/2}\}\varphi_0\chi_0 d\mathbf{r}\right|^2 d\omega_k, \quad (2)$$

with functions ϕ_1 normalized to unity. In the case of collisions without exchange the function ϕ_1 coincides with ϕ_0. Scattering amplitudes f_1 and f_2 contain, in general, exchange terms in spin and charge variables. Hence during the scattering process changes may take place in the spin and charge states of the nucleons.

3. The integrals in the expressions (1) and (2) cannot be calculated for large q since in this case values of $r \sim 1/q$ are important while the functions ϕ_p and ϕ_0 are known only for $r > r_0$, where r_0 is the range of the interaction forces. For what follows only the dependence of Eq. (1) on the interaction energy of the nucleons is essential. This dependence may be easily found for the case that $\hbar q$ is large compared to the momentum of the particles in the deuteron and compared to the momentum P. In this case in the integrals of Eq. (1) the region of small $r (\sim 1/q)$ is essential, and the probability of finding the nucleons with relative wave vector $\mathbf{P}$ which lies in the interval $d\mathbf{P}$, is

$$dw_p = C_1 |\varphi_P(\mathbf{r}_1)|^2 d\mathbf{P}; \quad r_1 \sim 1/q. \quad (3)$$

4. Let us consider the case of a non-exchange collision. Then one has in the final state (besides the fast nucleon) a slow neutron and a proton. As is easy to obtain from the theory of scattering of neutrons by protons*,

$$|\varphi_P(r_1)|^2 = \frac{A}{E+\varepsilon}\left\{1 + O\left(\frac{P^2 r_0^2}{\hbar^2}\right)\right\}, \qquad P^2 \ll P_{1,2}^2,$$

where A does not depend on the energy, E is the energy of relative motion of the nucleons, $\epsilon = \epsilon_0 =$ 2.2 MeV for parallel spins and $\epsilon = \epsilon_1 =$ 0.07 MeV for antiparallel spins of neutron and proton. Substituting this expression into (3), it is easy to obtain

$$dw_p^{np} = C_{np}\left\{\frac{1}{E+\varepsilon_0} + \frac{a}{E+\varepsilon_1}\right\} d\mathbf{P}. \quad (4)$$

The quantity a determines the amount of admixture of the component depending on the spin in the non-exchange scattering amplitude. The angular distribution of the nucleons in their center-of-mass system is spherically symmetrical.

Formula (4) shows that the energy distribution of the nucleons has a maximum at energies of the order of ϵ.

5. When, as a result of the exchange interaction with the incident fast particle two slow neutrons are formed, it can be seen from (3) that they must be in an S-state (functions with non-zero orbital momentum are small for small distances r_1). Then, according to the exclusion principle, their spins are anti-parallel, and during the collision a change of spin must occur (in the deuteron the spins of the nucleons are parallel).

The distribution in relative energies is given by the expression

$$dw_p^{nn} = C_{nn} d\mathbf{P}/(E+\varepsilon). \quad (5)$$

---

* If $r_1 < r_0$ the dependence of $\phi_p(r_1)^2$ on the energy is determined by the dependence on the energy of the expression $\phi_p(r_0)^2$ since when $r < r_0$ one can neglect the energy E compared to depth of potential well.

The quantity ϵ is in this case unknown.

6. In the case of an exchange collision with formation of two slow protons the function $\phi_p(r_1)$ may be obtained from the theory of proton-proton scattering[1,2]:

$$\varphi_P(r_1) = \frac{\hbar}{r_1}\sqrt{\frac{F(\eta)}{M}}\left\{F^2(\eta)\,E + \frac{\hbar^2}{M}\left[-\frac{1}{a} - \frac{h(\eta)}{R} + \gamma E\right]^2\right\}^{-1/4},$$

where

$$F(\eta) = \frac{2\pi\eta}{e^{2\pi\eta}-1}, \qquad \eta = \frac{e^2}{\hbar v},$$

$$h(\eta) = \mathrm{Re}\,\frac{\Gamma'(-i\eta)}{\Gamma(-i\eta)} - \lg\eta,$$

$$R = \frac{\hbar^2}{Me^2} = 2.9\cdot10^{-12}\ \text{см}, \quad a = -7.7\cdot10^{-13}\ \text{см},$$

$$\gamma = 3.4\cdot10^{11}\ \text{MeV}^{-1}\ \text{см}^{-1}.$$

Substituting this expression into (3), we obtain

$$dw_P^{pp} = C_{pp}\frac{F(\eta)\,d\mathbf{P}}{F^2(\eta)\,E + \frac{\hbar^2}{M}\left[-\frac{1}{a} - \frac{h(\eta)}{R} + \gamma E\right]^2}. \qquad (6)$$

As in the case of two neutrons, the spins of the protons are antiparallel, and the distribution does not depend on the angle of the vector $\mathbf{P}$.

7. Formula (3) is also applicable in the case when a high energy deuteron is incident on a nucleus. The distribution of the two nucleons according to energies of relative motion is given by the expression (4) if the charge of the nucleons does not change, and by expression (5) or (6) if there is a change in the charge of one of the nucleons.

It is possible to calculate the angular correlation of the emergent nucleons. For this, it is necessary to integrate the expression dw with respect to the component of the vector $\mathbf{P}$ parallel to the vector $\mathbf{P}_0$. ($\mathbf{P}_0$ is the momentum of the center of mass of the two nucleons in the laboratory coordinate system.)

Introducing the longitudinal ($\mathbf{P}_1$) and transverse ($\mathbf{P}_2$) components of the relative momentum of the nucleons, we obtain

$$d\mathbf{P} = dP_1\,dP_2\,2\pi P_2,$$

$$f(\vartheta)\,d\vartheta = 2\pi P_2\int w_P\,dP_1\frac{dP_2}{d\vartheta}\,d\vartheta.$$

Here θ is the angle between the exit directions of the nucleons. It is easy to see that when $P \ll P_0$

$$\vartheta = 4P_2/P_0,$$

hence the angular distribution is given by the expression

$$f(\vartheta)\,d\vartheta = \frac{2\pi P_0^2}{16}\int_{-\infty}^{+\infty} w_P\,dP_1\vartheta d\vartheta.$$

For neutron and proton we obtain from (4)

$$f(\vartheta)\,d\vartheta = \frac{P_0^2}{16}C'_{np}\int_{-\infty}^{+\infty}\left\{\frac{1}{[(P_1^2+P_2^2)/M]+\varepsilon_0} + \frac{a'}{[(P_1^2+P_2^2)/M]+\varepsilon_1}\right\}dP_1 2\pi\vartheta\,d\vartheta \qquad (7)$$

$$= A_{np}\left\{\frac{1}{\sqrt{(4\varepsilon_0/E_0)+\vartheta^2}} + \frac{a'}{\sqrt{(4\varepsilon_1/E_0)+\vartheta^2}}\right\}\vartheta\,d\vartheta,$$

where E_0 is the energy of the center of mass of the two nucleons and is given by $E_0 = P_0^2/4M$. The quantity a' gives the fraction of the collisions which are accompanied by change of spin of the system neutron-proton in traversing the nucleus.

For two neutrons we obtain

$$f_{nn}(\vartheta)\,d\vartheta = A_{nn}\frac{\vartheta\,d\vartheta}{\sqrt{(4\varepsilon/E_0)+\vartheta^2}}. \qquad (8)$$

In the case of two protons emerging after the collision Eq. (6) must be integrated with respect to the longitudinal momentum P_1. Upon numerical integration of Eq. (6), we obtain

$$f_{pp}(\vartheta)\,d\vartheta = A_{pp}\Phi(E_2)\,\vartheta\,d\vartheta; \qquad (9)$$

here A_{pp} is a constant, and the "transverse" energy E_2 is related to the angle θ by the relation $E_2 = E_0\theta^2/4$, where E_0 is the energy of the incident deuteron. The function Φ which occurs in (9) may be presented in tabular form as follows:

E_2 (MeV)	0	1	2	3	4	5
Φ	1.00	0.82	0.59	0.40	0.34	0.31

[1] L.D. Landau and Ia. Smorodinskii, J. Exper. Theoret. Phys. **14**, 269 (1944)

[2] J. D. Jackson and J. M. Blatt, Rev. Mod. Phys. **22**, 77 (1950)

Equations (3)-(9) hold under the condition that $\theta \ll \theta_0$ where θ_0 is the angle of deflection of the momentum of the center of mass in traversing the nucleus. (This condition is equivalent to the condition used in deriving formula (3): $P \ll \hbar q$).

8. In deriving the distributions according to the energy of the relative motion and the formulas of angular correlation, we used only the fact that the probability of the process (for large q) is proportional to the square of the function of two nucleons at small distances. It may be assumed, therefore, that formulas (4)-(9) will apply not only in the case when nucleons with small interaction energy have been formed as a result of a collision of a deuteron with a nucleon or nucleus, but also in other cases (e.g., collisions of α-particles with nuclei).

9. Expressions (5) and (8) which give energy and angular correlations of two slow neutrons formed as a result of a neutron-deuteron collision, may be used for the measurement of the very important quantity ϵ, which characterizes the interaction of two neutrons with antiparallel spins.

For this purpose it may be more convenient to study the energy of distribution of fast protons which result from an exchange collision. The energy distribution of the protons can be easily obtained from the distribution (5), if we restrict ourselves to the region of proton energy where the energy of relative motion of the two neutrons is sufficiently small. From the laws of conservation of energy and momentum one has

$$E_0 = E_p + \frac{P_p^2}{4M} + E_{nn} = \frac{3}{2} E_p + E_{nn}, \qquad (10)$$

where E_p and P_p are the energy and the momentum, respectively, of the proton, and E_{nn} is the energy of the two neutrons in their center of mass system. Let us denote the maximum energy of the protons by $E_p^m = {}^2/_3 E_0$; then

$$E_p = E_p^m - {}^2/_3 E_{nn}. \qquad (11)$$

The energy distribution of the protons near E_p^m will be determined by the fact that the cross-section for the process is proportional to Eq. (5) and to the statistical weight of the final state,

$$f_p(E_p)\,dE_p = C_1 \frac{1}{E_{nn}+\varepsilon} P^2 \frac{dP}{dE_{nn}} dE_p = C \frac{\sqrt{E_{nn}}}{E_{nn}+\varepsilon} dE_p$$

Using (11), we obtain

$$f_p(E_p)\,dE_p = C \sqrt{{}^2/_3} \left[\sqrt{E_p^m - E_p} \,/\, (E_p^m - E_p + {}^2/_3\,\varepsilon) \right] dE_p. \qquad (12)$$

The distribution (12) has a maximum at $E_p^m - E_p = {}^2/_3\,\epsilon$.

If there exists a di-neutron, then along with distribution (12) there are monochromatic protons with energy given by $E_p' = E_p^m + {}^2/_3\,\epsilon$ [as is seen from (10)].

The cross-section σ_0 for formation of the di-neutron can be connected quantitatively with the cross-section for formation of two neutrons in the free state. In fact, the ratio of the cross-sections of these two processes is given by the ratio $\phi_p(r_1)^2 / \phi_0(r_1)^2$ where ϕ_0 is the function of the di-neutron.

The di-neutron function and the function ϕ_p must be expressed in the same form as for the system neutron-proton (replacing ϵ_0 by ϵ). The ratio of these expressions, as is easily seen from the theory of neutron-proton scattering and from deuteron theory, is given (for small r_1) by

$$\frac{|\varphi_p(r_1)|^2}{|\varphi_0(r_1)|^2} = \left(\frac{\hbar^2}{M}\right)^{3/2} \frac{2\pi}{\varepsilon^{1/2}} \frac{1}{E_{nn}+\varepsilon} \qquad (13)$$

with the functions ϕ_p normalized to unit volume and the function ϕ_0 normalized to unity. It is easily seen that with this normalization of the functions ϕ_p the ratio of the cross-sections will include the expression

$$\frac{3\pi}{(2\pi\hbar)^3} P^2 \frac{dP}{dE_{nn}} \sqrt{\frac{E_p}{E_p'}}\, dE_p, \qquad (14)$$

which arises from the ratio of the statistical weights of the free and bound states.

Using (14) and (13), we obtain

$$d\sigma = \sigma_0 \frac{3}{4\pi} \frac{\sqrt{E_{nn}}}{E_{nn}+\varepsilon} \sqrt{\frac{E_p}{E_p'\varepsilon}}\, dE_p$$

$$= \frac{\sigma_0}{2\pi} \sqrt{\frac{E_p'}{E_p'\varepsilon'}} \frac{\sqrt{E_p^m - E_p}}{E_p^m - E_p + \varepsilon'} dE_p; \quad \varepsilon' = {}^2/_3\,\varepsilon. \qquad (15)$$

Expression (15) holds only for energies E_p which are close to E_p^m. For a rough estimate of the total cross-section for formation of free parti-

cles and the cross-section for formation of the bound state, let us assume that the expression (15) is valid in the entire range of energies E_p. Then, integrating (15) with respect to E_p from zero to E_p^m, we obtain

$$\sigma_0 \Big/ \int d\sigma \approx 4\sqrt{\varepsilon' / E_p^m}. \qquad (16)$$

10. Formulas (10), (15) and (16) will also hold for the case of the energy distribution α-particles in the reaction:

$$H_3 + H_3 = n + n + \alpha.$$

The energy distribution of α-particles will have the same form as the distribution of protons in the reaction considered above: $n + H_2 = n + n + p$. The quantity ϵ' in the case of α-particles is $\epsilon' = 1/3\,\epsilon$. The chief difficulty in experiments of this kind is the necessity of resolving two maxima in the distribution curve (of the α-particles or protons). One maximum (at energy $E_p = E_p^m - 2/3\,\epsilon$ or $E_\alpha = E_\alpha^m - 1/3\,\epsilon$) corresponds to free neutrons while the other (at the energy $E_p = E_p^m + 2/3\,\epsilon$ or $E_\alpha = E_\alpha^m + 1/3\,\epsilon$) corresponds to the bound state of the two neutrons (if it exists).

Since the quantity ϵ is apparently very small (for two protons and for proton and neutron with antiparallel spins ϵ 100 keV), it follows that for a proof of the existence of a di-neutron an extremely precise determination of the energies of the α-particles (or protons) is necessary. This circumstance has not been taken into account in the experimental attempts to detect the di-neutron.

11. Expressions (15) and (16), obtained for the case of two neutrons, are, of course, valid also for the neutron-proton case, if by σ_0 one understands the cross-section for formation of the deuteron, and by $d\sigma$ the cross-section for formation of a free neutron and a free proton with parallel spins. It can be assumed that these expressions remain valid also for collisions of deuterons and of more complex particles with a nucleus. Equation (16) then gives an estimate of the ratio of the probability of formation of free nucleons to the probability of formation of the same nucleons in a bound state as a result of the nuclear reaction. The energy E_p^m is to be regarded as the maximum energy which is transferred to the nucleons in the given reaction. It is to be noted that an estimate of this ratio without taking into account of the nucleon interaction would be given by the ratio of the volume in the momentum space in the deuteron to that in the free state, i.e. it would have the form

$$\sigma_0 / \int d\sigma \sim (\varepsilon_0 / E^m)^{3/2}.$$

Taking into account the nucleon interaction, leads, as has been shown, to a much great probability of formation of the deuteron. Because of the resonance denominator in Eq. (4), one obtains the estimate given by (16). This formula explains the frequent appearance of deuterons in nuclear reactions.

The author expresses his gratitude to B. T. Geilikman, I.Ia. Pomeranchuk, and Ia.A. Smorodinskii for interesting discussions.

Translated by A. V. Bushkovitch
1

Meson Production at Energies Close to Threshold*

A. B. MIGDAL

(Submitted to JETP editor February 23, 1955)
J. Exper. Theoret. Phys. USSR 28, 10-12 (January, 1955)

The energy spectrum of mesons produced in the collisions of two nucleons is determined. The most probable events are those in which the nucleons are produced with very small relative energy. Consequently, the most probable energy of the mesons occurs close to the maximum energy permitted by conservation laws. The ratio between the cross section for the production of deuterons (in the reactions $p+p=n+\pi^+$; $n+p=p+n+\pi^0$; $n+n=n+p+\pi^-$) and the cross section for the production of free neutrons and protons with parallel spin is obtained.

1. THE cross section for the production of mesons with momentum $\mathbf{P}_\mu$ in the interval $d\mathbf{P}_\mu$, when the relative momentum of the nucleons, $\mathbf{P}_n$, lies in the interval of solid angle $d\omega_n$, is equal to

$$d\sigma = d\mathbf{P}_\mu P_n^2 (dP_n/dE_n)\, d\omega_n \left| \int \varphi_1^* H' \varphi_0 \, d\tau \right|^2. \quad (1)$$

Here ϕ_0 and ϕ_1 are the exact wave functions for the relative motion of the two nucleons in the initial and final states. Because the form of the operator H' will not be used, the expression (1) contains no hypothesis on the strength of the interaction between nucleon and meson field. The function ϕ_0 describes the state of larger relative momentum of the nucleons and changes sign in a distance of order of magnitude $\hbar/P_n^0 < r_0$, where r_0 is the interaction radius. Therefore, in the integration over the relative coordinates of the nucleons, distances less than r_0 play a role and the integral depends essentially on the behavior of the potential at short distances. This behavior is unknown at present. It is easily seen that the dependence of the cross section on the relative kinetic energy of the nucleons in the final state can be found without hypotheses on the form of interaction between the nucleons and the operator H'. In fact, if the functions ϕ in (1) are normalized per unit volume, then considered as functions of the complex variable P_n, they must have a pole for imaginary P_n corresponding to real or virtual binding of the system of two nucleons[1]. Therefore, the dependence of the integral in (1) on the relative energy of the nucleons in the final state, E_n, is given by the expression

$$\left| \int \varphi_1^* H' \varphi_0 d\tau \right|^2 = \frac{U(\mathbf{P}_n, \mathbf{P}_n^0, \mathbf{P}_\mu)}{E_n + \varepsilon}. \quad (2)$$

where P_n^0 is the initial relative momentum of the nucleons, and ϵ is the absolute value of the binding energy. From the theory of neutron-proton scattering one easily derives that

$$U(\mathbf{P}_n, \mathbf{P}_n^0, E_\mu) = U(0, \mathbf{P}_n^0, E_\mu)\,[1 + O(E_n/V_0)],$$

where V_0 is the depth of the potential well. The resonance denominator in Eq. (2) coincides with that which is found in the theory of neutron-proton scattering, and the cross section does not depend on the direction of the vector $\mathbf{P}_n$. (The case of two neutrons and two protons is considered below.) The quantity $\epsilon = \epsilon_0 = 2.2$ MeV for parallel spin and $\epsilon = \epsilon_1 = 0.07$ MeV for anti-parallel spin of the neutron and proton.

Using the laws of conservation of energy and momentum and integrating (1) over $d\omega_\mu\, d\omega_n$, we get

$$d\sigma = C(E_n^0, E_\mu) \quad (3)$$

$$= \frac{\sqrt{(E_\mu^m - E_\mu)\,E_\mu}}{E_\mu^m - E_\mu + \varepsilon'} \sqrt{1 + \frac{E_\mu}{2\mu c^2}} \left(1 + \frac{E_\mu}{\mu c^2}\right) dE_\mu;$$

$$E_\mu^m = \frac{E_n^0 - \mu c^2}{1 + (\mu/2M)}; \quad \varepsilon' = \frac{\varepsilon}{1 + (\mu/2M)},$$

where E_μ^m is the maximum energy of the mesons. For energies E_μ, close to the maximum (E_μ^m –

*Presented at the Theoretical Seminar of the Institute of Physical Problems, Academy of Sciences, USSR in October 1950.

Note in Proof: After this work was completed several papers appeared treating the same questions [see e.g., K. M. Watson, Phys. Rev. 88, 1163 (1952)].

[1] L. D. Landau and E. M. Lifshitz, *Quantum Mechanics*.

$E_\mu \ll E_\mu^m$) we can set $C(E_n^0, E_\mu) \approx C(E_n^0, E_\mu^m)$. As is seen from (3), the spectrum of mesons has a maximum at the energy $E_\mu \approx E_\mu^m - \epsilon'$.

2. We can get the ratio between the cross section (3) for parallel spin of the nucleons and the cross section corresponding to the production of a deuteron in the final state. Inside the range of nuclear forces ($r < r_0$) the functions ϕ for free and bound states of the neutron and proton differ only in a constant factor which is determined by the value of the functions at $r = r_0$ (if the energy of the nucleons can be neglected compared to the depth of the potential well V_0). Outside the range of forces the functions are known from the theory of the deuteron and the theory of neutron-proton scattering[2]. . It can be shown that

$$\left|\frac{\varphi_0(r_0)}{\varphi_{P_n}(r_0)}\right|^2 = \left(\frac{M}{\hbar^2}\right)^{1/2} \frac{\varepsilon_0^{1/2}}{2\pi} (E_n + \varepsilon_0)\left\{1 + O\left(\frac{\varepsilon}{V_0}\frac{E_n}{V_0}\right)\right\}. \tag{4}$$

Using (4), it is easy to obtain

$$d\sigma = \frac{\sigma_0}{2\pi\sqrt{[1+(\mu/2M)]\,\varepsilon_0 E'_\mu}} \times \frac{\sqrt{(E_\mu^m - E_\mu)E_\mu}}{(E_\mu^m - E_\mu + \varepsilon_0')} \frac{\sqrt{1+(E_\mu/2\mu c^2)}}{\sqrt{1+(E'_\mu/2\mu c^2)}} \times \frac{1+(E_\mu/\mu c^2)}{1+(E'_\mu/\mu c^2)} \frac{C(E_n^0 E_\mu)}{C(E_n^0 E'_\mu)} dE_\mu\, d\omega_\mu; \tag{5}$$

$$\varepsilon_0 = \frac{\varepsilon_0}{1+(\mu/M)}, \quad E'_\mu = E_\mu^m + \varepsilon_0;$$

Here σ_0 is the cross section for the production of deuterons per unit solid angle of the mesons. Near the upper end of the spectrum of mesons $C(E_n^0 E_\mu)/C(E_n^0 E'_\mu) \approx 1$. The experimental spectrum of mesons represents the superposition of two curves: the distribution (5) and the analogous distribution for anti-parallel spin of neutron and proton. Integrating (5) over dE_μ and $d\omega_\mu$ and assuming $C(E_n^0 E_\mu)$ to be an increasing function of E_μ we get the ratio

$$\int \sigma_0 d\omega_\mu \Big/ \int \sigma d\omega_\mu dE_\mu \geqslant 4\sqrt{\varepsilon_0/E_\mu^m}. \tag{6}$$

Equality in (6) corresponds to H' being independent of meson energy (under the restriction $E_\mu \ll \mu c^2$). If $H' \sim \sqrt{E_\mu}$ then

$$\int \sigma_0 d\omega_\mu \Big/ \int \sigma d\omega_\mu dE_\mu = {}^{16}/_3 \sqrt{\varepsilon_0/E_\mu^m}. \tag{6'}$$

3. When two neutrons appear in the final state (the reactions are then $p+n=n+n+\pi^+$ or $n+n=n+n+\pi^0$), then only the case of anti-parallel spin occurs with appreciable probability. Neutrons with parallel spin cannot, consistent with selection rules, appear in S states and, consequently, do not interact at low energy. Therefore, the cross section for the production of mesons with neutrons having parallel spin in the final state does not have a resonance factor (2) and is considerably smaller than the cross section for neutrons with anti-parallel spin. For the same reason as before this latter cross section does not depend on the direction of the vector $\mathbf{P}_n$. The distribution of mesons in energy is given by the expression (3). However, the quantity ϵ is unknown in this case.

4. In the case with two protons in the final state (the reactions are then $p+n=p+p+\pi^-$ or $p+p=p+p+\pi^0$), finding the energy dependence of the wave function at $r=r_0$ and using the results of the theory of proton scattering [3,4] it is easy to prove that :

$$d\sigma = C_1(E_n^0 E_\mu) \times \frac{F(\eta)\sqrt{(E_\mu^m - E_\mu)E_\mu}\sqrt{1+(E_\mu/2\mu c^2)}\,(1+E_\mu/\mu c^2)\,dE_\mu}{F^2(\eta)(E_\mu^m - E_\mu) - \frac{\hbar^2}{M+(\mu/2)}\left\{-\frac{1}{a} + \gamma E_n - \frac{h(\eta)}{R}\right\}^2} \tag{7}$$

$$F(\eta_l) = \frac{2\pi\eta}{e^{2\pi\eta}-1}; \quad \eta_l = \frac{e^2}{\hbar v_n};$$

$$h(\eta_l) = \mathrm{Re}\,\frac{\Gamma'(-i\eta)}{\Gamma(-i\eta)} - \ln\eta_l;$$

$$R = \frac{\hbar^2}{Me^2} = 2.9\cdot 10^{-12}\ \text{см}; \quad a = -7.7\cdot 10^{-13}\ \text{см};$$

$$\gamma = 3.4\cdot 10^{11}\ \text{MeV}^{-1}\ \text{см}^{-1}.$$

[2] Ia. A. Smorodinskii, J. Exper. Theoret. Phys. USSR 17, 941 (1947); Doklady Akad. Nauk SSSR 60, 217 (1948)

[3] L. D. Landau and Ia. Smorodinskii, J. Exper. Theoret. Phys. 14, 269 (1944).

[4] J. D. Jackson and J. M. Blatt, Revs. Mod. Phys. 22, 77 (1950).

The Coulomb repulsion of the protons, as can be seen from (7), significantly diminishes the spectrum of mesons near the upper limit as compared with the cases considered above. As in the case of two neutrons the spins of the protons are anti-parallel and the cross section is independent of the direction of the vector P_n.

5. The differential cross section σ_1 in the center of the mass system for the absorption of mesons by the deuteron is easily connected with the cross section σ_0, using the principle of detailed balance. A simple calculation gives

$$\sigma_1 = \sigma_0 (E_n^0) \frac{E_n^0}{E_\mu} \frac{[M + (\mu/2)]}{2\mu} \times \frac{\sqrt{1 + (E_\mu^0/\mu c^2)}}{\sqrt{1 + (E_\mu/2\mu c^2)}} \frac{[1 + (2E_n^0/\mu c^2)]}{[1 + (E_\mu/\mu c^2)]}; \quad (8)$$

$$E_n^0 = \mu c^2 + \frac{P_\mu^2}{4M} + E'_\mu - \varepsilon_0.$$

I express my thanks to N.M. Polievtov-Nikoladze and L.M. Soroke for interesting discussions.

Translated by A. S. Wightman
2

SOVIET PHYSICS-JETP VOLUME 1, NUMBER 1 JULY, 1955

Remarks on the Theory of Fusion

G. A. SOKOLIK
Moscow State University

(Submitted to JETP editor February 25, 1953)
J. Exper. Theoret. Phys. USSR 28, 13-16 (January, 1955)

A generalization of De Broglie's theory of fusion is given, which holds for infinite-dimensional as well as finite-dimensional wave equations.

IN de Broglie's theory of fusion, which generalizes the idea of the neutrino theory of light [1], a method of constructing particles with higher spin from particles with spin 1/2 was indicated [2].

In the present work, a point of view somewhat more general than the theory of fusion is proposed. The problem is formulated as follows: Consider two relativistically invariant equations, infinite-dimensional in general,

$$\gamma_\mu^{(1)} \frac{\partial \psi^{(1)}}{\partial x_\mu} + \varkappa' \psi^{(1)} = 0, \quad \gamma_\mu^{(2)} \frac{\partial \psi^{(2)}}{\partial x_\mu} + \varkappa'' \psi^{(2)} = 0, \quad (1)$$

They will generate two reducible representations of the Lorentz group $\tau^{(1)}$ and $\tau^{(2)}$. It is required to find the invariant equation corresponding to the Kronecker product $(\tau^{(1)} \times \tau^{(2)})$. In our arguments, we will use the results and notation of the work of Gel'fand and Iaglom [3].

[1] A. A. Sokolov, J. Exper. Theoret. Phys. USSR 7, 1055 (1937)

[2] L. De Broglie, Théorie générale des particules a spin (méthode de fusion), Paris, 1943

[3] I. Gel'fand and A. Iaglom, J. Exper. Theoret. Phys. USSR 18, 703 (1948)

1. For the following, we need the reduction formula for the direct product of two irreducible representations of the Lorentz group. The infinitesimal representation of the group is determined by the operators F^+, F^-, F^0, H^+, H^-, H^0. Their form for irreducible representations is given by numbers k_0, k_1 [3]. If k_0, k_1 are simultaneously integral or half integral real numbers, and $k_0 < k_1$, then the representations are finite-dimensional.

The space of the representation is given by basis vectors ξ_p^k, where the total momentum k, appearing as the weight of the sub-group of rotations H^+, H^-, H^0, runs through the series of numbers ($k = k_0$, $k_0 + 1$, $k_0 + 2$, . . .). In the finite-dimensional case, the sequence k breaks off at $k = k_0 - 1$ ($p = k, k-1, \ldots -k$). It is not difficult to prove that the infinitesimal representations of the group, τ_n, have two scalar operators Δ_1 and Δ_2 which commute with every operator of the representation and have the form

$$\Delta_1 = F^+F^- + F^{02} - H^+H^- - H^{02} - 2iH^0,$$
$$\Delta_2 = 2F^0H^0 + F^+H^- + F^-H^+. \quad (2)$$

These operators are given by the formulas

$$\Delta_1 \xi^k_p = (k_0^2 + k_1^2 - 1)\,\xi^k_p, \qquad (2')$$
$$\Delta_2 \xi^k_p = 2i(k_0 k_1)\,\xi^k_p.$$

The vectors $\xi^{(1)k_1}_{p_1}\xi^{(2)k_2}_{p_2}$, written in lexicographic order

$$(\xi^{(1)k_1}_{p_1}\xi^{(2)k_2}_{p_2} \prec \xi^{(1)l_1}_{m_1}\xi^{(2)l_2}_{m_2}, \quad \text{if}$$

$$k_1 < l_1 \quad \text{or} \quad k_1 = l_1,\ k_2 < l_2).$$

form a basis for the space of the product representation.

As is easily proved, the commutators among the operators Δ_1, Δ_2, given in (2), and the known scalar operator of the sub-group of rotations $[H^2 + k(k+1)]\,\xi^k_p = 0$, written in the basis $\xi^{(1)k_1}_{p_1}\xi^{(2)k_2}_{p_2}$ are simultaneously reduced to diagonal form by a matrix T. In the general case, T has the form: $T = AC$ where C is a matrix whose elements are finite-dimensional matrices $\| C^{k_1+k_2-\lambda}_{p_1 p_2} \|$ indexed by the parameters k_1, k_2. $C^{k_1+k_2-\lambda}_{p_1 p_2}$ denotes a Clebsch-Gordon coefficient [4]. A is a matrix commuting with H^2. (The particular form of A has to be determined for each separate case.) Hence, we have $\Delta_1' = T^{-1}\Delta_1 T$ and $\Delta_2' = T^{-1}\Delta_2 T$, where Δ_1' and Δ_2' are diagonal matrices.

From the proper values Δ_1' and Δ_2', we get, using formula (2), the weights $(\pm k_0^m, \pm k_1^m) = \tau_m$ of the representations into which $(\tau_n^{(1)} \times \tau_n^{(2)})$ reduces. The reduction works also for the infinite-dimensional case, but may be written especially simply in the case of finite-dimensional representations:

$$[(k_0' k_1') \times (k_0'' k_1'')] = (k_0' + k_0'',\ k_1' + k_1'' - 1) \qquad (3)$$
$$+ (k_0' + k_0'' + 1,\ k_1' + k_1'' - 2) + (k_0' + k_0'' - 1,$$
$$k_1' + k_1'' - 2) + (k_0' + k_0'' + 2,\ k_1' + k_1'' - 3)$$
$$+ (k_0' + k_0'',\ k_1' + k_1'' - 3)$$
$$+ (k_0' + k_0'' - 2,\ k_1' + k_1'' - 3) + \ldots$$

In the particular case in which $(k_0' k_1')$ and $(k_0'' k_1'')$ are half integers, (3) coincides with a formula of Cartan [5]. Finally, it is impossible, using the spinor formalism, to generalize the development of Cartan to the infinite-dimensional cases.

2. With the use of this formula, we can solve the problem posed above of constructing generalized equations for the product functions $(\psi^{(1)}\psi^{(2)})$. The representations $\tau^{(1)}$ and $\tau^{(2)}$ are reduced into irreducible components $\tau^{(1)} \sim \tau_1^{(1)} + \tau_2^{(1)} + \ldots$; $\tau^{(2)} \sim \tau_1^{(2)} + \tau_2^{(2)} + \ldots$. Taking the product $(\tau^{(1)} \times \tau^{(2)})$, and using the above mentioned reduction into irreducible representations, we get a direct sum of irreducible components τ_i. We use a matrix T, whose elements are the matrices $\| T^{\tau_i \tau_j} \|$, given in the preceding paragraph, where $(\tau_i \tau_j)$ are, as before, in lexicographic order.

As basis for the space of $(\tau_1^{(1)} \times \tau_2^{(2)})$, we take the vectors $g^k_{p\tau}$ connected with the vectors $\xi^{(1)k_1}_{p_1\tau_1}\xi^{(2)k_2}_{p_2\tau_2}$ by the formula:

$$g^k_{p\tau} = \sum_{\substack{k_1 k_2 \\ \tau_1 \tau_2 \\ p_1 + p_2 = p}} T^{k;\ k_1\ k_2}_{p\tau;\ p_1\tau_1 p_2\tau_2}\, \xi^{(1)k_1}_{p_1\tau_1}\xi^{(2)k_2}_{p_2\tau_2}. \qquad (4)$$

If, in the expression for the matrix T, we let $A = I$, where I is the unit matrix, we get from (4) the ordinary Clebsch-Gordon reduction. The expansion obtained in (4) determines the fundamental matrix γ_0, giving the generalized equation for the product functions:

$$\gamma^0 = \| c^k_{\tau\tau'}\delta_{pp'}\delta_{kk'} \|; \qquad (5)$$

the form of $c^k_{\tau\tau'}$ is found in Gel'fand and Iaglom [3]. The quantity γ^0 can be computed immediately in the basis $\xi^{(1)k_1}_{p_1\tau_1}\xi^{(2)k_2}_{p_2\tau_2}$ from the known condition of Lorentz invariance

$$\gamma^0 = [[\gamma^0 F^0] F^0]. \qquad (5')$$

To do this, we represent γ^0 in the form

$$\gamma^{0\prime}\xi^{(1)k_1}_{p_1\tau_1}\xi^{(2)k_2}_{p_2\tau_2} = \sum_{\tau_1'\tau_2'} c^{k_1 k_2\ ,\ ,}_{\tau_1\tau_2\tau_1'\tau_2'}\xi^{(1)k_1}_{p_1\tau_1'}\xi^{(2)k_2}_{p_2\tau_2'}, \qquad (6)$$

and use (5). Then we get 12 homogeneous equations relating the coefficients:

$$c^{k_1\pm 1 k_2}_{\tau_1\tau_2\tau_1'\tau_2'}, \quad c^{k_1\ k_2\pm 1}_{\tau_1\tau_2\tau_1'\tau_2'}, \quad c^{k_1\pm 1 k_2\pm 1}_{\tau_1\tau_2\tau_1'\tau_2'}, \qquad (7)$$
$$\ldots \quad c^{k_1\pm 1 k_2\pm 1}_{\tau_1\tau_2\tau_1'\tau_2'}, \quad c^{k_1\ k_2}_{\tau_1\tau_2\tau_1'\tau_2'}.$$

A somewhat tedious calculation shows that this system of equations has non-trivial solutions only when $(\tau_1\ \tau_2)$ and $(\tau_1'\ \tau_2')$ are connected by one of the following possible correspondences:

[4] van der Waerden, Die Gruppen Theoretische Methode in der Quanten Mechanik, Berlin, 1932

[5] E. Cartan, Leçons sur la Theorie des Spineurs, Paris, 1938

$$k_0'^{(1)} = k_0^{(1)},\ k_0'^{(2)} = k_0^{(2)},\ k_1'^{(1)} = k_1^{(1)} \pm 1,\ k_1'^{(2)} = k_1^{(2)} \pm 1,$$

or

$$k_0'^{(1)} = k_0^{(1)} \pm 1,\ k_0'^{(2)} = k_0^{(2)} \pm 1,\ k_1'^{(1)} = k_1^{(1)},\ k_1'^{(2)} = k_1^{(2)},$$

or

$$k_0'^{(1)} = k_0^{(1)} \pm 1,\ k_0'^{(2)} = k_0^{(2)},\ k_1'^{(1)} = k_1^{(1)},\ k_1'^{(2)} = k_1^{(2)} \pm 1,$$

or

$$k_0'^{(1)} = k_0^{(1)},\ k_0'^{(2)} = k_0^{(2)} \pm 1,\ k_1'^{(1)} = k_1^{(1)} \pm 1,\ k_1'^{(2)} = k_1^{(2)},$$

that is when $(\tau_1\ \tau_2)$ and $(\tau'_1 \tau'_2)$ are "linked" in pairs.

3. We now note the connection between the generalized equations for product functions, given by the formulas (5) and (5′) and the equations of the theory of De Broglie [2]. We consider the particular case of the fusion of two identical finite dimensional equations, whose matrices γ^0 are in diagonal form. Then the matrix β^0 determined by (5) and (5′), can be expressed in the form

$$\beta^0 = {}^1/_2(\gamma^0 I' + \gamma^{0\prime} I); \tag{8}$$

γ^0 and $\gamma^{0\prime}$ are labeled with different sets of indices; I and I' are the corresponding unit matrices. In this case, the proper values μ_i of the matrix β^0 are subject to the condition $\mu_i = 1/2(\lambda_k + \lambda_j)$ (λ_k, λ_j are the proper values of the matrix γ^0); distinct μ_i correspond to distinct pairs λ_k, λ_j. The condition (8) gives the well known representation of the theory of De Broglie [2].

Thus it is proved that the equations of De Broglie's theory of fusion are obtained from our generalized equations for product functions, while the fusion condition, introduced in (2) is not used in this derivation. As is proved in (2), De Broglie equations consisting of different spins are reducible in the absence of external fields.

As an example, we consider the fusion of two spinor equations, appearing in the basic theory of De Broglie. As is proved in reference 3, the Dirac equation is given by the representation $(-1/2, 3/2) = (1/2, 3/2)$ where γ^0 has the form:

$$\gamma^0 = \begin{Vmatrix} 0 & 1 & 0 & 0 \\ 1 & 0 & 0 & 0 \\ 0 & 0 & 0 & 1 \\ 0 & 0 & 1 & 0 \end{Vmatrix}$$

Multiplying the representations and using the reduction formula (3), we get the following irreducible representations (0 1), (0 1), (0 2), (0 2), (−1 2), (1 2). In order that the matrix γ^0 corresponding to this representation be reduced to diagonal form while the energy remains positive in agreement with the theorem of Pauli [6] it is necessary to represent the irreducible components in the form

$$(-1\ 2) = (0\ 2) = (1\ 2) \sim 1,$$
$$(0\ 1) = (0\ 2) \sim 2,$$
$$(0\ 1) \sim 3.$$

Thus, the equation for the product functions splits into two equations: a ten dimensional equation giving representations 1, and a five-dimensional giving representations 2. The representation 3 yields the trivial one-dimensional equation.

It is easily shown that the resulting equations coincide with the equations of Duffin [6]. As is well known, those equations describe particles with spin 1 or 0, and their matrices satisfy the relation (8). It is easy to see that the possibility of more general schemes of "coupled" irreducible representations gives irreducible equations. Here the energy will be positive definite only if supplementary conditions are imposed. In that case the equations also describe particles with spin 1 and 0.

We note that in the corresponding generalized equations for product functions consisting of different spins, in general, no reduction takes place, even in the absence of external fields; this follows from (3). This mixing of components can be interpreted as the existence of internal interaction in the "product" particles.

The new type of interaction proposed in the present work differs from ordinary interactions in that internal interaction connects the component irreducible representations of the Lorentz group, but not, as in the usual case, the components of the ψ-functions. Thus, there appears to be a possibility of giving the structure of elementary particles on the basis of representations of the Lorentz group, infinite dimensional ones in general. The connection between internal interaction and positive definiteness conditions has been considered in the same way in the work of Gurevitch [8]. It is necessary to remark, that in the theory of De Broglie, particles of higher spin are described by reducible equations, which are represented some-

[6] W. Pauli, Revs. Mod. Phys. **13**, 203 (1941)

[8] A. Gurevitch, J. Exper. Theoret. Phys. **24**, 149 (1953)

what artificially from the point of view of Gel'fand and Iaglom's theory of particles of higher spin. It is proposed that the consideration of the problem in the infinite-dimensional case can be connected with the general theory of non-local fields, giving vectors in hilbert space[7].

Translated by A. S. Wightman
3

In conclusion, I want to express my thanks to Professor D. D. Tvanenko for a series of remarks and numerous discussions of the results of this work.

[7] D. Ivanenko and A. Sokolov, Klassische Feld. Theorie, Berlin (1953)

SOVIET PHYSICS-JETP VOLUME 1, NUMBER 1 JULY, 1955

On Longitudinal Vibrations of Plasma, 1.

A. A. LUCHINA
Moscow State University

(Submitted to JETP editor February 17, 1954)
J. Exper. Theoret. Phys. USSR 28, 18-27 (January, 1955)

The problem of propogation of longitudinal waves in a plasma under given boundary conditions is solved. A "dispersion" equation which takes into account motion of the ions is obtained.

1. INTRODUCTION

IN studying the processes discovered by Langmuir, of vibrations in a plasma which arise because of the Coulomb interaction of charged particles, one usually considers only the motion of the electrons. The method proposed by Vlasov[1] for investigating specific electrical properties of plasma--the self-consistent field method--basically is applied only to them. Because of their large mass, the ions are considered as a positive background having no effect on the vibration of the electrons.

It is true that recently the necessity for considering ionic vibrations has been pointed out in several papers[2-4] However, no detailed investigations like those for electrons[5,6] exist in the literature*.

Ions can play a significant role in the vibrational properties of a plasma. In fact, since the mean free paths of electrons and ions are comparable, the squares of their transitional velocities are inversely proportional to their masses M/m. Therefore, during the passage of electrons and ions through a region of varying potential (an oscillating electrical double layer, etc.) the amplitude of vibration of the ions may turn out to be comparable to that of the electrons or even to exceed it, if the time for traversal of the region is smaller than the period of the variable potential. This behavior is clear, since the time for traversal of the region by the ions is M/m greater than for the electrons, although the acceleration given to the ion is a factor m/M smaller than that of an electron.

The ions play a special role when we consider the peculiar auto-oscillation process in plasma which leads to the possibility for occurrence of practically undamped waves, despite the occurrence of collisions[3]. The presence of two streams of charged particles (electrons and ions) with different velocities results in the appearance of undamped oscillations if the losses of energy from the wave due to collisions are compensated by a transfer of energy from the directed motion to the wave via the Coulomb interaction of the two particle streams.

A rigorous solution of the problem of longitudinal plasma oscillations (not considering the ions or collisions) was given in a paper of Landau[8] for the case where the initial deviation of the distribu-

[1] A. A. Vlasov, J. Exper. Theoret. Phys. USSR 8, 291 (1938); Scientific Reports, Moscow State University 75, Book II, part I (1945); Theory of Many Particles, State Publishing House, (1950)

[2] G. Ia. Miakishev, Dissertation, Moscow State University, (1952)

[3] M. E. Gertzenshtein, J. Exper. Theoret. Phys. USSR 23, 669 (1952)

[4] V. P. Silin, J. Exper. Theoret. Phys. USSR 23, 649 (1952)

[5] D. Bohm and E. P. Gross, Phys. Rev. 75, 1851, 1864, (1949)

[6] Yu. L. Klimontovich, Dissertation, Moscow State University (1951); J. Exper. Theoret. Phys. USSR 21, 1284, 1292 (1951)

* We consider the paper of Bazarov [e.g., see I. P. Bazarov, J. Exper. Theoret. Phys. USSR 21, 711 (1951)], which investigates the effect of the ions on the propagation of longitudinal waves in a plasma, to be unsatisfactory. In particular, in deriving the initial dispersion equation which is the basis of the investigation, an algebraic error is made as a result of which electronic and ionic terms which are proportional to the square of the charge have different signs in Bazarov's equation.

[8] L. D. Landau, J. Exper. Theoret. Phys. USSR 16, 574

tion function from equilibrium is given (initial value problem). Up to the present time there has been no formulation and rigorous solution of the problem of plasma oscillatior under assigned boundary conditions. This is precisely the problem which occurs when we consider plasma oscillations (e. g. in discharge tubes) which have stationary character.

The purpose of the present paper is to investigate stationary plasma oscillations caused by Coulomb forces, for given conditions at the boundary, and to analyze the part which ions play in the propagation of longitudinal waves in a plasma.

Keeping in mind that there are observed in plasmas sinusoidal oscillations with amplitudes not related to the magnitude of the ionization potential, an attempt is made in paper II (*v.* the following paper) to identify the longitudinal density waves considered here with the experimentally observed striations, and to compare the theory with experiment.

2. FORMULATION OF THE PROBLEM

The basis of all our later considerations is the set of kinetic equations for electrons and ions which takes into account the interaction of the charged particles by using the method of the self-consistent field in the form proposed by Vlasov [1]. Elastic collisions of charged particles with neutrals are included by means of a Boltzmann integral term.

The initial system of equations has the following form:

$$\frac{\partial f_1}{\partial t} + \mathbf{v}\frac{\partial f_1}{\partial \mathbf{r}} - \frac{e}{m}\operatorname{grad}(\varphi + \varphi_{ext.})\frac{\partial f_1}{\partial \mathbf{v}} = \iint (f_1' f_a' - f_1 f_a)\, V_1\, d\sigma_1 (d\mathbf{v}_a), \tag{1}$$

$$\frac{\partial f_2}{\partial t} + \mathbf{v}\frac{\partial f_2}{\partial \mathbf{r}} + \frac{e}{M}\operatorname{grad}(\varphi + \varphi_{ext.})\frac{\partial f_2}{\partial \mathbf{v}} = \iint (f_2' f_a' - f_2 f_a)\, V_2\, d\sigma_2 (d\mathbf{v}_a), \tag{2}$$

$$\Delta\varphi = -4\pi e\left(\int_{-\infty}^{+\infty} f_1 (d\mathbf{v}) - \int_{-\infty}^{+\infty} f_2 (d\mathbf{v})\right), \tag{3}$$

where $f_1 = f_1(\mathbf{r}, \mathbf{v}, t)$, $f_2 = f_2(\mathbf{r}, \mathbf{v}, t)$ and $f_a = f_a(\mathbf{r}, \mathbf{v}, t)$ are the distribution functions for electrons, ions and atoms in the spatial coordinate $\mathbf{r}$ and velocity $\mathbf{v}$, depending on the time t; V_1 is the relative velocity of electron and atom, V_2 the relative velocity of ion and atom; $d\sigma_1$ and $d\sigma_2$ are the differential cross sections for collision of electrons and ions with atoms; e is the algebraic value of the electron charge; m and M are the electron and ion masses; ϕ_{ext} is the potential of the external electric field in the interior of the plasma, which is responsible for the drift of electrons and ions; ϕ is the total potential of the self-consistent field.

An arbitrary disturbance in some portion of the plasma will be taken care of by assigning a corresponding boundary condition (concerning this, more later). In the absence of perturbations, the system of equations (1) to (3) determines a distribution of electrons f_{10}, and of ions f_{20}, which are time-independent. We shall consider a quasi-neutral plasma for which, in the absence of perturbations, the mean densities of ions and electrons are equal, i. e.

$$\int_{-\infty}^{+\infty} f_{10} (d\mathbf{v}) = \int_{-\infty}^{+\infty} f_{20} (d\mathbf{v}).$$

For the case of a uniform distribution of particles in space in the absence of perturbing forces, the system of equations (1) to (3) splits up into two independent equations:

$$-\frac{e}{m}\operatorname{grad}\varphi_{ext}\frac{\partial f_{10}}{\partial \mathbf{v}} = \iint (f_{10}' f_a' - f_{10} f_a)\, V_1\, d\sigma_1 (d\mathbf{v}_a), \tag{4}$$

$$\frac{e}{M}\operatorname{grad}\varphi_{ext}\frac{\partial f_{20}}{\partial \mathbf{v}} = \iint (f_{20}' f_a' - f_{20} f_a)\, V_2\, d\sigma_2 (d\mathbf{v}_a). \tag{5}$$

Equations like Eq. (4) have been solved by many authors. For weak constant currents, under the assumption that the cross section for elastic collision of electrons with gas atoms is inversely proportional to their velocity, the distribution f_{10} as shown in papers (6, 9) is Maxwellian around the drift speed of the electrons. Under the condition that the electrons, in moving through a free path, receive energy far in excess of the thermal energy of the gas atoms, the distribution has the form:

$$f_{10} = N\left(\frac{m}{2\pi\Theta_1}\right)^{3/2} \exp\left\{-\frac{m(\mathbf{v} - \mathbf{v}_{01})^2}{2\Theta_1}\right\}, \tag{6}$$

where N is the electron concentration, $\Theta_1 = kT_1$, k is the Boltzmann constant, T_1 is the absolute temperature of the electrons, $\mathbf{v}_{01}$ is the mean velocity of their directed motion.

---

[7] I. P. Bazarov, J. Exper. Theoret. Phys. USSR 21, 711 (1951)

[9] Taro Kihara, Revs. Mod. Phys. **24**, 45 (1952)

The applicability of such a distribution to the case of high currents ($|\mathbf{v}_{01}| \gtrsim \mathbf{v}_{te} = 2\Theta_1/m$) has not been established theoretically.

The distribution function f_{20} of the ions is much more difficult to find than the distribution function for the electrons. Investigations in this direction have been carried out either for very special cases or under crude physical assumptions (Kihara [9], Fok [10] and others). Still, the use of a Maxwell distribution for the ions does not lead to any clear discrepancy with experiment, and is used by many authors (for example, Vlasov [1] and Klimontovich [6]). In our calculations, we shall also use as a zeroth approximation (no perturbation) a Maxwell distribution for the ions:

$$f_{20} = N\left(\frac{M}{2\pi\Theta_2}\right)^{3/2} \exp\left\{-\frac{M(\mathbf{v}-\mathbf{v}_{02})^2}{2\Theta_2}\right\}, \quad (7)$$

where $\Theta_2 = kT_2$, T_2 is the absolute temperature of the ions, $\mathbf{v}_{02}$ is the drift velocity of the ions.

We carry through a linearization of the initial equations (1)-(3), assuming that the redistribution of the plasma particles due to a given perturbation in some part of the plasma is small. Thus, we set:

$$f_1 = f_{10} + f_{11}, \quad f_2 = f_{20} + f_{21}, \quad (8)$$

noting that $f_{11} \ll f_{10}$, $f_{21} \ll f_{20}$, $\phi \ll \phi_{ext}$. Then we obtain for f_{11} and f_{21} (in the case of small currents, determined by the potential ϕ_{ext}, the following system of equations:

$$\frac{\partial f_{11}}{\partial t} + \mathbf{v}\frac{\partial f_{11}}{\partial \mathbf{r}} - \frac{e}{m}\operatorname{grad}\varphi\frac{\partial f_{10}}{\partial \mathbf{v}} = -\frac{1}{\tau_1}f_{11}, \quad (9)$$

$$\frac{\partial f_{21}}{\partial t} + \mathbf{v}\frac{\partial f_{21}}{\partial \mathbf{r}} + \frac{e}{M}\operatorname{grad}\varphi\frac{\partial f_{20}}{\partial \mathbf{v}} = -\frac{1}{\tau_2}f_{21}, \quad (10)$$

$$\Delta\varphi = -4\pi e\left(\int_{-\infty}^{+\infty} f_{11}(d\mathbf{v}) - \int_{-\infty}^{+\infty} f_{21}(d\mathbf{v})\right). \quad (11)$$

The right side of Eq. (9) is the usual approximation of the Boltzmann term for the electrons, which has been used in many papers concerning plasmas ($1/\tau_1$ is the electron-atom collision frequency). In just this same way the right side of Eq. (10) is the first approximation to the Boltzmann term for the ions in the case of small perturbations (τ_2 is the mean free time for the ions).

Over the plane $x = 0$, we preassign a perturbation which is periodic in time with frequency ω (it is sufficient to consider a periodic perturbation, since, by virtue of the linearity of the system of equations, the solution in the case of an arbitrary perturbation can be represented in the form of a Fourier series or integral with known harmonics). Then the solution of the system of Eqs. (9)-(11) describes the process of propagation of the given disturbance into the plasma. Since we are considering a plane problem,

$$f_{11} = f_{11}(x, \mathbf{v}, t),$$
$$f_{21} = f_{21}(x, \mathbf{v}, t) \text{ and } \phi = \phi(x, t).$$

For convenience we integrate the system of equations over the y and z components of the velocity. Once more designating the functions $\int\int_{-\infty}^{+\infty} f_{11}\,d\eta d\zeta$ and $\int\int_{-\infty}^{+\infty} f_{21}\,d\eta d\zeta$ thus obtained by f_{11} and f_{21}, we obtain

$$\frac{\partial f_{11}}{\partial t} + \xi\frac{\partial f_{11}}{\partial x} - \frac{eN}{m}\frac{\partial\varphi}{\partial x}\frac{\partial F_{1,0}}{\partial\xi} = -\frac{1}{\tau_1}f_{11}, \quad (12)$$

$$\frac{\partial f_{21}}{\partial t} + \xi\frac{\partial f_{21}}{\partial x} + \frac{eN}{M}\frac{\partial\varphi}{\partial x}\frac{\partial F_{2,0}}{\partial\xi} = -\frac{1}{\tau_2}f_{21}, \quad (13)$$

$$\Delta\varphi = -4\pi e\left(\int_{-\infty}^{+\infty} f_{11}\,d\xi - \int_{-\infty}^{+\infty} f_{21}\,d\xi\right), \quad (14)$$

where

$$F_{1,0} = \left(\frac{m}{2\pi\Theta_1}\right)^{1/2}\exp\left\{-\frac{m(\xi-\xi_{01})^2}{2\Theta_1}\right\}; \quad (15)$$

$$F_{2,0} = \left(\frac{M}{2\pi\Theta_2}\right)^{1/2}\exp\left\{-\frac{M(\xi-\xi_{02})^2}{2\Theta_2}\right\}.$$

The problem we have formulated--the propagation in a plasma of longitudinal waves arising from a perturbation at the boundary $x = 0$ which varies periodically with frequency ω (a boundary value problem) which is analogous to the problem of Landau [8] in which he investigated the time behavior of a perturbation in a plasma (initial value problem). Therefore, generally speaking, we can also apply to our problem the method of solution of Landau, which makes use of one-sided Laplace transformations applied to the initial equations (the problem for the half-space [$x = 0$, $x = \infty$]). In our case this method requires that at $x = 0$ the functions

$$f_{11}(0, \xi, t), \quad f_{21}(0, \xi, t),$$
$$\phi(0, t), \quad (\partial\phi/\partial x)(0, t).$$

shall be given.

However, in specifying our boundary value

[10] V. A. Fok, J. Exper. Theoret. Phys. USSR 18, 1049 (1948)

[11] E. Hopf, Mathematical problems of radiative

problem* we can assign arbitrarily only the magnitude of the current of particles entering the medium through its boundary, so that we can assign the functions listed above only for positive values of ξ (we take the $+\xi$ axis along $+x$). The form of these functions for negative values of ξ is already determined by their form for $\xi > 0$, since the current of particles emerging from the medium across its boundary is automatically regulated by processes going on in its interior (collisions, Coulomb interactions, etc.). In our case the decisive role in this respect is played by the elastic collisions of the charged particles with neutrals; this is made clear by the fact that the solution of our linearized system of equations in which we neglect collisions ($1/\tau_1 = 1/\tau_2 = 0$) and use the method of Landau, does not lead to any auxiliary conditions of consistency which must be satisfied by the functions $f_{11}(0, \xi, t)$, $f_{21}(0, \xi, t)$. At the same time, if we include collisions, this same method leads to an auxiliary condition for consistency, which must be satisfied by the functions $f_{11}(0, \xi, t)$ and $f_{21}(0, \xi, t)$ because of the dependence of the form of these functions for $\xi < 0$ on their values for $\xi > 0$. It is therefore natural to choose a method of solution of the problem which goes with the direct assignment of the distribution function for the particles only for $\xi > 0$. Such a method of solution was suggested to us by N. N. Bogoliubov, and is carried through in the the following section.

First we simplify the equation system (12)-(14) by making use of the fact that a perturbation on the boundary which varies periodically with frequency ω, results in propagation in the plasma of a perturbation which varies in time with this same frequency. Setting

$$\begin{aligned} f_{11}(x, \xi, t) &= \psi_{11}(x, \xi)\, e^{-i\omega t}, \\ f_{21}(x, \xi, t) &= \psi_{21}(x, \xi)\, e^{-i\omega t}, \\ \varphi(x, t) &= \varphi_1(x)\, e^{-i\omega t}, \end{aligned} \tag{16}$$

we obtain for the functions ψ_{11}, ψ_{21}, ϕ_1 the following system of equations:

$$-i\omega\psi_{11} + \xi\frac{\partial\psi_{11}}{\partial x} - \frac{eN}{m}\frac{\partial\varphi_1}{\partial x}\frac{\partial F_{1,0}}{\partial\xi} = -\frac{1}{\tau_1}\psi_{11}, \tag{17}$$

$$-i\omega\psi_{21} + \xi\frac{\partial\psi_{21}}{\partial x} + \frac{eN}{M}\frac{\partial\varphi_1}{\partial x}\frac{\partial F_{2,0}}{\partial\xi} = -\frac{1}{\tau_{21}}\psi_{21}, \tag{18}$$

$$\Delta\varphi_1 = -4\pi e\left(\int_{-\infty}^{+\infty}\psi_{11}\,d\xi - \int_{-\infty}^{+\infty}\psi_{21}\,d\xi\right). \tag{19}$$

3. SOLUTION OF THE PROBLEM

We shall solve the system of equations (17)-(19), subjecting the functions ψ_{11} and ψ_{21} to the following boundary conditions:

$$\psi_{11}(0, \xi) = f_1(\xi), \quad \xi > 0; \tag{20}$$

$$\psi_{21}(0, \xi) = f_2(\xi), \quad \xi > 0; \tag{21}$$

$$\psi_{11}(\infty, \xi) = 0, \tag{22}$$

$$\psi_{21}(\infty, \xi) = 0. \tag{23}$$

The last two conditions correspond to absorption at infinity. We could also consider similarly the case of a totally reflecting wall at one of the boundaries, or other cases.

We also want to point out the close connection between the formulation of our present problem of propagation of longitudinal waves in a plasma and that of the well known problem of Milne [11-13] concerning the scattering and absorption of light in the atmosphere.

A solution of Eqs. (17) and (18) for the functions $\xi\psi_{11}(x, \xi)$, $\xi\psi_{21}(x, \xi)$ satisfying the boundary conditions (20)-(23), can be given in the form

$$\xi\psi_{11}(x, \xi) = \xi f_1(\xi)\exp\left\{-\frac{x}{\xi}\left(\frac{1}{\tau_1} - i\omega\right)\right\} \tag{24}$$

$$+ \frac{eN}{m}\int_0^x \exp\left\{-\frac{x - x'}{\xi}\left(\frac{1}{\tau_1} - i\omega\right)\right\}$$

$$\times \frac{\partial\varphi_1(x')}{\partial x'}\frac{\partial F_{1,0}(\xi)}{\partial\xi}\,dx', \quad \xi > 0,$$

$$\xi\psi_{11}(x, \xi) = -\frac{eN}{m}\int_x^\infty \exp\left\{-\frac{x - x'}{\xi}\left(\frac{1}{\tau_1} - i\omega\right)\right\}$$

*The specification of the boundary value problem was pointed out to us by A. N. Tikhonov and N. N. Bogoliubov.

[12] E. Titchmarsh, *Introduction to the Theory of Fourier Integrals* (1948)

[13] V. A. Fok, Matem. Sbornik **14**, 3 (1944)

$$\times \frac{\partial\varphi_1(x')}{\partial x'}\frac{\partial F_{1,0}(\xi)}{\partial\xi}dx', \quad \xi<0;$$

$$\xi\psi_{21}(x,\xi)=\xi f_2(\xi)\exp\left\{-\frac{x}{\xi}\left(\frac{1}{\tau_2}-i\omega\right)\right\}$$

$$-\frac{eN}{M}\int_0^x\exp\left\{-\frac{x-x'}{\xi}\left(\frac{1}{\tau_2}-i\omega\right)\right\}$$

$$\times \frac{\partial\varphi_1(x')}{\partial x'}\frac{\partial F_{2,0}(\xi)}{\partial\xi}dx', \quad \xi>0,$$

$$\xi\psi_{21}(x,\xi)=\frac{eN}{M}\int_x^\infty\exp\left\{-\frac{x-x'}{\xi}\left(\frac{1}{\tau_2}-i\omega\right)\right\} \tag{25}$$

$$\times \frac{\partial\varphi_1(x')}{\partial x'}\frac{\partial F_{2,0}(\xi)}{\partial\xi}dx', \quad \xi<0.$$

We introduce the following notation:

$$\int_0^\infty \xi f_1(\xi)\exp\left\{-\frac{x}{\xi}\left(\frac{1}{\tau_1}-i\omega\right)\right\}d\xi=u_1(x); \tag{26}$$

$$G_1(x)=\int_0^\infty\exp\left\{-\frac{x}{\xi}\left(\frac{1}{\tau_1}-i\omega\right)\right\} \tag{27}$$

$$\times\frac{\partial F_{1,0}(\xi)}{\partial\xi}d\xi, \quad x>0,$$

$$G_1(x)=-\int_{-\infty}^0\exp\left\{-\frac{x}{\xi}\left(\frac{1}{\tau_1}-i\omega\right)\right\}$$

$$\times\frac{\partial F_{1,0}(\xi)}{\partial\xi}d\xi, \quad x<0;$$

$$\int_0^\infty \xi f_2(\xi)\exp\left\{-\frac{x}{\xi}\left(\frac{1}{\tau_2}-i\omega\right)\right\}d\xi=u_2(x), \tag{28}$$

$$G_2(x)=\int_0^\infty\exp\left\{-\frac{x}{\xi}\left(\frac{1}{\tau_2}-i\omega\right)\right\} \tag{29}$$

$$\frac{\partial F_{2,0}(\xi)}{\partial\xi}d\xi, \quad x>0,$$

$$G_2(x)=\int_{-\infty}^0\exp\left\{-\frac{x}{\xi}\left(\frac{1}{\tau_2}-i\omega\right)\right\}$$

$$\times\frac{\partial F_{2,0}(\xi)}{\partial\xi}d\xi, \quad x<0.$$

Then

$$\int_{-\infty}^{+\infty}\xi\psi_{11}(x,\xi)\,d\xi=u_1(x) \tag{30}$$

$$+\frac{eN}{m}\int_0^\infty G_1(x-x')\frac{\partial\varphi_1(x')}{\partial x'}dx';$$

$$\int_{-\infty}^{+\infty}\xi\psi_{21}(x,\xi)\,d\xi=u_2(x) \tag{31}$$

$$-\frac{eN}{M}\int_0^\infty G_2(x-x')\frac{\partial\varphi_1(x')}{\partial x'}dx'.$$

In addition we make use of the equation of continuity associated with the system of equations (17)-(19):

$$\frac{\partial j_{11}(x)}{\partial x}\frac{1}{i\omega-(1/\tau_1)}+\frac{\partial j_{21}(x)}{\partial x}\frac{1}{i\omega-(1/\tau_2)}=\rho(x), \tag{32}$$

where

$$j_{11}(x)=e\int_{-\infty}^{+\infty}\xi\psi_{11}(x,\xi)\,d\xi, \tag{33}$$

$$j_{21}(x)=-e\int_{-\infty}^{+\infty}\xi\psi_{21}(x,\xi)\,d\xi,$$

$$\rho(x)=e\int_{-\infty}^{+\infty}\psi_{11}(x,\xi)\,d\xi-e\int_{-\infty}^{+\infty}\psi_{21}(x,\xi)\,d\xi.$$

Equations (32) and (19) lead to the relation

$$\frac{j_{11}(x)}{i\omega-(1/\tau_1)}+\frac{j_{21}(x)}{i\omega-(1/\tau_2)}=-\frac{1}{4\pi}\frac{\partial\varphi_1(x)}{\partial x}. \tag{34}$$

Setting

$$\frac{u_1(x)}{(1/\tau_1)-i\omega}-\frac{u_2(x)}{(1/\tau_2)-i\omega}=U(x), \tag{35}$$

we obtain from the relations (30), (31), and (34)

$$\frac{\partial\varphi_1(x)}{\partial x}=4\pi eU(x) \tag{36}$$

$$+\frac{4\pi Ne^2}{m}\int_0^\infty G_1(x-x')\frac{\partial\varphi_1(x')}{\partial x'}\frac{dx'}{(1/\tau_1)-i\omega}$$

$$+\frac{4\pi Ne^2}{M}\int_0^\infty G_2(x-x')$$

$$\times\frac{\partial\varphi_1(x')}{\partial x'}\frac{dx'}{(1/\tau_2)-i\omega}.$$

We define

$$\partial\varphi_1(x)/\partial x = f(x), \tag{37}$$

$$\frac{4\pi Ne^2}{m}\frac{G_1(x)}{(1/\tau_1)-i\omega}+\frac{4\pi Ne^2}{M}\frac{G_2(x)}{(1/\tau_2)-i\omega}=k(x), \tag{38}$$

$$4\pi eU(x)=g(x). \tag{39}$$

From (36), we obtain for $f(x)$ an integral equation of the form:

$$f(x)=g(x)+\int_0^\infty k(x-x')f(x')\,dx' \tag{40}$$

with the kernel

$$k(x)=\omega_{10}^2\int_0^\infty \exp\left\{-\frac{x}{\xi}\left(\frac{1}{\tau_1}-i\omega\right)\right\} \tag{41}$$

$$\times\frac{\partial F_{1,0}(\xi)}{\partial\xi}\frac{d\xi}{(1/\tau_1)-i\omega}$$

$$+\omega_{20}^2\int_0^\infty \exp\left\{-\frac{x}{\xi}\left(\frac{1}{\tau_2}-i\omega\right)\right\}$$

$$\times\frac{\partial F_{2,0}(\xi)}{\partial\xi}\frac{d\xi}{(1/\tau_2)-i\omega},\quad x>0,$$

$$k(x)=-\omega_{10}^2\int_{-\infty}^0 \exp\left\{-\frac{x}{\xi}\left(\frac{1}{\tau_1}-i\omega\right)\right\}$$

$$\times\frac{\partial F_{1,0}(\xi)}{\partial\xi}\frac{d\xi}{(1/\tau_1)-i\omega}$$

$$-\omega_{20}^2\int_{-\infty}^0 \exp\left\{-\frac{x}{\xi}\left(\frac{1}{\tau_2}-i\omega\right)\right\}$$

$$\times\frac{\partial F_{2,0}(\xi)}{\partial\xi}\frac{d\xi}{(1/\tau_2)-i\omega},\quad x<0,$$

where $\omega_{10}=\sqrt{4\pi Ne^2/m}$ and $\omega_{20}=\sqrt{4\pi Ne^2/M}$ are the Langmuir oscillation frequencies of the electrons and ions, respectively. The free term has the form

$$g(x)=4\pi e\int_0^\infty \xi f_1(\xi)\exp\left\{-\frac{x}{\xi}\left(\frac{1}{\tau_1}-i\omega\right)\right\} \tag{42}$$

$$\times\frac{d\xi}{(1/\tau_1)-i\omega}$$

$$-4\pi e\int_0^\infty \xi f_2(\xi)\exp\left\{-\frac{x}{\xi}\left(\frac{1}{\tau_2}-i\omega\right)\right\}$$

$$\times\frac{d\xi}{(1/\tau_2)-i\omega}.$$

Equations like (40) come up in many problems of mathematical physics [13]. For example, the previously mentioned Milne problem concerning the scattering and absorption of light in the atmosphere coincides with ours in its formulation and leads to an equation of this same type. An equation of this type was investigated in detail by Fok [13] who gives the method of solution, and proves the existence and uniqueness of a solution falling off at infinity ($x\to\infty$), under the following assumptions concerning the kernel $k(x)$ and the function $g(x)$*: the kernel itself and the functions $g(x)$, $k_1(x)=e^{c|x|}k(x)$, for some $c>0$, shall be absolutely integrable and have bounded variation in an infinite interval. If the equation $1-K(w)=0$ $\left(K(w)=\int_{-\infty}^{+\infty}k(x)\,e^{iwx}dx\right)$ has real roots in addition to com-

* Fok considered an equation with a symmetric kernel; but one can show that, without changing his argument essentially, the basic results remain valid also for an unsymmetric kernel.

plex roots, one must add to the previous conditions the requirement that these same conditions be satisfied by the function $(\ln g(x))\, x^{s-1} g(x)$ (where s is the maximum multiplicity of the root) and the orthogonality condition: $\int_0^\infty g(x)\,\gamma_r(x)\,dx = 0$ (where the $\gamma_r(x)$ are any linearly independent solutions of the homogeneous equation).

The asymptotic behavior of the solution is determined by the equation

$$1 - K(w) = 0 \tag{43}$$

or, defining

$$-iw = p, \quad \int_{-\infty}^{+\infty} e^{-px} k(x)\,dx = K(p), \tag{44}$$

by the equation

$$1 - K(p) = 0, \tag{45}$$

where $K(p)$ is analytic in the strip $-c < \mathrm{Re}\, p < c$: in fact for $x \to \infty$ the solution has the form

$$f(x) \sim \exp\{p_k x\}, \tag{46}$$

where p_k is that root of Eq. (45) with $\mathrm{Re}\, p < 0$ which is closest to the imaginary axis.

In order to apply Fok's method to the solution of our Eq. (40), we must first verify that the kernel $k(x)$ defined by (41) satisfies the required conditions.

Keeping in mind that particles with infinitely large velocities do not affect processes in the plasma, we shall, for convenience in applying the above mentioned method of solution, set

$$F_{1,0}(\xi) = F^M_{1,0}(\xi), \quad |\xi| < a, \tag{47}$$
$$F_{1,0}(\xi) = AF^M_{1,0}(\xi)\,\frac{\exp\{-N_{01}(\xi)\}}{\exp\{-m(\xi-\xi_{01})^2/2\Theta_1\}}, \quad |\xi| > a;$$

$$F_{2,0}(\xi) = F^M_{2,0}(\xi), \quad |\xi| < b, \tag{48}$$
$$F_{2,0}(\xi) = BF^M_{2,0}(\xi)\,\frac{\exp\{-N_{02}(\xi)\}}{\exp\{-M(\xi-\xi_{02})^2/2\Theta_2\}},$$

where

$$N_{01}(\xi) = \exp\{|\xi - \xi_{01}|^\alpha (m/2\Theta_1)^{\alpha/2}\}$$
$$N_{02}(\xi) = \exp\{|\xi - \xi_{02}|^\beta (M/2\Theta_2)^{\beta/2}\},$$

$F^m_{1,0}(\xi)$, $F^m_{2,0}(\xi)$ are Maxwellian velocity distributions for the electrons and ions, as given by Eq. (15); a, b, α, β are arbitrary constants satisfying the conditions: $a \gg 2|\xi_{01}|$, $b \gg 2|\xi_{02}|$, $0 < \alpha < 1$, $0 < \beta < 1$; the constants A and B are determined from the condition of continuity of the functions $F_{1,0}(\xi)$ and $F_{2,0}(\xi)$:

$$A = \frac{\exp\{-m(a-\xi_{01})^2/2\Theta_1\}}{\exp\{-N_{01}(a)\}}, \tag{49}$$

$$B = \frac{\exp\{-M(b-\xi_{02})^2/2\Theta_2\}}{\exp\{-N_{02}(b)\}}.$$

It is not difficult to see that $k(x)$ is a continuous function of x, since the integrals defining $k(x)$ converge uniformly in x and the functions in the integrands are continuous. Consequently we need only investigate the behavior of $k(x)$ at infinity. One can obtain an upper bound for the modulus of $k(x)$:

$$|k(x)| < C|x|\,e^{-c|x|}, \tag{50}$$

where

$$c = \min\{1/a\tau_1,\ 1/b\tau_2\}, \tag{51}$$

$$C = \max\Big\{2(1+A)\Big(\frac{m}{2\pi\Theta_1}\Big)^{1/2} \times \frac{\omega_{10}^2}{|(1/\tau_1) - i\omega|\,\tau_1(a - |\xi_{01}|)} \times 2(1+B)\Big(\frac{M}{2\pi\Theta_2}\Big)^{1/2} \times \frac{\omega_{20}^2}{|(1/\tau_2) - i\omega|\,\tau_2(b - |\xi_{02}|)}\Big\} \tag{52}$$

The estimate obtained for $k(x)$ shows the following:

1) $k(x)$ is an absolutely integrable function in the infinite interval $(-\infty, +\infty)$.

2) $e^{c|x|}k(x)$ is also an absolutely integrable function in the infinite interval $(-\infty, +\infty)$ for $0 < c' < c$.

Differentiating $k(x)$ under the integral sign, one can show in just this same way that $k'(x)$ is an absolutely integrable function in the infinite interval. At infinity, $k'(x)$ decreases no more slowly than an exponential with exponent $cx/2$. It is obvious that $\left\{e^{c''|x|}k(x)\right\}'$ is also absolutely integrable in the infinite interval for $c'' < c/2$. The condition of absolute integrability of the derivative is sufficient to make the function have bounded variation in the infinite interval. Consequently, the functions $k(x)$ and $e^{c''|x|}k(x)$ have bounded variation in that interval.

It is not hard to see that the function $g(x)$, defined in terms of the arbitrary functions $f_1(\xi)$, $f_2(\xi)$ by (42), also satisfies the requirements imposed, if $f_1(\xi)$ and $f_2(\xi)$ decrease sufficiently rapidly at infinity.

The preceeding discussion allows us to conclude that Fok's method applies to the solution of Eq. (40). Therefore we can assert that there exists a unique solution of (40), falling off at infinity, and that its asymptotic behavior is given by the "dispersion" Eq. (45).

We transform this last equation to a somewhat different form. For this purpose, we calculate $\int_{-\infty}^{+\infty} k(x)\, e^{-px}dx$, substituting for $k(x)$ its expression in (41). We carry out the computation for the electronic part of the kernel, $k_e(x)$.

$$\int_{-\infty}^{+\infty} k_e(x)\, e^{-px}dx = \omega_{10}^2 \int_0^\infty \left\{ \int_0^\infty \frac{\partial F_{1,0}}{\partial \xi} \frac{\exp\{-(x/\xi)[(1/\tau_1) - i\omega]\}}{(1/\tau_1) - i\omega}\, d\xi \right\} e^{-px}\, dx \tag{53}$$

$$- \omega_{10}^2 \int_{-\infty}^0 \left\{ \int_{-\infty}^0 \frac{\partial F_{1,0}}{\partial \xi} \times \frac{\exp\{-(x/\xi)[(1/\tau_1) - i\omega]\}}{(1/\tau_1) - i\omega}\, d\xi \right\} e^{-px}\, dx.$$

For values of p with $\mathrm{Re}\, p > 0$, we can, in computing the first integral, reverse the order of integration; then

$$\omega_{10}^2 \int_0^\infty \left\{ \int_0^\infty \frac{\partial F_{1,0}}{\partial \xi} \frac{\exp\{-(x/\xi)[(1/\tau_1) - i\omega]\}}{(1/\tau_1) - i\omega}\, d\xi \right\} \times e^{-px}\, dx \tag{54}$$

$$= -\frac{\omega_{10}^2}{p^2} \int_0^\infty \frac{\partial F_{1,0}}{\partial \xi} \frac{d\xi}{\xi - (i\omega/p) + (1/\tau_1 p)} + \frac{\omega_{10}^2}{p} \int_0^\infty \frac{\partial F_{1,0}}{\partial \xi} \frac{d\xi}{(1/\tau_1) - i\omega}.$$

We obtain a similar expression for the second integral, calculated for values of p with $\mathrm{Re}\, p < 0$:

$$-\omega_{10}^2 \int_{-\infty}^0 \left\{ \int_{-\infty}^0 \frac{\partial F_{1,0}}{\partial \xi} \exp\left\{-\frac{x}{\xi}\left(\frac{1}{\tau_1} - i\omega\right)\right\} \times \frac{d\xi}{(1/\tau_1) - i\omega} \right\} e^{-px}\, dx \tag{55}$$

$$= -\frac{\omega_{10}^2}{p^2} \int_{-\infty}^0 \frac{\partial F_{1,0}}{\partial \xi} \frac{d\xi}{\xi - (i\omega/p) + (1/\tau_1 p)} + \frac{\omega_{10}^2}{p} \int_{-\infty}^0 \frac{\partial F_{1,0}}{\partial \xi} \frac{d\xi}{(1/\tau_1) - i\omega}$$

But, since $\int_{-\infty}^{+\infty} k_e(x)\, e^{-px}\, dx$ is an analytic function of the complex variable p (cf. page 18) in the strip $-c'' < \mathrm{Re}\, p < c''$, we obtain the expression for $\int_{-\infty}^{+\infty} k_e(x) e^{-px}dx$ by analytic continuation of the sum of the integrals (54), (55) over the strip $-c'' < \mathrm{Re}\, p < c''$. The ionic part of $K(p)$ is calculated similarly. Finally we have

$$\int_{-\infty}^{+\infty} k(x)\, e^{-px}\, dx = -\frac{\omega_{10}^2}{p^2} \times \int_{C_1} \frac{\partial F_{1,0}}{\partial \xi} \frac{d\xi}{\xi - (i\omega/p) + (1/\tau_1 p)} \tag{56}$$

$$-\frac{\omega_{20}^2}{p^2}\int\limits_{C_2}\frac{\partial F_{2,0}}{\partial\xi}\frac{d\xi}{\xi-(i\omega/p)+(1/\tau_2 p)},$$

where the contours C_1 and C_2 go along the real axis from $\xi=-\infty$ to $\xi=+\infty$ circling the points $\xi_p=(i\omega/p)-(1/\tau_1 p)$ (for the contour C_1) and $\xi_p=(i\omega/p)-(1/\tau_2 p)$ (for contour C_2) from below.

Now the "dispersion" equation defining the asymptotic form of the solution for the longitudinal electric field produced in a plasma by a periodic perturbation at the boundary can be written in the form

$$1+\frac{\omega_{10}^2}{k^2}\int\limits_{C_1}\frac{\partial F_{1,0}}{\partial\xi}\frac{d\xi}{(\omega/k)+(i/\tau_1 k)-\xi}+\frac{\omega_{20}^2}{k^2}\int\limits_{C_2}\frac{\partial F_{2,0}}{\partial\xi}\frac{d\xi}{(\omega/k)+(i/\tau_2 k)-\xi}=0, \quad (57)$$

where $k=ip$, and the contour C_1 bypasses the point $\omega/k+i/\tau_1 k$, and the contour C_2 similarly bypasses the point $\omega/k+i/\tau_2 k$ from below.

At sufficiently large distances from the source of the perturbation, the distribution of field (and particles) will be approximated to sufficient accuracy by an expression of the form $A\exp\{i(\omega t-kx)\}$ (where k is the root of Eq.(57) which is closest to the imaginary axis). The quantity $2\pi/\mathrm{Re}\,k$ represents the spatial period of the propagating disturbance, while $\mathrm{Im}\,k$ is its logarithmic decrement*.

The last equation differs from the one obtained by Landau[8] for the dispersion of longitudinal waves in a plasma due to a given perturbation at the initial time, by terms which take into account the ions and the collisions of charged particles with neutrals. In addition, in Eq. (57) k is complex and ω is a real number ($\omega>0$), whereas in Landau's equation ω was complex and k was a real number.

In conclusion, I express my deep appreciation to N. N. Bogoliubov and G. Ia. Miakishev for the help they gave me in this work, and also to A. N. Tikhonov, M. V. Keldysh, M. F. Shirokov, and Iu. L. Rabinovich for discussion and valuable advice in completing the work.

Translated by M. Hamermesh
4

---

* The "dispersion" equation (57) also gives the criterion for occurrence of antidamped solutions, although a rigorous solution of the problem for this case (i.e., a determination of the amplitude) cannot be given within the realm of the linear theory.

On Longitudinal Vibrations of Plasma, II.

G. IA. MIAKISHEV AND A. A. LUCHINA
Moscow State University

(Submitted to JETP editor, February 17, 1954)
J. Exper. Theoret. Phys. USSR 28, 28-37 (January, 1955)

On the basis of the results of paper I, the dispersion properties of plasma are investigated in various special cases. It is shown that the motion of ions is of essential importance in most cases of propagation of longitudinal waves in discharge tubes. Values are found for the spatial period and logarithmic decrement as functions of the parameters of the discharge.

1. LONGITUDINAL VIBRATIONS OF PLASMA IN THE HIGH FREQUENCY REGION

FOR the case of plasma vibration at high frequency, the "dispersion" equation (57) of paper I simplifies considerably, and is easy to solve, so that the frequency dependence of the wave number and logarithmic decrement are obtained in explicit form. This equation, expressed in terms of dimensionless integration variables, has the form:

$$1 = -\frac{1}{k^2a_1^2} + \frac{1}{k^2a_1^2}\frac{\beta_1}{\sqrt{2\pi}}\int_{C_1}\frac{\exp\{-u^2/2\}\,du}{\beta_1-u} \quad (1)$$

$$-\frac{1}{k^2a_2^2} + \frac{1}{k^2a_2^2}\frac{\beta_2}{\sqrt{2\pi}}\int_{C_2}\frac{\exp\{-u^2/2\}\,du}{\beta_2-u},$$

where $a_1=\sqrt{\Theta_1/4\pi Ne^2}$ is the Debye length for the electrons, $a_2=\sqrt{\Theta_2/4\pi Ne^2}$ is the Debye length for the ions, $u=\sqrt{m/\Theta_1}(\xi-\xi_{01})$ in the integrals over contour C_1, $u=\sqrt{M/\Theta_2}(\xi-\xi_{02})$ in the integrals over contour C_2:

$$\beta_1 = \sqrt{\frac{m}{\Theta_1}}\left(\frac{\omega}{k}+\frac{i}{\tau_1 k}-\xi_{01}\right), \quad (2)$$

$$\beta_2 = \sqrt{\frac{M}{\Theta_2}}\left(\frac{\omega}{k}+\frac{i}{\tau_2 k}-\xi_{02}\right).$$

We shall look for a solution with small logarithmic decrement, i.e., we shall assume that

$$|\gamma| \ll |\varkappa| \quad (\varkappa + i\gamma = k). \quad (I)$$

In integrating along the contours C_1 and C_2 in Eq. (1), the points β_1 and β_2 are circled from below, so that each of these integrals can be written as the sum of an integral along the real axis between the limits $-\infty$ to $+\infty$, plus the residue of the integrand at the singularity, multiplied by πi [since, according to condition (I)

$$\mathrm{Re}\,\beta_1 \gg \mathrm{Im}\,\beta_1,$$

and

$$\mathrm{Re}\,\beta_2 \gg \mathrm{Im}\,\beta_2,$$

as can be seen from what follows]. Now Eq. (1) is expressed in the form:

$$1 = -\frac{1}{k^2a_1^2} + \frac{1}{k^2a_1^2}\frac{\beta_1}{\sqrt{2\pi}}\int_{-\infty}^{+\infty}\frac{\exp\{-u^2/2\}\,du}{\beta_1-u} \quad (3)$$

$$-i\sqrt{\frac{\pi}{2}}\frac{\beta_1}{a_1^2k^2}\exp\{-\beta_1^2/2\}$$

$$-\frac{1}{k^2a_2^2} + \frac{1}{k^2a_2^2}\frac{\beta_2}{\sqrt{2\pi}}\int_{-\infty}^{+\infty}\frac{\exp\{-u^2/2\}\,du}{\beta_2-u}$$

$$-i\sqrt{\frac{\pi}{2}}\frac{\beta_2}{a_2^2k^2}\exp\{-\beta_2^2/2\}.$$

Since we are considering the high frequency case, it is natural to introduce the conditions:

$$1/\tau_1 \ll \omega - \varkappa\xi_{01}, \qquad 1/\tau_2 \ll \omega - \varkappa\xi_{02}, \qquad \text{(II)}$$

which mean physically that the frequency, as measured in a coordinate system moving with the electron current, is much greater than the frequency of electron-atom collisions; and the frequency of vibration, measured in a coordinate system moving with the ion current, is much greater than the frequency of ion-atom collisions.

Keeping in mind conditions (I) and (II), we obtain the following values for β_1 and β_2 in zeroth approximation:

$$\beta_1 \approx \sqrt{\frac{m}{\Theta_1}}\left(\frac{\omega}{\varkappa} - \xi_{01}\right), \quad \beta_2 \approx \sqrt{\frac{M}{\Theta_2}}\left(\frac{\omega}{\varkappa} - \xi_{02}\right).$$

We also require that

$$\left|\frac{\omega}{\varkappa} - \xi_{01}\right| \gg \sqrt{\frac{\Theta_1}{m}}, \quad \left|\frac{\omega}{\varkappa} - \xi_{02}\right| \gg \sqrt{\frac{\Theta_2}{M}}, \qquad \text{(III)}$$

i.e., the phase velocity of the wave as measured in a coordinate system moving with the electron current shall be much greater than their mean thermal velocity, and that the phase velocity as measured in a system moving with the ions shall be much greater than the average thermal velocity of the ions. In this case, $|\beta_1| \gg 1$ and $|\beta_2| \gg 1$. The conditions (II) and (III) are a simple generalization of the analogous conditions that are introduced in solving the "dispersion" equation for high frequencies, when one neglects the ions and the drift of the charged particles.

Expanding the factors multiplying the exponentials in the integrands in Eq. (3) in powers of u/β_1 and u/β_2, and limiting ourselves to five terms in the expansion, we obtain:

$$1 = \frac{1}{k^2a_1^2\beta_1^2} + \frac{3}{k^2a_1^2\beta_1^4} - i\sqrt{\frac{\pi}{2}}\,\frac{\beta_1}{k^2a_1^2}\exp\{-\beta_1^2/2\} + \frac{1}{k^2a_2^2\beta_2^2} + \frac{3}{k^2a_2^2\beta_2^4} - i\sqrt{\frac{\pi}{2}}\,\frac{\beta_2}{k^2a_2^2}\exp\{-\beta_2^2/2\}. \qquad (4)$$

Separating into real and imaginary parts, we find in first approximation after a simple calculation, the well known dispersion equation relating the wave number κ to the vibration frequency ω, and the expression for the logarithmic decrement γ:

$$(\omega - \varkappa\xi_{01})^2 = \omega_{10}^2(1 + 3a_1^2\varkappa^2), \qquad (5)$$

$$\gamma = \frac{1}{\tau_1(\xi_{01} + 3a_1^2\omega_{10}\varkappa)} + \sqrt{\frac{\pi}{8}}\,\frac{\omega_{10}(1 + 3a_1^2\varkappa^2)^2}{\varkappa^3 a_1^3(\xi_{01} + 3a_1^2\omega_{10}\varkappa)} \times \exp\left\{-\frac{m\omega_{10}^2(1 + 3a_1^2\varkappa^2)}{2\Theta_1\varkappa^2}\right\}. \qquad (6)$$

Terms due to the ions will be of at least first order in the small quantity m/M compared to the electronic terms, and have therefore been omitted in deriving the relations (5) and (6).

These last relations were obtained under the assumption that the conditions (I)-(III) were fulfilled. It is easy to see that these conditions are fulfilled for sufficiently long wave lengths ($\kappa a_1 \ll 1$) at pressures sufficiently low so that

$$[\tau_1(\xi_{01} + 3a_1^2\omega_{10}\varkappa)]^{-1} \ll \varkappa.$$

The first term in the expression for the absorption coefficient is due to elastic collisions; the second represents the loss of energy, via Coulomb interaction, from electrons participating in the ordered motion, to electrons in random motion. Both the collisions and the loss of phase relation by the particles lead to damping of the disturbance as we move away from the source. In fact, the expression in the denominator of the right hand side of Eq. (6) is just the group velocity of the wave, in first approximation:

$$v_{gr} = d\omega/d\varkappa = \xi_{01} + 3a_1^2\omega_{10}\varkappa, \qquad (7)$$

which is positive, since its direction coincides with the direction of propagation of the disturbance. Thus, for a wave propagating away from the source, γ is positive, which represents a

damping. It is interesting that for very long wave lengths, as follows from (7), the perturbation propagates in the direction of the drift velocity of the electrons.

The linear absorption coefficient γ which we have obtained is related to the value of the time decrement [1] γ_t by:

$$\gamma = \gamma_t / v_{gr}. \tag{8}$$

Relation (8) is also satisfied for all the other cases considered in this paper, which indicates its universality.

2. LONGITUDINAL VIBRATIONS OF PLASMA IN THE LOW FREQUENCY REGION

Let us consider the case of excitation of plasma vibrations by a perturbation of low frequency. We include the limiting case $\omega = 0$, which corresponds to the appearance of a stationary spatial stratification in the particle distribution, under the action of a given jump of the potential at the boundary.

In the case we are now considering, where the frequency is low, and the average translational velocities of the electrons, ξ_{01}, and of the ions, ξ_{02}, are arbitrary, the integrals in Eq. (1) cannot be expressed in terms of elementary functions. They can however be expressed in terms of the error integral with complex argument [2].

Using Fok's relation [3]:

$$\frac{1}{\sqrt{2\pi}} \int_C \frac{e^{-u^2/2} du}{\beta - u} = \sqrt{2} e^{-\beta^2/2} \int_{-i\infty}^{\beta/\sqrt{2}} e^{z^2} dz - i\sqrt{2\pi} e^{-\beta^2/2}$$

and carrying out some simple transformations, we rewrite Eq. (1) in the form:

$$1 = -\frac{1}{k^2 a_1^2} - \frac{i\sqrt{\pi}}{k^2 a_1^2} (\alpha_1 + i\delta_1)(\alpha_3 + i\delta_3) \cdot \tag{9}$$
$$- \frac{1}{k^2 a_2^2} - \frac{i\sqrt{\pi}}{k^2 a_2^2} (\alpha_2 + i\delta_2)(\alpha_4 + i\delta_4),$$

where the following notation is used:

$$\beta_1 / \sqrt{2} = \alpha_1 + i\delta_1, \quad \beta_2 / \sqrt{2} = \alpha_2 + i\delta_2; \tag{10}$$

$$\exp\{-\beta_1^2/2\} \left(1 + \frac{2i}{\sqrt{\pi}} \int_0^{\beta_1/\sqrt{2}} e^{z^2} dz\right) = \alpha_3 + i\delta_3, \tag{11}$$

$$\exp\{-\beta_2^2/2\} \left(1 + \frac{2i}{\sqrt{\pi}} \int_0^{\beta_2/\sqrt{2}} e^{z^2} dz\right) = \alpha_1 + i\delta_4.$$

In Eq. (9) integrals of the type of (11) appear, for which tables are available.

Going over to dimensionless quantities, and choosing the Debye length for electrons, a_1, as unit of length, we will have in place of (9):

$$k^{*2} = -1 - (\Theta_1/\Theta_2) - i\sqrt{\pi}(\alpha_1 + i\delta_1)(\alpha_3 + i\delta_3) - (\Theta_1/\Theta_2) i\sqrt{\pi}(\alpha_2 + i\delta_2)(\alpha_4 + i\delta_4), \tag{12}$$

where k^* is the dimensionless complex wave number ($k^* = ka_1$). Equation (12) can be solved formally, giving κ^* and γ^* in terms of α_1, δ_1, α_2, δ_2, α_3, δ_3, α_4, δ_4. In fact, setting $\kappa^* = \kappa^* + i\gamma^*$ in Eq. (12) and separating real and imaginary parts, we get a pair of algebraic equations whose solution can be written in the form:

$$\kappa^* = \pm\sqrt{y}, \quad \gamma^* = \pm\sqrt{\bar{y}}, \tag{13}$$

where

$$y = (g_1 \pm \sqrt{g_1^2 + g_2^2})/2, \tag{14}$$

$$\bar{y} = (-g_1 \pm \sqrt{g_1^2 + g_2^2})/2. \tag{15}$$

---

[1] G. E. Gordeev, J. Exper. Theoret. Phys. USSR **22**, 230 (1952)

[2] V. N. Faddeeva and N. N. Terentiev, Tables of Values of the Probability Integral for Complex Argument, G.I.T.T.L. (Gov' T. Publ. Tech. Lit.), 1954; M. Born, Optics.

[3] V. A. Fok, Diffraction of Radio Waves, Publishing House, Acad. Sci. USSR, 1946.

For given κ^*, the sign of γ^* is uniquely determined by the sign of g_2, since

$$\gamma^* = g_2 / 2\kappa^*. \tag{16}$$

The relations (13)-(15) enable us to compute the period of the spatial inhomogeneity in the plasma, $\lambda^* = 2\pi / \kappa^*$, if we are given the damping coefficient γ^* and the frequency ω (in the general case, for a given frequency we get different values of the wave length λ^*, depending on the damping coefficient γ^*). For practical purposes, it is more convenient to give α_1 and δ_1 rather than ω and γ^*. Assigning α_1 and δ_1 determines the values of ω, γ^*, κ^* and correspondingly α_2, δ_2, α_3, δ_3, α_4 and δ_4. However, in the general case this dependence is not explicit. The values of α_2, δ_2 can be found immediately for given α_1 and δ_1 only if we neglect collisions (knowing α_2 and δ_2, we can find from the tables[2] values of α_3, δ_3, α_4, δ_4, and corresponding to these κ^*, γ^* and ω). Actually, since β_2 is related to β_1 by the relation

$$\beta_2 = \sqrt{\frac{M}{m}\frac{\Theta_1}{\Theta_2}}\,\beta_1 \tag{17}$$

$$+ \sqrt{\frac{M}{\Theta_2}}\,\frac{i}{k}\left(\frac{1}{\tau_2} - \frac{1}{\tau_1}\right) + \sqrt{\frac{M}{\Theta_2}}\,(\xi_{01} - \xi_{02}),$$

β_1 immediately determines β_2 if $\sqrt{\frac{M}{\Theta_2}}\,\frac{i}{k}\left(\frac{1}{\tau_2} - \frac{1}{\tau_1}\right) = 0$

Inclusion of this term makes it very difficult to establish the relation between ω, κ^* and γ^*, which we must know in order to match values of these quantities which will satisfy the "dispersion" equation. Consequently, finding an exact solution of the "dispersion" equation in the general case is practically impossible.

The fact that collisions were not considered in using the approximation of the Boltzmann integral to calculate the first approximation for the distribution function, cannot have any decisive effect on the value of the space period of a vibration process in the plasma if that process is the result of Coulomb interaction between the particles.*

However, if we are investigating absorption, the collisions can no longer be ignored, so that, having dropped them, we must renounce any attempt to find the value of the logarithmic decrement. All we can do in this respect is to show the existence of waves with increasing amplitude in the absence of collisions.

In this same way we can show the possibility for occurrence of undamped or weakly damped waves, despite the considerable absorption due to collisions.

We consider in detail the case $\omega = 0$. Here all the calculations simplify considerably, since in this case α_1 and δ_1 are uniquely determined by the parameters of the discharge, and we can then find κ^* and determine the sign of γ^* (as we pointed out above, it is meaningless to determine a numerical value for γ^* if we neglect collisions). It is typical that, for the case of $\omega = 0$, the values of κ^* and γ^* are determined uniquely, whereas in the general case of $\omega \neq 0$, there is a whole sequence of values of κ^* and γ^* which correspond to a definite frequency.

Assuming that the experimentally observed stratified illumination of the positive column (striations) could be due to the presence of a longitudinal density wave, we can compare the values of $\lambda = \lambda^* a_1$ thus obtained with the experimental values. In this interpretation, the case of $\omega = 0$ corresponds to fixed striations, the case of $\omega \neq 0$ to moving ones.

The comparison of theory with experiment is made difficult by the lack of precise information concerning some of the discharge parameters which are used in the theory. Usually in experiments on gas discharges only the following data are given: the electron concentration N, which is approximately equal to the ion concentration, the dimensions of the tube, the current I to the anode (or the current density j), the electron temperature T_1, and the spatial period of striation λ_s.

In our formulas there appear the expressions, not for the currents, but rather for the average velocities of the directed motion of electrons and ions. This velocity for the electrons can be determined from the current density j by the familiar relation:

$$j = \frac{1}{1{,}36}\,Ne\,\xi_{01}. \tag{18}$$

The order of magnitude of the ionic drift velocity can be determined from the simplest gas-kinetic considerations:

$$\xi_{02} = -\,{}^1\!/_2 \sqrt{m / M}\,\xi_{01}. \tag{19}$$

* This last does not mean that in the present theory the space period does not depend at all on the number of collisions. This dependence enters implicitly into the expression for the zeroth approximation to the distribution function: the velocity of drift and the concentration of charged particles are determined by it.

Table 1

Gas	N electrons per cm^3	T_1 °K	Pressure in cm Hg	Radius R or cross section S of tube	j or I
N_2^{14}	2×10^8	3×10^4	0.16	3.9 cm	0.27 mA/cm^2
Ne^{20}	10^{10}	3×10^4	1–2	3.5 "	$\frac{Ne}{1.36}$ 4×10^6 "
H_2^4	4×10^9	1.2×10^4	0.63	1.1 "	8mA
$Hg^{200.6}$	1.77×10^{10}	3×10^4	3×10^{-3}	0.6×0.4 cm^2	20mA

Gas	λ_s in cm	λ in cm for $T_2 = 1/10\ T_1$	λ in cm for $T_2 = 1/5\ T_1$	λ in cm for $T_2 = 1/2\ T_1$	λ in cm for $T_2 = 300$°K	Literature references
N_2^{14}	6	1.2	2.9	24	0.12	[7]
Ne^{20}	2.5	0.45	1.1	10.70	0.044	[8-9]
H_2^4	0.9	0.16	0.45	3.20	0.041	[10]
$Hg^{200.6}$	0.2	0.04	0.085	0.56	0.013	[11]

We still need to know the ion temperature, which also is not determined in experiments on striations. Apparently it is impossible to speak of the ion temperature in a plasma without specific information about the current distribution. Thus the ion temperature must be investigated separately in each experiment.

For orientation, we have used those data on ion temperatures which are available in the literature [4-6]. In accordance with this information, we shall compute the periods of striations setting the ion temperature T_2 equal, in turn, to $(1/10)T_1$, $(1/5)\ T_1$, $(1/2)T_1$ and room temperature.

The experimental data[7-11] in Table 1 are given along with the value of the space period computed theoretically for the ion temperatures shown there.

Table 1 shows that, for slightly non-isothermal plasma ($T_1 / T_2 \approx 2-10$) the space period of stationary striations as calculated theoretically agrees in order of magnitude with the experimental value. There is of course no expectation of exact agreement of theory and experiment, since our formulation of the problem is highly idealized.

4 L. Tonks, M. Mott-Smith and I. Langmuir, Phys. Rev **28**, 104 (1926).
5 L. Tonks and I. Langmuir, Phys. Rev. **34**, iuy (1929).
6 V. F. Kovalenko, D.A. Rozhanskii and L.A. Sena, Zh. Tekhn. Fiz. **4**, 1271-1688 (1934).
7 D. Oettingen, Ann. d. Phys., **19**, 519(1934)
8 A. A. Zaitsev, Vestn. M.G.U. (Moscow St. Univ.) ser. phys. math. and nat. sci., **10**, 41 (1951).
9 A. A. Zaitsev and Iu. L. Klimontovich, Vestn. M.G.U. (Moscow St. Univ.) ser. phys. math. and nat. sci., **12**, 59 (1951).
10 H. Paul, Z. Phys. **97**, 330 (1953).
11 H. J. Merill and H. W. Webb, Phys. Rev. **55**, 1069 (1939).

In particular, the effect of the radius of the tube on the period of striations has not been considered.

Nevertheless, order of magnitude calculations are still of interest, since for striation periods smaller than the tube diameter (which is the case for the experiments considered), we should expect that the tube radius should not seriously affect the space period. Calculations of the space period ommiting the ions show that the contribution of the ions to the value of λ will be the same in order of magnitude as that of the electrons. Consequently in this case the motion of the ions cannot be neglected.

In the case of highly non-isothermal plasma ($T_2 = 300\,^\circ$K), only the ionic vibrations are important. This can be shown by comparing the value of the period computed taking account of the ions with the value for the electrons alone.

We should also point out that in the case of electrons alone, the damping coefficient γ is always positive, ($g_2 > 0$), for positive values of κ, i.e., damping occurs. Since the inclusion of collisions leads to even greater damping, spatial layering is not possible in this case. Joint oscillations of electrons and ions lead to negative values of γ ($g_2 < 0$). This increase in amplitude, compensating the damping caused by collisions, can result in undamped waves.

A special feature of the results obtained is the occurrence of stationary striations for $|\xi_{01}| < 0.93 v_{Te} = 0.93\sqrt{2\Theta_1/m}$, in complete accord with experiment. The point is that, in several papers on the theory of striations, a condition has been presented for the existence of stationary striations

$$\xi_{01} \geqslant 0.93\, v_{Te},$$

supposedly following from the kinetic equations. This condition was first derived by Vlasov[12] from a form of the dispersion equation which was not entirely correct, since it contained a divergent integral. But in a paper of Klimontovich[13], the same condition was obtained on the basis of a correct dispersion equation. By considering an unbounded plasma, and neglecting collisions, Klimontovich arrived at the result that in such a plasma there cannot occur a time-independent distribution of electric field of the form $E = E_0 e^{-px}$ ($p = \gamma + i\kappa$), for $|\gamma| > |\kappa|$. (The last condition is equivalent to the limitation on the drift velocity mentioned above). However, this condition states only that in an unbounded plasma there can exist no exponentially increasing or decreasing distribution of electron density; this assertion, though certainly correct, has nothing to do with the appearance of striations. First of all, when we take account of the boundary (as is done in this paper), solutions of the type $E = E_0 \exp\{-(\gamma + i\kappa)x\}$ with $|\gamma| > |\kappa|$ do exist and satisfy the dispersion equation. Furthermore the true criterion for occurrence of spatial periodicity will have the form: $|\kappa| > |\gamma|$, where the quantity γ must be calculated by taking account of collisions. This condition gives a relation between the values of the drift velocities of the particles, their thermal velocities, and the frequency of collision of charged particles with neutrals.

We have considered the case of the appearance of spatial periodicity in the distribution of the charge density under the action of a jump in potential at some point of the plasma ($\omega = 0$). If the perturbation on the boundary varies periodically with frequency ω, it will excite in the plasma a traveling wave with phase velocity ω/κ. For small phase velocities, namely for $|\omega/\kappa| \ll \xi_{02}$ the dispersion equation remains, in first approximation, the same as for case of $\omega = 0$. For such waves, the period of the traveling spatial inhomogeneity will be the same as for stationary striations. This result is in agreement with experiment.

Usually for plasma in gas discharge tubes, $|\xi_{01}| \sim 10^6 - 10^8$ cm/sec, $|\xi_{02}| \sim 10^4 - 10^6$ cm/sec. For the centimeter wave region, the condition imposed on the phase velocity of the wave corresponds to the frequency range $\omega < 10^4 - 10^6$ c.p.s., to which the results of this section are therefore applicable.

3. THE CASE OF HIGH DRIFT VELOCITIES

For high drift velocity of the electrons, the problem of propagation in the plasma of a periodically varying perturbation, including effects of collisions of electrons and ions with gas atoms, can be completely solved by a method of successive approximations (just as in the case of high frequencies). In this case, the "dispersion" equation enables us to give explicitly the dependence of the space period of the inhomogeneity and the damping coefficient on the vibration frequency and the parameters of the discharge.

We shall assume that the drift velocity of the

12 A. Vlasov, Theory of Many Particles, Govt. Publ. House 1950.

13 Iu. L. Klimontovich, Journal of Experimental and Theoretical Physics., 21, 1292 (1951).

electrons is much greater than their thermal velocity, i.e.,

$$|\xi_{01}| \gg v_{Te} = \sqrt{2\Theta_1/m}. \tag{20}$$

A similar relation will hold for the ions:

$$|\xi_{02}| \gg v_{Ti} = \sqrt{2\Theta_2/M}. \tag{21}$$

We also assume that the following conditions are satisfied:

$$|\omega/\varkappa| \ll |\xi_{02}|, \quad |1/\tau_2\varkappa| \ll |\xi_{02}|. \tag{22}$$

Then, expanding the denominators of the integrands in Eq. (57) of paper I in powers of the small parameters,

$$\alpha = (\xi - \xi_{01})/\left(\xi_{01} - \frac{\omega}{k} - \frac{i}{\tau_1 k}\right)$$

and

$$\beta = (\xi - \xi_{02})/\left(\xi_{02} - \frac{\omega}{k} - \frac{i}{\tau_2 k}\right)$$

and limiting ourselves to the first approximation in computing the integrals, we obtain

$$k^2 = \left[\omega_{10}^2/\xi_{01}^2\left(1 - \frac{\omega}{k\xi_{01}} - \frac{i}{\tau_1 k\xi_{01}}\right)^2\right] \tag{23}$$

$$+ \left[\omega_{20}^2/\xi_{02}^2\left(1 - \frac{\omega}{k\xi_{02}} - \frac{i}{\tau_2 k\xi_{02}}\right)^2\right]$$

$$+ \sqrt{\frac{\pi}{2}}\,\omega_{10}^2\left[\left(\frac{m}{\Theta_1}\right)^{3/2}\left(\xi_{01} - \frac{\omega}{k} - \frac{i}{\tau_1 k}\right)\right.$$

$$\times \left.\exp\left\{-\frac{m}{2\Theta_1}\left(\xi_{01} - \frac{\omega}{k} - \frac{i}{\tau_1 k}\right)^2\right\}\right]$$

$$+ \sqrt{\frac{\pi}{2}}\,\omega_{20}^2\left[\left(\frac{M}{\Theta_2}\right)^{3/2}\left(\xi_{02} - \frac{\omega}{k} - \frac{i}{\tau_2 k}\right)\right.$$

$$\times \left.\exp\left\{-\frac{M}{2\Theta_2}\left(\xi_{02} - \frac{\omega}{k} - \frac{i}{\tau_2 k}\right)^2\right\}\right].$$

The solution of Eq. (23) for positive values of $\varkappa$, satisfying the condition (22) in the frequency range $\omega \ll \omega_{20}$ and $1/\tau_2 \ll \omega_{20}$, up to the terms of first order in the small quantities $\omega/k\xi_{01}$, $\omega/k\xi_{02}$, $1/\tau_1 k\xi_{01}$ and $1/\tau_2 k\xi_{02}$, has the form:

$$\varkappa = \sqrt{\frac{\omega_{10}^2}{\xi_{01}^2} + \frac{\omega_{20}^2}{\xi_{02}^2}} + \frac{\omega}{\xi_{01}}\frac{1}{1 + (\omega_{20}^2/\omega_{10}^2)(\xi_{01}^2/\xi_{02}^2)} \tag{24}$$

$$+ \frac{\omega}{\xi_{02}}\frac{1}{1 + (\omega_{10}^2/\omega_{20}^2)(\xi_{02}^2/\xi_{01}^2)},$$

$$\gamma = \frac{1}{\tau_1\xi_{01}}\frac{1}{1 + (\omega_{20}^2/\omega_{10}^2)(\xi_{01}^2/\xi_{02}^2)} \tag{25}$$

$$+ \frac{1}{\tau_2\xi_{02}}\frac{1}{(\omega_{10}^2/\omega_{20}^2)(\xi_{02}^2/\xi_{01}^2) + 1}$$

$$+ \sqrt{\frac{\pi}{2}}\,\frac{m\xi_{01}|\xi_{01}|}{2\Theta_1 a_1}\,\frac{\exp\{-m\xi_{01}^2/2\Theta_1\}}{\sqrt{1 + (\omega_{20}^2/\omega_{10}^2)(\xi_{01}^2/\xi_{02}^2)}}$$

$$+ \sqrt{\frac{\pi}{2}}\,\frac{M\xi_{02}|\xi_{02}|}{2\Theta_2 a_2}\,\frac{\exp\{-M\xi_{02}^2/2\Theta_2\}}{\sqrt{(\omega_{10}^2/\omega_{02}^2)(\xi_{02}^2/\xi_{01}^2) + 1}}.$$

From the relations (24), (25), we see that the ions play an essential part in this case of propagation of a perturbation in the plasma. Thus their contribution to value of the space period is the same order of magnitude as the contribution of the electrons. The direction of propagation of the disturbance is determined entirely by the ionic component, and in fact coincides with the direction of drift of the ions; i.e., the disturbance propagates only in the direction of the cathode. This last statement follows from the expression for the group velocity, which is a consequence of Eq. (24):

$$v_{gr} = \left[\frac{1}{\xi_{02}}\frac{1}{(\omega_{10}^2/\omega_{20}^2)(\xi_{02}^2/\xi_{01}^2) + 1}\right. \tag{26}$$

$$\left. + \frac{1}{\xi_{01}}\frac{1}{1 + (\omega_{20}^2/\omega_{10}^2)(\xi_{01}^2/\xi_{02}^2)}\right]^{-1} \approx {}^5/_4\xi_{02}.$$

Let us examine Eq. (25) for the damping coefficient in detail. The first two terms in it are due to elastic collisions of electrons and ions with neutral gas molecules, the remainder are caused by the

Coulomb interaction, with the wave, of randomly moving electrons and ions. Here the collisions of the ions with molecules play a dominant role compared with collisions of electrons with molecules. As we know, collisions lead to damping of the wave. As for the last two terms in the expression for γ, the modulus of their ratio can be greater or less than unity, depending on the temperatures of electrons and ions; thus for $\Theta_1 < 4\Theta_1$, the ionic term exceeds the electric one, while for $\Theta_1 > 4\Theta_2$ the electronic term can far exceed the ionic term, so that the latter can be neglected. The electronic term appears in (25) with a minus sign, i.e., it makes possible an increase in the amplitude of the wave. Consequently, in this last case, because of the Coulomb interaction of the electron and ion currents, there results a decrease in the damping, or even the ocurrence of waves with rising amplitude ($\gamma < 0$). This will occur if:

$$l_e > a_1 \frac{v_{Te}^2}{\xi_{01}^2} \exp\left\{\frac{\xi_{01}^2}{v_{Te}^2}\right\}, \qquad (27)$$

where $l_e = \xi_{01}\tau_1$ is the mean free path of the electrons.

Condition (27) is fulfilled for $l_e \gg a_1$. As l_e decreases, the terms in γ due to collisions increase until, for l_e less than $a_1(v_{Te}^2/\xi_{01}^2)\exp\{\xi_{01}^2/v_{Te}^2\}$, the damping coefficient is of the same order as the terms due to collisions, and has a positive sign. It is still meaningful to speak of a space-periodic distribution of the charged particles (fixed or moving) in this case, if $l_e \gg \xi_{01}/\omega_{10} > a_1$ since then $\gamma \ll \kappa$.

Thus spatial periodicity in the distribution of particle density, potentials, etc., can exist only for $l_e > a_1$, which coincides with the criterion given by many authors[13,14].

According to the paper of Zaitsev et al[8,9], for certain special cases there exists a region near the anode in which the drift velocity of the electrons is comparable to the thermal velocity or even exceeds it. This effect, which is caused by the large potential gradient at the anode, enables us to compare the results of the present section with experiment. According to Zaitsev's data, for anode striations (i.e. striations moving from the anode to the cathode), $N \approx 10^8 - 10^9$ electrons/cm^3, (in the positive column $N \approx 10^{10}$ electrons/cm^3), $|\xi_{01}| = 10^8$cm/sec, $T = 3 \cdot 10^4$ °K ($|\xi_{01}| > v_{Te}$), $\lambda_s = 2.5$ mm. The calculated value for the period, from formula (24) for $\omega < 10^5 - 10^6$ c.p.s. in zeroth approximation is: $\lambda = 5$ mm for $N = 10^8$ el./cm^3, and $\lambda = 1.6$ mm for $N = 10^9$ el./cm^3. The agreement of theory with experiment is good, considering that the concentration in the experiment is not known exactly. In this frequency region, the period hardly depends on the frequency and is the same as the period of fixed spatial inhomogeneities, as the experiments show.

It is interesting to note that the expression (24) gives the correct qualitative dependence of the space period on pressure. In fact, we have from (24), approximately, $\lambda \approx (2\pi/\sqrt{5})(\xi_{01}/\omega_{10})$. Since ξ_{01} increases with decreasing pressure, while the concentration decreases, λ increases with decreasing pressure.

The decrease of λ with pressure also occurs in the case of $\omega = 0$, discussed in the second section. For $v_{Te} \approx \xi_{01}$ we can obtain from (13) the following expression for the space period:

$$\lambda = A\sqrt{\Theta_1/Ne^2},$$

where A is a numerical factor. So, with increasing N, the space period decreases.

More complicated is the case of $v_{Te} \gg \xi_{01}$. Here one cannot draw any definite conclusions concerning the pressure dependence of λ. The result will depend on the relative rates of change of ξ_{01} and N with pressure.

In addition to considering these special cases (large drift velocity, high and low frequencies of vibration), we also found general conditions under which the motion of the ions can be disregarded completely. These conditions, obtained from analysis of the "dispersion" equation (57) of paper I, have the following form:

$$\omega \gg \omega_{20}, \quad \omega \gg 1/\tau_2; \qquad (28)$$

$$\omega/\varkappa \gg \xi_{02}, \quad \omega/\varkappa \gg v_{Ti}.$$

As expected, the motion of the ions can be neglected for sufficiently high oscillation frequencies.

We take the opportunity to express our gratitude to A. A. Zaitsev for the interest he has shown in this work, and for his advice. We are also grateful to V. N. Faddeeva for preparing the tables of the probability integral of complex argument.

Translated by M. Hamermesh

[13] Iu. L. Klimontovich, J. Exper. Theoret. Phys. USSR **21**, 1292 (1951)

[14] A. I. Akhiezer and Ia. B. Feinberg, Doklady Akad. Nauk SSSR **69**, 555 (1949)

SOVIET PHYSICS-JETP VOLUME 1, NUMBER 1 JULY, 1955

Resonance Absorption of Ultrasound in Paramagnetic Salts

S. A. AL'TSHULER
Kazan State University

(Submitted to JETP editor March 1, 1954)
J. Exper. Theoret. Phys. USSR 28, 38-48 (January, 1955)

A theory is given of resonance absorption of ultrasound in various paramagnetic salts under the assumption that spin-lattice interaction is caused by the modulation of the internal electric field of the crystal by the elastic vibrations of the lattice. The coefficient of sound absorption has been computed for salts of elements of the iron group (titanium-cesium and chromium alums), for salts of rare earth elements (cerium nitrate, praseodymium ethyl sulfate), and in salts whose magnetic ions are in the S state (iron alum). In certain cases the coefficient σ is so considerable that the effect of paramagnetic absorption of sound ought to be easily observable.

1. INTRODUCTION

IN the present work there is considered the resonance absorption of ultrasound in paramagnetic salts which occurs as the result of transitions between the energy levels of a spin system placed in a constant magnetic field. Such absorption takes place if the resonance condition

$$h\nu = g\beta H, \tag{1}$$

is satisfied, where ν is the ultrasonic frequency, g the spectroscopic splitting factor, β the magneton, and H the intensity of the applied magnetic field.

The phenomenon under consideration is analogous to the effect of paramagnetic resonance, discovered by Zavoiskii [1]. This latter phenomenon, as is well known, consists of the resonance absorption of the energy of a radio frequency electromagnetic field by the spin system, as a result of magnetic dipole transitions between sublevels, brought about by a constant magnetic field applied perpendicularly to a variable magnetic field. Equation (1) must be satisfied in this case also, but ν now represents the frequency of the variable magnetic field. The possibility of resonance absorption of the energy of sound vibrations by paramagnetic salts was also discussed by Zavoiskii.

The nature of the mechanism which brings about the transfer of the energy of sound vibrations to the paramagnetic particles is evidently the same as that in paramagnetic relaxation. In paramagnetic relaxation thermodynamic equilibrium is established by the transfer of energy of the magnetic atoms to the thermal vibrations of the lattice. This energy exchange between the spin system and the vibrations of the lattice is brought about by processes of second order, i. e., by the multiple scattering of phonons, at least down to liquid helium temperatures. Single phonon processes play a dominant role only at very low temperatures.

The resonance absorption of ultrasound can be considered as the reverse phenomenon of paramagnetic lattice relaxation, for it consists of the absorption by the lattice of the energy of vibration of a set of magnetic atoms. The forces which act on the magnetic atoms will change periodically, under the action of ultrasound, and transitions from one magnetic energy sublevel to another will occur. The high population of the lower sublevels causes the number of transitions connected with the absorption of energy to exceed the number of reverse processes. Equilibrium will be established as a result of transfer of the excess energy of the paramagnetic particles to the thermal vibrations of the lattice.

It must be kept in mind that the paramagnetic sound absorption results from first order processes which involve the complete absorption of phonons whose frequency satisfies the resonant condition (1). Therefore, calculation of the paramagnetic sound absorption coefficient is analogous to the computation of the relaxation time τ of the paramagnetic lattice at liquid helium temperatures. We can, therefore, immediately estimate the magnitude of this effect in solids.

The probability A of the absorption of a phonon per second under the action of the thermal vibration of the lattice is approximately $1/2\,\tau$. Furthermore, this probability is proportional to the number of vibrations per unit frequency interval, $\rho\nu$, at frequency ν, and to the mean value of the quantum number n_ν at the temperature T_0 of the crystal, since

$$A = A_0 \rho_\nu n_\nu, \tag{2}$$

[1] E. K. Zavoiskii, Sow. Phys. 10, 197 (1946)

$$\rho_\nu = 4\pi\nu^2 V / v^3, \quad n_\nu = kT_0 / h\nu.$$

Here V is the volume of the crystal and v is the velocity of sound. We shall consider the sound to be virtually monochromatic. If the mean width of sound frequency band is $\Delta\nu$, the intensity of the sound wave, i. e. the energy developed per second per square centimeter, will be equal to $I = I_\nu \Delta\nu$, where $I_\nu = v\rho_a n_a h\nu / V$. Here ρ_a and n_a have the same meanings as ρ_ν and n_ν in (2) but refer to the sound vibrations. The energy of these vibrations absorbed per unit volume of paramagnetic material per second at a temperature T is equal to

$$E = NA_0\rho_a n_\alpha \frac{(h\nu)^2}{kT} \frac{\Delta\nu}{\nu_{1/2}}, \qquad (3)$$

where N is the number of magnetic atoms per unit volume.

We have assumed that the interval $\Delta\nu$ is much less than the half width of the paramagnetic resonance absorption line, $\nu_{1/2}$. The factor $\frac{h\nu}{kT}$ defines the excess of absorption events over events of phonon emission. We obtain the sound absorption coefficient σ from (2) and (3):

$$\sigma = \frac{E}{I} = \frac{\hbar^2}{8\pi k^2} \frac{Nv^2}{\tau T_0 T\nu_{1/2}}. \qquad (4)$$

All measurements of the relaxation time T, carried out for the compounds

$$CrK(SO_4)_2 \cdot 12H_2O, \quad Gd_2(SO_4)_3 \cdot 8H_2O,$$
$$FeNH_4(SO_4)_2 \cdot 12H_2O, \quad CuK_2(SO_4)_2 \cdot 6H_2O,$$

at the temperatures of liquid helium [2] give values for τ close to 10^{-2} sec, increasing slightly with increase in the applied magnetic field. Hence we obtain a value of about 0.1 cm^{-1} for the coefficient σ at room temperature. Of course it must be recalled that frequencies higher than 10^9 / sec play a decisive role in the spin-lattice interactions that define the quantity τ, because of internal magnetic fields. Therefore an estimate of the absorption coefficient σ can be made for sound frequenices of the order 10^9 / sec., with the aid of (4); for lower frequencies, one must take into account the fact that σ is ordinarily proportional to the square of the frequency ν.

Thus, the effect we seek is of measurable size. We have therefore carried out calculations of the absorption coefficient σ for various substances. In most paramagnetic salts the internal electric field of the crystal plays a fundamental role in spin-lattice interactions. In these substances the sound vibrations of the lattice alter the electric field of the crystal and periodically react on the orbital motion of the electrons of the magnetic atom. Consequently a change results in the spin direction of the atom relative to the external magnetic field. We have considered only sound absorption resulting from the mechanism of spin-lattice interaction.

2. SALTS OF ELEMENTS OF THE IRON GROUP

First we introduce the usual formula for the coefficient of absorption. The probability per second that an atom undergoes transition from one magnetic level $\propto$ to another level β, absorbing in this process one quantum of lattice vibration, is equal to

$$A = \frac{4\pi^2}{h^2} \rho_a |\mathcal{H}_{\alpha,\ \beta;\ n_a-1,\ n_a}|^2. \qquad (5)$$

Here $\mathcal{H}_{\propto,\ \beta;\ n_a-1,\ n_a}$ is the matrix element of excitation, consisting of spin-lattice and possibly other interactions. The energy absorbed per unit volume of the paramagnetic specimen is

$$E = AN \frac{(h\nu)^2}{kT} \frac{\Delta\nu}{\nu_{1/2}}. \qquad (6)$$

Hence we obtain for the absorption coefficient

$$\sigma = \frac{4\pi^2}{h^2} \frac{Nh\nu V}{kTvn_a \nu_{1/2}} |\mathcal{H}_{\alpha,\ \beta;\ n_a-1,\ n_a}|^2. \qquad (7)$$

We assume that the sound absorption is related to the periodic variations of the electric field of the crystal under the action of the elastic vibrations of the lattice. In many salts the magnetic ion is surrounded by six water molecules, placed at the corners of an octahedron. The normal vibrations of such a group of molecules were investigated by Van Vleck [3]. If we denote by Q_k the normal coordinates of the system $Me{\times}6H_2O$, then it is shown that the energy of the spin-lattice interaction will depend linearly only on some 6 coordinates, so that, neglecting quadratic terms relative to Q_k, we can write

[2] H. C. Kramers, D. Bijl, C. J. Gorter, Physica 16, 65 (1950)

[3] J. H. Van Vleck, J. Chem. Phys. 7, 72 (1939)

$$\mathcal{H}_{\alpha,\beta;\,n_a-1,\,n_a}=\sum_{k=1}^{6}(\mathcal{H}_k)_{\alpha,\beta}(Q_k)_{n_a-1,\,n_a}. \quad (8)$$

The quantities Q_k will be linear functions of all $3N$ normal coordinates q_i which characterize the elastic waves of the lattice:

$$Q_k=\sum_i a_{ki}\,q_i, \quad (9)$$

where

$$\begin{aligned}
a_{1l}&=0;\\
a_{2l}&=u(\lambda_{x_l}\Phi_{x_l}-\lambda_{y_l}\Phi_{y_l});\\
a_{3l}&=u(\lambda_{x_l}\Phi_{x_l}+\lambda_{y_l}\Phi_{y_l}-2\lambda_{z_l}\Phi_{z_l})/\sqrt{3};\\
a_{4l}&=u(\lambda_{x_l}\Phi_{y_l}+\lambda_{y_l}\Phi_{x_l}+\lambda_{z_l}\Phi_{x_l}+\lambda_{x_l}\Phi_{z_l}\\
&\quad+\lambda_{z_l}\Phi_{y_l}+\lambda_{y_l}\Phi_{z_l})/\sqrt{3};\\
a_{5l}&=u(\lambda_{x_l}\Phi_{z_l}+\lambda_{z_l}\Phi_{x_l}-\lambda_{y_l}\Phi_{z_l}\\
&\quad-\lambda_{z_l}\Phi_{y_l})/\sqrt{2};\\
a_{6l}&=u(\lambda_{x_l}\Phi_{z_l}+\lambda_{z_l}\Phi_{x_l}+\lambda_{y_l}\Phi_{z_l}+\lambda_{z_l}\Phi_{y_l}\\
&\quad-2\lambda_{y_l}\Phi_{x_l}-2\lambda_{x_l}\Phi_{y_l})/\sqrt{6},
\end{aligned} \quad (10)$$

and

$$u=(2\pi\nu R/v)\sin\delta_l. \quad (11)$$

Here Φ_{x_i}, Φ_{y_i}, Φ_{z_i} and λ_{x_i}, λ_{y_i}, λ_{z_i} are the direction cosines of the polarization and the velocity of propagation of the wave, respectively, R is the equilibrium distance between the molecule of water and the magnetic ion, δ_i is a phase constant.

We assume that the magnetic field is parallel to the z axis and that the sound wave is propagated along the x axis. Then, substituting (8) in (7), and making use of (9), (10) and (11), we get, for the absorption coefficient of a wave propagated in a direction perpendicular to the magnetic field, the expression

$$\begin{aligned}
\sigma_\perp=\frac{2}{9}P\nu^2R^2\Big[&3|\mathcal{H}_2|^2+|\mathcal{H}_3|^2\\
&+\frac{1}{\sqrt{3}}(\mathcal{H}_2\mathcal{H}_3^*+\mathcal{H}_2^*\mathcal{H}_3)\\
&+2|\mathcal{H}_4|^2+\frac{3}{2}|\mathcal{H}_5|^2+\frac{5}{2}|\mathcal{H}_6|^2\\
&+\sqrt{\frac{3}{2}}(\mathcal{H}_4\mathcal{H}_5^*+\mathcal{H}_4^*\mathcal{H}_5)\\
&-\frac{1}{\sqrt{2}}(\mathcal{H}_4\mathcal{H}_6^*+\mathcal{H}_4^*\mathcal{H}_6)\\
&+\frac{\sqrt{3}}{2}(\mathcal{H}_5\mathcal{H}_6^*+\mathcal{H}_5^*\mathcal{H}_6)\Big]_{\alpha,\beta},
\end{aligned} \quad (12)$$

Here d is the density of the substance and P represents the factor $\pi^2N/kTv^3\nu l/_2 d$ which appears in all expressions for the coefficient of sound absorption in solids. We have carried out averages over all directions of polarization and over all possible values of δ_i. Similarly if the wave is propagated in a direction parallel to the magnetic field we obtain the expression*

$$\begin{aligned}
\sigma_\parallel=\frac{2}{9}P\nu^2R^2[&4|\mathcal{H}_3|^2+2|\mathcal{H}_4|^2+3|\mathcal{H}_5|^2\\
&+|\mathcal{H}_6|^2+2\sqrt{2}(\mathcal{H}_4\mathcal{H}_6^*+\mathcal{H}_6^*\mathcal{H}_6)]_{\alpha,\beta}.
\end{aligned} \quad (12')$$

We first consider the rather thoroughly investigated, (both theoretically and experimentally) titanium-cesium and chromium-potassium alums. The atom of titanium entering into the compounds $CsTi(SO_4)_2\cdot 12H_2O$ is found in the position ^2D. The strong field of cubic symmetry, created by the water molecules, splits the orbital energy level into a doublet and triplet, separated by an interval greater than 50, 000 cm $^{-1}$. The trigonal field created by the remaining atoms of the crystal and the spin-orbital interaction completely removes the orbital degeneracy. In the absence of an external magnetic field only the double spin degeneracy is preserved. We assume that the magnetic field is applied parallel to the trigonal axis of the crystal; the splitting of the lowest energy level will be defined by a g factor, equal to $^5/_4$ [4]. We are interested in the matrix element of excitation which combines these two magnetic sublevels. It is possible to obtain it by making use of the known calculations on the time of paramagnetic relaxation [5], if we include in the excitation operator the energy of the atom in the external magnetic field, the spin-orbit and orbit-lattice interactions. The first approximation shows this matrix element equal to zero. In the second approximation the matrix element of excitation is equal to

---

* Henceforth we shall denote by $\perp$ and $\parallel$ quantities relating to waves propagated in directions perpendicular and parallel, respectively, to the applied magnetic field.

[4] B. Bleaney and K. W. H. Steevens, Ann. Rep. Prog. Phys. 16, 108 (1952)

[5] J. H. Van Vleck, Phys. Rev. 57, 426 (1940)

$$\mathcal{H}_{-1/2,+1/2;n_a-1,n_a} = \frac{3}{2}\frac{\lambda g\beta H}{\delta^2}\left[\sqrt{6}a\,(iQ_2+Q_3) - \frac{1}{\sqrt{3}}b\,(iQ_5-Q_6)\right]_{n_a-1,n_a}, \quad (13)$$

where

$$a = -\frac{12}{7}\left(\frac{\bar{r}^2}{R^2}-\frac{25}{18}\frac{\bar{r}^4}{R^4}\right)\frac{e\mu}{R^3}\ ; \quad (14)$$

$$b = \frac{24}{7}\left(\frac{\bar{r}^2}{R^2}-\frac{5}{6}\frac{\bar{r}^4}{R^4}\right)\frac{e\mu}{R^3}\ .$$

Here r is the mean distance of the $3d$ electron from the nucleus, μ is the effective dipole moment of the water molecule, δ is the interval separating the two lowest orbit sublevels, λ is the constant of spin-orbit interaction. Hence we immediately obtain the value of $\mathcal{H}_k$, the substitution of which in (12) and (12′) gives us the following expression for the absorption coefficient .

$$\sigma = \alpha h^2 P\left(\frac{\lambda}{\delta^2}\right)^2\left(\frac{e\mu}{R^2}\right)^2\nu^4, \quad (15)$$

where

$$\alpha = 3\left(\frac{8}{7}\right)^2\left[11\left(\frac{\bar{r}^2}{R^2}\right)^2 - \frac{85}{3}\frac{\bar{r}^2\bar{r}^4}{R^6} + \frac{75}{4}\left(\frac{\bar{r}^4}{R^4}\right)^2\right].$$

The absorption coefficient does not depend on the angle between the constant magnetic field and the direction of propagation of the ultrasound. Making use of the following values for the quantities entering into this formula:

$\lambda = 154$ см$^{-1}$; $\delta = 500$ см$^{-1}$;
$v = 2.3\times10^5$ см/сек.; $d = 2$ г/см^3;
$R = 2\times10^{-8}$ см; $\bar{r}^2 = 1.23\times10^{-16}$ см^2;
$\bar{r}^4 = 2.46\times10^{-32}$ см^4; $\mu = 2\times10^{-18}$ CGSE;
$\nu_{1/2} = 1.8\times10^8$ сек.$^{-1}$; $T = 20°$K,

(taken in large part from Bleaney and Steevens [4] and Van Vleck [5]), we get for σ:

$$\sigma = 2.4\times10^{-38}\nu^4 \text{ см}^{-1}. \quad (16)$$

In estimating σ, we have taken $T = 20°$, since titanium-cesium alum possesses an anomalously short time for spin-lattice relaxation, so that resonance absorption is found only at low temperatures.

We proceed to chromium alum. The basic state of the triply ionized atom of chromium is ^4F. The splitting scheme of the energy levels by the electric field of the crystal and the external magnetic field is shown in Fig. 1. The strong cubic field produces a splitting of the orbit energy level into three sublevels, the lowest of which is single. The overall splitting Δ, according to Bleaney and Bowers[6] is 50,000/cm. If electron spin is taken into account, the degeneracy of the basic energy level associated with it is preserved in a field of cubic symmetry. The trigonal field splits the spin quadruplet into two Kramers doublets, the interval δ between them lying in the range 0.12 to 0.18 cm^{-1} for chromium alums of various types. The magnetic spin quantum numbers $\pm 3/2$ correspond to the lower doublet, the numbers $\pm 1/2$ to the upper.

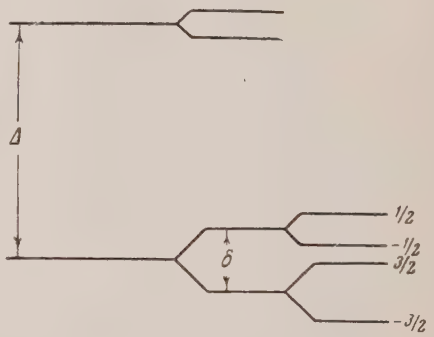

Fig. 1. Scheme of the successive splitting of the basic energy level of the Cr^{+++} ion because of its presence in the electric field of a crystal of cubic symmetry, in a weak field of trigonal symmetry and, in an external magnetic field.

The matrix element of excitation, which consists of spin-orbit and spin-lattice interaction, differs from zero only in the third approximation, and can be represented in the following form [5]:

$$\mathcal{H}_{\alpha,\beta;n_a-1,n_a} = \{\varepsilon_1[Q_3(2S_z^2-S_x^2-S_y^2) + \sqrt{3}Q_2(S_y^2-S_x^2)] + \varepsilon_2[Q_4(S_xS_y+S_yS_x) + Q_5(S_xS_z+S_zS_x) + Q_6(S_yS_z+S_zS_y)]\}_{\alpha,\beta;n_a-1,n_a}, \quad (17)$$

where

$$\varepsilon_1 = 54\sqrt{3}\frac{\lambda^2}{\Delta^2}\left(\frac{e\mu}{R^3}\right)\frac{\bar{r}^4}{R^4},$$

$$\varepsilon_2 = \frac{12\cdot324}{175}\frac{\lambda^2}{\Delta^2}\left(\frac{e\mu}{R^3}\right)\left(\frac{\bar{r}^2}{R^2}-\frac{55}{36}\frac{\bar{r}^4}{R^4}\right),$$

[6] B. Bleaney and K. D. Bowers, Proc. Phys. Soc. (London) **64A**, 1135 (1951)

S is the spin moment operator, $\alpha, \beta = \pm 1/2, \pm 3/2$.

In our approximation, only transitions between sublevels of different Kramers doublets are non-vanishing. Therefore the location of the absorption line will no longer be determined by Eq. (1), which refers to transitions between sublevels that are produced upon the imposition of an external magnetic field. With the help of (17) and (12), calculation leads to the following expression for the absorption coefficient:

$$\sigma = \alpha \left(\frac{e\mu}{R^2}\right)^2 \left(\frac{\lambda}{\Delta}\right)^4 P_\nu^2. \tag{18}$$

For transitions $-1/2 \to 3/2$ and $-3/2 \to 1/2$, the coefficient is equal to

$$\alpha'_\perp = 3\left(\frac{8\cdot 324}{175}\right)^2 \left[\left(\frac{\bar{r}^2}{R^2}\right) - \frac{55}{18}\frac{\bar{r}^2\bar{r}^4}{R^6} + 82\left(\frac{\bar{r}^4}{R^4}\right)^2\right], \tag{19}$$

$$\alpha'_\parallel = 3\left(\frac{8\cdot 324}{175}\right)^2 \left(\frac{\bar{r}^2}{R^2} - \frac{55}{36}\frac{\bar{r}^4}{R^4}\right)^2.$$

For transitions between sublevels $-3/2 \to -1/2$, $1/2 \to 3/2$, the coefficient α does not depend on the direction of the applied magnetic field, and is equal to $8\alpha'_\parallel$.

If, in estimating the numerical value of the absorption coefficient we assume that $\lambda = 88\ \text{cm}^{-1}$; $d = 1.7\ \text{gm/cm}^3$, $\nu_{1/2} = 1.03 \times 10^9\ \text{sec}^{-1}$, $T = 300^\circ\text{K}$, and that the other quantities have the same values as for titanium-cesium alums, we get

$$\sigma'_\perp = 0.80 \times 10^{-21} \nu^2\ \text{cm}^{-1};\ \sigma'_\parallel = 0.56 \times 10^{-23} \nu^2\ \text{cm}^{-1}. \tag{20}$$

For salts of titanium and chromium we obtained a different dependence of the magnitude of the absorption on the frequency of the sound. This behavior is explained by the fact that in the case of chromium alums the spin degeneracy is partially removed even in the absence of any external magnetic field.

3. SALTS OF RARE EARTH ELEMENTS

Spin-lattice interaction in salts of rare earth elements possesses a number of peculiarities which were considered in an earlier work of the author [7]. As an example, we consider cerium nitrate. The free triply ionized atom of cerium is in the state $^2F_{5/2}$. The six molecules of water which surround the magnetic ion evidently produce a field of cubic symmetry. This field splits the fundamental energy level into a doublet and a quadruplet, separated by a difference Δ (Fig. 2). A weaker trigonal field, produced by the remaining atoms of the crystal, splits the quadruplet into two doubly degenerate sublevels. Further splittings of the levels *ab*, *cd* and *fg* in an external magnetic field, applied parallel to the axis of the octahedron, have the values $^{11}/_3 g\beta H$, $g\beta H$, $^5/_3 g\beta H$, respectively.

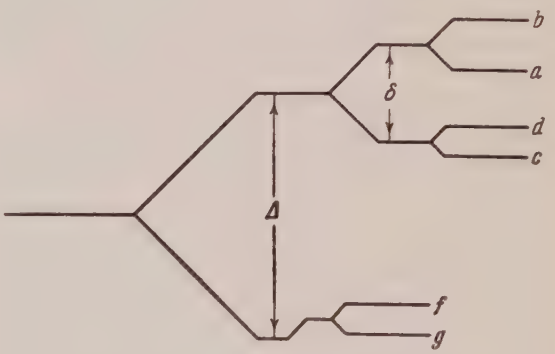

Fig. 2. Scheme of the successive splitting of the basic energy level of the Ce^{+++} ion because of its presence in the electric field of a crystal of cubic symmetry, in a weak field of trigonal symmetry, and in an external magnetic field.

We first consider absorption due to transitions between levels *f* and *g*. The matrix element of the interaction, which included the spin-lattice interaction and the potential of the trigonal field, differs from zero in the second approximation, and is equal to

$$\mathcal{H}_{f,g;\,n_a-1,\,n_a} = \frac{1}{8}\left(\frac{e\mu}{R^3}\right)\left(\frac{\bar{r}^2}{R^2} - \frac{9}{64}\frac{\bar{r}^4}{R^4}\right)^2 \tag{21}$$

$$\times \frac{(^5/_3 g\beta H)\,\delta}{\Delta^2}(Q_5 + iQ_6)_{n_a-1,\,n_a}.$$

For absorption coefficients we get, by the usual method,

$$\sigma_\parallel = \frac{1}{18}\left(\frac{\bar{r}^2}{R^2} - \frac{9}{64}\frac{\bar{r}^4}{R^4}\right)^2 \left(\frac{e\mu}{R^2}\right)^2 \frac{\hbar^2\delta^2 P}{\Delta^4}\nu^4, \tag{22}$$

$$\sigma_\perp = {}^1/_4\,\sigma_\parallel.$$

If we take $\nu_{1/2} = 1.6 \times 10^9/\text{sec}$. as the half width of the absorption line, and use the values given in reference 7 for the other quantities, we get (at

[7] S. A. Al'tshuler, J. Exper. Theoret. Phys. USSR 24, 681 (1953)

$T = 20°$ K)

$$\sigma_{\parallel} = 3 \cdot 10^{-44} \nu^4 \text{см}^{-1}. \qquad (22')$$

The matrix element of excitation for transitions between the sublevels *ab* has the same form as that for *fg*. The only difference is that the interval *ab* is $^{11}/_5$ times larger than the interval *fg*. As a consequence the absorption coefficient obtained for *fg* must be multiplied by $(^5/_{11})^2$.

Calculation shows that the probabilities of transitions between levels *cd* are zero. This result is related to our choice of a field of low symmetry (relative to the fundamental cubic field). With a field of another type we would have obtained absorption of the same order as for the other pair of levels.

Thus the absorption coefficient for cerium nitrate is shown to be very small. Such a result isexplained by the low symmetry of the electric field of the crystal, which leaves only the Kramers degeneracy of the energy level. This cannot be connected with changes in the electric field produced by the vibrations of the lattice. Otherwise it would be as if the electric field of the crystal had possessed such great symmetry that it could preserve the non-Kramers degeneracy of the energy levels. In such a case the spin-lattice interaction would differ from zero even in the first approximation and the absorption coefficient would be far larger.

Among the salts of the rare earths, most attention has thus far been given to the ethyl sulfates. In these cases the crystalline field possesses hexagonal symmetry. The Ian-Teller effect, which contributes to the low symmetry of the field, is so small [3] in the salts of the rare earths that it can be neglected. In atoms which have half integer spin, the field of hexagonal symmetry splits the energy levels so that only the Kramers degeneracy remains [8]. Therefore, in salts of cerium, neodymium and other elements, whose ions possess an odd number of electrons , the effect of resonance absorption of sound must be small. In atoms with an even number of electrons, the hexagonal field leaves certain energy levels doubly degenerate. For example, in praseodymium ethyl sulfate, the fundamental level of Pr^{+++} exhibits a non-Kramers doublet [9]. It is easy to estimate the sound absorption as a result of transitions between this pair of levels. If we assume that the matrix element of spin-lattice interaction for this doublet differs from zero in the first approximation, we get for the absorption coefficient,

$$\sigma = \gamma P \left(\frac{e\mu}{R^2}\right)^2 \left(\frac{\bar{r}^2}{R^2}\right)^2 \nu^2, \qquad (23)$$

where γ is a numerical coefficient of order unity. Taking $\nu_{1/2} = 2 \times 10^9$/sec as the width of the absorption line, we get, for 20°K,

$$\sigma \sim 10^{-15} \nu^2 \text{ см}^{-1}. \qquad (23')$$

We note that for salts of rare earth elements, the time of spin-lattice relaxation at room temperature appears to be very short [7]. Therefore observation of the sound absorption effect is possible only at low temperatures.

4. SALTS WITH MAGNETIC IONS IN THE *S* STATE

A special place is taken among paramagnetic salts by the salts of doubly ionized manganese and triply ionized iron and gadolinium. The magnetic ions of these salts are in the *S* state, for which reason the electric field of the crystal produces very small splitting of the fundamental level, not exceeding 1 cm^{-1}. It is also appropriate to consider the salts of iron whose ion is in the ^6S state. The Hamiltonian operator which gives the effect of the electric field of the crystal and the external magnetic field has the following form [10]:

$$\mathcal{H} = {}^1/_6 D [S_x^4 + S_y^4 + S_z^4 - {}^1/_3 S(S+1) \times (3S^2 + S - 1)] + g\beta H. \qquad (24)$$

For iron rubidium alums, $D = 0.0134$ cm^{-1} [11]. If the magnetic field is applied in the [100] direction, the non-vanishing matrix elements of $\mathcal{H}$ have the form

$$\begin{aligned} \mathcal{H}_{\pm^5/_2, \pm^5/_2} &= D \pm {}^5/_2 G, \\ \mathcal{H}_{\pm^3/_2, \pm^3/_2} &= -{}^3/_2 D \pm {}^3/_2 G, \\ \mathcal{H}_{\pm^1/_2, \pm^1/_2} &= D \pm {}^1/_2 G, \\ \mathcal{H}_{-^5/_2, {}^5/_2} &= \mathcal{H}_{-^3/_2, {}^5/_2} = \frac{\sqrt{5}}{2} D. \end{aligned} \qquad (25)$$

[8] H. Bethe, Ann. Physik 3, 133 (1929)

[9] B. Bleaney and H. E. D. Scovil, Phil. Mag. 43, 999 (1951)

[10] K. W. H. Steevens, Proc. Roy. Soc. **214**, 237 (1952)

[11] B. Bleaney and K. S. Trenar, Proc. Phys. Soc. (London) 65A, 560 (1952)

Here $G = g\beta H$.

The solution of the secular equation leads to the following eigenvalues and wave functions:

$$E_a = -{}^1/_2 D - {}^1/_2 G + \sqrt{(D-2G)^2 + {}^5/_4 D^2}; \quad (26)$$
$$\Psi_a = a_1\Phi_{-{}^3/_2} + a_2\Phi_{{}^3/_2};$$
$$E_b = -{}^1/_2 D + {}^1/_2 G + \sqrt{(D+2G)^2 + {}^5/_4 D^2};$$
$$\Psi_b = b_1\Phi_{-{}^3/_2} + b_2\Phi_{{}^3/_2};$$
$$E_c = D - {}^1/_2 G;$$
$$\Psi_c = \Phi_{-{}^1/_2};$$
$$E_d = D + {}^1/_2 G;$$
$$\Psi_d = \Phi_{{}^1/_2};$$
$$E_f = -{}^1/_2 D - {}^1/_2 G - \sqrt{(D-2G)^2 + {}^5/_4 D^2};$$
$$\Psi_f = f_1\Phi_{-{}^3/_2} + f_2\Phi_{{}^3/_2};$$
$$E_g = -{}^1/_2 D + {}^1/_2 G - \sqrt{(D+2G)^2 + {}^5/_4 D^2};$$
$$\Psi_g = g_1\Phi_{-{}^3/_2} + g_2\Phi_{{}^3/_2}.$$

The triply ionized atoms of iron and cerium have a similar energy level structure, owing to the fact that in their ground state both ions have a quantum number of total angular momentum equal to $^5/_2$. Therefore, making use of Eqs. (8) and (9) of our work, which illustrates paramagnetic relaxation in cerium salts [7], we get for the matrix elements of the operator of spin-lattice interaction (with the help of the wave functions (26)):

$$\mathcal{H}_{ab} = -\frac{3}{2}\sqrt{5}\,(a_1b_1 - a_2b_2)\left(\frac{\bar r^2}{R^2} - \frac{9}{64}\frac{\bar r^4}{R^4}\right) \quad (27)$$
$$\times \left(\frac{e\mu}{R^3}\right)(Q_5 + iQ_6) \equiv F_1(a, b);$$
$$\mathcal{H}_{ac} = \frac{3}{8}\sqrt{2}\left\{3\,(\sqrt{5}\,a_1 + 3a_2)\left(\frac{\bar r^2}{R^2} + \frac{45}{32}\frac{\bar r^4}{R^4}\right)Q_2\right.$$
$$\left. - 2i(\sqrt{5}\,a_1 - 3a_2)\left(\frac{\bar r^2}{R^2} + \frac{27}{32}\frac{\bar r^4}{R^4}\right)Q_4\right\}\frac{e\mu}{R^3}$$
$$\equiv F_2(a_1, a_2);$$
$$\mathcal{H}_{ad} = \frac{3}{2}\sqrt{2}\left\{a_2\frac{\bar r^2}{R^2} + \frac{9}{128}(7\sqrt{5}\,a_1 + 5a_2)\frac{\bar r^4}{R^4}\right\}$$
$$\times \left(\frac{e\mu}{R^3}\right)(Q_5 - iQ_6) \equiv F_3(a_2, a_1);$$
$$\mathcal{H}_{af} = -\frac{3}{4}\sqrt{3}\left\{(5a_1f_1 - a_2f_2)\frac{\bar r^2}{R^2}\right.$$
$$\left. - \frac{15}{64}[5a_1f_1 - 15a_2f_2 - 14\sqrt{5}(a_1f_2 + a_2f_1)]\frac{\bar r^4}{R^4}\right\}$$
$$\times \left(\frac{e\mu}{R^3}\right)Q_3 \equiv F_4(a, f);$$
$$\mathcal{H}_{ag} = F_1(a, g), \quad \mathcal{H}_{bc} = F_2(b_2, b_1);$$
$$\mathcal{H}_{bd} = F_3(b_1, b_2); \quad \mathcal{H}_{bf} = F_1(b, f);$$
$$\mathcal{H}_{bg} = F_4(b, g); \quad \mathcal{H}_{cd} = 0;$$
$$\mathcal{H}_{cf} = F_2(f_1, f_2); \quad \mathcal{H}_{cg} = F_3(g_1, g_2);$$
$$\mathcal{H}_{df} = F_3(f_2, f_1); \quad \mathcal{H}_{dg} = F_2(g_2, g_1).$$

With the help of (12), we get the sound absorption coefficient σ:

$$\sigma = \alpha P\,(e\mu / R^2)^2\nu^2. \quad (28)$$

If the magnetic field is applied perpendicularly to the direction of sound propagation, then the numerical coefficient will have the following values for the various pairs of levels:

$$\alpha_{ab} = 5\left[(a_1b_1 - a_2b_2)\left(\frac{\bar r^2}{R^2} - \frac{9}{64}\frac{\bar r^4}{R^4}\right)\right]^2 \quad (29)$$
$$\equiv \alpha_1(a, b);$$
$$\alpha_{ac} = 2\left[a_2\frac{\bar r^2}{R^2} + \frac{9}{128}(7\sqrt{5}\,a_1 + 5a_2)\frac{\bar r^4}{R^4}\right]^2$$
$$\equiv \alpha_2(a_2, a_1);$$
$$\alpha_{ad} = \frac{3}{2}\left[\frac{3}{4}(\sqrt{5}\,a_1 + 3a_2)\left(\frac{\bar r^2}{R^2} + \frac{45}{32}\frac{\bar r^4}{R^4}\right)\right]^2$$
$$= \alpha_3(a_1, a_2);$$
$$\alpha_{af} = \frac{9}{16}\left\{(5a_1f_1 - a_2f_2)\frac{\bar r^2}{R^2}\right.$$
$$- \frac{15}{64}[5a_1f_1 - 15a_2f_2$$
$$\left. - 14\sqrt{5}\,(a_1f_2 + a_2f_1)]\frac{\bar r^4}{R^4}\right\}^2 \equiv \alpha_4(a, f);$$
$$\alpha_{ag} = \alpha_1(a, g); \quad \alpha_{bc} = \alpha_2(b_2, b_1);$$
$$\alpha_{bd} = \alpha_3(b_2, b_1); \quad \alpha_{bf} = \alpha_1(b, f);$$
$$\alpha_{bg} = \alpha_4(b, g); \quad \alpha_{cd} = 0;$$
$$\alpha_{cf} = \alpha_3(f_1, f_2); \quad \alpha_{cg} = \alpha_2(g_1, g_2);$$
$$\alpha_{df} = \alpha_2(f_2, f_1); \quad \alpha_{dg} = \alpha_3(g_2, g_1);$$
$$\alpha_{fg} = \alpha_1(f, g).$$

If the magnetic field is applied parallel to the direction of sound propagation, then the numerical coefficient α, which we now denote by α', will be determined, according to Eqs. (27) by four functions α_i, if we give them the following values:

$$\alpha_1 = \alpha_1; \quad \alpha_2 = \frac{1}{2}(\sqrt{5}\,a_1 - 3a_2)^2 \quad (30)$$
$$\times \left(\frac{\bar r^2}{R^2} + \frac{27}{32}\frac{\bar r^4}{R^4}\right)^2;$$

$$\alpha_3' = \alpha_3; \quad \alpha_4' = 4\alpha_4.$$

In a strong magnetic field, which produces splittings much larger than does the electric field of the crystal, it is appropriate to characterize the energy levels by the values of the magnetic quantum number M. Thus, in this case,

$$a_1 = b_2 = f_2 = -g_1 = 1;$$
$$a_2 = b_1 = f_1 = g_2 = 0,$$

and for the coefficient $\propto$ we have

$$\Delta M = 1: \quad \alpha_{-3/2,-3/2} = \alpha_{3/2,3/2} = 5\left(\frac{\bar{r}^2}{R^2} - \frac{9}{64}\frac{\bar{r}^4}{R^4}\right)^2; \tag{31}$$

$$\alpha_{-3/2,-1/2} = \alpha_{1/2,3/2} = 2\left(\frac{\bar{r}^2}{R^2} + \frac{45}{128}\frac{\bar{r}^4}{R^4}\right)^2;$$

$$\alpha_{-1/2,1/2} = 0;$$

$$\Delta M = 2: \quad \alpha_{-3/2,-1/2} = \alpha_{1/2,3/2} = \frac{135}{2}\left(\frac{r^2}{R^2} + \frac{45}{32}\frac{\bar{r}^4}{R^4}\right)^2;$$

$$\alpha_{-3/2,1/2} = \alpha_{-1/2,3/2} = \frac{9}{5}\alpha_{1/2,3/2};$$

$$\Delta M = 3: \quad \alpha_{-3/2,1/2} = \alpha_{1/2,5/2} = 10\left(\frac{63}{128}\frac{\bar{r}^4}{R^4}\right)^2;$$

$$\alpha_{-3/2,3/2} = 0;$$

$$\Delta M = 4: \quad \alpha_{-3/2,3/2} = \alpha_{-3/2,5/2} = 5\left(\frac{315}{128}\frac{\bar{r}^4}{R^4}\right)^2;$$

$$\Delta M = 5: \quad \alpha_{-3/2,5/2} = 0.$$

It should be noted that transitions between neighboring sublevels are possible only under the action of transverse vibrations, and transitions for which $\Delta M = 2$ take place only under the action of longitudinal waves.

If a weak magnetic field is applied, then $a_1 = b_2 = -f_2 = -g_1 = \sqrt{5/6}$; $a_2 = b_1 = f_1 = g_2 = 1/\sqrt{6}$. In the limiting case of a vanishing magnetic field, the electric field splits the basic level of the iron ion into only two sublevels, for which the coefficient $\propto$ is equal to

$$\alpha = 25\left[\left(\frac{\bar{r}^2}{R^2}\right)^2 - \frac{5}{6}\frac{\bar{r}^2\bar{r}^4}{R^6} + 36\left(\frac{\bar{r}^4}{R^4}\right)^2\right]. \tag{32}$$

In order to compute the absorption coefficient according to the formulas that we have developed, the following circumstances must be considered. In the previous cases, the energy of interaction of the magnetic ion with the water molecules is of the order of $e\mu/R^2$. The effect of the electric field of the crystal on the ion, which is in the S state, is even weaker. We take this circumstance into account by attaching correspondingly smaller values of the dipole moment μ. In iron-rubidium alums, the crystalline field produces energy splitting approximately 10^{-6} that in the same salts with another cation. Therefore, taking $\mu \sim 10^{-24}$, we get, for the absorption coefficient in the absence of a magnetic field,

$$\sigma = 10^{-24}\,\nu^2\ \text{см}^{-1}. \tag{32'}$$

It is necessary to show that in some cases the crystalline field creates a much greater splitting. Thus, for the gadolinium ion [12], it is two orders larger, which increases the absorption coefficient σ by 10^4.

As we have seen, the probability of phonon absorption depends very critically upon the magnitude of the spin-orbit interaction of the electrons on the magnetic atom and, in particular, on the character of the splitting of the fundamental energy level of this atom by the electric field of the crystal. Therefore the magnitude of the effect of resonant absorption of sound can change over wide ranges in going from one substance to another. Contemporary ultrasonic techniques permit the obtaining of frequencies of 10^9 cps, which makes possible the observation of the resonance paramagnetic absorption of sound, at least in certain substances.

---

[12] N. S. Garif'ianov, Doklady Akad. Nauk SSSR 84, 923 (1952)

Translated by R. T. Beyer
6

SOVIET PHYSICS-JETP VOLUME 1, NUMBER 1 JULY, 1955

On the Theory of Electronic and Nuclear Paramagnetic Resonance under the Action of Ultrasound

S. A. AL'TSHULER
Kazan State University

(Submitted to JETP editor, March 1, 1954)
J. Exper. Theoret. Phys. USSR 28, 49-60 (January 1955)

The theory of resonance absorption of ultrasound in different classes of paramagnetic substances (salts, rare-earth metals, salt solutions, and gases) is presented. We consider the different mechanisms of the spin-lattice interaction, and discuss the cause of the effect. The magnitude of the calculated coefficient shows that for a series of substances the effect can easily be observed, in other cases it is possible to use an indirect method of observation.

1. INTRODUCTION

IN the work of the author[1] on the theory of resonance absorption of ultrasound in different paramagnetic salts, there is an assumption that the spin-lattice interaction is caused by the modulation of the internal electric field of the crystal by the elastic vibrations of the lattice.

In this paper we consider, in the case of the absorption of ultrasound in salts, an assumption that the spin-lattice interaction is due to magnetic and exchange forces. In certain cases it turns out that this mechanism causes the greatest effect. We also calculate the resonance absorption effect of ultrasound in rare-earth metals, in some of which it proves to be extremely important. We also consider the resonance absorption of ultrasound caused by nuclear paramagnetism. As has been made clear this often gives a large effect that is observed directly, as well as by indirect methods*.

In our calculation we proceed from the following general formula for the sound absorption coefficient [1]:

$$\sigma = \frac{4\pi^2}{h^2}\frac{NhvV}{kTvn_a\nu_{1/2}}|\mathcal{H}_{\alpha,\beta;\,n_a-1,\,n_a}|^2. \qquad (1)$$

Where N is the number of magnetic atoms per unit volume, ν and v are the frequency and the velocity of propagation of sound, V and T are the volume and temperature of the paramagnetic body, $\nu_{1/2}$ is the half-width of the absorption line, $\mathcal{H}_{\alpha,\beta;\,n_a-1,\,n_a}$ is the matrix element of the spin-lattice interaction, acting between the magnetic sublevels α and β and the vibration state of the lattice characterized by the quantum numbers $n_a - 1$ and n_a.

The calculation of the absorption of sound starts from the assumption that the resonance condition is satisfied; this in the simplest case has the form

$$h\nu = g\beta H, \qquad (2)$$

where g is the spectroscopic splitting factor, β is the magneton, H is the intensity of the applied magnetic field.

2. MAGNETIC AND EXCHANGE INTERACTIONS

The first theory of paramagnetic relaxation was developed [2] by building from the assumption that the spin-lattice coupling is brought about by means of magnetic forces acting between the atoms of the crystal. Later, in samples of several paramagnetic salts[3] it was demonstrated that this mechanism was completely inadequate in explaining the observed values of the relaxation times. Another mechanism was introduced which we too used in a previous paper [1]. However, in certain paramagnetic substances the mechanism considered by Waller[2] played an essential role. Waller considered the case in which the atomic spin $S = \frac{1}{2}$. In addition it was easily seen, that the probability of the change of the spin orientation under the action of the oscillations of the internal magnetic field was proportional to the fourth power of the atomic magnetic moment. However, this probability was also

*Resonance absorption of ultrasound occurs not only in paramagnetic, but also in ferromagnetic and anti-ferromagnetic substances. The absence of a satisfactory theory of the spin-lattice interaction for ferro and anti-ferromagnetic substances makes it difficult to give a quantitative determination of the acoustic effect. It is known that the usual effect of the ferro and anti-ferromagnetic resonances is not less than the resonance absorption in paramagnetic substances. Hence we may expect that the resonance absorption of ultrasound in ferro and anti-ferromagnetic substances is also significant.

[1] S. A. Al'tshuler, J. Exper. Theoret. Phys. USSR 28, 38 (1955)

[2] J. Waller, Z. Phys. 79, 370 (1932)

[3] J. H. Van Vleck, Phys. Rev. 57, 426 (1940)

inversely proportional to a^9, where a denotes the equilibrium spacing between the magnetic atoms of the crystal. Hence it was clear that the magnetic forces could determine spin-lattice interactions in substances with large atomic magnetic moments and with a large density of magnetic atoms.

We take the usual expression for the atomic magnetic dipole interaction operator:

$$U_{kl} = g^2\beta^2\left[\frac{(S_k S_l)}{r_{kl}^3} - \frac{3(S_k r_{kl})(S_l r_{kl})}{r_{kl}^5}\right]. \quad (3)$$

To determine the absorption coefficient of sound we start from formula (1). Substituting in (1) the square of the spin-lattice interaction matrix element, if it is assumed that the sound wave is propagated along the x axis, one easily obtains the following formula[2].

$$|\mathcal{H}_{\alpha,\beta;\, n_a-1,\, n_a}|^2 = \frac{hn_a}{4\pi^2 M\nu}\sum_l\left(\frac{2\pi\nu r_{kl}}{v}\right)^2 |(U_{klx})_{\alpha,\beta}|^2, \quad (4)$$

where

$$U_{klx} = \partial U_{kl}/\partial x_{kl}, \quad (5)$$

the summation being carried out over all the magnetic atoms of the crystal. As usual, we apply this formula where the atoms comprise a simple cubic lattice. We are going to make use of the representation in which S_{kz} and S_{lz} are diagonal, and we denote by M_k and M_l the magnetic quantum numbers of the appropriate atoms. The operator U_{klx} will contain various terms of the type $S_{kq}S_{lp}$, non-diagonal matrix elements which differ from zero only in the following case:

$$(S_{kx}S_{lz})_{M_k,M_k+1;\, M_l,\, M_l} = \tfrac{1}{2}\sqrt{S(S+1)-M_k(M_k+1)}\, M_l \equiv t, \quad (6)$$

$$(S_{ky}S_{lz})_{M_k,\,M_k+1;M_l,M_l} = it;$$

$$(S_{kx}S_{lx})_{M_k,M_k+1;\,M_l,M_l+1} = \tfrac{1}{4}\sqrt{S(S+1)-M_k(M_k+1)}\times\sqrt{S(S+1)-M_l(M_l+1)} \equiv p,$$

$$(S_{kx}S_{ly})_{M_k,M_k+1;\,M_l,\,M_l+1} = (S_{ky}S_{lx})_{M_k,\,M_k+1;\,M_l,\,M_l+1} = ip, \quad (7)$$

$$(S_{ky}S_{ly})_{M_k,\,M_k+1;\,M_l,\,M_l+1} = -p.$$

At first we consider the absorption of sound by the allowed transition $\Delta M_k = 1$ and $\Delta M_l = 0$. With the aid of (3), (4), and (6) we find the absolute square of the matrix element U_{klx}:

$$|(U_{klx})_{M_k,\,M_k+1;\,M_l,\,M_l}|^2 = 9\frac{g^4\beta^4}{r_{kl}^{14}}\, z_{kl}^2\,[2x_{kl}^2(x_{kl}^2+y_{kl}^2) - 10\,x_{kl}^2 r_{kl}^2 + r_{kl}^4]\,t^2. \quad (8)$$

We carry out the averaging for various directions of propagation of sound relative to the axes of the crystal, and also for all values of M_k and M_l. Then we obtain

$$|(U_{klx})_{M_k,\,M_k+1;\,M_l,\,M_l}|^2 = \frac{759}{7}\,\frac{g^4\beta^4}{r_{kl}^8}\,\frac{1}{36}\,S(S+1)^2(2S+1). \quad (9)$$

We substitute this expression into (4) and then into (1) and taking into account the action of nearest neighbors only, we obtain for the absorption coefficient

$$\sigma = \gamma PZ(g^2\beta^2/a^3)^2\, S(S+1)^2(2S+1)\,\nu^2, \quad (10)$$

where Z is the number of nearest neighbor atoms in the crystal lattice, $\gamma\perp = 253/21$, d is the density of the substance, and $P = \pi^2 N/kTv^3\nu_{1/2}d$. Our calculation pertains to the absorption of sound vibrations, propagated perpendicular to the applied magnetic field, along the z axis. If we carry out the analogous calculation for waves that are parallel to the magnetic field then we obtain the same expression as (1) only with the coefficient $\gamma\parallel = 16/21$.

For the absorption coefficient, in the coupled double transition ($\Delta M_k = +1$; $\Delta M_l = +1$), we obtain

$$\sigma = \gamma PZ(g^2\beta^2/a^3)^2(S+1)^2(2S+1)^2\nu^2, \quad (11)$$

where $\gamma\perp = 40/7$, $\gamma\parallel = 40/21$. In this way it is found that the line-width which corresponds to the resonance condition

$$h\nu = 2g\beta H, \quad (12)$$

yields approximately the same intensity as for the usual normal line which is specified by condition (2).

As an example, we estimate the absorption coefficient σ from formula (10) for MnF_2. For a temperature $T = 300°K$, assuming $\nu_{1/2} = 10^9$ sec^{-1}, we obtain

$$\sigma = 0.7 \cdot 10^{-19} \nu^2 \text{ см}^{-1}. \qquad (10')$$

The action of a magnetic force in the spin-lattice interaction is appreciable in substances with large densities of magnetic atoms. But in these substances there is also a large exchange force. The usual operator of the exchange interaction gives the following isotropic form:

$$\sum_l I(r_{kl})(S_k S_l).$$

This matrix does not have non-diagonal elements, and therefore isotropic exchange forces cannot directly influence a spin-lattice interaction**. However there are found in certain paramagnetic substances anisotropic exchange forces[4] that are able to play an essential role. For example, these forces are involved in the explanation of the magnetic substance $NiSiF_6 \cdot 6H_2O$[5], where the exchange interaction operator has the dipole form

$$\mathcal{H}_{об} = \sum_l A(r_{kl}) \qquad (13)$$
$$\times [(S_k S_l) - 3 r_{kl}^{-2} (S_k r_{kl})(S_l r_{kl})].$$

Then the calculation is precisely analogous to the calculation we employed in the magnetic case . We only know the dependence of the integral A on the atomic spacing. If we make the natural assumption that $A(r) = A_0\ (a)\, e^{-r/r_0}$ where $r_0 \sim a$, then the matrix element of the disturbance goes over to the expression $[\,(2/a) + (1/r_0)\,]$. If we assume that it equals $3/a$ we obtain for the coefficient of sound absorption the same formulas (10) and (11), but $(g^2\beta^2/a^3)$ is replaced by $[\,A(a)\,]^2$. For the transition between neighboring energy levels the coefficient γ is equal to

$$\gamma_\perp = 391/105, \qquad \gamma_\parallel = 8/21.$$

The detailed comparison of the experiments for paramagnetic resonance and the theoretical calculations carried out by Glebashev[6], for a wide range of substances, showed that the exchange integral lies between the limits 10^{-17}– 10^{-18} erg. In such a case the exchange force may increase the value of the calculated absorption coefficient over the action of magnetic interaction alone by one or two orders of magnitude.

3. RARE-EARTH METALS

The paramagnetism of the rare-earth metals depends on the deep lying internal atomic $4f$ electrons; the action of the conduction electrons is insignificant. Hence there exist great similarities between the magnetic properties of rare-earth metals and the salts of these elements. The author[7] by means of a comparison of the theoretical calculations with the experiments for the paramagnetic resonance in metallic cerium, praseodymium and neodymium has established that the atoms of these metals are triply ionized and the splitting of their energy levels is determined by electric fields having the same symmetry as the crystal lattice.

We carry out the calculation of the absorption coefficient of sound in rare-earth metals assuming that the spin-lattice interaction definitely modulates the electrical field of the vibrating lattice. At first we confine ourselves to the metals possessing cubic lattices, of which there are β-cerium, β-praseodymium, europium and ytterbium. For calculating the absorption coefficient we must use formulae (1), (4) and (5), only it is neccessary to understand that by U_{kl} is meant the energy of $4f$ electrons in electric fields, created by neighboring metallic ions. Taking into account the interaction of the six nearest neighbors and considering that the sound waves are propagated along the x axis, we find for U_{klx} the following expression:

$$U_{klx} = \frac{3ee'}{a^4} \qquad (14)$$
$$\times [u_x(r^2 - 3x^2) + 2u_y xy + 2u_z xz],$$

where r is the radius vector connecting $4f$ electron to the nucleus, x,y,z are components of this vector e' is the effective ionic charge, a is the lattice constant, u is the unit vector, along the direction of the atomic vibrations.

β-cerium. The energy levels and wave functions found in an electric field of cubic symmetry and an external magnetic field are specified in formula (26) of reference 1, for Ce^{+++} and Fe^{+++} which have total angular momentum of 5/2. This formula allows

** The average internal magnetic fields of crystals, and consequently the resulting absorption line-width $\nu_{1/2}$ is highly dependent on isotropic exchange forces. Hence this force indirectly influences the absorption of ultrasound and the spin-lattice interaction.

[4] W. Opechowski, Physica 14, 234 (1948)

[5] J. F. Ollom and J. H. Van Vleck, Physica 17, 205 (1951)

[6] G. Y. Glebashev, Dissertation, Kazan State University, 1954

[7] S. A. Al'tshuler, J. Exper. Theoret. Phys. USSR 26, 439 (1954)

us to simplify the calculation, if we take into account that the Zeeman splitting is by far weaker than that caused by the electric field. We calculate with the aid of the given functions and show that in first approximation only the following nondiagonal matrix elements differ from zero:

$$(U_{klx})_{ac} = (U_{klx})_{bd} = \frac{4\sqrt{3}}{105}(-3u_x + 2iu_y)\left(\frac{ee'}{a^2}\right)\frac{\overline{r}^2}{a^2}, \quad (15)$$

$$(U_{klx})_{ad} = (U_{klx})_{bc} = \frac{4\sqrt{3}}{105}u_z\left(\frac{ee'}{a^2}\right)\frac{\overline{r}^2}{a^2}.$$

Hence when we average for different directions of polarization, we find

$$|(U_{klx})_{ac}|^2 = 13\,|(U_{klx})_{ad}|^2 = 13\left(\frac{4}{105}\frac{ee'}{a^2}\frac{\overline{r}^2}{a^2}\right)^2. \quad (16)$$

Substituting (16) into (4) and (1) we find the absorption coefficient of sound in a magnetic field perpendicular to the direction of propagation of the waves

$$\sigma = \gamma P\left(\frac{ee'}{a}\right)^2\left(\frac{\overline{r}^2}{a^2}\right)^2\nu^2, \quad (17)$$

where

$$\gamma_{ac} = \gamma_{bd} = 13\,(8/105)^2,\ \gamma_{ad} = \gamma_{bc} = (8/105)^2.$$

If the sound wave is parallel to the magnetic field, then $\gamma_{ac} = \gamma_{bc} = \gamma_{ad} = \gamma_{bd} = 2(8/105)^2$. This formula is correct for any metal having a cubic lattice, except that the γ factors have different values. The numerical value of the coefficient σ is difficult to obtain since as yet we have not given the magnitude of the effective charge. If we assume $e' = e$ and for γ we take the maximum value, then for $T = 300\,^\circ$K we find

$$\sigma \sim 10^{-16}\nu^2 \ \text{см}^{-1}. \quad (17')$$

The differences $E_a - E_c$ and $E_b - E_d$ are equal and fit a single absorption line, whose position is necessarily strongly dependent on the direction of the external magnetic field relative to the axes of the crystal. On turning the magnetic field from the [100] direction to along the [111] direction, the value of the spacing $E_a - E_c = E_b - E_d$ is changed from $4/3g\beta H$ to $1/3g\beta H$. Hence in polycrystalline samples this absorption line has a half-width of the order of $g\beta H$.

The position of other absorption lines is slightly dependent on the direction of the magnetic field relative to the crystal axes, because the change of the interval $E_a - E_d = E_b - E_c$ goes only from $7/3g\beta H$ to $8/3g\beta H$.

β-praseodymium. In an electric field of cubic symmetry the energy levels of praseodymium split into four components: one singlet, one doublet and two triplets. The resultant splitting in a magnetic field does not depend on the direction of this field relative to the crystal axes. The perturbation method leads to the following values for the energy and wave functions:

$$E^{(\alpha)}_{1,3} = \frac{7}{27}\Delta \pm \frac{1}{2}G + \frac{189}{80}\frac{G^2}{\Delta}; \quad (18)$$

$$\Psi^{(\alpha)}_{1,3} = \frac{1}{\sqrt{8}}(\Phi_{\mp 3} + \sqrt{7}\,\Phi_{\pm 1});$$

$$E^{(\alpha)}_2 = \frac{7}{27}\Delta + \frac{864}{35}\frac{G^2}{\Delta};$$

$$\Psi^{(\alpha)}_2 = \frac{1}{\sqrt{2}}(\Phi_{-4} - \Phi_4);$$

$$E^{(\beta)} = \frac{14}{27}\Delta + \frac{180}{7}\frac{G^2}{\Delta};$$

$$\Psi^{(\beta)} = \frac{1}{\sqrt{24}}(\sqrt{5}\,\Phi_{-4} + \sqrt{14}\,\Phi_0 + \sqrt{5}\,\Phi_4);$$

$$E^{(\gamma)}_{1,2} = \frac{2}{27}\Delta \pm \frac{36}{5}\frac{G^2}{\Delta};$$

$$\Psi^{(\gamma)}_1 = \frac{1}{\sqrt{24}}(\sqrt{7}\,\Phi_{-4} - \sqrt{10}\,\Phi_0 + \sqrt{7}\,\Phi_4);$$

$$\Psi^{(\gamma)}_2 = \frac{1}{\sqrt{2}}(\Phi_{-2} + \Phi_2);$$

$$E^{(\delta)}_{1,3} = -\frac{13}{27}\Delta \pm \frac{5}{2}G + \frac{189}{80}\frac{G^2}{\Delta};$$

$$\Psi^{(\delta)}_{1,3} = \pm\frac{1}{\sqrt{8}}(\sqrt{7}\,\Phi_{\mp 3} - \Phi_{\pm 1});$$

$$E^{(\delta)}_2 = -\frac{13}{27}\Delta - \frac{36}{5}\frac{G^2}{\Delta};$$

$$\Psi^{(\delta)}_2 = \frac{1}{\sqrt{2}}(\Phi_{-2} - \Phi_2).$$

Here Δ is the total value of the splitting of the main energy levels of Pr^{+++} in the electric field of the crystal. In a magnetic field perpendicular to the propagation direction of the sound

$$\gamma_{\alpha_1\alpha_3} = \frac{13}{3}\left(\frac{182}{275}\right)^2, \quad \gamma_{\alpha_1\alpha_2} = \gamma_{\alpha_2\alpha_3} = \frac{8}{27}\left(\frac{182}{275}\right)^2,$$

$$\gamma_{\delta_1\delta_3} = \frac{13}{27}\left(\frac{208}{275}\right)^2, \quad \gamma_{\delta_1\delta_2} = \gamma_{\delta_2\delta_3} = \frac{2}{3}\left(\frac{338}{825}\right)^2,$$

$$\gamma_{\gamma_1\gamma_2} = 13\left(\frac{416}{33\cdot 225}\right)^2.$$

If the direction of the field is parallel to the direction of motion of the sound wave then the only difference is in the following factors

$$\gamma_{\alpha_1\alpha_2} = \gamma_{\alpha_2\alpha_3} = \frac{16}{27}\left(\frac{182}{275}\right)^2, \ \gamma_{\delta_1\delta_3} = \gamma_{\delta_2\delta_3} = \frac{4}{3}\left(\frac{338}{825}\right)^2.$$

Particular interest exists in the absorption of sound in the resulting transition between the above levels γ_1 and γ_2, as the magnetic field splits the level γ only in the second approximation. The location of the absorption peak in this case is determined by the value of Δ. In this way the observation of this line allows an immediate evaluation of the magnitude of the electric field inside the crystal. We notice that with the aid of the ordinary paramagnetic resonance this is impossible since the magnetic dipole transition between the sublevels γ_1 and γ_2 is forbidden.

Europium. The angular momentum of triply ionized atoms of europium in the ground state is zero. At room temperature, however, there is a noticeable polulation of the first excited state with $J = 1$ separated from the ground state by 214 cm^{-1}. It is well known that the energy level $J = 1$ does not split in an electric field of cubic symmetry. Hence the splitting in an external magnetic field is the same as for the free atom.

The factor γ has the following values

$$(\gamma_\perp)_{-1,1} = 0.52;\ (\gamma_\perp)_{-1,0} = (\gamma_\perp)_{0,1} = 0.08;$$
$$(\gamma_\parallel)_{-1,0} = (\gamma_\parallel)_{0,1} = 0.16;$$
$$(\gamma_\parallel)_{-1,1} = 0.$$

Ytterbium. In the ground state the ytterbium ion has $J = 7/2$, the same as ionic gadolinium. Hence we take advantage of the calculated energy and wave functions for gadolinium[8]:

$$E^{(a)}_{1,2} = \pm \frac{3}{2} G;$$
$$\Psi^{(a)}_{1,2} = \frac{1}{2}\left(\sqrt{3}\,\Phi_{\pm 5/2} - \Phi_{\mp 3/2}\right);$$
$$E^{(b)}_{1,4} = \frac{5}{8}\Delta \pm \frac{11}{6} G;$$
$$\Psi^{(b)}_{1,4} = \sqrt{\frac{7}{2}}\left(\Phi_{\pm 7/2} - \sqrt{\frac{5}{7}}\,\Phi_{\mp 1/2}\right);$$
$$E^{(b)}_{2,3} = \frac{5}{8}\Delta \pm \frac{1}{2} G;$$
$$\Psi^{(b)}_{2,3} = \frac{1}{2}\left(\Phi_{\pm 5/2} + \sqrt{3}\,\Phi_{\mp 3/2}\right);$$
$$E^{(c)}_{1,2} = \Delta \pm \frac{7}{6} G;$$
$$\Psi^{(c)}_{1,2} = \sqrt{\frac{5}{12}}\left(\Phi_{\pm 7/2} + \sqrt{\frac{7}{5}}\,\Phi_{\mp 1/2}\right).$$

With the aid of these wave functions the factors that are non-zero are found to have the following values

$$(\gamma_\perp)_{b_1 b_3} = (\gamma_\perp)_{b_2 b_4} = 13/(21)^2;$$
$$(\gamma_\parallel)_{b_1 b_2} = (\gamma_\parallel)_{b_3 b_4} = (4/7)^2.$$

We now consider metals with hexagonal lattices. At first we concern ourselves with α-Ce, Nd, Dy and Er whose ions have an odd number of electrons. In these ions electric fields of hexagonal symmetry cause complete splitting of the energy levels, retaining only the Kramers degeneracy. Since this degeneracy is not removed by the electric field the spin-lattice coupling can only emerge in second approximation. Hence the effect of paramagnetic resonance in ultrasound in these metals is $(g\beta H/\Delta)^2$ times weaker than in metals with cubic lattices. All that we have said also applies to samarium whose lattice is tetragonal.

A special case is presented by gadolinium whose ions are in the S state. The spin-lattice interaction in Gd^{+++} appears to depend on magnetic and exchange forces.

The ions of metallic α-Pr, Tb, Ho, Pm contain even numbers of electrons. Certain energy levels of these ions retain their double (non-Kramers) degeneracy in an electric field of hexagonal symmetry, which may be removed in a field of lower symmetry. In this case the spin-lattice interaction is different from zero in the first approximation. The effect on the absorption of sound will be of the same order as in metals of cubic lattices.

The study of the resonance absorption of ultrasound in rare-earth metals has a special interest, as the investigation of the absorption of electromagnetic waves in metals is extremely difficult to carry out because of the skin-effect.

4. NUCLEAR PARAMAGNETIC RESONANCE IN ULTRASOUND

Resonance absorption of ultrasound obviously takes place not only in "electronic" paramagnetics but also in substances possessing nuclear paramagnetism. We attempt to estimate the magnitude of this effect.

To begin with, we will consider solid bodies (non-metallic). The exchange of energy between the elastic vibrations of the lattice and the system of nuclear spins, due to a magnetic nuclear interaction, gives an effect whose value can be calculated from formula (10). Thereby it is only necessary to keep in mind that in the first place β is the nuclear magneton; this decreases the absorption coefficient by $\sim 10^{12}$. In the second place, $\nu_{1/2}$ now means the line-width of the nuclear resonance, which causes an increase of approximately 10^5. A more careful numerical calculation

[8] C. Kittel and J. M. Guttinger, Phys. Rev. 73,162 (1948)

carried out for the NaBr, gives $\sigma \sim 10^{-25}\nu^2 \text{cm}^{-1}$. Thus the absorption of ultrasound by the action of magnetic fields is extremely slight.

It is known that in many cases the spin-lattice coupling is caused by a quadrupole interaction [9]. The order of magnitude of the absorption coefficient of sound, caused by quadrupole forces, may be determined from formula (10) if we replace $g^2\beta^2$ by e^2Q. If we take into account that $\beta \sim 10^{-23}\text{G/cm}^3$, and $Q \sim 10^{-25}\text{cm}^2$, then for some substances the resulting $\sigma = 10^{-20}\nu^2\text{cm}^{-1}$. This value is exceedingly small since for an applied static magnetic field $\sim 10^4$ oersteds, as is seen from condition (2), we are obliged to employ an alternating field of frequency 10^7 cycles per sec.

We may expect a large effect in liquids . As is known from the theory of spin-lattice interactions in liquids[10], it follows that whereas in solid bodies the spectrum of thermal vibration frequencies determines a correspondingly small intensity from condition (3), in liquids the thermal motion contains oscillations of these frequencies with enormous intensities. In the case of solids we could, in comparison with the intensity of sound vibrations, neglect the thermal oscillations of these frequencies. Now we must properly reject this assumption, and then the probability of absorbing energy quanta of sound vibrations has an order of magnitude equal to $\frac{1}{2}\tau$ (τ is the time of spin-lattice relaxation).

The energy of sound waves, absorbed per unit volume of a substance in one second is obviously equal to

$$\frac{1}{2\tau} N h\nu \frac{h\nu}{kT} \frac{\Delta\nu}{\nu_{1/2}},$$

and hence for the absorption coefficient we have (I is the intensity of sound vibrations)

$$\sigma = N(h\nu)^2 \Delta\nu / 2\tau kTI\nu_{1/2}. \qquad (19)$$

We check, as an example, the proton resonance in water. By means of the addition of a paramagnetic salt the time of the spin-lattice relaxation may easily be brought to 10^{-4} seconds.

If $\nu = 3 \times 10^7$ cycles per sec. and the frequency interval and half-width $\nu_{1/2}$ are approximately the same, then in one second the energy absorbed ~ 360 ergs. It is easily calculated that the intensity of sound and thermal vibrations are comparable, if $I \approx 10^5$ ergs/cm^{3}sec; and therefore we find $\sigma \sim 0.01$ cm^{-1}. An increase in the sound intensity causes a disappearance of the effect because of saturation (cf. below). It is necessary to keep in mind that in so far as the spin-lattice interaction in water is produced by magnetic forces, then we have two absorption lines, whose locations are determined by equations (2) and (12), wherein the second line, as was easily derived in reference (10), has twice the intensity of the first.

It is well known that in the usual phenomenon of nuclear magnetic resonance we frequently observe a saturation effect, which consists in the fact that the spin-lattice interaction does not enable a transfer of all of the energy, absorbed by the spin system, to the thermal vibrations of the lattice. Consequently the population of the upper magnetic levels increases and the absorption of energy from the electromagnetic field decreases. An analogous effect is possible in the case of paramagnetic resonances for ultrasound. For simplicity we assume that we have only two magnetic levels and let A stand for the transition probability between them per second under the action of ultrasound. We denote by n the excess population of the lower level and let n_0 stand for the excess which corresponds to thermal equilibrium for the lattice temperature. In the absence of ultrasound, as is well known, the process of establishing equilibrium is set forth in the equation

$$dn/dt = (n_0 - n)/\tau,$$

where we may consider that τ determines the time of spin-lattice relaxation. If there is a sound field in the substance, then the equation takes the form

$$\frac{dn}{dt} = \frac{n_0 - n}{\tau} - 2nA, \qquad (20)$$

from which it follows that in the stationary state ($dn/dt = 0$)

$$n/n_0 = 1/(1 + 2A\tau). \qquad (21)$$

This value is usually called the saturation factor. If $n/n_0 \gg 1$, it is clear that the absorption of ultrasound is vanishingly small.

In liquids $A = (1/2\tau)(\Delta\nu/\nu_{1/2})$, the factor n/n_0 is nearly $\frac{1}{2}$ and consequently saturation is feeble. In solids it is easy to calculate the following expression for the transition probability:

$$A = I\sigma kT / N(h\nu)^2. \qquad (22)$$

[9] R. V. Pound, Phys. Rev. 79, 585 (1950)

[10] N. Blombergen, E. M. Purcell and R. V. Pound, Phys. Rev. 73, 678 (1948)

The numerical value shows that with an intensity of the order of $1 W/cm^2$ for a frequency 10^7 cycles per sec. we obtain a strong saturation. This fact may be used for the indirect detection of the absorption of ultrasound by nuclei. Suppose that we are observing the usual effect of the resonance absorption of an electromagnetic field of frequency ν. Then we superimpose a sufficiently strong acoustic field of the same frequency and the effect may be canceled.

With the aid of formulae (21) and (22) the possibility of the saturation effect for electric paramagnetic resonance for ultrasound can also be explained. In certain substances, which possess a large sound absorption coefficient σ, saturation may be approached under experimental conditions.

5. CONCLUSION

We have considered the resonance absorption of ultrasound in the main types of paramagnetic substances. For metals we considered only the rare-earths. In other metals the effect we have investigated is small. In metals that do not have available deep lying *f*-electrons with uncompensated spins, paramagnetism is due to the outer atomic electrons, which participate in conduction. In consequence of this the translational motion will also participate in the exchange of energy between the lattice vibrations and the electronic spins, observed in an applied magnetic field. Since the average energy of translational motion far exceeds the magnetic energy of the electrons, then clearly the absorption of sound cannot substantially depend on the magnetic field intensity; it will not have the sharply defined resonance character.

In the foregoing section we considered the nuclear effect in liquids. Formula (19) can only be applied for estimating the electronic resonance absorption of sound in liquid solutions of paramagnetic salts. In this case the number of absorbing atoms N is considerably smaller than in the case of nuclear resonances, the half width of the absorption line is on the other hand much larger. Hence the absorption coefficient is comparatively small, in spite of the considerably much shorter time of spin-lattice relaxation ($\tau \sim 10^{-8}$ sec). In truth electronic resonance permits the use of very high frequencies, which may make the effect observable, at the present time, by a sensitive arrangement.

The theory of spin-lattice interaction, developed for liquids, may be applied also to gases. With the aid of formula (20) of reference (10) we find that the time of paramagnetic relaxation for gases for atmospheric pressure and for room temperature is equal to $\tau \sim 10^{-6}$ sec. From formula (19) it follows that the absorption coefficient is very small [order of magnitude $10^{-20}(\nu 2/l)\,cm^{-1}$], if we take advantage of what is known from experiments on paramagnetic resonance in oxygen[11] where the value of $\nu_{1/2} = 0.05\ cm^{-1}$.

It is of interest to compare these considerations to the paramagnetic resonances for electromagnetic waves.

1. To begin with, we compare the magnitudes of both effects. The coefficient of absorption of energy in an electromagnetic field[12] is equal to

$$\sigma_e = \frac{8\pi^2}{c}\nu\chi''. \tag{23}$$

Where χ'' is the imaginary part of the complex magnetic susceptibility. If by χ_0 we denote the static susceptibility, then for maximum absorption $\chi'' \approx \chi_0 \nu/\nu_{1/2}$, and consequently,

$$\sigma_e = \frac{8\pi^2}{c\nu_{1/2}}\chi_0\nu^2. \tag{24}$$

At "electronic" paramagnetic frequencies $\nu_{1/2} \sim 10^9$ cycles per sec, $\chi_0 \sim 10^{-5}$ and hence $\sigma \sim 10^{-22}\nu^2\ cm^{-1}$. For the absorption coefficient of ultrasound for many substances we also derive the expression, proportional to ν^2, in which the proportionality factor is strongly dependent on the magnitude of the matrix element of the spin-lattice interaction. If this matrix element differs from zero in the first approximation, the for the coefficient of sound absorption σ we obtain a value exceeding σ_e. Under the requirements of higher approximations then usually σ_e and σ have values of the same order.

We make the observation, that throughout we calculated the average absorption coefficient for solids for longitudinal and transverse waves. Generally speaking, the transition probabilities between magnetic sublevels under the action of acoustic vibrations of the first type are very greatly surpassed by those for vibrations of the second type. Thus, for example, if the magnetic field is perpendicular to the direction of propagation of sound waves, then the absorption of sound in the resulting transition between sublevels *ad* and *bc of* β-cerium is possible only

---

[11] R. Beringer and J. G. Castle, Phys. Rev. **78**, 581 (1950); **81**, **82** (1951)

[12] J. C. Gorter, *Paramagnetic Relaxation* (1949), pg. 41

under the action of transverse oscillations.

2. In the case of the usual paramagnetic resonance the probability of absorbing a photon is a maximum if the alternating magnetic field is perpendicular to the static field; this probability decreases to zero if the magnetic fields are set parallel to one another. The probability of absorbing phonons is slightly dependent on the direction of the magnetic field. All the changes in the direction of this field may vary the order of magnitude of the effect.

3. The absorption of ultrasonic frequencies is a possible result of transitions between those sublevels for which the magnetic dipole transitions are forbidden. Hence, for example, in substances with pure spin paramagnetism the probability of absorbing photons is large only for transitions coupled by changes of the magnetic quantum numbers of the atoms by unity, where we know that only one resonance line appears. The probability of absorbing phonons has the same order both for transitions in which the magnetic quantum numbers of two interacting atoms change by unity, and those which are connected with changes of the quantum numbers of single atoms. Hence two observable absorption lines exist here.

4. The line widths of paramagnetic resonances both for ultrasound as well as for electromagnetic waves depend on the same factors. If the spin-lattice interaction is stronger than the spin-spin interaction, the half-width is of the order of $\sim 1/2\pi\tau$ and hence is strongly temperature dependent. If the spin coupling is stronger than the coupling to the lattice vibrations, then the line-width depends on the magnetic dipole interaction, exchange forces, electric fields of the ions and is not temperature dependent. Although the broadening of the absorption line in both phenomena is explained by the same forces, the form of one line can differ considerably from the other in the second case considered. This is explained by the fact that for the two phenomena we deal with one and the same band of energy levels, which produce magnetic and other interactions. However, the rules which determine the transition probability between these levels, under the action of ultrasound and under the action of an external alternating magnetic field, are completely different in nature. Thus, for example, the resonance line for the absorption of an electromagnetic field narrows under the action of an isotropic exchange force, as is well known [13]. Proof of this narrowing is based upon the fact that the second moment of the absorption line does not depend on the exchange force; this follows from the fact that the matrix S_x, which determines the probability of the magnetic dipole transition, commutes with the exchange interaction operator $A\Sigma S_i S_k$.

Evidently, the transition under the action of ultrasound may lead to an absorption line, the second moment of which depends on exchange forces. Nevertheless, the order of the absorption line-width is the same in both effects.

We note still another case in what follows. Comparatively small sensitivity of the ultrasonic method of investigation makes it desirable to use an indirect method of detecting paramagnetic resonances in ultrasound. Some of these were discussed in a previous section. We indicate one possibility. Paramagnetic resonance absorption of ultrasound will be accompanied by magnetization of substances which may be evaluated with the help of the coefficient of high frequency susceptibility χ'. From the investigation of the usual paramagnetic resonances it is known, that if the static magnetic field is changed, then the maximum change χ' is approximately equal to the value χ'', for maximum absorption. However with the help of (23) and (24) we at once find $\chi' \sim c\sigma/8\pi^2\nu$. The change in magnetization under the action of ultrasound may pro bably be observed by the use of the usual method of measuring χ' of Zavoiskii[14] or by nuclear induction [15].

In conclusion we note that the calculation of the spin-lattice interaction, which determines the magnitude of the effect of resonance absorption of ultrasound in paramagnetic substances can not lay claim to any great precision. The purpose was to arrange the calculation as an estimate of the order of magnitude of the effect and to establish the essential mechanism. The most interesting result which permits investigation is the explanation of the nature of the determinable characteristic constant of the spin-lattice interaction in various classes of paramagnetic bodies.

[13] J. H. Van Vleck, Phys. Rev. 74, 1168 (1948)

[14] E. K. Zavoiskii, J. Exper. Theoret. Phys. USSR 17, 155 (1947)

[15] F. Bloch, W. W. Hansen, and M. Packard, Phys. Rev. 70, 474 (1946)

Translated by B. Hamermesh
7

The Regression of the Centers of the Latent Photographic Image

B. I. KAZANTSEV AND P. V. MEIKLIAR
Moscow State Pedagogical Institute
(Submitted to JETP editor February 5, 1954)
J. Exper. Theoret. Phys. USSR **28**, 70-76 (January, 1955)

The time dependence of the regression of the centers of the latent photographic image and the subcenters has been investigated. It has been shown that the regression process is subject to a law similar to that of the relaxation of photo-conductivity and the damping of luminescence in crystals of silver halide.

THE regression of the centers of the latent image in plates with thick emulsion strata is manifested in the fact that the capacity for the development of emulsion crystals which have been subjected to the action of ionizing particles [1,2] or light [3] gets reduced in accordance with the length of time of storage.

The analogous effect, in such an ostensible form, is, however, not observed in the ordinary photographical plates. In their emulsion layers the centers of the latent image are more stable and regress but little with the passing of time. The same centers of the latent image in the case of the development delayed over some period of time after the cessation of light action are less stable and subject to apparent regression. Such centers are often called the subcenters of the latent image.

This work is devoted to the analysis of the regression of the centers of the latent image and the subcenters.

THE METHOD OF EXPERIMENTATION

A definite exposure was given to a photographic plate, either continuous, lasting 100 sec (t_0), or intermittent, dividing the same exposure time into two batches of illumination with a certain dark interval between them.

As the time (t_1) of the first exposure we took 10 sec, 20 sec, 30 sec, and so on. The time (t_2) of the second exposure was accordingly 90 sec, 80 sec, 70 sec, and so on. In each case $t_1 + t_2 = t_0$, or 100 sec. The time τ of the dark interval was changed alternately from 1 to 30 days. Illumination was from an incandescent lamp operated through a light stabilizer.

A sensitometric graphite wedge with the constant of 0.15 for white light and 0.17 for the blue was kept in front of the photographic plate. The development was carried in the Chibisov's developer. The constancy of the temperature of the development with the precision up to 0.5^0 was secured by means of a thermostatic control. The measurements on the resulting sensitograms were taken by means of the photo electric densitometer evaluating the diffusive density (D). The measurements were carried on the diapositive (2^0 H&D), line reproduction (2^0 GOST), and isoorthochromatic (31 units GOST) plates. Through the medium of the sensitograms the characteristic curves of $D = f(\lg H)$ were drawn with $\lg H$ (the value of the logarithm of the quantity of illumination) plotted in relative units.

THE RESULTS OF THE EXPERIMENTS

The comparisons were made of the characteristic curve obtained with the uninterrupted illumination lasting 100 sec with the characteristic curves obtained with this exposure divided into two batches of illumination of different durations, i. e. for various values t_1/t_0.

In all cases the curve of the intermittent illumination was shifted with respect to the curve of the uninterrupted illumination in the direction of greater values of $\lg H$ (Fig. 1). This shift we were e-

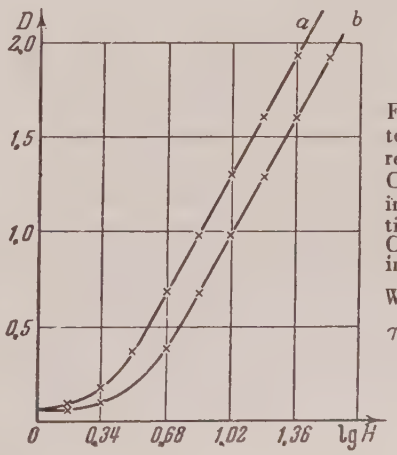

Fig. 1. The characteristic curves of reproduction plates. Curve a - for the uninterrupted illumination; Curve b - for the intermittent illumination; With $t_1/t_0 = 0.5$ and $\tau = 6$ days.

[1] M. Blau, Sitz. Ber. Acad. Wiss. Wien **140**, 623 (1931)

[2] H. Farraggi and G. Albouy, Compt. Rend. **226**, 717 (1948)

[3] L. Winand and L. Falla, Bull. Roy. Soc. Sci. Liège **18**, 184 (1949)

valuating by $\Delta \lg H$ of some definite value of optical density.

In Fig. 2 the relations are shown between $\Delta \lg H$ and t_1/t_0 obtained for the three different dark intervals, for the diapositive plates (for D =1).

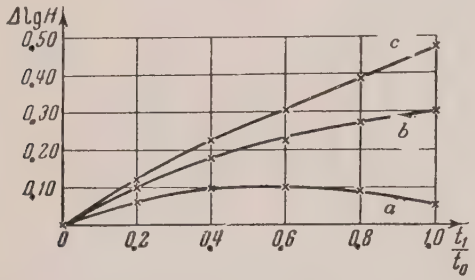

Fig. 2. The curves showing the relation between $\Delta \lg H$ and t_1/t_0 for the diapositive plates (for $D = 1$).
a for $t = 1$ day; *b* for $t = 6$ days; *c* for $t = 20$ days

In Fig. 3 the same relations appear for the reproduction plates (for $D = 1.5$). It becomes apparent from the examination of these curves that the regression of the subcenters of the latent image is most prominent for a certain intermediate value (t_1/t_0) max. and that this value of (t_1/t_0) max. increases with the increase in duration of the dark interval τ.

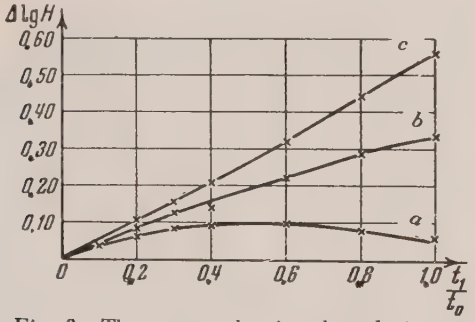

Fig. 3. The curves showing the relation between $\Delta \lg H$ and t_1/t_0 for the reproduction plates (for $D = 1.5$).
a for $t = 1$ day; *b* for $t = 7$ days; *c* for $t = 20$ days.

The results of the experiments may be expressed in a somewhat different way. Let H_0 be the quantity of illumination necessary to effect a certain density when the illumination is continuous and the development carried out immediately upon the the exposure , and N_0 be the number of atoms of silver found within the centers of latent image in the emulsion crystals, producing this density, so that $H_0 = CN_0$. If the development takes place after the lapse of time τ upon the exposition, then by that time the number of atoms of silver in the center will be N. Hence the effect of the development would be such as if the quantity of illumination $H = CN$ were in continuous action through an uninterrupted exposure and with development carried out immediately after the exposure. This means that

$$\Delta \lg H = \lg \frac{H_0}{H} = \lg \frac{N_0}{N} .$$

Hence we may write that

$$\frac{N}{N_0} = \frac{1}{\text{anti lg}\,(\Delta \lg H)} .$$

Now it is possible to draw some conclusions concerning the mechanism of the regression from the relation existing between N/N_0 and τ.

At the present time there are two theories [4] of the regression. According to the first of these the regression is an effect of the oxidation produced by the oxygen found in the air. It is also commonly accepted that the presence of the vapor of water intensifies this reaction.

According to the second theory the regression is an effect of the combination of atoms of silver found in the latent image with the atoms of bromide. If the first of these two theories is correct, i. e., if the mechanism of the regression is monomolecular, then the number dN of atoms of silver participating in the regression during the interval dt is given by

$$dN = -kN\,dt. \tag{1}$$

If the bromosilver or bimolecular theory is true, then the respective number of atoms of silver participating in the regression is

$$dN = -kN^2\,dt. \tag{2}$$

In both cases k is the coefficient of proportionality.

The root of the first equation will be

$$N/N_0 = e^{-k\tau}, \tag{3}$$

and of the second,

$$N/N_0 = (1 + N_0 k\tau)^{-1}. \tag{4}$$

The experiments prove that neither of these two equations is true. As an illustration Figures 4 and

[4] H. Farraggi and G. Albouy, *Photographic Registration of Ionic Radiations, 223*

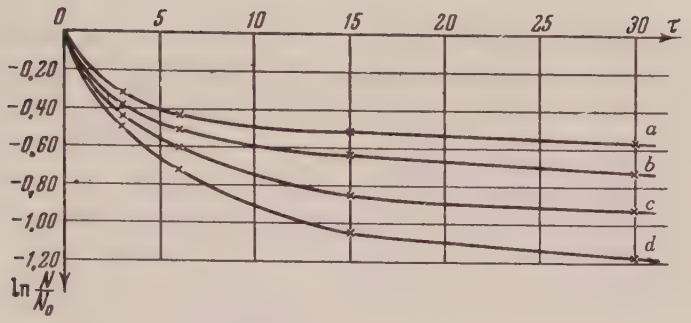

Fig. 4. The curves showing the relation between $\ln (N/N_0)$ and τ for the diapositive plates. The curve a for $t_1/t_0 = 0.4$; b for $t_1/t_0 = 0.6$; c for $t_1/t_0 = 0.8$; d for $t_1/t_0 = 1.0$

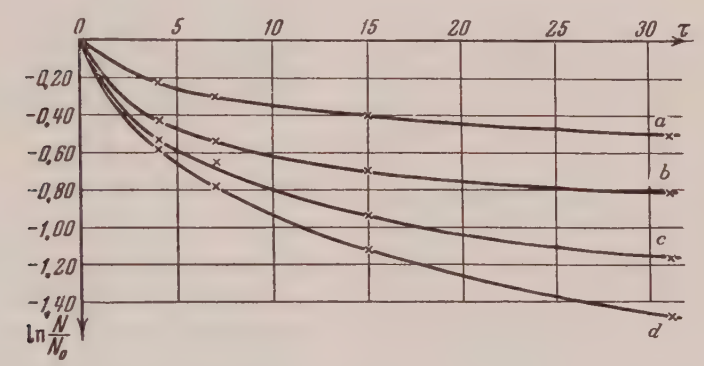

Fig. 5. The curves showing the relation between $\ln (N/N_0)$ and τ for the reproduction plates. The curve a for $t_1/t_0 = 0.4$; b for $t_1/t_0 = 0.6$; c for $t_1/t_0 = 0.8$; d for $t_1/t_0 = 1.0$

5 show the curves of relation between $\ln (N/N_0)$ and τ for the diapositive and the reproduction plates with various t_1/t_0. This relation would be linear if Eq. (3) were correct.

Meikliar has shown that in the process of the relaxation of the photoconductivity in crystals of silver halide the following equation holds:

$$\frac{\Delta\sigma}{\Delta\sigma_0} = \frac{1}{(1+at)^{\alpha}},$$

where $a \approx 10^3$ for thin monocrystals and $0.2 < \alpha < 0.5$. It is interesting to note that a similar law also governs the process of the regression of the centers of the latent image.

For this process the relation has the following form

$$\frac{N}{N_0} = \frac{1}{(1+N_0 k\tau)^{\alpha}}. \qquad (5)$$

The proof of the correctness of the Eq. (5) is found in the curve plotted for the values showing the relation between the reciprocal of the logarithmic derivative and τ. It should be linear since it appears from the Eq. (5) that

$$-\frac{1}{d\ln (N/N_0)/d\tau} = \frac{1}{\alpha}\tau + \frac{1}{N_0 k\alpha}$$

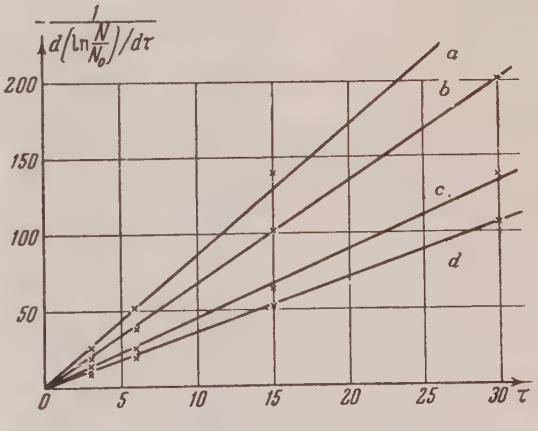

Fig. 6. The graph showing the relation between $-\frac{1}{d\ln (N/N_0)/d\tau}$ and τ for the diapositive plates. The line a for $t_1/t_0 = 0.4$; b for $t_1/t_0 = 0.6$; c for $t_1/t_0 = 0.8$; d for $t_1/t_0 = 1.0$

The results of such an examination are shown in Fig. 6 for the diapositive plates, in Fig. 7 for the reproduction plates, and in Fig. 8 for the Polish photographic paper "Photon".

The values lg H on the paper "Photon" were evaluated visually by comparing the changes of densities in the sensitogram produced after the regression had taken place with those of the sensitogram obtained immediately after the exposition.

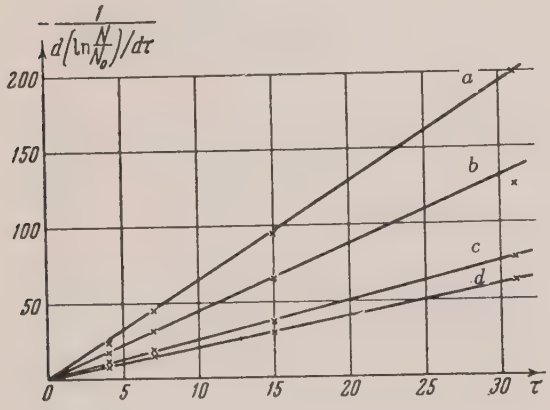

Fig. 7. The graph showing the relation between $-\frac{1}{d \ln (N/N_0)/d\tau}$ and τ for the reproduction plates. The line a for $t_1/t_0 = 0.4$; b for $t_1/t_0 = 0.6$; c for $t_1/t_0 = 0.8$; d for $t_1/t_0 = 1.0$

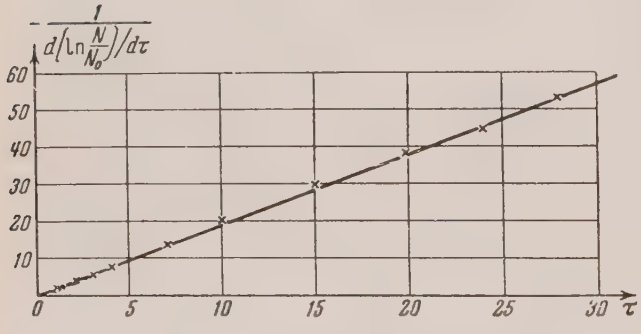

Fig. 8. The graph showing the relation between $-\frac{1}{d \ln (N/N_0)/d\tau}$ and τ for the photographic paper "Photon"

The resulting values α are found within the same limits as those taking place for the relaxation of the photo-conductivity. This is well illustrated by means of the following table.

Table

Values of α

t_1/t_0	Photomaterials		
	Diapositive Plates	Reproduction Plates	Photo Paper "Photon"
1.0	0.28	0.50	0.52
0.8	0.22	0.39	-
0.6	0.15	0.23 - 0.25	-
0.4	0.12	0.16	-

Since the value $N_0 k$ is great, the quantity $1/N_0 k \propto$ must be very small. Hence the lines in Figs. 6, 7, and 8 pass practically through the origin of the coordinates, which means that the following relation is essentially correct:

$$N/N_0 = c\tau^{-\alpha},$$

where

$$c = 1/(N_0 k)^{\tau}.$$

From the resulting data one may deduce that the kinetics of the regression of the centers of the latent image is similar to the kinetics of the photoconductivity [5] and the luminescence [6]. From this it may also be deduced that the kinetics of the regression are determined by the electronic part of this process, which is bimolecular in its character.

This is in accordance with the data by Cherdyntsev [7] who found that bimolecular reaction of the type $(1/m) - (1/m_0) = \text{const.}\ t$ takes place in the thermal destruction of minute particles of silver preliminarily discharged through the photochemical process. Our conclusions are also in agreement with the results of the work by Hedges and Mitchell [8]. These authors have shown that under the action of light the crystals of silver bromide discharge the atoms of bromide. These atoms not only can enter into a combination with the photolithic silver but also destroy the silver particles with which the crystals were previously dusted.

The results of the experiments showing the in-

[5] P. V. Meikliar, J. Exper. Theoret. Phys. USSR 21, 42 (1951)

[6] S. I. Golub, Doklady Akad. Nauk SSSR 60, 1153 (1948), works of the State University of Odessa 3, 41 (1951)

[7] S. V. Cherdyntsev, J. of Phys. Chem. USSR 15, 419 (1941)

[8] J. M. Hedges and J. W. Mitchell, Phil. Mag. 44, 357 (1953)

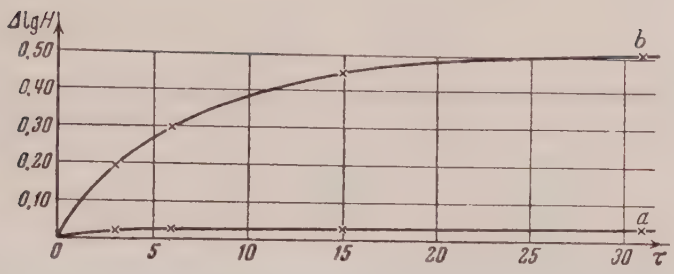

Fig. 9. The regression curve of the diapositive plates.
a - curve for the plate processed with 3% solution of borax.
b - same for the unprocessed plate.

crease of the regression in the atmosphere of oxygen, especially when it is filled with the vapor of water, and the decrease of the regression in the vacuum are often cited in support of the oxidation theory of the regression. It seems to us that these results are not yet sufficient to prove the oxidation theory. Any sharp change in the medium which surrounds the emulsion crystal is apt to affect the kinetics of the processes taking place on its surface irrespective of their mechanical nature.

Thus in the work by Bube [9] it has been shown that the presence of water vapor decreases considerably the time of the relaxation of the photo-

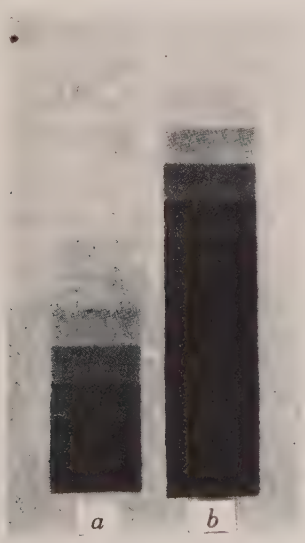

Fig. 10. The sensitograms produced on photo paper "Photon".
a - for the development carried out after a lapse of 6 days upon the exposure.
b - for the development carried out immediately after the exposure.

conductivity in the Cd S crystal, also that the time of relaxation increases in the vacuum. In other words, the presence of water vapor increases the velocity of the recombination of perforated electrons and decreases it in the vacuum.

It is known [4] that the regression of the traces left by ionizing particles within plates with thick strata decreases when the plates are treated with borax. A similar effect has also been observed for the regression taking place in the ordinary plates. This is seen in Fig. 9, where the curve *b* relates to the regression in the unprocessed diapositive plates, and the curve *a* relates to the regression in the plates treated with borax.

In Fig. 10 are given two sensitograms, one produced on the paper "Photon" with the exposure made just before the development (*b*), and the other one for the regression which took place during 6 days of storage (*a*).

Similar sensitograms appear in Fig. 11 for the paper preliminarily treated with 3% solution of borax

Fig. 11. The sensitograms produced on photo paper "Photon" treated with 3% solution of borax.
a - for the development carried out after a lapse of 6 days upon the exposure.
b - for the development carried out immediately after the exposure.

[9] R. Bube, Phys. Rev. 83, 393 (1951) J. Chem. Phys. 21, 1409 (1953)

Translated by V. J. Doberly.

A Magnetometer Which Makes Use of the Magnetic Resonance of Protons

N. I. LEONTIEV

(Submitted to JETP editor February 11, 1954)
J. Exper. Theoret. Phys. USSR 28, 77-84 (January, 1955)

A magnetometer is described which utilizes the nuclear absorption effect of protons. This meter is provided with automatic calibration circuits, which permit the measurement of the field intensity with an accuracy of $\pm 0.006\%$ Fields of application in which the apparatus could be used are indicated.

INTRODUCTION

IN several investigations a need arises for the measurement and stabilization of static magnetic fields and for the measurement of their homogeneity with a high degree of accuracy. Among the different apparatus offered for the solution of these problems, the simplest and the most accurate ones are those which utilize the nuclear magnetic resonance.

A magnetic field meter can be constructed based on the principles of the utilization of the nuclear induction effect [1] or of the nuclear absorption effect [2].

We will examine the advantages of the nuclear absorption effect in its use as a basis for the construction of a magnetic field meter. Let us place a few atoms of a para- or a diamagnetic substance in a uniform magnetic field H_0 directed along the z-axis. The magnitude of the field is such as to prevent any interaction between the nuclear spin magnetic moment and the magnetic moment of the outer electronic shells of the atom. At the same time let us act on these atoms by means of an alternating field. $H = 2H_m \cos \omega_r t$ which oscillates with the Larmor precession frequency and which is directed perpendicularly to the field H_0. Two cases can be considered here, according to the magnitude of the amplitude H_m.

1) H_m large, $H_m \gg \dfrac{1}{|\gamma|(T_1T_2)^{1/2}}$, where γ = nuclear gyromagnetic ratio, i. e., the ratio of the nuclear magnetic moment to the mechanical moment, T_1 = relaxation time, i. e., the time for attaining the thermal equilibrium, T_2 = period of precession of the nuclear moment in the interatomic field. A strong radiofrequency field will produce a rotation of the magnetization vector around the field H_0 synchronous with the field (precession).

This vector will deviate from the z-axis in direct proportion to the proximity of H_0 to the resonance field H_r, according to the Larmor precession equation:

$$H_r = \frac{\omega_r}{2\pi\gamma'} \qquad (1)$$

where γ' = gyromagnetic ratio in cgs units. For $H_0 = H_r$ the magnetization vector will make an angle of 90° with the z direction. If one measures the induction emf which appears in the coil which envelops the substance (the axis of the coil being directed along the y-axis), its maximum will correspond to the resonance condition ($H_0 = H_r$). By using the method of nuclear induction, we can make a magnetic field meter in which the measurement of H_0 is reduced to the measurement of ω_r. If an adequate frequency standard is available, ω_r may be measured to a high degree of accuracy.

2) H_m is small. The induction effect is then very small, but the conditions for the observation of the resonance absorption of the electromagnetic energy of the alternating field become optimum. The maximum of energy absorption lies in the region of resonance frequency as determined by Eq. (1). This effect is called the nuclear absorption effect and can also be utilized in the construction of a magnetic field meter in which the measurement of the field is reduced to a measurement of frequency.

It is not feasible to build a magnetic field meter which utilizes the induction resonance effect, because in order to detect a weakly oscillating field around the y-axis in presence of a strong field H_m along the x-axis it is necessary to introduce a series of regulating elements into the sample holder of the apparatus and then to shield the same carefully [3]. The sample holder of the magnetic field meter which utilizes the nuclear absorption effect can be made smaller and therefore can measure fields in greater detail.

[1] F. Bloch, Phys. Rev. 70, 460 (1946)

[2] H. C. Torrey, E. M. Purcell and R. V. Pound, Phys. Rev. 69, 680 (1946)

[3] F. Bloch, W. W. Hansen and M. Packard, Phys. Rev. 70, 474 (1946)

GENERAL DESCRIPTION OF THE APPARATUS

We built an apparatus which utilizes the nuclear absorption effect of protons, their γ' ratio being accurately known. Fig. 1 is a block diagram of the apparatus.

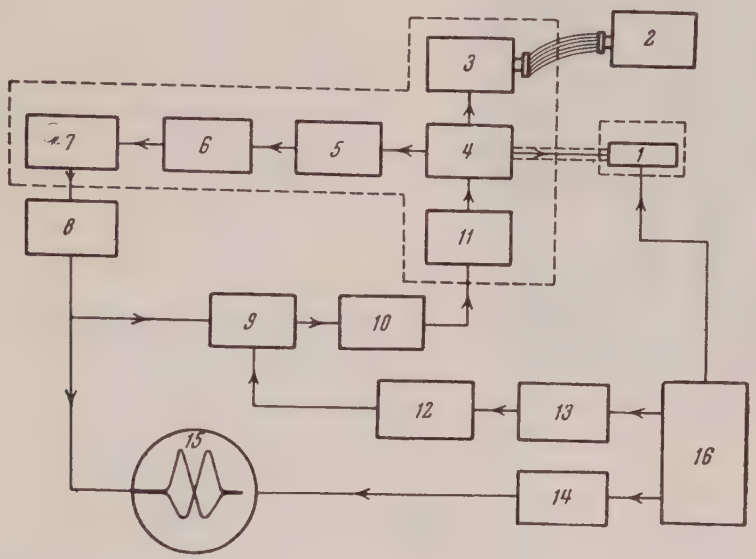

Fig. 1. Block diagram of the magnetic field meter: 1-sample holder, 2-heterodyne wavemeter, 3-buffer stage, 4-oscillator, 5-detector, 6-differentiating circuit, 7, 8-signal amplifiers, 9-phase detector, 10-differential amplifier, 11-reactance tube, 12-square wave pulse generator, 13, 14-phase changers, 15-cathode-ray tube, 16-50 cycle source.

The sample holder is a thin-walled copper box which acts as an electrical and mechanical shield. A plastic toroidal vial is placed in this box of following dimensions; external diameter 15 mm, internal diameter 3 mm, height 6 mm, wall thickness 0.2 mm. The vial is filled with a 10% solution of ferric chloride and a coil is wound around it to serve as the inductive coil of the oscillator. This coil is coupled to the oscillator by a coaxial cable of 500 mm in length, which makes it possible to measure the field intensity at any point in the gap of a magnet of a diameter up to 1m and also to make quick changes of coils. The apparatus has 3 interchangeable sample holders with 3 coils wound around the vial in "PESHO 0.22" cable. The long wave, medium wave and short wave coils have 38, 22 and 6 turns respectively. The vial is surrounded by a plastic cover of 24 mm diameter, on which the modulating coil is wound. This coil has 250 turns of "PE 0.2" cable. The modulating coil is fed by a. c. out of the 50 cycle mains. The modulation amplitude can be smoothly varied by varying the current in the coil from 0 to 120 mA. The current is controlled by means of a device on the front panel of the meter. For measurements the sample holder is placed in the gap region of the magnet in such a manner as to make the axis of the modulating coil coincide with the axis of the measured field. To each value of the field, a value of the oscillator frequency ω_r can be found such that a pulse signal will appear on the oscillograph scree which corresponds to a quantum jump of the proton to a neighboring Zeeman level. Equation (1) is valid here. The oscilloscope beam is displayed along the horizontal axis by applying a voltage in phase and synchronous with modulating potential.

If the apparatus is made so that the impulses appear at times

$$t_0, t_0 + \frac{T_{\text{mod}}}{2}, t_0 + T_{\text{mod}}, \ldots,$$

the modulating field will contribute no distortions to the measurement and $H_0 = H_r$ (Fig. 2). This condition corresponds to a calibration of the apparatus such that the peaks of coinciding pulses lie exactly in the center of the screen (during one modulation period 2 pulses appear on the screen). In our apparatus the pulses are differentiated and the base-point is selected as being the intersection of the near fronts of the differentiated pulses. From Fig. 2 one can see that the position of the base point on the screen corresponds to the positio

of the peaks of non-differentiated simultaneous pulses.

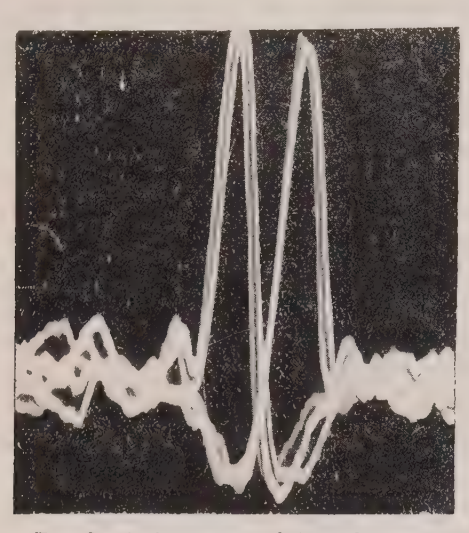

Fig. 2. A photograph of the pulse signal on the screen of the indicator tube.

The calibration of the apparatus reduces to a smooth variation of the oscillator frequency until the base-point is placed at the center of the screen, or, more exactly, in the middle of the sweep line, with a symmetrical modulating potential. Before the appearance of a pulse on the screen the calibration is performed by means of a vernier which modifies the capacity of the oscillator tuned circuit, while the sweep control (exact positioning of the base-point at the center of the screen) is obtained by means of automatic calibration circuits. By measuring the frequency of the oscillator (by means of the heterodyne wavemeter) it is easy to calculate the field intensity:

$$H_0 = 234.864\, f_r$$

where H_0 = field intensity in gauss, f_r = frequency in Mc/sec.

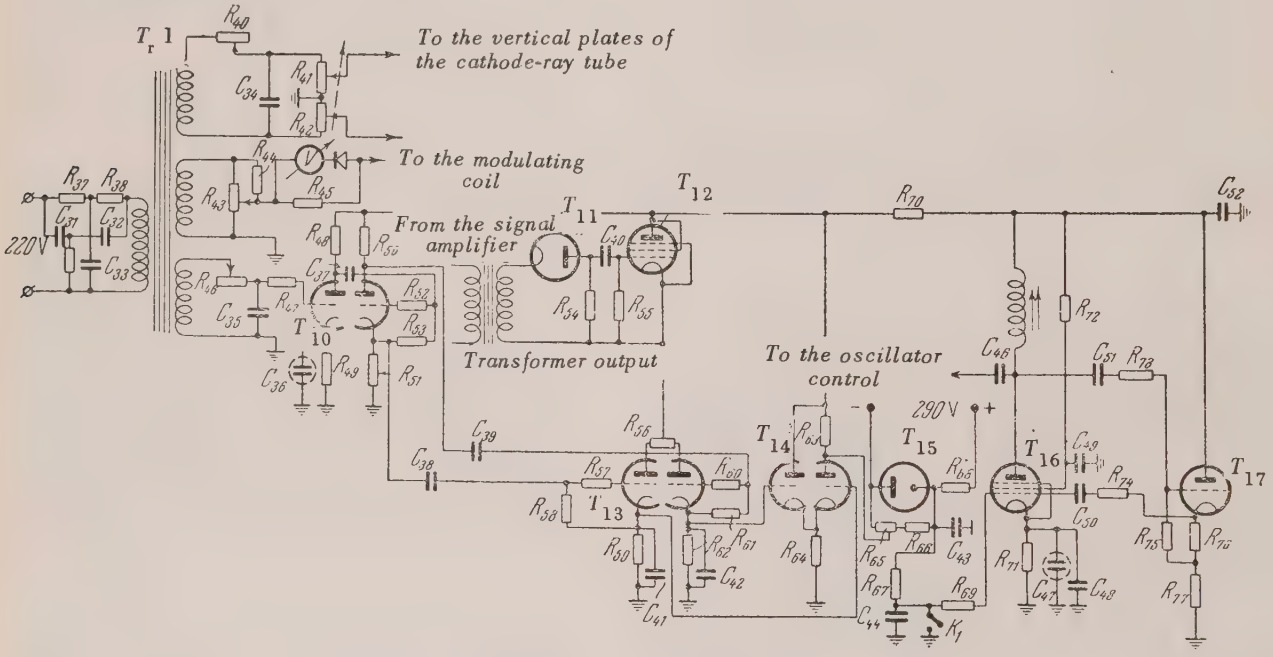

Fig. 3. Principal scheme of the automatic sweep control circuit. R_{37}, R_{38}, R_{73} - 1k Ω; R_{39} - 500 Ω; R_{40}, R_{46} - 5k Ω; R_{41}, R_{42} - 820 k Ω; R_{43} - 10 k Ω; R_{44}; R_{45} - 10 Ω; R_{46} - 5 k Ω; R_{47}, R_{52}, R_{54}, R_{55}, R_{56}, R_{57}, R_{58}, R_{60}, R_{61}, R_{77} - 510 k Ω; R_{48}, R_{50}, R_{51}, R_{66} - 100 k Ω; R_{49}, R_{71} - 2 k Ω; R_{53}, R_{63} - 1 MΩ; R_{59}, R_{62} - 51 k Ω; R_{64} - 30 k Ω; R_{65} - 160 k Ω; R_{67} - 10 MΩ; R_{68} - 12.5 k Ω; R_{69}, R_{72} - 50 k Ω; R_{70} - 24 k Ω; R_{74} - 400 k Ω; R_{75} - 70 k Ω; R_{76} - 200 k Ω; C_{31}, C_{32} - 1 μF; C_{33}, C_{44} - 2 μF; C_{34}, C_{35}, C_{43} - 0.25 μF; C_{36}, C_{47} - 100 μF; C_{37}, C_{38}, C_{39} - 0.5 μF; C_{40} - 0.02 μF; C_{41}, C_{42} - 12 μF; C_{46} - 20 μμF; C_{48}, C_{50}, C_{52} - 1000 μμF; C_{49} - 0.01 μF; C_{51} - 60 μμF; T_{10}, T_{13}, T_{14} - 6N9M; T_{11} - 6(KH)6; T_{12}, T_{16} - 6(ZH)3P; T_{15} - SG4S; T_{17} - 6(ZH)5

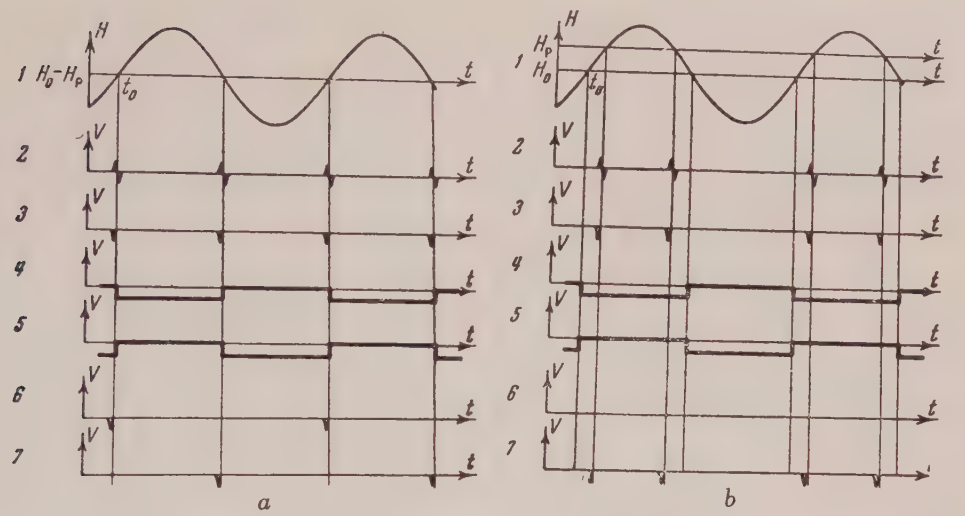

Fig. 4. Potential diagrams: *a)* $H_0 = H_r$, *b)* $H_0 \mp H_r$

1) Total intensity of the measured and the modulating fields
2) Signal on the cathode-ray tube
3) Potential on the grid of the tube T_{12}
4) Potential on the grid of the right-hand half of the tube T_{13}
5) Potential on the grid of the left-hand half of the tube T_{13}
6) Potential on the resistor R_{62}
7) Potential on the resistor R_{59}

AUTOMATIC CALIBRATION CIRCUIT

The basic part of the automatic sweep control circuit is the phase detector[4] (tubes T_{12} and T_{13}, Fig. 3.).

Square pulses in opposite phases are fed to the right and left-hand side circuits of the tube T_{13}. The pulses are formed by the square wave generator by using a potential in phase with, and synchronous to, the modulating voltage. The width of the square pulse is equal to the duration of a half-period of the modulating potential.

The amplitude of the square phase is such that at each moment one half of the tube T_{13} is non-conducting and the other is conducting. The pulse which is fed to the grid of T_{12} comes from the resistor R_{59} or from R_{62}, depending on which half of T_{13} is conducting. Figure (4a) gives the potential diagrams for the case when frequency of the generator corresponds to $H_0 = H_r$. One can see from Fig. (4) that the same number of pulses appears on the resistors R_{59} and R_{62}. Figure (4*b*) gives the potential diagrams for the case when the apparatus is not exactly tuned and the measured field is not equal to the resonance field. In this case no pulses will appear across R_{59}, all going to the resistor R_{62}. The potentials across R_{59} and R_{62} are integrated by the condensers C_{41} and C_{42}; the difference between these potentials, which changes in sign according to the direction of deviation of the oscillator frequency from the resonance frequency, is transmitted to the "deviation cascade" (reactance tube). The deviation cascade calibrates the generator frequency in order to keep it at the f_r value.

A general scheme of the automatic calibration circuits appears in Fig. (3). The voltage from the power transformer is applied to the horizontal deflection plates of the cathode-ray tube, the modulating coil and the square wave generator.

A double T filter is introduced into the primary circuit of the power transformer in order to obtain a better potential pattern in the secondary winding. The filter is tuned to the third harmonic of the circuit. The resistor R_{40} and the capacity C_{34} constitute a simple phase changer. It compensates for the phase shift between the modulating coil and the cathode-ray tube sweep circuits. The resistor R_{46} and the capacity C_{35} represent another phase changer which compensates the phase shift between the square wave generator and the modulating coil circuits. Two stages in the T_{10} tube circuit transform the sine signal into a square wave. The resistor R_{49} following the cathode of the first tube permits one to obtain a positive and

[4] N. A. Shuster, Rev. Sci. Instr. 22, 254 (1951)

a negative pulse of the same width. The square pulses are transmitted respectively to the right-hand and the left-hand side triodes of the T_{13} tube of the phase detector. By means of the potentiometer R_{56}, on changing the T_{13} tube, one can always calibrate the phase detector so that with the signal absent the voltage across R_{59} is always equal to the voltage across R_{62}. The tube T_{11} cuts off the negative part of the differentiated signal pulse. On the anode of the differential amplifier T_{14} a voltage is obtained proportional to the difference of voltages obtained respectively across R_{59} and R_{62}. The magnitude of the constant anode voltage of the right-hand side of T_{14} is neutralized by the voltage drop across the resistor R_{66} and a part of the variable resistor R_{65} in parallel with the voltage stabilizer tube T_{15}. The voltage across the voltage stabilizer is provided by a separate rectifier. By means of the potentiometer R_{65} (on changing T_{15}) a zero potential is established between the grid of T_{16} and the ground. With a correct tuning of the automatic calibration circuit the voltage between the grid of the T_{16} tube and the ground will be zero (for in this case the base point lies exactly at the center of the screen), or will be negative (the base point is deflected to the right of the center), or positive (b. p. deflected to the left). On deflection of the base point to the border of the screen this voltage is ± 25 V. The parameters of the "deviation cascade" [5] (tubes T_{16} and T_{17}) are such that on changing the voltage on the grid of the tube T_{16} from -2 to -6 V, with a constant modulating voltage, the frequency of the oscillator changes so as to make the base-point traverse the whole screen from one extremity to the other. With a deviation on the T_{16} tube equal to -3.75 V, which is obtained by the deviating resistor R_{71} ($2k\,\Omega$), the operating point of the deviation cascade will lie in the middle of the linear part of the characteristic deviation curve. A negative voltage with respect to the ground, applied to the grid of T_{16} will make the base point deviate to the left; a positive voltage, to the right. With such calibration of the automatic circuit the base point will be automatically positioned at the center of the screen, provided a previous manual calibration brings the pulses at least up to the border of the screen. The time constant of the automatic calibration circuits is such that the base point moves from one border of the screen to the other in a time interval of one minute. To shorten the observation time and to obtain a greater accuracy it is necessary to bring the base point as near as possible to the center of the screen by manual tuning. A tumbler switch K, grounds the circuit of the T_{16} tube and thus disconnects the whole automatic calibration circuit.

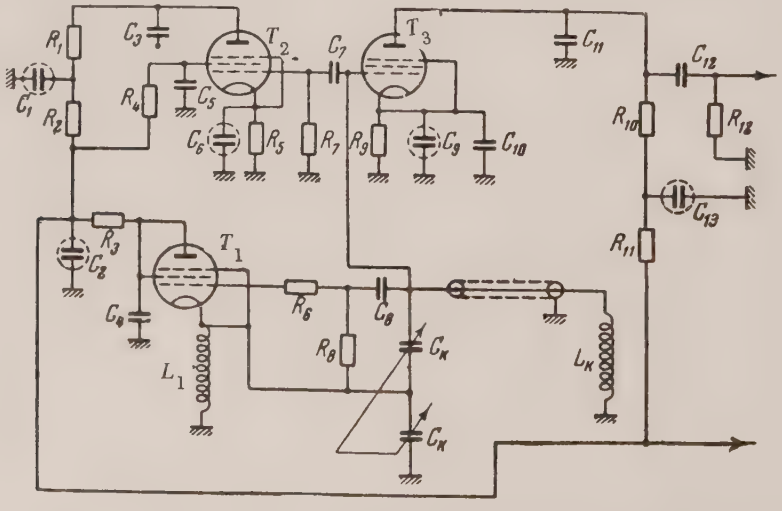

Fig. 5. Main circuit diagram of the oscillator, detector and the buffer stage. R_1 - 500 Ω; R_2 - 1 kΩ; R_3, R_9, R_{11} - 24 kΩ; R_4 - 50 kΩ; R_5 - 500 Ω; R_6 - 325 Ω; R_7 - 1 MΩ; R_8 - 70 kΩ; R_{10}, R_{12} - 100 kΩ; C_1, C_2 - 10 μF; C_3 - 20 μμF; C_4, C_5, C_{11} - 0.01 μF; C_6, C_9 - 100 μF; C_7 - 100 μμF; C_8, C_{12} - 60 μμF; C_{10} - 0.005 μF; C_{13} - 10 μF; C_k - 17 ÷ 550 μμF; T_1, T_2, T_3 - 6(ZH)3P; L_1 - 10 μH

[5] H. D. Holerich, Electronics **4**, 120 (1948)

OSCILLATOR AND THE OTHER STAGES OF THE METER

The oscillator consists of a (ZH) 3 tube, connected as a triode, in a capacitively coupled circuit (tube T_1, Fig. 5). This circuit allows the coupling of the control coil, which lies in the gas of the magnet which is being measured, with a coaxial cable with a grounded external lead. The resistance of the feedback coupling, R_6 regulates the amplitude characteristic of the oscillator according to the frequency sweep range. A block of 3 variable condensers and 3 variable coils on the oscillator covers a range of frequencies from 4.25 to 30 Mc/sec, corresponding to fields from 1000 to 7000 oersteds. The oscillator allows the broadening of the measurement range in both directions, if additional exchange coils are provided. A preliminary reading of the frequency is made on the vernier and the final reading is made on the heterodyne wave meter.

The tube T_3 constitutes the anode detector. The use of the T_1 tube as an oscillator (grid, cathode, screen grid) and as a detector (cathode, grid, anode), simultaneously, gives worse results, because it is difficult to find a value for the deviation voltage which is at the same time optimum throughout a large frequency range both for the oscillator and the detector.

The buffer stage (tube T_2) permits one to eliminate any influence of the heterodyne wavemeter on the oscillator, because of the weak coupling and of the small amplification factor.

The resistor R_{12} and the capacity C_{12} constitute a differentiating circuit, from which the signal goes to the signal amplifier, which has 5 stages. The output stage has a push-pull transformer coupling. The transformer is provided with 2 secondary windings. One applies the signal to the vertical deflecting plates of the cathode-ray tube, the other applies the signal to the input of the phase detector. The maximum amplification factor of the amplifier is about 10^6. The potentiometer in the circuit of the third stage permits a smooth regulation of the amplification factor. The transmission band of the amplifier is from 30-20,000 cps, with a sharp decrease of the amplification on the edges of the band.

The anode voltages of all the tubes are stabilized by an electronic stabilizer, which supplies a 265 V, 80 mA regulated voltage, with a noise of 2-3 mV. The filaments of T_1, T_2, T_3, T_{16} and T_{17} (figs. 3 and 5) are connected in series and are fed from a 0.3 B 17-3B rectifier with a selenium column. The total power utilized by the apparatus is 160 W. A cathode-ray tube of the 13L037 type was employed for visualization purposes. The supply circuit of this tube is analagous to that in the EO-4 oscillograph.

The actual construction of the apparatus employs two racks: the smaller one contains the oscillator, the detector, 2 signal amplifier stages, the buffer and the deviation stages; the other contains the remaining circuits. This construction permits use of the apparatus in the case where there is little space left near the magnet whose field is to be measured. The racks are interconnected by means of 2 cables. One transmits the signal and the other (a multiple cable) provides the supply and the reactance tube voltages.

APPLICATIONS OF THE APPARATUS

The above descrived meter has been used for exact measurements with permanent magnets. Measurements on one of them (of 24,000 oersteds), over many days, after a previous magnetic aging and maintained at a constant temperature, have shown that the maximum deviation from the mean value of 10 measurements constitutes + 0.006% The same degree of accuracy can be obtained by observing the sound tone in the phones of the heterodyne wavemeter by connecting it to the buffer stage. On connecting the automatic calibration circuit the frequency of the generator does not stay constant: it changes slowly about its mean value. The maximum frequency deviation which can thus be detected is 600 cps with a generator frequency of 10 Mc/sec this constitutes 0.006%. On measuring stronger fields the relative frequency oscillation is less. The absolute precision of the apparatus was not verified, because no other methods were available which would measure the magnetic field with the same accuracy as ours. Besides the measurements with permanent magnets, measurements have been effected on the aging of permanent magnets, the variations of the intensity of the field of an electromagnet fed by a storage battery of great capacity, and of the homogeneity of the field of a magnet. The apparatus can also be used for the measurement of instantaneous values of alternating fields.

The author expresses his deep gratefulness to Dr. V. Shiuttse for help with this work.

Translated by B. Cimbleris
10

The Problem of Calculating the Internal Field in Polycrystalline Dipole Dielectrics in the Case of Relaxation Polarization

G. I. SKANAVI AND A. N. GUBKIN
P.N. Lebedev Institute of Physics, Academy of Sciences, USSR
(Submitted to JETP editor Jan 19, 1954)
J. Exper. Theoret. Phys. USSR 28, 85-95 (Jan., 1955)

A method is proposed for calculating the internal field for the case of relaxation polarization in dipolar polycrystalline dielectrics. The parameters characterizing the relaxation polarization are computed for the particular case of organic dipolar polycrystals.

IT is known that only in relatively rare cases (non-polar liquids, diatomic cubic crystals) can the acting (local) field in liquid and solid dielectrics be determined, in first approximation, by the well-known Lorentz equation

$$E = E_{av} + \frac{4\pi}{3} I, \tag{1}$$

where I is the electric moment per unit volume.

If the structure of the crystal is known, it is possible to find the internal field using the method of structural coefficients[1].

This article represents an effort to determine the internal-field coefficients for dielectrics of complex and unknown structure from experimental data on the relaxation polarization. Such a determination is of interest for two reasons. First, it permits greater precision in the evaluation of those parameters characteristic of relaxation polarization, which are of substantial significance in themselves (potential barrier that limits the motion of the relaxing dipole or ion group, or the natural frequencies of these groups). Second, it gives an idea of the behavior of the field acting in a polycrystalline dipolar dielectric, how it differs from the Lorentz field, and how it is related to the values of the dielectric constants at zero and infinite frequencies.

According to the Lorentz method, the acting field can be represented in the form of a sum:

$$E = E_{av} + \frac{4\pi}{3} I + E_{add} \tag{2}$$

where E_{add} is the additional field due to the particles within the Lorentz sphere. Using the method of structural coefficients[1] it is possible to represent the field acting on the ith particle as follows:

$$E_i = E_{av} + \frac{4\pi}{3} I + \sum_{k=1}^{m} \alpha_k C_{ik} E_k + \sum_{k=1}^{m'} \alpha'_k C'_{ik} E_k. \tag{3}$$

Here α_k is the relaxation polarizability of the kth dipole group (or of the group of weakly-coupled ions); α'_k is the elastic polarizability of the kth group of particles; C_{ik} are the structural coefficients, accounting for the dipole distribution in the lattice; C'_{ik} are the structural coefficients accounting for the elastically-bound particles in the lattice; m is the number of dipole groups differently distributed in the crystal cell; m' is the number of particle groups differently distributed in the crystal cell and having "elastic" polarization; E_k is the field acting on the kth particle located in the vicinity of the ith particle under consideration (i varies from 1 to m'; $m \geq m'$).

Assuming that all particles in the dielectric are under the influence of the same averaged local field, Eq. (3) can be written:

$$E = \frac{1}{m'} \sum_{i=1}^{m'} E_i = E_{av} + \frac{4\pi}{3} I + \frac{1}{m'} \sum_{i=1}^{m'} \sum_{k=1}^{m} \alpha_k C_{ik} E_k + \frac{1}{m'} \sum_{i=1}^{m'} \sum_{k=1}^{m'} \alpha'_k C'_{ik} E_k. \tag{4}$$

Since we do not know the structural coefficients (not knowing the lattice structure) let us

[1] G. I. Skanavi, J. Exper. Theoret. Phys. 17, 399 (1947)

introduce the generalized coefficients β_1 and β_2 of the internal field:

$$E = E_{av} + \beta_1 I_{rel} + \beta_2 I_0, \tag{5}$$

where I_{rel} and I_0 are the electric moments per unit volume, due to the relaxation and to the displacement polarization respectively.

According to Eq. (4), the generalized coefficients can be expressed in terms of the structural coefficients

$$\beta_1 = \frac{4\pi}{3} + \frac{1}{m' I_{rel}} \sum_{i=1}^{m'} \sum_{k=1}^{m} \frac{C_{ik} I_{relk}}{n_k}, \tag{6}$$

$$\beta_2 = \frac{4\pi}{3} + \frac{1}{m' I_0} \sum_{i=1}^{m'} \sum_{k=1}^{m'} \frac{C'_{ik} I_{0k}}{n_{0k}}. \tag{7}$$

Here I_{relk} and I_{ok} are electric moments per unit volume, due respectively to the relaxation and displacement polarizations of the kth-group particles.

For the case of linear polarization considered in this article, the electric moment per unit volume is proportional to the acting field strength, and the coefficients β_1 and β_2 are therefore independent of the field.

According to Fröhlich[2], who generalized Kirkwood's equation for polar fluids to include the case of dipolar solids, the basic quantity characterizing the relaxation polarization in crystalline dipolar substances is not the individual dipole or group of dipoles, as in the case of dipolar liquids, but the individual crystalline cell, which has a certain effective dipole $\mathbf{m}_j$, depending on the orientations of the dipoles contained in the cell. This difference between crystalline dipolar substances and dipolar liquids is due to the difference in the construction of the crystal and the liquid.

In evaluating the interaction between dipoles, we shall assume, in agreement with Kirkwood and Fröhlich, that a sphere surrounding a given cell with a fixed dipole moment $\mathbf{m}_j$ has a dipole moment $\mathbf{m}_j^*$. In the first approximation, we shall characterize the relaxation polarization of the dipolar crystalline cells by a single potential barrier, and consequently, by a single relaxation time. This is permissible if the density with which which the values of relaxation time are grouped about the probable value is sufficiently high.

Assuming that each crystalline dipolar unit cell has only two equilibrium positions, corresponding to opposite directions of the electric moments, the equation for relaxation polarization[3] can be used in the following simple form:

$$\frac{d(\Delta N_j)}{dt} \frac{e^{U/kT}}{\nu} = -\Delta N_j (e^{\Delta U_j/kT} + e^{-\Delta U_j/kT}) + \frac{N_0}{6} (e^{\Delta U_j/kT} - e^{-\Delta U_j/kT}), \tag{8}$$

where ΔN_j is the increase per cm^3 in the number of crystalline cells (due to the superposition of the external field) having a dipole moment $\mathbf{m}_j$ directed along the field; N_0 is the total number of crystalline cells per cm^3 in the dielectric ν is the natural frequency of the effective dipole of the crystalline cell; U is the potential barrier restricting the orientation of the unit cell; and ΔU_j is the change in the potential barrier due to the external field.

For a given dipole direction in the unit cell, the dipole moment per unit volume produced by the relaxation polarization equals

$$I_{relj} = 2\Delta N_j \mathbf{m}_j. \tag{9}$$

Multiplying both halves of Eq. (8) by $2\mathbf{m}_j$ we obtain

$$\frac{e^{U/kT}}{\nu} \frac{dI_{relj}}{dt} = -I_{relj} (e^{\Delta U_j/kT} + e^{-\Delta U_j/kT}) + \frac{N_0 \mathbf{m}_j}{3} (e^{\Delta U_j/kT} - e^{-\Delta U_j/kT}).$$

If $\Delta U_j \ll kT$, we have

$$\tau \frac{d I_{relj}}{dt} = -I_{relj} + \frac{N_0}{3} \mathbf{m}_j \frac{\Delta U_j}{kT},$$

where

$$\tau = (1/2\nu)\, e^{U/kT}$$

Considering that the energy of a dipole unit cell is an external electric field is determined (because of the interaction between dipole cells) not by the dipole moment $\mathbf{m}_j$ of the cell itself, but by the dipole moment $\mathbf{m}_j^*$ of the sphere surrounding the given cell, and assuming the dipole moment of the cell itself to be fixed, we have

[2] H. Fröhlich, Theory of Dielectrics: Dielectric Constant and Dielectric Loss, Oxford, 1949.

[3] G. I. Skanavi, Fisika Dielektrikov (Physics of Dielectrics), GITTL, 1949.

$$\Delta U_j = \mathfrak{m}_j^* \cdot E$$

hence

$$\tau = \frac{dI_{\text{relj}}}{dt} = -I_{\text{relj}} + \frac{N_0}{3}\frac{\mathfrak{m}_j \cdot \mathfrak{m}^*_j}{kT}\,\mathrm{E}.$$

Averaging over all possible dipole orientations, taking into account the probability of finding the dipoles in a given configuration, and considering that the internal field has the same direction as I_{rel} and I_0 [see Eq.(5)], we obtain finally

$$\tau\frac{dI_{\text{rel}}}{dt} = -I_{\text{rel}} + BE, \tag{10}$$

where

$$\mathrm{B} = N_0\frac{\overline{(\mathfrak{m}\mathfrak{m}^*)}}{3kT}.$$

Replacing E of Eq. (10) by its value in (5):

$$\tau(dI_{\text{rel}}/dt) = -I_{\text{rel}} + BE_{\text{av}} + \beta_1 BI_{\text{pen}} + \beta_2 BI_0. \tag{11}$$

To solve (11) it is essential to express I_0 in terms of E_{av} and I_{rel}.
For the general case,

$$I_0 = \sum_{k=1}^{m'} I_{0k} = n_2\alpha_1 E_1 + n_2\alpha_2 E_2 + \ldots + n_{m'}\alpha_{m'}E_{m'}.$$

Here $\alpha_1, \alpha_2 \ldots \alpha_{m'}$ are the elastic polarizabilities. Introducing, as before, an averaged acting field

$$E = \frac{1}{m'}\sum_{i=1}^{m'} E_i,$$

we obtain

$$I_0 = E\left[n_1\alpha_1 m' E_1\left(\sum_{i=1}^{m'} E_i\right)^{-1} + n_2\alpha_2 m' E_2\left(\sum_{i=1}^{m'} E_i\right)^{-1} \ldots + n_{m'}\alpha_{m'}m'E_{m'}\left(\sum_{i=1}^{m'} E_i\right)^{-1}\right] \tag{12}$$

The sum in the brackets can be replaced by the product of the equivalent quantities $n_{\text{eq}}\alpha_{\text{eq}}$,

$$I_0 = n_{\text{eq}}\,\alpha_{\text{eq}}E. \tag{13}$$

Using (5), (11), and (13), and making some simple transformations, we obtain a fundamental equation

$$\tau(dI_{\text{rel}}/dt) = -I_{\text{rel}}[1 - \beta_1 B(1+A)] + E_{\text{av}}B(1+A). \tag{14}$$

Here

$$A = \beta_2 n_{\text{eq}}\alpha_{\text{eq}}/(1 - \beta_2\, n_{\text{eq}}\,\alpha_{\text{eq}} \tag{15}$$

Solving Eq. (14) for the case of a static field, we obtain

$$I_{\text{rel}} = \frac{B(1+A)}{\gamma}(1 - e^{-t\gamma/\tau})E_{\text{av}}$$

where

$$\gamma = 1 - \beta_1 B(1+A), \tag{16}$$

and the quantity $\theta = \tau/\gamma$ is the time constant of the relaxation polarization.

If the external field is periodic and in its steady-state we obtain:

$$E_{\text{av}} = E_m e^{i\omega t}, \quad I_{\text{rel}} = I_m e^{i(\omega t - \delta)}.$$

For the case of linear polarization we have

$$\tau(dI_{\text{rel}}/dt) = i\omega\tau I_{\text{rel}} \tag{17}$$

Equating (17) and (14) and separating real and imaginary parts, we get

$$I^*_{\text{rel}} = \frac{\gamma B(1+A)E_{\text{av}}}{\gamma^2 + \omega^2\tau^2} - i\frac{B(1+A)\omega\tau E_{\text{av}}}{\gamma^2 + \omega^2\tau^2}. \tag{18}$$

Using the relationships

$$\varepsilon^* = 1 + 4\pi I^*_{\text{rel}}/E_{\text{av}} \quad \text{and} \quad \varepsilon^* = \varepsilon' - i\varepsilon'',$$

where ϵ^* and I^* are the complex expressions for the dielectric constant and the total electric moment per unit volume respectively, and making use of Eq. (18), we obtain, after separating the real and imaginary parts of the expressions for ϵ' and ϵ'':

$$\varepsilon' = 1 + \frac{4\pi A}{\beta_2} + \frac{4\pi B\,(1+A)\,(1+(\beta_1/\beta_2)\,A)\,\gamma}{\gamma^2+\omega^2\tau^2}\,; \quad (19)$$

$$\varepsilon'' = \frac{4\pi\omega\tau B\,(1+A)\,(1+(\beta_1/\beta_2)\,A)}{\gamma^2+\omega^2\tau^2} \quad (20)$$

For $\omega \to \infty$ we have

$$\varepsilon_\infty = 1 + 4\pi A/\beta_2. \quad (21)$$

For $\omega = 0$ we have

$$\varepsilon_0 = 1 + \frac{4\pi A}{\beta_2} + \frac{4\pi B\,(1+A)\,(1+(\beta_1/\beta_2)A)}{\gamma}\,. \quad (22)$$

Using Eq. (21) and (22), as well as (19) and (20), we can express ϵ' and ϵ'' in terms of ϵ_0 and ϵ_∞ (the dielectric constants at zero and infinite frequency) *

$$\varepsilon' = \varepsilon_\infty + \frac{(\varepsilon_0-\varepsilon_\infty)\,\gamma^2}{\gamma^2+\omega^2\tau^2}\,, \quad (23)$$

$$\varepsilon'' = \frac{(\varepsilon_0-\varepsilon_\infty)\,\omega\tau\gamma}{\gamma^2+\omega^2\tau^2}\,. \quad (24)$$

It follows from Eqs. (23) and (24) that

$$\tan\delta = \frac{\varepsilon''}{\varepsilon'} = \frac{\omega\tau\,(\varepsilon_0-\varepsilon_\infty)\,\gamma}{\varepsilon_0\gamma^2+\varepsilon_\infty\omega^2\tau^2}$$

whenever the conductivity is low.

The frequency-temperature value at which tan δ is maximum can be obtained by differentiating tan δ with respect to $\omega\tau$ and setting the result equal to zero. This value is:

$$(\omega\tau)_m = \sqrt{\varepsilon_0/\varepsilon_\infty}\,\gamma.$$

Comparison of equations (19) and (20) with (23) and (24) yields

$$\varepsilon_0-\varepsilon_\infty)\,\gamma = 4\pi B\,(1+A)\,[1+(\beta_1/\beta_2)\,A]. \quad (25)$$

The relationship between the quantities β_1, β_2, γ, and B can be found by using Eqs. (16), (21), and (25). This relationship is of the form:

$$\beta_1 = \frac{4\pi\,(\varepsilon_0-\varepsilon_\infty)}{B\,(\varepsilon_0-1)\,[4\pi+(\varepsilon_\infty-1)\,\beta_2]} - \frac{4\pi}{\varepsilon_0-1}\,; \quad (26)$$

$$\gamma = \frac{\beta_1\,(\varepsilon_\infty-1)+4\pi}{\beta_1\,(\varepsilon_0-1)+4\pi}\,. \quad (27)$$

The unknowns in (26) and (27) are β_1, β_2, γ, and $B = N_0\,\overline{\mathbf{m}\cdot\mathbf{m}^*}\,/3kT$. . The value of B can be determined from Fröhlich's basic equation for the polarization of dipolar substances

$$\frac{(\varepsilon_0-\varepsilon_\infty)\,(2\varepsilon_0+\varepsilon_\infty)}{9\varepsilon_0} = \frac{4\pi}{3}\,N_0\,\frac{\overline{\mathbf{m}\cdot\mathbf{m}^*}}{3kT}\,. \quad (28)$$

Substituting the value of B obtained from (28), we get for (26):

$$\beta_1 = \frac{48\pi^2\varepsilon_0}{(\varepsilon_0-1)\,(2\varepsilon_0+\varepsilon_\infty)\,[4\pi+(\varepsilon_\infty-1)\,\beta_2]} - \frac{4\pi}{(\varepsilon_0-1)}\,. \quad (29)$$

If the dielectric consists of a mixture of a polar polycrystalline compound and a non-polar filler, this will affect, to first approximation, only the value of B In this case B can be determined from Kirkwood's equation, obtained for the case of a mixture of a polar polymer with a non-polar one[4]. This equation has been generalized by us, in analogy with Fröhlich's equation, to read:

$$\frac{(\varepsilon_0-1)\,(2\varepsilon_0+1)}{9\varepsilon_0} - \frac{(\varepsilon_\infty-1)\,(2\varepsilon_\infty+1)}{9\varepsilon_\infty} = \frac{4\pi}{3}\,N_0\,\frac{\overline{\mathbf{m}\cdot\mathbf{m}^*}}{3kT}\,. \quad (30)$$

In this case we obtain, instead of Eq. (29), the following expression:

$$\beta_1 = \frac{48\pi^2\varepsilon_0\varepsilon_\infty}{(2\varepsilon_0\varepsilon_\infty+1)\,(\varepsilon_0-1)\,[4\pi+\beta_2\,(\varepsilon_\infty-1)]} - \frac{4\pi}{(\varepsilon_0-1)}\,. \quad (31)$$

If one of the three quantities β_1,β_2, or γ is known, Eqs. (27), (29), and(31) become the basic equations from which the other two quantities can be determined.

In the general case, the coefficient β_2 can be determined from Eqs. (15) and (21):

$$\beta_2 = \frac{1}{n_{eq}\,\alpha_{eq}} - \frac{4\pi}{\varepsilon_\infty-1}$$

* If $\gamma = (\epsilon_\infty+2)/(\epsilon_0+2)$, Eqs. (23) and (24) reduce to the corresponding Debye equations. Substituting the value of B obtained from (28), we get for (26):

[4] J. Kirkwood and R. Fuoss, Journ. Chem. Phys. 9, 329 (1941)

If the fields E_i differ little from the averaged field E, Eq. (12) yields

$$n_{eq}\alpha_{eq} \approx \sum_{i=1}^{i=m'} n_i\alpha_i,$$

hence

$$\beta_2 = \left(\sum_{i=1}^{m'} n_i\alpha_i\right)^{-1} = 4\pi(\varepsilon_\infty - 1)^{-1}.$$

Consequently, if the concentration and polarizabilities of the elastically-polarized particles are known, the coefficient β_2 can be determined; then the coefficient β_1 and the parameter γ can be expressed in terms of ϵ_0 and ϵ_∞, i.e., the stated problem can be solved. On the other hand, if the composition of the dielectric is complicated and unknown, the coefficient β_2 cannot be calculated with sufficient accuracy, and an expression for the internal-field coefficients in terms of ϵ_0 and ϵ_∞ can be derived only for special cases.

For the special case of dielec rics that contain no ions (for example, organic substances), i.e., dielectrics having only electron-displacement polarization at $\omega \to \infty$, it is possible to assume

$$\beta_2 = 4\pi/3.$$

In fact it follows from Eq. (4) that

$$E = E_{av} + \frac{4\pi}{3} I_{rel} + \frac{4\pi}{3} I_0 + E'_{add} + E''_{add}$$

where

$$E'_{add} = \frac{1}{m'} \sum_{i=1}^{m'} \sum_{k=1}^{m} \alpha_k C_{ik} E_i,$$

$$E''_{add} = \frac{1}{m'} \sum_{i=1}^{m'} \sum_{k=1}^{m'} \alpha'_k C'_{ik} E_i.$$

If $\omega \to \infty$

$$E = E_{av} + \frac{4\pi}{3} I_0 + E''_{add}$$

It can be shown[3] that a dielectric having polarization of the electron-displacement type, and having a low refractive index, obeys the Clausius-Mossotti equation. It is therefore possible to assume for this case

$$E''_{add} \approx 0,$$

i.e., the electron polarization does not contribute to E_{add}, and consequently it follows from (7) that $\beta_2 = 4\pi/3$. In addition, if ϵ_∞ has the usual range (2-4), then

$$\sum_{i=1}^{m'} n_i\alpha_i = \frac{3(\varepsilon_\infty - 1)}{4\pi(\varepsilon_\infty + 2)} \sim 0.1,$$

corresponding to $n \sim 10^{22}$ cm^{-3} and $\alpha \sim 10^{-23}$ cm^3, which are of the correct order of magnitude (the electron polarizability of a molecule of solid dielectric equals approximately the cube of the molecular radius[3]). Using this approximation ($\beta_2 = 4\pi/3$), we obtain the following expressions instead of (29) and (23):

$$\beta_1 = \frac{4\pi[9\varepsilon_0 - (\varepsilon_\infty + 2)(2\varepsilon_0 + \varepsilon_\infty)]}{(2\varepsilon_0 + \varepsilon_\infty)(\varepsilon_\infty + 2)(\varepsilon_0 - 1)}, \quad (32)$$

$$\beta_1 = \frac{4\pi[9\varepsilon_0\varepsilon_\infty - (2\varepsilon_0\varepsilon_\infty + 1)(\varepsilon_\infty + 2)]}{(2\varepsilon_0\varepsilon_\infty + 1)(\varepsilon_\infty + 2)(\varepsilon_0 - 1)}, \quad (33)$$

These permit determining β_1 and γ [from Eq. (27)], provided ϵ_0 and ϵ_∞ are known. Obviously $\beta_1 \neq 4\pi/3$ and $\gamma \neq (\epsilon_\infty + 2)/(\epsilon_0 + 2)$, and the resultant equations differ considerably from the known Debye equations.

Equations (32) and (33) make it possible to study the variation of β_1 with ϵ_0 and ϵ_∞. It follows from (32) that $\beta_1 = 0$ whenever

$$\varepsilon_0 = \varepsilon_\infty(\varepsilon_\infty + 2)/(5 - 2\varepsilon_\infty). \quad (34)$$

This condition can be satisfied if ϵ_∞ varies between 1 and 2.5 (ϵ_0 varies accordingly between 1 and ∞). As ϵ_0 varies within this range, the sign of β_1 depends on the value of ϵ_0: if $\epsilon_0 > \epsilon_\infty > (\epsilon_\infty + 2)/(5 - 2\epsilon_\infty)$, then $\beta_1 > 0$; otherwise $\beta_1 < 0$. On the other hand, if $\epsilon_\infty \geqslant 2.5$, then $\beta_1 \leqslant 0$ always (Fig. 1). Equation (32) can be represented graphically by a family of curves $\beta_1 = \phi(\epsilon_0)$ for various values of the parameter ϵ_∞. Fig. 2 shows such curves for $\epsilon_\infty = 2,3$, and 4. It can be seen from Fig. 2 that if $\epsilon_\infty \geqslant 2.5$ the absolute magnitude of β_1 diminishes as ϵ_0 increases, and that it passes through its maximum when $\epsilon_\infty < 2.5$.

If a polycrystalline dipolar dielectric having only electron and dipolar polarizations satisfies Eq. (34), the average field acting on it can be shown to equal

$$E = E_{av} + \frac{4\pi}{3} I_0, \quad (35)$$

the presence of relaxation polarization notwithstanding. Such dielectrics obey the following simple relationship between ϵ_0 and ϵ_∞:

$$\frac{\varepsilon_0 - 1}{\varepsilon_\infty + 2} = \frac{4\pi}{3}\left[\sum_{i=1}^{m'} n_i \alpha_i + N_0\, \alpha_{rel}\right],$$

where $\alpha_{rel} = \overline{\mathbf{m}\cdot\mathbf{m}^*}/3kT$ is the relaxation polarizability of a single crystal cell. In these cases the parameter γ becomes unity [see Eq. (27)] and the calculation of the characteristics of the relaxation polarization is considerably simplified [5].

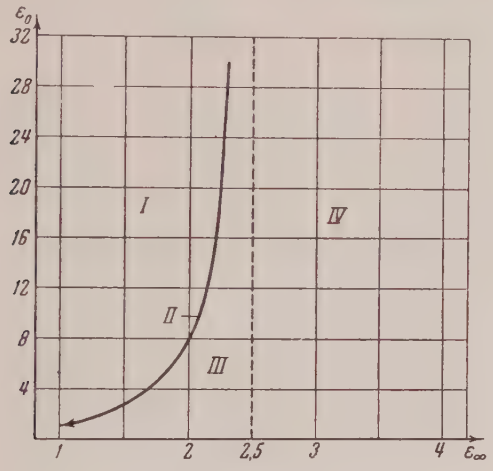

Fig. 1. Graphic representation of Eq. (34): I—domain values of ε_0 and ε_∞ for which $\beta_1 > 0$; III and IV—$\beta_1 < 0$; curve II corresponds to the condition $\beta_1 = 0$.

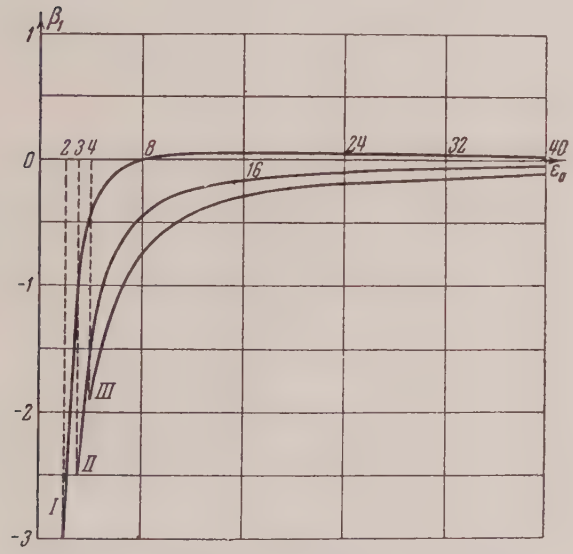

Fig. 2. Variation of β_1 with ε_0 for various constant values of ε_∞ [Eq. (32)]; I—$\varepsilon_\infty = 2$; II—$\varepsilon_\infty = 3$; III—$\varepsilon_\infty = 4$.

[5] G. I. Skanavi and A. N. Gubkin, J. Exper. Theoret. Phys. USSR 27, 742 (1954)

Equation (33) permits analogous calculation of the coefficient β_1 for a mixture of polar and non-polar substances. Computations show that the coefficient β_1 can vanish also in this case; β_1 is always negative when $\varepsilon_\infty \geqslant 2.5$, and decreases in absolute magnitude with increasing ε_0 for a given value of $\varepsilon_\infty \geqslant 2.5$.

If ε_0 is sufficiently large, β_1 may become a very small quantity; this holds for both pure dipolar polycrystals [Eq. (32)] and a mixture of polar and non-polar substances [Eq. (33)]. Thus, for example, if $\varepsilon_\infty = 3$ and $\varepsilon_0 = 100$, a value $\beta_1 = -0.01$ is obtained from both equations (32) and (33). The negative sign of the coefficient β_1 indicates that the relaxation polarization reduces the acting field.

Knowing the coefficients β_1 and β_2 of the internal field, it is possible to determine from Eq. (5) the extent to which the acting field deviates from the acting macroscopic one. In fact, assuming as before $\beta_2 = 4\pi/3$, and using

$$I_0 = \frac{\varepsilon_\infty - 1}{4\pi} E_{av} \quad \text{and} \quad I_{rel} = \frac{\varepsilon' - \varepsilon_\infty}{4\pi} E_{av},$$

where ε' is the dielectric constant for a given frequency ω, it is easy to obtain an expression for the acting field in terms of its average macroscopic value:

$$E = \left[\frac{(\varepsilon_\infty + 2)}{3} + \beta_1 \frac{(\varepsilon' - \varepsilon_\infty)}{4\pi}\right] E_{av}. \qquad (36)$$

Evidently this expression differs from the corresponding expression for the case when the internal field equals the Lorentz field:

$$E = \frac{\varepsilon' + 2}{3} E_{av}, \qquad (37)$$

If $\varepsilon_\infty = 3$, $\varepsilon' = 15$, and $\beta_1 = -0.1$, Eq. (35) yields $E = 1.6 E_{av}$, while Eq. (37) yields $E = 6 E_{av}$ for the same case. On the other hand, if $\beta_1 = 0$ [see condition (34)], we obtain $E = [(\varepsilon_\infty + 2)/3] E_{av}$, which corresponds to the acting field (35).

Thus, in the case of a clearly pronounced relaxation polarization, the acting field differs much less from the average macroscopic field than from the acting Lorentz field.

Table 1 lists the values of coefficient β_1 and parameter γ computed in the manner given above for oleo-waxes of various degrees of plasticity, using data from our previous work [5].

In the case of oleo-wax compound 1, which contained the minimum amount of the amorphous phase, the coefficient β_1 was computed from Eq. (32). Equation (33) was used for compounds 2,3

Table 1

Hydrogenized castor oils (oleo-waxes)	Experimental data[5]			19°C			45°C		
				β_1,	γ		β_1,	γ	
	ϵ_∞	ϵ_o at 19°C	ϵ_o at 45°C	Eq. (32) for Comp. #1 Eq. (33) for Comp. #2,3,4.	$\frac{\epsilon_\infty + 2}{\epsilon_o + 2}$	Eq. (27)	Eq. (32) for Comp. #1 Eq. (33) for Comp. #2,3,4.	$\frac{\epsilon_\infty + 2}{\epsilon_o + 2}$	Eq. (27)
Compound 1	3.4	21.8	25.2	-0.14	0.23	1.27	-0.12	0.20	1.26
" 2	3.2	13.3	14.1	-0.15	0.34	1.14	-0.13	0.32	1.13
" 3	3.2	11.9	13.0	-0.17	0.37	1.13	-0.15	0.35	1.14
" 4	3.8	5.5	5.5	-0.68	0.77	1.12	-0.68	0.77	1.12

Table 2

Hydrogenized castor oils (oleo-waxes)	Frequency corresponding to maximum tan δ		Relaxation time $10^6.\tau$ sec.		Activation energy, U. eV	Natural frequency sec^{-1}
	19°C	45°C	19°C	45°C		
Compound 1	25 100	91 200	2.0	0.6	0.38	0.8×10^{11}
" 2	19 950	50 120	1.9	0.8	0.28	1.7×10^{9}
" 3	19 950	50 120	1.7	0.7	0.26	1.0×10^{9}
" 4	12 590	22 390	1.7	1.0	0.18	3.4×10^{7}

and 4, which contained some amount of amorphous non-polar filling. For the sake of comparison, the table contains the values of the coefficient $\gamma = (\epsilon_\infty + 2)/(\epsilon_o + 2)$.

It is evident from table 1 that the coefficients β_1 and γ, obtained with the above method from experimental values of ϵ_∞ and ϵ_o, differ sharply from the values $\beta_1 = 4\pi/3$ and $\gamma = (\epsilon_\infty + 2)/(\epsilon_o + 2)$, used in the theory of relaxation polarization and based on the use of a Lorentz acting field.

Once the coefficient β_1 is determined, the general equations for computing the characteristics of relaxation polarization[5] can be used to find the activation energy, the relaxation time, and the natural frequency of the dipolar unit cell. Such computations were made for the four oleo-wax compounds at two temperatures (Table 2).

It can be seen from Table 2 that the relaxation time is of the order of 10^{-5} seconds for oleo-waxes of various degrees of plasticity, and hardly changes with the composition of the substance. On the other hand, calculations in which the internal field was assumed not to differ from the Lorentz field[5] show a gradual increase of τ with the plasticity of the compound. The activation energy decreases as the plasticity of the compound increases. In all but compound 4 the activation energy obtained is somewhat lower than the value obtained by previous computations[5]. As the plasticity of the compound increases, the natural frequency of the dipolar unit cell drops from a value on the order of 10^{11} to values on the order of 10^7 sec^{-1}. Compared with the natural frequency computed in reference [5], the results obtained by the method given here are lower by approximately a factor of ten.

The method given in refernce [5] for computing the increase in the relaxation time does not involve the internal field. The method is thus applicable also to the present case. On the other hand, application of the theory of absolute reaction rates (see[5]) gives results that differ somewhat from those obtained when the Lorentz field is used, inasmuch as the use of a different internal field causes that theory to be premised on different

Table 3

Hydrogenized castor oils (oleo-waxes)	T, °K	Relaxation time, $\tau.10^5$ seconds	ΔF, kgm-calories	ΔS cal/deg	ΔH, kgm-calories
Compound 1	292 318	2.0 0.6	10.8 11.0	-9.9 -9.8	7.9
Compound 2	292 318	1.9 0.8	10.8 11.2	-17.8 -17.6	5.6
Compound 3	292 318	1.7 0.7	10.7 11.1	-17.1 -17.0	5.7
Compound 4	292 318	1.7 1.0	10.7 11.4	-25.7 -25.8	3.2

values of relaxation time τ.

Table 3 lists the values of the difference in heat content, difference in entropy, and difference in free energy for an internal field differing from the Lorentz field. It can be seen from Table 3 that the absolute magnitudes of the activation entropy are higher than those obtained in reference [5]. This can most probably be explained by the fact that the present work accounts more fully for the interaction between the dipole groups.

The method presented above for determining the internal-field coefficients can also be used for liquid dipolar dielectrics. It would then be necessary to consider the polar liquid molecule instead of the dipolar cell of the crystal.

$$\mathbf{m} = \vec{\mu}, \quad \mathbf{m}^* = \vec{\mu}^*,$$

where $\vec{\mu}$ is the dipole moment of the molecule, and $\vec{\mu}^*$ is the dipole moment of the sphere surrounding a given molecule, provided its dipole moment has a fixed direction; since all dipole directions are equivalent in a liquid, we have $\overline{\mathbf{m}\cdot\mathbf{m}} = \vec{\mu}\vec{\mu}^*$.

In this case, Fröhlich's general equation (28) reduces to Kirkwood's equation for polar liquids (see [2])

$$\frac{(\varepsilon_0 - \varepsilon_\infty)(2\varepsilon_0 + \varepsilon_\infty)}{9\varepsilon_0} = \frac{4\pi}{3} N_0 \frac{\vec{\mu}\cdot\vec{\mu}^*}{3kT},$$

where N_0 is the number of dipoles per cm^3, and the quantity B entering into the relaxation equations equals

$$B = N_0 \frac{\vec{\mu}\cdot\vec{\mu}^*}{3kT}.$$

Taking the above into account, it is possible to derive analogously Eqs. (29) and (31), which will then be valid also for liquid dielectrics.

Translated by J. G. Adashko
11

A Self-Quenching Light Meter

S. F. RODIONOV, M. S. KHAIKIN AND A. I. SHAL'NIKOV
Institute for Physical Problems of the Academy of Sciences, USSR

(Submitted to JETP editor March 31, 1954)
J. Exper. Theoret. Phys. USSR 28, 223-227 (February, 1955)

A description is given of a self-quenching light meter and the special characteristics of meters with platinum, aluminum and magnesium photocathodes.

1. THE photon meter[1], which at this time is the most sensitive instrument for the measurement of ultraviolet light, is used successfully in many investigations that require the precise determination of low intensity light. The mass production of this instrument is impeded by the large number of rejects. A considerable number of these rejects suffer from too steep counting characteristics and instability. A long aging process is required to make them acceptable. Stabilization of counting characteristics may be achieved by the use of quenching (gas) mixtures of the type used in self-quenching meters[2].

In this paper we describe a self-quenching photor meter with very stable counting characteristics and good sensitivity that can be used industrially. Tests on the production of self-quenching meters under laboratory conditions indicate that if the proper technical production methods are used, one may expect perfect output and good reproducibility of meter characteristics.

We made and tested about 40 such self-quenching meters. Their utilization in the laboratory and under field conditions over a period of several years indicates good stability and working dependability. Cases of changes in the properties of properly used meters were not observed.

Figure 1 shows the scheme we used for our self-quenching meter. Other similar circuits are possible. Three batteries connected in series served as a source of voltage. The voltage could be varied between 600 and 900 volts by means of a two megohm potentiometer. This interval was sufficient to cover the requirements of all of our light meters. An electrostatic voltmeter was used to measure the working potential. The output terminals of the meter circuit were connected either to an oscillograph or to a counting circuit. The magnitude of the pulses put out by the meter circuit was of the order of one volt.

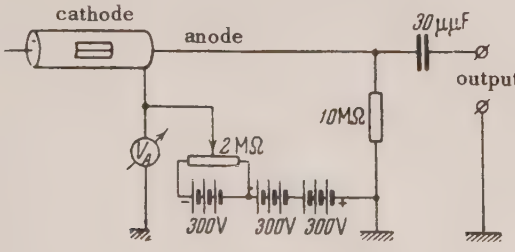

Fig. 1. Circuit diagram of the meter

2. The meter is of cylindrical form. The body consists of a tube, the mid part of which is made of quartz and the ends of molybdenum glass. The two are joined together by means of transition glass. The cathode material is chosen to satisfy the spectral requirements of the meter. We used platinum, aluminum and magnesium. The tube is filled with 85% argon and 15% methyl or ethyl vapor to a pressure of 65 to 70 mm of Hg. The entire tube is then encased in a metal setting and provided with a two prong socket.

3. The magnitude that correctly and uniquely describes the light sensitivity of the meter is the ratio of the number of impulses in the meter circuit produced by the incident light to the corresponding number of photons. This magnitude ϵ_λ is given by

$$\epsilon_\lambda = n_\lambda / N_\lambda \qquad (1)$$

where N_λ is the intensity of light in quanta per second, that is, the number of quanta of a given wavelength that pass through the cell window per second, and n_λ is the difference in the number of pulses per second when light shines on the meter and the number of pulses per second in the dark (due to background radiation). The magnitude ϵ_λ may be identified as a measure of photoelectric emission only if the meter is 100% efficient, that is, if each photoelectron is counted.

The magnitude ϵ_λ will now on be called the *spectral sensitivity* of the meter. The determination of ϵ_λ in absolute units depends on the determination of N_λ, a difficult measurement, particularly

[1] S. F. Rodionov and A. I. Shal'nikov, J. Exper. Theoret. Phys. USSR 5, 160 (1935)

[2] H. F. Neuert and K. A. Lauterjung, Reichber Phys. 1 17, (1944)

in the ultraviolet region. It is not convenient in this connection to use light sources of known spectral energy distribution (such as models of black body radiators, or incandescent lamps), because the changes in the emission characteristics of ordinarily used emitters (tungsten, for example) leads to large and unknown errors, particularly in the ultraviolet and infrared regions. To test the sensitivity of our meters, we used light sources whose spectral characteristics were determined in absolute units by means of sensitive thermal (radiation) detectors. (This method, previously described by one of the authors[3], was reconfirmed in the present work.) Then, with the same experimental arrangement and a fixed attenuation of the source, the meter was substituted for the thermoreceptor and its sensitivity in the corresponding spectral region was measured.

As a source of light we used a 25 watt hydrogen tube especially prepared for us. In some measurements we also used the Mercury-Argon tube PRK-2. The optical system consisted of a double quartz monochromator that was built up from two quartz monochromators of equal angular dispersion. The diagram of the optical system is shown in Fig. 2. The light source was placed directly in front of the input slit *I*. The light receptors, the thermal indicator of our meter, was placed after the output slit *III*.

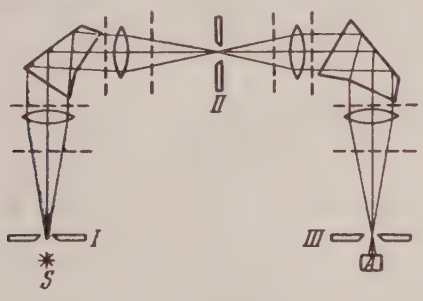

Fig. 2. Schematic diagram of the optical system for the measurement of meter sensitivity.

To determine the absolute intensity of the source, we used calibrated thermoelements and thermopiles with quartz windows followed by photoelectric amplification of the thermocurrent. A similar system has recently been brought to a high state of perfection by Kozyrev[4]. The thermoelement or thermopile was connected to a galvanometer. The light reflected from the mirror of this galvanometer impinges on a compensated photoelectric system having a second galvanometer in its output. The ratio of the current in the second galvanometer to that in the first represents the amplification of the photoelectric-optical system (the current amplification factor). A special check was made of the linear dependence of this ratio on the current in the first galvanometer.

Special measurements were made to ascertain the spectral nonsensitivity of the thermal elements. The results of these measurements are shown in Fig. 3. This figure represents, in rela-

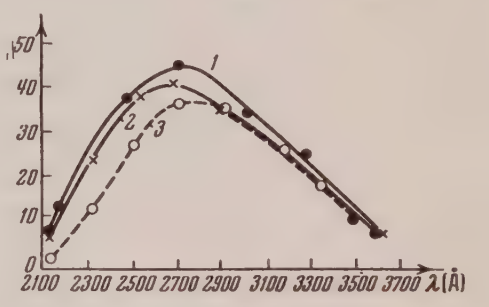

Fig. 3. Energy distribution in the hydrogen spectrum.

tive units, the energy spectrum of the hydrogen tube, measured under similar conditions, using as receptor *1)* the thermopile FAI, *2)* the Kipp thermopile and *3)* the thermoelement LETI[4]. As is seen from the diagram, the third receptor proved selective because, as was shown later, its surface blackening was defective (the reflection coefficient in the region 2100 to 2900 Å was too large). The coincidence of the curves obtained from the first two receptors was checked by means of controlled measurements on their surface reflectivities. The results fully justified the interchange of data obtained by means of the first two receptors.

Table 1 represents a summary of the data on the distribution of energy in the hydrogen spectrum in absolute units. These were obtained with the aid of the photo-optical amplifier.

If n_T is the current measured by the second galvanometer in the photo-optical system (expressed in scale divisions); I_λ the light intensity in ergs per second that emerges from the slit system *I, II, III*; $d_I = d_{II} = 0.2$ mm and $d_{III} = 0.4$ mm; it follows that:

$$I_\lambda = n_T (R_T + R_r) \alpha / \beta\gamma \qquad (2)$$

where α = the sensitivity of the first galvanometer

[3] S. F. Rodionov, J. Exper. Theoret. Phys. USSR 10, 294 (1940)

[4] B. M. Kozyrev, Usp. Fiz. Nauk 44, 173 (1951)

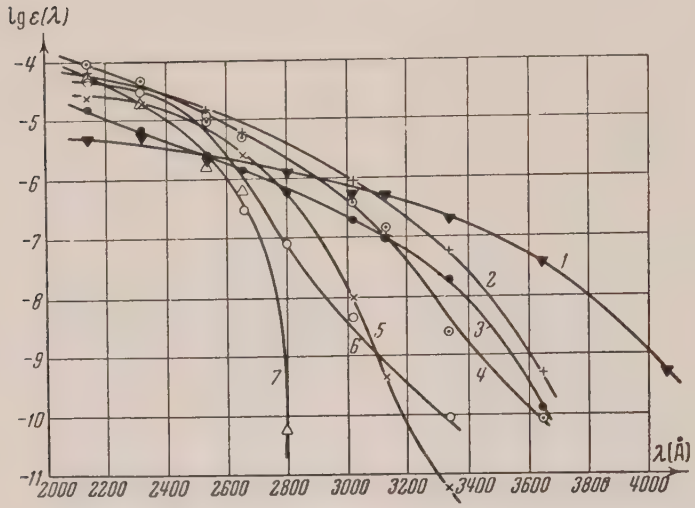

Fig. 4. Spectral sensitivity of self-quenching light meters. *1* – M-1, *2* – A-4, *3* – A-3, *4* – A-6, *5* – P-6, *6* – P-7, *7* – P-10.

TABLE I. Current in the tube was 25 ma

λ in Å	n_T in scale divisions	I_λ ergs/second	$N_\lambda \times 10^{-10}$ quanta/second
2145	11	0.123	1.32
2318	43	0.480	5.60
2537	76	0.850	10.80
2655	82	0.920	12.20
2803	80	0.842	12.60
3022	64	0.715	10.80
3130	52	0.580	9.07
3340	32	0.358	6.20
3650	12	0.134	2.43
4000	8	0.089	1.78

β = the current amplification of the photo-optical system

R_T = the resistance of the thermopile or the thermoelement

R_r = the internal resistance of the first galvanometer

γ = the sensitivity of the thermopile or thermoelement in volts/erg.

The constants for one of our systems, using the FAI thermopile, are: $\alpha = 0.5 \times 10^{-3}$ amperes per scale division, $\beta = 580.5$, $R_T = 30$ ohms, $R_r = 35$ ohms and $\gamma = 10^{-3}$ volts per erg.

Having ascertained in absolute units the energy distribution of our source, we could then attenuate it a known amount and measure it with our meter. That is, we could establish the value of ϵ_λ in Eq. (1).

As light attenuators we used thin metal screens (mesh), whose attenuation was measured very carefully. They were placed in the optical system so that the width of the light beam was considerably larger than the cell size of the screen (see Fig. 2). Such neutral attenuators, as was previously shown[3], give excellent results. In this way we established the linearity of our meter (that is, the dependence of n_λ on light intensity) to a sufficiently high degree.

The spectral characteristics of our self-quenching meters with photocathodes of different metals are shown in Fig. 4, where we plot Log ϵ_λ vs. λ in Å.

The use of platinum cathodes (meters P-6, P-7 and P-10), aluminum cathodes (meters A-3, A-4 and A-6) and magnesium cathodes (meter M-1), allow, as is seen from Fig. 4, the rather sharp separation of three spectral regions, 2100 to 2800 Å, 2100 to 3500 Å and 2100 to 4000 Å, where it is particularly convenient to use the meters of the described type as integrating photometers. The results shown in Fig. 4 indicate that the sensitivity of the tested meters compare well with previous measurements[3] and are normal for the photoeffect from clean metal surfaces. At the wavelength of 2000 Å, this sensitivity is of the order 10^{-4} electrons per quantum or about 7×10^{-5} coulombs per calorie.

The typical working characteristics of self-quenching light meters are shown in Fig. 5. The lower curve corresponds to the dark background activity, the upper curve was obtained with some illumination. There is a good plateau over the range of about 100 volts.

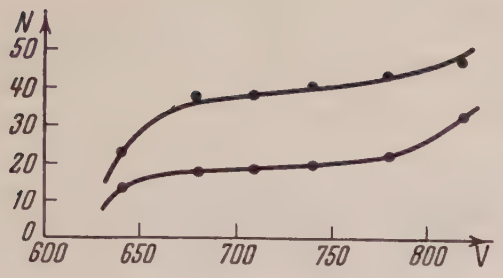

Fig. 5. Working characteristics of the meter.

The dark background count of different meters varies between 3 and 15 counts per minute. The magnitude of this background activity depends, of course, on the size of the meter. If the working volume of the meter is a cylinder 1.0 cm in diameter, 2.5 cm high, the background count is about 9 pulses per minute.

In this study we did not undertake the detailed study of self-quenching light meters. One may expect that the meters described in this paper will have characteristics similar to those of ordinary self-quenching meters of the type used in measuring hard radiation.

Some of our meters that have been in use for a long time already show signs of aging and fatigue, due no doubt to the exhaustion of the quenching components of the gas mixture. It may also be that the photocell itself shows the effects of aging.

Unfortunately, our experience to date is not enough for a more detailed judgement. We hope to return to this subject when more experience is gathered on the utilization of the self-quenching light meters.

The design and construction of the self- quenching meters was done at the Institute for Physical Problems, Academy of Science of the USSR, by A. I. Shal'nikov and M. S. Khaikin. The measurements of the spectral sensitivity of the meters were done at the Institute of Physics, Leningrad State University, by F. Rodionov.

Translated by M. M. Kessler
32

Additional footnote:

S. F. Rodionov and E. N. Pavlova, Doklady Akad. Nauk SSSR 79, 961 (1951)

Scattering of Mesons by Nucleons in the Theory of Radiation Damping

A. S. MARTYNOV
P. N. Lebedev Physical Institute, Academy of Sciences, USSR

(Submitted to JETP editor March 9, 1954)
J. Exper. Theoret. Phys. USSR **28**, 287-290 (March, 1955)

When radiation damping is taken into account, a qualitative improvement is obtained in the picture given by perturbation theory in the lowest nonvanishing order (the appearance of characteristic maxima in the energy dependence of total cross sections, etc.). However quantitative agreement with experiment is still lacking.

EXPERIMENTALLY, scattering of mesons by nucleons has been studied by various methods [1-3] (see also review article of Silin and Fainberg[4]) Mesons of bombarding energies from 35 to 230 MeV have been considered. We shall not enter into the well known results of these investigations, but will only point out two characteristic features, namely, that at low energies (E_μ = 35 MeV) the following relation is satisfied by the cross sections:

$$\sigma^{(\alpha)} : \sigma^{(\gamma)} : \sigma^{(\beta)} \approx 2 : 1 : 1; \quad \sigma^{(\gamma)} \approx \sigma^{(\beta)},$$

whereas at higher energies (E_μ = 120 MeV) this relation takes the form:

$$\sigma^{(\alpha)} : \sigma^{(\gamma)} : \sigma^{(\beta)} \approx 9 : 2 : 1.$$

Here $\sigma^{(\alpha)}, \sigma^{(\beta)}, \sigma^{(\gamma)}$, represent cross sections for the following processes, respectively,

$$\pi^+ + p \to \pi^+ + p, \qquad (\alpha)$$

$$\pi^- + p \to \pi^- + p, \qquad (\beta)$$

$$\pi^- + p \to \pi^0 + n. \qquad (\gamma)$$

There are known in literature various attempts at theoretical explanation of the data on scattering of mesons by nucleons[4]. In the article Biswas[5], the conclusion is reached that, by taking into account radiation damping, a picture is obtained for the scattering of mesons by protons that is close to experiment. We show below that this conclusion is wrong. The results of Biswas are essentially based on conclusions reached in the works of Cornaldesi and Field [6,7] where errors were comitted in performing the reduction over spin states (when deriving the differential cross section). As a result of these errors pseudoscalar coupling led to an increase of the total scattering cross section with an increase in the energy E_μ of the bombarding meson. This contradicts the results of numerous other investigations.

In the present work use is made of the theory of radiation damping in a covariant form. All calculations are performed according to the perfected methods of perturbation theory [8-11]; a pseudoscalar meson field is chosen and the coupling between the meson field and the nucleon is taken to be a linear combination of pseudoscalar and pseudovector couplings.

To calculate the radiation damping (which is the purpose of this work) one must solve the integral equation which defines the scattering matrix R:

$$R = K - (i/2)\,KR. \qquad (1)$$

Equation (1) follows from

$$S = 1 - iR, \quad S = \left(1 - \frac{i}{2}K\right) \Big/ \left(1 + \frac{i}{2}K\right),$$

where $S = 1 + \sum_{n=1}^{\infty} S_n$ is the unitary collision matrix, $K = \sum_{n=0}^{\infty} K_n$ is a hermitian operator (see Schwinger [12]).

[1] H. L. Anderson, E. Fermi, R. Martin, and D.E. Nagle, Phys. Rev. **91**, 155 (1953)

[2] C. E. Angell and J. P. Perry, Phys. Rev. **90**, 724 (1953)

[3] A. Roberts and J. Tinlot, Phys. Rev. **90**, 951 (1953)

[4] V. P. Silin and V. Ia. Fainberg, Usp. Fiz. Nauk **50**, 325 (1953)

[5] S. N. Biswas, Ind. Journ. Phys. **26**, 617 (1953)

[6] E. Corinaldesi and G. Field, Phil. Mag. **40**, 1159 (1949)

[7] E. Corinaldesi and G. Field, Phil. Mag. **41**, 364 (1949)

[8] J. Pirenne, Phys. Rev. **86**, 395 (1952)

[9] N. Fukuda and T. Mijazina, Prog. Theor. Phys. **5**, 849 (1950)

[10] F. Dyson, Phys. Rev. **75**, 1736 (1949)

[11] R. P. Feynman, Phys. Rev. **76**, 749 (1949)

[12] J. Schwinger, Phys. Rev. **74**, 1439 (1948)

We solve Eq. (1) in the lowest nonvanishing order of approximation for second order processes (scattering processes), i.e.,the equation

$$R_2 = K_2 - (i/2)\,K_2 R_2, \qquad (2)$$

where K_2 is the first nonvanishing term in the expansion of K. In the second term on the right hand side of Eq. (2) a sum over all intermediate states of the same energy and charge is understood.

To obtain the scattering amplitude one needs a clear picture of K_2. It is known[8] that $K_2 = iS_2$; thus, given the matrix elements of S_2, we can obtain those of K_2.

As is well known one obtains from Eq. (2) an integral equation containing a nonseparable kernel which leads to well known difficulties in obtaining a solution. However, taking advantage of the smallness of certain quantities (for example the quantity $x_1 = 2l^2/(2E\epsilon - \mu^2)$; for $E_\mu \lesssim 180$ MeV we have $x_1 \leq 1/8$), one can obtain an approximate integral equation with a separable kernel. For process (α) this equation is:

$$X_{fi}(\theta) = \frac{f^2}{\mu^2} M \Big\{ \Big[(G_1' - x_1\cos\theta)\Big(\frac{W}{M}\gamma_4 - 1\Big) - 2(\Gamma y + 1)(1 + x_1\cos\theta)\Big](1 - x_1\cos\theta) - i\omega \int_0^\pi \Big[(G_1' - x_1\cos\theta\cos\theta')\Big(\frac{W}{M}\gamma_4 - 1\Big) - 2(\Gamma y + 1)(1 + x_1\cos\theta\cos\theta')\Big] (E\gamma_4 + M) X_{fi}(\theta')\sin\theta' d\theta' \Big\} \qquad (3)$$

where l = momentum of the meson or nucleon in the center of mass system; μ, M the masses of meson and nucleon; ϵ, E total energies of meson and nucleon; g, f pseudoscalar and pseudovector coupling constants, respectively,

$$h = c = 1;\quad G_1' = f(E, \varepsilon, l);$$

$$\Gamma = \frac{\mu}{M};\quad y = -\frac{g}{f};$$

$$W = E + \varepsilon;\quad \omega = \frac{l}{8\pi W}.$$

Equation (3) is reduced by standard methods to a system of two algebraic equations. The matrices γ_μ are assumed to be numbers close to unity. The solution of Eq. (3) has the following form:

$$X_{fi}(\theta) = \frac{f^2}{\mu^2} M \Big\{ \Big[f_1(\theta) + \frac{A + iB}{L + iM} + \frac{A_1 + iB_1}{L_1 + iM_1}\cos\theta \Big] + \Big[f_2(\theta) + \frac{C + iD}{L + iM} + \frac{C_1 + iD_1}{L_1 + iM_1}\cos\theta \Big]\gamma_4 \Big\}, \qquad (4)$$

where $f_1(\theta) = \alpha_3 + \beta_3\cos\theta + \bar{\gamma}_3\cos^2\theta$;

$f_2(\theta) = \alpha_4 + \beta_4\cos\theta + \bar{\gamma}_4\cos^2\theta$,

and A, B,.. $\bar{\gamma}_3$, $\bar{\gamma}_4$ are expressions depending on $E, \epsilon, l, y, \omega, f^2$.

The integral equations for processes (β) and (γ) reduce to a system of four algebraic equations; the solutions are similar to (4). The differential scattering cross section, for process (α),for example,looks as follows in the center of mass system:

$$\frac{d\sigma^{(\alpha)}}{d\Omega} = \frac{1}{2}\frac{M^2}{W^2}|X_{fi}(\theta)|^2.$$

Since the resulting expression for the differential scattering cross section is very cumbersome, we do not write it out in full.

For purposes of numerical calculations we write the differential scattering cross sections as follows:

$$d\sigma^{(\alpha)}/d\Omega = \varkappa(\bar{A}_1 + \bar{B}_1\cos\theta + \bar{C}_1\cos^2\theta + \bar{D}_1\cos^3\theta + \bar{E}_1\cos^4\theta + \bar{F}_1\cos^5\theta); \qquad (5)$$

$$d\sigma^{(\beta)}/d\Omega = \varkappa(\bar{A}_2 + \bar{B}_2\cos\theta);$$

$$d\sigma^{(\gamma)}/d\Omega = \varkappa(\bar{A}_3 + \bar{B}_3\cos\theta + \bar{C}_3\cos^2\theta + \bar{D}_3\cos^3\theta + \bar{E}_3\cos^4\theta + \bar{F}_3\cos^5\theta),$$

where

$$\varkappa = 2\pi f^4\Big(\frac{h}{\mu c}\Big)^2\frac{M^2}{W^2}\frac{x\gamma}{2};\quad x = \frac{E}{\mu};\quad \gamma = \frac{M}{\mu},$$

and $\bar{A}_1 = A_1 + A_1^I$,...; $\bar{F}_3 = F_3 + F_3^I$.

Here, the first term in $\bar{A}_1,\ldots,\bar{F}_3$ is obtained by neglecting radiation damping, the second being the correction due to the damping.

Differential cross sections were computed for two energies E_μ -- 42 and 112 MeV -- of the bombarding meson in the laboratory coordinate system. Numerical estimates have shown that the coefficients C_1, D_1, E_1, F_1, B_2, E_3, F_3 are small in comcomparison with A_1, B_1, A_2, A_3, B_3, C_3. Assuming that at low energies ($E_\mu = 42$ MeV) the influence of radiation damping is small, and comparing

numerical data with those of other authors[1-3] we obtain in an unique way the constants y and f^2.

The numerical data indicate that values $y < 0$ are unacceptable, because they do not lead to values of $\sigma^{(\alpha)}/\sigma^{(\beta)}$ as given by experiments[2,3]. The calculation gives $\sigma^{(\alpha)}/\sigma^{(\beta)} > 1$ for $E_\mu = 42$ MeV, whereas the experimental value is of the order of ½; in addition, $d\sigma^{(\alpha)}/d\Omega$ shows a sharp forward directionality for $y < 0$. It also follows from the numerical data that $y = 10$ and 3 are inadmissible values: for these values of y, the total scattering cross sections increase with the energy of the bombarding mesons more slowly than the experiments indicate [1-3]. Using the value $y = 1.5$, we get satisfactory agreement with the experimental value of $\sigma^{(\alpha)}/(\sigma^{(\beta)} + \sigma^{(\gamma)})$, namely: $\sigma^{(\alpha)}/(\sigma^{(\beta)} + \sigma^{(\gamma)}) \approx 1$; $\sigma^{(\beta)} \gtrsim \sigma^{(\gamma)}$.

As far as angular distributions are concerned, one finds that with $y = 1.5$, $E_\mu = 42$ MeV, $d\sigma^{(\alpha)}/d\Omega$ indicates that the mesons are scattered predominantly in the backward direction, $d\sigma^{(\beta)}/d\Omega$ indicates an isotropic distribution, and $d\sigma^{(\gamma)}/d\Omega$ indicates that the mesons are scattered in a backward direction, in the center of mass system. At low energies angular distributions have not been directly measured and therefore it is not clear whether the above results contradict experiment or not. However the few investigations [2,3] (see review article, reference 4) indicate that in the energy region $E_\mu = 30$ MeV, and for small angles, the interference between nuclear and electromagnetic interactions must be considered.

The results obtained for angular distributions for $E_\mu = 42$ MeV are qualitatively valid also for $E_\mu = 112$ MeV (disregarding damping). In this case the coefficient C_1 in $d\sigma^{(\alpha)}/d\Omega$ is relatively small, although the angular distribution indicates a backward directionality.

We note that the relation between the coefficients A_3, B_3, C_3, in Eq. (5) for $d\sigma^{(\gamma)}/d\Omega$ ($A_3 < B_3 < C_3$) is the opposite of that for $d\sigma^{(\alpha)}/d\Omega$, i.e., closer to the experimental results. Furthermore, the calculated $d\sigma^{(\beta)}/d\Omega$ disagrees with the angular distribution of π^- - mesons as given by experiments: π^- - mesons are scattered mostly forward. Also, the calculated value of $\sigma^{(\alpha)}/(\sigma^{(\beta)} + \sigma^{(\gamma)})$ disagrees with the experimental value.

Using the best values of the constants: $y = 1.5$, $f^2 = 0.51$, one can compute the coefficients A_1^r, ..., F_3^r, which account for the damping. The corrections due to the damping turn out to be of the order of a few percent; hence it is clear that they cannot change the relation $\sigma^{(\alpha)}/(\sigma^{(\beta)} + \sigma^{(\gamma)}) < 1$ which we obtain for $E_\mu = 112$ MeV and $y = 1.5$, and therefore cannot explain the experimental relation $\sigma^{(\alpha)}/(\sigma^{(\beta)} + \sigma^{(\gamma)}) \approx 3$ for $E_\mu = 120$ MeV. We therefore deduce that quantum theory of radiation damping in the above treated approximation does not lead to quantitative agreement with experiment, although it does predict certain qualitative features (for example, the passage of the total cross section through a maximum, etc.).

The author wishes to thank Professor M. A. Markov and A. M. Baldin for continuous help and interest in this work and also I. A. Lebedev and L. Ia. Zhil'tsov for performing the numerical calculations.

Note added in proof: Analogous results are obtained in the recently published paper by Zharkov[13], where the same problem is treated by different mathematical methods.

[13] G. F. Zharkov, J. Exper. Theoret. Phys. USSR 27, 296 (1954)

Translated by A: M. Bincer
49

SOVIET PHYSICS-JETP VOLUME 1, NUMBER 1 JULY, 1955

Dependence of the Electrical Conductivity and Electron Emission on the Energy of a Metal in the Process of its Heating by a Current of High Density

L. N. Borodovskaia and S. V. Lebedev
P. N. Lebedev Physical Institute, Academy of Sciences, USSR
(Submitted to JETP editor August 1, 1953)
J. Exper. Theoret. Phys. USSR 28, 96-110 (January, 1955)

Upon heating of nickel wires by a current of 6×10^4 - 5×10^6 A/cm^2 phenomena were discovered which were of the same nature as those previously observed in tungsten [1-3]. Moreover, upon investigation of the dependence of the wire resistance R on the introduced energy E, discontinuities were discovered in the curve $R = R(E)$. The location of these with respect to resistance and energy does not change with a change in density of the heating current (Ni, W, Au, constantan). An investigation of emission showed that an anomalously high emission from unbroken wires can drop even if the rate of energy arrival in the wires exceeds the energy losses at melting point temperature in the case of stationary heating. Data are supplied, characterizing the speed of emission decay after interruption of the heating current.

IN the experiments considered below, the previously applied method [1-3] of recording and compilation of oscillograms was improved, thus increasing the accuracy of the data obtained.

We recall that $V_R(t) = i(t)R(t)$ - the voltage on the examined wire and $V_r(t) = i(t)r$ - the voltage at constant resistance r permit us to find the current $i(t) = V_r(t)/r$, the resistance of the examined wire $R(t) = [V_R(t)/V_r(t)]r$ and the energy entering in the time t

$$E(t) = \frac{1}{r}\int_{t_1}^{t} V_R(t)\, V_r(t)\, dt,$$

where t_1 is the time of switching on of the heating current i. It is assumed that the rate of energy arrival considerably exceeds its losses $i^2 \gg i_m^2$ (i_m is the maximum current, which the examined wire withstands on steady-state heating, i. e., the current which compensates for maximum losses). For nickel of 0.015 cm diameter in vacuum i_m = 1A, in air i_m = 3A.

Experiments on emission measurements were made according to the scheme shown in Fig. 1. The anode current I_a from the examined wire was determined from the oscillograms of the voltage $V_\rho(t) = \rho_a I_a(t)$, decreasing at a constant resistance ρ_a.

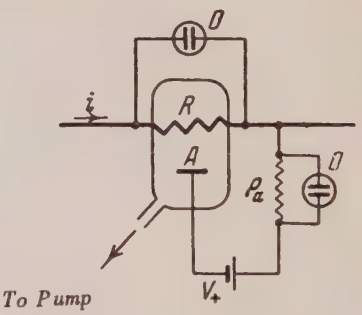

Fig. 1. Schematic of emission measurements. R - examined wire, A - anode, V_+ - anode battery, ρ_a - a constant resistance, O - oscillograph.

1. DEPENDENCE OF THE RESISTANCE ON ENERGY

Nickel wires were heated in transformer oil, air or vacuum by current pulses of high density. Qualitatively, the shape of the oscillograms $V_R(t) = i(t)R(t)$ obtained here, coincides with corresponding oscillograms taken on tungsten (Fig. 2). The presence of a region of small dR/dE followed by a jump R at the moment t_c - an explosion- is characteristic for these oscillograms (in our oscillograms a small dR/dE corresponds to a small dV_R/dt and a jump R corresponds to a jump V_R). Breaks in the oscillogram* as shown in Fig. 2 are designated by the numbers *1, 2, 3, 4, 5* and

[1] S. V. Lebedev and S. E. Khaikin, J. Exper. Theoret. Phys. USSR 26, 629 (1954)

[2] S. V. Lebedev and S. E. Khaikin, J. Exper. Theoret. Phys. USSR 26, 723 (1954)

[3] S. V. Lebedev, J. Exper. Theoret. Phys. USSR 27, 605 (1954)

* The presence of sharp breaks in the oscillograms $V_R(t)$ shows that the changes dR/dt take place simultaneously through the whole volume of the wire or, in any case, in the major part of its volume. Therefore, the oscillograms characterize a change in the specific resistance of the metal under investigation.

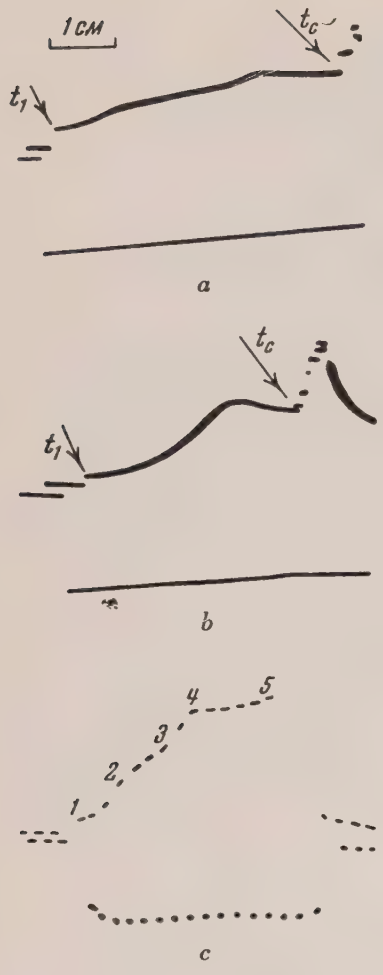

Fig. 2. Oscillograms $V_R(t) = R(t)i(t)$ (top curves) and $V_r(t) = ri(t)$ (bottom curves) for wires of length l and diameter d in oil.

a - Nickel: $d = 0.008$ cm; $l = 1.1$ cm; $j(t_1) = 10^6$ A/cm^2; $r = 2\Omega$, sensitivity of the oscillograph $a = 75$ V/cm ($a_R \sim a_r = a$), time scale $b = 7.9 \times 10^{-5}$ sec/cm.
b - Tungsten: $d = 0.006$ cm; $l = 0.46$ cm; $j(t_1) = 1.8 \times 10^6$ A/cm^2; $r = 2\Omega$; $a = 75$ V/cm; $b = 7.9 \times 10^{-5}$ sec/cm.
c - Nickel: $d = 0.015$ cm; $l = 2.15$ cm; $j = 5 \times 10^6$ A/cm^2; $r = 0.5\Omega$; the time markings are made with a frequency $\nu = 7.7 \times 10^{-5}$ sec^{-1}. At the start of the photograph $a_R = 470$ and $a_r = 425$ V/cm, at the end $a_R = 440$ and $a_r = 385$ V/cm. The zero lines are parallel straight lines forming a continuation of horizontal segments at the start of the oscillograms.

In tests 2c; 3a; 3b; 3c, the zero lines for $V_r(t)$ also go through a horizontal part at the end of the oscillogram $V_r(t)$ [the end of the oscillograms $V_R(t)$ in these tests is above the zero line].

they correspond to time intervals t_c, t_2, t_3, t_4, t_5. The Figure 5 (or t_5) marks the moment preceding t_c in cases where the jump R is not visible or not clearly expressed. The character of the change in the shape of the oscillograms of nickel and tungsten as a function of a change in current density is the same: the ratio of the time interval $t_c - t_4$, during which dR/dE is small, and the total heating time $t_c - t_1$ decreases with a decrease in current density j (Fig. 3). When j decreases below 2×10^5 A/cm^2 in the oscillograms for nickel (Figs. 3*d*, 3*e*) the region of small dR/dE is not visible. Unlike the region $t > t_4$, the dependence of R on E in the region $t < t_4$ is not altered by a change of j from 6×10^4 to 5×10^6 A/cm^2.

A break in the curve $R(E)$ can also be seen in oscillograms for nickel as well as at point *4* at point *3*. Up to this point no peculiarities in the dependence of R on E can be seen, while $R(t_3) = R_3 \approx R^s_{mp}$ and $E(t_3) = E_3 \approx W_h$, i. e., the values of resistance and energy in point *3* are such as would normally correspond to a start of fusion (R^s_{mp} and R^l_{mp} are the resistances of the wires at the melting point temperature in the solid and in the liquid state, W_h - the energy to heat it to melting point temperature, W_{fus} the heat of fusion). The energy entering the wire in the time interval $t_4 - t_3$ is approximatley equal to W_{fus}, but the change in resistance during the transition from point *3* to point *4*, R_4/R_3, is found to be smaller than the tabulated value[4] of R^l_{mp}/R^s_{mp}. Actually, according to tabulated data for nickel wire of 0.015 cm diameter, per centimeter length, $W_H = 1.39$ joule, $W_{fus} = 0.46$ joule, $R^l_{mp}/R^s_{mp} = 1.94$ (the value $R^l_{mp}/R^s_{mp} = 1.94$ is quoted in reference 4 on p. 295. Data on the resistance of liquid nickel are shown below in Table 2. Values of W_H and W_{fus} are taken from Seitz[5], p. 30, and reference 6, v. 1, p. 129. But, according to data obtained in our experiments,

[4] Encyclopedia of Metalphysics, edited by Masing, v. 1., Moscow, 1937

[5] F. Seitz, *Modern Theory of Solid State*

[6] *Technical Encyclopedia*, Tables of phys. - chem. and technological data, Moscow, (1931)

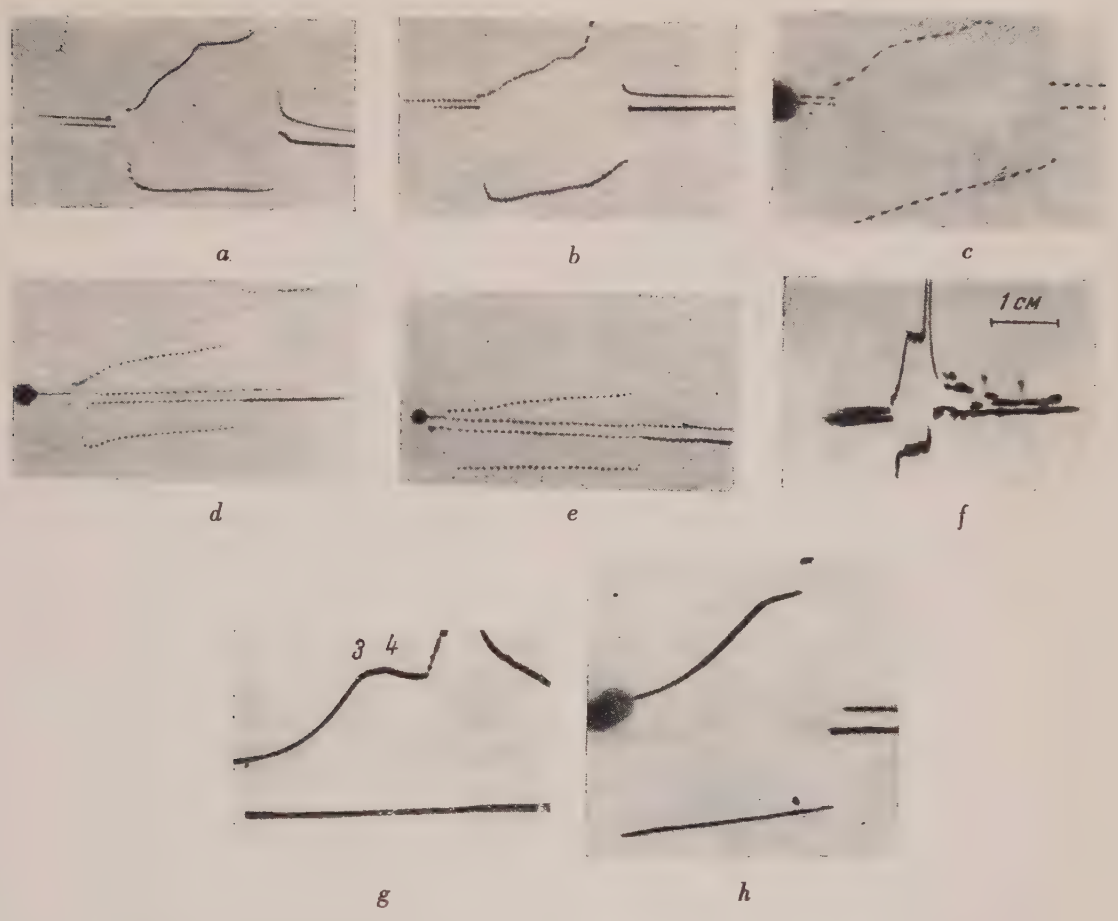

Fig. 3. Oscillograms $V_R(t)$ (upper curves) and $V_r(t)$ (bottom curves) for nickel and tungsten.

a - Nickel: $j = 5 \times 10^6$ in oil ($d = 0.015$; $l = 1.8$; $r = 0.5$; $a = 560$; $b = 2.6 \times 10^{-5}$).

b - Nickel: $j = 2 \times 10^6$ in oil ($d = 0.015$; $l = 2.35$; $r = 2$; $a = 160$, $\nu = 2.6 \times 10^5$).

c - Nickel: $j = 7.10^5$ in oil ($d = 0.015$; $l = 2.85$; $r = 1.22$; $a = 117$; $\nu = 2 \times 10^4$)

d - Nickel: $j = 2 \times 10^5$ in air ($d = 0.015$; $l = 2.85$; $r = 0.72$; $a = 64$; $\nu = 5 \times 10^3$).

e - Nickel: $j = 6 \times 10^4$ in air ($d = 0.015$; $l = 5.25$; $r = 2$; $a = 50$; $\nu = 5 \times 10^2$).

f - Tungsten: $j = 7 \times 10^6$ in water ($d = 0.0077$; $l = 0.75$; $r = 0.225$; $a_R = 650$; $a_r = 155$; $b = 24.5 \times 10^{-6}$).

g - Tungsten: $j = 1.2 \times 10^6$ in oil ($d = 0.006$; $l = 1.07$; $r = 2$; $a = 110$; $b = 1.2 \times 10^{-5}$).

h - Tungsten: $j = 3.5 \times 10^5$ in oil ($d = 0.006$; $l = 3$; $r = 9.5$; $a = 70$; $b = 9.6 \times 10^{-4}$). j - A/cm^2 - average current density; l and d centimeters; ν - sec^{-1}; r - Ω. a - V/cm and b sec/cm - average value of sensitivity and time scale. In experiments 3d and 3e the zero lines were traced during the writing of the oscillogram. In all other oscillograms the location of the zero lines is explained in the caption of Fig. 2.

$E_3 = 1.40$ joule $\approx W_H$; $E_4 = 1.82$ joule $\approx W_H + W_{fus}$; $R_3 = 0.36 \approx R^s_{mp}$; $R_4 = 0.46$. Consequently $R_4/R_3 = 1.3$ (Table 1). The value of $R^s_{mp} = 0.35$ was obtained at the instant of fusion of the investigated wire on slow heating in vacuum. The suitability of tabulated values of W_H and W_{fus} for the types of nickel used by us can be checked in the following way. In vacuum tests with $j \approx 10^5$ A/cm^2 (Fig. 3*e*, Table 1) the arrival of energy is stopped at the instant t_4, when $E = W_H + W_{fus}$, the wire being completely liquified as a result of the test (being totally converted into little balls). It can be seen directly from this that at the instant t_4, the energy $E = W_H$

$+ W_{fus}$ was actually introduced into the metal. However, the tabulated value * $R^l_{mp}/R^s_{mp} = 1.94$ for normal fusion could not be checked with our method, because on slow heating the wire disintegrates before it has time to melt completely.

The similarity in the behavior of tungsten and nickel is completed by the fact that it is also possible to separate , for tungsten, a region similar to the region (3,4) of nickel. For example, in the experiment with a tungsten wire of 0.006 cm diameter, 1 cm length at $j = 1.2 \times 10^6$ A/cm^2, the oscillogram of which is shown in Fig. 3g, values are obtained for $R_3 = 3.72\,\Omega$; $R_4 = 4.02\,\Omega$; $E_4 - E_3 = 0.15$ joule. On the other hand, it was measured at the instant of fusion of the tested wire upon slow heating in vacuum that $R^s_{mp} = 3.74\,\Omega$ per centimeter length and the tabulated value $W_{fus} = 0.137$ joule per centimeter length. Thus for tungsten too **, $R_3 \approx R^s_{mp}$ and $E_4 - E_3 = W_{fus}$.

The points *3* and *4* can also be seen on the oscillograms of experiments with gold. The measurements in these experiments were less precise than in those made with nickel, but qualitatively the results were the same: the values of R_3, R_4 E_3 and E_4 do not change when the current density is changed from 2.5×10^5 A/cm^2 to 3.6×10^6 A/cm^2 and $E_3 \approx W_H$, $E_4 - E_3 \approx W_{fus}$. The value R_4/R_3 was found in this case to be equal to 1.94, whereas, according to tabulated data for gold, $R^l_{mp}/R^s_{mp} = 2.28$.

The break in the oscillograms $V_R(t)$, observed on nickel at point *2* corresponds to the Curie point and is naturally absent in the case of tungsten and gold.

The results of tests with nickel are shown in Fig. 4. The usual dependence of resistance on the energy for solid and liquid nickel (see reference 4, p. 295) is shown as a solid curve. The dotted line, initially coinciding with the full line, corresponds to data obtained at large j. For current

Table 1*

Nickel, diameter 0.015 cm, length 1 cm

i A	j A/cm^2	$t_2 - t_1$ sec	R_2 Ω	E_2 joule	$t_3 - t_1$ sec	R_3 Ω	E_3 joule	$t_4 - t_1$ sec	R_4 Ω	E_4 joule	$t_5 - t_4$ sec	$E_5 - E_4$ joule	E total joule
900	5×10^6	5×10^{-6}	0.18	0.37	1×10^{-5}	0.35	1.42	1.1×10^{-5}	0.46	1.77	6.5×10^{-6}	1.98	3.75
350	2×10^6	2×10^{-5}	0.17	0.31	5×10^{-5}	0.35	1.30	5.6×10^{-5}	0.48	1.76	1.2×10^{-5}	0.66	2.42
125	7×10^5	1.5×10^{-4}	0.18	0.34	4×10^{-4}	0.35	1.38	5×10^{-4}	0.45	1.77	0.6×10^{-4}	0.27	2.04
42	2×10^5	1.3×10^{-3}	0.20	0.32	4×10^{-3}	0.36	1.46	5×10^{-3}	0.46	1.90	—	—	1.90
17	9×10^4	1.1×10^{-2}	0.20	0.40	2.5×10^{-2}	0.36	1.46	3×10^{-2}	0.48	1.96	—	—	1.96
11	6×10^4	2.5×10^{-2}	0.20	0.38	6×10^{-2}	0.36	1.38	7×10^{-2}	0.42	1.75	—	—	1.75
			0.19 ±0.01	0.36 ±0.03		0.36 ±0.01	1.40 ±0.05		0.46 ±0.02	1.82 ±0.08			

* The value and the density of the current are indicated as an approximation, since the current changed during the experiment (see for example, Fig. 3). In each line are recorded average results of several tests. (The change of α_R, α_r and b throughout the oscillogram was taken into account for the calculations.)

* *Note added in proof:* [see N. P. Mokrovskii and A. R. Regel, Zh. Tekhn. Fiz. 23, 2121 (1953)] A value of $R^l_{mp}/R^s_{mp} = 1.3$ is given for nickel, which is different from the tabulated value[4] $R^l_{mp}/R^s_{mp} = 1.94$ and coincident with the value of R_4/R_3 measured by us.

** *Note added on proof:* If it is assumed that the ratio R_4/R_3 is characteristic for the change in resistance on melting (as it can, seemingly, be concluded for nickel from the values of E_3, E_4, R_3 and their comparison with the data [see N. P. Mokrovskii and A. R. Regel, Zh. Tekhn. Fiz. 23, 2121 (1953)],) we obtain, for tungsten, $R^l_{mp}/R^s_{mp} = 1.08$.

densities from 6×10^4 to 2×10^5 A/cm^2 the graph is valid only for $E \leq W_H + W_{fus}$. [At a current $6 \times 10^4 - 2 \times 10^5$ A/cm^2 in vacuum experiments, the current stops at the instant t_4 ($E_4 \approx W_H + W_{fus}$), which indicates a destruction of the wire. In the case of experiments in air an arc is started between parts of the wire upon destruction, after which the measurements of R and E become unreliable*. The oscillograms of the experiments are the same in air and in vacuum up to the moment of destruction of the wire. The experiments were not conducted in oil at these j, because it was impossible to measure the energy without accounting for the losses**.] The complete dotted curve corresponds to the process up to the instant of explosion for $j = 5 \times 10^6$ A/cm^2. In case of smaller current density the explosion occurs at lower energy.

Let us note that the value of energy at which an explosion takes place for a given j was changing from test to test more than other measured values. Sometimes the region of explosion had the appearance of individual steps, probably corresponding to a non-simultaneous explosion of different segments of the wire.

2. EMISSION

Emission measurements were made on nickel wires with $j = 1 \times 10^5$ A/cm^2, according to the scheme shown in Fig. 1. The anode current I_a, measured by means of oscillograms, and divided by the surface area of the wire S, reaches a magnitude of 1.6×10^{-4} A/cm^2 whereas the normal emission of pure nickel at the melting point temperature $I_{mp} = 3 \times 10^{-6}$ A/cm^2.

The normal emission is calculated by means of the formula

$$I = AT^2 e^{-\phi/kT}$$

with $\phi = 7.4 \times 10^{-12}$ erg, $A = 30$ A/cm^{2}deg^2, $T = 1725^0$K.
Thus I_a/S is fifty times larger than I_{mp}.

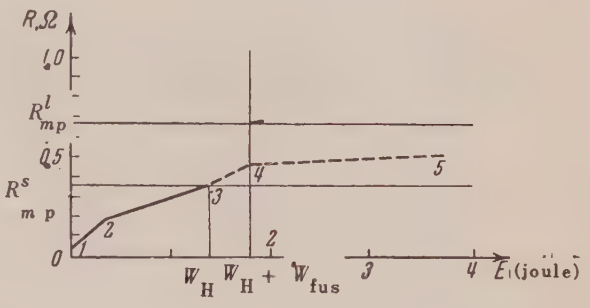

Fig. 4. Comparison of the normal dependence of R on E (solid line) with the dependence between these values at large j (dotted line coinciding with the solid line up to point *3*). The numbers *1*, *2*, *3*, *4*, *5* on the curve mark the same states as on the oscillograms Fig. 2c. Nickel, diameter 0.015 cm length - 1 cm.

The vacuum in these tests was approximately 10^{-6} mm Hg. The wires were degassed at yellow heat for several hours. The lead-in connections and the anode were degassed at red heat. A typical oscillogram of the current I_a under these conditions is shown in Fig. 5*a*. As it can be seen from the oscillograms of Fig. 5, the current I_a, having reached a maximum, decreases, even though the energy of the wire continues to increase. Actually the current $i = 17$ A, while losses at the melting point temperature are compensated by the current $i_m = 1$ A. The interruption of the current i occurred here automatically (because of destruction of the wire) at the moment t_4. The oscillogram $V_R(t)$ shows that the wire is not destroyed up to the instant t_4, and that the drop of I_a with increasing energy takes place in the region *3*, *4*. (The second peak of I_a is related to the destruction of the wire at the instant t_4.)

The magnitude of the current and the character of its dependence on time remain also approximately the same in those cases when the current i is interrupted somewhat before the instant t_4 and the wire is not destroyed. In such cases one can succeed in making several tests with the same small piece of wire. The results of repeated tests are similar. Consequently, the observed drop I_a cannot be explained by the cleaning of the wire surface during the test. In Fig. 5*b* are shown two oscillograms, obtained in repeated tests on the same wire. The reproducibility of the results was

* The electric resistance to breakdown of the gap between the parts of a disintegrating nickel wire is larger in vacuum than in air. The reverse can be observed for tungsten wires of high emission.

** For nickel of 0.015 cm in diameter in oil, $i_m = 6$A, while for $j = 10^5$ A/cm^2, $i = 20$A. While measuring i_m in oil, convection currents were created which changed the cooling conditions of the wire as compared to the conditions in pulsed tests. At low j this circumstance makes it difficult to evaluate energy losses in pulsed tests from the value i_m.

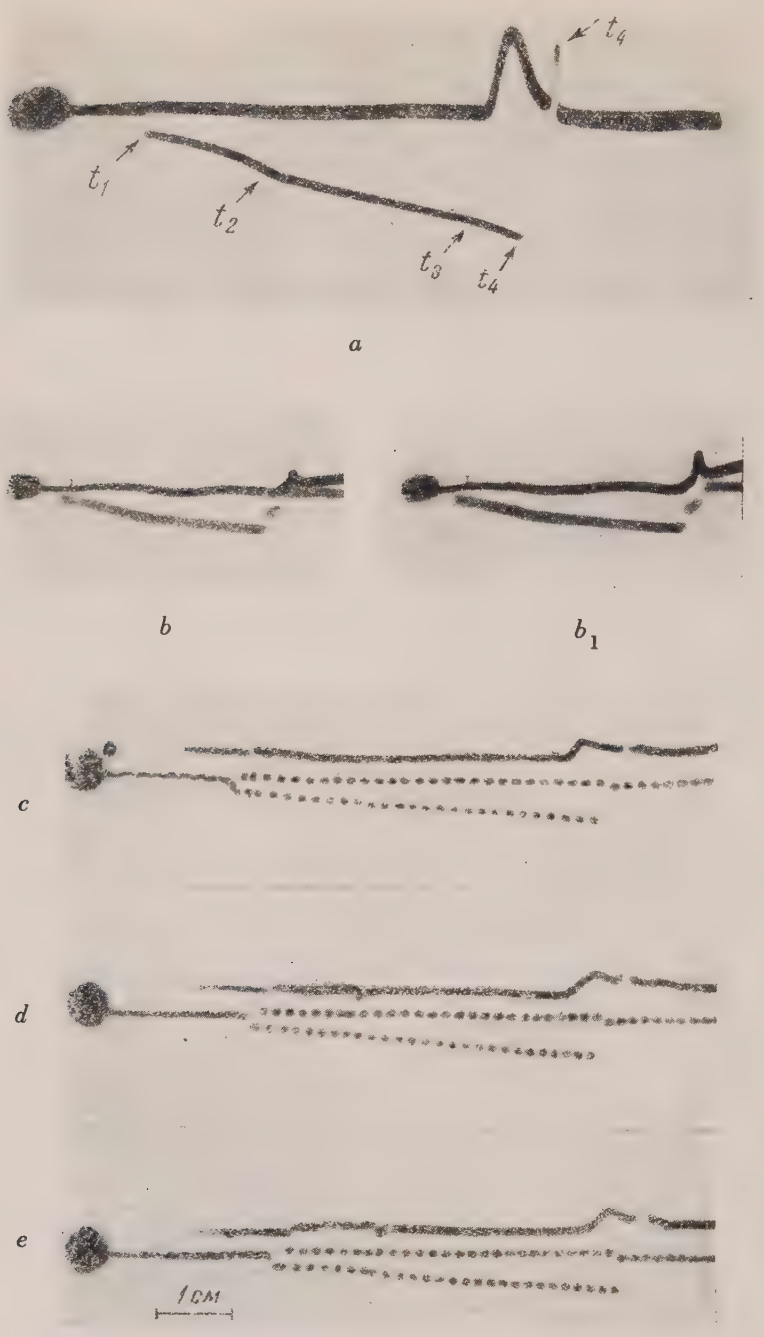

Fig. 5. Oscillograms $V_\rho(t) = \rho_a I_a(t)$ (upper curves) and $V_R(t)$ (lower curves) of nickel wire $d = 0.015$ cm (the upper curves are displaced to the right relative to the lower curves). $j = 10^5$ A/cm^2, j decreasing 3 - 5% from the time of starting t_1 to the instant of interruption t_i. In experiments *c*, *d*, *e*, $l \approx 1$ cm, $V_+ = 70$ V; $\rho_a = 10^6\ \Omega$; $a = 24.5$ V/cm; $\nu = 10^3$ sec^{-1}. In experiments *a*, *c*, *d*, *e*, the wires are destroyed and in experiments *b* and b_1 they are not destroyed. The horizontal part of the oscillograms $V_\rho(t)$ up to the rise coincides with the zero line. In Fig. 5 *a*, *b*, b_1, the zero lines of the oscillograms $V_R(t)$ and $V_\rho(t)$ are almost coinciding straight lines. In Fig. 5, *c*, *d*, *e* the location of the zero lines of the oscillograms $V_R(t)$ is recorded during the photography.

Fig. 6. Oscillograms $V_\rho(t)$ (upper curves) and $V_r(t)$ (lower curves). Tungsten: $d = 0.01$ cm, $r = 2\Omega$; $a = 52$ V/cm; $b = 5.7 \times 10^{-4}$ sec/cm. The wires are not destroyed during the experiment. The configuration of the electrodes in experiments 6 *a*, *b*, *c*, is different. The upper oscillogram is displaced with relation to the lower by 0.3 cm to the left.
a - $i(t_1) = 59$ A; $l = 0.75$ cm; $\rho_a = 200\,\Omega$; $V_+ = 300$ V; $I_a^{max} = 5.7$ A/cm^2;
b - $i(t_1) = 56$ A; $l = 0.2$ cm; $\rho_a = 2600\,\Omega$; $V_+ = 1000$ V; $I_a^{max} = 5$ A/cm^2;
c - $i(t_1) = 63$ A; $l = 0.5$ cm; $\rho_a = 200\,\Omega$; $V_+ = 300$ V; $I_a^{max} = 12.7$ A/cm^2. The zero lines of the oscillograms $V_\rho(t)$ and $V_r(t)$ are parallel straight lines. For $V_\rho(t)$ the zero lines are directed lengthwise along the horizontal segments at the start of the oscillograms $V_\rho(t)$. For $V_r(t)$ the zero lines are about 0.15 cm below the zero lines of the oscillograms $V_\rho(t)$.

also good in tests with destroyed wires. These tests (5 *c*, *d*, *e*) were made under the same conditions, the variation in the value of I_a approximately corresponding to the difference in length of the wire. The drop of I_a with an increase in wire energy also shows that the large value of I_a is not connected with the appearance of a discharge between wire and anode. In fact a discharge could not be extinguished when the energy of the wire was increased, because the conditions for its formation become more and more favorable.

Thus the measured anode current appears to be a current of abnormal emission, the characteristics of which are its large value, and the possibility of a decrease with increasing energy of the metal.

The drop in emission with rising energy is also observed in the case of tungsten, although the emission current density is here several orders of magnitude larger than in nickel. Examples of such tests are shown in Fig. 6 *a* and *c*. In test 6 *a*, the drop of I_a begins at a current value $i = 13$ A, while the current which compensates the losses is $i_m = 3$ A. The areas of the oscillograms marked by arrows correspond to a current I_a^*, limited by space charge (region of validity of the law of Boguslavskii - Langmuir[P]). It was previously clarified that I_a large compared to I_a^* is caused by the state of the cathode and not by secondary currents[7]. Therefore, a drop in I_a indicates a drop in emission.

If emission is determined from the formula $I = A T^2 e^{-\phi/kT}$ large values ($I > I_{mp}$) can be explained by the overheating of the metal above melting point temperature for regular values of A and ϕ or by overheating of the electron gas alone. However, the drop in emission with an increase in the energy of the metal can only be explained by a change of $A = A_0(1 - K)$ and ϕ (which under ordinary circumstances practically do not change with a change of T) or a decrease of the electron

[P] In our experiments with nickel deviations from the law of Boguslavskii - Langmuir cannot be observed, since $I_{mp} < I_a^*$

[7] S. V. Lebedev, J. Exper. Theoret. Phys. USSR 27, 487 (1954)

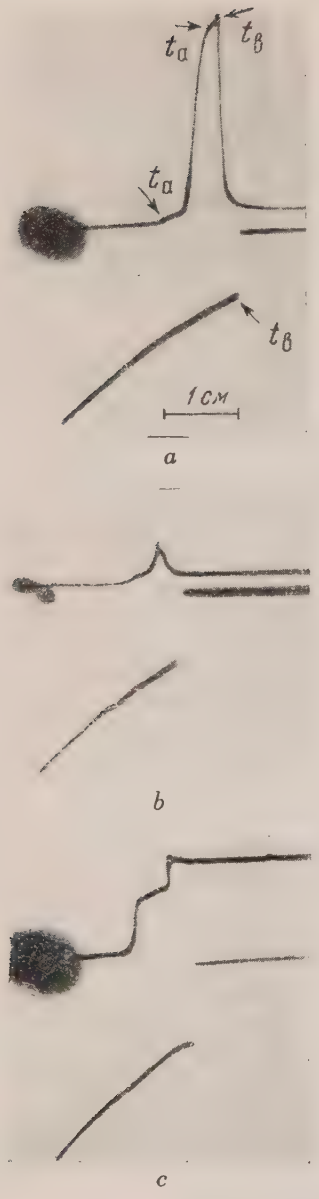

Fig. 7. Oscillograms $V_\rho(t)$ (upper curves) and $V_r(t)$ (lower curves). Tungsten: $d = 0.01$ cm; $l = 0.5$ cm; $i(t_1) = 63$ A; $r = 2\Omega$; $a = 52$ V/cm; $b = 5.7 \times 10^{-4}$ sec/cm. The wires are not destroyed. The configuration of the electrodes is different in experiments *a*, *b*, *c*. The upper oscillogram is displaced with relation to the lower by 0.3 cm to the left.

a - $\rho_a = 500\Omega$; $V_+ = 200$ V; $I_a^{max} = 10$ A/cm^2.
b - $\rho_a = 200\Omega$; $V_+ = 300$ V; $I_a^{max} = 5.3$ A/cm^2.
c - $\rho_a = 7000\Omega$; $V_+ = 200$ V; $I_a^{max} = 0.38$ A/cm^2

The zero lines for $V_\rho(t)$ are straight lines, directed lengthwise along the horizontal segments at the start of the oscillograms $V_\rho(t)$. The zero lines for $V_r(t)$ are straight lines directed along the horizontal segments at the end of the oscillograms $V_r(t)$.

temperature for $i > i_m$. In this manner, if this formula is valid, the experiments under study confirm the assumption that the observed anomalies are caused by a change in the properties of the metal and not by its overheating to a higher than melting point temperature.

The large value of current I_a ($50\, I_{mp}$, $100\, I_{mp}$ [2]) cannot be explained by a small value of the average reflection coefficient $\bar{K}$, and indicates an abnormally low value of the work function ϕ, or an overheating of the electron gas with respect to the lattice. The surplus of electron energy connected with a rise of their temperature above the temperature of the lattice or with their excitation [3] can be sufficient to cause a large increase in emission and, at the same time, be insufficient to lead to a considerable change in the dependence of R on E. Therefore, the absence of noticeable anomalies of the dependence of R on E for $j \leq 5 \times 10^6$ A/cm^2 (part 1) does not disprove the assumption of an energy excess of the electrons. This fact can be cited against the supposition of an overheating of the electron gas, namely, that the abnormal anode current decreases too slowly after the decrease of current i: as was pointed out in reference 7, $I_a > I_a^*$ for $\sim 10^{-5}$ sec after an interruption of the current i.

One can try to explain the drop in emission with the rise in energy by a fusion of the metal, assuming that the emission of the liquid metal is smaller than that of the solid metal at the same temperature*. However, whereas the drop in emission with a rise in energy is observed in experiment 6 *c*, it is not observed in experiment 7 *a*** although the heating current $i(t)$, initially the same in both tests, decreases more steeply in test 6 *c* from a certain moment on. This signifies that, beginning at that instant, the rate of energy intake becomes larger in 7 *a* than in 6 *c*. Therefore the

* *Note added on proof:* It was observed in [see V. G. Bol'shov and L. N. Dobretsov, Doklady Akad. Nauk SSSR 98, 193 (1954)] that the thermal emission current does not show a jump during transition through the melting point.

** In experiment 6 *c*, the drop of I_a is observed at $i \approx 5\, i_m$. In test 7 *a* the drop occurs only after complete interruption of current i.

Table 2

	ρ_{20} Ωcm	$\overset{s}{\rho_{mp}}$ Ωcm	$\overset{l}{\rho_{mp}}$ Ωcm	$\overset{l}{\rho_{1500}}$ Ωcm	Bibliography
Tabulated values for nickel	6.9×10^{-6}	55×10^{-6}	107×10^{-6}	—	[4] p. 295
	6.9×10^{-6}	—	—	109×10^{-6}	[6] v. I, p. 127, 129
	7.24×10^{-6}	—	108×10^{-6}	—	[6] v. IV, p. 335
	8.7×10^{-6}	—	—	—	[8] p. 86
Our wire * Diameter 0.015 cm	8.5×10^{-6}	63×10^{-6}	—	—	Measured under usual conditions
	ρ_1 Ωcm	ρ_3 Ωcm	ρ_4 Ωcm		
Our wire ** Diameter 0.015 cm	—	64×10^{-6}	81.5×10^{-6}		Measured at large j's
		$\pm2\times10^{-6}$	$\pm4\times10^{-6}$		

*All data, given in the present paper (except experiment 2*a*) were obtained on this type of nickel.

** The start of the oscillogram is distorted.

[8] Espe and Knoll, *Technology of Electro-vacuum Materials*, Moscow (1939)

melting in 7*a* must occur earlier than in 6*c*, and the drop in anode current caused by it should have been observed in 7*a* even before the time of interruption of the current *i*. (It must also be remembered that in 7*a*, as well as in 6*c*, the wire remains intact after the end of the experiment.)

The oscillograms of Fig. 7*a*, *b*, *c* show that the drop in anode current $|dI_a/dt|$ after interruption of the current is the faster, the larger I_a/I_a^*. For example it can be seen in Fig. 7*a* that $|dI_a/dt|$ decreases when I_a/I_a^* is approaching unity. The same can be seen by comparing various oscillograms: in test 7*a* at $I_a^{max}/I_a^* = 30$, I_a drops almost by a factor of 30 in a time interval not exceeding 2×10^{-4} sec, whereas in test 7*c* with $I_a^{max}/I_a^* = 1.5$, a drop in I_a is almost unnoticeable.

The character of the dependence of the decrease of I_a on the value of I_a/I_a^* remains the same in the case when the current *i* is not instantly interrupted but drops sufficiently fast. Thus, for example, in test 6*b* with $I_a^{max}/I_a^* = 2.7$, there is no drop of I_a. (The value of $|dI_a/dt|$ after complete interruption is found to be larger than under incomplete interruption*.)

The speed of decrease of current I_a is not given by the magnitude of this current. For example, in experiments 6*a*, *b*, the speed of decay of current I_a is completely different, although its maximum value is almost the same in both cases and is equal respectively to 5.7 and 5 A/cm^2. (Experiment 6*b* was conducted with $V_+ = 1000$ V but it was also repeated with $V_+ = 500$ V and $V_+ = 250$ V. The value of I_a^{max} was thereby changed, but the ratio I_a^{max}/I_a^* remained equal to 2.7, and in all these cases no noticeable drop in I_a was observed. Therefore the difference in the speed of decay of I_a in tests 6*a* and 6*b* cannot be explained by a difference in V_+.)

Thus the disappearance of anode current anom-

* In reference 7 [e.g., see S. V. Lebedev, J. Exper. Theoret. Phys. USSR 27, 487 (1954)] (Fig. 3), I_a does not drop during $t_2 - t_1 \sim 10^{-5}$ sec after interruption of the current j. It seems that the drop of I_a is hindered by a weak repeated pulse $j' \sim j/150 \sim 7\times10^4$ A/cm^2 given by the network L, C at $t_1 \leq t \leq t_2$ (see $V_r(t)$ in reference 7, Fig. 3, *zh*, upper curve).

Table 3

	ρ_{20} Ωcm $\times 10^6$	ρ^l_{mp} Ωcm $\times 10^6$	ρ_4 Ωcm $\times 10^6$	
Pure Au	2.4	30.82	—	[6] v. IV, p. 335
Our wire, diameter 0.01 cm	3.45	—	—	Measured under usual conditions
Same	—	—	26.2 ± 1.2	Measured at large j's

alies (i. e., the disappearance of an increase in I_a as compared to I^*_a) takes place the faster, the larger is I_a/I^*_a, independently of the magnitude of the anode current.

3. CONSIDERATION FOR POSSIBLE IMPURITIES IN THE METAL

The question can arise whether the peculiarities discovered in the behavior of metals can be explained by impurities contained in them. As it is known, impurities strongly influence the electrical conductivity of a metal. It can be seen on the top part of Table 2 that the specific resistance ρ_{20} of our wire at 20° C is very little different from the specific resistance of pure nickel. In emission anomalies we considered not only the absolute value of anode current, but also the unusual character of the curve $I_a = I_a(E)$. However the drop in emission with increasing energy cannot be explained by the presence of impurities. It is obvious that the dependence of the value of energy $E(t_c)$ (at which the metal explodes) on the density of the heating current also cannot be explained by the presence of impurities.

The situation is different as far as the difference of R_4 and the tabulated value of R^l_{mp} is concerned. Insofar as the difference between these values is not changed with a change in j and the value of R^l_{mp} for the investigated wire was not rechecked by us, it is possible that the tabulated value of R^l_{mp} (which we used) is not applicable to the type of wire investigated. It is known, however, that small additions to nickel of other metals (copper in particular) increase its specific resistance in the liquid state[4]. Consequently, for nickel with an additive, R^l_{mp} must be rather somewhat larger but not smaller than in pure nickel (Table 2).

Let us note that for nickel with $\rho_{20} = 14 \times 10^{-6}$ Ω cm, known to contain an added amount of Mn, the shape of the oscillograms and the value of the ratio R_4/R_3 are found to be the same as for pure nickel (Fig. 2*a*). Moreover, the transition of the type $R_3 - R_4$ and the region of small dR/dE following it, which terminates in an explosion, are observed also constantan, in which case $R_4/R_3 = 1.3$. On the other hand, the tabulated value for nickel is $R^l_{mp}/R^s_{mp} = 1.94$; for constantan* it seems that this value is also larger than 1.3.

Thus the difference between the value of R_4 determined by us and the value of R^l_{mp} listed in the tables cannot be explained by the presence of impurities. According to our measurements on gold $R_4/R_3 = 1.94$ while according to tabulated values $R^l_{mp}/R^s_{mp} = 2.28$. However, the break in the curve $R(E)$ at point *3* on the oscillograms for gold is not expressed very definitely and the determination of the value R_3 may be unreliable. As a control let us compare the value of ρ_4 found in our oscillograms with ρ^l_{mp} (Table 3). Judging from the value ρ_{20}, the investigated type of gold contained an impurity. But, as it was already indicated, an impurity should not decrease the value ρ^l_{mp}. Therefore, in this case also, ρ_4 is somewhat smaller than the tabulated value of ρ^l_{mp}.

---

* The constantan wire investigated by us had $\rho_{20} = 48 \times 10^{-6}$ Ωcm, $\rho^s_{mp} = 58 \times 10^{-6}$ Ωcm. According to tabulated data for the alloy 40% Ni and 60% Cu for which $\rho_{20} = 50 \times 10^{-6}$ Ωcm, in the liquid state $\rho_{1500} = 85 \times 10^{-6}$ Ω cm. For other concentrations of the alloy Cu - Ni for which $\rho_{20} \approx 50 \times 10^{-6}$ Ωcm, $\rho^l_{mp} > 85 \times 10^{-6}$ Ωcm [see *Encyclopedia of Metalphysics*, edited by Masing, v. 1, Moscow (1937), p. 306]. For example, for the alloy 65% Ni and 35% Cu with $\rho_{20} = 50 \times 10^{-6}$ Ωcm and $T_{mp} = 1358°$ C it is known that $\rho^l_{mp} = 136.7 \times 10^{-6}$ Ω cm, and $\rho_{1400} = 138.5 \times 10^{-6}$ Ωcm [see *Technical Encyclopedia*, Tables of phys - chem. and technological data, Moscow (1931), v. V, p. 50].

4. COMPARISON OF RESULTS WITH DATA OBTAINED BY OTHER AUTHORS

1. In the paper of Khaikin and Bene[9] results are shown of an investigation of the melting of tin rods, heated by a current $j \approx 10^3 - 1.4 \times 10^3$ A/cm^2 and cooled on the surface by a jet of air. It was found that polycrystalline rods begin to melt from the inside and single crystal rods from the surface.

The conditions of these tests differed basically from the conditions of the discussed experiments made with $j > 6 \times 10^4$ A/cm^2 only in current density.

The results of these experiments coincide qualitatively with the results of our experiments with interrupted impulses for tungsten[3] in the sense that the metal does not melt, although it should be liquid according to the energy introduced into it. (In their paper, Khaikin and Bene observed that the single crystal is molten only at the surface, where the temperature is lower than inside, and in reference 3 the wires did not melt with $E = W_H + W_{fus}$.) It is true that, from the qualitative point of view, the difference here is quite considerable. If, for example, we recalculate the excess of energy, $E - W_H \approx W_{fus}$, observed in the experiments of reference 3, at a temperature for the usual value of specific heat, we obtain a value of $\sim 1000^0$ and not $1 - 2^0$ as estimated in reference 9 (for small j). However, it is possible in our experiments to interrupt the heating current earlier; then, obviously, one can obtain as small an excess of energy as desired.

Khaikin and Bene[9] concluded that they observe an overheating of a solid body. It seems to us, that if one starts with such a concept, one can not explain all the phenomena which we observe. In particular, for the case of an overheating of the metal, a drop in emission with an increase in energy is incomprehensible (see Sec. 2). One could assume that the losses in energy increase as a result of the overheating and that the drop in emission is tied to a cooling of the wire. Then in tests 6*a*, *c* the losses should exceed the losses at the melting point by more than 16 times ($i = 4.3 i_m$ and $i = 5 i_m$). The order of magnitude of the necessary temperature can be estimated by assuming that the wire is heated uniformly and emits as a black body. Then a temperature is obtained which is twice as high as the melting point temperature of tungsten, i. e., it exceeds its boiling temperature ($T_{mp} \approx 3650^0$ K, $T_{bp} \approx 6200^0$K*). However, the overheating of a non-melting metal over its boiling point temperature appears to be unlikely. Moreover a large overheating probably would have caused a large increase in the resistance of the wire, because the dependence of R on E upon overheating should remain of the same character as in a metal below the melting point. Actually, the resistance of the wire during the drop in emission differs from R^s_{mp} by not more than 10%, while the wire remains intact after the experiment. We note that in experiments with tungsten we cannot definitely indicate the start of the drop in current I_a with relation to points *3* and *4* since these points do not appear in experiments 6 and 7, and such experiments were not repeated with an improved technique of taking the oscillograms V_R.

2. Ignat'eva and Kalashnikov[10] studied the dependence of $R = R(E)$ in metals with j as high as 5×10^6 A/cm^2, using the same method as in our experiments. It is stated in this paper that the resistance of transition metals, measured at high current density, is much larger than the resistance at ordinary current, i. e., there is a violation of Ohm's law. In this case the increase in R has its maximum value at the instant of switching the high current on, i. e., when the metal has not yet received any appreciable energy from the current (for example, with $j \approx 5 \times 10^6$ A/cm^2 for platinum, $[V_R(t_1)/V_r(t_1)]r = 5R_{20}$).

In our experiment such an effect was much smaller (for example, from oscillogram 4*c* for nickel at $j = 5 \times 10^6$ A/cm^2, $[V_R(t_1)/V_r(t_1)]r = 1.15\, R_{20}$). Here the experiment shows that the increase of $[V_R(t_1)/V_r(t_1)]r$ over R_{20} at the start of the oscillograms is considerably modified by a change in the configuration of the wires of the segment of the network, located between the terminals of the plates of the oscillograph. Therefore we believe that the difference between $[V_R(t_1)/V_r(t_1)]r$ and R_{20} cannot be considered as characteristic of the condition of the metal and the statement about the dependence of resistance on the current density seems erroneous to us. The error, in our opinion, is due

* When the length of the tungsten wire is changed from one to several centimeters, the current i_m is changed only by a small amount. Consequently, the losses of energy due to thermal conduction through the ends of the wire are small compared to radiation losses even at the melting point of tungsten.

[9] S. E. Khaikin and N. P. Bene, Doklady Akad. Nauk SSSR 23, 31 (1939)

[10] L. A. Ignat'eva and S. G. Kalashnikov, J. Exper. Theoret. Phys. USSR 22, 385 (1952)

to the fact that, during some time after the start of the current i, V_R and V are considerably different from iR and ir, because of the influence of the inductance L of the segments of the network between the connection points of the oscillograph plates[1,3] ** We believe that it is not possible to determine R and E from the initial parts of the oscillograms from the formulas

$$R = \frac{V_R}{V_r} r$$

and

$$E(t) = \frac{1}{r} \int_{t_1}^{t} V_R(t)\, V_r(t)\, dt.$$

In the later regions of our oscillograms, in which these formulas are valid, there are no signs of deviation from Ohm's law.

It was also concluded in reference 10 that, for a sufficient increase in current density, the energy necessary to start melting is decreased, which is confirmed by the course of the curve IV (see reference 10, Fig. 9, p. 395). However, the displacement of the entire curve along the energy axis is observed only for the curve taken at $j = 4.2 \times 10^6$ A/cm^2. Its course is very different from the course of all other curves shown in Fig. 9, including that of the curve taken at $j = 3.9 \times 10^6$ A/cm^2. For all these curves the values of R and E at point *3* (in our terminology) are equal, and do not differ to any extent from the usual relationship between R and E, before the onset of melting. The values of R and E are also equal in these curves at the point *4*. These results coincide with our results obtained at $6 \times 10^4 \leq j \leq 5 \times 10^6$ A/cm^2 for nickel.

The decrease in energy E_3 observed by the authors in reference 10 at the transition to large j's was never observed by us*.

** Upon cooling the wire with liquid air while keeping the other test conditions the same, we observed an increase in the deviation of $[V_R(t_1)/V_r(t_1)]r$ from the value of R_{20}. This can be explained by the fact that at the start of the oscillogram, when di/dt is large, the difference between $V_R/Ri = (L\frac{di}{dt} + Ri)/Ri$ and unity increases with a reduction in R. The increase in j at constant i increases the rate of heating and displaces the working regions of the oscillograms to the region of distortions of V_R and V_r.

* Our early experiments in measuring the dependence $R = R(E)$ [e.g., see S. V. Lebedev and S. E. Khaikin, J. Exper. Theoret. Phys. USSR 26, 629 (1954)] rather indicate an increase in this energy with increasing j above 5×10^6 A/cm^2 than its decrease.

CONCLUSIONS

1. At current densities $6 \times 10^4 \leq j \leq 5 \times 10^6$ A/cm^2 the character of the dependence of R on E for nickel appears to be the same as for tungsten. The breaking point *4* separates the curve $R = R(E)$ into two parts, so that for $t \leq t_4$ the function $R(E)$ does not change with a change in j, but for $t > t_4$ the shape of the curve $R(E)$ depends on j. The value of the energy $E(t_c)$ at which R increases abruptly, decreases when j is decreased.

2. At the breaking point *3* of the curve $R = R(E)$ the values of energy and resistance correspond to the start of melting of the metal under ordinary conditions. The value of energy in point *4* corresponds to the end of the melting of the metal under ordinary conditions. A comparison of the measured value of the resistance of the metal in the liquid state at the melting point R^l_{mp} is difficult, because the value R^l_{mp} has not been checked by us.

3. An increased electron emission is observed on nickel as well as on tungsten. The anode current, measured upon heating the nickel wire by a current pulse $\sim 10^5$ A/cm^2, is 50 times larger than the nickel emission at the melting point and the nickel wire is not destroyed.

4. A drop in emission is observed on nickel and on tungsten, while the intake of energy into the observed wire is many times larger than energy losses, measured during stationary heating in vacuum at the melting point temperature.

5. In experiments with tungsten, after an abrupt interruption of the heating current, the large anode current I_a decreases, coming close to the value I^*_a, corresponding to the law of Boguslavskii - Langmuir. Here the rate of decrease of I_a/I^*_a appears to be larger, the larger the value of I_a/I^*_a independently of the value of I_a.

It was not possible to discern the breaking points in the curve $R = R(E)$ (points *3* and *4*) in our former experiments on tungsten, because the oscillograms were not sufficiently sharp. The presence of these points shows that the drop of dR/dE observed on tungsten near $R = R^s_{mp}$, does not occur smoothly, but by jumps. These jumps correspond to the start and the end of the melting process, if it is assumed that there is only 8% change in the resistance of tungsten on melting. (I.e., the change is very small in comparison with other metals.) This assumption is more natural, as the ratio R_4/R_3 does not change with a change of the current density in large limits. Thus our former supposition[1,3] that the drop of dR/dE in tungsten near $R = R^s_{mp}$ is anomalous, is probably wrong.

Other phenomena*, observed in our previous experiments with tungsten at large current densities and not observed under ordinary conditions, depend considerably on the current density. These phenomena were considered by us as indications of an anomalous state of the tungsten caused by a flow of current of high density. The dependence of energy at the instant of explosion - $E(t_c)$ - on j and emission anomalies is observed in the experiments treated in present paper, not only on tungsten, but also on nickel. New peculiarities of emission (see point 4 of the Conclusions) were discovered which we also could not explain by means of a supposition that the metal is in a normal state. We note that the conditions of the experiments on nickel and on tungsten were materially different because of the considerable difference in melting point temperature (for example the measured anode currents were different by several orders of magnitude). The identical character of the phenomena observed in these metals near $R = R^s_{mp}$ shows that they are caused by processes in metals independent of the value of their melting point temperature.

* The dependence on the energy $E(t_c)$ on j(t) [e.g., see S. V. Lebedev and S. E. Khaikin, J. Exper. Theoret. Phys. USSR 26, 629 (1954) and S. V. Lebedev, J. Exper. Theoret. Phys. USSR 27, 605 (1954)], anomalies of emission [e.g., see S. V. Lebedev and S. E. Khaikin, J. Exper. Theoret. Phys. USSR 27, 487 (1954)], peculiarities of melting in experiments with interrupted pulses [e.g., see S. V. Lebedev, J. Exper. Theoret. Phys. USSR 27, 605 (1954)].

Translated by S. Paskwer
12

SOVIET PHYSICS-JETP VOLUME 1, NUMBER 1 JULY, 1955

The Wave Function of the Lowest State of a System of Interacting Bose Particles

N. N. Bogoliubov and D. N. Zubarev
Mathematical Institute of the Academy of Sciences, USSR

(Submitted to JETP editor June 13, 1954)
J. Exper. Theoret. Phys. USSR 28, 129-139 (1955)

The wave function and the energy of the lowest state of a slightly non-ideal Bose gas are determined by means of the method of " auxiliary variables ", with accuracy to terms of second order relative to the smallness of the parameter of the energy of interaction.

I. INTRODUCTION

THE problem of the investigation of the wave of a system of a large number of interacting Bose particles arose in connection with attempts at the formation of a microscopic theory of the superfluidity of He II. In spite of a series of successes in this direction[1,2] we are today still far from the completion of such a microscopic theory.

If we select as a model for the liquid helium a slightly non-ideal degenerate Bose gas, then it is possible, as one of us has shown[2], to explain the phenomenon of the superfluidity of He II by the properties of the energy spectrum of such a system. However, inasmuch as the slightly non-ideal Bose gas cannot be regarded an entirely satisfactory model of liquid helium, the necessity arises of improving the theory of the non-ideal Bose gas, taking into account interactions that are not small. Up to the present time only such systems with weak interactions between particles have been studied theoretically.

Wave functions of the lowest state of a system consisting of a large number of weakly interacting Bose particles have been determined by Bijl[3]. However the results of his work are in error because of the lack of validity of the approximations used (i.e., terms that are not small in magnitude have been neglected).

In the present work the correct wave functions of the lowest state of a Bose system with weak interaction have been determined by means of the method of "auxiliary variables" with accuracy to terms of second order of smallness.

[1] L.D. Landau, J. Exper. Theor. Phys. USSR 11, 592 (1941).

[2] N.N. Bogoliubov, Izv. Akad. Nauk SSSR, Ser. Fiz. 11, 77 (1947).

[3] A. Bijl, Physica 7, 869 (1940).

II. APPLICATION OF THE METHOD OF AUXILIARY VARIABLES TO BOSE SYSTEMS

We consider N interacting particles, without spin that obey to Bose-Einstein statistics. To describe the system we introduce the variables $\rho_{\mathbf{k}}$, the Fourier coefficients of the density operator, according to the formula

$$\rho_{\mathbf{k}} = \frac{1}{\sqrt{N}} \sum_{j=1}^{N} e^{-i\mathbf{k}\cdot\mathbf{r}_j} \qquad (\mathbf{k} \neq 0). \quad (2.1)$$

The quantity $\rho_0 = \sqrt{N}$ is a constant and cannot be employed as a variable. $1/\sqrt{N}$ is a normalizing factor.

The variables $\rho_{\mathbf{k}}$ appear to be natural "collective" variables for describing oscillatory processes in systems that consist of a large number of interacting particles, and were applied earlier to systems of Fermi particles in the works of Zubarev[4], Tomonaga[5], and Pines and Bohm[6]

We shall seek a wave function of the systems in the form

$$\varphi(t, \rho_{\mathbf{k}_1} \ldots \rho_{\mathbf{k}_i} \ldots), \qquad (2.2)$$

which does not contain explicitly coordinates of the particles but only the auxiliary variables $\rho_{\mathbf{k}}$. This representation of the wave function we shall call the $\rho_{\mathbf{k}}$-representation in what follows. This is a feasible arrangement since the wave function of the system is symmetric relative to the coördinates $\mathbf{r}_1, \ldots, \mathbf{r}_N$ and $\rho_{\mathbf{k}}$ is also a symmetric function of the coördinates particles.

The number of variables in the wave function (2.2) is infinite, and they are not independent. In order to go over to the usual representation of the wave functions, it is necessary to substitute Eq. (2.1) for $\rho_{\mathbf{k}}$ in Eq. (2.2); the resultant function will be symmetric relative to $\mathbf{r}_j$.

The Schrödinger equation for a system of N particles has the form

$$i\hbar \frac{\partial \varphi}{\partial t} = -\frac{\hbar^2}{2m} \sum_{j=1}^{N} \Delta_{\mathbf{r}_j} \varphi + \frac{1}{2} \sum_{\substack{j_1, j_2 \\ j_1 \neq j_2}} \Phi(|\mathbf{r}_{j_1} - \mathbf{r}_{j_2}|)\varphi. \qquad (2.3)$$

It is now required to put this equation in the $\rho_{\mathbf{k}}$-representation for a system of Bose particles.

We express the interaction operator in terms of the variables $\rho_{\mathbf{k}}$:

$$\frac{1}{2} \sum_{j_1 \neq j_2} \Phi(|\mathbf{r}_{j_1} - \mathbf{r}_{j_2}|) = \sum_{\mathbf{k} \neq 0} \frac{N}{2V} \nu(k) \rho_{\mathbf{k}} \rho_{-\mathbf{k}} + \frac{N^2}{2V} \nu(0) - \sum_{\mathbf{k}} \frac{N}{2V} \nu(k), \qquad (2.4)$$

where $\nu(k) = \int \Phi(r) e^{-i\mathbf{k}\cdot\mathbf{r}} d\mathbf{r}$ is the Fourier coefficient of the energy of interaction. We introduce the Bose-Einstein kinetic energy operator in the $\rho_{\mathbf{k}}$ representation, carrying out the differentiation of the function (2.2) as an implicit function of the $\mathbf{r}_j$:

$$T = \frac{1}{\sqrt{N}} \sum_{\substack{\mathbf{k}_1, \mathbf{k}_2 \\ \mathbf{k}_1 + \mathbf{k}_2 \neq 0}} \frac{\hbar^2}{2m} (\mathbf{k}_1 \mathbf{k}_2) \rho_{\mathbf{k}_1 + \mathbf{k}_2} \frac{\partial^2}{\partial \rho_{\mathbf{k}_1} \partial \rho_{\mathbf{k}_2}} + \sum_{\mathbf{k}} \frac{\hbar^2 k^2}{2m} \left(-\frac{\partial^2}{\partial \rho_{\mathbf{k}} \partial \rho_{-\mathbf{k}}} + \rho_{\mathbf{k}} \frac{\partial}{\partial \rho_{\mathbf{k}}} \right). \qquad (2.5)$$

Making use of the Eqs. (2.4), (2.5) for the potential and kinetic energy, we write the Schrödinger equation in the $\rho_{\mathbf{k}}$ representation in the form

$$i\hbar \frac{\partial \varphi}{\partial t} = \sum_{\mathbf{k} \neq 0} \left\{ \frac{\hbar^2 k^2}{2m} \left(-\frac{\partial^2 \varphi}{\partial \rho_{\mathbf{k}} \partial \rho_{-\mathbf{k}}} + \rho_{\mathbf{k}} \frac{\partial \varphi}{\partial \rho_{\mathbf{k}}} \right) + \frac{1}{2} \frac{N}{V} \nu(k) \rho_{\mathbf{k}} \rho_{-\mathbf{k}} \varphi \right\} + \frac{1}{\sqrt{N}} \times \sum_{\substack{\mathbf{k}_1, \mathbf{k}_2 \\ \mathbf{k}_1 + \mathbf{k}_2 \neq 0}} \frac{\hbar^2}{2m} (\mathbf{k}_1 \mathbf{k}_2) \rho_{\mathbf{k}_1 + \mathbf{k}_2} \frac{\partial^2 \varphi}{\partial \rho_{\mathbf{k}_1} \partial \rho_{\mathbf{k}_2}} + \left\{ \frac{N^2}{2V} \nu(0) - \frac{N}{2V} \sum_{\mathbf{k}} \nu(k) \right\} \varphi. \qquad (2.6)$$

We have thus shown that if the function (2.2) is a solution of Eq. (2.6) in which the $\rho_{\mathbf{k}}$ are the independent variables, then the function

$$\varphi\left(t, \ldots \frac{1}{\sqrt{N}} \sum_{j=1}^{N} \exp\{-i(\mathbf{k}\mathbf{r}_j)\}, \ldots\right)$$ is a solution of the Schrödinger equation, symmetric relative to $\mathbf{r}_1, \ldots, \mathbf{r}_N$. We can therefore work with Eq. (2.6) in what follows, regarding the ρ_{kj} as the independent variables.

The Hamiltonian operator in Eq. (2.6) is non-

---

[4] D.N. Zubarev, J. Exper. Theor. Phys. USSR **25**, 548 (1953).

[5] S. Tomonaga, Prog. Theor. Phys. **5**, 544 (1950).

[6] D. Pines and D. Bohm, Phys. Rev. **82**, 625 (1951). **85**, 338 (1952); **92**, 609(1953).

Hermitian, since the transformation to the variables ρ_k is not a canonical one. The principal part of the Hamiltonian can be made Hermitian if we introduce a new wave function Φ by the substitution

$$\Phi = \exp\left\{-\frac{1}{4}\sum_{\mathbf{k}}\rho_{\mathbf{k}}\rho_{-\mathbf{k}}\right\}\varphi. \tag{2.7}$$

Then Eq. (2.6) takes the form

$$i\hbar\frac{\partial\Phi}{\partial t} = \left\{\sum_{\mathbf{k}\neq 0}\left[-\frac{\hbar^2k^2}{2m}\frac{\partial^2}{\partial\rho_{\mathbf{k}}\partial\rho_{-\mathbf{k}}} + \frac{1}{2}\left(\frac{N}{V}v(k) + \frac{\hbar^2k^2}{4m}\right)\rho_{\mathbf{k}}\rho_{-\mathbf{k}}\right] + \frac{1}{V\bar{N}}\right. \tag{2.8}$$

$$\times\sum_{\substack{\mathbf{k}_1,\,\mathbf{k}_2\\ \mathbf{k}_1+\mathbf{k}_2\neq 0}}\frac{\hbar^2}{2m}(\mathbf{k}_1\mathbf{k}_2)\rho_{\mathbf{k}_1+\mathbf{k}_2}\left(\frac{\partial}{\partial\rho_{\mathbf{k}_1}} + \frac{\rho_{-\mathbf{k}_1}}{2}\right)\left(\frac{\partial}{\partial\rho_{\mathbf{k}_2}} + \frac{\rho_{-\mathbf{k}_2}}{2}\right)$$

$$\left. - \sum_{\mathbf{k}}\left(\frac{\hbar^2k^2}{4m} + \frac{Nv(k)}{2V}\right) + \frac{N^2}{2V}v(0)\right\}\Phi.$$

Transforming to the variables $q_{\mathbf{k}}$,

$$\rho_{\mathbf{k}} = \sqrt{2}\,\lambda_{\mathbf{k}}q_{\mathbf{k}}, \tag{2.9}$$

$$\lambda_{\mathbf{k}}^4\left(\frac{N}{V}v(k) + \frac{\hbar^2k^2}{4m}\right) = \frac{\hbar^2k^2}{4m}, \tag{2.10}$$

and we obtain Eq. (2.8) in the form

$$i\hbar\frac{\partial\Phi}{\partial t} = \left\{\frac{1}{2}\sum_{\mathbf{k}}E(k)\left(-\frac{\partial^2}{\partial q_{\mathbf{k}}\partial q_{-\mathbf{k}}} + q_{\mathbf{k}}q_{-\mathbf{k}}\right)\right. \tag{2.11}$$

$$+\frac{i}{V\bar{N}}\sum_{\substack{\mathbf{k}_1,\,\mathbf{k}_2\\ \mathbf{k}_1+\mathbf{k}_2\neq 0}}\frac{\hbar^2}{2m}(\mathbf{k}_1\mathbf{k}_2)\frac{\lambda_{\mathbf{k}_1+\mathbf{k}_2}}{\sqrt{2}\lambda_{\mathbf{k}_1}\lambda_{\mathbf{k}_2}}q_{\mathbf{k}_1+\mathbf{k}_2}\left(\frac{\partial}{\partial q_{\mathbf{k}_1}}\right.$$

$$\left. + \lambda_{\mathbf{k}_1}^2q_{-\mathbf{k}_1}\right)\left(\frac{\partial}{\partial q_{\mathbf{k}_2}} + \lambda_{\mathbf{k}_2}q_{-\mathbf{k}_2}\right) + \frac{N^2}{2V}v(0)$$

$$\left. - \sum_{\mathbf{k}}\left(\frac{\hbar^2k^2}{4m} + \frac{N}{2V}v(k)\right)\right\}\Phi,$$

where

$$E(k) = \sqrt{\frac{N}{V}v(k)\frac{\hbar^2k^2}{m} + \left(\frac{\hbar^2k^2}{2m}\right)^2} \tag{2.12}$$

We introduce the Bose operators

$$b_{\mathbf{k}} = \frac{1}{\sqrt{2}}\left(\frac{\partial}{\partial q_{-\mathbf{k}}} + q_{\mathbf{k}}\right), \tag{2.13}$$

$$b_{\mathbf{k}}^+ = \frac{1}{\sqrt{2}}\left(-\frac{\partial}{\partial q_{\mathbf{k}}} + q_{-\mathbf{k}}\right),$$

with the help of which the Schrödinger equation for a system of interacting Bose particles can be written in the form

$$i\hbar\frac{\partial\Phi}{\partial t} = \left\{\sum_{\mathbf{k}}E(k)b_{\mathbf{k}}^+b_{\mathbf{k}} + \frac{1}{V\bar{N}}\right. \tag{2.14}$$

$$\times\sum_{\substack{\mathbf{k}_1,\,\mathbf{k}_2\\ \mathbf{k}_1+\mathbf{k}_2\neq 0}}\frac{\hbar^2}{8m}(\mathbf{k}_1\mathbf{k}_2)\frac{\lambda_{\mathbf{k}_1+\mathbf{k}_2}}{\lambda_{\mathbf{k}_1}\lambda_{\mathbf{k}_2}}(b_{\mathbf{k}_1+\mathbf{k}_2} + b_{-\mathbf{k}_1-\mathbf{k}_2}^+)$$

$$\times[(1+\lambda_{\mathbf{k}_1}^2)b_{-\mathbf{k}_1} + (\lambda_{\mathbf{k}_1}^2-1)b_{\mathbf{k}_1}^+][(1+\lambda_{\mathbf{k}_2}^2)b_{-\mathbf{k}_2}$$

$$\left. +(\lambda_{\mathbf{k}_2}^2-1)b_{\mathbf{k}_2}^+]\right\}\Phi,$$

where the constant E_0,

$$E_0 = \frac{N^2}{2V}v(0) + \frac{1}{2}\sum_{\mathbf{k}}\left(E(k) - \frac{\hbar^2k^2}{2m} - \frac{N}{V}v(k)\right) \tag{2.15}$$

has been eliminated by means of the substitution

$$\Phi \to \Phi\exp\{E_0t/i\hbar\}.$$

Thus the Hamiltonian of a system of interacting Bose particles consists of two parts: the diagonal part, which represents the sum of the Bose density fluctuation operators (or elementary phonon excitations) with energy $E(k)$, and a non-diagonal part, that describes the phonon interaction. The energy of the elementary excitations in a Bose gas agrees with the obtained earlier[2].

The first sum in Eqs. (2.6), (2.8), (2.11), (2.14) represents the principal part of the Hamiltonian, the second sum is the secondary (and, in general, small) part of the Hamiltonian. If the interaction between phonons tends to zero, then $\lambda_{\mathbf{k}}^2 \to 1$. In this event, sizeable terms remain in the second sum of Eq. (2.14). These terms contain the operators $(b_{\mathbf{k}_1+\mathbf{k}_2} + b_{-\mathbf{k}_1-\mathbf{k}_2}^+)b_{-\mathbf{k}_1}b_{-\mathbf{k}_2}$. However, inasmuch as we are interested only in the wave function of the lowest state, this term can be omitted, since it has no effect on the wave function of the vacuum.

3. THE RELATION BETWEEN THE METHOD OF "AUXILIARY VARIABLES" AND THE METHOD OF BIJL

Bijl's method [3] consists of the following. An approximate wave function of the lowest level of a system of N Bose particles is required which satisfies the Schrödinger equation (2.3). The interaction energy between the particles is assumed to be small, proportional to a parameter ϵ. We choose as the zeroth approximation a uniform particle distribution density. The usual method in the theory of excitation, in which a decomposition of the desired wave function is expressed in a series of powers of ϵ, is not suitable here, since the corrections to the wave function of the zeroth approximation turn out not to be small, and to be

proportional to a positive power of the total number of particles, N. For sufficiently large N, the correction can therefore be arbitrarily large. Bijl showed that it is possible to avoid this difficulty by expressing the logarithm of the wave function in powers of ϵ, rather than the wave function itself.

Setting

$$\varphi = e^S, \tag{3.1}$$

Bijl sought a new unknown function S in a power series in ϵ. We shall attempt to calculate S without making use of this decomposition. This precaution is necessary, because the coefficients for the neglected terms, which are proportional to ϵ^2, are not small, and cannot be disregarded.

If we substitute (3.1) in Schrödinger's equation we obtain the following for the logarithm of the wave function:

$$-\frac{\hbar^2}{2m}\sum_{j=1}^{N}\Delta_j S - \frac{\hbar^2}{2m}\sum_{j=1}^{N}(\nabla_j S)^2 \tag{3.2}$$
$$+\frac{1}{2}\sum_{j_1 \neq j_2}\Phi(|\mathbf{r}_{j_1}-\mathbf{r}_{j_2}|) = E.$$

In this equation, Bijl neglected the second term (proportional to ϵ^2); we keep this term.

We first seek S in the form of a sum of binary functions:

$$S(\mathbf{r}_1, \ldots, \mathbf{r}_N) = \sum_{j_1 j_2} S(|\mathbf{r}_{j_1}-\mathbf{r}_{j_2}|). \tag{3.3}$$

We decompose the function $S(r)$ in a Fourier series

$$S(r) = \frac{1}{V}\sum_{\mathbf{k}} \sigma(k)\, e^{i(\mathbf{kr})}, \tag{3.4}$$

and write (3.3) in the form

$$S(\mathbf{r}_1, \ldots, \mathbf{r}_N) = \frac{N}{V}\sum_{\mathbf{k}} \sigma(k)\, \rho_{\mathbf{k}}\rho_{-\mathbf{k}}. \tag{3.5}$$

making use of Eq. (2.1). With the help of Eqs. (2.4) and (3.5), Eq. (3.2) becomes

$$\frac{N}{V}\sum_{\mathbf{k}}\left(\frac{\hbar^2 k^2}{m}\sigma(k) + \frac{\nu(k)}{2}\right)\rho_{\mathbf{k}}\rho_{-\mathbf{k}} \tag{3.6}$$
$$+\frac{2}{N}\left(\frac{N}{V}\right)^2 \sum_{\mathbf{k}_1\mathbf{k}_2;\, j} \sigma(k_1)\sigma(k_2)\frac{\hbar^2(\mathbf{k}_1\mathbf{k}_2)}{m}$$
$$\exp\{-i(\mathbf{k}_1+\mathbf{k}_2)\mathbf{r}_j\}\,\rho_{-\mathbf{k}_1}\rho_{-\mathbf{k}_2} = E - E_0,$$

where

$$E_0 = \frac{1}{2}\frac{N^2}{V}\nu(0) - \frac{1}{2}\sum_{\mathbf{k}}\frac{N}{V}\nu(k) \tag{3.7}$$
$$+\frac{N}{V}\sum_{\mathbf{k}}\sigma(k)\frac{\hbar^2 k^2}{m}.$$

An exact solution of Eq. (3.6) is difficult, but it is possible to simplify the procedure if we leave only the principle part (corresponding to $\mathbf{k}_1+\mathbf{k}_2=0$) in the second sum. This procedure is equivalent to a neglect of the correlation between particles. For the present, we accept this rough approximation, since it permits us to establish a simple connection between the method of "auxiliary variables" and the method of Bijl. Below, in Sec. 4, a more rigorous method is given for obtaining the wave function of the lowest state of a system of Bose particles.

After some simplification Eq. (3.6) takes the form

$$\frac{N}{V}\sum_{\mathbf{k}}\left\{-2\frac{N}{V}\frac{\hbar^2 k^2}{m}\sigma^2(k) + \frac{\hbar^2 k^2}{m}\sigma(k) + \frac{\nu(k)}{2}\right\} \tag{3.8}$$
$$\times\, \rho_{\mathbf{k}}\rho_{-\mathbf{k}} = E - E_0,$$

which can be satisfied by setting

$$-\frac{2N}{V}\frac{\hbar^2 k^2}{m}\sigma^2(k) + \frac{\hbar^2 k^2}{m}\sigma(k) + \frac{\nu(k)}{2} = 0, \tag{3.9}$$

whence

$$\sigma(k) = \frac{1}{4n} - \frac{1}{4n}\frac{\sqrt{n\nu(k)(\hbar^2 k^2/m) + (\hbar^2 k^2/2m)^2}}{\hbar^2 k^2/2m}, \tag{3.10}$$
$$n = \frac{N}{V}.$$

The negative sign is chosen for the radical since we are interested in the minimum value of the energy.

The logarithm of the wave function of the lowest state will be

$$S = \sum_{\mathbf{k}}\frac{1}{4} \tag{3.11}$$
$$\times\left\{1 - \frac{\sqrt{n\nu(k)(\hbar^2 k^2/m) + (\hbar^2 k^2/2m)^2}}{\hbar^2 k^2/2m}\right\}\rho_{\mathbf{k}}\rho_{-\mathbf{k}}$$

and the corresponding wave function is

$$\rho_0 = \exp\left\{\frac{1}{4}\sum_{\mathbf{k}}\rho_{\mathbf{k}}\rho_{-\mathbf{k}}\right\} \tag{3.12}$$
$$\times\ \exp\left\{-\frac{1}{4}\sum_{\mathbf{k}}\frac{E(k)}{\hbar^2 k^2/2m}\rho_{\mathbf{k}}\rho_{-\mathbf{k}}\right\},$$

where $E(k)$ is the energy of elementary excitations in the weakly non-ideal Bose gas, given by Eq. (2.12).

The first factor in the wave function (3.12) is

identical to the factor which we introduced in the wave function of the lowest state in order to make the principal part of the Hamiltonian (2.6) Hermitian. It can be demonstrated by direct substitution that the function (3.12) satisfies the principal part of Eq. (2.6).

If we neglect the term in Eq. (3.9) which is quadratic in $\sigma(k)$, we get Bijl's result:

$$\sigma(k) = -mv(k)/2\hbar^2k^2. \tag{3.13}$$

The logarithm of the wave function of the lowest state in this case is

$$S = \sum_{\mathbf{k}} -\frac{mv(k)n}{2\hbar^2k^2}\rho_{\mathbf{k}}\rho_{-\mathbf{k}} \tag{3.14}$$

and the corresponding wave function is

$$\varphi_0 = \exp\left\{-\frac{n}{4}\sum_{\mathbf{k}}\frac{v(k)}{\hbar^2k^2/2m}\rho_{\mathbf{k}}\rho_{-\mathbf{k}}\right\}. \tag{3.15}$$

The function (3.16) satisfies the differential equation

$$\sum_{\mathbf{k}}\left\{\frac{\hbar^2k^2}{2m}\rho_{\mathbf{k}}\frac{\partial\varphi}{\partial\rho_{\mathbf{k}}} + \frac{1}{2}nv(k)\rho_{\mathbf{k}}\rho_{-\mathbf{k}}\varphi\right\} \tag{3.16}$$

$$= (E - E_0')\varphi,$$

where

$$E_0' = \frac{N^2}{2V}v(0) - \frac{1}{2}\sum_{\mathbf{k}}nv(k).$$

Equation (3.16) differs from the principal part of Eq. (2.8) in that part of the kinetic energy operator of the phonons is missing from it:

$$-\frac{\hbar^2k^2}{2m}\frac{\partial^2}{\partial\rho_{\mathbf{k}}\partial\rho_{-\mathbf{k}}}$$

This omission is unjustified, and, consequently, Bijl's method always gives a rough approximation to the wave function of lowest order of the system of Bose particles. Thus the doubt expressed by Landau and Lifshits[7] on the validity of one of the author's results[2], since they did not agree with those of Bijl [3], is unjustified.

Making use of (2.4) and (2.1), and carrying out the integration over the variable $\mathbf{k}$, we write the logarithm of the wave function in the form

$$S = -\frac{m}{2\hbar^2}\frac{1}{4\pi}\sum_{i,j}\int\frac{\Phi(r)\,d\mathbf{r}}{|\mathbf{r}_i - \mathbf{r}_j - \mathbf{r}|}, \tag{3.17}$$

or, after integration over the angular variables,

$$S = -\frac{m}{\hbar^2}\frac{1}{2}\sum_{i,j}\left\{\int_{r_{ij}}^{\infty}\Phi(r)\,r\,dr + \frac{1}{r_{ij}}\int_0^{r_{ij}}\Phi(r)\,r^2dr\right\}, \tag{3.18}$$

$$r_{ij} = |r_i - r_j|.$$

This form of the wave function coincides with that deduced by Bijl[3].

In obtaining Eq. (3.18) from Eq. (3.14), we have carried out a five-fold integration over the three variables $\mathbf{k}$ and the two angular variables of the radius vector $\mathbf{r}$. It also would have been possible to obtain Eq. (3.18) directly, by solving the Schrödinger equation in the variables $\mathbf{r}j$, neglecting the quadratic terms in S, as was done by Bijl[3].

The equation (3.11) for the logarithm of the wave function can also be written in the form

$$S = -\frac{1}{4\pi^2}\frac{m}{\hbar^2n} \times \sum_{i,j}\frac{1}{r_{ij}}\int_0^{\infty}\left\{E(k) - \frac{\hbar^2k^2}{2m}\right\}\frac{\sin kr_{ij}}{k}\,dk, \tag{3.19}$$

where the integration has been carried out over the angular variables.

4. THE WAVE FUNCTIONS OF THE LOWEST STATE OF A SYSTEM OF INTERACTING BOSE PARTICLES

In the preceding section, we detrmined the zeroth approximation wave function of the lowest state of a system of interacting Bose particles, making more precise the method of Bijl. We now return to the more systematic method of the Bose system, which makes possible the determination of the wave functions of the lowest state in the form of a decomposition in powers of a parameter of the smallness of interaction.

As a subsidiary problem, we determine the eigenfunctions of the operator

$$H_0 = \frac{1}{2}\sum_{\mathbf{k}}E(k)\left(-\frac{\partial^2}{\partial q_{\mathbf{k}}\partial q_{-\mathbf{k}}} + q_{\mathbf{k}}q_{-\mathbf{k}}\right), \tag{4.1}$$

which is the principal part of the Hamiltonian (2.11) The equation for the eigenfunctions of Eq. (4.1) can be written in the form

$$\frac{1}{2}\sum_{\mathbf{k}}E(k)\left\{-\frac{1}{4}\left(\frac{\partial^2}{(\partial q_{\mathbf{k}}^c)^2} + \frac{\partial^2}{(\partial q_{\mathbf{k}}^s)^2}\right) + (q_{\mathbf{k}}^c)^2 + (q_{\mathbf{k}}^s)^2\right\}\Phi = \mathcal{E}\Phi, \tag{4.2}$$

[7] L. D. Landau and E. M. Lifshits, *Statistical Physics*, 2nd edition.

where $q_{\mathbf{k}}^c$ and $q_{\mathbf{k}}^s$ are the real and imaginary parts of $q_{\mathbf{k}}$. The eigenfunctions of Eq. (4.2) have the form

$$\Phi_{n_1,n_2} = \prod_{(\mathbf{k})}{}' \exp\{-q_{\mathbf{k}}q_{-\mathbf{k}}\} \tag{4.3}$$

$$\times \quad H_{n_1}(\sqrt{2}\,q_{\mathbf{k}}^c) H_{n_2}(\sqrt{2}\,q_{\mathbf{k}}^s).$$

Here n_1, n_2 are positive integers; H_n are the Hermitian polynomials; $\prod_{(\mathbf{k})}{}'$ denotes that the product omits the $\mathbf{k}$ which lie in the hemisphere (for example, $k_z > 0$), since $q_{\mathbf{k}}^c$ and $q_{\mathbf{k}}^s$ are connected by the relations $q_{\mathbf{k}}^c = q_{-\mathbf{k}}^c$ and $q_{\mathbf{k}}^s = -q_{-\mathbf{k}}^s$.

The function (4.3) corresponds to the energy

$$\mathcal{E} = \sum \frac{E(k)}{2}(1 + n_1 + n_2). \tag{4.4}$$

In the lowest energy state, $n_1 = n_2 = 0$ and the eigenfunction of (4.3) will be

$$\Phi_0 = \exp\left\{-\frac{1}{2}\sum_{\mathbf{k}} q_{\mathbf{k}}q_{-\mathbf{k}}\right\} \tag{4.5}$$

$$= \exp\left\{-\sum_{\mathbf{k}}\frac{\rho_{\mathbf{k}}\rho_{-\mathbf{k}}}{4\lambda_{\mathbf{k}}^2}\right\}.$$

By means of Eq. (2.7) we get for the wave function of the lowest state

$$\varphi_0 = \exp\left\{\frac{1}{4}\sum_{\mathbf{k}}\left(1 - \frac{1}{\lambda_{\mathbf{k}}^2}\right)\rho_{\mathbf{k}}\rho_{-\mathbf{k}}\right\}, \tag{4.6}$$

which coincides with the function (3.12) obtained earlier, since we have, from Eqs. (2.10) and (2.12):

$$E(k) = \hbar^2k^2/\lambda_{\mathbf{k}}^2 2m. \tag{4.7}$$

One can verify directly that the wave function (4.5) corresponds to the lowest energy level by demonstrating that the $b_{\mathbf{k}}$ --the operators of "annihilation" of phonons -- yield zero when they operate on (4.5)

The wave function of the state in which there is one phonon with wave number $\mathbf{k}$ is

$$\Phi_{\mathbf{k}} = b_{\mathbf{k}}^+\Phi_0 = \sqrt{2}\,q_{-\mathbf{k}}\Phi_0 \tag{4.8}$$

$$= \frac{1}{\lambda_{\mathbf{k}}}\frac{1}{\sqrt{N}}\sum_{j=1}^{N}\exp\{i(\mathbf{k}\mathbf{r}_j)\}\,\Phi_0.$$

In a similar way we can obtain the wave function of the state in which n phonons are present. We note that the $\rho_{\mathbf{k}}$ appear in the eigenfunctions of the ideal Bose gas, corresponding to the energy $\hbar^2k^2/2m$.

The wave functions (4.5), (4.6) and (4.8) of the lowest and excited states of a Bose gas are wave functions of zero approximation only, and are not of sufficient accuracy to permit us to find wave functions of arbitrary approximation. We shall now give an account of the method of constructing such functions for the lowest energy state of the system.

The Schrödinger equation for the system of interacting Bose particles in the $\rho_{\mathbf{k}}$ representation (2.14) can be written in the form

$$\{H_0 + H_1 + H_2\}\,\Phi = \mathcal{E}\Phi, \tag{4.9}$$

where

$$H_0 = \sum_{\mathbf{k}} E(k)\,b_{\mathbf{k}}^+b_{\mathbf{k}} + \frac{1}{\sqrt{N}} \tag{4.10}$$

$$\times \sum_{\substack{\mathbf{k}_1,\mathbf{k}_2\\ \mathbf{k}_1+\mathbf{k}_2\neq 0}} \frac{\hbar^2}{8m}(\mathbf{k}_1\mathbf{k}_2)\frac{\lambda_{\mathbf{k}_1+\mathbf{k}_2}}{\lambda_{\mathbf{k}_1}\lambda_{\mathbf{k}_2}}(b_{\mathbf{k}_1+\mathbf{k}_2} + b_{-\mathbf{k}_1-\mathbf{k}_2}^+)$$

$$\times(1 + \lambda_{\mathbf{k}_1}^2)(1 + \lambda_{\mathbf{k}_2}^2)\,b_{-\mathbf{k}_1}b_{-\mathbf{k}_2};$$

$$H_1 = -\frac{1}{\sqrt{N}}$$

$$\times \sum_{\substack{\mathbf{k}_1,\mathbf{k}_2\\ \mathbf{k}_1+\mathbf{k}_2\neq 0}} \frac{\hbar^2}{8m}(\mathbf{k}_1\mathbf{k}_2)\frac{\lambda_{\mathbf{k}_1+\mathbf{k}_2}}{\lambda_{\mathbf{k}_1}\lambda_{\mathbf{k}_2}}(b_{\mathbf{k}_1+\mathbf{k}_2} + b_{-\mathbf{k}_1-\mathbf{k}_2}^+)$$

$$\times[(1 + \lambda_{\mathbf{k}_1}^2)(1 - \lambda_{\mathbf{k}_2}^2)\,b_{\mathbf{k}_2}^+b_{-\mathbf{k}_1}$$

$$+ (1 + \lambda_{\mathbf{k}_2}^2)(1 - \lambda_{\mathbf{k}_1}^2)\,b_{\mathbf{k}_1}^+b_{-\mathbf{k}_2}],$$

$$H_2 = \frac{1}{\sqrt{N}}\sum\frac{\hbar^2}{8m}(\mathbf{k}_1\mathbf{k}_2)\frac{\lambda_{\mathbf{k}_1+\mathbf{k}_2}}{\lambda_{\mathbf{k}_1}\lambda_{\mathbf{k}_2}}$$

$$\times(b_{\mathbf{k}_1+\mathbf{k}_2} + b_{-\mathbf{k}_1-\mathbf{k}_2}^+)(1 - \lambda_{\mathbf{k}_1}^2)(1 - \lambda_{\mathbf{k}_2}^2)\,b_{\mathbf{k}_1}^+b_{\mathbf{k}_2}^+;$$

$$\mathcal{E} = E - E_0.$$

Here the Hamiltonian operator is divided into three parts: H_0, H_1, and H_2, corresponding to the zero, first, and second order relative to the small parameter

$$1 - \lambda_{\mathbf{k}}^2 = 1 - \sqrt{\frac{\hbar^2k^2/4m}{n\nu(k) + (\hbar^2k^2/4m)}}. \tag{4.11}$$

In the zeroth approximation we get the equation

$$H_0\Phi = \mathcal{E}\Phi, \tag{4.12}$$

which has the "vaccum" solution given in Eq. (4.5), $\Phi = \Phi_0$, $\mathcal{E}_0 = 0$.

The second, non-ideal part of the operator H_0 yields zero in operating Φ_0, and does not change

the wave function in zeroth approximation.

We attempt to solve the equation (4.9) with the aid of the theory of excitations. We seek a solution of Eq. (4.9) in the form

$$\Phi = \Phi_0 + \Phi_1 + \Phi_2 + \ldots; \qquad (4.13)$$
$$\mathcal{E} = \mathcal{E}_0 + \mathcal{E}_1 + \mathcal{E}_2 + \ldots,$$

where $\Phi_1, \Phi_2, \ldots$; $\mathcal{E}_1, \mathcal{E}_2, \ldots$ are the corrections of the first and second order to the wave function and the energy of the lowest state. Substituting Eq. (4.13) and comparing the terms of corresponding order, we get the following equations for the functions Φ_1, Φ_2:

$$(H_0 - \mathcal{E}_0)\Phi_1 = (\mathcal{E}_1 - H_1)\Phi_0, \qquad (4.14)$$
$$(H_0 - \mathcal{E}_0)\Phi_2 = (\mathcal{E}_1 - H_1)\Phi_1 + (\mathcal{E}_2 - H_2)\Phi_0,$$

Inasmuch as

$$H_1\Phi_0 = 0,$$

the first equation of the set (4.14) is satisfied for $\Phi_1 = 0$, $\mathcal{E}_1 = 0$, the corrections of the first approximation become zero. The second equation of the set (4.14), which gives ,i.e., the corrections to the wave function and the energy of the lowest state can be written in the form

$$(H_0 - \mathcal{E}_0)\Phi_2 = \mathcal{E}_2\Phi_0 - \frac{1}{V\overline{N}} \qquad (4.15)$$
$$\times \sum_{\substack{k_1, k_2 \\ k_1 + k_2 \neq 0}} \frac{\hbar^2}{8m}(\mathbf{k}_1\mathbf{k}_2)\frac{\lambda_{k_1+k_2}}{\lambda_{k_1}\lambda_{k_2}}(1-\lambda_{k_1}^2)$$
$$\times (1-\lambda_{k_2}^2) b^+_{-k_1-k_2} b^+_{k_1} b^+_{k_2}\Phi_0.$$

We seek the solution of this equation in the form of a decomposition in the operator $b^+_{\mathbf{k}}$

$$\Phi_2 = \sum_{\mathbf{k}} L(\mathbf{k}) b^+_{\mathbf{k}}\Phi_0 \qquad (4.16)$$
$$+ \sum_{k_1, k_2} M(\mathbf{k}_1, \mathbf{k}_2) b^+_{k_1} b^+_{k_2}\Phi_0$$
$$+ \sum_{\substack{k_1, k_2 \\ k_1 + k_2 \neq 0}} N(\mathbf{k}_1, \mathbf{k}_2) b^+_{-k_1-k_2} b^+_{k_1} b^+_{k_2}\Phi_0,$$

where the functions $L(\mathbf{k})$, $M(\mathbf{k}_1, \mathbf{k}_2)$, $N(\mathbf{k}_1, \mathbf{k}_2)$ are to be determined.

Substituting (4.16) in Eqs. (4.15) and equating coefficients for terms which contain identical operators, we get the following set of equations for the unknown functions L, M, N and $\mathcal{E}_2$:

$$E(\mathbf{k})L(\mathbf{k}) = \frac{1}{V\overline{N}}\sum_{\mathbf{k}'}\frac{\hbar^2}{4m}(\mathbf{k}', \mathbf{k}+\mathbf{k}') \qquad (4.17)$$
$$\times \frac{\lambda_k}{\lambda_{k'+k}\lambda_{k'}}(1+\lambda^2_{k+k'})(1+\lambda^2_{k'}) \times M(\mathbf{k}+\mathbf{k}', -\mathbf{k}'),$$

$$\{E(\mathbf{k}_1) + E(\mathbf{k}_2)\} M(\mathbf{k}_1, \mathbf{k}_2)$$
$$= \delta^{-k_2}_{k_1}\frac{1}{V\overline{N}}\sum_{\mathbf{k}_2'}\frac{\hbar^2}{4m}(\mathbf{k}_2', \mathbf{k}_1 + \mathbf{k}_2')\frac{\lambda_{k_1}}{\lambda_{k_1+k_2'}\lambda_{k_2'}}$$
$$\times (1+\lambda^2_{k_1+k_2'})(1+\lambda^2_{k_2'})\{N(-\mathbf{k}_1 - \mathbf{k}_2', -\mathbf{k}_2')$$
$$+ N(\mathbf{k}_1, \mathbf{k}_2') + N(\mathbf{k}_2', \mathbf{k}_1)\},$$

$$\{E(\mathbf{k}_1+\mathbf{k}_2) + E(\mathbf{k}_1) + E(\mathbf{k}_2)\} N(\mathbf{k}_1, \mathbf{k}_2) \qquad (4.18)$$
$$= -\frac{1}{V\overline{N}}\frac{\hbar^2}{8m}(\mathbf{k}_1\mathbf{k}_2)\frac{\lambda_{k_1+k_2}}{\lambda_{k_1}\lambda_{k_2}}(1-\lambda^2_{k_1})(1-\lambda^2_{k_2});$$

$$\mathcal{E}_2 = \frac{1}{V\overline{N}}\sum_{\substack{k_1, k_2 \\ k_1+k_2\neq 0}}\frac{\hbar^2}{4m}(\mathbf{k}_1\mathbf{k}_2)(1+\lambda^2_{k_1})$$
$$\times (1+\lambda^2_{k_2})\frac{\lambda_{k_1+k_2}}{\lambda_{k_1}\lambda_{k_2}}\{N(-\mathbf{k}_1, -\mathbf{k}_2) +$$
$$+ N(\mathbf{k}_1+\mathbf{k}_2, -\mathbf{k}_2) + N(-\mathbf{k}_1, \mathbf{k}_1+\mathbf{k}_2)\}.$$

We see from the second equation of (4.17) that the function $M(\mathbf{k}+\mathbf{k}', -\mathbf{k}')$ is different from zero only for $\mathbf{k} = 0$, which is impossible, since $\mathbf{k} \neq 0$, by assumption; consequently $L(k) = 0$.

We find the value of $\mathcal{E}_2$ from Eq. (4.18):

$$\mathcal{E}_2 = -\frac{2}{N} \qquad (4.19)$$
$$\times \sum_{\substack{k_1, k_2 \\ k_1+k_2\neq 0}}\left(\frac{\hbar^2}{8m}\right)^2\frac{(\mathbf{k}_1\mathbf{k}_2)(1+\lambda^2_{k_1})(1+\lambda^2_{k_2})\lambda_{k_1+k_2}}{\lambda_{k_1}\lambda_{k_2}\{E(\mathbf{k}_1+\mathbf{k}_2)+E(\mathbf{k}_1)+E(\mathbf{k}_2)\}}$$
$$\times \left\{(\mathbf{k}_1\mathbf{k}_2)\frac{\lambda_{k_1+k_2}}{\lambda_{k_1}\lambda_{k_2}} \times (1-\lambda^2_{k_1})(1-\lambda^2_{k_2})\right.$$
$$- (\mathbf{k}_2, \mathbf{k}_1+\mathbf{k}_2)\frac{\lambda_{k_1}}{\lambda_{k_1+k_2}\lambda_{k_2}}(1-\lambda^2_{k_1+k_2})(1-\lambda^2_{k_2})$$
$$\left. - (\mathbf{k}_1, \mathbf{k}_1+\mathbf{k}_2)\frac{\lambda_{k_2}}{\lambda_{k_1+k_2}\lambda_{k_1}}(1-\lambda^2_{k_1+k_2})(1-\lambda^2_{k_1})\right\}$$

Because of the practical continuity of the spectrum, we can go from the summation to integration in Eq. (4.19) and obtain an expression for $\mathcal{E}_2$ in the form

$$\mathcal{E}_2 = -\frac{2N}{(2\pi)^6 n^2}\left(\frac{\hbar^2}{8m}\right)^2 \qquad (4.20)$$
$$\times \iint \frac{(\mathbf{k}_1\mathbf{k}_2)\lambda^2_{k_1+k_2}(1-\lambda^4_{k_1})(1-\lambda^4_{k_2})d\mathbf{k}_1 d\mathbf{k}_2}{\lambda^2_{k_1}\lambda^2_{k_2}\{E(\mathbf{k}_1+\mathbf{k}_2)+E(\mathbf{k}_1)+E(\mathbf{k}_2)\}}$$

$$+\frac{4N}{(2\pi)^6 n^2}\left(\frac{\hbar^2}{8m}\right)^2$$

$$\iint \frac{(\mathbf{k}_1, \mathbf{k}_1+\mathbf{k}_2)(\mathbf{k}_1\mathbf{k}_2)(1-\lambda_{\mathbf{k}_1}^4)(1-\lambda_{\mathbf{k}_1+\mathbf{k}_2}^2)(1+\lambda_{\mathbf{k}_2}^2)\,d\mathbf{k}_1 d\mathbf{k}_2}{\lambda_{\mathbf{k}_1}^2\{E(\mathbf{k}_1+\mathbf{k}_2)+E(\mathbf{k}_1)+E(\mathbf{k}_2)\}}.$$

For second order corrections to the wave function of the lowest state, we get

$$\Phi_2 = \frac{-2}{N}\sum_{\mathbf{k}_1,\mathbf{k}_2}\left(\frac{\hbar^2}{8m}\right)^2 \tag{4.21}$$

$$\frac{(\mathbf{k}_1\mathbf{k}_2)(\mathbf{k}_2, \mathbf{k}_1+\mathbf{k}_2)(1+\lambda_{\mathbf{k}_1+\mathbf{k}_2}^2)(1-\lambda_{\mathbf{k}_1}^2)(1-\lambda_{\mathbf{k}_2}^4)\,b_{\mathbf{k}_1}^+ b_{-\mathbf{k}_1}^+\Phi_0}{\lambda_{\mathbf{k}_2}^2 E(\mathbf{k}_1)\{E(\mathbf{k}_1+\mathbf{k}_2)+E(\mathbf{k}_1)+E(\mathbf{k}_2)\}}$$

$$-\frac{1}{\sqrt{N}}$$

$$\sum_{\substack{\mathbf{k}_1,\mathbf{k}_2\\ \mathbf{k}_1+\mathbf{k}_2\neq 0}}\frac{\hbar^2}{8m}\,\frac{(\mathbf{k}_1\mathbf{k}_2)\lambda_{\mathbf{k}_1+\mathbf{k}_2}(1-\lambda_{\mathbf{k}_1}^2)(1-\lambda_{\mathbf{k}_2}^2)\,b_{-\mathbf{k}_1-\mathbf{k}_2}^+ b_{\mathbf{k}_1}^+ b_{\mathbf{k}_2}^+\Phi_0}{\lambda_{\mathbf{k}_1}\lambda_{\mathbf{k}_2}\{E(\mathbf{k}_1+\mathbf{k}_2)+E(\mathbf{k}_1)+E(\mathbf{k}_2)\}}$$

$$+\frac{1}{N}\sum_{\mathbf{k}_1,\mathbf{k}_2}\left(\frac{\hbar^2}{8m}\right)^2$$

$$\times\,\frac{(\mathbf{k}_2,\mathbf{k}_1+\mathbf{k}_2)^2\lambda_{\mathbf{k}_1}^2(1-\lambda_{\mathbf{k}_1+\mathbf{k}_2}^4)(1-\lambda_{\mathbf{k}_2}^4)\,b_{\mathbf{k}_1}^+ b_{-\mathbf{k}_1}^+\Phi_0}{\lambda_{\mathbf{k}_1+\mathbf{k}_2}^2\lambda_{\mathbf{k}_2}^2 E(\mathbf{k}_1)\{E(\mathbf{k}_1+\mathbf{k}_2)+E(\mathbf{k}_1)+E(\mathbf{k}_2)\}}.$$

With the aid of Eqs. (4.5), (2.13), (2.9) and (2.1) we can represent (4.21) in the form of an explicit function of coordinates.

By a suitable method we can determine Φ_3 and higher terms of the decomposition of the wave function of the lowest state of the Bose gas in powers of the parameter of the smallness of the interaction.

The method of the "auxiliary variables" developed above for application to the Bose gas has a simple relation to the method of approximate second quantization of the weakly non-ideal Bose gas [2].

We express ρ_k (2.1) in the representation of second quantization in momentum space:

$$\rho_{\mathbf{k}} = \frac{1}{\sqrt{N}}\sum_{\mathbf{f}} a_{\mathbf{f}-\mathbf{k}}^+ a_{\mathbf{f}} \quad (\mathbf{k}\neq 0), \tag{4.22}$$

where a_f^+, a_f are Bose operators. We separate in Eq. (4.22) terms which contain Bose operators with zero momentum and write ρ_k in the form

$$\rho_{\mathbf{k}} = \frac{a_{-\mathbf{k}}^+ a_0}{\sqrt{N}} + \frac{a_0^+ a_{\mathbf{k}}}{\sqrt{N}} + \frac{1}{\sqrt{N}}\sum_{\substack{\mathbf{f}\\ (\mathbf{f}\neq 0,\ \mathbf{f}\neq\mathbf{k})}} a_{\mathbf{f}-\mathbf{k}}^+ a_{\mathbf{f}}. \tag{4.23}$$

The first two terms in (4.23) represent the Bose operators b_k and b_k^+ which were used in our previous work [2].

We note that the wave function of the elementary excitations of the zeroth approximation (4.8) is identical in form with the function hypothesized by Feynman in his work on the theory of superfluidity of He II [8]. The correlation function of the zeroth approximation, which can be calculated with the help of the variation derivative of the energy of the lowest state (2.15) with respect to the function of interaction by the relation

$$g(r) = \frac{2V}{N^2}\,\frac{\delta E_0}{\delta\Phi(r)}, \tag{4.24}$$

is also identical to the correlation function calculated by Feynman. Thus we see that the results of Feynman agree with the zeroth approximation of our method. The further development of the methods of the present work can serve as the basis for improving the theory of superfluidity of He II.

Translated by R. T. Beyer
22

[8] R. P. Feynman, Phys. Rev. 94, 262 (1954)

SOVIET PHYSICS - JETP VOLUME 1, NUMBER 1 JULY, 1955

The Structure of Superconductors VIII. X-ray and Metallographic Investigations of the System Bismuth - Rhodium.

N. N. ZHURAVLEV AND G. S. ZHDANOV
Moscow Institute of Engineering Physics

(Submitted to JETP editor February 24, 1954)
J. Exper. Theoret. Phys. USSR 28, 228 - 236 (February, 1955)

The system Bi-Rh has been investigated metallographically and by x-rays and has been found to contain three compounds: BiRh, Bi_2Rh in two modifications, and Bi_4Rh in three modifications. Crystals have been obtained and the primitive cell and space group determined for α-Bi_4Rh and the primitive cell for α- and β-Bi_2Rh.

THE structural diagram of the system bismuth-rhodium (Fig. 1) has been determined by

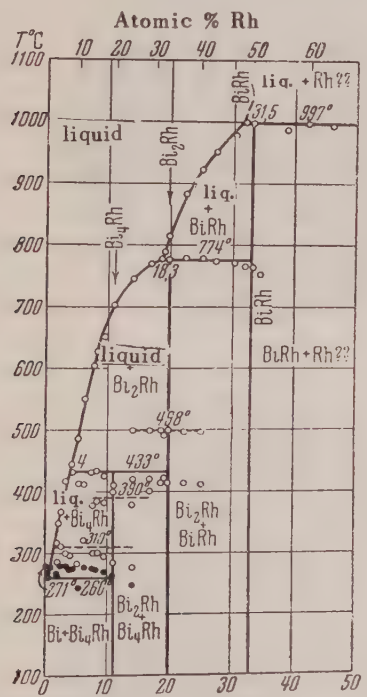

Fig. 1. Diagram of the System Bi - Rh

Rode[1] on the basis of thermal and metallographic analysis.

According to the findings of Alekseevskii[2], all compounds in this system (Bi_4Rh, Bi_2Rh and BiRh) can be obtained in the superconducting state. However a series of essential questions has remained obscure. The majority of alloys having the compositions Bi_2Rh and Bi_4Rh had superconducting transition temperatures T_k in the vicinity of 3.4° K. In some cases alloys of composition Bi_4Rh passed into the superconducting state at temperatures in the neighborhood of 2.9° K. For a series of specimens of Bi_4Rh it was possible to observe both transition points to the superconducting state. After annealing, alloys of composition Bi_4Rh and Bi_2Rh lost the capability of becoming superconducting while annealed alloys of composition BiRh preserved this capability. The temperature T_k for annealed as well as for unannealed alloys of composition BiRh lies in the vicinity of 2° K although the transition temperature in various specimens varies within a range of several tenths of a degree. These small fluctuations, as has been shown by the work of one of us with Glagoleva[3], can be explained by small changes in phase composition under annealing, since BiRh constitutes a phase of variable composition. The clarification of the other points mentioned above required a deeper investigation of this system and the employement of both metallographic methods of inquiry, x-ray methods of analysis as well as measurement of micro-hardness and, in individual cases, of the density of compounds.

Preparation of Alloys. Bismuth of purity 99.95% and rhodium of analyticaly purity (domestic sources) were employed for the preparation of the alloys. Part of the alloys were prepared in the laboratory of N. E. Alekseevskii at the Institute for Physical Problems of the Academy of Sciences, USSR, and part in the laboratory of the Moscow In-

[1] E. J. Rode, Communications of the Platinum Institute 7, 21 (1929)

[2] N. E. Alekseevskii, n. V. Brandt and T. I. Kostina, Izv. Akad. Nauk SSSR, Phys. Ser. 16, 233 (1952)

[3] V. P. Glagoleva and G. S. Zhdanov, J. Exper. Theoret. Phys. USSR 25, 485 (1953)

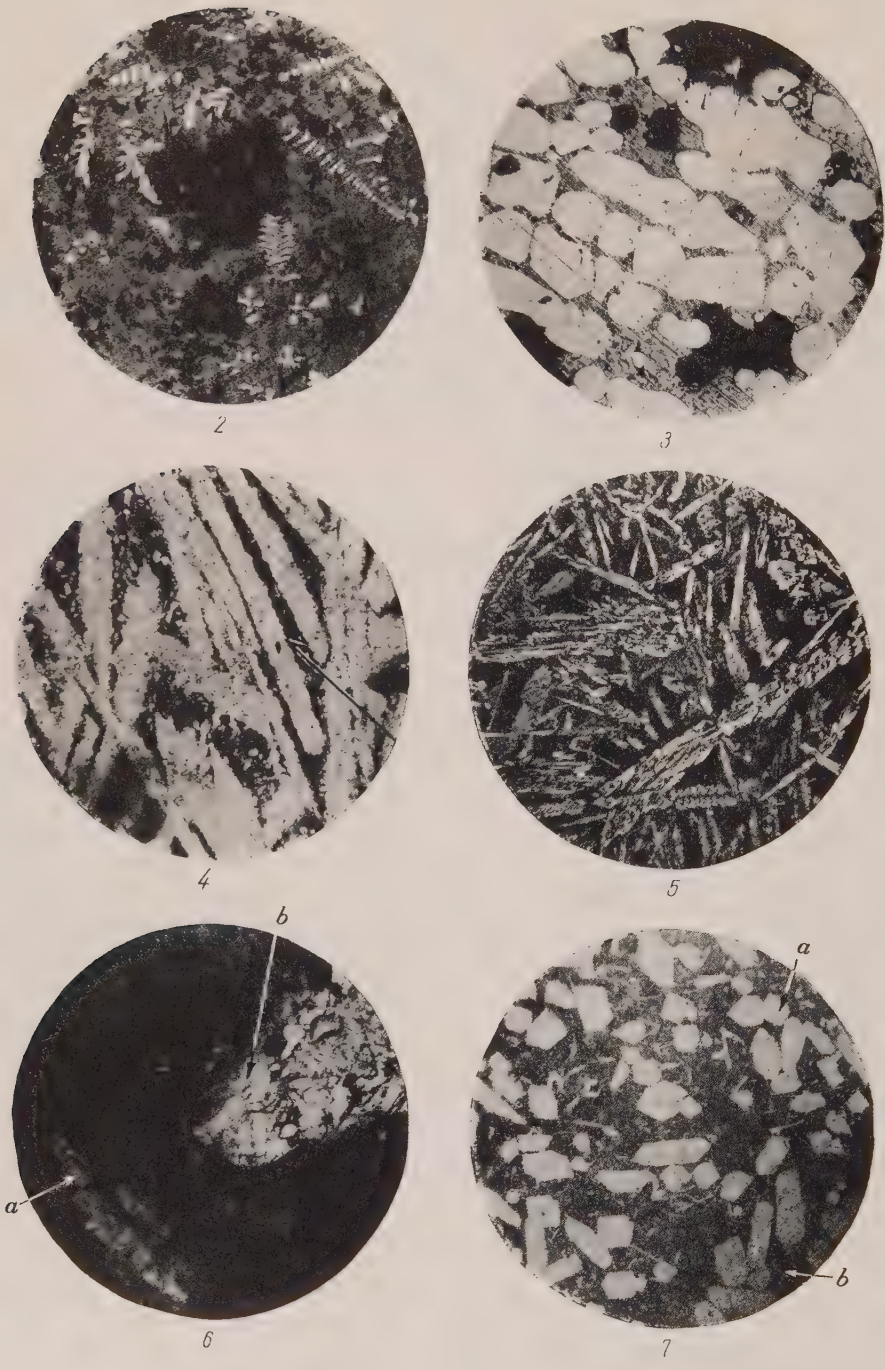

Fig. 2. 43 % Rh by wt. Etched by concentrated HNO_3. Magnification 134.
Fig. 3. 70 % Rh by wt. Etched by concentrated HNO_3. Magnification 57.
Fig. 4. 11.01 % Rh by wt. Etched by KI + I. Magnification 57.
Fig. 5. 3.5 % Rh by wt. Etched by KI + I. Magnification 57.
Fig. 6. Surface of laminar and needle shaped crystals. Magnification 57.
Fig. 7. 3.5 % Rh by wt. Etched by KI + I. Magnification 134.

stitute for Engineering Physics. Melting was carried out in an atmosphere of inert gas (helium, argon) in sealed quartz ampules in a high frequency furnace, in a resistance furnace and in a gas jet flame.

The alloying of bismuth with rhodium was carried out in various proportions by weight. Annealed alloys were investigated as well as those quenched at various temperatures and at various rates of cooling.

Microstructure. For the preparation of section slides alloys were poured over sulphur or over a special cement. A solution of iodine in potassium iodide was employed as an etching agent for metallographic analysis principally for alloys with a large content of bismuth, and nitric acid and aqua regia were employed for alloys rich in rhodium.

The microstructures which we observed in the region from approximately pure bismuth to 50% rhodium by weight were similar to those adduced in reference 1.

Alloys rich in rhodium, which were not investigated by Rode, show a double phased structure. Alloys ranging from the compound BiRh to pure rhodium consist of a mixture of crystals of BiRh in rhodium, the number of rhodium crystals increasing with the rise in the total content of rhodium in the alloy. Rhodium can crystallize in the form of dendrites (Fig. 2) as well as in single crystals of irregular shape (Fig. 3). X-raygrams taken by using x-radiation from copper on alloys rich in rhodium support the metallographic observations.

Precise x-raygrams were obtained from alloys which were rich in rhodium and which were annealed for 50 hours at a temperature of 1100° C, using x-radiation from copper in an RKU camera of diameter 114 mm. These x-raygrams were used to determine the lattice period of rhodium crystals in the alloy. Within the limits of experimental error the magnitude of this period coincides with the period of pure rhodium, a result which indicates the negligible solubility of bismuth in rhodium in contrast to our findings of significant solubility of bismuth[4], as well as of antimony and lead[5] in palladium. It is interesting to note that while rhodium and palladium have the same crystal structure, comparable lattice parameters and atomic radii, and are neighbors in the Periodic Table, they behave differently with respect to solubility of bismuth. Doubtless this result is connected with the differences in the electronic structures of the atoms of rhodium and palladium and shows the inadequacy of purely geometrical investigations of solid solutions, an inadequacy one often finds in the metallographic literature.

THE COMPOUND Bi_4Rh AND ITS POLYMORPHIC MODIFICATIONS

Alloys corresponding to the composition Bi_4Rh (11.01% Rh by weight), under customary conditions of cooling, turn out to be heterogeneous as a consequence of the incompleteness of the peritectic reaction. Sections obtained from such alloys show the existence of several phases. On the microphotograph of Fig. 4 there are seen initial separations of Bi_2Rh which did not succeed in reacting with the liquid alloy, and which appear as gray dendrites surrounded by a later growth of a thin (1-10 μ) film of crystals of Bi_4Rh (shown by the arrow in the Figure). The dark etched places correspond to the eutectic which is composed principally of bismuth (99.3% by weight). In all probability, the film of Bi_4Rh obstructs the entry of crystals of Bi_2Rh into reaction with the bismuth of the eutectic. Continued heating at a temperature sufficient for the conduct of a process of diffusion between the bismuth of the eutectic and Bi_2Rh permits the reaction to go to completion, resulting in the formation of the low-temperature modification of Bi_4Rh. According to the observations of Alekseevskii[2], and our findings, this temperature lies above 100° C. A heterogeneous alloy of Bi_4Rh annealed for 16 hours at a temperature of 200° C, after annealing, showed a uniform structure under metallographic and x-ray analysis. Alloys obtained through different rates of cooling differ with respect to the number of phases.

A powder x-raygram obtained from a conventionally cooled specimen shows, on a strong background, many weak lines which are hard to measure. The interpretation of this x-raygram is extremely intricate, since all three phases have complex structures with a large number of superimposed lines. In addition to the large number of lines and their superpositions, there is involved the effect of line diffusion, ensuing from the smallness of the crystals of Bi_4Rh and from stresses.

As noted by Rode, a well defined temperature pause occurs in the alloy at the temperature $\sim 310°$, and a weakly defined one at the temperature $\sim 390°$; these correspond, according to Rode's surmise, to polymorphic transformations of Bi_4Rh.

Investigations by Alekseevskii[2] on the super-

[4] N. N. Zhuravlev and G. S. Zhdanov, J. Exper. Theoret. Phys. USSR 25, 485 (1953)

[5] M. Hansen, *The Structure of Binary Alloys* (1941)

conducting properties of alloys of this composition showed that only the unannealed specimens passed into the superconducting state thus indicating the presence of polymorphic transformations. We made an attempt to obtain a high temperature modification of Bi_4Rh by way of quenching, in water at 20°C and in ethyl alcohol at – 55°C, crystals of the low temperature modification of Bi_4Rh heated to various temperatures from 300° to 430°C. This attempt did not lead to the expected results.

It is interesting to note that x-raygrams taken from quenched crystals had clearer lines than those taken from crystals separated from annealed alloys. This fact is indicative of the relaxation of stresses in the crystals. It was decided to obtain quenched crystals of Bi_4Rh by separation from the alloy ingot. To this end, an alloy containing 3.5% by weight of Rh was used on the basis that, irrespective of the rapidity of cooling of such an alloy from a temperature slightly (10-20°) lower than the melting point of Bi_4Rh (433°), a two-phase alloy would be formed consisting of the eutectic and crystals of Bi_4Rh. Such an alloy was obtained. Figure 5 is a microphotograph showing crystals of Bi_4Rh imbedded in a mass of eutectic. Crystals of Bi_4Rh were separated in the form of a black powder by dissolving the bismuth in dilute nitric acid. From the powder x-raygram of the crystals separated in this way it is difficult to judge the crystal structure, since the photographs show weak lines on a strong background. Evidently the cause of this appearance of the x-raygrams is tied to the smallness of the crystals (1-25 μ as determined from the microphotographs) and the magnitude of the stresses in the crystals, both of which lead to strong diffusion of lines.

Crystals of larger size were obtained from a later melt, which was cooled less rapidly. Crystals of Bi_4Rh, separated by the process of dissolving bismuth in dilute nitric acid, had dominantly needle shaped forms, a fact which has also been noted by Rossler (see reference 5). In the mass of needle shaped crystals there were also observed single crystals in the form of thin laminas. Observation of the needle shaped crystals under a microscope disclosed growths of needles in the form of "brooms", growths in the form of packets of crystals, as well as single needles. Cross sections of needle shaped crystals are rectangular or close thereto.

In the microphotograph shown in Fig. 6, the arrow *a* points to a packet growth of crystals of Bi_4Rh; the rectangularity of the crystal cross sections can also be seen. Probably these crystals are associated with one of the orthogonal systems. Microscopic investigation of the laminar crystals shows that they are of a character significantly different from the needle shaped ones and probably belong to a third modification of Bi_4Rh. Arrow *b* in Fig. 6 shows a laminar crystal whose plane lies in the plane of the microphotograph. It is interesting to point out that on the laminar crystals which have been studied, cleavage lines can clearly be observed inclined at angles of approximately 120°. This fact allows the presumption that these crystals belong to the hexagonal system with the hexagonal axis being located at right angles to the plane of the lamina.

The discovery of three habit forms for the crystals of Bi_4Rh underlies the possibility of the existence of three modifications of the compound Bi_4Rh which we will call α (low temperature), β (needle shaped) and γ (laminar). Modifications β-Bi_4Rh and γ-Bi_4Rh can be obtained by rapid cooling from temperatures in the interval 310-390° for β-Bi_4Rh (in accord with the structural diagram) and in the interval 390-433° for γ-Bi_4Rh. The quenching temperatures must be reached by cooling the alloy from a temperature higher than the melting point of Bi_4Rh (433°), this being essential if crystals of the α- modification are to be eliminated.

Crystals obtained from an alloy of composition 3.5% by weight of rhodium, and quenched at a temperature of 350° C, had primarily the needle shaped form and represented β-Bi_4Rh. Crystals obtained from an alloy of the same composition, but quenched at a temperature of 420° C, had primarily laminar form and represented γ-Bi_4Rh. In Fig. 7 a microphotograph is shown of an alloy of composition 3.5% rhodium by weight, quenched at a temperature of 350° C, in which the needle shaped crystals can be seen in cross section (arrow *a*) among the mass of eutectic and, in small amount, the laminar crystals (arrow *b*).

As mentioned previously, attempts to obtain the modifications β and γ-Bi_4Rh by annealing crystals of α-Bi_4Rh in the intervals of temperatures 310-390° and 390-433°, and by subsequent quenching in water and in ethyl alcohol, did not succeed. Experiments were also made to obtain these modifications by way of annealing and quenching heterogeneous alloys containing bismuth along with α-Bi_4Rh. Heterogeneous alloys were obtained of compositions 3.5 and 9% rhodium by weight, containing the eutectic and crystals of α-Bi_4Rh; these alloys were heated in argon

filled glass ampules up to the temperature 400-420° C and held for 3-6 hours, after which they were quickly cooled in water. After such quenching the alloy became very friable; it was possible to separate single crystals from it by mechanical means. By measurement of microhardness, and checking by x-ray analysis, it was established that these crystals represent ∝- Bi_4Rh. The friability of bismuth attests to the great rapidity of cooling, which it was not possible to obtain in cooling alloys in quartz ampules. It is interesting to note that alloys of composition 3.5% rhodium by weight, cooled from higher temperature, broke up into powder as if disintegrating. The quenching of pure bismuth at the temperature 700°C produced this effect and could evidently be explained by the increase in volume of bismuth on crystallization. Accordingly, to obtain high temperature modifications of Bi_4Rh from crystals of ∝-Bi_4Rh, it is probably essential that a prolonged period of time be allowed for the conduct of the process of diffusion through which these modifications are produced. The reverse diffusion process for the passage of high temperature modifications of Bi_4Rh into ∝-Bi_4Rh, as was mentioned previously, takes place at temperatures exceeding 100°C.

Powder x-raygrams of the three modifications, obtained on irradiation by K∝- copper, have distinct dispositions of lines pointing to the existence of distinct crystalline structures.

THE PRODUCTION OF CRYSTALS AND STRUCTURAL STUDIES OF THE MODIFICATION ∝-Bi_4Rh.

Crystals of ∝-Bi_4Rh were obtained by growth in the mother liquor and subsequent separation by way of dissolving the bismuth. An alloy consisting of 3% rhodium by weight was chosen which, with appropriate heat treatment, contained the eutectic and crystals of ∝-Bi_4Rh. The alloy was prepared in a quartz ampule containing argon. Melting was carried out in a resistance furnace. The temperature of the furnace was carried to 650-700°C, the rhodium dissolved in the bismuth, and the furnace was slowly cooled to a temperature of 350-400°C. The alloy was held at this temperature for two hours (in order that the reaction might be fully completed) and was then cooled to room temperature, together with the furnace. Phase composition was checked by metallographic analysis. If the existence of two phases was detected the alloy was annealed at 300-350°C for 20-40 hours. As a result of such heat treatment there were formed large crystals of ∝-Bi_4Rh with linear sections of 0.3-0.5 mm. In Fig. 8 there is shown a microphotograph of such an alloy; on the dark background of the etched eutectic are seen the bright crystals ∝-Bi_4Rh. The crystals of ∝-Bi_4Rh were separated from the alloy by dissolving the bismuth in 25% nitric acid. The crystals of ∝-Bi_4Rh are silver-gray in color, crystallize in polyhedral shapes, the faces of which give good optical reflections. The more perfect of the separated crystals were chosen for x-ray structural studies. It was established by Laue diagrams that the crystals belong to the cubic system and the diffraction class $O_h = m3m$, and by vibration x-raygrams that the crystals have a body-centered unit cell with the period $a = 14.9 \pm 0.2$ Å. After greater precision was attained by the method of Umanskii and Kvitka[6] through the reflection of 1860 at the angle 78° 59′ from the radiation of copper in a camera of diameter 144.4 mm, it was found that

$$a = 14.928 \pm 0.005 \text{ Å}.$$

X-ray density $\sigma_x = 11.24$ gm/cm^3. The unit cell contains 24 weight units which corresponds to 120 atoms of bismuth and rhodium. As a result of the indications of the series of vibration and rotation x-raygrams the extinction law was established, and from this followed x-ray group No. 115[7], containing the single-space group O_h^{10}— $Ia3d$.

THE COMPOUND Bi_2Rh AND ITS POLYMORPHIC MODIFICATIONS

According to the structural diagram (Fig. 1) the compound Bi_2Rh is formed by a peritectic reaction. Conventionally cooled alloys turn out to be heterogeneous as a consequence of the incompleteness of the peritectic reaction. Alloys obtained by different rates of cooling differ with respect to the number of phases. In such alloys the fundamental phase is the high temperature modification β-Bi_2Rh, with small quantities of Bi_4Rh, and, occasionally, bismuth and BiRh. Figure 9 shows a microphotograph of a conventionally cooled alloy where the basic gray mass consists of β-Bi_2Rh, the bright dendrites are BiRh, and the strongly etched dark places are Bi_4Rh. A powder x-raygram obtained from such an alloy shows, on a strong background, many weak lines which are difficult to measure.

[6] M. M. Umanskii and S. S. Kvitka, Izv. Akad. Nauk SSSR, Phys. Ser. 15, 153 (1953)

[7] G. S. Zhdanov and V. A. Pospelov, J. Exper. Theoret. Phys. USSR 15, 709 (1945)

Fig. 8. 3 % Rh by wt. Etched by KI + I. Magnification 57.
Fig. 9. 19.81 % Rh by wt. Etched by concentrated HNO_3. Magnification 255.
Fig. 10. 17 % Rh by wt. Etched by 35 % HNO_3. Magnification 57.
Fig. 11. Section of a high temperature modification. Magnification 57.
Fig. 12. Surface of the alloy 21.5 % Rh by wt. Magnification 55.

Crystals were obtained of the low and high temperature modifications of Bi_2Rh. To obtain α-Bi_2Rh an alloy containing 17% by weight of rhodium was employed. The alloy was prepared in a quartz ampule in an atmosphere of argon. Melting was carried out in a resistance furnace. The temperature of the furnace was carried to 900-1000°C, the rhodium dissolved in bismuth, and the furnace was slowly cooled to a temperature of 450-480°C. The alloy was held at this temperature for 15-20 hours, after which it was cooled together with the furnace. In Fig. 10 is presented a microphotograph of such an alloy in which the large light crystals are those of α-Bi_2Rh and the etched places, Bi_4Rh and bismuth. Crystals of α-Bi_2Rh were separated from the alloy by dissolving the Bi_2Rh and bismuth in 35% nitric acid at 40-50°C. Crystals of α-Bi_2Rh had laminar form, were of a dull gray color, and the faces were not reflecting. Powder x-raygrams of such crystals show the presence of many clear lines. Through a preliminary structural x-ray study, carried out with a monocrystalline growth, it is possible to assign the crystal α-Bi_2Rh to the rhombic system with the periods:

$$a = 5.9 \pm 0.3\ \text{Å},\ b = 6.8 \pm 0.3\ \text{Å},\ c = 7.2 \pm 0.3\ \text{Å}.$$

The elementary cell contains 4 parts by weight, that is, 12 atoms.

Alloys containing the high temperature modification of Bi_2Rh have a flaky character. From ingots of the alloy it is possible to split off mechanically very thin (several hundredths of a millimeter) laminas with good optical reflections. Figure 11 shows a microphotograph of a split from such an alloy. In spite of the great care which was used, it was not possible to separate, by mechanical means, crystals of β-Bi_2Rh which would be useful for x-ray study, because the laminas were too easily deformed during the separation. In order to obtain underformed crystals of β-Bi_2Rh, alloys were employed whose composition was richer in bismuth than would correspond to stoichiometric proportions. As was mentioned previously, such alloys, under rapid cooling, are characterized by reticular and needle shaped structures of crystals of β-Bi_2Rh surrounded by thin layers of crystals of Bi_4Rh (Fig. 5). In the spacesbetween crystals the lattice is filled with bismuth. The thickness of the layers of crystals of Bi_4Rh depends on the rapidity of cooling of the alloys. Crystals of β-Bi_2Rh were separated by dissolving bismuth and Bi_4Rh in dilute nitric acid.

According to the structural diagram, and as was shown above, the compound Bi_2Rh can exist in two modifications: α-Bi_2Rh formed as a result of slow cooling of the alloys and β-Bi_2Rh obtained as a result of rapid cooling of the alloys. The passage of the crystals of β-Bi_2Rh into α-Bi_2Rh takes place comparatively rapidly under annealing of the crystals of β-Bi_2Rh at temperatures not exceeding 498°C. The reverse passage of α-Bi_2Rh into β-Bi_2Rh requires more prolonged annealing in the temperature interval 498-774°C. Probably β-Bi_2Rh exists in some region of concentrations. The variation in microhardness of the crystals of α-Bi_2Rh in various alloys over a wide range (70-330 kg/mm^2) can be explained in the light of this fact.

Co-crystallization of the two modifications of Bi_2Rh was observed by us on the surface of ingots of the alloy containing a shortage of rhodium in proportion to the stoichiometric composition of Bi_2Rh. If we exclude the effect of differences in the rate of cooling in various parts of the alloy, then the co-crystallization can be viewed as an indication of the difference in the composition of the different modifications. Figure 12 shows a microphotograph of the surface of an alloy containing 21.5% by weight of rhodium in which the large dark rhombic crystals correspond to α-Bi_2Rh (probably α-Bi_2Rh crystallizes in the form of rhombic bipyramids) while the light laminar crystals correspond to β-Bi_2Rh. There were also observed a small quantity of the dendrites of BiRh shown by the arrow in Fig. 12*b*.

THE COMPOSITION BiRh

Investigation of phase composition in the region of the compound BiRh supports the structural diagram of Rode. Facts about the solubility of bismuth in BiRh and the crystal structure of BiRh were published in reference 3.

DENSITY AND MICROHARDNESS OF COMPOUNDS

Table I lists the densities σ_x calculated from the results of x-ray analysis and σ_{hydr} determined by hydrostatic weighing in carbon tetrachloride of the crystals of Bi_4Rh and Bi_2Rh. The density of BiRh is reduced from the data of Glagoleva and Zhdanov[3].

Microhardness of the compounds was measured on the apparatus PMT-3 with a constant loading of 10 gms on the indentor. Measurements were carried out on crystals in the alloys as well as on crystals separated from the alloys and in an isolated state. Measurements were made on several specimens from

TABLE I

Compound	At Room Temperature gms/cm³	
	σ_{hydr}	σ_x
α-Bi_4Rh	11.0	11.24
β-Bi_4Rh	10.7	—
γ-Bi_4Rh	10.7	—
α-Bi_2Rh	12.2	12
β-Bi_2Rh	11.4	11.6
BiRh	12.5	12.65

TABLE II

Compound	Mean microhardness in kg/mm²	Limits of variation of microhardness
α-Bi_4Rh	105	95—115
β-Bi_4Rh	65	60—70
γ-Bi_4Rh	40*	30—55
α-Bi_2Rh	230	210—260
β-Bi_2Rh	45	40—50
BiRh	410	370—450

* Measured with a load of 5 gms on the identor.

various alloys and the results were averaged. The conditions of measurement and the preparation of the surfaces of the specimens were the same within practical limits.

Table II lists the mean microhardness and the limits of its variation for isolated crystals of the compounds.

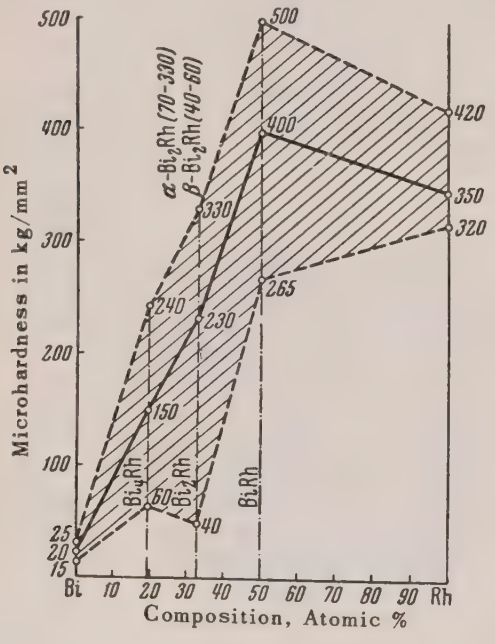

Fig. 13. Plot of the microhardness of crystals of compounds in the alloy.

In Fig. 13 is given a plot of the microhardness of compounds in the system bismuth-rhodium; the thick line gives the mean microhardness, while the dashed line gives the limits of variation of the microhardness, which fall within the limits of accuracy of the measurements. The results can be explained in a number of ways:

1) for the compound BiRh the small range of hardness may be explained by the solubility of bismuth in BiRh[3];

2) for Bi_2Rh and Bi_4Rh it is necessary to take into account the existence of several modifications with different hardness, as well as the effect of the size of crystals in the alloy; moreover, for Bi_2Rh the possibility of the existence in the compound of some homogeneous region is not to be excluded;

3) the microhardness of rhodium is measured on crystals of rhodium in alloys rich in rhodium; the range of microhardness can be explained by the effect of crystal size.

Figure 13 shows that in the system bismuth-rhodium the mean microhardness of the compounds increases with a rise in the content of rhodium, and that the microhardness of the compound (BiRh) rich in rhodium is greater than the microhardness of crystals of rhodium in the alloy. Similarly to the microhardness, there can be noted the increase in density of the low temperature modifications of the compounds with an increase in their rhodium content.

CONCLUSIONS

1. In the system bismuth-rhodium the existence of three compounds is confirmed: Bi_4Rh, Bi_2Rh and BiRh.

2. The compound Bi_4Rh has three modifications: α (low temperature) — with crystals in the form of polyhedra, β (medium temperature) — with needle shaped crystals and γ (high temperature) — with laminar crystals.

α-Bi_4Rh crystallizes in the cubic system with the period $a = 14.928 \pm 0.005$ Å. The elementary cell contains 24 parts by weight, which corresponds to 120 atoms; $\sigma_x = 11.24$ gm/cm³. The space

group is $O_h^{10} - Ia3d$. By habit the crystals of β-Bi_4Rh belong to the orthogonal system, while those of γ-Bi_4Rh belong to the hexagonal system.

3. The compound Bi_2Rh has two modifications: α (low temperature) and β (high temperature). α-Bi_2Rh crystallizes in the rhombic system: $a = 5.9 \pm 0.3$ Å; $b = 6.8 \pm 0.3$ Å; $c = 7.2 \pm 0.3$ Å. In the elementary cell there are four parts by weight, or 12 atoms: $\sigma_x = 12.1$ gm/cm^3; β-Bi_2Rh crystallizes in the monoclinic system: $a = 16.2 \pm 0.1$ Å; $b = 7.0 \pm 0.1$ Å; $c = 10.3 \pm 0.1$ Å; $\beta = 92°30'$. In the elementary cell there are 16 parts by weight, or 48 atoms; $\sigma_x = 11.6$ gm/cm^3 (see Supplement).

4. Alloys rich in rhodium have a two phase character consisting of BiRh and rhodium.

5. The solubility of bismuth in rhodium is very slight and cannot be shown by x-ray analysis.

6. The density and microhardness of compounds in the system bismuth-rhodium have been determined.

We express deep gratitude to Prof. N. E. Alekseevskii and to V. P. Glagoleva for productive collaboration and for joint discussion of the results of the work. We also express thanks to I. I. Lifanov and N. P. Ivanova, E. I. Michurina and N. S. Seryeiko for assistance in the preparation of alloys, preparation of x-raygrams and microsections.

SUPPLEMENT

THE X-RAY DETERMINATION OF THE ELEMENTARY CELL OF β-Bi_2Rh.

Crystals of β-Bi_2Rh constitute thin laminas with two reflecting faces. Through a Laue diagram the crystals of β-Bi_2Rh was placed in the monoclinic system. The period along the monoclinic axis b, lying in the plane of the lamina, was obtained by a rotation x-raygram, $b = 7.0 \pm 0.1$ Å. The periods a, c and the angle between them, were determined from the evolvement of three layer lines from an x-ray goniometer with a cylindrical film while the crystal was rotated about the axis b. It was found:

$a = 16.2 \pm 0.1$ Å; $c = 10.5 \pm 0.1$ Å; $\beta = 92°30''$

X-ray density $\sigma_x = 11.6$ gm/cm^3, with the number of parts by weight per unit cell being $Z = 16$, corresponding to 48 atoms.

Translated by N. E. Golovin
33

SOVIET PHYSICS-JETP VOLUME 1, NUMBER 1 JULY, 1955

The Problem of the Superconductivity of the Compounds Bi_4Rh and Bi_2Rh

N. E. Alekseevskii, G. S. Zhdanov and N. N. Zhuravlev
The Institute for Physical Problems of the Academy of Sciences, USSR
The Moscow Institute of Engineering Physics
(Submitted to JETP editor February 24, 1954)
J. Exper. Theoret. Phys. USSR 28, 237-240 (February, 1955)

The temperature of transition into the superconducting state of the crystals of β and α-Bi_4Rh are determined. An explanation is given of unstable behavior of the superconducting alloys of bismuth with rhodium.

As reported earlier [1], alloys of composition Bi_4Rh and Bi_2Rh show superconductivity when they have not been annealed, and have transition temperatures, independent of composition, lying in the vicinity of 2.9° and 3.4 °K. Specimens of the same composition which have been annealed do not show superconductivity. In order that the specimens may again become superconducting, it is necessary to remelt them. It was also noted that the majority of specimens of Bi_4Rh and Bi_2Rh, after the second remelting, gave a transition temperature in the neighborhood of 3.4 °K. In the case of several specimens of alloys of composition Bi_4Rh, it was possible to observe a discontinuity in the critical field curve corresponding to the existence of two points of transition into the superconducting state from $T_k = 3.4$ and $T_k = 2.9°$ K.

The fact that, after annealing, specimens lost the capacity of becoming superconducting was considered to be indicative of the existence of superconducting high temperature modifications of the compound Bi_2Rh and Bi_4Rh. The disappearance of superconductivity in annealed speci-

[1] N. E. Alekseevskii, N. B. Brandt and T. I. Kostina, Izv. Akad. Nauk SSSR Ser. Fiz. 16, 233 (1952)

mens is explained by the polymorphic transformation of the modifications mentioned above.

The loss of superconductivity after annealing at temperatures slightly above 100 °C, as well as the sharp change in the coefficient of expansion in the temperature interval 100-120 °C, which was discovered during dilatometric measurements of two specimens of Bi_4Rh*, give some indication of the presence of polymorphic transformations in this temperature region.

Metallographic and x-raygraphic investigations[2] of alloys in the neighborhood of compositions Bi_4Rh and Bi_2Rh were confirmed by the existence of several modifications of these compounds with points of polymorphic transition in agreement with the structural diagram of this system first investigated by Rode[3]. Investigation of the compound Bi_4Rh showed that it can be obtained in three modifications : α- Bi_4Rh-low temperature, β-Bi_4Rh-middle temperature and γ-Bi_4Rh- high temperature form.

Crystals of α-Bi_4Rh (separated from annealed alloys with 3% by weight of rhodium) crystallize into the cubic system with the period $a = 14.928 \pm 0.005$ Å. The elementary cell contains 24 parts by weight, or 120 atoms of rhodium and bismuth; $\sigma_x = 11.24$ gm/cm^3. The space group is O_h^{10} - $Ia3d$. The α modification of Bi_4Rh does not become superconducting down to the temperature 0.1 °K[4]. Crystals of β-Bi_4Rh separated from an alloy containing 3.5% of rhodium by weight, and quenched at a temperature of 300 °- 390 °C, pass into the superconducting state at the temperature $T = 3.2$ °K. Crystals of γ- Bi_4Rh separated from the same alloy and quenched from a temperature close to the melting point of this compound, show superconductivity at $T = 2.7$ °K.

The transition temperatures of specimens previously observed at 3.4 ° and 2.9 °K obviously were determined by the presence in them of the β and γ phases. The higher T_k of these specimens (in comparison with the T_k of the pure phases) most probably can be explained either by the partial solution of other components of the alloy in the superconducting compound, or by the great internal stresses arising in a heterogeneous specimen.

The compound Bi_2Rh can be obtained in two modifications: α-Bi_2Rh-low temperature and β-Bi_2Rh -the high temperature form. Crystals of α-Bi_2Rh (separated from annealed alloys containing 17% of rhodium by weight) crystallize into the rhombic system with the periods $a = 5.9 \pm 0.34$ Å; $b = 6.8 \pm 0.3$ Å and $c = 7.2 \pm 0.3$ Å. The elementary cell contains 4 parts by weight, $\sigma_x = 12.1$ gm/cm^3. Crystals of α-Bi_2Rh do not pass into the superconducting state down to the temperature 1.34 °K. Crystals of β-Bi_2Rh, separated from an alloy containing 14 to 17% by weight of rhodium, quenched from a temperature close to the melting point of this compound, crystallize into the monoclinic system with the parameters $a = 16.2 \pm 0.1$ Å; $c = 10.5 \pm 0.1$ Å; $\beta = 92°30'$; $\sigma_x = 11.6$ gm/cm^3 Crystals of β-Bi_2Rh also do not pass into the superconducting state down to the temperature 1.27 °K.

In addition to the well-defined determination of the temperature of transition into the superconducting state, it is possible, in some degree, to explain the behavior of alloys obtained under various conditions and having the compositions Bi_2Rh and Bi_4Rh.

As has been shown in the work cited in references 1 and 2, alloys of composition Bi_4Rh cooled in the conventional way have a heterogeneous character. Depending on the rapidity of cooling, it is possible to observe in such alloys the presence of two modifications of Bi_2Rh and three modifications of Bi_4Rh. Annealing of alloys of composition Bi_4Rh at temperatures above 100 °C leads to homogeneous structures. Moreover, the changes (loss of superconductivity, a sharp change in the coefficient of expansion) noted in the work of reference 1 under annealing above 100 °C probably are better explained by the continuation of the peritectic reaction producing α-Bi_4Rh.

For specimens of composition Bi_4Rh there are possible five basic variants in the phase composition of the alloys, depending on the conditions of cooling.

First Variant. At rapid rates of cooling the reaction between crystals of Bi_2Rh and Bi does not go to completion. The speed of cooling is such that only the formation of γ-Bi_4Rh is possible. In such specimens there is only one transition point corresponding to γ-Bi_4Rh. To this variant corresponds specimen No. 1 and the specimen remelted after annealing No. 6[1].

On Fig. 1 is shown a microphotograph of an alloy of composition 9% rhodium by weight characterizing the first variant of phase composition. On the microphotograph can be seen bright crystals

[2] N. N. Zhuravlev and G. S. Zhdanov, J. Exper. Theoret. Phys. USSR 28, 228 (1951); Sov. Phys. 1,91 (1955)

[3] E. J. Rode, Communications of the Platinum Institute 7, 21 (1929)

[4] N. E. Alekseevskii and Iu. P. Gaidukov, J. Exper. Theoret. Phys. USSR 25, 383 (1953)

* Dilatometric measurements were carried out in the laboratory of P. G. Strelkov.

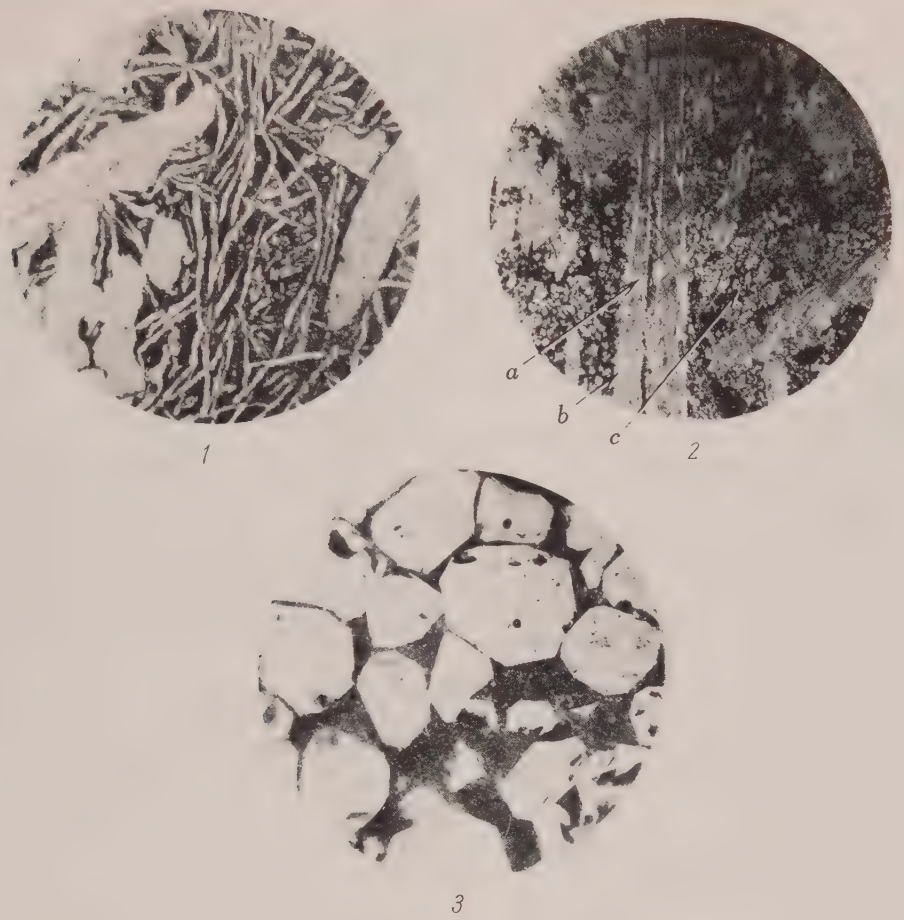

Fig. 1. Composition of 9% Rh by wt. Etched KI + I. Magnification 134.

Fig. 2. Composition of 11% Rh by wt. Etched KI + I. Magnification 57.

Fig. 3. Composition of 9% Rh by wt. Etched KI + I. Magnification 57.

surrounded by a film. The bright crystals represent β-Bi_2Rh with a microhardness of 40-60 kg/mm^2. The coating represents γ–Bi_4Rh with a microhardness of 30-55 kg/mm^2. The etched places correspond to the eutectic containing principally bismuth (99.3% by weight).

Second Variant. At rates of cooling slower than in the first case, the reactions between the crystals of Bi_2Rh and bismuth are carried out to a greater extent but are not completed; under such circumstances the formation of the modifications α, β and γ-Bi_4Rh is possible. Such specimens have two points of transition into superconductivity corresponding to $T_k = 3.2\,^\circ K$ for β-Bi_4Rh and $T_k = 2.7\,^\circ K$ for γ-Bi_4Rh. To this variant correspond samples No. 4 and No. 6 obtained in quartz ampules.

In Fig. 2 is shown a microphotograph of an alloy of composition 11% rhodium by weight, characterizing the second variant of phase composition. On the microphotograph the long gray crystals represent β-Bi_2Rh with a microhardness of 40-60 kg/mm^2 (shown by the arrow *a*). The lighter film of longish crystals with a microhardness of 30-55 kg/mm^2 represent γ-Bi_4Rh (arrow *b*). The small four-sided crystals with a microhardness of 60-70 kg/mm^2 represent β-Bi_4Rh (arrow *c*), the small polyhedral crystals -α-Bi_4Rh with a microhardness of 90-200 kg/mm^2 (the upper limit of hardness is raised because of the influence of crystal size). The etched places are the bismuth of the eutectic

Third Variant. The reaction between crystals of Bi_2Rh and bismuth has proceeded to completion. The speed of cooling is sufficient for the formation of crystals of β and γ-Bi_4Rh. Such specimens have two points of transition into the superconducting state corresponding to β and

γ-Bi_4Rh.

The metallographic picture is close to that shown in Fig. 2, the difference being merely that the longish crystals have smaller microhardness and lighter coloring. To differentiate between crystals of β-Bi_4Rh and γ-Bi_4Rh is difficult since they look similar on microsections and have similar values of the microhardness. In a hetergeneous alloy it is not possible to do this even by x-ray analysis. This variant of phase composition is observed in cases in which the alloy is heated to a temperature higher than the melting temperature of Bi_4Rh by 150-200°, and is then cooled to a temperature a little lower than the melting point of Bi_4Rh, is held at this temperature for some time sufficient for the reaction between Bi_2Rh and bismuth to be completed, and is then rapidly cooled.

Fourth Variant. The reaction between the crystals of Bi_2Rh and the bismuth of the eutectic has run to completion. The speed of cooling suffices for the formation of crystals of β-Bi_4Rh, but is not sufficient for the formation of γ-Bi_4Rh. In such specimens there is only one transition point corresponding to β-Bi_4Rh. Specimen No. 2, melted in a thick-walled quartz ampule, corresponds to this variant, and specimens No. 8 and 9 prepared in graphite crucibles.

Fifth Variant. The reaction between crystals of Bi_2Rh and the bismuth of the eutectic has run to completion. The speed of cooling is too small for the formation of crystals of β and γ-Bi_4Rh. The specimens are not superconducting. As an example, we have specimen No. 7 which was melted in a thick-walled porcelain container. In Fig. 3 is shown a microphotograph of an alloy of composition 9% rhodium by weight, characterizing the fifth variant of phase composition. In the microphotograph, in the mass of etched eutectic, can be seen bright polyhedral crystals of α-Bi_4Rh with a microhardness of 90-120 kg/mm^2.

Similar to the alloys of composition Bi_4Rh, the alloys of composition Bi_2Rh, when conventionally cooled, also have a heterogeneous character. It is sufficient to point out that under various conditions of preparation of the alloys, in addition to the modifications mentioned above, at very rapid rates of cooling, it is possible to form crystals of Bi_2Rh which can give one more point of transition into superconductivity ~ 2°K, as was mentioned in reference 5. Alloys of composition Bi_2Rh obtained by us through conventional cooling, as was mentioned above, had heterogeneous character and consisted primarily of crystals of Bi_2Rh and β-Bi_4Rh. The latter were responsible for the superconductivity of these alloys. As examples, can serve specimen No. 1 melted in a quartz ampule, and specimens No. 3 and No. 4 melted in graphite crucibles.

In conclusion we express thanks to I. I. Lifanov and to N. P. Ivanov for assistance in the experiments.

---

[5] N. E. Alekseevskii, N. B. Brandt and T. I. Kostina, J. Exper. Theoret. Phys. USSR 21, 951 (1951)

Translated by N. E. Golovin
34

SOVIET PHYSICS-JETP VOLUME 1, NUMBER 1 JULY, 1955

The Theory of the Electrical Resistivity of Ordered Alloys

M. A. KRIVOGLAZ AND Z. A. MATYSINA
Metallo-physics Laboratory, Academy of Sciences, Ukrainian SSR
(Submitted to JETP editor February 16, 1954)
J. Exper. Theoret. Phys. USSR 28, 61-69 (January, 1955)

The residual electrical resistivity of binary ordered alloys is examined in light of the many electron theory. It has been shown that the relation between the resistivity and the composition of the alloy and the degree of order is the same as in the one electron approximation. The correlation in alloys has also been calculated.

1. INTRODUCTION

THE quantum mechanical theory of the residual resistivity of disordered alloys was developed by Nordheim[1]. The theory of the residual resistivity of ordered solid solutions was constructed by Smirnov[2] for the general case of binary alloys of different structure, of arbitrary composition and degree of distant order. This article also explains the observations of the experimental dependence of the residual resistivity ρ_0 on the composition of the alloy and the degree of distant order. In the calculation of ρ_0 in references 1 and 2, two basic simplifying assumptions were made. In the first place, it was assumed that the absolute value of the difference $(V_A - V_B)$ of energies of interaction of valence electrons with the atoms of an alloy of the first and second type was sufficiently small. In the second place, it was assumed that the problem could be solved by the one electron approximation, i.e., the real system of interacting electrons could be replaced by a system of noninteracting electrons, moving in a potential field that is created by the ionic crystal lattices of the metal and by the remaining electrons.

The first of the indicated assumptions apparently is satisfied with sufficient exactness for many alloys. However, as has been noted repeatedly, the solution of the many electron problem with the help of the one electron approximation does not appear to have a theoretical basis in the case of metals. Among the results of theoretical examinations, some electronic properties of metals (for example, the possibility of passing electrons through an ideal crystal lattice without scattering, the appearance of the optical dispersion formula of metals) agree in the many electron and in the one electron theories[3,4]. In the present article, it is shown that the results in references 1 and 2, for the dependence of the residual resistivity upon the composition of the alloy and the degree of the order, are preserved also in the many electron theory, if only the assumption about the smallness of $(V_A - V_B)$ is used.

In articles 1 and 2, in calculating ρ_0, the coupling between the filling up of the various sites of a crystal lattice by atoms of the alloy was not taken into account, i.e., it was assumed that the atoms of the alloy are in a disordered distribution at the sites of a sublattice of the given type. In the particular cases of alloys with simple cubic lattices of stoichiometric systems, the coupling was studied with the help of the one electron approximation[5]. In the present article, formulas are developed for the residual resistivity, taking correlations into account; these are suitable for alloys of various structures and arbitrary composition.

2. DETERMINATION OF THE PROBABILITIES OF QUANTUM TRANSITIONS OF ELECTRONS FOR CONDUCTION UNDER THE ACTION OF DISORDER IN THE LOCATION OF THE ATOMS

We examine the binary ordered alloys A-B with the Brava-type crystal lattice having two types of sites in a well-ordered structure. Let us assume that this alloy was annealed at some temperature, as a result of which some equilibrium distribution of the atoms A and B at the junctions of the crystal lattice was established. Let us examine the electrical resistivity of this alloy, which has been quickly quenched to such a low temperature that the effect of the vibrations of the crystal lattice of the alloy on the movement of the electrons is negligibly small, so that one can assume that the ions are attached to the lattice sites.

For the identification of the stationary states of the system, strictly speaking, we should have

[1] L. Nordheim, Ann. Physik. 9, 607 (1931)

[2] A. A. Smirnov, J. Exper. Theoret. Phys. 17, 743 (1947)

[3] S. V. Vonsovskii, Izv. Akad. Nauk SSSR, Ser. Fiz. 12, 337 (1948); Usp. Fiz. Nauk 48, 289 (1952)

[4] A. V. Sokolov, J. Exper. Theoret. Phys. USSR 25, 341 (1953)

[5] S. G. Ryzhanov, J. Exper. Theoret. Phys. USSR 9, 4 (1939)

solved the Schrödinger equation for all the electrons of the metal in the field of all the nuclei. Since, however, the inner electrons of the ions of the metal are bound considerably stronger than the valence electrons, and since they exist in discrete energy levels, it is possible to use the adiabatic assumption. According to this assumption, one can study the motion of the strongly bound electrons for given coordinates $\mathbf{r}_i$ of the conducting electrons. Afterwards, it is necessary to include this energy of the strongly bound electrons, which depends on $\mathbf{r}_i$, as a term in the potential energy of the conducting electrons. It is not possible to take the strongly bound electrons into account otherwise. In this case, we mean by strongly bound electrons, electrons lying in such deep electron shells of alloy atoms that the shells are practically unpolarized. All the remaining electrons refer to conduction electrons. This separation of valence electrons into a discrete subsystem is necessary so that it will be possible to formulate for just these electrons the smallness condition for the difference in interaction energy of the electrons with the ions in the lattice of different kinds:

$$|V_A - V_B| \sim \xi. \tag{1}$$

Here the smallness of the parameter ξ implies that the solutions of the Schrödinger equation with the potential energies V_A and V_B differ by a small amount. The equation for a stationary system of N_e valence electrons in the field of the alloy ions has the form:

$$\left[-\frac{\hbar^2}{2m}\sum_i \Delta_i + \sum_i V(\mathbf{r}_i) + \sum_{i<k}\frac{e^2}{|\mathbf{r}_i - \mathbf{r}_k|}\right] \tag{2}$$

$$\times\ \psi_n(\ldots \mathbf{r}_i \ldots) = E_n \psi_n(\ldots \mathbf{r}_i \ldots),$$

where $-\frac{\hbar^2}{2m}\Delta_i$ is the kinetic energy operator for the ith electron, $V(\mathbf{r}_i)$ is the potential energy of the ith electron in the field of the ions. As a zeroth approximation, as is customary[1,2], we shall take the state of the system of electrons, which are in the field of the completely ordered crystal lattice, consisting of effective ions. In this state, each effective ion creates a potential equal to average potential of the ions and alloy, occurring at the site of the given type. The perturbing function of the zeroth approximation is determined from the equation

$$\left[-\frac{\hbar^2}{2m}\sum_i \Delta_i + \sum_i \overline{V}(\mathbf{r}_i) + \sum_{i<k}\frac{e^2}{|\mathbf{r}_i - \mathbf{r}_k|}\right] \tag{3}$$

$$\times\ \psi_n^0(\ldots \mathbf{r}_i \ldots) = E_n^0 \psi_n^0(\ldots \mathbf{r}_i \ldots).$$

Equation (3) describes the motion of the system of electrons in the region of the periodic field $V(\mathbf{r}_i)$, creating the effective ions. Using only the properties of the symmetric transformations, it is possible, as is known, to reduce the solution of Eq. (3) to the following form:

$$\psi_n^0(\ldots \mathbf{r}_i \ldots) \tag{4}$$

$$= \sum_P (-1)^P P \exp\left[i\sum_{i=1}^{N_e} \mathbf{k}_i \mathbf{r}_i\right] u_n(\ldots \mathbf{r}_i \ldots),$$

where

$$P\exp\left[i\sum_{i=1}^{N_e} \mathbf{k}_i \mathbf{r}_i\right] u_n(\ldots \mathbf{r}_i \ldots)$$

results from the function

$$\exp\left[i\sum_{i=1}^{N_e} \mathbf{k}_i \mathbf{r}_i\right] u_n(\ldots \mathbf{r}_i \ldots)$$ by means of some permutations of position coordinates, $\sum_P$ denotes the summation over all permutations, and $(-1)^P$ equals $+1$ for an even number of transformations, corresponding to a given permutation, and equals -1 if the number of transformations is odd. The function $u_n(\ldots \mathbf{r}_i \ldots)$ remains unchanged for a displacement of all the electrons by the lattice constant a:

$$u_n(\ldots \mathbf{r}_i + \mathbf{a} \ldots) = u_n(\ldots \mathbf{r}_i \ldots). \tag{5}$$

under the action of the perturbation energy

$$V'(\mathbf{r}_1 \ldots \mathbf{r}_{N_e}) = \sum_{i=1}^{N_e} [V(\mathbf{r}_i) - \overline{V}(\mathbf{r}_i)] \tag{6}$$

the system can change from ψ_n^0 to another state, that is described by the wave function

$$\psi_m^0(\ldots \mathbf{r}_i \ldots) \tag{7}$$

$$= \sum_P (-1)^P P \exp\left[i\sum_{i=1}^{N_e} \mathbf{k}_i' \mathbf{r}_i\right] u_m(\ldots \mathbf{r}_i \ldots).$$

The probability of this transition is proportional to the square of the modulus of the matrix element

$$V'_{nm} = \int \psi_n^{0*} V' \psi_m^0 d\tau_1 \ldots d\tau_{N_e} \tag{8}$$

$$= \sum_{i=1}^{N_e} \int \Phi_{nm}(\mathbf{r}_i)\, \Delta V(\mathbf{r}_i)\, d\tau_i,$$

where

$$\Delta V(\mathbf{r}_i) = V(\mathbf{r}_i) - \overline{V}(\mathbf{r}_i), \tag{9}$$

$$\Phi_{nm}(\mathbf{r}_i) = \int \psi_n^{0*}(\mathbf{r}_1 \ldots \mathbf{r}_{N_e})\, \psi_m^0(\mathbf{r}_1 \ldots \mathbf{r}_{N_e}) \tag{10}$$

$$d\tau_1 \ldots d\tau_{i-1} d\tau_{i+1} \ldots d\tau_{N_e}.$$

Owing to the symmetry properties of the wave functions of the system relative to the periodic coordinates of the different electrons, the form of the function $\Phi_{nm}(\mathbf{r}_i)$ is not dependent upon the number i. Using Eq. (4) and the cyclic conditions, it is easy to see that

$$\Phi_{nm}(\mathbf{r} + \mathbf{a}) = e^{i\mathbf{q}\mathbf{a}}\Phi_{nm}(\mathbf{r}), \tag{11}$$

where

$$\mathbf{q} = \sum_i (\mathbf{k}_i' - \mathbf{k}_i).$$

Consequently, it is possible to introduce $\Phi_{nm}(\mathbf{r})$ in the form

$$\Phi_{nm}(\mathbf{r}) = e^{i\mathbf{q}\mathbf{r}} U_{nm}(\mathbf{r}), \tag{12}$$

where $U_{nm}(\mathbf{r})$ is a periodic function with period $\mathbf{a}$.

The potential energy of the ith electron $V(\mathbf{r}_i)$, as also in references 1 and 2, can be introduced in the form of a sum of potential energies which are formed by the separate ions of the alloy,

$$V(\mathbf{r}_i) = \sum_{s\chi} V^{\chi s}(\mathbf{r}_i - \mathbf{R}_s - \mathbf{h}_\chi), \tag{13}$$

where $\mathbf{R}_s$ denotes the vector drawn to the first site of the sth crystal cell, $\mathbf{h}_\chi$ is the vector, leading from the first site of the cell to the site of number χ of this cell, $V^{\chi s}$ is the potential energy of the electron in the field of the ion, occurring at the site of number χ of the sth cell, equaling V_A or V_B respectively, if atom A or B exists at this site. The summation in Eq. (13) is carried over all the sites of the crystal lattice of the alloy. The average of the potential energy $V(\mathbf{r}_i)$ equals

$$\overline{V}(\mathbf{r}_i) = \sum_{s\chi} \overline{V}^{\chi}(\mathbf{r}_i - \mathbf{R}_s - \mathbf{h}_\chi), \tag{14}$$

where V^{χ} is the potential energy of the electron in the field of the effective ion, denoted by the site number χ. This energy is not related to the number of the cell s.

Substituting in Eq. (8) the Eqs. (12), (9), (13), and (14) and making in each term the change of variables

$$\mathbf{r}_i - \mathbf{R}_s - \mathbf{h}_\chi \to \mathbf{r}_i,$$

we obtain

$$V'_{nm} = N_e \sum_{s\chi} \exp\{i\mathbf{q}\mathbf{R}_{s\chi}\}(V^{\chi s}_{nm} - \overline{V}^{\chi}_{nm}). \tag{15}$$

Here

$$V^{\chi s}_{nm} = \int \exp\{i\mathbf{q}\mathbf{r}_i'\}\, V^{\chi s}(\mathbf{r}_i') \times U_{nm}(\mathbf{r}_i' + \mathbf{h}_\chi)\, d\tau_i', \tag{16}$$

$$\overline{V}^{\chi}_{nm} = \int \exp\{i\mathbf{q}\mathbf{r}_i'\}\, \overline{V}^{\chi}(\mathbf{r}_i') \times U_{nm}(\mathbf{r}_i' + \mathbf{h}_\chi)\, d\tau_i', \tag{17}$$

$\mathbf{R}_{s\chi} = \mathbf{R}_s + \mathbf{h}_\chi$ is the radius vector of the site of number χ of the s th cell, $V^{\chi s}_{nm}$ equals V_{Anm} or V_{Bnm} depending on which atom occurs at the given site.

The square modulus of the matrix element $|V'_{nm}|^2$ on the basis of Eq. (15), equals

$$|V'_{nm}|^2 = N_e^2 \Big\{ \sum_{\chi s} (V^{\chi s}_{nm} - \overline{V}^{\chi}_{nm}) \times (V^{\chi s *}_{nm} - \overline{V}^{\chi *}_{nm}) + \sum_{\chi s \neq \chi' s'} \exp\{i\mathbf{q}(\mathbf{R}_{\chi s} - \mathbf{R}_{\chi' s'})\} (V^{\chi s}_{nm} - \overline{V}^{\chi}_{nm}) \times (V^{\chi' s' *}_{nm} - \overline{V}^{\chi' *}_{nm}) \Big\}. \tag{18}$$

The first sum in Eq. (18) specifies the residual resistivity of the alloy in which there is the absence of coupling. This is the form of the sum calculated by Smirnov[2]. From this the following results have been obtained:

$$\sum_{\chi s} (V^{\chi s}_{mn} - \overline{V}^{\chi}_{nm})(V^{\chi s *}_{nm} - \overline{V}^{\chi *}_{nm}) = N' \Big[p_A^{(1)} p_B^{(1)} \sum_{\chi_1 = 1}^{\lambda_1} \Delta^{\chi_1}_{nm} + p_A^{(2)} p_B^{(2)} \sum_{\chi_2 = 1}^{\lambda_2} \Delta^{\chi_2}_{nm} \Big]. \tag{19}$$

Here

$$\Delta^{\chi j}_{nm} = \left| V^{\chi j}_{Anm} - V^{\chi j}_{Bnm} \right|^2 \tag{20}$$

$$= \left| \int e^{i\mathbf{qr}} \left[V_A(\mathbf{r}) - V_B(\mathbf{r}) \right] U_{nm}(\mathbf{r} + \mathbf{h}_{\chi j})\, d\tau \right|^2,$$

$p_{\alpha}^{(j)}$ is the substitution probability of a site of the jth kind by an atom α ($j = 1,2$; $\alpha = A,B$), χ_j is the number of the site of the jth kind, and N' is the number of cells in the crystal lattice. The function $U_{nm}(\mathbf{r} + \mathbf{h}_{\chi j})$ is different from $U_{nm}(\mathbf{r})$ by the order of magnitude of $|V_A - V_B|$. Therefore, as also in reference 2, the terms of all the $\Delta_{nm}^{\chi_j}$ are mutually equal

$$\Delta_{nm}^{\chi_1} \approx \Delta_{nm}^{\chi_2} \approx \Delta_{nm}. \tag{21}$$

correct to the cubic terms in $V_A - V_B$. Then Eq. (19) can be converted to the form:

$$\sum_{\chi s} (V_{nm}^{\chi s} - \overline{V}_{nm}^{\chi})(V_{nm}^{\chi s *} - \overline{V}_{nm}^{\chi *}) \tag{22}$$

$$= N\Delta_{nm} \left[c_1 c_2 - \frac{\nu}{1-\nu} \gamma^2 \eta^2 \right],$$

as was also done in reference 2. Here N is the number of sites of the crystal lattice of the alloy, c_1 and c_2 are the relative atomic concentrations of atom A and B in the alloy ($c_1 + c_2 = 1$), $\eta = (p_A^{(1)} - c_1)/\gamma$ is the degree of distant order, ν is the ratio of the number of sites of the first kind to the total number of sites:

$$\gamma = \begin{cases} \dfrac{1-\nu}{\nu} c_1 & \text{where} \quad c_1 \leqslant \nu, \\ c_2 & \text{where} \quad c_1 \geqslant \nu. \end{cases} \tag{23}$$

The second sum in Eq. (18) equals zero, if coupling exists in the alloy [2]. If it is assumed that the coupling in the alloy is small, then it is possible, when computing this sum, to restrict the coupling parameter* to the linear terms. Therefore, we retain in the indicated sum only those terms that correspond to nearest neighbors. The remaining terms contain terms of a higher degree of smallness relative to the coupling parameter. Under these assumptions, the unknown sum can be put into the form:

$$\sum_{\chi s \neq \chi' s'} \exp\{i\mathbf{q}(\mathbf{R}_{\chi s} - \mathbf{R}_{\chi' s'})\} \tag{24}$$

$$\times (V_{nm}^{\chi s} - \overline{V}_{nm}^{\chi})(V_{nm}^{\chi' s' *} - V_{nm}^{\chi' *})$$

$$\approx \sum_{k=1}^{z} \exp\{i\mathbf{q}\delta\mathbf{R}_k\} \sum_{\chi s} (\overline{V_{nm}^{\chi s} V_{nm}^{\chi' s' *}} - \overline{V_{nm}^{\chi}}\,\overline{V_{nm}^{\chi' *}}).$$

Here the summation over χs, $\chi' s'$ is divided into a sum in which $\delta\mathbf{R}_k = \mathbf{R}_{\chi s} - \mathbf{R}_{\chi' s'}$ is constant. The summation over k is carried over all z nearest neighbors of a given site χs. At this site $\chi' s'$ is determined by the assignment of χs and k. The sum

$$\sum_{s} (\overline{V_{nm}^{\chi s} V_{nm}^{\chi' s' *}} - \overline{V_{nm}^{\chi}}\,\overline{V_{nm}^{\chi' *}})$$

depends only upon the kind of site χ and χ'. Introducing the probability $p_{\alpha\beta}^{(jl)}$ of the displacement of neighboring sites of type j and l ($j,l = 1,2$) to atoms α and β respectively, ($\alpha,\beta = A,B$), the indicated sum can be transformed to the form:

$$\sum_{s} (\overline{V_{nm}^{\chi s} V_{nm}^{\chi' s' *}} - \overline{V_{nm}^{\chi}}\,\overline{V_{nm}^{\chi' *}}) \tag{25}$$

$$= N' \left[p_{AA}^{(jl)} V_{Anm}^{\chi_j} V_{Anm}^{\chi'_l *} + p_{AB}^{(jl)} V_{Anm}^{\chi_j} V_{Bnm}^{\chi'_l *} \right.$$

$$+ p_{BA}^{(jl)} V_{Bnm}^{\chi_j} V_{Anm}^{\chi'_l *} + p_{BB}^{(jl)} V_{Bnm}^{\chi_j} V_{Bnm}^{\chi'_l *}$$

$$- \left(p_A^{(j)} V_{Anm}^{\chi_j} + p_B^{(j)} V_{Bnm}^{\chi_j}\right)$$

$$\left. \left(p_A^{(l)} V_{Anm}^{\chi'_l *} + p_B^{(l)} V_{Bnm}^{\chi'_l *}\right) \right].$$

Here it is understood that the site numbers χ and χ' refer, respectively, to sites of the type j and l. By introducing the values ε^{jl}, which are determined by the relation

$$\varepsilon^{jl} = p_{AB}^{(jl)} - p_A^{(j)} p_B^{(l)} = p_{BA}^{(jl)} - p_B^{(j)} p_A^{(l)} \tag{26}$$

$$= -(p_{AA}^{(jl)} - p_A^{(j)} p_A^{(l)}) = -(p_{BB}^{(jl)} - p_B^{(j)} p_B^{(l)}),$$

Eq. (25) takes on the simpler form:

$$\sum_{s} (\overline{V_{nm}^{\chi s} V_{nm}^{\chi' s' *}} - \overline{V_{nm}^{\chi'}}\,\overline{V_{nm}^{\chi' *}}) \tag{27}$$

$$= -N' \varepsilon^{jl} \left(V_{Anm}^{\chi_j} - V_{Bnm}^{\chi_j}\right)$$

$$\left(V_{Anm}^{\chi' l *} - V_{Bnm}^{\chi'_l *}\right) \approx -N' \varepsilon^{jl} \Delta_{nm}.$$

In the last equation $(V_{Anm}^{\chi_j} - V_{Bnm}^{\chi_j})\left(V_{Anm}^{\chi'_l *} - V_{Bnm}^{\chi'_l *}\right)$ is replaced by Δ_{nm}, which is correct only to the third order of the $|V_A - V_B|$ terms. Performing

* The coupling parameter can be chosen, for example, in the same way as in reference 6.

the summations over χ and k in Eq. (24) and taking into account Eq. (27), we obtain the following expression for Eq. (24)

$$\sum_{\chi s \neq \chi' s'} \exp\{iq\ (\mathbf{R}_{\chi s} - \mathbf{R}_{\chi' s'})\}\ (V_{nm}^{\chi s} - \overline{V_{nm}^{\chi}}) \quad (28)$$

$$(V_{nm}^{\chi' s'*} - \overline{V_{nm}^{\chi'*}}) \approx -\Big[N_1 \varepsilon^{11} \sum_{k_1=1}^{z_1} \cos\ \mathbf{q}\delta\mathbf{R}_{k_1}$$

$$+\ N_2 \varepsilon^{22} \sum_{k_2=1}^{z_2} \cos\ \mathbf{q}\delta\mathbf{R}_{k_2}$$

$$+\ 2N_1 \varepsilon^{12} \sum_{k_3=1}^{z_3} \cos\ \mathbf{q}\delta\mathbf{R}_{k_3} \Big]\ \Delta_{nm}.$$

Here $N_1 = \nu N$ is the number of sites of the first type, $N_2 = (1-\nu)N$ is the number of sites of the second kind, z_1 is the number of sites of the first kind, adjacent to the sites of the first kind, z_2 is the number of sites of the second kind adjacent to the sites of the second kind, and z_3 is the number of sites of the second kind adjacent to the sites of the first kind.

If q is sufficiently small, such that for all k

$$\mathbf{q}\delta\mathbf{R}_k \ll 1, \quad (29)$$

then on the basis of Eqs. (18), (22), and (28), the quadratic modulus of the matrix element $|V_m'|^2$ equals

$$|V_{nm}'|^2 = a_{nm} f(c, \eta, \varepsilon), \quad (30)$$

where

$$a_{nm} = N_e^2 N \Delta_{nm}, \quad (31)$$

$$f(c, \eta, \varepsilon) = c_1 c_2 - \frac{\nu}{1-\nu}\gamma^2\eta^2 - \nu z_1 \varepsilon^{11}$$

$$-(1-\nu)\, z_2 \varepsilon^{22} - 2\nu z_3 \varepsilon^{12}$$

and ϵ denotes the set of values ϵ^{11}, ϵ^{22}, and ϵ^{12}. Here the coefficients, a_{nm}, correct to the terms of the highest (third) order of smallness relative to the $|V_A - V_B|$, do not depend upon c, η, and ϵ, i.e., they are single valued for all the quantum transitions. The latter case is essentially for what follows. In the case of the one electron approximation, inequalities similar to (29) are satisfied for all the quantum transitions in the case of "poor metals", i.e., of metals with a small number of valence electrons. If the number of valence electrons is large and the quantum transitions, for which the condition (29) is not fulfilled, play an essential role, then the coupling correction in Eq. (30) and (31) is too large in absolute magnitude. However, the basic contribution to the quadratic modulus of the matrix elements $|V'_{nm}|^2$ is the term (22), the calculation of which does not have a bearing on the condition (29) of small q. Therefore, without the coupling calculations in the alloy, Eq. (30) is correct for any q.

3. CALCULATION OF THE RESIDUAL RESISTIVITY

The average value of the electron current density can be determined by the equation:

$$I = \sum_{nm} w_{nm} I_{nm}, \quad (32)$$

where the series of values ω_{nm} introduces the matrix density, formulated by the wave functions ψ_n^0, which are determined by Eq. (4), and I_{nm} is the matrix element of the current density operator. In the absence of an electric field, the average electron current density equals zero, i.e.,

$$\sum_{nm} w_{nm}^0 I_{nm} = 0, \quad (33)$$

where ω_{nm}^0 designates the matrix density without the external field. If a large field F is applied to the metal, then the matrix element ω_{nm} can be written in the form:

$$w_{nm} = w_{nm}^0 + \Delta w_{nm}, \quad (34)$$

while the average current density equals

$$I = \sum_{nm} \Delta w_{nm} I_{nm}. \quad (35)$$

The values of $\Delta\omega_{nm}$ are determined from the stationary condition, which requires

$$dw_{nm}/dt = 0. \quad (36)$$

in order that the matrix density does not change with time. Further, as in the derivation of the kinetic equation, we take into consideration the fact that the system of electrons exists in states of dynamic equilibrium, and the value of ω_{nm} change because of the presence of the field, also because of the diffusion of electrons on heterogeneities combined with an incompletely ordered distribution in an alloy of two types of atoms. The transformation of ω_{nm} per unit of time is some function of the field as a consequence of the first reason. The decomposition of this function into a power series in F does not include the zero

order and can be written in the following form:

$$(\partial w_{nm}/\partial t)_{\text{field}} = \alpha_{nm}F + \dots \quad (37)$$

Since, according to Eqs. (30) and (31), the probabilities of any quantum transitions are proportional to the same function $f(c, \eta, \epsilon)$, then the change in ω_{nm} per unit time, connected with the heterogeneities of the alloy, is also proportional to this function:

$$(\partial w_{nm}/\partial t)_{\text{alloy}} = \lambda_{nm} f(c, \eta, \varepsilon), \quad (38)$$

where λ_{nm} in the assumed approximation ($|V_A - V_B|$ small) does not depend upon c, η, or ϵ. The coefficients λ_{nm} appear as functions of the matrix elements of the density operator. The separation of these coefficients into a series in increments of $\Delta\omega_{pr}$ has the form:

$$\lambda_{nm} = \sum_{pr} \mu_{prnm}\Delta w_{pr} + \dots \quad (39)$$

Here the zeroth order term is zero, since in the absence of an electric field, Eq. (38) reduces to zero. From Eqs. (36), (37), (38), and (39), we obtain a system of equations for the determination of the values of $\Delta\omega_{pr}$:

$$f(c, \eta, \varepsilon) \sum_{p,r} \mu_{prnm}\Delta w_{pr} + \alpha_{nm}F = 0. \quad (40)$$

Here the higher order terms of the decompositions (37) and (39) are rejected, which is justified for not too large fields, when Ohm's law is obeyed. The solution of the system of equations (40) has the form:

$$\Delta w_{pr} = c_{pr} \frac{F}{f(c, \eta, \varepsilon)}. \quad (41)$$

Substituting the solution into Eq. (35), we obtain the final expression for the average density of electric current

$$I = \frac{F}{f(c, \eta, \varepsilon)} \sum_{nm} c_{nm} I_{nm}. \quad (42)$$

Hence, the residual resistivity of the alloy equals

$$\rho_0 = A f(c, \eta, \varepsilon), \quad (43)$$

where the constant A does not depend upon c, η, or ϵ.

It is evident, from Eq. (43), that the many electron theory, once the condition (29) is satisfied leads to a similar relation for the residual resistivity for a compound alloy, the degree of the distant order, and correlation in the alloy, as does the one electron approximation. According to this, the coefficient A, proportional to $|V_A - V_B|^2$ in the many electron theory, determines the same parameter as it does in the one electron theory.

Equation (31) for $f(c, \eta, \epsilon)$ takes a special form in the two cases:

1. For an inhomogeneous alloy, $\eta = 0$ and the function $f(c, \eta, \epsilon)$ equals

$$f(c, \varepsilon) = c_1 c_2 - z\varepsilon. \quad (44)$$

Here the value of ϵ, determined by Eq. (26), is the same in an inhomogeneous alloy, for any neighboring sites, regardless of type, and z is the coordination number. The meaning of ϵ can be estimated with the aid of the statistical theory of conduction, taking into account the interaction only between nearest neighbors. According to Lifshitz[6] ϵ equals

$$\varepsilon = c_1^2 c_2^2 \frac{W}{kT}, \quad (45)$$

correct to the quadratic terms relative to W/kT, where the energy of ordering $W = 2|v_{AB}| - |v_{AA}| - |v_{BB}|$ ($v_{\alpha\beta}$ is the energy of interaction of neighboring atoms α and β).

Equations (44) and (43), with $\epsilon = 0$, change to the corresponding equations in reference 1, not taking into account the coupling in the alloy. From the Eqs. (43), (44), and (45), it follows that the coupling (of nearest neighbors) diminishes the residual resistivity of ordered alloys ($W > 0$) and increases the residual resistivity of disordered alloys ($W < 0$). The effect of the nearest neighbor increases with a drop in the temperature T, at which the alloy was quenched. For given temperatures the coupling calculation gives a much larger correction to the electroresistivity, the nearer the composition of the alloys to the stoichiometric. We note that the correction of ρ_0, corresponding to the coupling calculation, is perhaps much too large. For example, at $c_1 = c_2 = \frac{1}{2}$, $W/kT = 1/z$ (the temperature T is four times greater than the ordering temperature), the coupling diminishes in ordered alloys (in the case of "poor metals") by 25 per cent. (In the case of metals, in which the number of current carriers is not small, the coupling appears less influenced by the ordering). It would be interesting experiment-

[6] I. M. Lifshitz, J. Exper. Theoret. Phys. USSR 9, 481 (1939)

ally to find the effect of nearest neighbors on the residual resistivity of alloys and to investigate this effect at different temperatures of annealing and different systems of alloys.

It should be noted that the reduced equations (44) and (45) cease to be correct at temperatures approximating the ordering temperatures, in which case the correction term $z\epsilon$ in Eq. (44) proves to be fairly large. In this case, it is not possible to restrict oneself to the linear terms relative to W/kT. The coupling not only between near neighbors must be considered.

2. In the case of the ordered alloy, in which each site is surrounded by neighboring sites only of a different type (for example, in alloys with a volume centered cubic lattice type, β-brass, alloys with a simple cubic lattice, etc.) $\epsilon^{11} = \epsilon^{22} = 0$, $\nu = \frac{1}{2}$, $z_3 = z$ and the function $f(c, \eta, \epsilon)$ can be written in the form:

$$f(c, \eta, \varepsilon) = c_1 c_2 - \gamma^2 \eta_i^2 - z\varepsilon^{12}. \qquad (46)$$

In this case the value of ϵ^{12} in the approximation of nearest neighbors similar to Eq. (45), is equal to

$$\varepsilon^{12} = (c_1^2 - \gamma^2 \eta_i^2)(c_2^2 - \gamma^2 \eta_i^2) \frac{W}{kT}. \qquad (47)$$

with exactness to the quadratic terms relative to to W/kT. Equation (46) is accurate only at temperatures considerably lower than the annealing temperature, for η close to unity, when the correction $z\epsilon^{12}$ is small. If it is assumed in this equation that $\epsilon^{12} = 0$, then Eq. (43) converts to the appropriate expression of reference 2. In the general case, the expression for ρ_0 in reference 2 results from Eqs. (43) and (31) when $\epsilon^{ij} = 0$.

In conclusion, we wish express our deep thanks to Prof. A. A. Smirnov for the repeated discussions of the article and his valuable advice.

Translated by D. F. Edwards
8

SOVIET PHYSICS - JETP VOLUME 1, NUMBER 1 JULY, 1955

The Conditions of Formation and Stability of Films at the Electrodes in Dielectrics

IA. N. PERSHITS
Pskov State Teacher's Institute
(Submitted to JETP editor May 25, 1953)
J. Exper. Theoret. Phys. USSR 28, 181-190 (February, 1955)

The conditions for formation and destruction of films at the electrodes in dielectrics were studied with respect to their dependence on the type of heat treatment and on the action of the electric field. A connection between the change of electrical conductance produced by impurities and the change of properties of the electrode films was discovered and investigated.

1. GENERAL REMARKS

CLARIFICATION of the condition for formation and destruction of films at the electrodes in self-forming dielectrics is of considerable interest; for occurrences at the electrodes in dielectrics and semi-conductors have a bearing on the possibility of application of technically important devices (electrolytic condensers and rectifiers, high-temperature insulation, etc.).

Researches conducted earlier[1] on the electrical conductivity of quartz and of alkali-halide crystals showed that phenomena connected with the formation and destruction of a film at the anode lead to an extremely complex variation of the current with time. In the present work these researches are extended to a series of other dielectrics: porcelain, Eternit (an asbestos cement), mica and asbestos. Besides the previously used method of successive changes of the direction of the electric field, a new method was applied, which enables one to examine in succession the separate important features of the process of formation of the dielectric.

In the study of the variation of current with time, two similar specimens were clamped in an iron frame, a second electrode was placed between them. Thus the two specimens were connected in parallel; this eliminated the necessity for using insulation. The frame was placed in a tubular electric furnace. The constancy of the temperature was carefully controlled; a compensation scheme of thermocouple connection was used for this purpose. For photographic recording of the variation of current with time, the apparatus used was a string electrometer, shunted with a wire resistance, and a rotating drum with a photographic film. During the photographing, the commutation of the voltage occurred only in the circuit of the dielectric under study. In the photographs, therefore, the curves for currents in both directions were obtained on one side of the zero position; this facilitated their comparison.

The object under study was subjected to prolonged electrolysis (30-60 min), and then the variation of current with time was recorded in the "permeable" and the "shut-off" directions.

In Figs. 1 and 2 are shown curves of the variation with time of the "permeable" and "shut-off" current in fused quartz. From Fig. 1 it is evident that in the specimen of fused quartz (temperature 550° C, $E = 120$ V/cm), subjected to prolonged electrolysis, after a change of direction of the field there develops a "permeable" current that increases abruptly and passes through a maximum (coefficient of unipolarity $K = 10$). Such dependence of the "permeable" current on time occurs in all the dielectrics studied. At the same time, as we shall see later, even in a single specimen the character of the current in the "permeable" direction depends on the previous treatment; specifically, on the action of the electric field and on the type of heat treatment.

The most characteristic features, for all the dielectrics, are the curves of variation of current with time after a repeated change of direction of the field ("shut-off" current). For different dielectrics these curves may differ in the rate of fall of current, but the character of the variation is quite similar for different dieclectrics. Comparison of the curves drawn in Figs. 2*a* and 2*b* shows that the rate of decrease of current in the "shut-off" direction depends on the duration of the current in the "permeable" direction. This rule is so general that it leads us to surmise the presence of an electrode film in the dielectric even when none can be observed by probe measurements of the potential distribution.

It has already been established by probe measurements[1] that the dependence shown in Figs. 1 and 2 is connected with the destruction and restoration of a film at the anode, produced by electrolysis of the dielectric. In the present work, as a result of a

[1] Ia. N. Pershits, J. Exper. Theoret. Phys. USSR 17, 251 (1947)

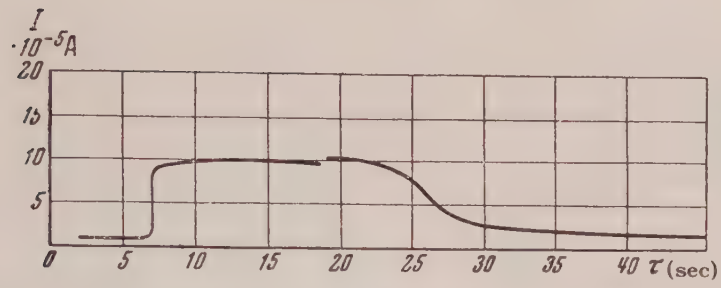

Fig. 1. Variation of current with time for "permeable" and "shut-off" currents. Rising curve (at left), "permeable" current"; falling curve (at right), "shut-off" current.

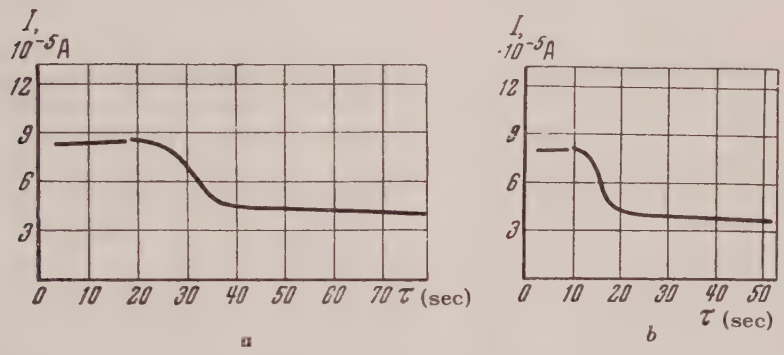

Fig. 2. Dependence of current in the "shut-off" direction on duration of current in the "permeable" direction. Duration of "permeable" current: *a*, 14 sec; *b*, 7 sec.

study of different dielectrics, we arrived at the following conclusions, the basis of which we will give below:

1) In the electrolysis it is possible for two high-resistance films to be formed at the electrodes: a cathodic and an anodic. The cathodic film is stable; the anodic is unstable and completely determines the observed unipolar phenomena.

2) The degree of stability of the anodic film and its resistance depend on the conditions of formation of the film, and specifically on the character of the previous heat treatment and the time of action of the electric field.

3) Certain conditions (heating, electrolysis), which contribute to an increase of resistance of the electrode film, produce a simultaneous increase of conductivity of the specimen itself.

4) The magnitude of the coefficient of unipolarity for a given dielectric depends on the conditions of heat treatment and the action of the electric field.

2. CATHODIC AND ANODIC HIGH-RESISTANCE FILMS

Simultaneous formation of high-resistance films on the cathode and the anode was observed in E-ternit. We shall describe one of the experiments. On specimens of Eternit (17 × 10 × 4 mm) there were deposited on one side (17 × 10 mm) continuous graphite electrodes, and on the opposite side pairs of similar graphite electrodes, separated by a thin strip of the pure dielectric. Two specimens were clamped in an iron frame in such a way that both continuous electrodes butted against the frame, whose holder served to connect these electrodes to one of the terminals of the current source. The small graphite electrodes were face to face; between them were placed iron plates, which served to connect the specimens to the other terminal of the current source. In Fig. 3 is shown the wiring diagram of the specimens. Shown in black in the diagram are the plates that cover the graphite electrodes deposited on the Eternit specimens. The terminal *C* is connected to the continuous electrode, terminals *A* and *B* to the small electrodes. Hereafter these same letters will represent the corresponding electrodes. By means of a switch it was possible to connect electrodes *AC* or *BC* to the current source. The frame was placed in a tubular furnace and heated to a temperature of 580° C.

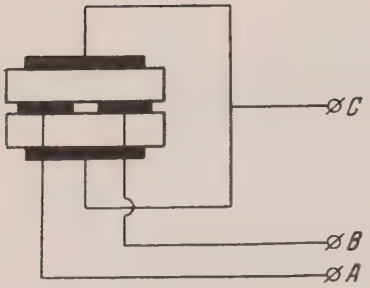

Fig. 3. Wiring diagram of specimens with auxiliary electrode (*B*).

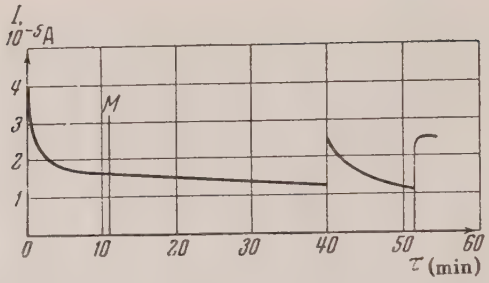

Fig. 4. Change of current in Eternit during and after formation of a cathodic film.

With equal areas of electrodes *A* and *B*, the initial currents existing at the instant of application of a field between electrodes *A* and *C* or *B* and *C*, were also equal (for $E = 225$ V/cm, $I_A = I_B = 4 \times 10^{-5}$ A). Initially the electric field was applied in such a direction that electrode *A* was the anode, electrode *C* the cathode; the auxiliary electrode *B* remained free. Eleven minutes after the beginning of electrolysis, the current had diminished to 1.6×10^{-5} A. At this time the "permeable" current was equal to 3.2×10^{-5} A. On the replacement of electrode *A* by electrode *B*, the current was also equal to 3.2×10^{-5} A (Fig. 4, point *M*). As a result of further electrolysis, the current between electrodes *A* and *C* for the "shut-off" direction became equal to 1.2×10^{-5} A, and for the "permeable" 2.4×10^{-5} A; but upon replacement of *A* by electrode *B* the value 2.4×10^{-5} A was again obtained for the current. Subsequent formation of the specimen between electrodes *B* and *C* led to a corresponding decrease of the current, but the "permeable" current in this case was equal to the current passing between electrodes *B* and *C* at the instant of application of the field (2.4×10^{-5} A). The process described is shown in Fig. 4.

In These experiments, two circumstances are noteworthy: a) passage of current through the specimen between electrodes *A* and *C* has an effect on the conductance of the specimen between electrodes *B* and *C*; b) at any instant of time the initial value of the current passing through electrode *B* is equal to the value of the "permeable" current passing through electrode *A*. The decrease of conductance of the specimen between electrodes *B* and *C*, when current flows between electrodes *A (+)* and *C (−)*, shows that the electrolysis is accompanied either by an increase of resistance near the cathode, i.e., by creation of a cathodic film, or by decrease of the volume conductivity. The latter hypothesis is easily excluded by means of a similar control experiment in which electrode *C* serves as anode. In this case electrolysis between electrodes *A (−)* and *C (+)* also produce a decrease of conductance between *B (−)* and *C (+)* in consequence of the creation of an anodic film on electrode *C*; but now after change of the direction of the field between electrodes *A* and *C* ("permeable" current), the current between electrodes *B* and *C* is equal to the value that was measured upon first application of the field, i.e., before formation. From this it is also clear that the anodic film is easily destroyed by an electric field in the "permeable" direction.

Concerning the cathodic film it is so far possible only to conclude that it either is not destroyed at all, or is incompletely destroyed, since both in this and in the other case the "permeable" current is less than the current that passes through the unformed specimen. However, it is not hard to show that only on the anode does there form a film on which the electric field has an effect, and that the cathodic film is comparatively stable. For this purpose, after passage of "permeable" current between electrodes *A (−)* and *C (+)* we pass current in the "shut-off" direction between *B (+)* and *C (−)*. The characteristic variation with time of the "shut-off" current is not observed in this case. But if we apply to the electrodes a difference of potential as in the control experiment mentioned above, then replacement of electrode *A* by electrode *B* after passage of current in the "permeable" direction produces in the "shut-off" direction a decrease in current according to the characteristic curve, dependent on the duration of current in the "permeable" direction.

Experiments conducted on porcelain showed that after electrolysis of brief duration (~ 10 min, $t = 340°$ C), the initial value of "permeable" current was appreciably less than the initial value of current passing through the specimen at the instant of application of the field. However, investiga-

tions conducted by the method described above disclosed that in porcelain no high-resistance film forms on the cathode. Thus in one of the experiments ($t = 250°$ C, $E = 180$ V/cm) the initial values of the currents for electrodes A and B were equal to 2.4×10^{-5} A. During 42 minutes of electrolysis the current between electrodes A (+) and C (−) decreased to 1×10^{-5} A, and the "permeable" current between these electrodes was equal to 1.5×10^{-5} A; but the current between electrodes B and C upon switching on of electrode B did not decrease as compared with the initial value of the currents.

Observation of the character of the currents upon change of electrodes, by the method indicated above, showed that in porcelain all the changes connected with change of direction of the field occur only at the anode.

3. STABILITY AND RESISTANCE OF ELECTRODE FILMS

In the study of electrode films, one is impressed by the diverse character of the curves of "permeable" current. From photographs presented in Ref. 1 and and from Figs. 1 and 2 of the present article, it is evident that even in a single dielectric (quartz) these curves may be different. Furthermore it appeared that for all dielectrics, the course of the variation of the "permeable" current with time is determined by the conditions of preparation of the specimen. A change of direction of the field after prolonged electrolysis always gives a "permeable" current that rises more or less, and subsequent reversals give a smaller rise and then a constant current. This effect is very noticeable in the photographs in Ref. 1 (Fig. 8, quartz). It is more marked in Eternit and particularly in porcelain. In Fig. 5 are shown three curves of "permeable" current for Eternit specimens. The first curve was obtained after prolonged electrolysis, the second and third after the subsequent brief electrolysis (2-3 min) necessary for restoration of the anodic film destroyed by current in the "permeable" direction. Comparison of the curves shows that in consequence of the reversals there is a change of character of the curves: upon subsequent reversals, the values of "permeable" current very appreciably exceed the "permeable" current that passed after the first change of direction of the field.

Detailed study of the dependence of "permeable" current on the preceding preparation showed that the character of the curves is determined by the degree of stability of the anodic film. Special experiments with use of an auxiliary electrode showed

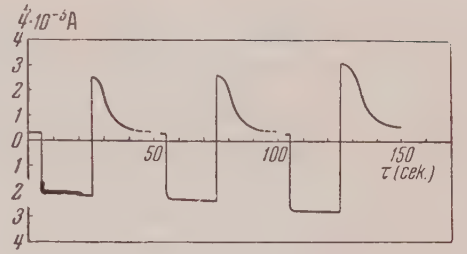

Fig. 5.

that passage of current in the "permeable" direction is always accompanied by growth of the film on the new anode ["permeable" current between C(+) and A (−) is accompanied by decrease of conductance between C and B]. But this film, originating during the short time of passage of current in the "permeable" direction, is comparatively unstable (in Eternit), and after a change of direction of the field it disappears practically instantaneously.

If, despite the increase of resistance of the new anodic film, an increasing or even constant "permeable" current is observed, sometimes over an extended time (1-2 min), this means that the passage of "permeable" current is in this case connected with a destruction of relatively stable components of the anodic film. This disappearance of a tight film on one electrode and growth of a not very stable one on the other causes a peculiar unipolar effect, which in different dielectrics has a different relative magnitude. From Fig. 1 (quartz) and Fig. 5 (Eternit) it is clear that the fall of the current in the "shut-off" direction after reversal of the field starts from a value larger than the maximum current in the "permeable" direction. This effect is particularly pronounced in those dielectrics in which short-duration electrolysis does not cause formation of stable components of film at an electrode (for example, in Eternit). In this case the high resistance on the new anode exists only for current of one direction; and since passage of current is accompanied by a diminution of resistance at the other electrode, upon change of direction of the field to the "shut-off" direction the resistance of the specimen as a whole is less than the resistance for "permeable" current. Venderovich and Lapkin [2], measuring the distribution of potential in porcelain, found that the poorly conducting film gradually disappears on change of direction of the field. The authors cited used specimens that had undergone prolonged electrolysis.

[2] A. M. Venderovich and B. Lapkin, J. Exper. Theoret. Phys. USSR 9, 46 (1939)

In this case there forms on the anode in porcelain a comparatively stable film; however, an appreciable part of the film, as our experiments have shown, is always very unstable even in porcelain.

To solve the problem of the formation of a stable component an of its relation to the unstable, we again used and auxiliary electrode.

The specimens were formed initially at temperature 320° C; the following values of current were obtained: in the "shut-off" direction, $I_A = 2 \times 10^{-5}$ A; in the "permeable", $I_C = 8 \times 10^{-5}$A; between the common electrode C and the auxiliary electrode B, $I_B = 16 \times 10^{-5}$ A. Under these conditions there formed a relatively stable electrode film. Then the temperature was raised to 420° C for a few minutes, and as the result of brief electrolysis the following currents were measured: $I_A = 5.2 \times 10^{-5}$ A; I_C increasing from 24×10^{-5} A to 40×10^{-5} A; $I_B = 40 \times 10^{-5}$ A. That is, as a result of comparatively rapid annealing at a higher temperature, the anodic film became not very stable. Further observations were made after 1 hour (Fig. 6*a*) and after 2 hours (Fig. 6*b*) in an applied field ($E = 180$ V/cm). It was found that in both cases $I_B = 56 \times 10^{-5}$ A. The large difference between the currents passing through electrode A in the "permeable" direction and through electrode B shows clearly that in this case the tight component is large; furthermore it increases in proportion to the passage of current.

It is very interesting that the current passing through the auxiliary electrode not only did not decrease, but actually increased a little (from 40×10^{-5} A to 56×10^{-5} A).

This at once shows that the decrease of current upon prolonged electrolysis in the "shut-off" and "permeable" directions is connected with the growth and enlargement of a stable electrode film, and not with any volumetric effect.

The stability of the electrode film and its resistance are much influenced by the heat treatment of the specimen. The character of the curves of "permeable" current, and also the values of the currents in the two directions at a given temperature, depend on the previous heat treatment.

In all cases a cooling of the specimen, especially of one previously annealed at a higher temperature than that of the measurements (580° C for Eternit), produces an appreciable increase of stability of the film at the anode and an increase of resistance of the specimen for currents in the "shut-off" and "permeable" directions. As a result of such treatment, there is also an increase of resistance of a specimen that has no electrode film. The procedure of cooling and subsequent heating of the specimen produces quite the same change in character of the "permeable" current curves as does prolonged electrolysis.

To study this phenomenon, the frame with the specimens was quickly withdrawn from the hot furnace, and then reinserted after partial or complete cooling. The cooling was done both in an applied field and without a field. The reheating was usually done with the field off. The electrolysis after the new heating was continued for only a few minutes; for such duration of the electrolysis, without preliminary cooling, the effect of the tight film was not noticeable. The procedure in these measurements was briefly as follows: After prolonged electrolysis, the stability of the film is decreased by a series of successive changes of direction of the field; then follow the cooling and the reheating.

In order to determine the effect of cooling on the magnitude of the electrical conductance, the specimens were subjected to electrolysis of such duration that a practically stationary current was obtained, i.e., such in each case that in the interval of time necessary for the repeated electrolysis, no noticeable change of current occurred. By use of the auxiliary electrode, it was possible to compare the change of resistance of the films and of the specimen itself.

In Table 1 are presented the data on specimens of Eternit with various preliminary treatments; for all specimens, the highest temperature used in the heating was 720°C.

It is evident from the table that the cooling-heating cycle was accompanied by an appreciable decrease of the electrical conductance with respect to currents in the "shut-off" and "permeable" directions, and also a decrease of conductivity of the specimen itself without regard to films at the electrodes. There is no doubt that, in Eternit, the resistance of the electrode film changes very greatly as a result of cooling and subsequent heating.

A diminution of conductance of electrode films and of the specimens themselves, after annealing at a high temperature, cooling and reheating, was observed also in other dielectrics (porcelain, asbestos, mica, rock salt).

4. FORMATION OF ELECTRODE FILMS AND INCREASE OF CONDUCTANCE OF DIELECTRICS

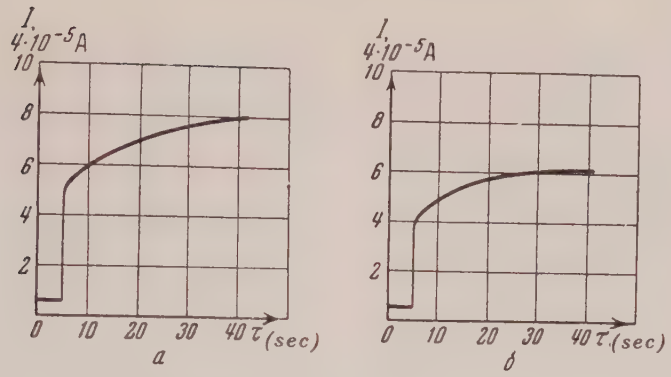

Fig. 6. Change of "permeable" current as result of the action of an electric field.

Table 1

Temperature of Measurement °C	Before Cooling 1×10^5 A			After Cooling 1×10^5 A			%			Remarks
	I_A	I_C	I_B	I_A'	I_C'	I_B'	$\frac{I_A'}{I_A}$	$\frac{I_C'}{I_C}$	$\frac{I_B'}{I_B}$	
580	3.2	12	13.2	2.4	10	12	75	83	90	Partial Cooling
580	2.8	11.2	14.4	2	8.8	12	71	79	83	
580	4	14	(a)	3	11.2	---	75	80	---	
580	1.6	8.8	(a)	1.2	8	---	75	91	---	
580	1.6	9.2	(a)	1	8	---	62	87	---	Complete Cooling
580	1.6	8.8	(a)	1	7.6	---	62	86	---	
580	1.2	10.8	(a)	0.8	8.8	---	67	81	---	
720	9.2	56	64	7.6	48	56	82	86	88	Partial Cooling

(a) Without the additional electrode

The electrolysis of a self-forming dielectric, previously annealed at an elevated temperature, is accompanied by two processes, which have opposite effects on its electrical conductance: a) an increase of the conductivity of the specimen; b) a rise in the resistance of the electrode film. The increase of conductivity is usually masked by the marked rise in resistance of the electrode film; but the observations and special experiments confirm that the conductivity of the annealed specimen increases upon subsequent action of the electric field.

In Eternit, as a result of annealing at an elevated temperature and of subsequent electrolysis, the "permeable" current is often no smaller than the initial current, passing at the instant of application of the field; with short-duration electrolysis (1-2 min), the "permeable" current may even exceed the initial current.

Special control experiments showed that even at high temperatures a cathodic film is formed; therefore it may be hypothesized that the increase of "permeable" current under such treatment is the result of an increase of conductivity of the specimen itself. This hypothesis was confirmed by special experiments. In one of the experiments, porcelain was annealed a long time at temperature 420° C. The specimen had an auxiliary electrode. At the instant of application of the field (E = 180 V/cm), the current between electrodes A-C and B-C was equal to 1.6×10^{-3}A. After a two-minute electrolysis, the "permeable" current was equal to 2×10^{-3} A, and in a few seconds it rose to 2.4×10^{-3} A; the current between the control electrode B and the common cathode C was equal to 3×10^{-3} A (until now no current had passed between B and C): i.e., as a result of electrolysis of the annealed specimen, the electrical conductance in-

creased almost twofold.

An increase of conductivity of the specimen, with simultaneous creation of a high-resistance film, fully explains why, in many dielectrics, the creation of electrode films may not be accompanied by a decrease of the current passing through the specimen. In connection with this, a phenomenon observed in asbestos is interesting. Specimens with a supplementary electrode were heated to 780° C. A brief switching in showed that a current of 2×10^{-5} A existed in each of the electrodes A and B. Twenty-six minutes after the start of electrolysis, the current strength between electrodes A and C was still equal to 2×10^{-5} A; but instantaneous switching in of control electrode B clearly showed that creation of an electrode film was occurring on electrode A, since at this time the current between B and C had risen to 4×10^{-5} A. As a result of electrolysis of longer duration, the current in the "shut-off" and "permeable" directions decreased (after 75 min, $I_A = 0.8 \times 10^{-5}$A, $I_C = 1.2 \times 10^{-5}$A), but the current through the control electrode remained equal to 4×10^{-5}A.

Observations of the same sort showed that in alkali-halide crystals (rock salt), the creation of films at the electrodes can even be accompanied by an increase of the current passing through the specimen.

5. ON THE COEFFICIENT OF UNIPOLARITY

The opposite influence of the two factors mentioned—i.e., the increase of conductivity of the specimen and the rise in resistance of the electrode film—and also the phenomenon of fixation of the electrode film under the action of the field, and the increase of resistance of the film and of the specimen itself upon lowering of the temperature, make up the very complicated picture that is observed on passage of current in dielectrics at high temperatures, and that gives the "history" of the specimen.

From the discussion above it is clear that the coefficient of unipolarity at a given temperature and at constant field must depend on the previous history of the specimen. For Eternit (17 × 10 × 4 mm), at temperature 580° C and field E = 225 V/cm, as a result of prolonged electrolysis (30-60 min) we have $K \approx 2$. With increase of electrolysis time, the currents in the "permeable" and "shut-off" directions decrease, but this does not lead to a noticeable change in the coefficient of unipolarity. With increase of the temperature to 720° C and annealing at this temperature for one to two hours, after subsequent electrolysis at temperature 580° C it was found that $K \approx 4$. With the same heating, accompanied by electrolysis and subsequent lowering of the temperature to 580° C (with field applied), the value $K \approx 10$ was obtained. In porcelain (16 × 10 × 5 mm), annealing at a high temperature, with simultaneous action of the field (E = 180 V/cm), produced an even greater change in the coefficient of unipolarity. With increase of temperature from 300 to 420° C, with subsequent lowering of temperature to 300° C after prolonged electrolysis, the coefficient of unipolarity changed from $K = 4$ to $K = 23$.

The observed increase of the coefficient of unipolarity, measured at a single temperature, is due to a decrease of current in the "shut-off" direction and an increase of current in the "permeable" direction. If a specimen, initially subjected only to heat treatment at an elevated temperature (720°C) and to electrolysis at a reduced temperature (580°C), is then subjected to the action of field and heating, the rise in the coefficient of unipolarity (at t = 580°C) in this case is invariably accompanied by a decrease of current in the "shut-off" direction.

CONCLUSION

The phenomena connected with the formation and destruction of electrode films can be explained in the following way: impurities, present in the dielectric or diffusing into the specimen at the high temperature[3,4], exist in it in the form of colloidal particles[5,6], and partly in a dissociated state; the possible concentration of impurity ions depends on temperature.

At an elevated temperature, the ions migrate to the electrodes and, by giving up their charges, become transformed to neutral particles. Since, upon passage of current and lowering of temperature, the concentration of impurity ions near the electrode may exceed the equilibrium concentration possible at the given temperature, a coagulation occurs, and this leads to an increase in the stability of the electrode film and an increase of its resistance. In

[3] B. M. Gokhberg and A. V. Ioffe, Zh. R. F.-Kh. O. 62, 433 (1930); J. Exper. Theoret. Phys. USSR 1, 264 (1931); 3, 303 (1933)

[4] B. M. Gokhberg, J. Exper. Theoret. Phys. USSR 7, 1031, 1044 (1937)

[5] R. Mattai, Z. Phys. 68, 85 (1931)

[6] A. Edner, Z. Phys. 73, 623 (1932)

the same way it is possible to explain the decrease of electrical conductivity observed on lowering of the temperature, and dependent on impurities that result from annealing of the dielectric at an elevated temperature.

Upon change of the direction of the electric field, free ions leave the anode; this disturbs the equilibrium in the film. As a result, additional ionization occurs, which may continue until the anodic film is completely destroyed. A similar process of destruction of a colloidal film is observed visually in the formation of a colored film on the boundary of two dielectrics (one of which must be an alkali-halide crystal[7]).

Simultaneously with the destruction of the more stable film on one electrode, a not very stable film is formed on the other. The motion of the ions emitted by the anodic film progresses in the form of a cloud, in which the concentration of impurity ions is increased as compared with the concentration in the whole volume of the dielectric. Upon a new change of direction of the field, there again occurs an immobilization of ions at the boundary, which leads to a growth of the electrode film.

[7] Ia. N. Pershits, J. Exper. Theoret. Phys. USSR 24, 347 (1953)

The observed changes of the coefficient of unipolarity can be explained in the following way: a) annealing at the more elevated temperature increases the number of impurity ions free to participate in the creation of an electrode film; b) the electric field, by transporting ions to the electrode, increases the number of ions that become immobilized in the electrode film.

Several authors[2], on the basis of the researches of Warburg and Tegetmeier[8], are inclined to ascribe the creation of electrode films at the anode in all cases to the migration of cations, which leave the anode and thus create a high-resistance film. From this point of view it is hardly possible to explain the effect of annealing and of the electric field; therefore it seems to us more probably that the anodic film, in the dielectrics studied, is created as the result of the migration of anions. The role of electronic conduction is also not excluded in these phenomena. The electronic component of conductivity may have a large value in the neighborhood of the electrode film, where a very strong electric field is created.

[8] E. Warburg and F. Tegetmeier, Wied. Ann. 32, 447 (1887); 35, 445 (1888)

Translated by W. F. Brown, Jr.
27

SOVIET PHYSICS - JETP VOLUME 1, NUMBER 1 JULY, 1955

Construction of a Distribution Function by the Method of Quasi - Fields

IU. A. GOL'FAND
P. N. Lebedev Institute of Physics, Academy of Sciences, USSR

(Submitted to JETP editor July 10, 1954)
J. Exper. Theoret. Phys. USSR 28, 140-150 (February, 1955)

The method of quasi - fields is developed, by means of which an expression can be constructed for the distribution function. It is shown that the distribution function obtained in this fashion is the same as that of the ordinary theory. A closed expression for the distribution function is given in the form of an infinite-multiple integral.

INTRODUCTION

AN outstanding peculiarity of the present state of the quantum theory of wave fields is the excellent agreement between the theory of quantum electrodynamics with experimental data, while at the same time the results of meson theory (by meson theory we mean the present theory of the interaction of π-mesons with the field of the nucleus) have only the most general and qualitative character, and cannot be brought into any satisfactory quantitative agreement with experiment. There are two basic viewpoints relative to the origin of this failure of meson theory. The first is that meson theory, based on a formal analogy with electrodynamics, is not adequate for the physical facts, and the simple transposition of electrodynamic concepts into the field of meson phenomena is not adequate; and accordingly for construction of a proper meson theory, a new method is necessary, based on a fundamental reconstruction of our ideas as to the nature of the interaction between mesons and nuclei.

Such a viewpoint seems to us to be very probably true; however, there is also a second possibility. All mathematical methods of modern electrodynamics use, to some degree or other, an analysis of physical quantities in a power series in the charge e. This might be done directly in the form of a perturbation theory [1-3] or by means of a summing of several parts of a number of perturbation theories with the aid of solutions of integral equations [4,5] in all cases neglecting magnitudes of the order of some power of e. The success of electrodynamics at present is based on the smallness of the constant e, and as a result, on the possibility of confining oneself to a small number of approximations for obtaining very good quantitative agreement with experiment. In meson theory, in view of the large value of the binding constant, such a method may not be altogether applicable, or at least applicable only within a limited region (for example, very small meson energies). Hence for meson theory, the problem of first order importance is the search for "precise" solutions, that is, solutions not based on an assumption as to the smallness of the binding constant. The efforts of a large number of theoreticians have been concentrated in this direction; however, a solution of the problem encounters formidable mathematical difficulties and at present is far from satisfactory. Thus the second viewpoint as to the source of the failure of meson theory is essentially that the theory is basically correct, and that the cause of the divergence of theoretical predictions from experiment comes from inadequate mathematical methods.

As long as it is not possible to make a correct approach to the problem of a "precise" solution, and therefore not possible to distinguish the results which stem from the basic theory, from those which are introduced because of approximate mathematical methods, it will be very difficult to make a final pronouncement on the degree of correctness of meson theory.

In this work the attempt is made to construct a new procedure in quantum field theory. The physical ideas basic to this procedure are certain general conceptions regarding the state of free particles. As was done in Feynman's method [2] for "virtual" particles, we shall describe the state of a free particle by a 4-vector of energy-impulse, p_μ, the components of which are not connected by a relation of the type $p^2 = m^2$. The method of Feynman leads to considerable simpli-

[1] J. Schwinger, Phys. Rev. **74**, 1439 (1948); **75**, 651 (1949); **76**, 790 (1949)

[2] R. P. Feynman, Phys. Rev. **76**, 749, 769 (1949)

[3] F. J. Dyson, Phys. Rev. **75**, 1736 (1949)

[4] S. F. Edwards, Phys. Rev. **90**, 284 (1953)

[5] L. D. Landau, A. A. Abrikosov and I. M. Khalatnikov, Doklady Akad. Nauk SSSR **95**, 497, 773, 1177 (1954)

fication of the results in comparison with the non-covariant theory of excitation. However, his theory has an essential inadequacy in that it is based on the model of a "one-particle" rather than a secondary-quantized theory, and hence leads to complex expressions for processes with a large number of real or virtual particles. In contrast with Feynman, we construct a secondary-quantized scheme, an advantage of which is that it makes possible a simple and uniform consideration of the properties of a system with an arbitrary number of particles. The resulting formalism is altogether relativistically invariant and very simple in form.

The theory is constructed according to the following pattern: The formal structure of the theory is developed (the quasi-field framework). Then, by use of Hamilton's method, an expression is set up for the fundamental-operator S, by means of which the distribution function is determined for a system of interacting particles. It is shown that the distribution functions obtained by this method are identical with those of the ordinary theory.

Because of the simplicity of the formalism, the theory goes further into the computation of the distribution functions, and finally yields expressions for them in the form of infinite-multiple integrals. Analogous expressions, including infinite-multiple integrals, were obtained in the solution of the equations of Schwinger[6], in the work of Gel'fand and Minlos[7] and Fradkin[8].

The appearance in the theory of infinite-multiple integrals obviously comes from the essential problem of field theory. Hence one of the central problems in the further development of the theory is the investigation of the properties of such integrals and approximate methods for their evaluation.

So far no considerable results have been achieved along this line. Infinite-multiple integrals comprise in themselves a new mathematical concept, and the possibility of using them effectively is of necessity connected with a major upheaval in mathematics. Thus, for the solution of the problem of quantum theory of fields, it is necessary to take a new and possibly very difficult step.

1. THE CONCEPT OF THE STATE OF A PARTICLE

For clarity we will speak below of the pseudo-scalar meson theory with a pseudo-scalar symmetrical variant of interaction. However, as will be evident later, the method being elaborated is not limited to the given variation of the meson theory, but is obviously applicable for all kinds of other variations of interaction both in Fermi fields and Bose fields, as well as in the case of the interaction of several fields.

We will use a system of units in which $\hbar = c = 1$. For the Dirac matrix, we use the form of Feynman[2]. The 4-vector a_μ we shall fix by the four actual components, and the scalar product of two vectors we write in the form

$$ab = a_\mu b_\mu = a_4 b_4 - a_1 b_1 - a_2 b_2 - a_3 b_3.$$

We indicate the scalar product of the vector a_μ with the matrix vector γ_μ by the symbol

$$\hat{a} = \gamma_\mu a_\mu.$$

The point of departure of the development of the method is the general concept of the state of a free particle. The state of a nucleon is specified by the following physical quantities: the 4-vector of the energy-impulse p_μ, the spin variable α and the variable isotopic spin ρ. Further, the components of the vector p_μ are not connected by the relation $p^2 = m^2$, and can take arbitrary values independently of one another. The varying quantity α takes four independent values rather than 2 as in the ordinary theory. The variable ρ takes two values, corresponding to the proton and neutron states. The states of the antinucleons are determined in exactly the same way as those of the nucleons. The state of a meson is determined by the 4-vector of energy-impulse k_μ and variable isotopic spin r. The components of the vector k_μ are not connected by a relation $k^2 = \mu^2$ and can take independently arbitrary values. The variable r can have three values corresponding to charge states of the π-meson.

Creation and annihilation operators are introduced for construction of the secondary-quantized scheme. For nucleons two kinds of creation operators are necessary: $a^+_{\alpha\rho}(p)$, $b^+_{\alpha\rho}(p)$, and, corresponding to them, annihilation operators $a_{\alpha\rho}(p)$, $b_{\alpha\rho}(p)$. Operators for creation and annihilation of mesons are designated $c^+_r(k)$ and $c_r(k)$. We note that the operators a^+ and a, etc., are not assumed Hermitian conjugates. More than this, in the following we will not be concerned with Hermitian properties in the operators and therefore will not introduce the idea of Hermitian conjugates. In relation to the Lorentz transformation, the operators a and b^+ behave like the Dirac bi-spinor ψ, and the operators a and b like the bi-spinor $\bar{\psi}$, operators c^+ and c are pseudo-scalar. In rotation in isotopic space a^+, a, b^+ and b are transformed like spinors, and c^+ and c, like

[6] J. Schwinger, Proc. Nat. Acad. Sci. 37, 452 (1951)

[7] I. M. Gel'fand and R. A. Minlos, Doklady Akad. Nauk SSSR 97, 209 (1954)

[8] E. S. Fradkin, Doklady Akad. Nauk SSSR 98, 47 (1954)

vectors. The operators of creation and annihilation obey the following commutation conditions:

$$[a_{\alpha\rho}(p),\ a^{+}_{\beta\sigma}(q)]_{+} = i\delta_{\alpha\beta}\delta_{\rho\sigma}\delta(p-q),$$
$$[b_{\alpha\rho}(p),\ b^{+}_{\beta\sigma}(q)]_{+} = i\delta_{\alpha\beta}\delta_{\rho\sigma}\delta(p-q), \qquad (1.1)$$
$$[c_r(k),\ c^{+}_s(l)] = i\delta_{rs}\delta(k-l).$$

Here only those commutation brackets are written that differ from zero. In the remaining cases, the nucleon operators anti-commute among themselves and commute with the meson operators, while the meson operators commute with one another.

Now that the operators of creation and annihilation have been determined, we can fix the state of a vacuum Φ_0 as the state in which there is no particle. The mathematical property of a vacuum is fixed by the equations

$$a\Phi_0 = b\Phi_0 = c\Phi_0 = 0. \qquad (1.2)$$

Different products of operators of creation, acting on a vacuum, generate a state with the specified number of particles. As is commonly done, we assume the state resulting from this arrangement as a basis in space for all states of a system of nucleon and meson fields.

The mean value over a vacuum of a certain operator A is determined in a natural manner, as expressed through operators of creation and annihilation. This mean value we will designate by the symbol $<A>_0$. In computing the mean in a vacuum, the normalization condition must be used

$$(\Phi_0,\ \Phi_0) = \langle 1\rangle_0 = 1.$$

2. THE QUASI-FIELD FRAMEWORK

We now specifiy operators playing in our scheme the role of field operators of the ordinary theory. Although hereafter we will be concerned only with quasi-fields, we reserve for them the designation used in the ordinary formalism for field operators. Operators of the quasi-field are fixed by the following Fourier integrals*.

The nucleon operators of the quasi-field are

$$\psi_\rho(x) = \frac{1}{(2\pi)^2}\int \{(\hat{p}-m)^{-1/2}a_\rho(p)\,e^{-ipx} + (\hat{p}+m)^{-1/2}b^{+}_\rho(p)e^{ipx}\}\,dp, \qquad (2.1)$$

$$\bar{\psi}_\rho(x) = \frac{1}{(2\pi)^2}\int \{a^{+}_\rho(p)(\hat{p}-m)^{-1/2}e^{ipx} + b_\rho(p)(\hat{p}+m)^{-1/2}e^{-ipx}\}\,dp.$$

The quasi-field meson operator is

$$\varphi_r(x) = \frac{1}{(2\pi)^2}\int (k^2-\mu^2)^{-1/2}\{c_r(k)e^{-ikx} + c^{+}_r(k)e^{ikx}\}\,dk. \qquad (2.2)$$

In Eqs. (2.1 and (2.2) the integration is carried out throughout the entire 4-dimensional momentum space. Inasmuch as the integrands have singularities at points lying on the surfaces $p^2 = m^2$ and $k^2 = \mu^2$ (m and μ are the masses of nucleon and meson respectively), for removal of duality of mass values we assume a difference in mass in the form of infinitesimally small negative imaginary particles.

The square roots of the Dirac matrices appearing in Eq. (2.1) are fixed by the equations:

$$(\hat{p}-m)^{-1/2} = \frac{\hat{p}+m-i\sqrt{p^2-m^2}}{\sqrt{2(m-i\sqrt{p^2-m^2})(p^2-m^2)}},$$
$$(\hat{p}+m)^{-1/2} = i\frac{\hat{p}-m+i\sqrt{p^2-m^2}}{\sqrt{2(m-i\sqrt{p^2-m^2})(p^2-m^2)}}.$$

The identity of mass values in the determination of the square root will hereafter play no part.

We notice that the operators of the quasi-field [Eqs. (2.1) and (2.2)] do not satisfy any kind of differential equation, and the equations of motion for the operators are nowhere used in the scheme developed here. In the following we depend on the commutation properties of the operators of the quasi-field (only the non-trivial commutation brackets are written out):

$$[\psi_{\alpha\rho}(x),\ \bar{\psi}_{\beta\sigma}(y)]_{+} = 0,$$
$$[\varphi_r(x),\ \varphi_s(y)] = 0. \qquad (2.3)$$

The remaining commutation brackets rotate to 0 in a trivial manner. In this way all the operators of the quasi-field at two arbitrary 4-parameter points x and y either commute or anti-commute among themselves.

The meaning of the operators of the quasi-field appears on computation of the vacuum averages of the product of two operators (only the magnitudes different from 0 are written):

$$\langle\bar{\psi}_{\alpha\rho}(x)\psi_{\beta\sigma}(y)\rangle_0 = -\langle\psi_{\beta\sigma}(y)\bar{\psi}_{\alpha\rho}(x)\rangle_0 = {}^1/_2\,\delta_{\rho\sigma}S^{F}(y-x), \qquad (2.4)$$

* After sending the paper to the editor, the author found works in which analogous operators were considered [e.g., see Iu. V. Novozhilov, Doklady Akad. Nauk SSSR 99, 533, 723 (1954) and S. Coester, Phys. Rev. 95, 1318 (1954)].

$$\langle \varphi_r(x)\varphi_s(y)\rangle_0 = {}^1/_2\,\delta_{rs}D^F(x-y).$$

Here S^F and D^F are the well known Feynman functions (see, for example, reference 9). Equations (2.3) and (2.4) follow readily from Eqs. (2.1), (2.2) and (1.1).

Relations (2.4) serve as a connecting link between the formalism of the quasi-field and the ordinary formalism. Actually, Eq. (2.4) leads to the known relations of field theory, if the symbols ψ and ϕ stand for the ordinary field operators in the interaction considered, and in place of the product, if the T-product of the operators is used.

By virtue of Eq. (2.3), the T-product for the quasi-field coincides with the ordinary product. It is possible to eliminate from the theory the idea of the T- product, which leads to considerable simplification.

3. THE FUNDAMENTAL OPERATOR

We formulate in terms of the quasi-field the analogue of the S- matrix, written in the form due to Dyson[3]. For this we determine the interaction operator of the field, which for a symmetrical pseudo-scalar meson theory, has the form

$$K(x) = ig\bar{\psi}(x)\gamma_5\tau_r\psi(x)\varphi_r(x). \qquad (3.1)$$

The fundamental operator S is determined by the equation

$$S = \exp\left\{-i\int (x)\,dx\right\}. \qquad (3.2)$$

We notice certain peculiarities of Eq. (3.2). First, by virtue of Eq. (2.3), the quantities $K(x)$ at different points of space commute with one another. Hence, in Eq. (3.2), only quantities are involved that commute, so that the exponential function can be considered in the algebraic sense rather than the symbolic sense, as is done in the references 10 and 11. Second, the integral in the exponent of Eq. (3.2) is distributed in all of 4-dimensional space. This fact insures the validity of the conservation of the 4-momentum in each elementary interaction. If, in place of the quasi-field, one should set up the ordinary field operators, the corresponding integral would transform to 0 by virtue of the existence of relations of the type $p^2 = m^2$, which naturally does not occur in our case.

In what follows, it will be appropriate for us to make the transition from coordinate representation to momentum. Also we introduce into the space of the 4-momentum a cubic lattice with 4-dimensional volume $(2\pi)^4/\Omega$ and will refer all quantities to the nodes of the lattice. To shorten the writing, we will use the complex indices

$$\lambda = (p, \alpha, \rho), \quad l = (k, r),$$

and agree that symbols of the type $-\gamma$ and $-l$ stand for the quantities

$$-\lambda = (-p, \alpha, \rho), \quad -l = (-k, r).$$

We replace the operators of creation and annihilation, introduced in Sec. 1, by the operators

$$a^+_\lambda = \frac{(2\pi)^2}{\sqrt{\Omega}}\,a^+_{\alpha\rho}(p) \qquad \text{etc.},$$

satisfying, by virtue of Eq. (1.1), the commutation relations

$$[a_\lambda, a^+_\mu]_+ = [b_\lambda, b^+_\mu]_+ = i\delta_{\mu\nu}, \qquad [c_l, c^+_m] = i\delta_{lm}. \qquad (3.3)$$

After obvious development, we obtain the following expression for S:

$$S = e^K, \qquad (3.4)$$

$$\times K = i\sum_{\mu\nu l}(a^+_\mu - ib_{-\mu})\,\Gamma^l_{\mu\nu}(b^+_{-\nu} + ia_\nu) \qquad (3.5)$$

$$(c^+_l + c_{-l}),$$

$$\Gamma^l_{\mu\nu} = -\frac{g}{\sqrt{\Omega}}(\hat{p} - m)^{-1/2}\gamma_5(\hat{q} - m)^{-1/2} \qquad (3.6)$$

$$\tau_r(k^2 - \mu^2)^{-1/2}\,\delta_{p-q+k}$$

$$\mu = (p, \alpha, \rho), \quad \nu = (q, \beta, \sigma), \quad l = (k, r).$$

In Eq. (3.6) the matrix indices of the Dirac matrix, and the matrix of the isotopic spin τ_r are not written out explicitly. We notice that only Eq. (3.6) is specific for a given variant of the meson theory. In what follows we will not depend on the concrete form of Γ, and hence our derivation will hold for all other variants of the theory.

4. DISTRIBUTION FUNCTION

Through the fundamental operator S the distribution function is determined for an arbitrary

[9] A. I. Akhiezer and V. B. Berestetskii, *Quantum Electrodynamics*, Moscow (1953)

[10] R. P. Feynman, Phys. Rev. **84**, 108 (1951)

[11] I. Fujiwara, Progr. Theor. Phys. **7**, 433 (1952)

system of interacting particles. To be concrete, we consider the particular case in which both initially and finally the states of the system consist of mesons and nucleons; however, all the deliberations clearly carry over to the general case. We determine the distribution function for our case by the expression

$$K(x_1' x_2';\ x_1 x_2) = \langle \varphi(x_1')\psi(x_2') \times S\varphi(x_1)\bar{\psi}(x_2)\rangle_0. \tag{4.1}$$

We show that Eq. (4.1) is in identical agreement with the corresponding expression of the ordinary theory. For this, we consider the Nth term of the expansion of Eq. (4.1) in a series in powers of g. According to Eqs. (3.1) and (3.2) this term is equal to

$$K_N(x_1', x_2';\ x_1 x_2) = \frac{g^N}{N!}\int dt_1 \ldots \int dt_N \langle \varphi(x_1')\psi(x_2')\bar{\psi}(t_1)\gamma_s\tau_{r_1}\psi(t_1)\varphi_{r_1}(t_1)\ldots \bar{\psi}(t_N)\gamma_s\tau_{r_N}\psi(t_N)\varphi_{r_N}(t_N)\varphi(x_1)\bar{\psi}(x_2)\rangle_0. \tag{4.2}$$

The vacuum average, appearing under the integral sign, in conformity with Wick's theorem [12] (this theorem is valid also for the quasi-field), is equal to the sum of all possible components, in which all operators are connected in pairs. Yet, on the one hand, every system of connection corresponds to some Feynman diagram, and conversely; and, on the other hand, in conformity with Eq. (2.4), the equation for connection of operators of the quasi-field agree with the corresponding expressions for ordinary fields. From this it follows that in Eq. (4.2) contributions are summed of all the Feynman diagrams of the Nth order, and in this fashion our assertion is demonstrated.

Points x_i and x_i' correspond to the free ends of the outer lines of the diagram, the points t correspond to the ends of the inner lines, and the integration is carried out over them.

By means of the propagation function $K(x_1' x_2';\ x_1 x_2)$ the elements of the S-matrix can be directly computed by Feynman's rule [2] for the process of scattering of mesons by nucleons.

For later applications it is rather convenient to transform Eq. (4.1). We take advantage of the fact that, by virtue of Eqs. (3.1), (3.2) and (2.3), the operator S commutes with all the operators of the quasi-field; and we transpose the operators $\varphi(x_1)$ and $\psi(x_2)$ over to the left of S. Then

$$K(x_1' x_2';\ x_1 x_2) = \langle \varphi(x_1')\varphi(x_1)\psi(x_2')\bar{\psi}(x_2) S\rangle_0 = (\bar{\Phi}_0 | \varphi(x_1')\varphi(x_1)\psi(x_2')\bar{\psi}(x_2) | \Psi_0), \tag{4.3}$$

where

$$\Psi_0 = S\Phi_0 \tag{4.4}$$

In this manner the determination of the propagation function boils down to the computation of the vector Ψ_0, after which the problem takes on an algebraic character. Essentially the vector Ψ_0 does not depend on the specific process to which the given propagation function is related.

5. THE RESOLVING OPERATION

The vector Ψ_0, determined in the foregoing section, as well as all vectors in state space, can be put in the form

$$\Psi_0 = U\Phi_0, \tag{5.1}$$

where the operator U is expressed only through the operators of particle creation. If we compare Eqs. (4.4) and (5.1), we see that to the operator S, which is expressed in terms of operators of creation as well as operators of annihilation, there corresponds the operator U which contains only operators of creation. The transformation from the operator S to the operator U, we will call the resolution of operator S and define the transformation symbol $U = S > 0$. A further problem will be to devise certain general methods of resolution.

On the basis of relations which are valid for arbitrary operators x and a:

$$e^x a e^{-x} = \sum_{n=0}^{\infty} \frac{1}{n!}\left[{}^n x,\ a\right]. \tag{5.2}$$

[for proof of Eq. (5.2) see Appendix I] and the corresponding commutation Eq. (3.3), it is easy to establish the validity of the following equations:

$$e^P a_\lambda^+ e^{-P} = a_\lambda^+ - ib_{-\lambda},\ e^P b_{-\lambda}^+ e^{-P} = b_{-\lambda}^+ + ia_{-\lambda},\ e^Q c_i^+ e^{-Q} = c_i^+ + c_{-i} \tag{5.3}$$

where

$$P = \sum_\mu a_\mu b_{-\mu}, \tag{5.4}$$

[12] G. C. Wick, Phys. Rev. 80, 268 (1950)

$$Q = -\frac{i}{2}\sum_m c_m c_{-m}.$$

From Eqs. (5.3), (3.4) and (3.5) it follows that the operator S can be expressed in the form

$$S = e^{P+Q}\, e^{K_0}\, e^{-(P+Q)}, \tag{5.5}$$

where the operator

$$K_0 = i\sum_{\mu\nu l} a_\mu^+ \Gamma_{\mu\nu}^l\, b_{-\nu}^+ c_l^+ \tag{5.6}$$

contains only the operators of creation.

We introduce the symbol

$$\sum_{\mu\nu} a_\mu^+ \Lambda_{\mu\nu}\, b_{-\nu}^+ = a^+ \Lambda b^+,$$

where Λ is a matrix. Then K_0 can be written in the two equivalent forms

$$K_0 = i\sum_l x_l c_l^+ = a^+\Gamma(c^+)\, b^+, \tag{5.7}$$

where

$$x_l = a^+\Gamma^l b^+, \tag{5.8}$$
$$\Gamma(c^+) = i\sum_l \Gamma^l c_l^+.$$

From the properties of the vacuum [Eq. (1.2)] it follows that in resolution, one can reject terms in which an operator of annihilation is found on the right side. Hence, from Eqs. (5.5) and (5.4) comes the relation

$$S\rangle_0 = e^{P+Q}\, e^{K_0}\rangle_0. \tag{5.9}$$

6. "DIFFUSION" EQUATIONS

We have for resolution expressions of the type in Eq. (5.9) for which it is characteristic that all operators of annihilation are to the left of the creation operators. Let $F(c^+)$ be some function of the meson creation operators. Then

$$QF\rangle_0 = -\frac{i}{2}\sum_m [c_m, [c_{-m}, F]]$$
$$= \frac{i}{2}\sum_m \frac{\partial^2 F}{\partial c_m^+\, \partial c_{-m}^+},$$

that is, the resolution operator Q, standing on the left of the function depending on c^+, acts like the differential operator

$$Q = \frac{i}{2}\sum_m \frac{\partial^2}{\partial c_m^+\, \partial c_{-m}^+}. \tag{6.1}$$

Likewise, if $F(a^+, b^+)$ is a function of nucleon operators of creation, in the resolution of which the overall number of operators a^+ and b^+ s even, then

$$PF\rangle_0 = \sum_\mu [a_\mu, [b_{-\mu}, F]]_+, \tag{6.2}$$

that is, P can also be considered a differential operator, but with this difference, that differentiation is carried out with respect to the anti-commuting variables* a^+ and b^+.

Hence, in view of Eq. (5.9),

$$U = S\rangle_0 = e^P e^Q e^{K_0}, \tag{6.3}$$

where P and Q are operators whose actions are determined by Eqs. (6.1) and (6.2). For evaluating expressions of the type of Eq. (6.3) we use the following relation. If F_0 is some function, and L is a linear operator, the function

$$F = e^L F_0$$

can be considered a solution of the equation

$$\partial F/\partial z = LF \qquad \text{for} \qquad z = 0,\ F = F_0 \tag{6.4}$$

if we set $z = 1$. Equation (6.4) has the character of a "diffusion" equation. Analogous equations are used for computing S-matrices in references 12 and 13.

In light of the simple character of the operator Q, the computation of $e^Q e^{K_0}$ can be carried out directly. We consider the case $L = P$. In this we are limited to a class of functions F depending on the variables

$$x_n = a^+\Lambda^n b^+ \quad (n = 1, 2, \ldots).$$

Operator P does not develop a function of this class, and Eq. (6.4) takes the form of Eq. (6.5). [The notation is introduced $\lambda_n = \mathrm{Sp}\,\Lambda^n = \sum_\mu (\Lambda^n)_{\mu\mu}$. The derivation of Eq. (6.5) is shown in Appendix II.]

---

* We will not introduce any special symbolism for this differentiation.

[13] S. Hori, Progr. Theor. Phys. 7, 578 (1952)

$$\frac{\partial F}{\partial z} = -\sum_{m,n=1}^{\infty} x_{m+n} \frac{\partial^2 F}{\partial x_m \partial x_n} + \sum_{n=1}^{\infty} \lambda_n \frac{\partial F}{\partial x_n} . \quad (6.5)$$

The solution of Eq. (6.5) for $F_0 = e^{x_1}$ is equal to

$$F(z) = \exp\left\{\sum_{n=1}^{\infty} (-1)^{n-1} \left(x_n z^{n-1} + \lambda_n \frac{z^n}{n}\right)\right\}. \quad (6.6)$$

7. THE EXPRESSION FOR THE OPERATOR U

Taking into account Eqs. (5.7), (5.8) and (6.1), it is easy to establish the equality

$$e^{Q} e^{K_0} \equiv e^{Q} \exp\left\{i \sum_l x_l c_l^+\right\} = \exp\left\{i \sum_l (x_l c_l^+ - {}^1/_2 x_l x_{-l})\right\}. \quad (7.1)$$

Further, from Eq. (6.6), for $z = 1$ and $\Lambda = \Gamma(c^+)$, it follows that

$$e^{P} e^{K_0} \equiv e^{P} \exp\{a^+ \Gamma(c^+) b^+\} = \exp\left\{\sum_{n=1}^{\infty} (-1)^{n-1} [a^+ \Gamma^n(c^+) b^+ + \frac{1}{n} \mathrm{Sp}\, \Gamma^n(c^+)]\right\}. \quad (7.2)$$

Results analogous to Eqs. (7.1) and (7.2) and corresponding to resolution of one of the fields are achieved by the methods of ordinary theory in references 10 and 14.

Simultaneous resolution of two fields is performed as follows: We consider the formal expansion of e^{K_0} in an infinite-product Fourier integral

$$e^{K_0} \equiv \exp\left\{i \sum_l x_l c_l^+\right\} = \int \exp\left\{i \sum_l x_l s_l\right\} \exp\left\{i \sum_l c_l^+ t_l\right\} \times \exp\left\{-i \sum_l s_l t_l\right\} ds\, dt = \int \exp\{a^+ \Gamma(s) b^+\} \exp\left\{i \sum_l c_l^+ t_l\right\} \times \exp\left\{-i \sum_l s_l t_l\right\} ds dt, \quad (7.3)$$

where

$$ds = \prod_l \frac{ds_l}{\sqrt{2\pi}}, \qquad dt = \prod_l \frac{dt_l}{\sqrt{2\pi}} .$$

In Eq. (7.3) variables pertaining to nucleons and mesons are separated. Applying the results of Eqs. (7.1) and (7.2), we obtain, in conformity with Eq. (6.3),

$$U = e^{P+Q} e^{K_0} = \int \exp\left\{\sum_{n=1}^{\infty} (-1)^{n-1} \left[a^+ \Gamma^n(s) b^+ + \frac{1}{n} \mathrm{Sp}\, \Gamma^n(s)\right]\right\} \times \exp\left\{i \sum_l c_l^+ t_l - s_l t_l - \frac{1}{2} t_l t_l\right\} ds dt.$$

Integration with respect to t can be carried out directly inasmuch as the infinite-product integral is broken down into the product of double integrals. As a result we obtain the following infinite product expression

$$U = \int \exp\left\{\sum_{n=1}^{\infty} (-1)^{n-1} \left[a^+ \Gamma^n(s) b^+ + \frac{1}{n} \mathrm{Sp}\, \Gamma^n(s)\right]\right\} \times \exp\left\{\frac{i}{2} \sum_l (c_l^+ - s_l)(c_{-l}^+ - s_{-l})\right\} ds. \quad (7.4)$$

By means of Eqs. (7.4) and (5.1) it is easy to obtain the distribution function as was shown in Sec. 4. Analogous expressions for the distribution functions were obtained by Fradkin[8] from Schwinger's theory[6].

In conclusion the author expresses his deep gratitude to Academician I. E. Tamm for his great influence on this work and for general review of the results.

APPENDIX

I. DEMONSTRATION OF EQ. (5.2)

In Eq. (5.2), the repeated commutator $\left[{}^n x, a\right]$ is determined by the recurrent relations

$$\left[{}^0 x, a\right] = a, \quad \left[{}^{n+1} x, a\right] = \left[x, \left[{}^n x, a\right]\right].$$

The formula is easily demonstrated by the induction method

[14] K. Yamazaki, Progr. Theor. Phys. 7, 449 (1952)

$$\left[\overset{n}{x},\ a\right] = \sum_{p+q=n} (-1)^q \binom{n}{q} x^p a x^q.$$

Hence

$$e^x a e^{-x} = \sum_{p,\ q=0}^{\infty} \frac{(-1)^q}{p!\ q!} x^p a x^q$$

$$= \sum_{n=0}^{\infty} \frac{1}{n!} \sum_{p+q=n} (-1)^q \binom{n}{q} x^p a x^q$$

$$= \sum_{n=0}^{\infty} \frac{1}{n!} \left[\overset{n}{x},\ a\right].$$

II. DERIVATION OF EQ. (6.5)

Let the operator a have the property that the commutator $[a, x_n]$ commute with operators x_m for all m and n. Then the following relation holds*

$$[a,\ F(x_1,\ x_2,\ \ldots)] = \sum [a,\ x_n] \frac{\partial F}{\partial x_n}, \qquad \text{(A)}$$

proof of which is almost obvious.

Expression (A), in particular, is applicable for $a = a_\mu$ and $a = b_{-\mu}$. Inasmuch as the operators a^+ and b^+ occur in pairs in the expressions for x_n, the action of the operator P on the function F is determined by Eq. (6.2).

For direct computation, use is made of (A) and the relation:

$$[a,\ bc]_+ = [a,\ b]_+ c - b\,[a,\ c],$$
$$[a,\ bc] = [a,\ b]_+ c - b\,[a,\ c]_+,$$

We then get

$$PF = -\sum_{m,\ n} a^+ \Lambda^{m+n} b^+ \frac{\partial^2 F}{\partial x_m \partial x_n}$$

$$+ \sum_n \mathrm{Sp}\, \Lambda^n \frac{\partial F}{\partial x_n},$$

which agrees with the right side of Eq. (6.5).

Translated by D. T. Williams
23

* The derivatives $\partial F / \partial x_n$ have the ordinary meaning since the operators x_n commute with one another.

New Means of Control of Compensating the Earth's Magnetic Field in Investigations on a Vertical Astatic Magnetometer

A. I. Drokin
Krasoiarsk State Teacher's Institute

(Submitted to JETP editor May 7, 1953)
J. Exper. Theoret. Phys. USSR 28, 199-200 (February, 1955)

A new method is given for checking the required intensity of a current in the windings of a vertical astatic magnetometer for compensating the vertical components of the earth's magnetic field and other external parasitic fields.

THE method offered here is based on the utilization of the magnetic temperature hysteresis[1-5], i.e.,on the irreversible variation of the intensity of magnetization in a weak, steady magnetic field upon heating and cooling of a ferromagnetic specimen.

Figures 1 and 2 display, respectively, the curves for the magnetic temperature hysteresis of specimens of Fe-Si alloy and polycrystalline nickel in a field of 0.06 oersted, according to Shur and Baranova [4], taken with the use of an A type cycle, i.e. heating followed by cooling.

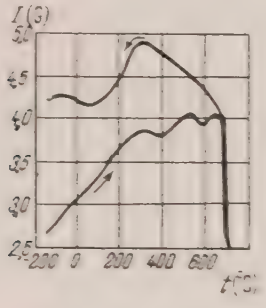

Fig 1. Magnetic temperature hysteresis of a sample of of iron-silicon alloy (3.7% Si) He = 0.06 oersted

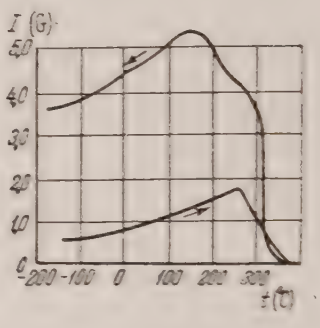

Fig. 2. Magnetic temperature hysteresis of a sample of polycrystalline nickel. H_e = 0.06 oersted

It is observed from these Figures that, as one approaches the Curie point, the magnetization of the samples grows suddenly up to a maximum (Hopkinson's effect [6]), and then falls down to zero. On cooling, a sudden increase in magnetization appears again, with a maximum which lies far above the Hopkinson's maximum.

If these phenomena are observed in absence of current in the magnetizing coil of the magnetometer, it is obvious that the sample lies in a weak steady field due to the vertical component of earth's magnetism or in a constant parasitic magnetic field. On selecting the appropriate current in the compensating winding of the magnetometer one can achieve a situation such that a crossing of the Curie point on cooling will not be followed by an increase in the magnetization of the sample. At the same time this will serve as a proof of the full compensation of the influence of the vertical component of the earth's magnetic field and of any external parasitic fields.

[1] Ia. S. Shur and V. I. Drozhzhina, J. Exper. Theoret. Phys. USSR 17, 607 (1947)

[2] V. I. Drozhzhina and Ia. S. Shur, Izv. Akad. Nauk. SSSR Ser. Fiz. 11, 539 (1947)

[3] Ia. S. Shur, N. A. Baranova and V. A. Zaikova, Doklady Akad. Nauk. SSSR 81, 557 (1951)

[4] Ia. S. Shur and N. A. Baranova, J. Exper. Theoret. Phys. USSR 20, 183 (1950)

[5] S. V. Vonsovskii and Ia. S. Shur, *Ferromagnetism*-Moscow 1948, p. 426

[6] Hopkinson, Phil. Trans. 153, 443 (1889)

Thus, if one investigates with the magnometer a process related to temperature change, then, in order to select the right current in the compensating winding, there is no need to build a complicated additional device such as a ballistic coil in series with a galvanometer [7], i.e. an induction inclinator[8], or an arrangement of switches and potentiometers in the magnetic circuit in order to obtain in it an alternating current with a smoothly damped amplitude. If one studies a process at room temperature, in order to choose the current in the compensating windings, one substitutes a nickel sample (Curie point 360 °C) for the original one, by placing it inside of the bifilar winding of the furnace; this is much simpler to do than to manufacture an induction inclinator or to arrange a set of potentiometers which would smoothly decrease the amplitude of the alternating current.

Thus, on working with a vertical magnetometer, for compensating the external fields one has first to compensate the effect of the magnetic fields of the magnetometer coils on the astatic suspension; this is achieved by moving the movable coil of the magnetometer [1] and by using a shunt in the magnetic circuit [9]. Then, with the magnetizing circuit open, the sample is placed in the fixed coil and is heated up to a temperature above the Curie point. The light spot reflected from the mirror of the static suspension is to be positioned on the division of the scale which corresponds to a zero magnetization of the specimen. After that, current is fed into the compensating coil and the furnace is disconnected.

On the cooling of the sample the crossing of the Curie point is usually followed by a deviation of the spot in a direction which depends on the intensity of the current in the compensating winding. By repeating similar operations one can select a "compensating current" of a magnitude such that the crossing of the Curie point on cooling of the sample will not be followed by a deviation of the spot from the zero position.

There is no need to cool the sample down to the room temperature on each operation. For Ni, for instance, it is sufficient to cool down to 320 °C to detect a deviation of the spot from the zero position of magnetization. Therefore, the time lost in each operation is not more than 3-5 minutes and the total time for compensating the vertical field components is about 20-25 minutes, i.e., almost the same as that in using an induction inclinator.

The accuracy of compensation by the proposed method is increased considerably because the very high sensitivity of the static suspension is utilized. Fields of the order of 10^{-4} oersted are "caught" by this method; with a magnetizing field of 0.015 oersted this represents a relative error of only 0.6%.

If the dimensions of the magnetometer coil permit the making of a very sensitive induction inclinator, the proposed method can be used to control the correctness of the compensation of the vertical components of earth's magnetic field and external parasitic fields.

---

[7] *Spezialny Fizicheskii Praktikum*, Moscow State Univ. 2, 115 (1945)

[8] *O. D. Khvol'son Kurs Fiziki (Course in Physics)* 4, 2 (Rikker Edition) (1915) p. 164

[9] J. Richard and R. M. Bozorth, J. Opt. Soc. Amer. 10, 593 (1925)

Translated by B. Cimbleris
29

The Proton Component of Cosmic Rays at 3200 Meters Above Sea Level

N. M. KOCHARIAN
Physical Institute, Academy of Sciences, Armenian SSR
(Submitted to JETP editor February 8, 1954)
J. Exper. Theoret. Phys. USSR 28, 160-170 (February, 1954)

The momentum spectrum of protons at an altitude of 3200 meters above sea level was obtained in the range of momenta $0.4 \leq p \leq$ BeV/c. The absorption lengths of the protons in air and in lead are determined. The spectrum of protons generated in lead is investigated.

1. DESCRIPTION OF THE APPARATUS

THE results reported in this paper are based on measurements made with two versions of a magnetic spectrometer. The first was described in detail previously[1]. The second, which provides great accuracy, will be described briefly here.

The particle momenta were measured in a field produced by an electromagnet, of strength 5800 oersteds, vertical length 80 cm, width 20 cm, and gap 10 cm (Fig. 1). Four trays of coordinate counters, K_1, K_2, K_3 and K_4, were used to determine the radii of curvature of the particle trajectories. The counters in trays K_1, K_3 and K_4 determined the radius of curvature, while those in tray K_2 served to check the accuracy of these determinations. In order to improve the accuracy of determination of the particle paths the counters were distributed in two layers in the trays[2]. These counters were 10 cm long and were of inside diameter $d = 4.6$ mm. From the point of view of specifying the path of the particles, these counters were equivalent to counters of diameter $^1/_3 d = 1.53$ mm distributed in a single layer. The counters in trays K_2 and K_3 were made of aluminum to reduce multiple scattering effects. The other counters had copper cathodes.

So that particles scattered from the poles of the magnet could be rejected, the counters, T, 1 cm in diameter, were placed on the poles at intervals of 3 cm, as indicated in Fig. 1. Two plates of lead, Π and Π', 5 cm in thickness, and 1 cm in thickness respectively, a total of 68 gm/cm^2, were placed above the magnet. These were removed for some of the measurements.

Seven double layer trays of copper-walled counters were located underneath the magnetic field, with absorbers Π_1, Π_2, Π_3, Π_4, Π_5 and Π_6 placed between these, as shown in Fig. 1. The first of these, Π_1, consisting of 4 cm of lead, was for the purpose of absorbing electrons, while the other absorbers were, respectively, 1, 4.2, 1.8, 6 and 2 cm of copper. Thus the total thickness of absorbers was $0.28\,\lambda_{Pb} + 1.23\,\lambda_{Cu}$, where λ_{Pb} and λ_{Cu} are the nuclear interaction lengths, assumed to be 160 gm/cm^2 and 108 gm/cm^2, respectively.

All of the counters, with the exception of those in K_{11} and T were individually connected to neon bulbs. The system was actuated only when a particle passed through counters in each of the trays K_1, K_3 and K_4. When this occurred the appropriate neon bulbs indicated through which particular counters the particle had passed. The mean square error of momentum determination in this assembly, due to the finite size of the counters and to multiple scattering in the counter walls, is given by

$$\sigma = \sqrt{(0.035p)^2 + \left(\frac{0.018}{\beta}\right)^2}. \qquad (1)$$

where β is the particle velocity in units of the velocity of light and p the particle momentum in units of BeV/c.

2. MOMENTUM SPECTRUM OF THE PROTONS

Using the arrangement described previously[1], 6085 protons were observed which had momenta ≥ 0.4 BeV/c and which were stopped in copper and lead absorbers of an equivalent thickness for ionization of 198 gm/cm^2. Of these 6085 protons, 1740 had momenta $\gtrsim$ BeV/c and were stopped in the absorbers by nuclear collisions. Table 1 shows the distribution of these particles by range.

The protons and mesons were well separated in each of the range intervals of Table 1. For this rea-

[1] N. M. Kocharian, M. G. Aivazian, Z. A. Kirakosian and S. D. Kaitmazov, Doklady Akad. Nauk Armenian SSR 17, 33 (1953)

[2] N. M. Kocharian, P. S. Saakian, M. G. Aivazian, Z. A. Kirakosian and S. D. Kaitmazov, J. Exper. Theoret. Phys. USSR 23, 532 (1952)

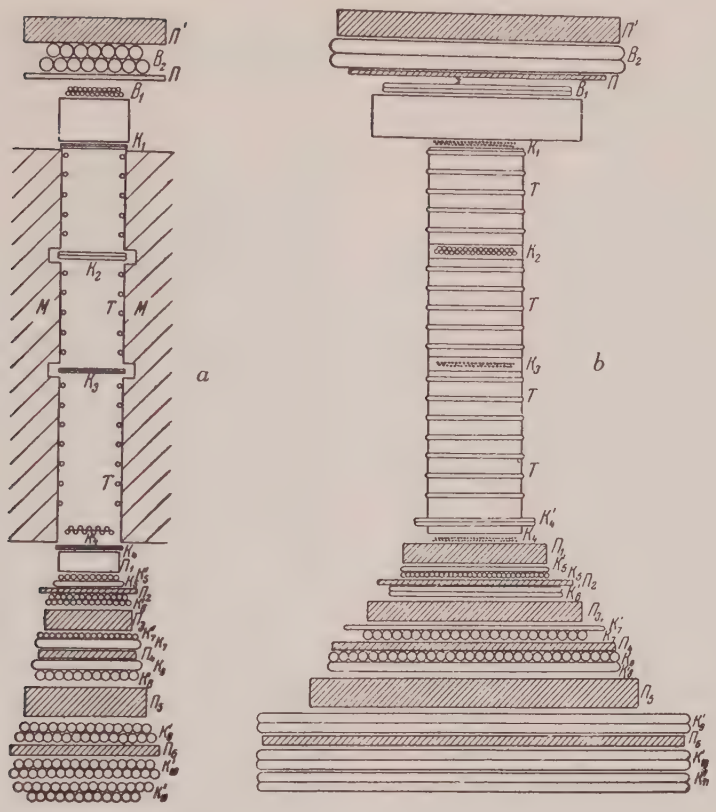

Fig. 1. Layout of the magnetic spectrometer, *a)* in the vertical plane parallel to the magnetic field, and *b)* in the vertical plane perpendicular to the field.

Table 1

Number of Protons Stopped in the Indicated Range Intervals

Range in gm/cm^2	Number of Stopped Particles		
	Ionizing	Nuclear	Total
11.3 Pb $\leqq R \leqq$ 57 Pb	1867	901	2768
57 Pb $\leqq R \leqq$ 57 $\leqq$ Pb + 22 Cu	636	473	1109
57 Pb + 22 Cu $\leqq R \leqq$ 57 Pb + 48.4 Cu .	480	415	895
57 Pb + 48.4 Cu $\leqq R \leqq$ 57 Pb + 101.7 Cu	661	652	1313

son it was possible to derive the momentum spectrum of the protons stopped in the absorbers. This spectrum would not necessarily be the true spectrum of the vertical proton flux, however. In order to obtain the true specturm it is necessary to divide the observed numbers in the differential spectrum by the probability of the particles stopping in the system of absorbers. Let "w" represent this probability. Involved in w is the probability that all of the products of nuclear interactions of protons with $p \geq 1$ BeV/c terminate in the absorbers, and hence do not set off counters in the last tray underneath all of the absorbers. This probability is a function of the energy of the particles.

Since protons of momentum $p \leq 1$ BeV/c necessarily will stop in the absorbers because of ioniza-

tion loss, in such a case $w = 1$, and the observed spectrum is the true one.

In order to evaluate w for $p > 1$ BeV/c a careful analysis was performed of the nuclear showers produced by the protons in the absorbers underneath the magnet. This analysis led to the conclusion that in most cases penetrating showers were produced by protons of $p > 3$ BeV/c. Penetrating showers were here defined to be those events in which more than one counter was set off in one of the trays situated between absorbers, and in which at least one of the products penetrated at least one of the following absorbers. In cases of momentum $p \leq 2$ BeV/c only very rarely was more than one counter in a tray set off. This implies that for such momenta the star products had little energy and so were usually absorbed in the same absorber wherein they were formed. In the rare cases at these momenta that such an event did occur, the star products were almost always absorbed in the next following absorber. Hence, it can be asserted with great confidence that particles with momenta $p \leq 2$ BeV/c are not capable of producing any appreciable number of fast secondaries able to penetrate all of the absorbers. From this it follows that the number of protons with momenta $1 \leq p \leq 2$ BeV/c which are not stopped in the absorbers by ionization is equal to the number of stars produced by particles in this range of momenta. Here, by stars are meant those inelastic collision events that give rise to more than one secondary. Thus, in the momentum range $1 \leq p \leq 2$ BeV/c the probability of stopping, w, approaches the probability of nuclear interaction, since at these momenta practically all protons suffering inelastic collisions are stopped in the absorbers along with their secondaries. Consequently, for $1 \leq p \leq 2$ BeV/c,

$$w = 1 - e^{-x_0/\lambda}, \tag{2}$$

where x_0 is the total thickness of absorbers and λ the inelastic nuclear scattering length.

Laboratory experiments on the scattering of fast neutrons[3] at energies of several tens of MeV show that the inelastic scattering length λ_a, increases with increasing energy. It first increases rapidly, but then at about 200 MeV approaches a constant value, $2\lambda_0$, where λ_0 is the inelastic scattering length corresponding to the geometrical cross section of the nuclei. Recent experiments[4,5] show that this constancy holds up to proton energies of 2.2 BeV. Thus, in the momentum range under discussion, $1 \leq p \leq 2$ BeV/c, it is correct to take $\lambda_a = 2\lambda_0$, and, for the experimental arrangement used,

$$w = 1 - e^{-x_0/2\lambda_0} = 0.48. \tag{3}$$

On the basis of Eq. (3) the deduction of the true differential spectrum from the observed numbers of protons stopped in the absorbers can be extended to momenta of the order of 2 BeV/c. For momenta $p \geq 2$ BeV/c, the probability, w, will not have the simple form of Eq. (3).

In Fig. 2 is shown the differential momentum spectrum of protons on a log-log plot. The abscissa is labeled in units BeV/c, while the ordinate indicates the intensity of the vertical flux of protons in air per unit momentum interval. The circles plotted are the results of the experiment described above, while the dots represent the results of the second version of the measurements. As is evident in the Figure, the spectrum can be approximated in the region $1.2 \leq p \leq 2$ BeV/c by a function of the form

$$N(p)\,dp = \frac{a}{p^{\gamma}}\,dp \tag{4}$$

with $\gamma = 2.65 \pm 0.23$, and $a = 1.46 \pm 0.16 \times 10^{-3}$, where p is in units of BeV/c. For values of $p \leq 1.2$ BeV/c the inclination of the curve de-

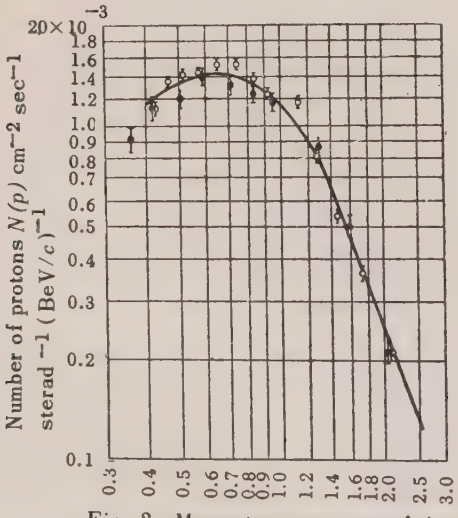

Fig. 2. Momentum spectrum of the vertical flux of protons in air at 3200 meters above sea level.

[3] V. I. Gol'danskii, A. L. Liubimov, and B. V. Medvedev, Usp. fiz. nauk **49**, 3 (1953)

[4] L. W. Smith, C. P. Leavitt, A. M. Shapiro, C. E. Schwartz and M. Wotring, Bull. Am. Phys. Soc. **28**, 15 (1953)

[5] G. A. Snow, T. Coor, D. A. Hill, W. F. Hornyak and L. W. Smith, Bull. Am. Phys. Soc. **29**, 54 (1954)

creases, and becomes zero at $p = 0.7$ BeV/c.

The intensities of the vertical proton flux are $J_0 = 0.806 \pm 0.012 \times 10^{-3}$, $0.606 \pm 0.013 \times 10^{-3}$ and 0.281×10^{-3} cm^{-2} sec^{-1} sterad^{-1} in the momentum intervals $0.4 \leq p \leq 1$ BeV/c, $1 \leq p \leq 2$ BeV/c, and $p \geq 2$ BeV/c, respectively.

In order to increase the accuracy of the above determinations additional measurements were made, using the apparatus described in Sec. 1, which permitted more precise determination of particle momenta. In 267 hours 1581 particles of $p \geq 0.35$ BeV/c were observed. Of the total number of stopped particles, 492 had momenta $p \geq 1.11$ BeV/c and were stopped by nuclear collision. Within the limits of error the results of the two experiments are in agreement.

The author is not familiar with other work in which the proton component was studied at mountain altitudes with sufficient care and attention to detail. An attempt has been made[6] to determine the proton spectrum with a cloud-chamber. Not included in this spectrum was the momentum interval $p \geq 1.2$ BeV/c, for which we found the power law dependence with exponent $\gamma = 2.65$. In the work cited the particles were identified by their ionization, and for this reason it was difficult, for $p \geq 0.5$ BeV/c, to separate unambiguously the protons from the mesons (as was noted by the authors). For this reason the shape of the spectrum is strongly distorted. There the maximum occurs at about $p = 0.4$ BeV/c and then falls off at higher momenta, as compared with our spectrum where the maximum is at about $p = 0.7$ BeV/c and begins to fall off above a value of p of about 0.8 BeV/c.

The proton spectrum at 3400 m was carefully investigated by others[7]. The spectrum was calculated by an analysis of the positive excess in the hard component of cosmic rays. For $p \geq 2$ BeV/c the spectrum obeys a power law with exponent $\gamma = 2.5 \pm 0.5$. Although the general features of this spectrum resemble ours, the intensity of protons is approximately one-and-a-half times larger. Perhaps the explanation lies in the insufficient accuracy of the method used. It should be noted, however, that the intensity of the proton flux calculated in that paper[7] from experimental data of the paper previously cited[6] agrees well with our results.

Now the intensity of the total flux of protons with $p > 1$ BeV/c can be calculated. The total intensity for such particles is given by

$$I = 2\pi \int_0^{\pi/2} J(\theta) \sin\theta \, d\theta \qquad (5)$$

$$= 2\pi J_0 \int_0^{\pi/2} \exp\left[\frac{x}{z}(1 - \sec\theta)\right] \sin\theta \, d\theta,$$

where J_0 is the intensity of the vertical proton flux. We have, above, that $J_0 = 0.887 \times 10^{-2}$ cm^{-2} sec^{-1} sterad^{-1}. From the angular distribution of protons obtained in a previous work[8] we had $L = 120$ gm/cm^2. Substituting these quantities into Eq. (5), one obtains

$$I = 0.69 \times 10^{-3} \text{ cm}^{-2} \text{ sec}^{-1}$$

3. THE ABSORPTION LENGTH OF PROTONS IN AIR

The absorption length in air of the proton component can be calculated from comparison of the observed intensity of protons at 3200 m with the intensities at other altitudes. By the absorption length we mean here the reciprocal of the absorption coefficient for protons of greater than the given energy. We assume that the absorption of particles is according to an exponential law

$$n(p, s_2) = n(p, s_1) e^{-(s_2 - s_1)/L}, \qquad (6)$$

where $n(p, s_1)$ and $n(p, s_2)$ are the intensities of the vertical flux of protons with momenta greater than p, at depths s_1 and s_2 measured from the top of the atmosphere, while L is the absorption length for protons of momenta greater than p.

Solving Eq. (6) for L gives

$$L = \frac{s_2 - s_1}{\ln n(p, s_1) - \ln n(p, s_2)}. \qquad (7)$$

Since the integral spectra at the depths s_1 and s_2 have the form

$$n(p, s_1) = \frac{a_1}{\gamma_1 - 1} p^{1-\gamma_1};$$

and

$$n(p, s_2) = \frac{a_2}{\gamma_2 - 1} p^{1-\gamma_2},$$

[6] C. E. Miller, J. E. Henderson, D. S. Potter, J. Todd, Jr. and W. Wotring, Phys. Rev. 79, 459 (1950)

[7] W. L. Whittemore and R. P. Shutt, Phys. Rev. 86, 940 (1952)

[8] N. M. Kocharian, M. T. Aivazian, Z. A. Kirakosian and S. D. Kaitmazov, J. Exper. Theoret. Phys. USSR 25, 364 (1953)

respectively, then Eq. (7) can be re-written

$$L = \frac{s_2 - s_1}{\ln\left(\frac{a_1}{a_2}\right) + \ln\frac{(\gamma_2 - 1)}{(\gamma_1 - 1)} + (\gamma_2 - \gamma_1)\ln p}. \qquad (9)$$

At the same time one may consider a differential absorption length, which can be defined by the following expression:

$$l = \frac{s_2 - s_1}{\ln N(p, s_1) - \ln N(p, s_2)}, \qquad (10)$$

where $N(p, s_1)$ and $N(p, s_2)$ are the ordinates of the differential momentum spectra at depths s_1 and s_2.

In another work[9], the values of the differential momentum spectrum at sea level was found to be $N(p, 1030) = 0.91 \pm 0.19 \times 10^{-4}$ and $1.21 \pm 0.23 \times 10^{-4}$ cm^{-2} sec^{-1} sterad^{-1} (BeV/c)$^{-1}$ for momenta $0.59 \leq p \leq 0.77$ BeV/c and $0.77 \leq p \leq 0.93$ BeV/c, respectively. For the same momentum intervals at a depth $s = 705$ gm/cm^2, the corresponding quantities were found here to be $1.52 \pm 0.03 \times 10^{-3}$ and $1.38 \pm 0.04 \times 10^{-3}$ cm^{-2} sec^{-1} sterad^{-1} (BeV/c)$^{-1}$. Inserting these values into Eq. (10), one obtains

$$l(p) = \begin{cases} (116 \pm 9)\ \text{GM/CM}^2 \\ \qquad \text{for} \quad p \approx 0.7\ \text{BeV}/c, \\ (133 \pm 10)\ \text{GM/CM}^2 \\ \qquad \text{for} \quad p \approx 0.85\ \text{BeV}/c. \end{cases} \qquad (11)$$

Measurements have been made previously[9] of the proton intensities at 2750 m (depth $s = 750$ gm/cm^2). The results reported were that $N(p, 750) = 0.96 \pm 0.12 \times 10^{-3}$ and $0.79 \pm 0.12 \times 10^{-3}$ cm^{-2} sec^{-1} sterad^{-1} (BeV/c)$^{-1}$ for $0.59 \leq p \leq 0.77$ and $0.77 \leq p \leq 0.93$ BeV/c, respectively.

These can be compared with the results of the present study. Using Eq. (11) to correct the latter to the same depth: viz.,

$$N(p, 750) = N(p, 705)\, e^{-x/L}$$

$$= \begin{cases} (1.05 \pm 0.11) \cdot 10^{-3} & \text{for} \quad p = 0.68\ \text{BeV}/c, \\ (1.00 \pm 0.11) \cdot 10^{-3} & \text{for} \quad p = 0.85\ \text{BeV}/c, \end{cases}$$

where $x = 750 - 705 = 45$ gm/cm^2. The two sets of results are seen to be consistent within the experimental errors.

In another study[10] the proton spectrum at sea level was measured with a magnetic spectrometer, and it was found that the intensity at $p = 0.7$ BeV/c was about 10^{-4} cm^{-2} sec^{-1} sterad^{-1} (BeV/c)$^{-1}$. Comparison with the results of this work at 3200 m leads to

$$l(0.7) = 119 \text{gm/cm}^2.$$

The expected error in this result is large, as the statistical errors in the results of the work[10] were appreciable.

Now let us consider the absorption length of protons and the comparison of the integral spectra at different atmospheric depths. At sea level it was found[10] that the intensity of protons of momenta $p \geq 1$ BeV/c was 0.55×10^{-4}cm^{-2}sec^{-1} sterad^{-1}, while at 3200 m we obtained $n(1705) = 0.887 \pm 0.01 \times 10^{-3}$ cm^{-2} sec^{-1} sterad^{-1}, which results imply an absorption length $L = 118$ gm/cm^2. This value appears to be low. In the work cited[10] the number of protons observed to stop in the absorbers had to be divided by the probability of their being stopped; viz., by $1 - e^{-x/L}$, where L was taken to be 160 gm/cm^2. According to our method of calculation it would have been necessary to use instead $1 - e^{-x/320}$. Since the total thickness of absorbers in that experiment was 226 gm/cm^2, one should correct the observed intensities by $(1 - e^{-x/160}) / (1 - e^{-x/320}) = 1.5$. Consequently, the sea level intensity of protons with $p \geq 1$ BeV/c would be $0.55 \times 1.5 = 0.83 \times 10^{-4}$ cm^{-2} sec^{-1} sterad^{-1}, and from this value one obtains $L = 137$ gm/cm^2.

It is of interest to compare the intensity of the primary component with that of the protons at the depth $s = 705$ gm/cm^2. We shall proceed from the results of Vernov et al[11]. It was found that the energy spectrum of the primaries can be approximated by a power law with $\gamma = 2$ and that their flux at 31° latitude was 1.8 min^{-1} cm^{-2} sterad^{-1}. At that latitude the cutoff energy for protons is about 6.8 BeV, while at the geomagnetic latitude of 35°, where our experiments were conducted, cutoff occurs at about 5.3 BeV energy, or 6.2 BeV/c momentum; from the 31° flux one can derive the flux at 35°, which comes out to be 0.0383 particle cm^{-2} sec^{-1} sterad^{-1}. On the other hand one can calculate from the spectrum observed

9 A. Z. Rosen, Phys. Rev. 93, 211 (1954)

10 M. G. Mylroi and J. G. Wilson, Proc. Phys. Soc. 64A, 404 (1951)

11 S. I. Vernov and A. I. Charakhchian, Doklady Akad. Nauk SSSR 91, 487 (1953)

Table 2

Spectra of protons above and below 68 gm/cm^2 of lead, and the absorption lengths in lead.

Momenta in BeV/c	$N_1(p)\times10^3$	$N_2(p)\times10^3$	$n_1(p)\times10^3$	$n_2(p)\times10^3$	$l(p)$	$L(p)$
0.502	1.15	0.740	1.59	1.17	154	222
0.587	1.22	0.744	1.49	1.11	137	230
0.707	1.22	0.786	1.34	1.02	155	252
0.826	1.16	0.830	1.05	0.824	204	280
0.977	1.05	0.798	0.884	0.701	247	293
1.14	0.99	0.764	0.713	0.576	258	318
1.30	0.85	0.673	0.574	0.463	290	316
1.57	0.504	0.411	0.419	0.338	333	316
2.04	0.212	0.172	0.273	0.220	325	315

at 3200 m for protons with $p < 2$ BeV/c that the flux of those with $p \geq 6.2$ BeV/c is 4.33×10^{-5} particle cm^{-2} sec^{-1} sterad^{-1} if it is assumed that the observed power law holds for the higher momenta. One should compare the primary flux with the total number of nucleons at 3200 m, or twice the number of protons; viz., 8.66×10^{-5} particle cm^{-2}sec^{-1}sterad^{-1}. Using these values, one obtains for the absorption length in air of protons with $p \geq 6.2$ BeV/c the value $L = 115$ gm/cm^2.

4. ABSORPTION LENGTH OF PROTONS IN LEAD

Using the second version of the spectrometer with 68 gm/cm^2 of lead above the magnet, 2742 protons with $p \geq 0.35$ BeV/c were observed in 523 hours. The spectrum obtained under lead was compared with that in air, and the results of this comparison are shown in Table 2. In this table $N_1(p)$ and $N_2(p)$ are the values of the differential spectra in air and under lead, respectively, and $n_1(p)$ and $n_2(p)$ the number of protons with momenta greater than p. In the last two columns the differential, l, and the integral, L, absorption lengths in lead are given as functions of the momentum.

It has been seen from Table 2 that both l and L increase with momentum, the latter reaching a constant value of

$$L = (315 \pm 49) \ \text{GM}/\text{CM}^2. \qquad (12)$$

for $p \geq 1$ BeV/c. These measured values of the absorption lengths are not immediately comparable with those obtained by others, as, for example, the photographic emulsion measurements [12-14] of the absorption lengths of the N-component of cosmic rays. In these studies the absorption length of the N-component was found to be appreciably (sometimes three times) larger than the interaction length λ_0 corresponding to the geometrical cross section, while in the present work it was found that the absorption length of protons was only 1 $^1/_2$ to 2 times larger. The reason for the difference between the proton and the N-component results may be due to the inclusion in the latter of meson, deuteron and heavier particle interactions, which tend to increase the absorption lengths.

5. SPECTRUM OF THE PROTONS PRODUCED BY NEUTRONS IN A THIN PLATE OF LEAD*

In the second arrangement of the experiment, two lead plates, 5 and 1 cm in thickness were placed above the magnet. Between these, as indicated in Fig. 1, was a double layer of counters whose detection efficiency for charged particles was practically 100%. In this way we were able to study protons and Π-mesons produced in a thin (11.3 gm/cm^2) layer of lead.

[12] J. C. Barton, Proc. Phys. Soc. **64A**, 1042 (1951)

[13] T. G. Stinchcomb, Phys. Rev. **83**, 422 (1951)

[14] S. A. Azimov, N. A. Dobrotin, A. L. Liubimov and K. P. Ryzhkova, Izv. Akad. Nauk SSSR, Ser. Fiz **42**, 80 (1953)

* *Note added in proof:* The spectrum of protons generated by neutrons in thick plates of lead has been studied by Dadaian and Mirzon [e.g., see A. G. Dadaian and G. I. Mirzon, Doklady Akad. Nauk SSSR **86**, 259 (1952)].

In 523 hours 146 protons were observed that originated in the 1 cm lead plate and were absorbed in the absorbers underneath the magnet. Of these, 114 particles had momenta $p \geq 0.35$ BeV/c, and 17 protons with $p \geq 1.13$ BeV/c stopped as a result of nuclear interaction. In order to derive the true spectrum of the protons produced in lead it is necessary to consider the ionization losses of the particles in the absorbers in which they were born. This was done approximately by assuming that the protons were generated uniformly throughout the thickness of the plate.

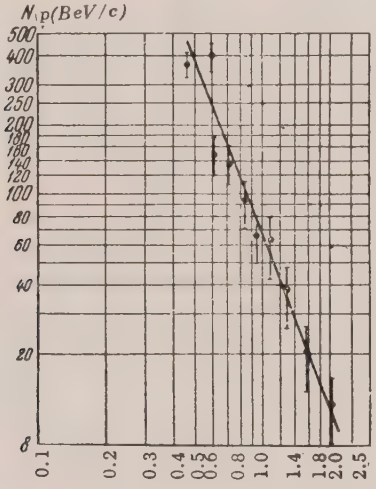

Fig. 3. Pulse spectrum of protons produced by neutrons in lead of thickness 11.3 gm/cm^2.

The curve of Fig. 3 was obtained by analyzing the data as described in Sec. 2. It is seen that the spectrum of the generated protons can be approximated by the power law

$$N(p)\,dp \sim p^{-\gamma}dp$$

where $\gamma = 2.55 \pm 0.3$. The number of protons of momentum $1.0 \leq p \leq 2.33$ BeV/c was 34, and those of $p \geq 1$ BeV/c (430 MeV) was 46. Assuming that the same law holds for $p \geq 2.33$ BeV/c, one obtains that the number of these is 12. In order to calculate the number of protons with momentum $p \geq 1$ BeV/c produced in 1 cm of lead, one must divide the number 46 by $s\,\omega\,t\,x\,k = 3.38 \times 10^7$ cm^2 sterad sec gm/cm^2, where $s = 140.8$ cm^2 is the area of the coordinate counters, $\omega = 0.0144$ sterad the solid angle of the apparatus, $t = 523$ hours $= 1.88 \times 10^6$ sec the time of observation, $x = 11.3$ gm/cm^2 the thickness of the lead plate, and $k = 0.78$ the overall counting efficiency. Since these observations of the production of protons were made under 5 cm of lead, the number observed must be multiplied by a factor $e^{62/315}$, where 315 is the absorption length of protons in lead. Thus one obtains

$$n = 1.66 \times 10^{-6} \text{ protons cm}^{-2}\text{ sec}^{-1}\text{ sterad}^{-1}\,(\text{gm/cm}^2)^{-1}.$$

Π-mesons are created in the lead as well as protons. In this experiment it was assumed that observed particles were mesons if they were negatively charged, or if, though positively charged, they exhibited a greater deflection than that of protons stopping in the same absorbers. There were 17 negatively charged and 12 positively charged particles with deflections greater than that of the protons, implying that in this range of the spectrum the ratio of negative to positive mesons was 1.5. However, 3 negative particles were observed with deflections about the same as that of the protons, so that if the same ratio holds there must also have been two positive mesons. Thus, the total number of Π-mesons observed was 34 and their momentum was $p \geq 0.16$ BeV/c ($E \geq 73$ MeV), if we assume that the mesons were produced, on the average, at a depth of 5.6 gm/cm^2 in the lead. Considering the efficiency of the apparatus one concludes that the number with $E \geq 73$ MeV was 54. Assuming that the spectrum of the mesons produced is the same as that previously reported[15], one can calculate that the number that penetrated through all of the absorbers without stopping was about 4. Consequently, there were 58 mesons and 46 protons with $E \geq 430$ MeV, and from the spectrum of the protons produced one concludes that there were about 40 protons with $E > 500$ MeV.

From this it may be concluded that in lead the ratio of mesons to protons in nuclear stars is 1.5, as compared with about 3 in photographic emulsions[16]. The explanation of this difference may be that in lead the mesons created may suffer secondary interactions in the nucleus, thus losing a considerable part of their energy, or perhaps being completely absorbed. In the course of these investigations there occurred instances where several of the coordinate counters in a tray were set off simultaneously in a way which precluded an unambiguous interpretation of the particle momenta, but this happened in less than 7% of the cases. Conse-

[15] J. G. Wilson et al, Progress in Cosmic Ray Physics, Amsterdam (1952), pp. 358 and 360

[16] W. O. Lock and Yekutieli, Phil. Mag. **43**, 231 (1952)

quently, the number of shower particles observed was for all practical purposes the total number of shower particles that were produced in the layer of lead during the time of observation (523 hours).

Translated by V. A. Nedzel
25

SOVIET PHYSICS - JETP VOLUME 1, NUMBER 1 JULY, 1955

On the Theory of Energy Losses of Charged Particles Traversing a Ferromagnetic Material

D. IVANENKO AND V. N. TSYTOVICH
Moscow State University

(Submitted to JETP editor March 5, 1954)
J. Exper. Theoret. Phys. USSR 28, 291-296 (March, 1955)

An investigation of the effect of saturation of the energy losses of a charged particle passing through a ferromagnetic material is presented[1-3]. An analysis of the separation of the losses into ionization losses and Cerenkov radiation losses is also given.

THE energy losses of a charged particle passing through a ferromagnetic material has been investigated in a series of papers[1-3].

It is known[4,5] that when high velocity charged particles traverse a dielectric the energy losses approach saturation. These energy losses do not increase without limit as the energy of the charged particle increases but they are higher in materials which have a lower electron density. In addition to this, at higher velocities the losses by Cerenkov radiation play a special role[6-8].

For the case of a charged particle traversing a dielectric the analysis of the separation of the losses into ionization losses and Cerenkov radiation losses showed the essential dependence of this separation on the value of the damping coefficients in the dispersion formulas, which coefficients must not be assumed equal to zero[8,9].

The analogous situation can be expected to occur in the analysis of the separation of the losses into ionization losses and Cerenkov radiation losses when a particle traverses a ferromagnetic material. In addition, in a ferromagnetic material as in a dielectric, the question of this separation cannot be calculated correctly if the effect of damping is not considered finite[9].

When a high velocity charged particle traverses a substance, the loss of its energy depends essentially on the interaction between the atoms of the substance. In a ferromagnetic material the magnetic properties are determined, first, by an exchange interaction of the electrons of the substance (exchange energy) and secondly, by a magnetic interaction of the elementary magnetic moments (energy of magnetic anisotropy(see, for example, Vonsovskii and Shur[10]). In the following discussion, however, it will be shown the exchange interaction is not essential for the energy losses of charged particles which pass through a ferromagnetic material. A relatively small energy of magnetic isotropy, however, gives a contribution to the energy losses, but it is negligibly small in comparison to the ionization losses and Cerenkov radiation losses associated with the dielectric constant ϵ of the ferromagnetic material. Also included are some unexpected results of the analysis of the energy losses in a ferromagnetic material. We note also that the effect of saturation of the losses in a ferromagnetic material is analogous to the effect of saturation of the losses in a dielectric, where the losses in the ultra relativistic region depend only on the number of electrons, but not on the character of their coupling in the material.

If point charged particles, moving in a medium characterized by values of dielectric constant and

[1] D. Ivanenko and B. C. Gurgenidze, Doklady Akad. Nauk SSSR 67, 997 (1949)

[2] D. Ivanenko and B. C. Gurgenidze, Vestn. Moscow State University 2, 69 (1950)

[3] Ch. Weizsäcker, Ann. Physik 17, 869 (1933)

[4] E. Fermi, Phys. Rev. 53, 485 (1940)

[5] N. Bohr, Atomic Particles Traversing Media (1950)

[6] P. A. Cherenkov, Doklady Akad. Nauk SSSR 2, 451 (1934)

[7] I. M. Frank and I. E. Tamm, Doklady Akad. Nauk SSSR 14, 107 (1937)

[8] M. Schönberg, Nuovo Cim. 8, 159 (1951)

[9] P. Budini, Nuovo Cim. 10, 236 (1953)

[10] S. V. Vonsovskiĭ and Y. S. Shur, *Ferromagnetism*, Moscow (1948)

permeability ϵ and μ, have their kinematics denoted by $\mathbf{r}_\xi(t)$ and $\mathbf{v}_\xi(t)$ (position and velocity of the particle) then the potentials of the field obey the equations:

$$\nabla^2 \mathbf{A} - \frac{\varepsilon\mu}{c^2}\frac{\partial^2 \mathbf{A}}{\partial t^2} = -\frac{4\pi\mu}{c} e\mathbf{v}_\xi \delta(\mathbf{r} - \mathbf{r}_\xi), \tag{1}$$

$$\nabla^2 \phi - \frac{\varepsilon\mu}{c^2}\frac{\partial^2 \phi}{\partial t^2} = -\frac{4\pi}{\varepsilon} e\delta(\mathbf{r} - \mathbf{r}_\xi). \tag{2}$$

Since we are interested in both ionization losses and Cerenkov radiation losses we will consider the values of ϵ and μ to be complex.

It is well known [11,12] that in calculating Green's function of the field equations for transparent media, a well-defined expression is not obtained because of the presence of poles on the real axis in the expression of the integrand. In order to circumvent these poles correctly we can use either retarded, advanced, or other types of functions [13,14]. In the cases we are considering, because of the complex values of ϵ and μ, the poles of the integrand of the Green's function will not lie on the real axis. The requirements for radiation will be fulfilled if the coefficients in the imaginary part of ϵ and μ are positive ($\phi = e^{-i\omega t}\phi_0$). The latter circumstance, corresponding to a dissipation of energy by moving elementary charges and currents, is dependent upon a given value of ϵ and μ. The condition of positive coefficients in the imaginary parts of ϵ and μ, where the damping goes to zero, leads directly to a retarded potential for the transparent media.

Thus for the Green's function of Eqs. (1) and (2) we obtain the expression:

$$G = \frac{1}{16\pi^4} \cdot \int \frac{1}{k^2 - (\varepsilon\mu\omega^2/c^2)} \exp\{i\mathbf{k}\mathbf{R} - i\omega T\}\, d\omega d^3k, \tag{3}$$

where $\mathbf{R} = \mathbf{r} - \mathbf{r}'$, $T = t - t'$. Hence, for the potentials ϕ and $\mathbf{A}$, we have

$$\phi = \frac{e}{4\pi^3}\int \frac{\exp\{i\mathbf{k}\mathbf{R}_\xi - i\omega T\}}{\varepsilon(\omega)\,[k^2 - (\omega^2\varepsilon\mu/c^2)]}\, d\omega d^3k dt', \tag{4}$$

$$\mathbf{A} = \frac{e}{4\pi^3}\int \frac{\exp\{i\mathbf{k}\mathbf{R}_\xi - i\omega T\}}{c\,[k^2 - (\omega^2\varepsilon\mu/c^2)]}\, \mu(\omega)\,\mathbf{v}_\xi d\omega d^3k dt'. \tag{5}$$

Here

$$\mathbf{R}_\xi = \mathbf{r} - \mathbf{r}_\xi(t').$$

The potentials in Eqs. (4) and (5) permit finding the energy losses for any moving charged particles $\mathbf{r}_\xi(t)$, $\mathbf{v}_\xi(t)$. With these we can develop, in particular, the theory dealing with the analysis of the energy losses of charged particles having relativistic motion in a magnetic field in certain transparent media (recombination phenomena of the electrons "luminescence" and "superlight", that is, Cerenkov radiation [12]).

In case of uniform motion along the z axis, we have

$$\phi = \frac{e}{\pi}\int \frac{d\varkappa}{\varepsilon} \exp\{i\varkappa(z - vt)\}\, K_0(\zeta r), \tag{6}$$

where

$$K_0(\zeta r) = \frac{\pi i}{2} H_0^{(1)}(i\zeta r), \qquad \varkappa = \frac{\omega}{v}. \tag{7}$$

Here

$$\zeta = \varkappa\sqrt{1 - \varepsilon\mu\beta^2}\ \ \mathrm{Sign}\,\mathrm{Re}\,\varkappa\sqrt{1 - \varepsilon\mu\beta^2}, \tag{8}$$

and $H_0^{(1)}$ is a cylindrical function.

For determining the energy losses due to collisions with the parameter of the collision greater than b, we calculate the flux of the Poynting vector through the surface of a cylinder of radius b, which surrounds the trajectory of the particle:

$$W_b = \frac{c}{4\pi v}\int_b [\mathbf{E}\mathbf{H}]\, d\mathbf{S} \tag{9}$$

$$= \frac{2e^2}{\pi v^2}\,\mathrm{Re}\int_0^\infty i\omega d\omega \left(\frac{1}{\varepsilon} - \mu\beta^2\right)\zeta^* b K_0(\zeta b) K_1(\zeta^* b).$$

Here $\mathbf{E}$ and $\mathbf{H}$ are the values of the electric and magnetic intensities created by the charged particle, $d\mathbf{S}$ is an element of surface of the cylinder. In the derivation of Eq. (9) we used the relations [11]

$$A_x = A_y = 0, \quad A_z = \varepsilon\mu\beta\phi;$$

$$E_z = \frac{\partial\phi}{\partial z}(\varepsilon\mu\beta^2 - 1), \quad E_x = -\frac{\partial\phi}{\partial x},$$

$$E_y = -\frac{\partial}{\partial y}\phi, \quad H_z = 0;$$

$$H_x = \varepsilon\beta\frac{\partial\phi}{\partial y}, \quad H_y = -\varepsilon\beta\frac{\partial\phi}{\partial x},$$

and used for ϕ the expression (6), as well as the formulas:

---

[11] D. Ivanenko and A. Sokolov, *Classical Theory of Fields*, Moscow, 2nd ed. (1951)

[12] V. N. Tsytovich, Vestn. Moscow State University 11 27 (1951)

[13] R. Feynman, Phys. Rev. 76, 749 (1949)

[14] Article edited by D. Ivanenko: "Most Recent Developments in Quantum Electrodynamics", Moscow (1954)

$$K_1(z) = -\frac{\partial}{\partial z} K_0(z); \quad \varepsilon(-\omega) = \varepsilon^*(\omega);$$

$$\mu(-\omega) = \mu^*(\omega).$$

In the following we shall consider the small value of the collision parameter which limits us in Eq. (9) to the first members of the series for the Bessel functions $K_0(\zeta b)$ and $K_1(\zeta^* b)$:

$$K_1(\zeta^* b) = \frac{1}{\zeta^* b} \quad K_0(\zeta b) = \frac{1}{2} \ln \frac{4}{3.17\zeta^2 b^2}. \tag{10}$$

The relations in Eq. (10) can be used if $|\zeta| b \ll 1$. For a ferromagnetic material, with $\epsilon = 1$ and μ determined by the dispersion formula[15] the generalized classical formula of Arkadév is used [see below, Eq. (19)]. This condition is given for ultrarelativistic motion by

$$\frac{\omega}{c} |\sqrt{1 - \beta^2 \mu_{max}}| b \ll 1, \tag{11}$$

where μ_{max} is the maximum value of the magnetic permeability occurring in the region near the resonance frequency ω_0. If we neglect damping, then condition (11) is violated. Therefore in the following it is very essential to have a finite value of the damping. However, in the final result, after combining the ionization losses and the Cerenkov radiation losses, the damping can be neglected. The situation here is somewhat more complex than in the case of dielectrics[16], because the ranges of the integration with respect to frequency for Cerenkov radiation losses and for ionization losses partly overlap.

Thus, for a small range of the papameter we have

$$W_b = \frac{e^2}{\pi v^2} \operatorname{Re} \int_0^\infty i\omega d\omega \left(\frac{1}{\varepsilon} - \mu\beta^2\right) \ln \frac{4}{3.17\zeta^2 b^2}. \tag{12}$$

Assuming $\varepsilon = 1$, $\mu = \operatorname{Re}\mu + i \operatorname{Im}\mu$, $\gamma = \sqrt{3.17}$

$$\tan\phi = -\frac{\beta^2 \operatorname{Im}\mu}{1 - \beta^2 \operatorname{Re}\mu}, \tag{13}$$

we have

$$W_b = \frac{2e^2}{\pi v^2} \int_0^\infty \omega d\omega \left\{ \operatorname{Im}\mu\beta^2 \ln \frac{2v}{\gamma\omega |\sqrt{1 - \beta^2\mu}| b} + \frac{\phi}{2}(1 - \operatorname{Re}\mu\beta^2) \right\}. \tag{14}$$

For small values of the damping coefficient, instead of Eq. (13), we can write

$$\phi = \frac{\beta^2 \operatorname{Im}\mu}{\beta^2 \operatorname{Re}\mu - 1} - \pi \quad \text{when } \beta^2 \operatorname{Re}\mu > 1; \tag{15}$$

$$\phi = -\frac{\beta^2 \operatorname{Im}\mu}{1 - \beta^2 \operatorname{Re}\mu} \quad \text{when } \beta^2 \operatorname{Re}\mu < 1. \tag{16}$$

The relation (15) corresponds to the Cerenkov frequency, and Eq. (16) to the Bohr frequency.

Substituting Eqs. (15) and (16) in Eq. (14) we obtain the formulas for ionization and Cerenkov radiation losses in a ferromagnetic material with $\epsilon = 1$:

$$W^{Cer} = \frac{e^2}{v^2} \int_{\operatorname{Re}\mu\beta^2 > 1} (1 - \operatorname{Re}\mu\beta^2) \omega d\omega, \tag{17}$$

$$W_b^{Ion} = \frac{e^2}{\pi c^2} \tag{18}$$

$$\int_0^\infty \omega d\omega \operatorname{Im}\mu \left\{ \ln \frac{4v^2}{3,17\omega^2 b^2 |1 - \mu\beta^2|} - 1 \right\}.$$

In the following we will assume a concrete dispersion formula for the magnetic permeability*.

$$\mu = 1 + \frac{4\pi}{\beta} \frac{1 - i\gamma x}{1 - x^2 - 2i\gamma x}, \tag{19}$$

where

$$x = \frac{\omega}{\omega_0}, \quad \omega_0 = \frac{e}{mc} \beta I_s, \quad \gamma = \frac{e}{mc} \beta\varepsilon, \quad \beta = \frac{2k}{I_s^2},$$

I_s is the spontaneous magnetization, k is the coefficient of magnetic anisotropy, m is the mass of the electron.

We now stop to analyze the ionization losses [Eq. (18)]. Assuming the value of μ in the logarithmic part is equal to unity, we obtain the formula for the ionization losses, neglecting the polarization effect[9]. In the calculation of the ionization losses the value of μ is essentially the value near resonance[9]. Therefore we set

$$\mu = 1 + \frac{\mu_0 - 1}{1 - x^2 - 2i\gamma x} \tag{20}$$

---

[15] L. D. Landau and E. M. Lifshits, Sow. Phys 8, 157 (1935)

[16] P. Kunin, Article in "Mesons", edited by I. Tamm, Moscow (1947)

* We emphasize that in Refs. 1 and 10 [e.g., see Ref. 1, D. Ivanenko and B. C. Gurgenidze, Doklady Akad. Nauk SSSR 67, 997 (1949) and Ref. 10, S. V. Vonsovskii and Y. S. Shur, *Ferromagnetism*, Moscow (1948)] there was a typographical error in the expression of the relationship between μ and frequency. We use this occasion to note that the paper of Sitenko [e.g., see Ref. 17, A. G. Sitenko, Zh. Tekhn. Fiz. 23, 2200 (1953)], to which our attention was directed after the present paper was sent to the printer, is devoted to a closely related problem. However, the final results of the indicated paper do not agree with the reduced Eqs. (23) and (24), apparently as a result of some terms neglected in the calculations of Sitenko.

[17] A. G. Sitenko, Zh. Tekhn. Fiz. 23, 2200 (1953)

and we obtain the analogue of the Bloch formula[18,19] (see also Budini[9]) for the ionization losses in a ferromagnetic material with

$$W_b^{\text{Ion}} = \frac{e^2\omega_0^2(\mu_0 - 1)}{2c^2}\left\{\ln\frac{4v^2}{3{,}17\omega_0^2 b^2(1-\beta^2)} - 1\right\}. \quad (21)$$

In deducing Eq. (21) we use the relation

$$\int x \operatorname{Im}\mu dx = \frac{\pi}{2}(\mu_0 - 1). \quad (22)$$

The logarithmic rise of the ionization losses follows from Eq. (21).

Taking into account the effect of polarization and combining the total ionization losses with the Cerenkov radiation losses we can neglect the damping in the final result. Then we have

$$W_b = \frac{e^2\omega_0^2}{2c^2}(\mu_0 - 1)\left\{\ln\frac{4v^2}{3{,}17\, b^2\omega_0^2} - \ln(1-\beta^2) - 1\right\}, \quad \beta < \frac{1}{\sqrt{\mu_0}}, \quad (23)$$

$$W_b = \frac{e^2\omega_0^2}{2c^2}(\mu_0 - 1)\left\{\ln\frac{4v^2}{3{,}17 b^2\omega_0^2} - \ln\beta^2\,(\mu_0 - 1) - \frac{1-\beta^2}{\beta^2(\mu_0 - 1)}\right\}, \beta > \frac{1}{\sqrt{\mu_0}}, \quad (24)$$

The total losses, as is easily seen from Eqs. (23) and (24), in contrast to Eq. (21), approach saturation at high velocities, while in the limiting case of ultrarelativistic motion the losses depend on the value of the coefficient of magnetic anisotropy. Actually, in the ultrarelativistic case Eq. (13) gives

$$W_b(v \sim c) = \frac{2\pi n e^4}{mv^2}\left(\frac{2k^0}{mc^2}\right)\ln\frac{mc^2}{3{,}17\pi b^2 e^2 n}\left(\frac{mc^2}{2k^0}\right). \quad (25)$$

Here n is the electron density of the medium, and $k^0 = k/n$ denotes a value which is the order of the energy of interaction of two elementary magnetic dipoles at a separation of the lattice constant, and in comparison with the rest energy of the electron is a negligibly small value $\sim 10^{-9}$.

The value of the spontaneous magnetization I_s of the ferromagnetic material does not occur in Eq. (14). Only the energy of magnetic anisotropy associated with the magnetic interaction of elementary magnetic dipoles plays an essential part for losses when $v/c \sim 1$ (see above).

Comparing Eq. (25) with the formula obtained by Fermi[4] for the energy losses in dielectrics,

$$W_b(v \sim c) = \frac{2\pi n e^4}{mv^2}\ln\frac{mc^2}{3{,}17\pi b^2 e^2 n}, \quad (26)$$

we see that it is possible to neglect the energy losses connected with the magnetic permeability in the ultrarelativistic case. This is particularly clear when, in the calculation of the losses according to Eq. (12), use is made of Eq. (11) together with the concrete dispersion formula

$$\varepsilon = 1 + \frac{4\pi n e^2}{m}\frac{1}{\omega_0^2 - \omega^2 - 2t\gamma'\omega}. \quad (27)$$

then

$$W_b(v \sim c) = \frac{4\pi n e^4}{mc^2}\left(1 + \frac{2k^0}{mc^2}\right)\ln\frac{mc^2}{3{,}17\pi b^2 e^2 n\left(1 + \frac{2k^0}{mc^2}\right)}. \quad (28)$$

Since a ferromagnetic material is usually a metal, it is expedient to consider the energy losses of a particle traversing a ferromagnetic material as losses in a conducting medium.

We note in conclusion that with the aid of Eq. (12) formulas may be obtained by an analogous method for the ionization and Cerenkov radiation losses both for a charged particle traversing a ferroelectric material and a magnetized particle traversing ferromagnetic material.

Translated by F. P. Dickey
50

[18] F. Bloch, Ann. Physik 16, 285 (1933)
[19] F. Bloch, Z. Phys. 81, 363 (1933)

SOVIET PHYSICS-JETP VOLUME 1, NUMBER 1 JULY, 1955

The Mean Free Path of a Non-Localized Exciton in an Atomic Crystal

A. I. Ansel'm and Iu. A. Firsov
Leningrad Physical-Technical Institute
(Submitted to JETP editor March 1, 1954)
J. Exper. Theoret. Phys. USSR 28, 151-159 (February, 1955)

The mean free path of a non-localized exciton in an atomic crystal is calculated under the assumption of interaction with thermal lattice vibrations.

INTRODUCTION

FRENKEL[1] first introduced the concept of excited electrons of dielectric crystals, which are not accompanied by a current of charged carriers, and formulated a quantitative theory of that phenomenon. Thus, the excited electron, by virtue of the translational symmetry of the crystal, does not remain bound to a particular point in the lattice, but can behave as a quasi-particle, possessing a wave vector $\mathbf{k}$ and a certain quasi-momentum $\mathbf{p} = \hbar\mathbf{k}$. Frenkel called these quasi-particles excitons.

Frenkel[2] also introduced the concept of existence of two types of excitons, non-localized and localized. Non-localized excitons may be characterized as those that move in the excited crystal not accompanied by a localized or bound deformation of the lattice. Conversely, the localized exciton behaves as if, to quote Frenkel's figurative expression, "it were carrying the heavy burden of atomic displacements". Quite recently, Dykman and Pekar[3] have shown that states corresponding to non-localized and localized excitons are obtained automatically if one takes into account the polarization conditions in an ionic crystal. It has also been found that the localized excitons are formed in an ionic crystal only if fairly rigid conditions are satisfied, namely, if the ratio of the effective masses of the hole and the electron is larger than ten. After the appearance of Frenkel's original work, a number of research papers devoted to the theory of the exciton were published. These papers dealt mainly with the basic point of the theory of the exciton – the conditions for its existence[4]. Wannier[5] has shown that the states of a non-localized exciton can be regarded as similar to the bound hydrogen-like states of an electron and a hole experiencing mutual Coulomb attraction. However, this condition may be regarded as a direct consequence of the effective mass method. One should not neglect to mention the investigations of Davydov[6], who generalized the concept of the exciton and applied it to the study of spectra of molecular crystals.

In studying the internal photoelectric effect in copper oxide, Zhuze and Ryvkin[7] arrived at the conclusion that their observations could not be interpreted without the introduction of the exciton concept. Further, the experimental investigations of the external photoelectric effect. conducted by Apker and Taft[8] should be mentioned; the exciton concept is necessary, in the authors' opinion, to explain their results adequately. Finally, the work of Gross[9] and his co-workers permits us, apparently, to speak of a direct experimental proof of the existence of the exciton. Thus, the excitons are becoming not merely theoretically permissible states of a crystal, but, evidently, ones that can be observed experimentally. It thus appears timely to conduct a more detailed study of the properties of the exciton; attention should first be given to the determination of the mean free path of the exciton, which determines the speed of migration of energy excitation in a crystal. The paper dealing with the interactions of the excitons and the phonons[10], published some time ago, contains only numerical values of the mean free path of the exciton in various crystals. In the present study, the mean free path of a non-localized exciton is computed, on the basis of its interaction with the acoustic

[1] Ia. I. Frenkel, Phys. Rev. 37, 17, 1276 (1931)

[2] Ia. I. Frenkel, J. Exper. Theoret. Phys. USSR 6, 647 (1936)

[3] I. M. Dikman and S. I. Pekar, Trudy In. Fiz. Akad. Nauk SSSR 3, 92 (1952)

[4] J. C. Slater and W. Shockley, Phys. Rev. 50, 705 (1936); W. R. Heller and A. Marcus, Phys. Rev. 84, 809 (1951)

[5] G. H. Wannier, Phys. Rev. 52, 191 (1937)

[6] A. S. Davydov, *Theory of the Absorption of Light in Molecular Crystals*, Kiev (1951)

[7] V. P. Zhuze and S. M. Ryvkin, Izv. Akad. Nauk SSSR, Ser. Fiz. 16, 93 (1952)

[8] L. Apker and E. Taft, Phys. Rev. 72, 964 (1950); Phys. Rev. 81, 698 (1951); Phys. Rev. 82, 814 (1951)

[9] E. F. Gross and I. A. Karryev, Doklady Akad. Nauk SSSR 84, 471 (1952)

[10] P. Leurgans and J. Bardeen, Phys. Rev. 87, 200 (1952)

branch of vibrations. It is assumed here that the internal state of the exciton is not changed by either its emission or absorption of phonons. We are not considering any of the competing processes, such as the disappearance of the non-localized exciton by the way of transition into a localized state, or the recombination of an electron and a hole accompanied by the transformation of the excitation energy into heat and light.

WAVE FUNCTION OF THE EXCITON AND ITS INTERACTION WITH PHONONS

Using the approximate method of effective mass, the wave function of a non-localized exciton of lowest excited state can be given by

$$\psi_{exc}=\frac{1}{\sqrt{V}}e^{i\mathbf{kR}}\frac{1}{\sqrt{\pi a_{exc}^3}}e^{-\rho/a_{exc}} \tag{1}$$

Here V is the fundamental cell of the crystal, $\mathbf{k}$ is the wave vector of forward motion of the exciton, $\mathbf{R}$ and $\vec{\rho}$ are the radius vectors of the center of inertia of the exciton and position of the electron with respect to the hole, that is,

$$\mathbf{R}=\frac{\mu_1\mathbf{r}_1+\mu_2\mathbf{r}_2}{\mu_1+\mu_2},\quad \vec{\rho}=\mathbf{r}_1-\mathbf{r}_2, \tag{2}$$

where μ_1, μ_2 and $\mathbf{r}_1$, $\mathbf{r}_2$ are the effective masses and radius vectors of the electron and hole (in what follows, the index 1 will refer to the electron and 2 to the hole), a_{exc} is the "radius of the exciton"

$$a_{exc}=\varkappa\hbar^2/\mu e^2, \tag{3}$$

where $\varkappa$ is the optical dielectric constant and $\mu=\mu_1\mu_2/(\mu_1+\mu_2)$ is the reduced mass. If $\mu_1=\mu_2=m_e$ = the mass of the free electron, then a_{exc} is $2\varkappa$ times as large as the atomic unit of length, equal to 0.53×10^{-8} cm. The large size of the ψ-cloud of the exciton justifies the approximate method of the effective mass. The state of the exciton [Eq. (1)] corresponds to an energy

$$E_0=\frac{\hbar^2k^2}{2\mu_{exc}}-\frac{\mu e^4}{2\varkappa^2\hbar^2}=\varepsilon-\Delta E, \tag{4}$$

where the mass of the exciton $\mu_{exc}=\mu_1+\mu_2$. The internal energy of the exciton ΔE is $2\varkappa^2$ times (for $\mu_1=\mu_2=m_e$) lower than the ionization energy of a hydrogen atom, that is, it is comparable to thermal energies, even for not too high temperatures.

In what follows we will be interested only in such collisions between excitons and phonons for which internal excitation or dissociation of the exciton will not occur. For collisions of the exciton, possessing a wave vector $\mathbf{k}$, with a phonon having a wave vector $\mathbf{q}$, and for minimal internal excitation of the exciton, we have the conservation laws

$$\mathbf{k}\pm\mathbf{q}=\mathbf{k}', \tag{5}$$

$$\frac{\hbar^2k^2}{2\mu_{exc}}\pm\hbar v_0q=\frac{\hbar^2k'^2}{2\mu_{exc}}+\frac{3}{4}\Delta E, \tag{6}$$

where v_0 is the velocity of sound, and the upper sign corresponds to absorption, the lower to emission of a phonon.

From Eqs. (5) and (6) follows

$$q=\mp\left(k\cos\theta-\frac{\mu_{exc}v_0}{\hbar}\right)\pm\sqrt{\left(k\cos\theta-\frac{\mu_{exc}v_0}{\hbar}\right)^2-\frac{3\mu_{exc}\Delta E}{2\hbar^2}},$$

where θ is the angle between $\mathbf{k}$ and $\mathbf{q}$. It is easy to see that for absolute temperatures of more than a few degrees, θ not too near $\pi/2$, $k\cos\theta\gg\mu_{exc}v_0/\hbar$ for the overwhelming majority of excitons which are in thermal equilibrium with the lattice, and, consequently,

$$q=\mp k\cos\theta\pm\sqrt{k^2\cos^2\theta-(3\mu_{exc}\Delta E/2\hbar^2)}.$$

In order that excitation may not take place, it is necessary that the expression occurring under the radical be negative, that is,

$$\frac{8}{3}\frac{\varkappa^2\hbar^2\varepsilon}{\mu e^4}=\gamma\leqslant1. \tag{7}$$

For the overwhelming number of excitons we can substitute $\epsilon\approx k_0T$ in this expression. Then a criterion of the applicability of the theory can be seen to be

$$\bar{\gamma}=\frac{8}{3}\frac{\varkappa^2\hbar^2k_0T}{\mu e^4}\leqslant1. \tag{7a}$$

If $\mu_1=\mu_2=m_e$ and $\varkappa=15$, then $\bar{\gamma}=k_0T/0.023\,\text{eV}$, from which it can be seen that this theory is applicable only for temperatures lower than room temperature.

Considering such collisions of excitons with phonons, for which excitation (dissociation) of the excitons does not occur, we must set $\Delta E=0$ in Eq. (6), whence

$$q=\mp2k\cos\theta\pm2\mu_{exc}v_0/\hbar.$$

If we again neglect the term $2\mu_{exc}v_0/\hbar$, then

$$\cos\theta = \mp q/2k, \tag{8}$$

where the upper sign corresponds to the absorption, the lower to the emission, of a phonon. From Eq. (8) it can be seen that phonons with wave vectors $\mathbf{q} \approx \mathbf{k}$ in general interact with the excitons. As q is positive by definition, it follows from Eq. (8) that the wave vector of the phonons can vary between the limits of $q_{min} = 0$ to $q_{max} = 2k$.

PROBABILITY OF TRANSITION OF AN EXCITON $W_{kk'}$ BY ABSORPTION AND EMISSION OF PHONONS

For the calculation of the probability of transition of an exciton from a state with wave vector $\mathbf{k}$ to a state $\mathbf{k}'$ by collision with a phonon, we assume as the perturbation energy the deformation potential of Bardeen and Shockley [11]

$$U(\mathbf{r}_1, \mathbf{r}_2) = C_1\Delta(\mathbf{r}_1) - C_2\Delta(\mathbf{r}_2). \tag{9}$$

Here C_1 and C_2 are constants of the order of magnitude of the energy of the atom, that is, 1 - 10 V and $\Delta(\mathbf{r}) = \operatorname{div}\mathbf{u}$, the relative contraction, where $\mathbf{u}(\mathbf{r})$ is the displacement of a given point of the isotropic continuum. We will assume $C_1 > 0$ and $C_2 > 0$, and generally $C_1 \neq C_2$.

We investigate the elastic harmonic wave (phonon)

$$\mathbf{u}(\mathbf{r}) = \frac{1}{\sqrt{N}}\mathbf{e}_{qj}\left[a_{qj}e^{i(qr)} + a^*_{qj}e^{-i(qr)}\right]. \tag{10}$$

Here N is the number of atoms in the unit volume of the crystal, $\mathbf{e}_{qj}$ is the vector of polarization, a_{qj} and a^*_{qj} are the normal coordinates (amplitudes) of the vibrations.

Substituting Eq. (10) in Eq. (9), transforming from the coordinates $\mathbf{r}_1$ and $\mathbf{r}_2$ to $\vec{\rho}$ and $\mathbf{R}$, we obtain

$$U(\mathbf{r}_1, \mathbf{r}_2) = U_p(\vec{\rho}, \mathbf{R}) \tag{11}$$

$$= \frac{1}{\sqrt{N}}a_q q e^{i(qR)}\left[C_1\exp\left\{i\frac{\mu_2}{\mu_1+\mu_2}(\mathbf{q}\vec{\rho})\right\}\right.$$

$$\left. - C_2\exp\left\{-\frac{\mu_1}{\mu_1+\mu_2}(\mathbf{q}\vec{\rho})\right\}\right] + \text{compl. conj.}$$

where we have made use of the fact that only longitudinal elastic waves interact with the exciton. The complete unperturbed wave function of the crystal has the form

$$\Psi(\mathbf{k}, N_q) = \tag{12}$$

$$\frac{1}{\sqrt{V}}e^{i(\mathbf{kR})}\frac{1}{\sqrt{\pi a^3_{exc}}}e^{-\rho/a_{exc}}\prod_{\mathbf{q}}\psi_{N_q}(a_q),$$

where $\psi_{N_q}(a_q)$ is the oscillator wave function of the normal vibrations of the crystal (N_q is the quantum number of the oscillator with frequency $\omega_q = \nu_0 q$).

The matrix elements of the transition are

$$M_{kk'} = \int \Psi^*(\mathbf{k}', N'_q)\, U_p(\vec{\rho}, \mathbf{R}) \tag{13}$$

$$\Psi(\mathbf{k}, N_q)\, da_{\mathbf{q}} d\mathbf{R} d\vec{\rho}.$$

Integration over $da_{\mathbf{q}}$ and $d\mathbf{R}$ gives

$$(a_q)_{N_q-1,\,N_q} = \sqrt{\frac{\hbar}{2M\omega_q}N_q}\ ; \tag{14}$$

$$(a^*_q)_{N_q+1,\,N_q} = \sqrt{\frac{\hbar}{2M\omega_q}(N_q+1)}\ ;$$

$$\frac{1}{V}\int_V e^{i(\mathbf{k}\pm\mathbf{q}-\mathbf{k}',\mathbf{R})}d\mathbf{R} = \begin{cases}1, & \text{if } \mathbf{k}' = \mathbf{k}\pm\mathbf{q},\\ 0, & \text{if } \mathbf{k}' \neq \mathbf{k}\pm\mathbf{q}.\end{cases} \tag{15}$$

Here M is the mass of an atom of the crystal. It can be seen that Eq. (15) expresses the law of conservation of momentum [Eq. (5)] for the collision of an exciton and a phonon.

The integral remaining over $d\vec{\rho}$ from Eq. (13) can be seen to be

$$I = \frac{1}{\pi a^3_{exc}}\int \exp\left\{\pm i\frac{\mu_{1,2}}{\mu_1+\mu_2}(\mathbf{q}\vec{\rho})\right\} \tag{16}$$

$$\times\ \exp\left\{-\frac{2\rho}{a_{exc}}\right\}d\vec{\rho}$$

$$= \frac{1}{\pi a^3_{exc}}\int \exp\{i(\mathbf{q}_1\vec{\rho})\}\exp\left\{-\frac{2\rho}{a_{exc}}\right\}\rho^2 d\rho\, d\Omega,$$

where $\mathbf{q}_1 = \pm\dfrac{\mu_{1,2}}{\mu_1+\mu_2}\mathbf{q}$ and $d\Omega$ is the element of solid angle.

For integration over $d\rho$ the function $\rho^2\exp\left\{-2\rho/a_{exc}\right\}$ has a maximum of $\rho = a_{exc}$. Consequently it is desirable to evaluate the magnitude of the quantity

$$|q_1 a_{exc}| = \frac{\mu_{1,2}}{\mu_1+\mu_2}q\frac{\varkappa\hbar^2}{\mu e^2} \approx \frac{\sqrt{3}}{2}\frac{\mu_{1,2}}{\sqrt{\mu_1\mu_2}}\sqrt{\gamma}, \tag{17}$$

where we have used the condition that in general excitons interact with phonons with $q \approx k$.

Equation (17) shows that in the limits of applicability of the theory ($\gamma \leq 1$) the magnitude $|q_1 a_{exc}|$ is of the order of unity. It can be seen that it may be equal to 2 - 3, depending on the ratio between μ_1 and μ_2, the effective masses of the

[11] J. Bardeen and W. Shockley, Phys. Rev. 80, 72 (1950)

electrons and holes; therefore, in the general case it is impossible to assume $|q_1 a_{exc}| \ll 1$, if $q_1 a_{exc} \ll 1$, which does not contradict the conditions of applicability of the theory, then $l = 1$ and the matrix element $M_{kk'}$ has the same appearance, both for electron and hole separately. It can easily be seen that for this case the mean free path of the exciton is equal to

$$l = \frac{\pi M v_0^2 \hbar^4}{\Omega_0 \mu_{exc}^2 (C_1 - C_2)^2 k_0 T} = l_0, \tag{18}$$

where Ω_0 is the volume of the crystal cell. This expression is analogous to the expression for the mean free path of an electron hole[12], if one merely replaces $\mu_1 (\mu_2)$ and $C_1 (C_2)$ by $\mu_{exc} = \mu_1 + \mu_2$ and $C_1 - C_2$. It is obvious that $q_1 a_{exc} \ll 1$ is realized for the great majority of excitations with $\bar{\gamma} \ll 1$, that is with low temperatures and small dielectric constant κ.

Carrying out the integration of Eq. (16) we obtain

$$I = [1 + \beta_{1,2}^2 q^2]^{-2}, \tag{19}$$

where

$$\beta_1 = \frac{1}{4} \frac{\varkappa \hbar^2}{\mu_1 e^2} = \left[\frac{\mu_2}{2(\mu_1 + \mu_2)} \right] a_{exc}, \tag{19a}$$

and similarly for β_2. Thus $\beta_{1,2}$ is of the order of magnitude of a_{exc}. As a result, the probability of transition of an exciton, coupled with emission of absorption of a phonon, contains the factor

$$\Phi(q) = \left\{ \frac{C_1}{[1 + \beta_1^2 q^2]^2} - \frac{C_2'}{[1 + \beta_2^2 q^2]^2} \right\}^2 \tag{20}$$

$$= \frac{C_1^2}{[1 + \beta_1^2 q^2]^4} + \frac{C_2^2}{[1 + \beta_2^2 q^2]^4}$$

$$- \frac{2 C_1 C_2}{[1 + \beta_1^2 q^2]^2 [1 + \beta_2^2 q^2]^2}.$$

Calculating by the usual method[13], we obtain for the probability of transition, with absorption and emission of a phonon, the expressions

$$W_{kk'}^{+} = \pi \frac{\Phi(q) q}{N M v_0} N_q \delta(\varepsilon_{k'} - \varepsilon_k - \hbar v_0 q); \tag{21}$$

$$W_{kk'}^{-} = \pi \frac{\Phi(q) q}{N M v_0} (N_q + 1) \delta(\varepsilon_{k'} - \varepsilon_k + \hbar v_0 q), \tag{21a}$$

where δ is the delta function, expressing the law of conservation of energy for the collision.

MEAN FREE PATH OF AN EXCITON

For high temperatures (for our case exceeding several degrees Kelvin) the relaxation time τ may be calculated from the formula[14]

$$\frac{1}{\tau} = - \sum_q \frac{\Delta k_x(q)}{k_x} [W_{kk'}^{+} + W_{kk'}^{-}] \tag{22}$$

where $\Delta k_x = k_x' - k_x$ is the change in the component of the wave vector due to the collision.

We subsitute in Eq. (21) N_q for the mean number of phonons in equilibrium. From the Planck formula we have

$$\bar{N}_q = [\exp(\hbar v_0 q / k_0 T) - 1]^{-1}. \tag{23}$$

Taking into account that for the phonons, which mainly interact with excitons, $\hbar v_0 q / k_0 T \approx \hbar v_0 k / k_0 T \ll 1$,

we obtain

$$\bar{N}_q \approx \bar{N}_q + 1 \approx k_0 T / \hbar v_0 q. \tag{24}$$

Replacing the summation in Eq. (22) by an integration in polar coordinates, with the polar axis coinciding with $\mathbf{k}$, we get

$$\frac{1}{\tau} = - \frac{\pi k_0 T}{N M v_0^2 \hbar} \frac{v}{(2\pi)^3} \int \frac{\Delta k_x}{k_x} \Phi(q) \tag{25}$$

$$\times [\delta(\varepsilon_{k'} - \varepsilon_k - \hbar v_0 q)$$

$$+ \delta(\varepsilon_{k'} - \varepsilon + \hbar v_0 q)] q^2 dq \sin\theta d\theta d\varphi.$$

Integrating over ϕ, on which only $\Delta k_x / k_x$ depends, gives

$$\int_0^{2\pi} \frac{\Delta k_x}{k_x} d\varphi = - 2\pi q^2 / 2k^2. \tag{26}$$

Integrating over θ eliminates the delta functions and gives a factor $\mu_{exc} / \hbar^2 kq$ in place of each of them. Thus the mean free path of an exciton $l = \tau v = \tau \hbar k / \mu_{exc}$ is given by

$$\frac{1}{l} = \frac{\Omega_0 \mu_{exc}^2 (C_1 - C_2)^2 k_0 T}{\pi M v_0^2 \hbar^4} \frac{1}{4k^4} \int_0^{2k} \frac{\Phi(q)}{(C_1 - C_2)^2} q^3 dq. \tag{27}$$

We examine first the particular case when $\mu_1 = \mu_2 = \mu^*$, then

[12] B. I. Davydov and I. M. Shmushkevich, Usp. Fiz. Nauk 24, 21 (1940)

[13] H. Bethe and A. Sommerfeld, Electron Theory of Metals, Handbuch der Physik, vol. 24, p. 2

[14] H. Fröhlich, Proc. Roy. Soc. 160A, 230 (1937)

$$\Phi(q) = (C_1 - C_2)^2/[1 + \beta^2 q^2]^4, \qquad (20a)$$

where

$$\beta = {}^1/_4 a_{exc}.$$

Substituting this form of $\Phi(q)$ in Eq. (27) and carrying out the integration, we obtain

$$l = \frac{\pi M v_0^2 \hbar^4}{\Omega_0 \mu_{exc}^2 (C_1 - C_2)^2 k_0 T} \frac{(1 + b\varepsilon)^3}{1 + {}^1/_3 b\varepsilon}, \qquad (18a)$$

where $\epsilon = \hbar^2 k^2/2\mu_{exc}$ is the energy of the exciton and $b = [\mu^* e^4/4\kappa^2\hbar^2]^{-1}$. It can be easily seen that for the criterion (7) to be justified it is necessary that $\epsilon \leq 0.75/b$. From Eq. (18a) it is seen that for the particular case considered here the mean free path of the exciton is a monotonic function of the energy. For small values of the energy ϵ the numerical value of l is given by Eq. (18). For the maximum energy $\epsilon_{max} = 0.75/b$ the expression for l is 4.3 times larger.

For the general case a simple calculation gives

$$\frac{1}{4k^4}\int_0^{2k} \frac{\Phi(q)}{(C_1 - C_2)^2} q^3 dq = \left(\frac{C_1}{C_1 - C_2}\right)^2 \frac{1 + {}^1/_3 b_1\varepsilon}{(1 + b_1\varepsilon)^3} \qquad (28)$$

$$+ \left(\frac{C_2}{C_1 - C_2}\right)^2 \frac{1 + {}^1/_3 b_2\varepsilon}{(1 + b_2\varepsilon)^3} - \frac{2C_1C_2}{(C_1 - C_2)^2} \frac{2}{(b_1 - b_2)^2\varepsilon^2}$$

$$\times\left[\frac{b_1 + b_2}{b_1 - b_2} \ln \frac{1 + b_1\varepsilon}{1 + b_2\varepsilon} - \frac{b_1\varepsilon + b_2\varepsilon + 2b_1b_2\varepsilon^2}{(1 + b_1\varepsilon)(1 + b_2\varepsilon)}\right],$$

where ϵ is the energy of the exciton and

$$b_1 = \left(\frac{\mu_1}{\mu_1 + \mu_2} \frac{\mu_1 e^4}{2\hbar^2\kappa^2}\right)^{-1}, \quad b_2 = \left(\frac{\mu_2}{\mu_1 + \mu_2} \frac{\mu_2 e^4}{2\hbar^2\kappa^2}\right)^{-1} \qquad (29)$$

are coefficients, with dimensions of inverse energy and of the order of magnitude of the inverse of the internal energy of the exciton.

It seems expedient to write Eq. (27) in the form

$$l = \frac{\pi M v_0^2 \hbar^4}{\Omega_0 (\mu_1 + \mu_2)^2 (C_1 - C_2)^2 k_0 T} F(z; s, g) = l_0 F \qquad (30)$$

where

$$z = b_2\varepsilon, \quad s = C_1/(C_1 - C_2), \quad g = \mu_2/\mu_1 \qquad (30a)$$

and

$$\frac{1}{F(z; s, g)} = s^2 \frac{1 + {}^1/_3 g^2 z}{(1 + g^2 z)^3} + (s - 1)^2 \frac{1 + {}^1/_3 z}{(1 + z)^3} \qquad (30b)$$

$$- 2s(s - 1) \frac{2}{(g^2 - 1)^2 z^2}\left[\frac{g^2 + 1}{g^2 - 1} \ln \frac{1 + g^2 z}{1 + z}\right.$$

$$\left. - \frac{(g^2 + 1) z + 2g^2 z^2}{(1 + z)(1 + g^2 z)}\right].$$

It should be noted that $z = b_2\epsilon = {}^3/_4(\mu_1/\mu_2)\gamma \approx \gamma/g$, but $\gamma \leq 1$, from which

$$0 \leqslant z \leqslant 1/g. \qquad (30c)$$

It can be easily seen that for $z \to 0$, the function F converges to unity for all values of s, that is, Eq. (30) transforms into Eq. (18).

We see from Eq. (30) that the mean free path of excitons, just as that for electrons (holes), is inversely proportional to the absolute temperature. On the other hand the mean free path of an exciton, in contrast to that of an electron (hole), depends on its energy.

Since this problem is completely symmetrical with respect to the electron and the hole, let us consider only the case of $g > 1$, which corresponds physically to the more probable assumption that the effective mass of the hole μ_2 is larger than the effective mass of the electron μ_1. It appears that $C_1 > C_2$, as it can be imagined that, for a given relative change in the volume of a crystal, the displacement of the lower edge of the conduction band is larger than the displacement of the upper edge of the valence band.

To give visually an idea of the behavior of the function $F(z; s, g)$ for various values of its arguments, graphs of $F(z)$ for several values of g and s have been constructed. In Fig. 1 the behavior of $F(z)$ is depicted, for $g = 3$, and several values of s, from unity ($C_2 = 0$) to infinity ($C_1 = C_2$). Figure 2 shows the same relationship, for $g = 9$.

In the case of $s = 1$ ($C_2 = 0$), the function is

$$F(z) = (1 + g^2 z)^3/(1 + {}^1/_3 g^2 z).$$

If $C_1 = C_2 = C$, and consequently, $s = \infty$, then

$$\frac{(C_1 - C_2)^2}{F(z)} = C^2\left\{\frac{1 + {}^1/_3 g^2 z}{(1 + g^2 z)^3} + \frac{1 + {}^1/_3 z}{(1 + z)^3}\right.$$

$$- \frac{4}{(g^2 - 1)^2 z^2}\left[\frac{g^2 + 1}{g^2 - 1} \ln \frac{1 + g^2 z}{1 + z}\right.$$

$$\left.\left. - \frac{(g^2 + 1) z + 2g^2 z^2}{(1 + z)(1 + g^2 z)}\right]\right\},$$

and in this case we shall designate as $F(z)$ the inverse of the quantity contained in the brackets on the right hand side.

In discussing the graphs shown it is necessary

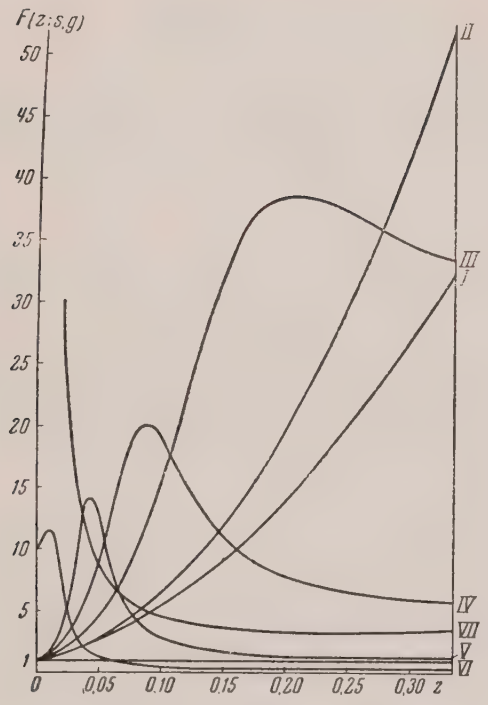

Fig. 1. $g = 3$. *I:* $s = 1$; $C_2 = 0$; *II:* $\phi s = 1.1$; $C_1 = 11C_2$; *III:* $s = 1.5$; $C_1 = 3C_2$; *IV:* $s = 2$; $C_1 = 2C_2$; *V:* $s = 3$; $C_1 = 1.5\,C_2$; *VI:* $s = 11$; $C_1 = 1.1\,C_2$; *VII:* $s = \infty$; $C_1 = C_2$. The ordinates of curve *VI* are magnified 10 times.

to keep in mind that the ordinates of the curves *VI* in Figs. 1 and 2 are magnified ten times, while the ordinates of the curves *I* and *II* in Fig. 2 are reduced ten times. Also, the curve *VII* for $s = \infty$ is not shown in Fig. 2, as it is similar to the curve *VII* in Fig. 1. The ordinates of the curve *VI* of Fig. 2 are of the order of 0.014 for values of $z > 0.02$.

Now if we regard l_0 as given (i.e., the difference $C_1 - C_2$ is given), then a number of conclusions can be drawn concerning the behavior of the dimensionless factor F, which, when multiplied by l_0, determines the mean free path of the exciton. We see that in all cases, when C_1 is of the order C_2, i.e., their difference is of the same order of magnitude (curves *III*, *IV*, and *V*), the function $F(z)$ has a maximum in the energy interval in which the excitons can exist, thus increasing the mean free path (with respect to l_0) by a factor of 10 - 40. The larger the value of C_1 as compared to C_2, the

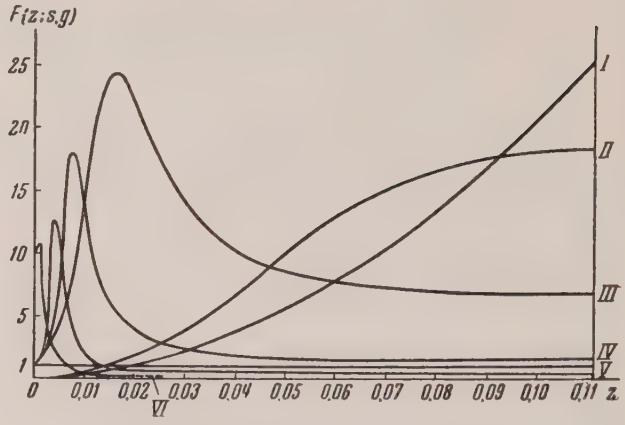

Fig. 2. $g = 9$. Curves *I-VI* are calculated for the same values of the parameter s, as in Fig. 1. The ordinates for curves *I* and *II* have been reduced 10 times, those for curve *VI* have been magnified 10 times.

higher will be the values of the exciton energy at which the length of the mean free path reaches its maximum. In the cases when C_1 differs only slightly from C_2 (curves *VI*), and the energy of the exciton is not overly small, its mean free path is several dozen times smaller than l_0.

Let us determine the temperature T_m, which corresponds to the energy $\epsilon = k_0 T_m$ for which F has a maximum, for the case of $g = \mu_2/\mu_1 = 3$ and $s = 2$. Assuming, for example, $\kappa = 15$ and $\mu_2 = 2m_e$, we obtain $T_m = 96°\,\mathrm{K}$. It is easy to see that for $g = 9$, the maxima of F are located, generally speaking, at somewhat lower temperatures, of the order of 10–20°K.

We see that the dependence of the length of the mean free path of the exciton on energy is materially connected with the relative magnitude of the effective masses of the electron and the hole, and of the interaction constants C_1 and C_2. Of course, no exact quantitative determinations of the mean free path of the exciton can be made unless the constants μ_1, μ_2, C_1, C_2 are known. As far as that is concerned, the conditions are similar to those encountered in considering the theory of the mean free path of an electron (hole).

The corresponding calculations for an exciton in a polar crystal will be published in the very near future.

Translated by O. L. Tiffany
24

SOVIET PHYSICS - JETP VOLUME 1, NUMBER 1 JULY, 1955

The Statistical Theory of Heavy Nuclei and of Nuclear Forces

F. I. KLIGMAN
Kiev Technological Institute of Light Industry
(Submitted to JETP editor December 15, 1953)
J. Exper. Theoret. Phys. USSR 28, 297-307 (March, 1955)

A statistical method representing a semi-classical approximation employing the self-consistent field method is developed for application to heavy nuclei. The method takes into consideration unfilled spin and charge states for various charge-symmetry functions of interaction between nucleons with the separation dependence having the form $-g^2e^{-\kappa r}/r$. Equations have been derived and analyzed both for the case of completely filled state of nucleons as well as for the "charge" or "spin" states. Formulas have been obtained for the basic "isotopic" and supplementary term of the equation expressing the energy of a nucleus. A discussion is included regarding the influence of various properties of nuclear forces on the behavior of a complex nuclei.

INTRODUCTION

THE investigation of a heavy nuclei by a statistical method which takes into account the properties of nuclear forces, predicted by theory and qualitatively substantiated for a system consisting of two nucleons, is of interest both for the explanation of properties of heavy nuclei, as well as for the study of nuclear interactions. A number of recent papers have been devoted to the study of nuclei using statistical methods. Ivanenko and others[1,2] used the methods of Thomas-Fermi in their analysis of nuclear shells. The nuclear potentials were considered to be functions of distance $f(r)$ of the type of Yukawa potential (without exchange and independent of spin). In the work of Kompaneets[3] the self - consistent method was applied to the study of a nucleus with saturation spins and charges, with an interaction function, representing one half the sum of ordinary exchange forces, having the same co-ordinate dependence $f(r)$.

In this paper a derivation for the statistical theory of nucleus is presented, which permits analysis of both the case of the saturation of spins and charges and the case where one or the other is incomplete for various charge-symmetry functions of interaction between nucleons (without regard to tensor forces). The solution obtained is in a general form in the sense that the derived formulas contain coefficients which depend upon the form of operator of the function of interaction, and therefore yield concrete results. An expression has been derived for the energy of a nucleus which takes into account the kinetic energy of nucleons the energy of "direct" and "exchange" interaction, as functions of two densities ρ_1 and ρ_2, which represent respectively the density of neutrons and protons under conditions of complete filling spins and incomplete saturation of charges, and densities of particles with spins directed "upward" and "downward", under the conditions of complete saturation of charges and incomplete saturation of spins. On the basis of the variation method and equation for nuclear potentials, a system of equations has been obtained which specifies the distribution of the total density of nucleons $\rho_0 = \rho_1 + \rho_2$ and the charge or spin density $\rho = \rho_1 - \rho_2$. In view of the small magnitude of ρ/ρ_0 equations have been obtained for ρ_0, in the first approximation which are independent of ρ, and which have the same form as they do in the case of complete saturation of spins and charges. In this case ρ is determined by linear differential equations with coefficients dependent upon ρ_0. Study of the equation for ρ_0 along with the equations for energy leads to the selection of interaction functions which insure complete saturation of nuclear forces; the ratio of "exchange" forces to "ordinary" has proven to equal four. By making use of the magnitude of the parameter g^2/κ, determined by the condition of existence of deuteron, the possibility is established that heavy nuclei can exist in stable state having binding energy proportional to A, and radii $R = r_0 A^{1/3}$ where r_0 is roughly equal to the radius of action of nuclear forces. On the basis of these parameters, which determine the interaction function of two nucleons, independently of the exact form of the potential

[1] D. D. Ivanenko and D. Rodichev, Doklady Akad. Nauk SSSR 70, 605 (1950)

[2] D. D. Ivanenko and A. A. Sokolov, Doklady Akad. Nauk SSSR 74, 33 (1950)

[3] A. S. Kompaneetz, Doklady Akad. Nauk SSSR 85, 301 (1952)

hole, expressions are also derived for "isotopic" and supplementary term $\delta(A, Z)$ of the semi-empirical equation for the energy of a nucleus [Ref. 4, Eq. (1.8)]. With the aid of the supplementary parameter -- having experimental value r_0 -- it is possible to compute coefficients of the various terms of the expression for the energy of nucleus and to estimate the mass of the meson. The parameter γ also appears in the theory, taking into account the dependence of nuclear forces due to spins. It has only a small quantitative effect on the results and is used merely for qualitative deductions made during analysis of distribution of ρ.

1. GENERAL THEORY

Let us examine the function of interaction between two nucleons expressed in the following form:

$$U_{1,2} = P(1,2)\, f(r_{1,2}), \tag{1}$$

where

$$f(r_{1,2}) = -g^2 (e^{-\varkappa r_{1,2}} / r_{1,2}); \tag{2}$$

P – an operator which can assume any one of the following forms:

$$P = P_0 = 1, \quad P = P_\sigma = \frac{1 + (\vec{\sigma}_1 \vec{\sigma}_2)}{2} \tag{3}$$

$$P = P_\tau = \frac{1 + (\vec{\tau}_1 \vec{\tau}_2)}{2},$$

$$P = P_r = -\frac{1 + (\vec{\sigma}_1 \vec{\sigma}_2)}{2} \frac{1 + (\vec{\tau}_1 \vec{\tau}_2)}{2},$$

or can be a linear combination of these quantities. Operators P_σ, P_τ, P_r correspond, as is known, to rearrangement of spin, charge and space coordinates of the two nucleons. Let us express the energy of a nucleus in the following form:

$$E = \int [T_1(\rho_1) + T_2(\rho_2)]\, d\tau \tag{4}$$

$$+ \frac{\alpha}{2} \int [A_1(\rho_1) + A_2(\rho_2)]\, d\tau$$

$$+ \alpha_{1,2} \int A_{1,2}(\rho_1, \rho_2)\, d\tau$$

$$+ \frac{\beta}{2} \iint [\rho_1(1)\rho_1(2) + \rho_2(1)\rho_2(2)] f(r_{1,2})\, d\tau_1\, d\tau_2$$

$$+ \beta_{1,2} \iint \rho_1(1)\rho_2(2) f(r_{1,2})\, d\tau_1\, d\tau_2,$$

where the first term represents kinetic energy:

$$T_1(\rho_1) + T_2(\rho_2) \tag{5}$$

$$= \frac{3}{10} \left(\frac{3}{\pi}\right)^{2/3} \frac{\pi^2 \hbar^2}{M} (\rho_1^{5/3} + \rho_2^{5/3});$$

the second and third terms are "exchange" interactions, respectively, for "like" and "unlike" particles, the fourth and fifth, analogous forms of "direct" interaction. The coefficients α, $\alpha_{1,2}$, β, $\beta_{1,2}$ depend upon the form of operator used in Eq. (1) and are computed in the same manner as the functions A_1, A_2, $A_{1,2}$, i.e., with the aid of the wave function Ψ of nucleus in the form of a determinant composed of the individual wave functions $\varphi_i(\mathbf{X}_i)$ of all N nucleons ($\mathbf{X}_i$ represents the various space co-ordinates, spin and charge co-ordinates of nucleons). It is assumed that

$$\phi(\mathbf{X}_i) = \psi_i(x_i, y_i, z_i)\, \eta_i(\vec{\sigma}_i)\, \zeta(\vec{\tau}_i), \tag{6}$$

where η and ζ are functions only of operators σ_z, τ_z respectively. The energy of interaction of all nucleons can be expressed as follows:

$$U = \frac{1}{2} \sum_{i=1}^{N} \sum_{j=1}^{N} \iint \varphi_i^*(1)\, \varphi_j^*(2)\, U_{1,2}\, \varphi_i \tag{7}$$

$$(1)\, \varphi_j(2)\, d\mathbf{X}_1\, d\mathbf{X}_2$$

$$- \frac{1}{2} \sum_{i=1}^{N} \sum_{j=1}^{N} \iint \varphi_j^*(1)\, \varphi_i^*(2)\, U_{1,2}\, \varphi_i$$

$$(1)\, \varphi_j(2)\, d\mathbf{X}_1\, d\mathbf{X}_2$$

$$= J + K = \frac{1}{2} \sum_{i,j} J_{i,j} + \frac{1}{2} \sum_{i,j} K_{i,j}.$$

Taking a summation over the spin and charge variables in the expressions for $J_{i,j}$ and $K_{i,j}$ from Eq. (7), and taking into account Eq. (6), we express the direct interaction J in Eq. (7) by ordinary densities

$$\rho_1 = \sum_{i=1}^{N_1} |\psi_i|^2, \quad \rho_2 = \sum_{j=1}^{N_2} |\psi_j|^2,$$

exchange interaction K by the mixed densities

$$\rho_1(1,2) = \sum_{i=1}^{N_1} \psi_i(1)\, \psi_i^*(2), \tag{8}$$

$$\rho_2(1,2) = \sum_{j=1}^{N_2} \psi_j(1)\, \psi_j^*(2)$$

[4] E. Fermi, *Nuclear Physics*

(N_1, N_2 -- the number of particles of both "types" correspondingly), and introduce the notation:

$$\iint |\rho_1(1,2)|^2 f(r_{1,2})\,d\tau_1\,d\tau_2 = \int A_1(\rho_1)\,d\tau, \quad (9)$$

$$\iint |\rho_2(1,2)|^2 f(r_{1,2})\,d\tau_1\,d\tau_2 = \int A_2(\rho_2)\,d\tau,$$

$$\iint \rho_1(1,2)\,\rho_2^*(1,2)\,f(r_{1,2})\,d\tau_1\,d\tau_2 = \int A_{1,2}(\rho_1,\rho_2)\,d\tau,$$

we derive the values of coefficients given in Table 1 for the four cases of Eq. (3).

In the case in which the operator $P(1,2)$ in Eq. (1) consists of a linear combination of any of the operators of Eq. (3), a situation which corresponds, physically, to the possible forms of interaction, the coefficients α, $\alpha_{1,2}$, β, $\beta_{1,2}$ are evaluated with the aid of the corresponding linear combinations from coefficients of Table 1. In Table 2 are represented the values of coefficients and some other quantities for a number of possibilities considered in the following Sections. In both tables in the column "Type of Saturation" line "a" corresponds to saturation of spins, line "b", to the saturation of charges.

The functions A_1, A_2 and $A_{1,2}$ were computed on the basis of Eqs. (2), (8) and (9), assuming that ψ_i, ψ_j have the form of plane waves, and substituting summation over i, j, by integration in momentum space p_1, p_2; the weight of each state was taken, as in Eq. (5), to be equal to two (two spin states or two charge states of nucleons). This computation is analogous to the computation of the exchange energy of an electron system (Ref. 5, Sec. 2) with the replacement of the Coulomb force by Eq. (2) and with consideration of the fact that the maximum momenta $p_{\mu,1}$, $p_{\mu,2}$ are, in our problem, different for particles of the two "types". Making use of the relation

$$\rho_1 = 2\,(4/3\,\pi p_{\mu,1}^3)\,/\,(2\pi\hbar)^3 \quad (10)$$

and analogous relation for ρ_2, we obtain the magnitudes of A_1, A_2, $A_{1,2}$ as functions of densities ρ_1 ans ρ_2:

$$A_{1,2} = -\frac{g^2\varkappa^4}{\pi^3}\left\{\left[\frac{1}{24} + \frac{\varepsilon^4}{4}\left(\rho_1^{2/3}\rho_2^{2/3} - \frac{1}{2}\rho_1^{4/3} - \frac{1}{2}\rho_2^{4/3}\right) + \frac{\varepsilon^2}{4}\left(\rho_1^{2/3} + \rho_2^{2/3}\right)\right]\ln\frac{1+\varepsilon^2(\rho_1^{1/3}+\rho_2^{1/3})^2}{1+\varepsilon^2(\rho_1^{1/3}-\rho_2^{1/3})^2}\right. \quad (11)$$

$$-\tfrac{2}{3}\varepsilon^3\left[(\rho_1+\rho_2)\ \arctan\ \varepsilon(\rho_1^{1/3}+\rho_2^{1/3}) - (\rho_1-\rho_2)\right.$$

$$\left.\times\ \arctan\ \varepsilon(\rho_1^{1/3}-\rho_2^{1/3})\right] - \tfrac{1}{6}\varepsilon^2\rho_1^{1/3}\rho_2^{1/3} + \frac{1}{2}\varepsilon^4(\rho_1^{1/3}\rho_2 + \rho_1\rho_2^{1/3})\Big\},$$

$$A_1 = -\frac{g^2\varkappa^4}{\pi^3}\left[\left(\frac{1}{24} + \frac{\varepsilon^2}{2}\rho_1^{2/3}\right)\right. \quad (12)$$

$$\left.\times\ \ln(1+4\varepsilon^2\rho_1^{2/3})\right.$$

---

[5] P. Gombas, *The Statistical Theory of the Atom and its Applications*

TABLE I

Operator	Type of Saturation	α	$\alpha_{1,2}$	β	$\beta_{1,2}$
$P_0=1$	a, b	$-1/2$	0	1	1
P_r	a, b	1	1	$-1/2$	0
P_σ	a	-1	0	$1/2$	$1/2$
	b	$-1/2$	$-1/2$	1	0
P_τ	a	$-1/2$	$-1/2$	1	0
	b	-1	0	$1/2$	$1/2$

TABLE II

Case No.	Operator	Value for various states of a system of two nucleons: Triplet l - even	Single l - even	Triplet - l odd	Single - l odd	Type of Saturation	α	$\alpha_{1,2}$	β	$\beta_{1,2}$	$\alpha+\alpha_{1,2}$	$\beta+\beta_{1,2}$	$\beta-\beta_{1,2}$
1	$\frac{1+P_r}{2}$	1	1	0	0	a, b	$\frac{1}{4}$	$\frac{1}{2}$	$\frac{1}{4}$	$\frac{1}{2}$	$\frac{3}{4}$	$\frac{3}{4}$	$-\frac{1}{4}$
2	$\frac{1+P_r}{2}(1+\gamma P_\sigma) = \frac{1+P_r}{2}+\frac{\gamma}{2}(P_\sigma-P_\tau)$	$1+\gamma$	$1-\gamma$	0	0	a	$\frac{1}{4}-\frac{\gamma}{4}$	$\frac{1}{2}+\frac{\gamma}{4}$	$\frac{1}{4}-\frac{\gamma}{4}$	$\frac{1}{2}+\frac{\gamma}{4}$	$\frac{3}{4}$	$\frac{3}{4}$	$-\left(\frac{1}{4}+\frac{\gamma}{2}\right)$
						b	$\frac{1}{4}+\frac{\gamma}{4}$	$\frac{1}{2}-\frac{\gamma}{4}$	$\frac{1}{4}+\frac{\gamma}{4}$	$\frac{1}{2}-\frac{\gamma}{4}$	$\frac{3}{4}$	$\frac{3}{4}$	$-\left(\frac{1}{4}-\frac{\gamma}{2}\right)$
3	$\frac{1+4P_r}{5}$	1	1	$-\frac{3}{5}$	$-\frac{3}{5}$	a, b	$\frac{7}{10}$	$\frac{4}{5}$	$-\frac{1}{5}$	$+\frac{1}{5}$	$\frac{3}{2}$	0	$-\frac{2}{5}$
4	$\frac{1+4P_r}{5}+\frac{\gamma}{2}(P_\sigma-P_\tau)$	$1+\gamma$	$1-\gamma$	$-\frac{3}{5}$	$-\frac{3}{5}$	a	$\frac{7}{10}-\frac{\gamma}{4}$	$\frac{4}{5}+\frac{\gamma}{4}$	$-\frac{1}{5}-\frac{\gamma}{4}$	$+\frac{1}{5}+\frac{\gamma}{4}$	$\frac{3}{2}$	0	$-\left(\frac{2}{5}+\frac{\gamma}{2}\right)$
						b	$\frac{7}{10}+\frac{\gamma}{4}$	$\frac{4}{5}-\frac{\gamma}{4}$	$-\frac{1}{5}+\frac{\gamma}{4}$	$+\frac{1}{5}-\frac{\gamma}{4}$	$\frac{3}{2}$	0	$-\left(\frac{2}{5}-\frac{\gamma}{2}\right)$

$$-\frac{4}{3}\varepsilon^3\rho_1 \arctan 2\varepsilon\rho_1^{1/3} + \varepsilon^4\rho_1^{4/3} - \frac{1}{6}\varepsilon^2\rho_1^{2/3}\Big],$$

$$\varepsilon = (3/\pi)^{1/3}(\pi/\varkappa); \tag{13}$$

A_2 is analogous to A_1, with ρ_1, substituted for ρ_2. For the case of saturation of spin and charge states $\rho_1 = \rho_2$, and $A_1 = A_2 = A_{1,2}$. Introducing new variables $\rho_0 = \rho_1 + \rho_2$ and $\rho = \rho_1 - \rho_2$ and at the same time decomposing Eqs. (5), (11) and (12) in powers of ρ/ρ_0, ignoring powers higher than the 2nd, we obtain an expression for the energy of nucleus [Eq. (4)] in the following form:

$$E = E_0 + E_I, \tag{14}$$

where

$$E_0 = {}^3/_{10}\, c_0 \int \rho_0^{5/3}\, d\tau - a_0(\alpha + \alpha_{1,2}) \tag{15}$$

$$\int [(1+3x^2)\ln(1+x^2) - 4x^3 \arctan x$$

$$+ {}^3/_2\, x^4 - x^2]\, d\tau - (g/4)(\beta + \beta_{1,2}) \int \rho_0 V_0\, d\tau,$$

$$E_I = \int \frac{\rho^2}{\rho_0^2}\Big\{\frac{1}{6}\, c_0 \rho_0^{5/3} - \frac{1}{3}\, a_0 [(\alpha + \alpha_{1,2}) \tag{16}$$

$$\times (x^4 - x^2 \ln(1+x^2)) - \alpha_{1,2}\, x^4 \ln(1+x^2)]\Big\}\, d\tau$$

$$- (g/4)(\beta - \beta_{1,2}) \int \rho V\, d\tau,$$

$$x = 2\pi \left(\frac{3}{2\pi}\right)^{1/3} \frac{\rho_0^{1/3}}{\varkappa}, \tag{17}$$

$$c_0 = \left(\frac{3}{2\pi}\right)^{2/3} \frac{\pi^2 \hbar^2}{M}, \quad a_0 = \frac{g^2 \varkappa^4}{24\pi^3}, \tag{18}$$

$$V_0(\mathbf{r}) = g \int \rho_0(\mathbf{r}') \frac{\exp\{-\varkappa |\mathbf{r} - \mathbf{r}'|\}}{|\mathbf{r} - \mathbf{r}'|}\, d\tau, \tag{19}$$

V is analogous to V_0, with $\rho_0(\mathbf{r}')$ substituted for $\rho(\mathbf{r}')$.

Making use of the variation method, the equation for ρ_0 and ρ is found from the condition

$$\delta E(\rho_0, \rho) = 0 \tag{20}$$

with the supplementary conditions

$$\int \rho_0\, d\tau = N = A = \text{const}, \tag{21a}$$

$$\int \rho\, d\tau = I = \text{const}, \tag{21b}$$

where I is the isotopic number $A - 2Z$, if ρ represents the charge density, and spin number $2s$ (s - the resultant spin in the components of $\hbar$) if ρ represents the spin state density.

On the basis of Eqs. (14) - (21) we obtain the following system of equations

$$\frac{1}{2}\, c_0 \rho_0^{5/3} - (\alpha + \alpha_{1,2}) \frac{2a_0}{\rho_0} [x^4 \tag{22a}$$

$$+ x^2 \ln(1+x^2) - 2x^3 \arctan x]$$

$$- \frac{g}{2}(\beta + \beta_{1,2})\, V_0 - \frac{1}{9}\frac{\rho^2}{\rho_0^2}\Big\{\frac{1}{2}\, c_0 \rho_0^{5/3}$$

$$- 2\,\frac{a_0}{\rho_0}\, x^4 \Big[\alpha\Big(\frac{2+x^2}{1+x^2} - 2\,\frac{\ln(1+x^2)}{x^2}\Big)$$

$$+ \alpha_{1,2}\Big(2 - 2\,\frac{\ln(1+x^2)}{x^2} - \ln(1+x^2)\Big)\Big]\Big\} = -\lambda_0,$$

$$\frac{\rho}{\rho_0}\Big\{\frac{1}{3}\, c_0 \rho_0^{5/3} - \frac{2}{3}\,\frac{a_0}{\rho_0}\, x^4 \Big[(\alpha + \alpha_{1,2}) \tag{22b}$$

$$\times \Big(1 - \frac{\ln(1+x^2)}{x^2}\Big) - \alpha_{1,2} \ln(1+x^2)\Big]\Big\}$$

$$- \frac{g}{2}(\beta - \beta_{1,2})\, V = -\lambda,$$

which must be solved simultaneously with the differential equations for nuclear potentials V_0 and V. Here λ_0 and λ are Lagrange's multipliers corresponding to the Eqs. (21a) and (21b).

2. NUCLEI WITH SATURATED SPINS AND CHARGES

The density distribution of nucleons ρ_0 is determined in this case ($\rho = 0$), on the basis of Eqs. (19) and (22a), by the following system of equations:

$$c_0 \rho_0^{5/3} - \frac{4a_0}{\rho_0}(\alpha + \alpha_{1,2})[x^4 + x^2 \ln(1+x^2) \tag{23}$$

$$- 2x^3 \arctan x] - (\beta + \beta_{1,2})\, g V_0 = -2\lambda_0,$$

$$\Delta V_0 - \varkappa^2 V_0 = -4\pi g \rho_0, \tag{24}$$

where V_0 must satisfy the condition of finiteness at the center of the nucleus and condition

$$(d/dr)[\ln(rV_0)]_{r=R} = -\varkappa$$

(R - radius of nucleus). The solution of this system depends upon the values of coefficients $\alpha + \alpha_{1,2}$ and $\beta + \beta_{1,2}$. On the basis of Eqs. (23) and (21a), Eq. (15) for the energy E_0 assumes the following form:

$$E_0 = \frac{1}{20} c_0 \int c_0^{2/3} d\tau - (\alpha + \alpha_{1,2}) a_0 \qquad (25a)$$

$$\int \varphi(x) d\tau - \frac{\lambda_0}{2} A,$$

where

$$\varphi(x) = (1 + 2x^2) \ln(1 + x^2) - 2x^3 \arctan x \qquad (25b)$$
$$+ {}^1/_2 x^4 - x^2.$$

Lagrange's multiplier λ_0 is connected with E_0 by the relation

$$\lambda_0 = -(\partial E/\partial A)_I = -(dE_0/dA) \qquad (26)$$

and represents the binding energy of one nucleon. If λ_0 does not depend on A, the effect of saturation takes place: $E_0 = -\lambda_0 A$, and it is this specific condition which limits the choice of the function of interaction. It is easy to see that saturation, without any doubt, takes place for forces which lead to the disappearance of direct interaction in Eq. (15), i.e., in the case $\beta + \beta_{1,2} = 0$. Actually, in this case, the term which contains V_0 in Eq. (23) also disappears, and ρ_0, determined by this equation, is constant within the bounds of the nuclei (the boundary conditions for V_0, on the basis of Eq. (24) and with constant density ρ_0 within a nucleus of radius R, with $\rho_0 = 0$ with $r > R$, are satisfied automatically here. From Eqs.(25a) and with the aid of (26), with $\rho_0 = \text{const}$, we obtain the following equation:

$$\lambda_0 = -\frac{1}{10} c_0 \rho_0^{2/3} + 2(\alpha + \alpha_{1,2}) \frac{a_0}{\rho_0} \varphi(x), \qquad (27)$$

Here, on the basis of Eq. (17),

$$x = 3(\pi/3)^{1/3} (1/\varkappa r_0), \qquad (28)$$

where r_0 — radius of the space belonging to one nucleon. From Eq. (23), with $\beta + \beta_{1,2} = 0$, and from Eq. (27), taking into account Eqs. (28) and (18), it is possible to determine λ_0 and r_0 through the constants g, κ, $\alpha + \alpha_{1,2}$; therefore λ_0 and r_0 do not depend on A in this case, which characterizes the effect of saturation. Excluding λ_0 from Eqs. (23), (27), and taking into consideration Eq. (28), we obtain the following equation:

$$x^3 = \frac{10}{\pi} \frac{M}{\hbar^2} \frac{g^2}{\varkappa} (\alpha + \alpha_{1,2}) f(x), \qquad (29a)$$

where

$$f(x) = 1 + \frac{x^2}{2} - \ln(1 + x^2) \qquad (29b)$$
$$- \frac{\ln(1 + x^2)}{x^2}.$$

The root of this equation X_0, and therefore also the magnitude of $1/\kappa r_0$ depend not on the exact value of g and κ, but merely on the magnitude of g^2/κ which on the basis of theory of deuteron is approximately constant.[1]

With the aid of relation $g^2/\kappa \approx \pi^2 \hbar^2/4M$, and employing operator 3, Table 2 (which satisfies the conditions $\beta + \beta_{1,2} = 0$), we find $\chi_0 = 5$; taking operator 4, likewise satisfying this condition, with $\gamma \approx 0.15$, $(1 + \gamma)(g^2/\kappa) = (g^2/\kappa)_{\text{tp}} \approx \pi^2 \hbar^2/4M$, we obtain $\chi_0 \approx 4$. On the basis of Eq. (28) an approximate equality is obtained for the radius of action of nuclear forces $1/\kappa$ and the radius of space available for one nucleon, r_0, which agrees with the experiment. The values of χ_0 determined in this manner, assure a positive value of λ_0 which can be computed on the basis of Eqs. (27) - (29) from the relation

$$\lambda_0 = \frac{3\pi}{10} \left(\frac{3}{\pi}\right)^{1/3} \frac{\hbar^2}{M} \frac{1}{r_0^2} \left[\frac{\varphi(x_0)}{x_0^2 f(x_0)} - \frac{1}{4}\right]. \qquad (30)$$

With $\chi_0 = 4$, $r_0 = 1.5 \times 10^{-13}$ cm we obtain for λ_0 the value of approximately 3 Me V. At that, from Eq. (28) $1/\kappa \approx 2 \times 10^{-13}$ cm, which corresponds to the mass of a meson $\mu \approx 200\, m_e$. The experimental value $\lambda_0 \approx 8$ Me V is obtained from Eq.(30) with $r_0 \approx 0.9 \times 10^{-13}$ cm. It should be noted that the magnitude of r_0 computed in this manner must actually be somewhat smaller than the experimental value, as a result of ignoring not only Coulomb forces of isotropic and surface effects but also the peculiarities of the method of variation.

It must also be pointed out that for the forces we have considered, which lead to saturation [i.e., to the disappearance of the term containing V_0 in Eqs. (15), (23)], the condition $\partial E_0/\partial R = 0$ is automatically satisfied, thus insuring stability of the surface of the nucleus.

Let us now examine the question regarding possible existence of a solution to the system of Eqs.(2 3) and (24) with $\beta + \beta_{1,2} \neq 0$ which gives approximately constant ρ_0 in the major part of volume, i.e., the solution, the zero approximation of which, within the nucleus (away from the shell), has the form:

$$\rho_0 = \text{const} = \frac{1}{{}^4/_3 \pi r_0^3}, \qquad V_0 = \frac{4\pi g \rho_0}{\varkappa^2}. \qquad (31)$$

If such a solution is possible then Eq. (27) remains roughly correct and with the condition (31) from Eqs. (23) and (27) we obtain the generalization (29) in the form

$$x^3 = \frac{10}{\pi}\frac{M}{\hbar^2}\frac{g^2}{\varkappa}\left[(\beta + \beta_{1,2})\frac{x^4}{6} + (\alpha + \alpha_{1,2})\, f(x)\right]; \tag{32}$$

which determines the equality $\chi = \chi_0$.

If operators 1, 2 (Table 2) are chosen, the solution of Eq. (32) is obtained in the form : $\chi = \chi_0 \approx 0.6$. From this $(1/\kappa): r_0 \approx 0.2$. Also λ turns out to be negative, i.e., this solution does not correspond to a stable state of the nuclei. On the basis of general considerations regarding the role of negative direct interaction and also on the basis of investigation of the polarity of second differential of E_0, we also come to the conclusion that it is impossible to have stable states of nuclei under the existence of forces whose expressions contain operators of type 1, 2, and which are saturated. The same applies to forces examined in Ref. 3, which differ from forces corresponding to operators of type 1 (Table 2) by the polarity of their exchange operator and which lead, therefore, to positive energy of exchange and to disappearance of the entire interaction for the condition of two nucleons with even l.

3. NUCLEI WITH UNSATURATED SPINS AND CHARGES

The distribution of spin or charge density ρ on the basis of Eq. (22b) is determined by the expression:

$$\rho = \frac{(g'/2)\,(\beta - \beta_{1,2})\, V - \lambda}{K(\rho_0)}, \tag{33}$$

where $K(\rho_0)$ is the expression in curly brackets in Eq. (22b), divided by ρ_0; moreover, V is related to ρ by the equation

$$\Delta V - \varkappa^2 V = -4\pi g\rho. \tag{34}$$

From Eqs. (33) and (34) we obtain the equation for potential V:

$$\Delta V - \mu^2 V = L, \tag{35}$$

where

$$\mu^2 = \varkappa^2 - 2\pi g^2 \frac{\beta - \beta_{1,2}}{K(\rho_0)}, \tag{36a}$$

$$L = 4\pi g\lambda / K(\rho_0), \tag{36b}$$

from Tables 1 and 2, K and μ^2 are positive for ordinary, exchange and "mixed" forces.

Assuming further that ρ_0 is approximately constant within the nucleus, we obtain solutions to Eq. (34) which are spherically-symmetrical and regular at the origin, of the form:

$$V = C\frac{\operatorname{sh}\mu r}{r} - \frac{L}{\mu^2}. \tag{37}$$

We then get, from Eqs. (33) and (36),

$$\rho = -\left(\frac{B\operatorname{sh}\mu r}{r} + \frac{1}{K}\frac{\varkappa^2}{\mu^2}\right)\lambda. \tag{38}$$

Constant C and the related constant B are determined from boundary condition

$$\left[\frac{d}{dr}\ \ln\ (rV)\right]_{r=R} = -\varkappa. \tag{39}$$

This yields

$$B = \frac{-(\beta - \beta_{1,2})\, 2\pi g^2}{K^2\mu^2}\,\frac{\varkappa R + 1}{\varkappa \operatorname{sh}\mu R + \mu \operatorname{ch}\mu R}. \tag{40}$$

On the basis of Eqs. (21a), (21b) and also (38) and (40), we obtain the following expression for λ:

$$\lambda = -\rho_0 KI/A\left[\left(1 - \frac{\varkappa^2}{\mu^2}\right)F(R) + \frac{\varkappa^2}{\mu^2}\right] = -b\frac{I}{A}, \tag{41}$$

where

$$F(R) = \frac{3}{(\mu R)^2}(1 + \varkappa R)\,\frac{1 - (\operatorname{th}\mu R/\mu R)}{1 + (\mu/\varkappa)\operatorname{th}\mu R}. \tag{42}$$

λ is negative since, for all forces of interest, $\mu^2 \geq \kappa^2$, $\mu R \gg 1$.

Further, taking into account the values of coefficients $\beta - \beta_{1,2}$ for the different cases (from Tables 1 and 2), we note that B is positive for exchange and "mixed" forces and is equal to zero for ordinary forces; therefore, Eq. (38) for distribution of ρ contains a term (determined by exchange forces) which increases from the center of the nucleus toward the periphery (with $\rho_0 \approx$ const). This means that "excess" neutrons in a nucleus with unsaturated charges and saturated spin states experience additional mutual repulsion; and similarly, mutual repulsion exists between "excess" nucleons with parallel spins in the case of saturation of charges and unsaturated spin states.

We wish to point out that the above effect of additional repulsion does not disappear even in the presence of spin dependence (for example, for the case of forces corresponding to operator 4, Table 2), as a result of the small magnitude of γ. How-

ever, the effect diminishes for the case of unsaturated spin states and saturation of charges and increases in the case of unsaturated charges and saturation of spin states because of the "spin" terms. This means that, for example, for a nucleus of type $A = 4n+2$, which is of great importance from the energy point of view, (if Coulomb forces and differences of mass of proton and neutron are ignored), a state exists with unsaturated spin states and saturated charges, which corresponds to a singlet charge state and triplet spin state with two "excess" nucleons (proton and neutron with parallel spin) in the shell model.

In this manner, the statistical model, as well as the free particle model, can explain the existence of nuclei of type "Z - odd, A - even" with spin equal to unity, by taking into account spin interaction.

The expression for E_I can be studied in more detail on the basis of the newly found distribution of ρ.

On the basis of Eqs. (16), (22b), (21b), we obtain

$$E_I = -(\lambda/2)\, I, \tag{43}$$

from which, taking into account the value of λ from Eq. (41), we obtain

$$E_I = +\frac{1}{2}\frac{\rho_0 K}{[1-(\varkappa^2/\mu^2)]\,F(R)+(\varkappa^2/\mu^2)}\frac{I^2}{A} \tag{44}$$

$$= +\frac{b}{2}\frac{I^2}{A}.$$

The magnitude of $F(R)$ is small for heavy nuclei and changes slowly with changes in $R = r_0 A^{1/3}$; for this reason the magnitude of b, which determines λ, and E_I, is practically independent of A.

From Eqs. (41) and (44) it follows that:

$$\lambda = -(\partial E_I/\partial I)_A = -(\partial E/\partial I)_A, \tag{45}$$

which is in accord with the physical meaning of the Lagrange multiplier λ which corresponds to condition (21b) of the variational problem. For the case in which ρ signifies charge density, $I = A - 2Z$, and Eq. (44) assumes the form

$$E_I = 2b\left(\frac{A}{2} - Z\right)^2 / A. \tag{46}$$

We have obtained, in this manner, the "isotopic" term of a semi-empirical formula for the energy of a nucleus [Ref. 4, Eq. (1.8)] with coefficient $2b$, determined by Eq. (44). This coefficient can be presented in a more expanded form by taking into account the value of $K\rho_0$, as well as Eqs. (18) and (28) and the relationship between ρ_0 and r_0:

$$2b = \left(\frac{3}{\pi}\right)^{1/3}\frac{1}{r_0^2} \tag{47}$$

$$\frac{\frac{\pi}{2}\frac{\hbar^2}{M}+\frac{g^2}{\varkappa}\frac{2}{x}\left[\alpha_{1,2}\ln(1+x^2)-(\alpha+\alpha_{1,2})\left(1-\frac{\ln(1+x^2)}{x^2}\right)\right]}{[1-(\varkappa^2/\mu^2)]\,F(R)+(\varkappa^2/\mu^2)}.$$

Also, on the basis of Eq. (36a)

$$\varkappa^2/\mu^2 = \psi/[\psi-(\beta-\beta_{1,2})(g^2/\varkappa)\,x], \tag{48}$$

where ψ is the numerator of the fraction in Eq. (47).

On the basis of these formulas it is possible to determine the numerical value of the coefficient $2b$ in Eq. (46) for different types of forces, consistent with the requirement $\rho_0 \approx$ const.

For the interaction which contains an operator of type 4, Table 2, with parameters r_0, g^2/κ, γ, we obtain from the previous section, $2b \approx 100$ Me V, which agrees in order of magnitude with the experimentally determined value of 77.3 Me V.

In the case when ρ signifies spin state density with saturation of charges, $I = 2S$ in Eqs. (43) - (45), and we obtain a positive term in the expression for the energy of the nucleus having the form:

$$E_S = 2bS^2/A \tag{49}$$

(S - resultant spin of the nucleus). But nuclei with saturated charges (the number of protons equal to the number of neutrons) and unsaturated spin states must belong to the group "A - even, Z - odd", and specifically for them, the additional empirical term in the expression $\delta(A, Z)$ for the energy of a nucleus [Ref. 4, Eqs. (1.8) and (1.9)] is positive.

The coefficient $2b$ is computed, by use of the same formulas (47), (48), as in the case of an isotopic member, but with different values of the coefficients $\alpha_{1,2}$, $\beta - \beta_{1,2}$ in correspondence with Table 2 (case "b" instead of case "a"). The computed magnitude of $2b$ in this case, with the operator and constants used in the computation of $2b$ for isotopic term is approximately 80 Me V.

Although Eq. (49) differs in appearance from the corresponding empirical term ($\sim A^{-3/4}$), it is interesting to note that for the heavier, stable nuclei of the type studied (N^{14}), we have the theoretical value $E_s \approx 6$ Me V, and the empirical, ≈ 4.7 Me V. The same type of correlation is obtained also for nuclei of other types.

Taking into consideration the roughness of our approximations, particularly for the case of unsaturated spin states (in connection with the neglected tensor forces), the correspondence in sign and order of magnitude of the theoretical formulas and empirical formulas indicates that the effect of unsaturated spin states, as also the isotopic effect, is correctly indicated by the statistical theory.

In closing we wish to call attention to the fact that the results of the present work indicate the applicability to research on the properties of heavy nuclei of the statistical method, which was developed here on the basis of nuclear forces that retain their basic properties predicted by meson theory (the type of distance function, exchange and spin terms). By choosing the parameters expressing these forces, corresponding both with the basic properties of the deuteron and the phenomenon of scattering of slow nucleons by nucleons, as well as with the property of saturation found in complex nuclei, proper orders of magnitude and sign have been obtained for various terms in the expression of binding energy of heavy nuclei. Also, the correct relationship between the radius of action of nuclear forces to the radius of space available to one nucleon has been found, as well as the explanation for the behavior of certain types of complex nuclei based on the analysis of influence of exchange and spin terms.

The method used here can be generalized to include tensor and Coulomb forces, which would improve the accuracy of the results of computations[6,7] dealing with the quadrupole moments of the nuclei. It must also be pointed out that, in the work reported by Gombas[8] which appeared after the preparation of this article, the statistical method is analyzed for application to nuclei with saturated spins. This work differs from ours both in the types of nuclear interactions (purely exchange forces between proton and neutron, and also, as in Bethe and Bacher[9], Sec. 6, spin dependent forces between like particles) and also in the method of derivation of theory (by means of solving various problems and analysis of related questions). The interactions studied by Gombas[8] are equivalent in their effect to saturation of forces, and have in their expressions operators of type 3, Table 2, given in this paper.

Taking into account the difficulties of interpreting experimental data pertaining to scattering of fast nucleons by nucleons[10] on the basis of semi-empirical nuclear forces, it may be appropriate to call attention to the semi-empirical character of the modern nuclear statistical theory the further refinement of which will be apparently concerned with the development of the meson theory of nuclear forces.

Translated by B. S. Maximoff
51

[6] F. I. Kligman, J. Exper. Theoret. Phys. USSR 14, 323 (1944)

[7] F. I. Kligman, J. Exper. Theoret. Phys. USSR 18, 346 (1948)

[8] P. Gombas, Usp. Fiz. Nauk 49, 385 (1953)

[9] H. A. Bethe and R. F. Bacher, *The Physics of Nuclei*, Revs. Mod. Phys.

[10] V. I. Gol'danskii, A. L. Liubimov and B. V. Medvedev, Usp. Fiz. Nauk 48, 531 (1952)

SOVIET PHYSICS - JETP VOLUME 1, NUMBER 1 JULY, 1955

On the Stability of a Homogeneous Phase. I General Theory

I. Z. FISHER
Byelorussia State University
(Submitted to JETP editor March 4, 1954)
J. Exper. Theoret. Phys. USSR **28**, 171-180 (March, 1955)

Necessary conditions for thermodynamic stability and sufficient conditions for the thermodynamic instability of a homogeneous phase are obtained in terms of the theory of the radial distribution function. The proposed problem of the determination of the radial distribution function is correctly formulated.

INTRODUCTION

THE use of partial distribution functions together with the "superposition approximation" allows the application of the general apparatus of the Gibbs canonical distribution--- which is of very little effectiveness in the case of the liquid state--- to a certain nonlinear problem concerning eigenfunctions and eigenvalues[1,2]. Let $F_1(q)$, $F_2(q, q')$, $F_3(q, q', q'')$ be the unitary, binary and ternary distribution functions, respectively. If we consider only a homogeneous phase (that is, a gas or a liquid), then the asymptotic expressions for the first two of these functions, when (by removal of all limits on the volume V up to infinity) the volume V of the system and the number of particles N of the system are allowed to increase without bound [but with $v = \lim (V/N) = \text{const}$], are

$$F_1(q) = 1; \quad F_2(q, q') = g(|q - q'|). \tag{1}$$

The function $g(r)$ is the so-called "radial distribution function". For the sake of simplicity we will assume the absence of strong external fields and will deal only with the simplest type of liquid (or gas), the intermolecular potential of which depends only on the distance between the centers of the two particles. If we allow that with sufficient exactitude, we may assume

$$F_3(q, q', q'') = g(|q - q'|) \tag{2}$$
$$g(|q - q''|)\, g(|q' - q''|)$$

("superposition approximation"), then the function $g(r)$ is determined by the intermolecular potential $\Phi(r)$ of the system, its temperature T and density $1/v$, by means of Bogoliubov's equation[1]

$$-kT \ln g(r) = \Phi(r) \tag{3}$$
$$+ \frac{\lambda}{r} \int_0^\infty \left\{ \int_{|r-\rho|}^{r+\rho} E(t)\, t\, dt \right\} (g(\rho) - 1)\, \rho\, d\rho,$$

where

$$E(t) = \int_\infty^t \Phi'(t)\, g(t)\, dt, \quad \lambda = 2\pi a^3/v. \tag{4}$$

Here k is Boltzmann's constant, and we have introduced the dimensionless unit of length $r' = r/a$, where a is a certain characteristic molecular distance, for example, the diameter of a particle. In (3), as also from here on, the prime on the r has been omitted.

The function $g(r)$ must, moreover, satisfy the normalization condition

$$\lim_{R \to \infty} \frac{1}{R^3} \int_0^R (g(r) - 1)\, r^2 dr = 0, \tag{5}$$

arising from (1) and from the significance of $F_1(q)$ and $F_2(q, q')$ in terms of probability.

Equations (3)---(5), taken together, present the complicated nonlinear problem of the determination of the eigenfunctions $g(r;\lambda)$ and the eigenvalues λ. The question of the spectrum of values λ (for a given temperature T) is very important for the theory of phase transitions from a homogeneous phase, as has already been pointed out by the author[3]. However, the problem of the determination of the spectrum of values λ for a given $\Phi(r)$ and T is unusually complex on account of the nonlinearity of Eqs. (3) and (4). It will be shown below that this problem can be solved, to a certain extent, by means of an investigation of the behavior of the solutions of Eq. (3) as $r \to \infty$. It will then become apparent that the problem defined by Eqs. (3)--(5) has, in a certain sense, not been formulated altogether correctly, and from this will arise the necessity of correctly formulating "boundary conditions" on Eq. (3). The present communication is devoted to

[1] N. N. Bogoliubov, *Problems of Dynamical Theory in Statistical Mechanics*, State technical publishing house, 1946.

[2] I. Z. Fisher, Usp. Fiz. Nauk **51**, 71 (1953)

[3] I. Z. Fisher, J. Exper. Theoret. Phys. USSR **21**, 942 (1951)

the solution of this problem. In the correctly formulated problem the discontinuous character of the spectrum of eigenvalues of the parameter λ arises automatically. In subsequent communications the general theory will be applied to the solution of actual problems of the liquid state.

2. BEHAVIOR OF THE RADIAL DISTRIBUTION FUNCTION AT GREAT DISTANCES

For what follows it is convenient to change over from the function $g(r)$ to the auxiliary function $u(r)$ such that

$$g(r) = e^{-\Phi(r)/kT} u(r). \tag{6}$$

If, at the same time, in place of $E(t)$ we introduce the function $\bar{E}(t)$ according to the relation

$$\bar{E}(t) = -\frac{1}{kT} E(t) = \int_{\infty}^{t} (e^{-\Phi(t)/kT})' u(t)\, dt, \tag{7}$$

we then obtain from (3) an equation determining $u(r)$,

$$r \ln u(r) = \lambda \int_0^{\infty} \left\{ \int_{|r-\rho|}^{r+\rho} \bar{E}(t)\, t dt \right\} \{e^{-\Phi(\rho)/kT} u(\rho) - 1\}\, \rho\, d\rho, \tag{8}$$

which contains only λ as a parameter of the integral equation (to employ the terminology of the theory of integral equations). The temperature enters into (8) in a more complicated manner, in the combination $e^{-\Phi(r)/kT}$, and must be given together with the potential $\Phi(r)$.

We are interested in the behavior of $g(r)$ or $u(r)$ as $r \to \infty$. The potential $\Phi(r)$ is assumed to approach zero sufficiently rapidly for $r \to \infty$. Then from (5) and (6) there follows the requirement that, in any case, $u(r) \to 1$ as $r \to \infty$. Hence we may set

$$u(r) = 1 + \varphi(r)\, r, \tag{9}$$

where $|\phi(r)/r| \to 0$ as $r \to \infty$. As a consequence of this we may linearize the logarithm in (8) for large r. Moreover, to the extent that $\bar{E}(t)$ rapidly approaches zero with increasing t, only the values of ρ which are near r will be of consequence in the expression under the integral, while for $r \to \infty$ we may replace $e^{-\Phi(\rho)/kT}$ by unity and extend the upper limit of the integral to infinity. If we denote

$$K(z) = \int_{|z|}^{\infty} \bar{E}(t)\, t dt \tag{10}$$

$$= {}^1/_2 \int_{|z|}^{\infty} (e^{-\Phi(t)/kT})' u(t) (z^2 - t^2)\, dt,$$

where the last expression is obtained by integrating by parts, taking account of (7), we finally arrive at the following equation determining $\phi(r)$ for $r \to \infty$:

$$\varphi(r) = \lambda \int_0^{\infty} K(|r-\rho|)\, \varphi(\rho)\, d\rho \qquad (r \to \infty). \tag{11}$$

In order to simplify the following discussion we now assume that the intermolecular forces have a finite radius of action, that is, that there exists a number σ such that for $r > \sigma$ we have $\Phi(r) \equiv 0$. This condition, we note, limits the generality of the problem only very slightly, since if $\Phi(r)$ extends to infinity (but falls off sufficiently rapidly), then the "radius of cut-off" may be chosen arbitrarily large. Moreover, in the final results of the theory it is not difficult to go over to the limit $\sigma \to \infty$. So,

$$\Phi(r) \equiv 0; \quad g(r) \equiv u(r) \qquad r > \sigma. \tag{12}$$

Then $\bar{E}(t) = K(t) = 0$ for $t > \sigma$ and in place of (10) and (11) we have

$$K(z) = {}^1/_2 \int_{|z|}^{\sigma} (e^{-\Phi(t)/kT})' u(t) (z^2 - t^2)\, dt, \tag{13}$$

$$\varphi(r) = \lambda \int_{r-\sigma}^{r+\sigma} K(|r-\rho|)\, \varphi(\rho)\, d\rho \qquad (r \gg \sigma). \tag{14}$$

In order to find the non-trivial solutions of this equation, we assume

$$\varphi(r) \sim e^{i\gamma r}. \tag{15}$$

Substitution into (14) leads to the equation for the determination of $\gamma = \gamma(\lambda)$

$$\lambda \mathcal{L}(\gamma) = 1 \qquad (\lambda > 0), \tag{16}$$

where $\mathcal{L}(\gamma)$ is the Fourier transform of the kernel $K(z)$

$$\mathcal{L}(\gamma) = \int_{-\sigma}^{\sigma} K(z)\, e^{i\gamma z} dz. \tag{17}$$

Equation (16), generally speaking, has for every $\lambda > 0$ several, or even infinitely many, roots, complex numbers in general: $\gamma_n = \beta_n(\lambda) + i\alpha_n(\lambda)$ ($n = 1,2,3.....$). From the nature of λ and $K(z)$ it follows that these roots occur in complex conjugate pairs, and from the evenness of the function $K(z)$ it follows that for every root $\gamma_n(\lambda)$ there is a corresponding root $-\gamma_n(\lambda)$. Hence we conclude that to each number n there correspond four roots: $\pm\beta_n$

$(\lambda) \pm i\alpha_n(\lambda)$. However, the roots with negative imaginary parts lead, according to (9), (12) and (15), to results for $g(r)$ which manifestly fail to satisfy the normalization condition (5), and therefore must be discarded. The two roots $\pm\beta_n(\lambda) + i|\alpha_n(\lambda)|$ then remain, and the corresponding $\phi(r)$ may be obtained essentially in the form

$$\varphi(r) = Ae^{-|\alpha|r}\cos(\beta r + \delta), \qquad (18)$$

where the numbers A and δ remain undetermined in the approximation under consideration. In accordance with (9) and (12), we then arrive at the following general form of the radial distribution function for large distances between particles

$$g(r) = 1 + \frac{1}{r}\sum_n A_n e^{-|\alpha_n|r}\cos(\beta_n r + \delta_n). \qquad (19)$$

This result corresponds to the known behavior of $g(r)$, found from experiments on the scattering of x-rays in liquids: with increasing r the functior $g(r)$ approaches unity with an oscillation which diminishes to zero. We wish to emphasize that expression (19) is true for all physically allowed values of λ. Smallness of λ (that is, smallness of the density) was not presupposed in the derivation of (19), and this distinguishes our result from the analogous results of other authors[4,5].

The function $\nu(r) \equiv g(r) - 1$ is the "correlation function" of statistical mechanics (see references 6,7), used in the calculation of fluctuations in the density. As is well known, a very rapid decrease in $\nu(r)$ with increasing r is required for the absence of correlation of the fluctuations in density in adjoining macroscopic volumes. According to (19) this requirement will be met if all the $|\alpha_n|$ are not zero and are sufficiently large. Moreover, the absence of correlation of the fluctuations in density in adjoining macroscopic volumes for a system in a state far from the limit of thermodynamic stability is rigidly derivable from Boltzmann's principle (see Leontovich[6]) and is confirmed by experiments on the scattering of light in liquids and gases. Hence for such states all the $|\alpha_n(\lambda)|$ in (19) are different from zero and we may introduce an enumeration of the roots γ_n of equation (16) in the order of the increasing magnitude of their imaginary parts:

$$0 < |\alpha_1(\lambda)| < |\alpha_2(\lambda)| < |\alpha_3(\lambda)| < \ldots \qquad (20)$$

This enumeration is preserved even in the case of very small $|\alpha_n|$, and we shall hold to it continuously below. Of course, for different values of λ the enumeration of the roots γ_n may be different. We note that for $\lambda \to \infty$ (that is, in the ideal gas approximation) we have $|\alpha_n| \to \infty$, as is clear from (16).

3. INSTABILITY OF STATES WITH $\alpha_1(\lambda) = 0$

We shall now show that states of the system for which $\alpha_1 = 0$ in (19) are thermodynamically absolutely unstable, that is, they do not correspond to a minimum free energy. As proof of this we need more than the single fact of the presence of correlation of the fluctuations in density in adjoining volumes. It is known, for example, that such correlations occur in the vicinity of the critical point (see references [6,7]), that is, in states which are of themselves stable.

Let us suppose that for a certain value of λ we have $\alpha_1(\lambda) = 0$, but $\alpha_2(\lambda) \neq 0$. Since in the subsequent estimates, due to their thermodynamic character, the behavior of $\nu(r)$ at small distances will not be of consequence, we can neglect the exponential members in (19) and write

$$\nu(r) = \frac{A_1}{r}\cos(\beta_1 r + \delta_1). \qquad (21)$$

We note at once that $\nu(r)$ is Green's function for all space of the linear differential operator

$$L(\varphi) = \Delta\varphi + \beta_1^2\varphi, \qquad (22)$$

where Δ is the Laplace operator.

We now assume that the state of the system with correlation function (21) is thermodynamically stable, so that there exists an equilibrium density of free energy $f_0(\lambda, T)$, the self free energy for which is $F = \int f_0 dV$. Let $f - f_0$ be the deviation of the equlibrium density of free energy from its own equilibrium value as a consequence of local fluctuations in density. Since in our case there is an evident correlation of the fluctuations in density in different regions, then, as is known from the general theory, the magnitude of $f - f_0$ will depend not only on the density itself, but also on the gradient of the density (see[6,7]). If ϕ is the relative density, then $f - f_0$ appears as a certain differential form in ϕ, and for small fluctuations this form will be quadratic: $f - f_0 = K(\phi, \phi)$. Let us use, further, the fundamental result of Leontovich, according to which the correlation function $\nu(r)$ is Green's function for all space of

---

[4] J. Kirkwood, J. Chem. Phys. 7, 919 (1939)

[5] M. Born and H. Green, Proc. Roy. Soc. A, 189, 455 (1947)

[6] M. A. Leontovich, *Statistical Mechanics*, State technical publishing house, 1944

[7] L. D. Landau and E. M. Lifshitz, *Statistical Physics*, State technical publishing house, 1951

the Euler-Laplace operator $L(\phi) \equiv$ corresponding to the quadratic differential form $K(\phi,\phi)$ (see[6]). Since we already know the function $\nu(r)$ and the operator $L(\phi)$, then by (22) we can readily set up the quadratic form $K(\phi, \phi)$ and also $f - f_0$. For the latter quantity we obtain

$$f - f_0 = B\{(\vec{\nabla}\varphi)^2 - \beta_1^2\varphi^2\}, \qquad (23)$$

where B is a certain constant (with respect to ϕ).

Thus to the correlation function (21) there corresponds an expression of indeterminate sign for $f - f_0$, and, consequently, f_0 cannot be a minimum in the density of free energy. The state of the system with $\alpha_1(\lambda) = 0$ is absolutely unstable, since a minimum free energy does not exist there.

4. INCORRECTNESS OF THE PROBLEM OF THE DETERMINATION OF $g(r)$ WITH THE REQUIREMENT OF NORMALIZATION IN EQ. (5)

The results obtained above may be formulated in a way which affirms that the necessary condition for the stability of a homogeneous phase is the absence of purely real solutions of Eq. (16), that is, the condition

$$|\operatorname{Im}\{\gamma_1(\lambda)\}| > 0 \quad \text{for} \quad \lambda > 0. \qquad (24)$$

Correspondingly, the condition

$$\operatorname{Im}\{\gamma_1(\lambda)\} = 0 \quad \text{for} \quad \lambda > 0, \qquad (25)$$

is sufficient for the instability of the system.

The question of the sufficiency of the first condition and the necessity of the second remains open, since it cannot be treated merely by investigation of the behavior of $g(r)$ as $r \to \infty$. If, in spite of this, we confine ourselves to such an investigation, as we are at present compelled to do, then the following circumstance is to be noted. The normalization condition (5) for the function $g(r)$ is somewhat limited, being superimposed on the behavior of the solution of Eq. (3) for $r \to \infty$. It is unsatisfactory that this limitation admits, along with the stable solutions, solutions which are unstable (that is, physically unreasonable) in the sense indicated above. Actually any function (19) with arbitrary $\alpha_n(\lambda)$ satisfies the condition (5), even if some or all of the α_n are zero. Hence we may say that the problem of the solution of Eq. (3) with the supplementary requirement (5) has been set up incorrectly since its answers are not those of the corresponding physical problem. Of course, the question now arises as to whether it is actually impossible to formulate the question of the solution of Eq. (3) on a physical basis in such a way that physically unreasonable solutions may not occur.

In the works of Born and Green[5], and of Kirkwood and his collaborators[4,8] on the theory of liquids, a more stringent requirement is introduced in place of the normalization condition (5), namely, the requirement of volume integrability of the function $g(r) - 1$:

$$\int_0^\infty [g(r) - 1]\, r^2 dr < +\infty. \qquad (26)$$

It is readily seen that this requirement is fulfilled only if $|\alpha_1| > 0$ in (19), and, consequently, it permits the separation of the solutions corresponding to stable states from those which are physically unreasonable. However, this requirement appears too strict, and for the purpose of distinguishing the stable solutions it would suffice to require the fulfillment of a less severe condition relative to the behavior of $g(r)$ for $r \to \infty$. What is even more essential is that it is not possible to prove this condition physically without previous knowledge of the solution of Eq. (3) in the form (19). Hence it is not suitable as an initial requirement on the solutions of Eq. (3) and as one capable of replacing condition (5). The latter is connected simply with the fact that the integrability requirement (26) does not arise immediately from the Gibbs canonical distribution, and hence is evidently supplementary---the above superposition approximation---restricted, superimposed on $g(r)$. Cosidering the connection of the left part of condition (26) with the isothermal compressibility of the system, one finds

$$\frac{4\pi}{v}\int_0^\infty [g(r) - 1]\, r^2 dr = \frac{kT}{v^2\left(-\partial p / \partial v\right)_T} - 1, \qquad (27)$$

erroneously*. Relation (27) is obtained from the comparison of two well-known equations for the squares of the fluctuations in the numbers of particles in a certain volume G:

$$\overline{(\Delta N_G)^2} = \bar{N}_G \frac{kT}{v^2\left(-\partial p / \partial v\right)_T}; \qquad (28)$$

$$\overline{(\Delta N_G)^2} = \bar{N}_G\left\{1 + \frac{\bar{N}_G}{V_G^2}\int_{(G)}\int_{(G)} \{g(|q_1 - q_2|) - 1\}\, dq_1\, dq_2\right\}, \qquad (29)$$

* The incorrect exposition of this equation is tolerated also by the author of the present paper in the survey[2].

[8] J. Kirkwood, E. Mann and B. Alder, J. Chem. Phys. 18, 1040 (1950)

with the latter having been rewritten in the form

$$\overline{(\Delta N_G)^2} = \overline{N}_G \left\{ 1 + \frac{4\pi}{v} \int_0^\infty [g(r) - 1] r^2 dr \right\}. \quad (30)$$

The erroneousness of Eq. (27), accepted in many works as one of the basic equations of the theory of liquids, is evident. Equation (28) clearly does not hold in the presence of the correlation of the fluctuations in different regions (see Leontovich[6]), and the exact Eq. (29) may be replaced by the approximate Eq.(30) only if the sufficiently rapid tendency of $g(r) - 1$ to zero for $r \to \infty$ is known beforehand. [For example, for a hypothetical function $g(r)$ of form $g(r) \sim 1 + Ar^n e^{-\alpha r}$ the condition (26) will be fulfilled for any $\alpha > 0$, but equations (28) and (27) will not hold for $n > 0$ and small α]. Hence Eq. (26), which does not arise from the general laws of statistical mechanics, is unacceptable as an initial supplementary requirement on the solution of Eq. (3).

The actual solution of the question of the correct presentation of the problem for Eq. (3) lies in an altogether different direction and is connected with the validity of the transition to the limit $N, V \to \infty$, which has already been accomplished in (3). At the basis of Eq. (3) lies the admission of (1), in particular the admission that the system under consideration is such that for removal to infinity of all walls bounding its volume V and the simultaneous preservation of its average density $(N/V) = 1/v$ unchanged, we get asymptotically $F_1(q) \to 1$. It is perfectly clear that a preliminary necessary condition for this must be the finiteness of the size of the walled layer of the system, where as a consequence of surface effects it is certain that $F_1(q) \neq 1$. In the opposite case Eq. (3) is devoid of physical meaning.

5. ON THE SIZE OF THE WALLED LAYER OF THE SYSTEM

Consider a molecular system of volume V and number of particles N, bounded, for example, by plane walls. Then let N and V increase without limit, keeping unchanged the relation $(V/N) = v$ and also the position of one of the walls. We consider the latter situated in the xOy plane, and the system itself extending in the direction of the positive Oz axis. In the limit we obtain a semi-infinite system occupying the entire right half-space. We will assume the wall to be ideal, although the final results would not be altered as long as the potential of the interaction of the wall on the particles had a sufficiently rapid fall-off. Conditions (1) do not hold in the neighborhood of the wall, and it is clear from symmetry considerations that $F_1(q) \equiv F_1(z)$. One may readily satisfy oneself that in our system the partial distribution functions satisfy equations completely analogous to those of Bogoliubov[1], but in which the integration extends only over the right half-space. For example, for $F_1(z)$ we obtain

$$kT \frac{dF_1(z)}{dz} + \frac{1}{v} \int_{(z'>0)} \frac{\partial \Phi(|q - q'|)}{\partial z} F_2(q,q')\, dqq' = 0 \quad (31)$$

in which the coordinates of the point q may be set equal to $(0,0,z)$. In order to obtain from this an approximate expression for $F_1(z)$, it is necessary to express $F_2(q,q')$ in terms of $F_1(z)$. The superposition approximation, which we are following, corresponds to a relation between F_1 and F_2 of form

$$F_2(q,q') = F_1(z) F_1(z') g(|q - q'|). \quad (32)$$

Actually, if we return to relations (1) and (2), we notice that, for example, $F_3(q,q',q'')$ may be interpreted as the binary distribution function for two particles for a given (and fixed) position of the third: $F_3(q,q',q'') \equiv F_2(q,q' \mid q'')$. Analogously $g(|q-q''|)$ may be interpreted as the unitary probability density of position of one of the particles for a given and maintained position of the second: $g(|q-q''|) \equiv F_1(q \mid q'')$. [We note that there is a similar universally prevalent representation of the radial function of the distribution $g(|q|) \equiv F_1(q \mid 0)$, although according to the definition it is necessary to connect it not with F_1 but with F_2: $g(|q-q''|) \equiv F_2(q, q'')$; both points of view are equally valid]. Hence relation (2) may be written thus:

$$F_2(q, q' \mid q'') = F_1(q \mid q'') F_1(q' \mid q'') g(|q - q'|). \quad (33)$$

That which is given and fixed beforehand in our problem is the position not of the third particle, but of the wall, and (33) is physically transformed into (32). Thus, allowing (32), we remain within the framework of the superposition approximation and do not introduce new limitations on the partial distribution functions.

Inserting (32) and (31), going over again to the dimensionless unit of length, and using relation (4), we easily integrate the resulting equation and obtain

$$kT \ln F_1(z) + \frac{\lambda}{2\pi} \int_{(z'>0)} E(|q - q'|) F_1(z')\, dq' = C. \quad (34)$$

Since we are considering a homogeneous phase, we must require that $F_1(z) \to 1$ for $z \to \infty$. This determines the constant of integration

$$C = 2\lambda \int_0^\infty E(\rho)\rho^2 d\rho. \tag{35}$$

If, as above, we go over from $g(r)$ and $E(t)$ to $u(r)$ and $\bar{E}(t)$ by means of relations (6) and (7), we obtain an equation for the determination of $F_1(z)$

$$\ln F_1(z) = -2\lambda \int_0^\infty \bar{E}(\rho)\rho^2 d\rho + \frac{\lambda}{2\pi} \tag{36}$$

$$\int_{(z'>0)} \bar{E}(|q-q'|) F_1(z')\, dq'.$$

The last member may be simplified by introduction of cylindrical coordinates z', ρ, ϕ in place of the cartesian coordinates $q' = (x', y, z')$. Then

$$\int_{(z'>0)} \bar{E}(|q-q'|) F_1(z')\, dq' \tag{37}$$

$$= 2\pi \int_0^\infty \left\{ \int_0^\infty \bar{E}[\sqrt{\rho^2 + (z-z')^2}]\, \rho d\rho \right\} F_1(z')\, dz'$$

$$= 2\pi \int_0^\infty \left\{ \int_{|z-z'|}^\infty \bar{E}(|t|)\, t dt \right\} F_1(z')\, dz'$$

$$= 2\pi \int_0^\infty K(|z-z'|) F_1(z')\, dz',$$

where the kernel $K(z)$ is identical with the kernel $K(z)$ in (10). Thus we have finally

$$\ln F_1(z) = -2\lambda \int_0^\infty \bar{E}(\rho)\rho^2 d\rho \tag{38}$$

$$+ \lambda \int_0^\infty K(|z-z'|) F_1(z')\, dz'.$$

Now let $z \to \infty$. Setting

$$F_1(z) = 1 + \psi(z) \tag{39}$$

and reckoning $|\psi(z)| < 1$, we readily simplify Eq. (38) and obtain

$$\psi(z) = \lambda \int_0^\infty K(|z-z'|)\psi(z')\, dz' \quad (z \to \infty). \tag{40}$$

This equation is identical with Eq. (11); whence it follows that the function $r[g(r)-1]$ for $r \to \infty$ behaves like the function $F_1(z) - 1$ for $z \to \infty$, a result of some importance for the theory of liquids.

If, as above, we allow the intermolecular forces to have a finite radius of action σ, then, in precisely the same way as in Sec. (2), we find

$$F_1(z) = 1 + \sum_n \bar{A}_n e^{-|\alpha_n| z} \cos(\beta_n z + \bar{\delta}_n), \tag{41}$$

where $\alpha_n(\lambda)$ and $\beta_n(\lambda)$ are the same as in (19), while the numbers $\bar{A}_n$ and $\bar{\delta}_n$ remain undetermined and possibly different from the corresponding A_n and δ_n in (19). Assuming the former enumeration of the $\alpha_n(\lambda)$ according to (20) to be correct, we see at once that the magnitude $|\alpha_1(\lambda)|^{-1}$ is the effective size of the walled layer of the system, in which $F_1(z)$ is notably different from unity. The special case $\alpha_1(\lambda) = 0$ considered in (3) thus corresponds to an infinitely extended "superficial layer".

We consider it necessary to remark, in order to avoid misunderstanding, that the periodic solution $F_1(z) \sim 1 + \bar{A}_1 \cos(\beta z + \bar{\delta}_1)$ appearing in (41) for $\alpha_1(\lambda) = 0$ has no relation to the crystalline state.

6. CONCLUSION

It is not difficult now to formulate the correct requirement which must be satisfied by the behavior of the solution of Eq. (3) for $r \to \infty$. Since Eq. (3) relates only the spatial properties of a homogeneous phase and requires for its correctness the identity $F_1(q) \equiv 1$, this indicates that in the problem of a system bounded by a plane wall the preliminary condition must be $F_1(z) \to 1$ for $z \to \infty$. Since, on the other hand, it appears that the behavior of $F_1(z) - 1$ for $z \to \infty$ in the problem of a system bounded by a wall is identical with the behavior of $r[g(r) - 1]$ for $r \to \infty$ in the problem of the unbounded system, we infer that the preliminary condition required for the correctness of Eq. (3) is that

$$r[g(r) - 1] \to 0 \quad \text{for} \quad r \to \infty. \tag{42}$$

It must be emphasized that this inference is obtained merely from a single comparison of Eqs. (11) and (40) and does not require for its establishment preliminary knowledge of the solutions of (19) and (41).

It is important to note that the nonfulfillment of the first of the conditions (1) necessarily brings with it the nonfulfillment of the second. Hence we may also say that the requirement (42) is a requirement that $g(|q-q'|) = F_2(q, q')$ (exactly, apart from terms which go to zero for $N \to \infty$). Nonfulfillment of condition (42) signifies, then, that $g(|q-q'|) \neq F_2(q, q')$. although $g(r)$, as a solu-

tion of the formally stated problem concerning Eq. (3), that is, of the purely mathematical problem, may possibly exist. However, it is clear that such a solution lacks physical meaning.

Thus we may say that the correctly presented mathematical problem of finding the radial distribution function $g(r)$ for a given intermolecular potential $\Phi(r)$ and given thermodynamic parameters T and λ, adequate to its physical content, is included in the solution of the problem of the eigenvalues λ and eigenfunctions $g(r;\lambda)$ of equation (3) under the additional requirement (42). The normalization requirement (5) is automatically fulfilled at the same time.

The solutions $g(r)$ considered above which correspond to thermodynamically absolutely unstable states do not belong to eigenvalues λ of the problem formulated in the indicated manner. The spectrum of eigenvalues λ now shows itself to be generally speaking, discontinuous, consisting of several continuous bands. The connection of this situation with the theory of phase transitions is evident. We will devote more attention to it in subsequent communications.

In conclusion we wish to remark, in order to avoid misunderstanding, that the states of the system were qualified by us in all the above as stable in a limited sense, that is, such a state may in reality prove to be only metastable. Correspondingly, instability is everywhere understood absolutely.

Translated by Brother Simon Peter, F.S.C.
26

Letters to the Editor

The Theory of Multiple Production of Particles at High Energy

S. Z. Belen'kii
P. N. Lebedev Institute of Physics, Academy of Sciences, USSR
(Submitted to JETP editor, July 24, 1955)
J. Exper. Theoret. Phys. USSR 28, 111-113 (January, 1955)

EXPERIMENTAL data obtained to date allows us to assert that the "nuclear charge" is conserved in all nuclear phenomena. In the investigation of phenomena of multiple production of nucleons at high energies[1] the conservation of the "nuclear charge" has been taken into account only for the assumption that particles and antiparticles are produced in equal numbers. Actually, in the collisions of nucleons with nuclei there are several initial nucleons (not less than two). We consider here in more detail the influence of the" nuclear charge" conservation on the production of heavy particles at high energies*.

Recent theoretical research has been carried out on the multiple production of particles, based on the methods of thermodynamics and hydrodynamics [3-5]. In nucleon-nucleon or nucleon-nucleus collisions, a system is formed in which a high energy is concentrated in a very small region. Then this system expands very rapidly and when its size has become sufficiently large, it decays into separate particles. The stage of decomposition depends on the temperature kT of the system with $kT \gtrsim m_\pi c^2$, where m_π is the π-meson mass. The density of particles of different kinds is given by the equations

$$n_{NN} = \frac{g_N}{2\pi^2}\left(\frac{kT}{\hbar c}\right)^3 F^+(z, y_{NN}), \quad (1)$$

$$n_{AN} = \frac{g_N}{2\pi^2}\left(\frac{kT}{\hbar c}\right)^3 F^+(z, y_{AN}), \quad (2)$$

$$n_\pi = \frac{g_\pi}{2\pi^2}\left(\frac{kT}{\hbar c}\right)^3 F^-(z, 0). \quad (3)$$

Here n_{NN} and n_{AN} are the densities of nucleons and antinucleons, n_π is the density of π-mesons, $g_N = 4$, $g_\pi = 3$,

$$F^\pm(z, y) = z^3 \int_0^\infty \frac{x^2\, dx}{\exp\{-y + z\sqrt{1+x^2}\} \pm 1}; \quad (4)$$

$z = Mc^2/kT$ for nucleons and $z = m_\pi c^2/kT$ for π-mesons, $y = \mu/kT$ where μ is the chemical potential.

The equilibrium condition with respect to pair production and pair annihilation will be $y_{NN} + y_{AN} = 0$. Thus, if we denote y_{NN} by y, then y_{AN} will be equal to $-y$.

We shall consider the case where $z > 1$ and $y < z$. In Eq. (4) we expand the denominator in a power series of $\exp\{y - z\sqrt{1+x^2}\}$, perform the integration and limit ourselves to the first term of the expansion, We obtain

$$F^+(z, y) = F^+(z, 0)\, e^y, \quad (5)$$

$$F^+(z, -y) = F^+(z, 0)\, e^{-y}.$$

Now it is not difficult to establish the following relations

$$\sinh y = \frac{N_{\pi 0}}{N_{N_0}}\frac{N_0}{N_\pi}; \qquad \cosh y = \frac{N_{\pi 0}}{N_{N_0}}\frac{N_N}{N_\pi}.$$

Here $N_{\pi 0}$ and N_{N0} are the total number of π-mesons and of nucleons and antinucleons produced in the system with the condition that the initial nucleons are not included, N_0 is the number of initial nucleons, N_π and N_N are the total numbers of π-mesons and of nucleons and antinucleons, where the existence of the initial nucleons is taken into account. Hence we obtain

$$N_N / N_\pi = \sqrt{(N_{N_0}/N_{\pi 0})^2 + (N_0/N_\pi)^2}. \quad (6)$$

The number of nucleons N_{NN} and the number N_{AN} of antinucleons are

$$N_{NN}/N_\pi = {}^1/_2\left[\sqrt{(N_{N_0}/N_{\pi 0})^2 + (N_0/N_\pi)^2} + N_0/N_{\pi 0}\right], \quad (7)$$

$$N_{AN}/N_\pi = {}^1/_2\left[\sqrt{(N_{N_0}/N_{\pi 0})^2 + (N_0/N_\pi)^2} - N_0/N_{\pi 0}\right].$$

*Schiff[2] has indicated that it is necessary to take into account the existence of the initial nucleons in the Fermi theory of multiple production; however he himself has not done so. It will be remembered that, according to Fermi, the decay of the system into separate particles takes place at the temperature $kT > Mc^2$ where M is the nucleon mass. Therefore in the frame of the Fermi theory the influence of the initial nucleons is not essential.

[1] E. Fermi, Prog. Theor. Phys. 5, 570 (1950)
[2] L. Schiff, Phys. Rev. 85, 374 (1952)
[3] L. D. Landau, Izv. Akad. Nauk. SSSR Ser. Fiz. 17, 51 (1953)
[4] I.L. Rozental and D.S. Chernavskii, Usp. Fiz. Nauk 52, 185 (1954)
[5] I. Ia. Pomeranchuk, Doklady Akad. Nauk SSSR 78, 889 (1951)

We turn now to the energy of the nucleons and π-mesons. It is easy to see that the ratio of the total energy density E_N of the nucleons and the antinucleons to E_π, the energy density of the π-mesons is equal to:

$$E_N / E_\pi = \sqrt{1 + (N_{\pi 0} / N_{N 0})^2 (N_0 / N_\pi)^2} E_{N 0} / E_{\pi 0}, \quad (8)$$

where E_{N0} and $E_{\pi 0}$ are the energy density of the nucleons and π-mesons for $N_0 = 0$. Equation (8) gives the ratio of the energy taken away by the nucleons and the π-mesons.

Let the critical temperature T_k at which the decay of the system into separate particles takes place, be equal to $1.2_\pi mc^2$. Then, according to a previous paper [6], $E_{N0}/E_{\pi 0} = 0.3$, $N_{N0}/N_{\pi 0} = 0.13$. If we take $N_0/N_\pi = 0.15$, then $E_N/E_\pi = 0.42$. If we suppose $N_0/N_\pi = 1$, then $E_N/E_\pi = 2.3$. This means that, for $N_\pi = N_0$, the nucleons carry away about 70% of the total energy. Thus the consideration of the initial nucleons gives a larger share of energy for the nucleons. This effect is particularly large for not too high energy values, i.e. when the numbe fof π-mesons produced is small. Qualitatively, the results obtained are in agreement with the experimental data obtained by Grigorov et al.[7] for energies of the order 10^{10} to 10^{11} eV. It is necessary however to emphasize that this theory represents only a rough approximation for such energies.

Equation (8) for the energy ratio contains two parameters: the temperature T_k of decay of the system into separate particles, and the ratio N_0/N_π. Both parameters are unknown. It is possible, however, to form a quantity which does not depend on N_0/N_π and the measurement of which would permit a direct determination of the decay temperature T_k of the system. It is not difficult to see that the energy attributed to each nucleon does not depend on the chemical potential, i.e., on the number of initial nucleons. (This is correct if we use a relativistic Maxwell-Boltzmann distribution instead of a Fermi distribution.) Let us consider now the following ratio of energies: the mean energy of the nucleons divided by the mean energy of the π-mesons. We call it α with $\alpha = (E_N/E_\pi)(n_\pi/n_N)$. This quantity depends only on the decay temperature T_k. Table 1 gives the value of α computed from our previous paper [6] for different temperatures T_k.

Collisions with nuclei can also produce heavier particles (the Λ-particles), possessing nucleon charges. These particles can be included in our consideration. If we suppose that these particles, like the nucleons, have spin ½, we obtain in particular that Eqs. (6) to (8) are still valid in the presence of Λ-particles, if we understand by N_N the sum of the numbers of nucleons, antinucleons, Λ-particles and anti-Λ-particles produced for $N_0 = 0$, and so on....In Table 2 we give the ratios N_{NN}/N_π, $N_{\Lambda N}/N_\pi$, N_{AN}/N_π, $N_{A\Lambda}/N_\pi$ (where $N_{\Lambda N}$ is the number of Λ-particles and $N_{A\Lambda}$ the number of anti-Λ-particles) for different values of N_0/N_π. For this computation, g_Λ has been taken equal to 4 and M_Λ (the Λ-particle mass) equal to 2200 m_e.

Table 1

kT in units of $m_\pi c^2$	α	kT in units of $m_\pi c^2$	α
$kT \ll m_\pi c^2$	6.8	1.5	2.16
0.5	3.76	2	1.83
0.7	3.28	3	1.6
0.8	2.92	4	1.4
1	2.65	$kT \gg m_\pi c^2$	1.17*

*This last value has been computed using a Fermi distribution for the nucleons and a Bose distribution for the π-mesons.

Table 2

kT in units of $m_\pi c^2$	$\frac{N_0}{N_\pi}$	$\frac{N_{NN}}{N_\pi}$	$\frac{N_{\Lambda N}}{N_\pi}$	$\frac{N_{AN}}{N_\pi}$	$\frac{N_{A\Lambda}}{N_\pi}$
1.2	0	0.063	0.027	0.063	0.027
	0.15	0.135	0.057	0.029	0.013
	0.30	0.23	0.096	0.018	0.008

In Table 2 we see that the existence of initial nucleons modifies essentially the ratio between the numbers of Λ-particles and antinucleons produced. For instance, for $kT_k = 1.2 m_\pi c^2$ and $N_0 = 0$, the number of antinucleons produced is 2.3 times larger than the number of Λ-particles produced. But for $N_0/N = 0.15$ (which corresponds to 3 initial nucleons when 20 π-mesons are produced) the number of Λ-particles is already twice the number of antinucleons. If the spin of the Λ-particles is larger than 1/2 and particles are formed at $T > T_k$, our quantitative relations are changed, but our qualitative deductions are still valid.

Translated by L. Michel
13

[6] S. Z. Belenkii, Doklady Akad. Nauk SSSR 99, 523 (1954)

[7] N. L. Grigorov and V. S. Murzin, Izv. Akad. Nauk SSSR, Ser. Fiz. 17, 21 (1953)

Relativistic Corrections to the Two Body Problem

V. N. TSYTOVICH
Moscow State University
(Submitted to JETP editor July 21, 1954)
J. Exper. Theoret. Phys. USSR 28, 113-115
(January, 1955)

RECENTLY wide application has been made of the method of finding propagation functions in quantum electrodynamics by means of variational derivatives at the sources [1]. This method, in particular, has been used for obtaining the relativistically covariant equation of motion of electron and positron, interacting through the electromagnetic field [2*] It has been shown also [4], that the Salpeter-Bethe [3] type of equation contains corrections to the energy levels of the hydrogen atom which are not contained in equations of the Berit [5] type. In the positronium atom these corrections have special importance since in this case, as distinguished from that of hydrogen, they have the same order of magnitude as the vacuum (radiative) corrections.

In the present communication we wish to point out the principal significance of taking into account the corrections due to the relativistic character of the two bodies in the case of interaction of positronium with external fields. Before taking up this question, we consider the method of finding the energy of interaction between particles by means of the relativistic equation for bound states [2,3]. In this equation there appears the interaction operator I.

$$(F_2^+ F_1^- - iI)\,\psi = 0, \tag{1}$$

$$F_2^+ = c\mathbf{p}_2\vec{\alpha}_2 + \beta_2 M_2^+ c^2 + e\alpha_{2\mu} A_\mu \quad (2),$$

$$F_2^- = c\mathbf{p}_1\vec{\alpha}_1 + \beta_1 M_1^- c^2 - e\alpha_{1\mu} A_\mu \quad (1)$$

where M_1^- and M_2^+ are mass operators.

Let us assume that we have somehow solved Eq. (1) for instantaneous interaction, and are interested in the energy of interaction of the electron and the positron between themselves and with the external field, conditioned by the perturbation ΔI in the quantity I appearing in (1), $I = I_0 + \Delta I$. To find the matrix elements of the perturbation energy we must determine the "scattering matrix for ΔI". For this it is sufficient to expand the wave function, governed by Eq. (1) with the inclusion of ΔI, in terms of the unperturbed wave functions [governed by (1) without ΔI]. It is more convenient, however, to deal with the solutions of the equation of type (1) since the expansion of the Green's function G of Eq. (1) in terms of the unperturbed G_0 has an extremely simple appearance:

$$G = G_0 + G_0\, i\Delta I G_0 + G_0\, i\Delta I G_0\, i\Delta I G_0 + \ldots \tag{2}$$

The relativistically covariant equation (1) contains different times for the particles, t_1 and t_2, so that if the external field is stationary we may go over to relative time $t = t_2 - t_1$ and common time $T = (t_1 + t_2)/2$. The scattering matrix, describing the scattering of bound systems from $T = -\infty$ to $T = +\infty$ during adiabatically isolated interaction ΔI, equals

$$S_{-\infty,\,+\infty} = G\,(T = +\infty,\ T = -\infty).$$

With the aid of $S_{-\infty,\,+\infty}$ we can find the transition amplitude from state n to state n', induced by the perturbation ΔI. We will regard as the effective perturbation energy V that energy in the equation for instantaneous interaction

$$(E - H_1 - H_2 - V)\,\varphi = -(\Lambda_+^{(1)} - \Lambda_-^{(2)})\,K(\mathbf{r})\,\varphi \tag{3}$$

(where $\phi = \psi|_{t=0}$, H_1 and H_2 are Hamiltonians for the free electron and positron, $K(\mathbf{r})$ is the potential of the instantaneous interaction, Λ_+ and Λ_- are projection operators), which leads to the same values of the scattering amplitudes as are obtained from $S_{-\infty,\,+\infty}$. In the first approximation of perturbation theory, as can be shown, the matrix elements of the effective perturbation energy have the form

$$V_{nn'} = \frac{1}{\hbar}\int \tilde{\psi}_{n'}(\mathbf{x}_1\mathbf{x}_2 t)\,\Delta I \psi_n(\mathbf{x}_1\mathbf{x}_2 t)\,d^3x_1\,d^3x_2\,dt, \tag{4}$$

where

$$\psi_n = \theta_n(t)\,\varphi_n;\quad \tilde{\psi} = \theta_n(-t)\,\varphi_n^+;\quad \varphi_n = \psi_n|_{t=0}. \tag{5}$$

Integration with respect to the relative time in (4) is easily performed with the aid of operator $\theta_n(t)$ describing the causal development in relative time. Its properties will be considered in a separate communication.

The energy of interaction between electron and positron which we have found by means of (4) exactly coincides with the energy found by Landau and Berestetskii [6] in the particular case of the absence of external field and with limitation to terms of order α^2.

Let us consider now the interaction of the positronium atom with the external electromagnetic field. We consider the case of weak fields when

the interaction with the external field can be treated as a perturbation. We regard the external fields as constants, i. e., we regard the potentials as linear functions of the coordinates. If only terms that are linear in the field are retained, then the operator for interaction with the external field ΔI_{ex} has the form

$$i\Delta I_{ex} = -e\alpha_{1\mu} A_\mu(1)\left(-\frac{\hbar}{2i}\frac{\partial}{\partial T}+\frac{\hbar}{i}\frac{\partial}{\partial t}-H_2\right) \quad (6)$$
$$+ e\alpha_{2\mu} A_\mu(2)\left(-\frac{\hbar}{2i}\frac{\partial}{\partial T}-\frac{\hbar}{i}\frac{\partial}{\partial t}-H_1\right).$$

The energy of interaction with the external field found by means of (6) in the first approximation exactly coincides with the energy found by us by the usual method in the first approximation of perturbation theory. It is important, however, to emphasize that by means of (6) corrections are obtained to this energy, connected with the relativistic two body problem and its influence on the interaction of positronium with external fields. For $n = 1$ they have the magnitude

$$(V_{ex}^{rel})_{ss'} = -\mu_0 \frac{\alpha^2}{12} <\sigma_{1z} - \sigma_{2z}>_{ss'} H_z, \quad (7)$$

where s characterizes the spin states σ_{1z} and σ_{2z} are Pauli matrices, $\alpha = e^2/\hbar c, \mu_0 = e\hbar/2mc$, H_z is the intensity of the magnetic field. This energy produces additional mixing of ortho and para states in positronium.

Since the operator for relative energy enters into operator (6), interest exists in the question to what degree the corrections which have been found are related to the operator $(\hbar/i)(\partial/\partial t)$ and, consequently, with the different times of the particles. If the energy of interaction associated with the part of operator (6) containing $(\hbar/i)(\partial/\partial t)$ is found separately, then exactly (7) is obtained.

The corrections found in this manner are of principal interest, since they are all related to the different times of the particles.

I wish to express my gratitude to Prof. A. A. Sokolov, M. M. Mirianashvili and Prof. D. D. Ivanenko for discussion of the question touched upon here.

Translated by B. Leaf
14

[1] J. Schwinger, Proc. Nat. Acad. Sci. 37, 452, 455, (1951)

[2] R. Karplus and A. Klein, Phys. Rev. 87, 848 (1952)

[3] E. Salpeter and H. Bethe, Phys. Rev. 84, 1232(1951); A. D. Galamin, J. Exper. Theoret. Phys. USSR 23, 488 (1952)

[4] E. Salpeter, Phys. Rev. 34, 533 (1929)

[5] G. Breit, Phys. Rev. 87, 328, (1952)

[6] V. B. Berestetskii and L. D. Landau, J. Exper. Theoret. Phys. 19, 673 (1949)

*The difference between this equation and the Salpeter-Bethe equation [3] is connected with calculation of the specific exchange interaction between electron and positron determined by their virtual annihilation.

Investigation of the Anisotropy of the Surface Resistance of Tin at Low Temperature

M. S. KHAIKIN
Institute for Physical Problems, Academy of Sciences USSR

(Received by JETP editor, July 2, 1954)
J. Exper. Theoret. Phys. USSR 28, 115-117
(January 1955)

RESULTS of investigations of the anisotropy of the surface resistance of tin at helium temperatures in normal and superconducting states are reported in the papers of Pippard [1-3]. In these studies the properties of the coaxial resonator (at a frequency of approximately 9400 mcs/sec) were experimentally investigated; the specimen under investigation serves as the internal conductor-cylindrical monocrystalline tin, 14 mm in length and 0.25 to approximately 1 mm in diameter, having a different angle of inclination of the major crystalline axis relative to the axis of the specimen. The dependence, arrived at in reference 1, of the active surface conductivity (at normal state) on the angle θ is shown in Figure 1 (solid curve; vertical dashes--Experimental points). A similar dependence of the reactive surface conductivity on the angle θ as well as the penetration depth of the electromagnetic field calculated from it is arrived at in reference 1. These experiments led Pippard to a conclusion as to the non-tensorial character of the anisotropic effects noted.

The principal significance of the above mentioned work is the necessity for careful and detailed consideration of these investigations as to the methods employed. As a first step it may be of interest to determine the experimental results one should expect if we assign a normal tensorial character to the anisotropy of surface conductivity of tin at helium temperatures. This article deals with this important question.

In the coaxial resonator the electrical oscillations may be produced along the axis (usual electromagnetic wave) as well as in the perpendicular direction. Keeping in mind the fundamental frequencies associated with these two types of resonance one

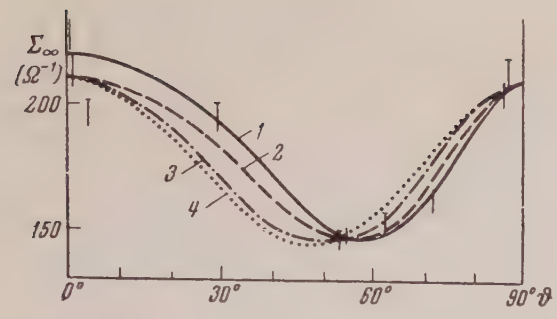

Dependence of active surface conductivity of the samples on the angle θ. 1- As found in reference 1 the vertical dashes indicate experimental points; 2-$f(\theta; 2)$; 3-$f(\theta; 1.4)$; 4-$f(\theta; 1.14)$. The measured curves disclose the high order of their correspondence with the values obtained from the curves of reference 1.

is led to consider the oscillation of a system with two degrees of freedom. In this case, the partial frequency of the transverse oscillation is one to two orders higher than that of the longitudinal oscillation (according to their real geometric dimensions). If the resonator is constructed from an isotropic conductor, then there is no relation between the transverse and longitudinal partial resonant frequencies, and they can be excited independently. If, on the other hand, the internal conductor of the resonator is anisotropic ($\theta \neq 0°$, $\theta \neq 90°$) then the separate resonances are related and the resonator may be excited as a coherent system.

Let us examine the mechanism connecting the longitudinal and the transverse resonances of the coaxial resonator, allowing the longitudinal external electrical field to excite the low frequency resonance of the system. As a consequence of the anisotropic conductivity of the internal conductor of the resonator, the electric field will induce displacement current at an angle to the axis of the resonator with a component of the displacement current perpendicular to the axis of the resonator (with sustained state of oscillation of the system, the current and the electrical excitation field will not be parallel to each other and to the axis of the resonator). Such forms of normal tensorial anisotropy lead to a relationship between the longitudinal and transverse resonances. There is no anisotropy evident and a relation between the resonances does not exist when $\theta = 0$; $\theta = 90°$, for all intermediate orientations of the crystalline axis a correlation exists, passing through a maximum as θ varies from 0° to 90°, and together with it the band width (damping) of the low frequency response passes through a maximum and its own frequency passes through a minimum at that same point.

This qualitative conclusion agrees fully with observations of Pippard[1] as shown in the diagram. The active conductivity of the sample was calculated as inversely proportional in magnitude to the band width of the resonator which, as is evident from the diagram, is maximum for the resonator with a sample having $\theta \approx 55°$.

A qualitative estimate of the effect of these relations on the properties observed in low frequency resonance may be quite simply carried out with respect to the dependence between the coupling and θ. The coupling increases the band width of the resonance (i.e. the longitudinal resonance) due to additional losses caused by the transverse component of the displacement current; these losses are proportional to the square of the average transverse current along the periphery of the sample. This transverse component is the current which would have appeared on an infinite plane surface of the same metal (with the same orientation of the crystal axis relative to the field, it is possible to consider the element in the lateral surface of the sample). Dependence of this component of the current upon θ can be easily found, if we know the anisotropy $\sigma_\parallel / \sigma_\perp$ of the conductivity of the metal. In this manner, the function $f(\theta, \sigma_\parallel/\sigma_\perp)$ is determined as proportional to the losses occuring at low frequencies (longitudinal resonance in connection with the transverse resonance). The agreement between the forms of the function (f) with the dependence of $\Sigma(\theta)$ in reference 1 (see diagram) is quite obvious.

The effect on the longitudinal resonance due to the coupling with transverse resonance may be considered as a complex resistance which has been introduced as proportional to the resistance of the resonator to the transverse current, i.e. is proportional to the surface resistance of the sample. Therefore, it is evident that the active and reactive resistances introduced are in the same ratio as the active and reactive resistances of the resonator to the longitudinal currents, which means that the relative effect of the coupling on the value observed for the reactive resistance of the sample (calculated from the displacement of the natural frequency of the resonator) must be same as that for the value of the active resistance. This conclusion is also in good agreement with the results presented by Pippard[1]

Therefore, it appears possible that the conclu - sion concerning the non-tensorial nature of the

anisotropy of the surface conductivity of metal at low temperatures and the non-tensorial anisotropy of the penetration depth of the electromagnetic field in superconductor, as arrived at in references 1-3, does not have sufficient experimental basis. The phenomena observed can be explained, at least qualitatively, on the basis of the above mentioned concept concerning the bond between the two fundamental oscillations of the coaxial resonator, with the aid of the usual tensorial anisotropic conductivity.

In any case, it should be most evident that there is a need for further and extensive investigations as to the anisotropy of surface conductivity at low temperatures before final conclusions as to its character can be formulated.

Translated by A. Andrews
15

[1] A. B. Pippard, Proc. Roy. Soc. A **203**, 98 (1950)
[2] A. B. Pippard, Proc. Roy. Soc. A **203**, 195 (1950)
[3] A. B. Pippard, Proc. Roy. Soc. A **203**, 210 (1950)
[4] T. E. Faber, Proc. Roy. Soc. A **219**, 75 (1953)

The Problem of the Invalidity of One Statistical Treatment of Quantum Mechanics

G. P. DISHKANT
Dnepropetrovsk State University
(Submitted to JETP editor March 9, 1954)
J. Exper. Theoret. Phys. USSR 28, 117
(January, 1955)

WIGNER and Szilard [1] have proposed a probability distribution in phase space of a quantum particle

$$F(q;p)=\frac{1}{2\pi}\int\psi^*\left(q-\frac{h\tau}{2}\right)e^{-i\tau p}\psi\left(q+\frac{h\tau}{2}\right)d\tau, \qquad (1)$$

satisfying the time-dependent equation

$$\frac{\partial F}{\partial t}+\frac{p}{m}\frac{\partial F}{\partial q}=\frac{i}{4\pi^2 h}\int\left[V\left(q-\frac{h\tau}{2}\right)\right. \qquad (2)$$

$$\left.-V\left(q+\frac{h\tau}{2}\right)\right]F(q;\eta)\,e^{i\tau(\eta-p)}d\eta d\tau.$$

Here q, p, m are coordinate, momentum and mass of of the particle; $V(q)$, its potential energy; h, Plank's constant; t, the time.

In an extension of this work [2] an interpretation of Eq. (2) has been given as the equation of a certain stochastic process of change of coordinate and momentum of a particle, i. e., a statistical treatment of quantum mechanics. For the validity of such a treatment it is necessary, in the first place, that $F(q;p)$, non-negative at a given moment of time, should remain non-negative at all later moments, proof of which was given by Bartlett (see Moyal [2]). However, in a recent work [3] it was correctly shown that F in general does not preserve its sign with the passage of time. From this follows the conclusion of the invalidity of the quantum mechanical treatment given by Moyal.

It is necessary only to point out Bartlett's error. Bartlett supposed that a quantum system possesses a cyclic coordinate θ (it is obvious that it is always possible formally to incorporate into a given system an additional cyclic degree of freedom). He takes the general solution of the time-dependent equation for such a system in the form

$$F(q,\theta;p,g)=\sum_{\mu}e^{i\mu(t+\theta/\omega)}F_{\mu}(q;p,g), \qquad (3)$$

where g and ω are the cyclic momentum and frequency; and F_μ, certain constant functions.

It is clear that if $F>0$ at a certain t and arbitrary θ, it will still be >0 at an arbitrary time. The error lies in the fact that the general solution of the time-dependent equation is

$$F(q,\theta;p,g)=\sum_{\mu_1\mu_2}e^{i\mu_1 t+i\mu_2\theta}F_{\mu_1\mu_2}(q;p,g). \qquad (4)$$

Therefore Bartlett's discussion necessarily applies only to a narrow class of solutions which actually preserve sign.

Translated by B. Leaf
16

[1] E. Wigner, Phys. Rev. **40**, 749 (1932)
[2] J. Moyal, Proc. Cambr. Phil. Soc. **45**, 99 (1949)
[3] T. Takabayasi, Prog. Theor. Phys. **10**, 121 (1953)

The Fermi Theory of Multiple Particle Production in Nucleon Encounters

I. L. ROZENTAL'
P. N. Lebedev Physical Institute, Academy of Sciences, USSR
(Submitted to JETP editor, Sept. 7, 1954)
J. Exper. Theoret. Phys. USSR **28**, 118-120
(January, 1955)

IN calculating the statistical weights of various states, Fermi [1] applied the law of conservation of energy in exact form, but the law of conservation of momentum only in approximate form. The purpose of the present work is the exact application of the law of conservation of momentum for two limiting cases: the non-relativistic limit

and the relativistic limit.

The statistical weight S_n of a state for n particles with zero spin is given by the expression

$$S_n = \left(\frac{V}{8\pi^3\hbar^3}\right)^n \frac{dQ_n(E_0)}{dE_0}, \qquad (1)$$

where V is the spatial volume and Q the volume in momentum space*. Our problem then reduces to the calculation of

$$dQ_n \; dE_0 = W_n(E_0).$$

We first calculate $W_n(E_0, P_0)$, taking into account that the total momentum P_0 of the system is different from zero. In the non-relativistic case we can write

$$W_n(E_0, P_0) = \underbrace{\int_{-\infty}^{\infty} \cdots \int_{-\infty}^{\infty}}_{3n} \delta\left(T - \frac{1}{2\mu}\sum_{i=1}^{n} p_r^2\right) \qquad (2)$$

$$\times \; \delta\left(P_{0x} - \sum_{r=1}^{n} p_{xr}\right) \times \delta\left(P_{0y} - \sum_{r=1}^{n} p_{yr}\right)$$

$$\times \delta\left(P_{0z} - \sum_{r=1}^{n} p_{zr}\right) \prod_{r=1}^{n} dp_{xr}\, dp_{yr}\, dp_{zr},$$

where T is the total kinetic energy of the system.

Making use of the integral representation of the δ function, we write Eq. (2) in the form

$$W_n(E_0, P_0) = \frac{1}{(2\pi)^4}\int_{-\infty}^{\infty} \exp\{-i\tau_1\}\, d\tau_1 \qquad (3)$$

$$\times \int_{-\infty}^{\infty} \exp\{-iP_{0x}\tau_2\}\, d\tau_2 \times \int_{-\infty}^{\infty} \exp\{-iP_{0y}\tau_3\}\, d\tau_3$$

$$\times \int_{-\infty}^{\infty} \exp\{-iP_{0z}\tau_4\}\, d\tau_4 \times \left[\iiint_{-\infty}^{\infty} \exp\left\{i\left[\frac{\tau_1 p^2}{2\mu} + \tau_2 p_x + \tau_2 p_y + \tau_2 p_z\right]\right\} dp_x\, dp_y\, dp_z\right]^n.$$

We evaluate the integral

$$I_1 = \iiint_{-\infty}^{\infty} \exp\left\{i\left[\frac{\tau_1 p^2}{2\mu} + \tau_2 p_x + \tau_3 p_y + \tau_4 p_z\right]\right\} \times dp_x dp_y dp_z.$$

Beginning with spherical coordinates and integrating over the angular variables, we obtain

$$I_1 = -\frac{2\pi i}{\tau}\int_{-\infty}^{\infty} x \exp\{i[\tau x + \alpha x^2]\}\, dx \qquad (4)$$

$$= \frac{\pi^{3/2}}{\sqrt{2}} \frac{i(1+i)\exp\{-i\tau^2/4\alpha\}}{\alpha^{3/2}};$$

$$\tau = \sqrt{\tau_2^2 + \tau_3^2 + \tau_4^2}, \qquad \alpha = \tau_1/2\mu.$$

We substitute Eq. (4) in (3) and again integrate over the angular variables in spherical coordinates:

$$W_n(E_0, P_0) = -\frac{(2\pi\mu)^{3/2} n}{(2\pi)^3}\left[\frac{i(1+i)}{\alpha^{1/2}}\right]^n \frac{i}{P_0} \qquad (5)$$

$$\times \int \frac{\exp\{-iT\tau_1\}}{\tau_1^{3/2 n}}\, d\tau_1$$

$$\times \int_{-\infty}^{\infty} \tau \exp\left\{-i\left[\frac{n\mu\tau^2}{2\tau_1} - \tau P_0\right]\right\} d\tau$$

$$= \frac{(2\pi\mu)^{3/2}(n-1)}{n^{3/2}[3/2(n-1)-1]!}\left(T - \frac{P_0^2}{2n\mu}\right)^{[3/2(n-1)-1]}$$

This equation can easily be generalized to the case in which the particles possess different masses $\mu_1, \ldots, \mu_n$:

$$W_n(E_0, P_0) = \frac{(2\pi)^{3/2}(n-1)}{[3/2(n-1)-1]!} \qquad (6)$$

$$\times \left(\frac{\mu_1\mu_2 \cdots \mu_n}{\mu_1 + \cdots + \mu_n}\right)^{3/2}$$

$$\times \left[T - \frac{P_0^2}{2(\mu_1 + \cdots + \mu_n)}\right]^{[3/2(n-1)-1]}$$

Further, we compute the function $W_n(E_0, P_0)$ for the relativistic limit. By analogy to (3) we can write

$$W_n(E_0, P_0) = \frac{1}{(2\pi)^4}\int_{-\infty}^{\infty} \exp\{-iE_0\tau_1\}\, d\tau_1 \qquad (7)$$

$$\times \int_{-\infty}^{\infty} \exp\{-iP_{0x}\tau_2\}\, d\tau_2$$

$$\times \int_{-\infty}^{\infty} \exp\{-iP_{0y}\tau_3\}\, d\tau_3 \int_{-\infty}^{\infty} \exp\{-P_{0z}\tau_4\}$$

$$\times d\tau_4 \left[\iiint_{-\infty}^{\infty} \exp\{i[\tau_1\sqrt{p_x^2 + p_y^2 + p_z^2}\right.$$

$$+\tau_2 p_x + \tau_3 p_y + \tau_4 p_z]\}\, dp_x dp_y dp_z\Big]^n.$$

We now evaluate I_2, the integral contained in square brackets:

$$I_2 = -\frac{2\pi i}{\tau}\int_{-\infty}^{\infty} x \exp\{i[\tau x + \tau_1 |x|]\}\, dx \qquad (8)$$

$$= -\frac{2\pi i}{\tau}\Big[\int_0^{\infty} x[\exp\{i(\tau_1+\tau)x\} - \exp\{i(\tau_1-\tau)x\}]\, dx\Big]$$

$$= -\frac{2\pi^2}{\tau}[\delta'_+(\tau_1+\tau) - \delta'_+(\tau_1-\tau)],$$

δ'_+ is the derivative of the δ_+ function. Finally,

$$I_2 = -8\pi i\tau_1/(\tau^2 - \tau_1^2). \qquad (9)$$

After substituting in Eq. (7) and integration over the angle variables, we get

$$W_n(E_0, P_0) = \frac{(-8\pi i)^n}{i(2\pi)^3 P_0}\int \exp\{-iE_0\tau_1\}\,\tau_1^n \qquad (10)$$

$$\times\, d\tau_1 \int \frac{x \exp\{-iP_{0x}\}}{(\tau_1^2 - x^2)^{2n}}\, dx.$$

We introduce the new variables $y = \tau_1 + x$, $z = \tau_1 - x$ and carry out the calculation at the point $y = x = 0$, obtaining the following after some simple transformations:

$$W_n(E_0, P_0) = \frac{\pi^{n-1}}{2^{n-2}}\frac{(E_0^2 - P_0^2)^{n-2}}{P_0} \qquad (11)$$

$$\times \sum_{r=0}^{n} C_n^r \frac{(E_0 - P_0)^r (E_0 + P_0)^{n-r}}{(n+r-2)!\,(2n-r-2)!}$$

$$\times\left[\frac{E_0 + P_0}{2n - r - 1} - \frac{E_0 - P_0}{n + r - 1}\right].$$

We now consider some applications of the formulas just developed. Frequently the phenomena which accompany particle collisions are studied in the center of mass coordinate system. In this case we must set $P_0 = 0$. Then we have

$$W_n(E_0, 0) = \frac{(2\mu\pi)^{3/2(n-1)}}{n^{3/2}[3/2(n-1)-1]!}\, T^{[3/2(n-1)-1]} \qquad (12)$$

in the limiting non-relativistic case, while in the limiting relativistic case we have

$$W_n(E_0, 0) = \left(\frac{\pi}{2}\right)^{n-1} E_0^{3n-4} \qquad (13)$$

$$\times \sum_{r=0}^{(n-1)/2} \frac{C_n^r [3n - 2 - (n-2r)^2]}{(n+r-1)!\,(2n-2-1)!} \qquad (n \text{ odd})$$

or $$W_n(E_0, 0) = \left(\frac{\pi}{2}\right)^{n-1} E_0^{3n-4}$$

$$\times \left\{ \sum_{r=0}^{(n/2)-1} \frac{C_n^r [3n - 2 - (n-2r)^2]}{(n+r-1)!\,(2n-r-1)!} + \frac{C_n^{n/2}}{(3/2\, n-1)!\,(3/2\, n-2)!}\right\} \qquad (n \text{ even})$$

An important characteristic of the collision is the probability $w_n(E_0, p)$ that one particular particle, created in a collision in which n particles are formed with a total energy E_0, has a momentum in the range p, $p + dp$. If we limit ourselves to statistical factors alone, then, omitting the multiplying factor $(V/8\pi^2\hbar^3)^n$, we can write the probability in the form

$$w_n(E_0, p)\, dp = 4\pi p^2 w_{n-1}\left[\left(T - \frac{p^2}{2\mu}\right), p\right] dp \qquad (14)$$

(non-relativistic case) and

$$w_n(E_0, p)\, dp = 4\pi p^2 w_{n-1}[(E_0 - p), p]\, dp \qquad (14')$$

(relativistic case).

Making use of Eqs. (5) and (11) we obtain

$$w_n(E_0, p) = \frac{4\pi(2\pi\mu)^{3/2(n-2)} p^2}{(n-1)^{3/2}[3/2(n-2)-1]!} \qquad (15)$$

$$\times \left[T - \frac{np^2}{2(n-1)\mu}\right]^{[3/2(n-2)-1]} dp$$

(non-relativistic case).

If the particles have different masses,

$$w_n(E_0, p) = \frac{4\pi(2\pi)^{3/2(n-2)} p^2}{[3/2(n-2)-1]!}\left(\frac{\mu_1 \ldots \mu_{n-1}}{\mu_1 + \ldots + \mu_{n-1}}\right)^{3/2} \qquad (16)$$

$$\times \left\{T - \frac{p^2}{2}\left[\frac{\mu_1 + \ldots + \mu_n}{\mu_n(\mu_1 + \ldots + \mu_{n-1})}\right]\right\} dp.$$

Finally,

$$w_n(E_0, p)\,dp = 2\pi\left(\frac{\pi}{2}\right)^{n-2}[E_0(E_0-2p)^{n-3}p \quad (17)$$

$$\times\sum_{r=0}^{n-1}\frac{C_{n-1}^{r}E_0^{n-r-1}(E_0-2p)^r}{(n+r-3)!\,(2n-r-4)!}$$

$$\times\left[\frac{E_0}{2n-r-3}-\frac{E_0-2p}{n+r-2}\right]dp$$

(relativistic case)

It should be observed that after the completion of the present work, the paper of Lepore and Stuart[2] appeared in which similar problems were investigated.

Translated by R. T. Beyer
17

[1] E. Fermi, Prog. Theor. Phys. 5, 570 (1950)

[2] J. V. Lepore and R. N. Stuart, Phys. Rev. 94, 1724 (1954)

* If the particles are identical, then the right side of Eq. (1) reduces to $n!$

The Fermi Distribution at Absolute Zero, Taking into Account the Interaction of Electrons with Zero Point Vibrations of the Lattice

V. L. Bonch-Bruevich
Moscow Electrotechnical Institute of Communication

(Submitted to JETP editor October 6, 1954)
J. Exper. Theoret. Phys. USSR 28, 121-122
(January, 1955)

THE method of Green's function developed in connection with problems of relativistic quantum field theory[1] can also be used in a number of other problems. In particular, the investigation of the distribution function for an electron gas which takes into account the interaction of the electrons with phonons is of considerable interest.

The Green's function is

$$G_{ss'}(x,y) = \frac{i}{\langle S\rangle_0}\langle T\{\psi_s(x)\,\psi^*_{s'}(y)\,S\}\rangle_0. \quad (1)$$

Here S denotes the S matrix, $x = \{x, x_0\}$, s, s' are spin indices, $\psi_s(x)$ is the wave function of the electronic field in the representation of the interaction. The Green's function (1), being decomposed into an arbitrary complete set of functions $\phi_\lambda(x)$ $\phi^*_\lambda(y)$ characterizes the electron distribution for $x_0 < y_0$, and the hole distribution for $x_0 > y_0$, in the terms of the parameter λ.

The S matrix is given by the usual expression

$$S = T\exp\left\{i\int L(x)\,dx\right\}, \quad (2)$$

where L is the Lagrangian of the interaction (in a system of units in which $\hbar = c = 1$, c = speed of sound). For a system of electrons interacting with acoustic vibrations [2],

$$L = \{g\psi^*_s(x)\,\psi_s(x) + \rho(x)\}\,\varphi(x);\ \varphi = \partial A(x)/\partial x_0, \quad (3)$$

where g is a coupling constant and $\rho(x)$ is the "external charge density",

$$A(x) = \frac{1}{V 2\pi^3}\int\frac{df}{|f|}[b_f\exp\{ifx - i|f|x_0\} \quad (4)$$

$$+ b^*_f\exp\{-ifx + i|f|x_0\}],$$

b^*_f, b_f are the Bose operators of "creation" and "annihilation" of phonons.

Integration over f is confined to the Debye limiting value of f_0. The equation for the Green's function can easily be found (for example, by the method given by Anderson[3]). It has the form

$$G_{s_1s_2}(x,y) = iK_{s_1s_2}(x,y) \quad (5)$$

$$-ig\int dz K_{s_1s'}(x,z)\,G_{s's_2}(z,y)\,a(z)$$

$$-\int dz\,dx' K_{s_1s'}(x,z)\,\Delta E_{s's''}(z,x')\,G_{s''s_2}(x',y).$$

Here the summation is carried out over the iterated spin indices;

$$a(z) = i\int F(z,z')\,\rho(z')\,dz'. \quad (6)$$

The functions $K_{ss'}(x,y)$ and $F(x,y)$ are the propagation functions of the "free" electron and phonon fields; E is the analog of the mass operator

$$\Delta E_{s's''}(z,x') \quad (7)$$

$$= -ig\int dz'\,dx''\,\frac{\delta a(z')}{\delta\rho(z)}F(z',z)\,G_{s's''}(z,x'')$$

$$\times[\delta G^{-1}_{s''s''}(x'',x')/\delta a(z')].$$

We have for the functions $K_{ss'}$ and F (under the condition of complete degeneracy of the electron gas)

$$K_{s_1s_2}(x,y) = \langle T\{\psi_{s_1}(x)\,\psi^*_{s_2}(y)\}\rangle_0 \quad (8)$$

$$= \delta_{s_1s_2}\frac{i}{(2\pi)^4}\int dp\int_L dp_0\,\frac{\exp\{i(\mathbf{p},\mathbf{x}-\mathbf{y}) - ip_0(x_0-y_0)\}}{p_0-(p^2/2m)}$$

$$\equiv \delta_{s_1s_2}K(x-y).$$

$$F(x,y) = \langle T\{\varphi(x)\,\varphi(y)\}\rangle_0 \qquad (9)$$
$$= \frac{1}{2\pi^3}\int d\mathbf{f}\,|\mathbf{f}|\exp\{i(\mathbf{f},\mathbf{x}-\mathbf{y}) - i|\mathbf{f}|\cdot|x_0-y_0|\}$$

(The curve L runs from $-\infty$ below the real axis, intersects it at the point $p_0 = E_\Phi$ and goes above the axis to $+\infty$; $E_\Phi = p_\Phi^2/2m$ is the Fermi energy).

In the theory of weak coupling it is customary to carry out an expansion in powers of the constant g. It is essential, however, that one decompose not the Green's function itself (this, generally speaking, is not admissible,) but the equation for it, i.e., the matrix ΔE. Expanding $\Delta E = \Delta E^{(0)} + g\Delta E^{(1)} + g^2\Delta E^{(2)} + \ldots$, we obtain

$$\Delta E^{(0)} = \Delta E^{(1)} = 0;\ \Delta E^{(2)}_{s's''} \qquad (10)$$
$$= -iF(x',z)\,K_{s's''}(z,x').$$

Equation (5) can easily be determined from this expression:

$$G_{s's''}(x,y) = \delta_{s's''}\frac{-1}{(2\pi)^4}\int d\mathbf{p} \qquad (11)$$
$$\cdot\int_L dp_0\,\frac{\exp\{i(\mathbf{p},\mathbf{x}-\mathbf{y}) - ip_0(x_0-y_0)\}}{p_0 - (p^2/2m) + ig^2 f(\mathbf{p},p_0)},$$

where

$$f(\mathbf{p},p_0) = \int K(x)\,F(-x)\exp\{i\,\mathbf{px} - ip_0x_0\}\,dx \qquad (12)$$

(we note that f is a purely imaginary function).

The energy spectrum of the electron which interacts with the zero point vibrations of the lattice is given by the expression

$$W(\mathbf{p}) = \frac{p^2}{2m} - ig^2 f(\mathbf{p},p_0^*), \qquad (13)$$

where p_0^* is the root of the equation

$$p_0 - \frac{p^2}{2m} + ig^2 f(\mathbf{p},p_0) = 0.$$

Computing the integral of (12) and integrating over p_0 in (13) (for $x_0 > y_0$) we obtain the energy spectrum and the hole distribution function in terms of the momentum $\Phi(p)$. Denoting by p_Φ the limiting momentum, we get the approximation below, with accuracy to small quantities of order m/p_Φ:

$$\Phi(\mathbf{p}) = 0,\ p < p_c, \qquad (14)$$
$$\Phi(\mathbf{p}) = \left[1 + \frac{2g^2m^2}{\pi^2}\left\{\ln\left(1+\frac{f_0^4}{4p^4}\right)\right.\right.$$
$$\left. + 2\left[\arctan\left(1+\frac{f_0}{p}\right) + \arctan\left(1-\frac{f_0}{p}\right) - \frac{\pi}{2}\right]\right.$$
$$\left.\left. + \frac{4}{3}\frac{(4p^2-f_0^2)\,f_0^2}{4p^4+f_0^4}\right\}\right]^{-1}, \qquad (15)$$

where

$$p_c = p_\Phi\left\{1 + \frac{2g^2m^2}{\pi^2}\left[\frac{2}{3}\frac{f_0^2}{p_\Phi^2}\right.\right. \qquad (16)$$
$$+ \frac{f_0^3}{3p_\Phi^3}\ln\frac{f_0^2+2f_0p_\Phi+2p_\Phi^2}{f_0^2-2f_0p_\Phi+2p_\Phi^2}$$
$$+ \frac{4}{3}\ln\left(1+\frac{f_0^4}{4p_\Phi^4}\right) + \frac{8}{3}\left(\operatorname{arctg}\left(1+\frac{f_0}{p_\Phi}\right)\right.$$
$$\left.\left.\left. + \operatorname{arctg}\left(1-\frac{f_0}{p_\Phi}\right) - \frac{\pi}{2}\right)\right]\right\}.$$

$$W(p) = \frac{p^2}{2m} - g^2\frac{m}{\pi^2 p}\left\{\frac{2}{3}pf_0^2\right. \qquad (17)$$
$$+ \frac{f_0^3}{3}\ln\frac{f_0^2+2f_0p+2p^2}{f_0^2-2f_0p+2p^2} + \frac{4}{3}p^3\ln\left(1+\frac{f_0^4}{4p^4}\right)$$
$$\left. + \frac{8}{3}p^3\left[\operatorname{arctg}\left(1+\frac{f_0}{p}\right) + \operatorname{arctg}\left(1-\frac{f_0}{p}\right) - \frac{\pi}{2}\right]\right\}.$$

These formulas are applicable for $m \ll p < E_\Phi + \frac{1}{2}m$ (i.e., in particular, close to the Fermi surface $p = p_\Phi$). Thus, because of the interaction with phonons, the Fermi distribution at absolute zero is somewhat broken up. Suitable calculations, associated with the application of the Green's function to the determination of distribution functions will be published in a separate paper.

Deep gratitude is expressed to N. N. Bogoliubov for discussion of the results and for his valuable advice.

Translated by R. T. Beyer
18

[1] J. Schwinger, Proc. Nat. Acad. Sci. **37**, 452 (1951)
[2] A. Salam, Prog. Theor. Phys. **9**, 550 (1953)
[3] J. Anderson, Phys. Rev. **94**, 703 (1954)

On the Paper of V. I. Karpman, "The Problem of the Connection Between the Method of Regularization and the Theory of Particles with Arbitrary Spin" [1]

IU. A. IAPPA
Leningrad State University

(Submitted to JETP editor January 23, 1954)
J. Exper. Theoret. Phys. USSR 28, 123-124
(January, 1955)

THE work of Karpman referred to in the title is devoted to a criticism of our note "The connection between the theory of regularization and the theory of particles with arbitrary spin" [2]. Karpman stated in his work that our results are in error. This letter is written to show that this statement of Karpman's is fundamentally the result of a misunderstanding. It was shown in reference 2 that the invariant δ - function introduced into the determination of the transformation relation of the second quantization for the fields described by the relativistically invariant equations in the case of finite size, satisfies a number of conditions, for each part of which there are conditions of regularization introduced by Pauli and Villers. This fact, the establishment of which is the basic result of the note [2], was not disproved, but rather confirmed in Karpman's comment. It may be presumed that this circumstance has a well-known physical interest in that the theory of particles having a mass spectrum represents, up to now, the only case in the theory of quantized fields, for which it has been shown that the "regularization" condition is obtained as a consequence of a certain conception of the properties of particles (the consequence of the idea that particles have a mass spectrum). In this sense the condition of regularization is obtained here more naturally, from the physical viewpoint, than in the theory with higher order derivatives, or even in the theory of "compensation" fields. This was precisely the point we made.

Karpman [1] showed that the adjustable relation, in spite of the presence of the regularization condition mentioned, following from the same structure of theory, contains certain divergent terms. However, this fact does not to any degree contradict the presence of a regularization condition in the case of particles with a mass spectrum. By the word "regularization" in reference 2 was implied only the presence of a number of regularization conditions. In order to be able to consider a concrete expression for physical quantities, it is necessary to solve all complex problems of normalization and regularization for particles with a mass spectrum. Reference 2 was not by any means designed to do this, as is evident from the nature of the note itself. The author regrets that there is an incorrect statement in the article, namely: ". . . analysis of the function $C(x)$ is characterized by an expansion of the function Δ_R into a series of terms vanishing as $x_s x^s \to 0$, and, in this manner, the function $C(x)$ itself is regularized . . . . ", which can lead to an error relative to the meaning of the term "regularization". All of Karpman's criticisms arise at this point.

It follows that the results of our earlier work relate not only to the establishment of the existence of proper regularization in the theory of particles with a mass spectrum, but to a new derivation of the adjustment relations of second quantization in that theory. These adjustment relations, brought out in reference 2, are a simpler method than was used previously by Pauli [3]; the result is a little different from that of Pauli. This difference is connected with the circumstance that in reference 2 the adjustment relations are subject to the natural requirement that they be the same in equations of the first order as in higher order equations, which requirement the wave function satisfies. In Karpman's work, nothing was said about this circumstance, which seems strange, inasmuch as to obtain the conditions of regularization of the adjustment relations in reference 1, it is necessary to go over to the viewpoint given in our work [2] with certain differences indicated above. It is also not clear, granting the basic results of our work, and its consequences, why Karpman did not mention this in the text of his work, taking notice only of the apparently erroneous results, and that in a footnote.

In conclusion, we present the derivation of Eq. 9 of reference 2, determining the operator F in the adjustment relations of the second quantization for a particle with mass spectrum. Let the equation for the eigenvalues of the matrix L^0 have the form:

$$L^0 \psi_r^{(0)} = \lambda_r \psi_r^{(0)}. \qquad (1)$$

Then, using the condition $S^{-1} L^\mu S l_\mu^0 = L^0$,

[1] V. I. Karpman, Doklady Akad. Nauk SSSR 89, 257 (1953)

[2] Iu. A. Iappa, Doklady Akad. Nauk SSSR 86, 51 (1952)

[3] W. Pauli, *Relativistic Theory of Elementary Particles*

we get

$$L^\mu t^0_\mu S\psi^{(0)}_r = \lambda_r S\psi^{(0)}_r; \tag{2}$$

$$S\psi^{(0)}_r \equiv \psi_r; \quad L^\mu t^0_\mu \psi_r = \lambda_r \psi_r; \tag{2'}$$

or, since it is possible to put

$$t^0_\mu = p_\mu / \sqrt{p^\lambda p_\lambda} \quad \text{(cf. reference 3)}, \tag{3}$$

$$L^\mu p_\mu \psi_r = \lambda_r \sqrt{p^\lambda p_\lambda}\, \psi_r.$$

Equation (3) has the form of an equation which is used to determine the eigenvalues and eigenfunctions of the matrix $L^\mu p_\mu$. The quantities $\varkappa_r = \lambda_r \sqrt{p^\lambda p_\lambda}$ would be, correspondingly, the roots of the characteristic equation that can be constructed by means of the matrix $L^\mu p_\mu$.

We will keep in mind the fact, established by Gel'fand and Iaglom, that to each value $+\lambda_r$ there corresponds a value $-\lambda_r$ in the spectrum of the matrix L^μ; and consequently to each $+\lambda_r \sqrt{p^\lambda p_\lambda}$ must correspond a $-\lambda_r \sqrt{p^\lambda p_\lambda}$ in the spectrum of the matrix $L^\mu p_\mu$. Accordingly, the minimal polynomial of the matrix $L^\mu p_\mu$ should have the form:

$$\Delta(\varkappa) = \prod_{i=1}^{s} (\varkappa^2 - \lambda_i p^\lambda p_\lambda) \tag{4}$$

or

$$\Delta(\varkappa) = \varkappa^{2s} + a_2 p^\lambda p_\lambda \varkappa^{2s-2} + \tag{5}$$

$$\ldots + a_{2s-2} (p^\lambda p_\lambda)^{s-1} \varkappa^2 + a_{2s} (p^\lambda p_\lambda)^s.$$

To derive the formula determining the operator F, we can then repeat, with appropriate changes, the derivation of the formula that determines the form of the "associated matrix". We will make the initial assumption that null eigenvalues are missing. We consider the expression $\phi(\kappa, x)$ of the formula

$$\varphi(\varkappa, x) = \frac{\Delta(\varkappa) - \Delta(x)}{\varkappa - x}. \tag{6}$$

After dividing in Eq. (6) we obtain

$$\varphi(\varkappa, x) = \varkappa^{2s-1} + x\varkappa^{2s-2} + (x^2 + a_2 p^\lambda p_\lambda)\varkappa^{2s-3} + \tag{7}$$

$$\ldots + [x^{2s-1} + a_2 p^\lambda p_\lambda x^{2s-3} + \ldots + a_{2s-2} (p^\lambda p_\lambda)^{s-1} x].$$

The matrix $L^\mu p_\mu$ has as a root the minimal polynomial

$$\Delta(L^\mu p_\mu) = \Delta(-L^\mu p_\mu) = 0. \tag{8}$$

According to Eqs. (6) and (8) we have

$$(L^\mu p_\mu + \varkappa)\, \varphi(\varkappa, -L^\mu p_\mu) = \Delta(\varkappa), \tag{9}$$

That is, (see reference 2, Eq. (8)) one can obtain

$$F = \varphi(\varkappa, -L^\mu p_\mu) \tag{10}$$

or

$$F = (-L^\mu p_\mu)^{2s-1} + \varkappa(-L^\mu p_\mu)^{2s-2} \tag{11}$$

$$+ (\varkappa^2 + a_2 p^\lambda p_\lambda)(-L^\mu p_\mu)^{2s-3} + \cdots$$

$$\ldots + [\varkappa^{2s-1} + a_2 p^\lambda p_\lambda \varkappa^{2s-3} + \cdots + a_{2s-2} (p^\lambda p_\lambda)^{s-1} \varkappa]\, E.$$

It is easily seen that when there is an n-fold zero eigenvalue, Eq. (9) is solved by use of the operator $F^1 = (L^\mu p_\mu)^n F$.

The operator F could be investigated in relation to the completion of the theorem of Pauli for the adjustment relations of the second quantization, which theorem is obtained by its help. The author hopes to return to a consideration of this question. It might be remarked that at present in the work of both Soviet (for example, see reference 3) and foreign (Bhaba, le Coutre) authors, there are several points of view on the problem of second quantization of the field of particles with a mass spectrum, so that the physical content of the corresponding problems is far from clear.

Translated by D. Williams
19

The Surface Tension of Liquid He^3 in the Temperature Range 0.93 - 3.34 °K

K. N. Zinov'eva
Institute of Physical Problems, Academy of Sciences, USSR
(Submitted to JETP editor October 4, 1954)
J. Exper. Theoret. Phys. USSR **28**, 125 (1955)

MEASUREMENTS of the surface tension of liquid He^3 have been carried out by the method of liquid rise in capillaries. Three capillaries were used in this research, each of length 2cm, and with diameters 0.360 mm, 0.224mm and 0.188 mm. The capillaries were carefully tested for uniform bore. The calibration of the capillaries was carried out within 1% by the usual method-- filling with mercury and measuring the length and weight of the mercury column. The capillaries were embedded in a glass test tube of 6 mm diameter and 30 mm length, at the end of which a resistance thermometer of phosphor bronze wire, diameter 40μ, was sealed in with platinum lead wires. The test tube was connected to a German silver tube of internal diameter 1.44 mm through a copper-glass connection. The He^3, whose purity was determined by mass spectrographic methods to be not less than 99.8%, was condensed along this tube, which leads across the trap of a Dewar into the test tube. This test tube was placed in the helium bath, which was constructed in similar fashion to that described by Peshkov[1]. This bath consisted of two Dewars placed one within the other. Temperature reduction was obtained by pumping.

Observation of the liquid level in the capillaries and in the test tube was made by means of a cathetometer which permitted measurement to within 0.01 mm. Actually the dispersion of the individual measurements at one temperature was large in several cases. Since the observation of the meniscus was carried out through seven glass layers, the form of the meniscus in the capillaries was not entirely clear, and the sight setting was made on some mean position of the interface. Distortions due to inhomogeneitis in the glass were detected by special measurements in which a straight edge of height 6.5 mm and with markings at each half millimeter was located inside the test tube in one of the experiments. The absolute error of the various measurements did not exceed 0.05 mm.

The coefficient of surface tension was computed by the equation

$$\alpha = \rho\, grh/2.$$

The density values of liquid He^3 were taken from Grilly, Hammel and Sydoriak [2]. The results of the three experiments, averaged at each temperature

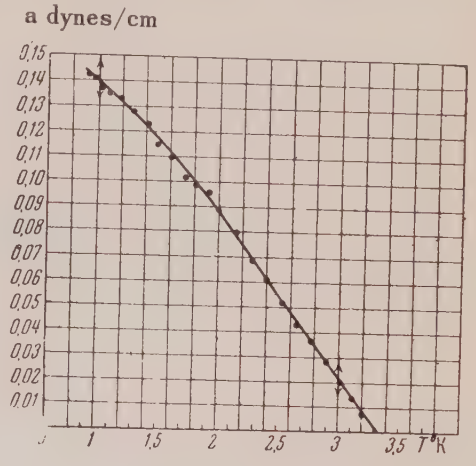

for all three capillaries, are shown in the figure. At very low temperatures, the mean error of measurement amounted to ±5%, with the maximum error ±7%. The maximum spread of the individual measurements is shown by the arrow on the graph.

The temperature of the liquid He^3 was determined by the resistance thermometer, which was first calibrated by the vapor pressure of He^3 (given by Abraham, Osborne and Weinstock[3]) and separately in He^4 (Mond Laboratory scale) with accuracy within 0.01 °K. Both scales agreed within the limits of error. Measurements of the surface tension of He^4 were carried out as a check on the method. Our results agreed well with the accepted values [4,5].

Comparison of the surface tension of He^3 and He^4 shows that the character of the temperature dependence of α in the region of investigation is the same in each case, but the curve for He^3 is displaced to the left by the difference in the critical temperatures (5.2° and 3.34 °K), and has the smaller slope. For T = 1 °K, the surface tension of He^3 is 2½ times less than for He^4.

Translated by R. T. Beyer
20

[1] V. P. Peshkov, J. Exper. Theoret. Phys. USSR **23**, 686 (1952)

[2] E. R. Grilly, E. F. Hammel and S. G. Sydoriak, Phys. Rev. **75**, 1103 (1949)

[3] B. M. Abraham, D. W. Osborne and W. Weinstock, Phys. Rev. **80**, 336 (1950)

[4] A. T. van Urk, W. H. Keesom and Kamerlingh Onnes, Leiden Comm. No. 179-a; Proc. Roy. Acad. Amsterdam **28**, 958 (1925)

[5] J. F. Allen and A. D. Misener, Proc. Camb. Phil. Soc. **34**, 299 (1938)

Rotation of Helium II at High Speeds

E. L. ANDRONIKASHVILI AND I. P. KAVERKIN
Institute for Physical Problems, Academy of Sciences, USSR
Institute of Physics, Academy of Sciences, Georgian SSR

(Submitted to JETP editor October 4, 1954)
J. Exper. Theoret. Phys. USSR 28, 126-127
(January, 1955)

1. IN uniform rotation a viscous liquid forms a parabolic meniscus whose depth depends only on the angular velocity and the radius r of the container

$$h = r^2\omega^2/2g, \tag{1}$$

where h is the depth of the meniscus and g is the acceleration due to gravity.

Since the superfluid component cannot perform motion in which curl $V_s \neq 0$ (as is proved by Landau's theory[1]), He II must be regarded as the only liquid whose meniscus depends on the density of its normal component, or, in the final analysis, on its temperature. Actually, in this case, the force which acts radially on a volume element of the liquid depends upon the density ρ_n of the normal component, while the force of gravity acting upon the same volume element is proportional to ρ (the density of the liquid as a whole). Therefore, the depth of the meniscus for He II must be expressed by the formula

$$h = \frac{\rho_n}{\rho}\frac{r^2\omega^2}{2g}. \tag{2}$$

2. We devised the following experiment to test this assumption[2]. A cylindrical plastic vessel, having an inner diameter of 27 mm and height 70 mm was turned on a lathe and then carefully polished. The base of the vessel was reinforced in a miniature ball bearing and ball thrust bearing pressed into a corresponding holder. (The glass and its base were regarded as a unit since it was turned from one piece of material, and the position of any component in the chuck of the lathe did not change during the entire machining process.) The apparatus was placed inside a helium dewar. Liquid helium was ladled into the container, after which it was rotated by means of a mechanical drive connected to a motor. The experiments covered the velocity range from 0.5 to 5 rev/sec, which, for the given radius, corresponds to 4 to 40 cm/sec for the tangental velocity of the glass. The depth of the meniscus was measured by a cathetometer and its shape was recorded with photographic equipment.

In this velocity range the depth of the meniscus was independent of the temperature and did not depart from the meniscus depth of normal liquids. This fact suggests that the expected phenomenon was not observed because of a transition through the critical velocity. Osborne[3] obtained similar results later and independently by carrying out a similar experiment for the velocity internal 35 to 70 cm/sec.

However, careful examination of the shape of meniscus enabled us to observe certain details not noted by Osborne. These details suggest that, even in the region of transcritical velocity, He II behaves very differently than a normal liquid.

Thus it was established that the meniscus which corresponds to speeds of rotation of 5 rev/sec has a conical recess at its center (Fig. 1) which is not found in normal liquids, including He I. Two cases were noted in which the meniscus was in a short time transformed into a vortex which extended to the edge of the container. However, it was not possible to record these on film. Also, we did not succeed in defining the precise conditions which led to the onset of such a vortex. Consequently, the vortices were not reproducible. Also not entirely normal was the process of untwisting , in which the peripheral part of the liquid was carried quickly along by the vessel and rose up, while the center part of the liquid continued to remain plane for about 120 sec. In the untwisting , the central part of the liquid had a conical meniscus which was maintained on the surface of the He II for 30 sec (Fig. 2).

3. All these facts suggest that in the critical region the superfluid condition is distorted, but does not vanish as such. Therefore, for a further study of this phenomenon, it was important to choose an experiment in which one of the characteristic properties of the superfluid would be displayed visibly. We chose the fountain effect for this purpose.

The experiment was carried out with the arrangement described above, with this difference, that a glass capillary, of length 148 mm and internal diameter 1.2 mm, was fastened along the axis of the cylinder. The lower part of the capillary was packed with iron oxide rouge. The

[1] L. D. Landau, J. Exper. Theoret. Phys. USSR 11, 596 (1941)

[2] E. L. Andronikashvili, Dissertation, Inst. Phys. Problems, Academy of Sciences, USSR (1948)

[3] D. V. Osborne, Proc. Phys. Soc. (London) 63A, 909 (1950)

Dependence of the quantities in the thermomechanical effect on the rotational velocity at different temperatures*

p pressure in mm Hg.	T^0K	n_1	h_1	n_2	h_2	n_3	h_3	n_4	h_4	n_5	h_5	n_6	h_6
30	2.1	0.24	135	1.6	134	3.3	135	6.8	135	12	135	16.2	135
20	1.95	0.24	120	2.2	120	4.8	120	7.1	120	10.5	120	17.2	120
10	1.74	0.24	105	1.6	105	5.2	105	8.5	105	10.8	105	15.5	105

* n = number of revolutions/sec; h = height of fountain of He, in mm of mercury.

Fig. 1. Meniscus of Rotating Helium II

Fig. 2. Meniscus of Rotating Helium II in the "Untwisting" process

capillary was rotated with the vessel.

Upon immersing the apparatus in liquid helium, a beam of light was directed on the rouge plug. As a result, a difference in level was established between the liquid in the capillary and in the container. This difference was measured by a cathetometer. Then the container was rotated. Under these conditions there was a lowering of the level of He II in the capillary by an amount which, in the limits of error of the experiment, did not differ from the displacement of the central part of the meniscus which was brought about by the rotation. This experiment covered the velocity range from 0.25 to 22 rev/sec and was repeated at different temperatures. The light intensity (which supplied the heat) was chosen separately in each case. As is evident from the table, the dependence of the thermomechanical effect on the rotational velocity is not observed up to velocities of 16 rev/sec, which corresponds to tangential speeds of 136 cm/sec.

In another experiment, this same capillary, rigidly fixed independently of the vessel, was displaced along its radius, thus playing the role of a stirrer. However, even in this case, the total rise of He II in the capillary changed insignificantly for a velocity change of 160 cm/sec.

From these experiments it follows that, in the transition through the critical velocity, the superfluid phenomenon not only does not disappear but that the quantitative characteristics, such as the thermomechanical effect and the quantity ρ_n/ρ connected with it, remain unchanged, and independent of the velocity of rotation, within the limits of error of measurement, up to very large velocities. It is thus possible to confirm that in the region of critical velocity the superfluid component maintains motion for which curl V_s differs from zero.

Translated by R. T. Beyer
21

Collisions of Fast Nucleons with Nuclei

E. L. Feinberg
P. N. Lebedev Institute of Physics, Academy of Sciences, USSR

(Submitted to JETP editor October 5, 1954)
J. Exper. Theoret. Phys. USSR 28, 241-242
(February, 1955)

In the investigations of collisions of nucleons and mesons (with energies of the order $10^{10} \div 10^{12}$ ev) with nuclei one occasionally finds the entire process with its attendant generation of new mesons (and possibly new nucleon pairs) represented as a cascade process within the nucleus or, in any case, as a process of successive collisions of the incident particle within the nucleus; the emission of new formed particles and nucleons being produced by the nucleons situated along the collision path. Occasionally, detailed calculations are exhibited which are based on the fact that after the collision, the primary particle and its products move through small angles relative to the initial direction of motion of the particle[1].

Nevertheless one cannot forget that, because of the wave properties of the particles, this view may be internally inconsistent. Let us consider, for example, the collision of two nucleons which produces in one event ν mesons, each with a mass μ and energy ϵ. If the collision cross section is of the order of π/μ^2, (where $\hbar = c = 1$, in the following) then the mean impact parameter is $1/\mu$, the momentum $q_\perp$ in the perpendicular direction, which is transferred to the nucleon by emission, has the order of μ and the energy carried away by these nucleons should be, on the average, comparatively small. Consequently, if we consider the momentum $q_\parallel$ in the longitudinal direction, which is transferred to the nucleon by emission, we can write

$$q_\parallel \approx \sqrt{E^2 - M^2} - \sqrt{(E-\nu\varepsilon)^2 - M^2}\cos\theta_M - \nu\sqrt{\varepsilon^2-\mu^2}\cos\theta_\mu \quad (1)$$

$$\approx \frac{M^2\nu\varepsilon}{2E(E-\nu\varepsilon)} + \frac{\nu\mu^2}{2\varepsilon} + \frac{1}{2}(\theta_M^2(E-\nu\varepsilon) + \theta_\mu^2\nu\varepsilon).$$

Here θ_M and θ_μ are the emergent angles of the nucleon and the mesons, and are considered small; in addition, all particles are assumed relativistic. Further considerations depend upon the emergent angles of the particles. Thus for example,

a) one occasionally assumes that

$$\theta_M \sim \theta_\mu \sim M/E. \quad (2)$$

It is easily seen that in this case, with sufficiently high energies, the quantity $q_\parallel$ can become quite small. Thus the effective extent of space within which the process occurs equals, according to the uncertainty relation, $1/q_\parallel$, and can become substantially greater than the extent of the core of

one nucleon. More precisely, it is sufficient that

$$q_{\parallel}(1/\mu) \ll 1. \tag{3}$$

Furthermore, if $q_{\parallel}(A^{1/3}/\mu) \ll 1,$ (4)

then this effective region elongates to a distance greater than the dimension of the entire nucleus. In these cases one cannot consider the collision of the incident nucleon and the generation of products as a collision with one nucleon in the nucleus. It is necessary to treat it as a process of simultaneous interaction within a "tube" or "channel" which has a cross section of π/μ^2 and which is cut out in the nucleus by the incident nucleon.

From Eqs. (1) - (4) one can easily obtain the conditions for the existence of such a collective interaction. Two cases are possible: 1) $\nu\epsilon \ll E$ and 2) $\nu\epsilon \sim E \sim E - \nu\epsilon$. For both cases, condition (3) has the form, after substitution of Eq. (2) into Eq. (1) and then Eq. (1) into Eq. (3):

$$\frac{M^2}{2E}\frac{1}{\mu} \ll 1, \quad E \gg M\frac{M}{2\mu} \sim 5\cdot 10^9 \text{ eV} \tag{3'}$$

[here one requires].

For condition (4), the threshold energy is multiplied by $A^{1/3}$. If the emergent angles are smaller than M/E, then the picture of successive collisions becomes inapplicable even earlier. If

b) the nucleons scatter with angles greater than $\theta_M \sim \sqrt{M/E}$ (isotropic in the center of mass system of both nucleons) then one finds

$$q_{\parallel} \sim M, \quad q_{\parallel}(A^{1/3}/\mu) \gg 1, \tag{5}$$

and the picture of successive collisions can be retained.

c) To the degree to which the impact parameter equals, in the mean, $1/\mu$ and $q_{\perp} \sim \mu$, then there is greater probability that the scattering angle of the nucleon is $\theta_M \sim \mu/M$. Then the decisive role is played by the emergent angle of the meson, θ_μ. If it equals $\sqrt{M/E}$ (this occurs, for example, in the case of isotropic emission of mesons in the center of mass system), then, as is plausible, the main role is played by the last term in Eq. (1):

$$q_{\parallel} \sim {}^1/_2 (M\nu\epsilon/E).$$

The picture of successive collisions is useful if the meson energy is not very small, that is, if

$$\nu\epsilon > 2(\mu/M)E. \tag{6}$$

If the mesons are emitted isotropically in the system of rest of the incident nucleon then $\theta_\mu \sim M/E$ and we again revert to case (a) and condition (3).

In this sense, only with a special mechanism of meson emission can we say that, in the realm of energies $E > 5 \times 10^9$ ev, successive collisions of a nucleon with different nucleons occur. The preceding considerations lose their force when $E \gtrsim 10^{12} \div 10^{13}$ ev[3], where the Fermi-Landau process[2] becomes operative.

Translated by A. Skumanich
35

[1] See, for example, *Cosmic Rays*, (edited by W. Heisenberg, Dover publications, 1948)

[2] E. Fermi, Progr. Theor. Phys. 5, 570 (1950); Izv. Akad. Nauk SSSR, Ser. Fiz. 17, 51 (1953)

[3] I. L. Rosental and D. S. Chernavskii, Usp. Fiz. Nauk 52, 185 (1954)

Improvement of the Quality of a Cavity Resonator By Means of Regeneration

N. G. Basov, V. G. Veselago and
M. E. Zhabatinski
P. N. Lebedev Physical Institute,
Academy of Sciences, USSR

(Submitted to JETP editor November 4, 1954)
J. Exper. Theoret. Phys. USSR 28, 242 (February, 1955)

In connection with the possibility of constructing a molecular oscillator[1,2] there arises the question of substantially improving the quality of cavity resonators. One possibility which can be utilized for this purpose is the construction of a superconducting type of cavity resonator[3]. Another is the adoption of the well known low frequency radio method of regeneration[4].

In experiments performed by us, a cavity resonator with a Q value of 4×10^4 was employed. This resonator was connected in a positive feedback loop with a microwave amplifier. By gradually increasing the gain modulus, the effective Q of the resonator increased and reached the value 3×10^6. This value was maintained for several hours; while a Q of 5×10^6 could be maintained for only 10 - 20 minutes. The Q values were measured with the help of a quartz frequency standard.

Further increase in the quality is restricted by the lack of stability in the amplifier system, which results from fluctuations in the gain modulus and, in particular, the phase shift.

The apparatus could have been changed so that with such periodic influences on the gain modulus one could employ the method of interrupted generation - - a scheme analogous to classical superregeneration.

A substantial improvement of the quality, without the utilization of superregeneration, can be obtained with the employment of negative feedback coupling. As is well known, the gain modulus and phase shift of the amplifier is determined by the fundamental parameters of the feedback loop. Thus a superimposed negative feedback can provide the necessary stable scheme.

Translated by A. Skumanich
36

[1] N. G. Basov and A. M. Prokhorov, J. Exper. Theoret. Phys. USSR 27, 431 (1954)

[2] J. R. Gordon, H. J. Zeiger and C. H. Townes, Phys. Rev. 95, 282 (1954)

[3] M. S. Khaikin, Doklady Akad. Nauk SSSR 75, 661 (1950)

[4] G. Barkgauzen, *Electron Tubes and Their Application in Engineering*, vol. III, Moscow (1938)

The Neutron Subshell in the Region of the Transuranic Elements

S. T. Larin and N. N. Kolesnikov
Moscow State University

(Submitted to JETP editor September 30, 1954)
J. Exper. Theoret. Phys. USSR 28, 243
(February, 1955)

At present the existence of neutron or proton shells or subshells in the region $N > 126$ and $Z > 82$ is not reliably established. There have been only a few scattered indications of the possibility of existence of weak subshells at $Z = 96$[1], $N = 148$[2] and $Z = 92$[3].

New data on the properties of isotopes of the transuranic elements, including the recently discovered elements 99 and 100 allows us to look into this question anew. The greatest interest in this respect is provided by the data on energies of α-decay. Using the experimental results of very recent papers[4-8] as well as of earlier papers[9,10], we constructed a diagram showing the dependence of the energy of the α-decay on the mass number A in the manner of the diagram of Seaborg et al[10]. Using the known β-decay energies of the nuclei 99^{254} [4] and Bk^{250} [5] and the α-decay energy of the nucleus 100^{254}, we calculated from the energy of the α-decay energy of 99^{254}, which is also indicated on the accompanying diagram. Points pertaining to the same element are connected by solid lines; points corresponding to nuclei with an equal number of neutrons are connected by dotted lines.

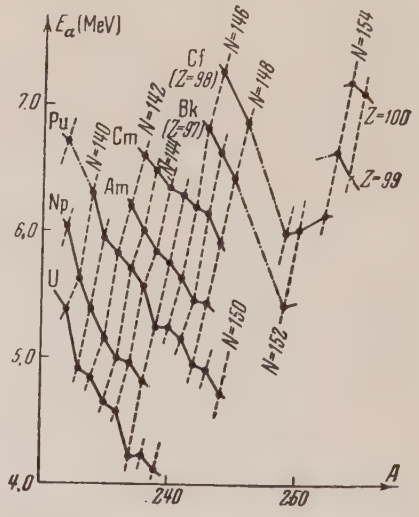

Dependence of α-decay energy E_α upon the Mass Number A

An examination of the diagram shows that for the element curium ($Z = 96$) a very slight decrease of α-decay energy takes place only for the lightweight isotopes; for the heavier isotopes (Cm^{242}, Cm^{243} and Cm^{244}) such is not observed. At the same time near $N = 150$ to 152 there is clearly visible a lowering of the α-decay energy with a subsequent increase; analogous to this, although on a smaller scale, are the jumps observed on a similar diagram near $N = 126$[10]. This is demonstrated most clearly by the considerable increase of α-decay energy of the nuclei with $N = 154$, especially for Cf^{252}, and also for 99^{253} and 100^{254}.

In connection with this we note that, according to the latest data[6,11], the nucleus Cf^{252}, proved to have a considerably lessened stability with respect to spontaneous fission, along with the above mentioned reduced stability with respect to α- decay.

Examination of lg τ as a function of the α-decay energy (the diagram of which is not shown here) indicates that the α-decays of nuclei Cf^{252}, 99^{253}, and 100^{254} are relatively more probable than for other neighboring nuclei; it is natural to connect this behavior with some increase of the radii of these nuclei after the subshell has been filled at $N = 150$ (or 152)[10,12].

The above facts point to the existence of a neutron subshell at $N = 150$ (or 152). According to the usual scheme of Mayer-Jensen, the following

sequence of levels (for the neutrons) could correspond to such a subshell:

$$\ldots 7i_{13/2}|_{126}\, 6g_{9/2},\ 7i_{11/2},\ 4s|_{150}\ldots$$

or

$$\ldots 7i_{13/2}|_{126}\, 6g_{9/2},\ 4s,\ 5d_{5/2},\ 6g_{7/2}|_{152}\ldots$$

We express our gratitude to Prof. D. D. Ivanenko for valuable suggestions and discussions.

Note during proof reading: After this communication was sent to press, we learned of a paper [13], the authors of which, on the basis of α-decay energy values (among others also those of Cf ^{248} published for the first time) come to the conclusion that a subshell exists at $N = 152$. In view of this paper, the second of our level sequences above should be considered the more probable one.

Translated by M. G. Jacobson
37

[1] G. T. Seaborg, Phys. Rev. 92, 1074 (1953)
[2] N. Kolesnikov, Doklady Akad. Nauk SSSR 97, 233 (1954)
[3] V. A. Kravtsov, Doklady Akad. Nauk SSSR 78, 43 (1955)
[4] G. R. Choppin et al, Phys. Rev. 94, 1080 (1954)
[5] A. Ghiorso et al, Phys.Rev. 94, 1081 (1954)
[6] H. Diamond et al, Phys. Rev. 94, 1083 (1954)
[7] M. H. Studier et al, Phys. Rev. 93, 1433 (1954)
[8] P. R. Fields et al, Phys. Rev. 94, 209 (1954)
[9] J. M. Hollander, I. Perlman, G. T. Seaborg, Revs. Mod. Phys. 25, 469 (1953)
[10] I. Perlman, A. Ghiorso and G. Seaborg, Phys. Rev. 77, 26 (1950)
[11] J. R. Huizenga, Phys. Rev. 94, 158 (1954)
[12] D. D. Ivanenko and S. I. Larin, J. Exper. Theoret. Phys. USSR 24, 359 (1953)
[13] A. Ghiorso et al, Phys. Rev. 95, 293 (1954)

The Problem of Spontaneous Fission and Beta-Stability

N. N. KOLESNIKOV AND S. I. LARKIN
Moscow State University

(Submitted to JETP editor September 30, 1954)
J. Exper. Theoret. Phys. USSR 28, 244-245
(February, 1955)

THE probability of fission of nuclei depends on the effective height of the potential barrier (that is, on the critical fission energy) and also on its width. Inasmuch as the critical fission energy, according to the theory of fission, is a function of the parameter $F = (Z^2/A)$, it can be expected that the probability of fission also will depend on this quantity. It was indicated by Seaborg [1] and others [2,3] that the relationship between the logarithm of the probability of spontaneous fission (or lg τ) and Z^2/A is nearly linear. However, further and more detailed investigation showed that such a relationship is at least not accurate. First, the uneven nuclei, which have a relatively low probability of spontaneous fission (in comparison with the even-even nuclei) do not fit into this general relationship. Second, and this is especially important, there is observed a maximum of stability with respect to spontaneous fission among the isotopes of a given element.

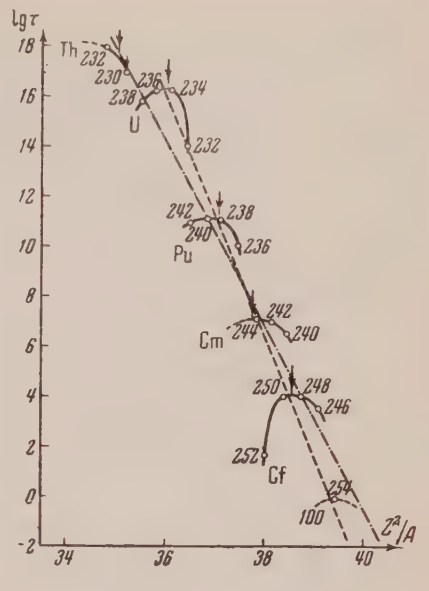

Dependence of lg τ (τ – in years) on Z^2/A

We wish to call attention to the fact that the maximum stability with respect to spontaneous fission fairly accurately coincides with the maximum of β-stability for the isotopes of a given element. We can convince ourselves of this, for instance, by examining the curve expressing lg τ as a function of Z^2/A (see accompanying figure). The experimental values for the lifetimes with respect to spontaneous fission τ are taken from the literature [4,5]. On the accompanying figure, points pertaining to isotopes of any one element are connected by solid lines. The curves obtained in this way sharply deviate from the linear relationship of Seaborg (the dash-dot line on the figure); they reach a maximum at some value of A and fall off both in the region of the lighter as well as of the heavier isotopes of the element. The latter fact is unexpected from the point of view of elementary fission theory.

Especially sharp bends of such curves are observed for the heavy isotpes of U and Cf. The maxima of the curves pertaining to single elements all lie almost on a straight line (the dotted line of the figure), and the values of Z^2/A corresponding to these maxima coincide very well with the values of Z^2/A^*. The values of A^* are taken from a stability curve, constructed from data on β-disintegration[6] and correspond to such A's, at which maximum β-stability is obtained for the isotopes of a given element. (The values of A^* are indicated on the figure by little arrows.) Note that in the case of thorium it is difficult to come to a definite conclusion at present, because of insufficient data, one of which is unreliable (Th^{230}).

The dependence of $\lg\tau$ on Z and A can be expressed by an empirical formula:

$$\lg\tau_{\text{years}} = -4.85\,(Z^2/A^*) + 191 - 0.063\,(A - A^*)^2. \quad (1)$$

The last term is added to make the formula applicable for nuclei which are not at the maximum of stability. Let us note that in the interval of mass numbers A under consideration, the values for A^* are given by the approximate relationship:

$$A^* \approx 2.5\ Z + 5. \quad (2)$$

Substitution of Eq. (2) into Eq. (1) shows that when $A \approx A^*$, $\lg\tau$ is approximately proportional to Z ($\lg\tau \sim Z$). This conclusion is confirmed also by a direct examination of the dependence of $\lg\tau$ upon Z.

A possible reason for the considerable deviations from the simple relationship of Seaborg above described is the incorrect form of the formula for the binding energy and hence also for the parameter Z^2/A. One of the most important factors, influencing the above described deviations, is the different susceptibility to deformation of the various nuclei[4]. It appears reasonable to consider that nuclei which are close to the β-stability curve and possess a greater binding energy with respect to other isobars, are less subject to deformation. On the contrary, nuclei which are located far away from the stability curve, and which have a lower binding energy, are more deformed. This deformation makes the crossing of the potential barrier easier. Such an explanation appears the nearer to the truth in view of the fact that the lower excited levels of the nuclei which are near the β-stability curve are elevated with respect to the levels of other isobars.

It is possible that some deviations from the relationship given by formula (1) in special cases are connected with the different deformations of the proton configuration (and also neutron configuration) inside the nuclei. The lower probability of spontaneous fission for uneven nuclei with respect to even-even nuclei[8] can apparently be explained in a similar manner, assuming their lower susceptibility to deformation. An assumption of this kind has already been made for the explanation of the differences in isotopic shifts between even and uneven isotopes.

For a series of valuable remarks and discussion of the problems of this paper, we express our gratitude to Professor D. D. Ivanenko.

Translated by M. G. Jacobson
38

[1] G. T. Seaborg, Phys. Rev. 85, 157 (1952)

[2] W. J. Whitehouse and W. Galbraith, Nature 169, 494 (1952)

[3] A. Ghiorso et al, Phys. Rev. 87, 163 (1952)

[4] J. R. Huizenga, Phys. Rev. 94, 158 (1954)

[5] A. Ghiorso et al, Phys. Rev. 94, 1081 (1954)

[6] N. N. Kolesnikov, Doklady Acad. Sci. USSR 97, 233 (1954)

[7] L. Willets, D. L. Hill, K. W. Ford, Phys. Rev. 91, 1488 (1953)

[8] D. L. Hill, J. A. Wheeler, Phys. Rev. 89, 1102 (1953)

On the Paper of G. M. Avak'iants "The Theory of the Transfer Equation in Strong Electric Fields." [1]

I. M. Tsidil'kovskii and F. G. Bass
Dagestan Branch of the Academy of Sciences of the USSR Makhachkala

(Submitted to JETP editor July 12, 1954)
J. Exper. Theoret. Phys. USSR 28, 245
(February, 1955)

THE necessity for a theoretical investigation of the properties of semi-conductors placed in strong electric fields has existed for a long time. The dependence of the electric conductivity obtained by Davydov[2], as is known, is not confirmed by experiment for many semi-conductors.

G. M. Avak'iants undertook the task of looking into the phenomena of transference in semi-conductors in which the electron gas is strongly heated. It should be noted that while investigation of galvanomagnetic phenomena is undoubtedly of interest, the same cannot be said of thermoelectric and of thermo- and photomagnetic effects. More than that,

the problem of investigation of these phenomena in a strong electric field appears to us one thought up especially for this occasion. In order to heat up the electron gas under conditions when primary current is absent, the author had to introduce artificially a strong electric field perpendicular to the primary temperature gradient (in the presence of a magnetic field in the direction of the latter). This immediately leads to a contradiction in the calculation of the electronic component of thermoconductivity, for instance. The calculation was carried out, as usual, with the assumption of absence of electric current in the specimen ($j = 0$). While doing this, however, the author did not account for the fact that a strong current is required in the semi-conductor in order to heat the electron gas.

Furthermore, in all formulas obtained, there enters a quantity χ^{ν}, which is dependent upon the electric and magnetic fields E and H, and, in the presence of a temperature gradient, also upon the coordinates r. Nevertheless, the calculations of χ^{ν} is carried out under the assumption that the symmetrical part of the distribution function f_0 does not depend on the magnetic field or on the coordinates, and the solution of Davydov is used for this case. We do not agree with Avak'iants, who states that "there is no necessity" for solving the equations of Davydov in the case in which f_0 depends on E, H and r. From the formulas of Davydov[3] it follows that for not very small magnetic fields (or small H at sufficiently low temperatures) the dependence of f_0 upon H cannot be neglected.

In calculating f_0, Avak'iants also neglects a term which accounts for the entrance of electrons into the zone of conductivity (or to local levels). This is justified only in those cases in which the concentration of electrons (holes) differs but little from the equilibrium condition. But, in a kinetic equation, under conditions where the semiconductor is in a strong electric field, not only the usual thermal ionization, but also the ionization by the field must be accounted for. Neglect of the terms expressing the ionization by the field, is, in our opinion, one of the basic causes of the disagreement between theory and experiment.

Thus, the papers of Avak'iants cannot interpret experimental results (for instance, the Pool* effect) and do not contribute, as it appears to us, anything new to the problem of behavior of semiconductors in strong electric fields.

Translated by M. G. Jacobson
39

* *Translator's note:* Probably misprint; correct reference probably is to Suhl effect.

[1] G. M. Avak'iants, J. Exper. Theoret. Phys. USSR 26, 562, 668 (1954)

[2] B. Y. Davydov, J. Exper. Theoret. Phys. USSR 6, 471 (1936)

[3] B. Y. Davydov, J. Exper. Theoret. Phys. USSR 7, 1069 (1937)

The Velocity of the Wave Front in Nonlinear Electrodynamics

L. G. Iakovlev
Moscow State University

(Submitted to JETP editor June 3, 1954)
J. Exper. Theoret. Phys. USSR 28, 246-248
(February, 1955)

IN papers by Blokhintsev[1] and Blokhintsev and Orlov[2], it is shown that for nonlinear electrodynamics and mesodynamics, the propagation of a signal (defined as the surface of a weak discontinuity in the field strength) can take place with a velocity greater than the velocity of light in the vacuum*. Both papers are based on the method of characteristics of systems of partial differential equations, going into detail in the case of plane waves. In view of the importance of this question, it is interesting to investigate it further and to simplify the method.

Sommerfeld[4] has investigated the velocity of the signal and of the wave front (the group and phase velocities**) in Maxwell-Lorentz linear electrodynamics. He showed that, in linear electrodynamics, the velocity of the front is always (independent of the medium) equal to the velocity of light in the vacuum***. This result is particularly easy to get by making use of a method pointed out by Levi-Civita. We shall apply the same method to nonlinear electrodynamics, since the equation for the velocity of the wave front can be derived simply and intuitively****.

As is well known, the equations of electrodynamics are gotten by the use of the variational principle from a Lagrangian depending on the first and second invariants of the field, that is,

$$L = L(K, I^2),$$

where

$$K \equiv \frac{1}{2}(E^2 - H^2), \quad I^2 \equiv (\mathbf{E}, \mathbf{H})^2.$$

First let us investigate the use of a plane wave. Let $E = E_x(z, t)$, $H = H_y(z, t)$, $E_y = E_z = H_x = H_z =$

Then the basic equations of the field take the form

$$\alpha \frac{\partial K}{\partial z} H + \alpha \frac{\partial K}{\partial t} E + \frac{\partial H}{\partial z} + \frac{\partial E}{\partial t} = 0; \qquad (1)$$

$$\frac{\partial E}{\partial z} + \frac{\partial H}{\partial t} = 0.$$

(the trivial equations $\partial E_y / \partial z = 0$ etc., are not written down). Above and in what follows we take the velocity of light $c = 1$,

$$\alpha \equiv \frac{\partial^2 L/\partial K^2}{\partial L/\partial K}, \quad \beta \equiv \frac{\partial^2 L/\partial K \partial I}{\partial L/\partial K}, \quad \gamma \equiv \frac{\partial^2 L/\partial I^2}{\partial L/\partial K}$$

In the case now under consideration, $\beta = \gamma = 0$.

Let the plane $z = \nu t$ be the surface of weak continuity of E_x and H_y moving with velocity ν. Denoting by Φ the change in the value of any quantity Φ on going through the surface of discontinuity, we have

$$[E] = 0, \ [H] = 0, \ [\partial E/\partial z] \equiv e \neq 0, \qquad (2)$$

$$[\partial H/\partial z] \equiv h \neq 0.$$

According to the method we are adopting, we must form the differences on crossing the surface of discontinuity for each of the equations,

$$E(z + \Delta z, \ t + \Delta t) = E(z, \ t) + \frac{\partial E}{\partial z} \Delta z + \frac{\partial E}{\partial t} \Delta t, \qquad (3)$$

$$H(z + \Delta z, \ t + \Delta t) = H(z, \ t) + \frac{\partial H}{\partial z} \Delta z + \frac{\partial H}{\partial t} \Delta t,$$

and then form the same differences for crossing the surface for each of Eqs. (1), where $\Delta z = \nu \Delta t$. Using Eqs. (2), we get the following formulas for substitution into Eqs. (1):

$$\frac{\partial_1}{\partial t} \to -v \frac{\partial}{\partial z}, \quad \frac{\partial E}{\partial z} \to e, \quad \frac{\partial H}{\partial z} \to h.$$

This gives

$$\alpha [\partial K/\partial z] (H - E\nu) + h - ev = 0, \quad e = hv, \qquad (4)$$

where $[\partial K/\partial z] = Ee - Hh$.

Solving Eq. (4) we find the velocity of the front (that of the surface of weak discontinuity),

$$v_{1,2} = \frac{\alpha EH \pm \sqrt{1 + \alpha (E^2 - H^2)}}{1 + \alpha E^2}. \qquad (5)$$

where $\partial K/\partial z = 0$ (that is, $E^2 - H^2 = f(t)$, or in particular, $E^2 - H^2 = 0$), we get from Eq. (4)

$$v_{1,2} = \pm 1. \qquad (6)$$

The velocity of a plane wave front is equal to the velocity of light in the vacuum in the following cases:

1) $\alpha = 0$, $\beta = 0$; i.e., for Lagrangians of the form

$$L = \text{const} \cdot K + f(I^2); \qquad (7)$$

2) $E^2 - H^2 = f(t)$ (i.e. $\partial K/\partial z = 0$). (8)

It is easy to show that for constants $E_x = E_0$ and $H_y = H_0$ and for variable $E_y = \epsilon$ and $H_x = h$, if $\epsilon \ll E_0$, $h \ll H_0$ ($\epsilon^2 \sim h^2 \sim \epsilon h \sim 0$) and if $\epsilon = h = 0$ on the surface of discontinuity of the derivatives $\partial E_y/\partial z$ and $\partial H_x/\partial z$, then the surface (the wave front of ϵ, h) is propagated with the velocity

$$v = \frac{-\gamma EH \pm \sqrt{\gamma (E^2 - H^2) - 1}}{1 - \gamma H^2}. \qquad (9)$$

If one assumes that the principle of superposition is valid for weak disturbances of the field, then any plane wave $\vec{\epsilon}$, $\mathbf{h}$, propagated in a constant field $\mathbf{E}_0, \mathbf{H}_0$, ($\mathbf{E}_0 \perp \mathbf{H}_0$; $\epsilon \ll E$, $h \ll H$) and perpendicular to the constant field, breaks up into two linear polarized rays ϵ_x, h_y and ϵ_y, h_x, each of which moves with velocities (5) and (9)*, respectively.

In the general case of the presence of all the components of the field strength, the present method [by using an equation of the form of Eq. (3) for each component] allows one easily to derive the following set of equations from the basic equations of the field:

$$\begin{aligned} Se + \Phi h_x + \Pi h_y &= 0, \\ Te + Dh_x + \Phi h_y &= 0, \\ Re - Th_x - Sh_y &= 0, \end{aligned} \qquad (10)$$

where

$$e \equiv \left[\frac{\partial E_z}{\partial z}\right] \neq 0, \ h_x \equiv \left[\frac{\partial H_x}{\partial z}\right] \neq 0, \ h_y \equiv \left[\frac{\partial H_y}{\partial z}\right] \neq 0;$$

$$S \equiv \alpha E_z H_z - \beta (E_y E_z - H_y H_z) - \gamma E_y E_z$$

$$- \{\alpha E_x E_z + \beta (E_x H_z + E_z H_x) + \gamma H_x H_z\} v,$$

$$\Phi \equiv \{\alpha E_x E_y + \beta (E_x H_y + E_y H_x) + \gamma H_x H_y\} v^2$$

$$+ \{\alpha (E_x H_x - E_y H_y) - \beta (E_x^2 - E_y^2 - H_x^2 + H_y^2)$$

$$+ \gamma (E_y H_y - E_x H_x)\} v - \alpha H_x H_y$$

$$+ \beta (E_x H_y + E_y H_x) - \gamma E_x E_y,$$

$$\Pi \equiv -(\alpha E_x^2 + 2\beta E_x H_x + \gamma H_x^2 + 1)v^2 + 2\{\alpha E_x H_y - \beta(E_x E_y - H_x H_y) - \gamma E_y H_x\}v - \alpha H_y^2 + 2\beta E_y H_y - \gamma E_y^2 + 1;$$

$$T \equiv \{\alpha E_y E_z + \beta(E_y H_z + E_z H_y) + \gamma H_y H_z\}v + \alpha E_z H_x - \beta(E_x E_z - H_x H_z) - \gamma E_x H_z;$$

$$D \equiv -(\alpha E_y^2 + 2\beta E_y H_y + \gamma H_y^2 + 1)v^2 + 2\{-\alpha E_y H_x + \beta(E_x E_y - H_x H_y) + \gamma E_x H_y\}v - \alpha H_x^2 + 2\beta E_x H_x - \gamma E_x^2 + 1,$$

$$R \equiv \alpha E_z^2 + 2\beta E_z H_z + \gamma H_z^2 + 1.$$

Equations (10) are homogeneous with respect to e, h_x, h_y. Therefore,

$$\begin{vmatrix} S & \Phi & \Pi \\ T & D & \Phi \\ R & -T & -S \end{vmatrix} = 0.$$

Expanding the determinant, we get

$$R(\Phi^2 - \Pi D) + S(T\Phi - SD) + T(S\Phi - T\Pi) = 0. \quad (11)$$

Substitution of the expressions for R, Φ, etc. into Eq. (11), leads to the equation for the velocity of the front [see Eq. (10) of Ref. 2]. Clearly, if $E = E_x$, $H = H_y$, $E_y = E_z = H_x = H_z = 0$, then Eq. (11) [just as Eq. (10) of Ref. 2] is unsuitable, for then $e = 0$, $h_x = 0$, $S = T = 0$, $R = 1$, and Eqs. (10) reduce to $\Pi = 0$, $\Phi = 0$, which give Eq. (5). Use of Eq. (11) would give $\Phi^2 - \Pi D = 0$ which leads to incorrect values of ν.

From the derived Eqs. (5) and (9), it is seen that nonlinear equations, generally speaking, give a velocity for the propagation of the wave front which is greater than the velocity of light in the vacuum (for a given choice of the Lagrangian). However, this leaves open the question of whether such a possibility really exists. We note that for a nonlinear Lagrangian, quantum electrodynamics gives a wave front velocity for a plane wave, which is not greater than the vacuum velocity of light.

Analogously, one can get an expression for the propagation velocity of a wave front in scalar or pseudoscalar mesodynamics. The field equation for $\phi = \phi(x, t)$ is

$$\phi'' - \ddot{\phi} - a\phi'^2\phi'' - a\dot{\phi}^2\ddot{\phi} + 2a\phi'\dot{\phi}\dot{\phi}' + \beta\phi(\phi'^2 - \dot{\phi}^2) + \gamma\phi = 0$$

Here

$$\phi' \equiv \frac{\partial\phi}{\partial x}, \dot{\phi} \equiv \frac{\partial\phi}{\partial t}, a \equiv \frac{\partial^2 L/\partial K^2}{\partial L/\partial K}, \beta \equiv \frac{\partial^2 L/\partial K \partial I}{\partial L/\partial K}, \gamma \equiv \frac{\partial^2 L/\partial I^2}{\partial L/\partial K},$$

$$K \equiv -\frac{1}{2}\phi'^2 + \frac{1}{2}\dot{\phi}^2, I^2 \equiv \frac{1}{2}\phi^2.$$

Making use of $[\phi] = 0$, $[\phi'] = [\dot{\phi}] = 0$, $[\phi''] \equiv \phi_{xx} \neq 0$ and the equations

$$\phi'(x + \Delta x, t + \Delta t) = \phi'(x, t) + \phi''\Delta x + \dot{\phi}'\Delta t,$$

$$\dot{\phi}(x + \Delta x, t + \Delta t) = \dot{\phi}(x, t) + \dot{\phi}'\Delta x + \ddot{\phi}\Delta t,$$

we get, by the same method,

$$(1 + a\dot{\phi}^2)\nu^2 + 2a\dot{\phi}\phi'\nu + a\phi'^2 - 1 = 0.$$

From this,

$$\nu = (-a\dot{\phi}\phi' \pm \sqrt{1 + 2aK})/(1 + a\dot{\phi}^2),$$

which follows from the formulas in Ref. 1.

All the results can be achieved by forming the differences of the divergence of the energy-momentum tensor across the surface of the discontinuity.

The author thanks Prof. D. D. Ivanenko for pointing out the importance of the problem and for advice during the investigation.

Translated by E. Saletan
40

* The question of the change of velocity of propagation of light in nonlinear electrodynamics was first investigated by Svirski [e.g., see Ref. 3, M. S. Svirski, Vestn. (Moscow State University) 3, 43 (1951)].

** It should be noted that there is a difference in terminology in Refs. 2 and 4 [e.g., see Ref. 2, D. I. Blokhintsev and V. V. Orlov, J. Exper. Theoret. Phys. USSR 25, 513 (1953) and Ref. 4, A. Sommerfeld, Ann. d. Phys. **44**, 177 (1914)]: in Ref. 4, the velocity of the signal means the actual group velocity, whereas in Ref. 2, it means the wave front velocity.

*** Sommerfeld showed that it is impossible to verify experimentally the result that only "forerunners" of extremely weak intensities travel at the vacuum velocity. However, using modern photoelements and amplifiers, it is possible that one can construct an experiment, for instance, to detect weak light pulses traveling without refraction through a plane parallel plate or prism. One can make use of the fact that the "forerunners" are unpolarized by a polarizer.

**** See Eq. (10) in Ref. 2 [e.g., D. I. Blokhintsev

and V. V. Orlov, J. Exper. Theoret. Phys. USSR 25, 513 (1953)]

* This situation was considered in a discussion with V. I. Skobelkin.

[1]D. I. Blokhintsev, Doklady Akad. Nauk SSSR 82, 553 (1952)

[2]D. I. Blokhintsev and V. V. Orlov, J. Exper. Theoret. Phys. USSR 25, 513 (1953)

[3]M. S. Svirski, Vestn. (Moscow State University) 3, 43 (1951)

[4]A. Sommerfeld, Ann. d. Phys. 44, 177 (1914)

The Problem of Obtaining a Metastable Modification of Thallium

E. I. Abaulina and N. V. Zavaritskii
Institute for Physical Problems, Academy of Sciences, USSR

(Submitted to JETP editor September 27, 1954)
J. Exper. Theoret. Phys. USSR 28, 230 (February, 1955)

An explanation as to the role played by the crystal lattice in the phenomenon of superconductivity may be found in various studies of the crystalline modification of one or another of the substances at low temperatures. In three well-known metals, thallium, titanium and zirconium, the α-modification exhibits superconductivity but β- modification has not been investigated at low temperatures.

One of the methods yielding a high temperature modification in metastable form is that of sudden quenching. This method of quenching pure substances has been treated by Sekito [1]. In this work an x-ray investigation was made of the modification of thallium (prepared by Kal'baum) which had received rapid cooling of the metal in ice water. As is known, at 235 °C, thallium undergoes allotropical changes in which the density due to hexagonal close packing changes to that of a body centered cubic[2]. Due to this quenching[1] the sample now exhibits a face centered lattice structure.

We have undertaken a low temperature study of the metastable modification of thallium (99.98% pure). The desired quenching may be achieved by several methods:

1. Thallium melted in a glass tube over a Bunsen-burner and plunged into ice water (method of reference 1).

2. To avoid crystallization of melted thallium in the α-modification, stable at 0 °C, the sample before quenching is slowly cooled in the oven from melting temperature (303 °C) to 290 °C. The sample is prepared by melting thallium in thin walled capillary tubes having a wall thickness of 0.1 mm.

3. For very rapid quenching the melted thallium is poured out under vacuum on a copper surface cooled to the temperature of liquid air.

Immediately after the preparation of the sample, x-ray analysis followed. It appears that x-ray analysis does not reveal any difference between the quenched sample and that of ordinary thallium. This likewise applies to the measured magnetic moment of the samples at the liquid temperature of helium. In all samples, in quenched as well as in unquenched, the transition to the superconducting state was observed at 2.38-2.4 °K. The marked absence of hysteresis (less than 1%) and the abrupt transition from superconductivity to the normal state is evidence of the absence of impurities occluded in the sample.

Analysis of the results of these methods shows that not one of the above methods lends itself to producing the thallium in metastable modification as in contrast of the statements found in reference 1. Thus the question of quenching pure thallium is left open.

The authors wish to thank A. I. Shal'nikov for his continued interest in this work and also his laboratory assistant N. V. Belov at the Institute of Crystallography for interpreting the x-ray analysis of the samples.

Translated by A. Andrews
42

[1] S. Sekito, Z. Krist 74, 189 (1930)

[2] H. Lipsona, A. R. Stoks. Nature 148, 437 (1941)

Possible Methods of Obtaining Active Molecules for a Molecular Oscillator

N. G. Basov and A. M. Prokhorov
P. N. Lebedev Institute of Physics, Academy of Sciences, USSR

(Submitted to JETP editor November 1, 1954)
J. Exper. Theoret. Phys. USSR 28, 249-250 (February, 1955)

As was shown in reference 1, one must use molecular beams in order to make a spectroscope with high resolving power. In this reference the possibility of constructing a molecular oscillator was investigated. Active molecules needed for self-excitation in the molecular oscillator were to be obtained by deflecting the molecular beam through inhomogeneous electric or magnetic fields. This method of obtaining active molecules has already been employed in the construction of a molecular oscillator [2]

There is yet another way of obtaining active molecules, namely, pre-exposure of the molecular beam to auxiliary high frequency fields which induce resonance transitions between different levels of the molecules. In Fig. 1 and Fig. 2 we illustrate the possible variants which utilize an exciting irradiation of frequency ν_{ex} for populating the upper level in order to obtain a scheme of self-excitation with the frequency ν_g.

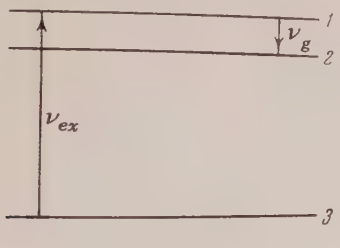

Fig. 1

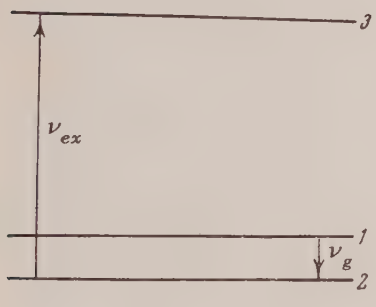

Fig. 2

In one case, illustrated by Fig. 1, active molecules in level 1 are obtained at the expense of molecules in level 3 through transitions induced by the high frequency field. If the high frequency field possesses sufficient energy, so that the effect nears saturation, then the number of active molecules equals

$$^1/_2 (N_3 - N_1) + N_1 - N_2, \quad (1)$$

where N_i is the number in the ith level.

The number of active molecules in level 1 increases with an increase of the energy difference between the first and third level relative to the energy difference between the first and the second levels. One must consider that the number of molecules in the levels is determined, in the case of thermodynamic equilibrium, by the Boltzman factor.

$$N_i \sim e^{-E_i / kT}, \quad (2)$$

where E_i is the energy of the ith level and T is the absolute temperature of the molecular beam.

These considerations are valid for the case illustrated in Fig. 2. Here, however, instead of an increase of the number of molecules in level 1, we have a decrease of the number in level 2. The number of active molecules equals, in this case,

$$^1/_2 (N_2 - N_3) + N_1 - N_2. \quad (3)$$

The method presented herein can be used, for example, in the following cases.

1) Level 1 and 2 appear as neighboring rotational levels belonging to one and the same vibrational state of the molecule, with level 3 belonging to a neighboring vibrational state. In this case the rotational quantum number of this level (level 3) differs from that of level 1 and 2 by $\Delta J = 0, \pm 1$.

It is convenient to use the transitions between the vibrational levels for which $\Delta J = \pm 1$, since this case does not impose too strict a requirement for the exciting irradiation to be monochromatic. Since transitions between vibrational levels fall in the infra-red region of the spectrum for most molecules, the exciting irradiation must belong to this frequency range. However, infra-red thermal sources in existence at the present time have insufficient power to produce a saturation effect.

2) Levels 1,2, and 3 are rotational levels of the molecule with asymmetric rotational momentum.

3) Levels 1 and 2 are hyperfine structures belonging to a given rotational state, and level 3 is a hyperfine level of a neighboring rotational level.

4) Levels 1 and 2 are specified by an inversion doublet belonging to a rotational level, and level 3 is one of the inversion levels of a neighboring rotational state.

The method presented here can be used to obtain a sufficient number of active molecules for the purpose of constructing a low frequency molecular oscillator.

Translated by A. Skumanich
41

[1] N. G. Basov and A. M. Prokhorov, J. Exper. Theoret. Phys. USSR **27**, 282 (1954)

[2] C. N. Townes et al, Phys. Rev. **95**, 282 (1954)

Luminescence of Organic Scintillators

I. M. ROZMAN

(Submitted to JETP editor September 8, 1954)
J. Exper. Theoret. Phys. **28**, 251-252 (February, 1955)

DESPITE a number of attempts in this direction, so far no satisfactory explanation has been offered for the low light energy output of organic

scintillators irradiated by slow electrons, α-particles and other slow charged particles[1-3]. In seeking a new approach to the problem, we have investigated the influence of the temperature and the nature of the surrounding gaseous medium on the scintillation output.

Below we give the results of our study of the luminescence output of plastic scintillators, prepared by polymerization of a 1.5% solution of 1,1,4,4- tetraphenyl-1, 3-butadiene in purified styrene (polymerization at high temperature and high pressure in the absence of a catalyzer and plasticizer). The scintillator was excited either by γ-rays from Co^{60} source or by α-particles from polonium. The luminosity was determined according to the mean current output of a FEIu-19 photomultiplier. The light was conducted from the scintillator to the photocathode of the multiplier by means of a polymethylmetacrylate rod, 280 mm long, enclosed in a textolite tube. With this arrangement the temperature of the photomultiplier remained virtually constant during the tests.

TABLE

Temperature dependence of the persistent luminescence (afterglow) of a plastic scintillator

Temperature °C	Photomultiplier current 15 sec after end of excitation	
	by γ-rays	by α-particles
—115	1.8	-
—121	6.0	—
—137	10.0	—
—150	17	1.7
—167	19	7.8
—188	22	13.2

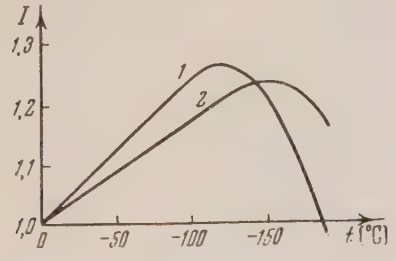

Fig. 1. Temperature dependence of the luminous intensity, I, of a plastic scintillator: 1- excited by γ-rays from a Co^{60} source; 2-excited by α-particles from a polonium source. Curves adjusted to coincide at 0°C.

Our data on the temperature dependence of luminescence for plastic scintillators Fig. 1, differ from those in scientific literature [2,4], particularly in that we observed a decrease in luminescence at lower temperatures. This decrease is accompanied by the appearance of a persistent luminescence (afterglow), the initial intensity of which increases as the temperature at which the scintillator is excited is reduced (see Table above). The attenuation of the persistent luminescence (afterglow) at three different temperatures, plotted to a semilogarithmic scale, is shown in Fig. 2. It will readily be seen that the attenuation law in the given time interval is not exponential[5,6] and that the extinction time is long.

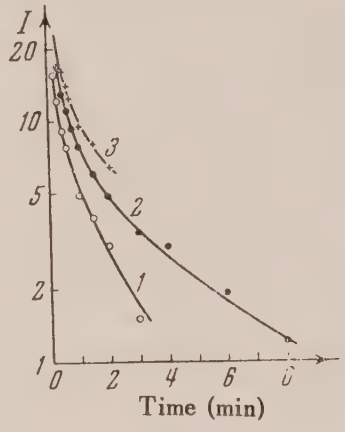

Fig. 2. Attenuation of persistent luminescence (afterglow) of a plastic scintillator, irradiated for 2 minutes by γ-rays from a Co^{60} source at the following temperatures: 1)-129°C, 2)-174 °C, 3)-188° C.

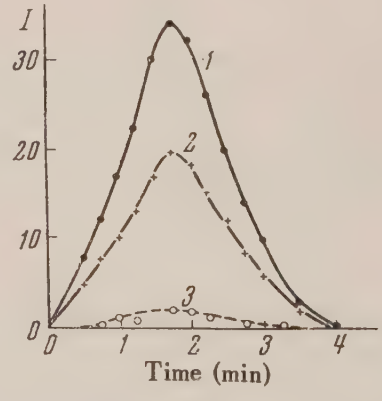

Fig. 3. Thermoluminescence of a plastic scintillator, excited at about -190° C by γ-rays from a Co^{60} source for 4 min (1), 2 min (2) and by α-particles from a polonium source for 2 min (3). Indicated times are from beginning of heating, [following extinction].

In some of our experiments the scintillator was rapidly heated after extinction of the afterglow: further light emission - thermoluminescence - was observed. The results of one such experiment are

shown in Fig. 3. The luminous intensity in Figs. 2 and 3 and in the table is given in the same units. The short term [initial response] luminescence at 0 °C with the scintillator excited by α-particles or γ-rays amounts to about 2500 such units.

The experimental results not only prove the existence of persistent luminescence (afterglow) and thermoluminescence for organic plastic scintillators excited at low temperatures by ionizing radiation, but also demonstrate that there are quantitative differences in the nature of the luminosity effects with α- as against γ- excitation. With α-excitation the decrease in short-term luminescence begins at a lower temperature than with γ-excitation and the afterglow intensity is appreciably lower. Thermoluminescence with α-particle excitation is relatively weak, particularly if we take into account the fact that the energy absorbed by the plastic scintillator with α-excitation exceeded the energy input with γ-ray excitation by a factor of 10. A possible reason for the difference is appreciable local heating of the scintillator in the α-particle track.

In any case it is obvious that temperature effects must be duly taken into account in any attempt to explain the dependence of the scintillation output on the speed and charge of the exciting particles.

Translated by E. Rosen
43

[1] J. B. Birks, *Scintillation Counters*, London, 1953

[2] S. C. Curran, *Luminescence and the Scintillation Counter*, London, 1953.

[3] G. F. Wright, Phys. Rev 91, 1282 (1953)

[4] Survey in Nucleonics 10, 32 (No. 3, 1952)

[5] V. A. Levshin, *Photoluminescence of Liquid and Solid Subtances*, Moscow, 1951

[6] V. A. Iastrebov, J. Exper. Theoret. Phys. USSR 21, 164 (1951); Dodlady Akad. Nauk SSSR 90, 1015 (1953)

F-Centers in Silver Halide Crystals

P. V. Meikliar

(Submitted to JETP editor September 16, 1954)
J. Exper. Theoret. Phys. USSR 28, 252-253 (February, 1954)

In a recently published article Grenishin[1] asserts that the absorption bands of AgBr at $\lambda = 420$-430 mμ (studied first by the writer in collaboration with Putseiko[2] and subsequently by the writer[3,4] alone) are in no way connected with the presence, in the silver halide crystals, of F-centers, similar to the F-centers found in the halides of alkali metals. By way of proof Grenishin cites the presumed temperature independence of the half-width of the absorption bands and the absence of vacant lattice sites in silver halides.

The first statement is erroneous: Grenishin used data taken from our report on experiments in which the temperature was varied only in a narrow interval. Experiments carried out by the writer in collaboration with Shimanskii[5] showed that when the temperature of AgBr is changed from 90-100 °C to 350 °C the half-width increases, on the average, by a factor of 1.6-1.7 and in the case of heating to 408 °C, by a factor of 1.8-1.9. Heating of an AgCl crystal also leads to a 1.6-fold increase in the half-width of the absorption band. This is clearly illustrated by the data listed in the table below*.

It will be seen from the table that the variation of the half-width of the F-center absorption band with the temperature is of the same order as for the halides of alkali metals[6].

As for the second statement, it is true that no vacant halide ion sites (such as occur in alkali metal halides) are formed by the mechanism of Schottky in silver halides. However, this is no proof that F-centers cannot form by the mechanism of de Boer. The writer has suggested a possible mechanism of the formation of F-centers in silver halides. By virtue of the close packing of the crystal lattice and the partially homeopolar nature of the bonds there is a certain probability of the transfer of an electron from the halide ion to the one of the six neighboring silver ions, with the subsequent escape of a halide atom and the formation of an F-center in its place. The activation energy for the process is approximately 0.15 eV[5]. Due to the low value of this activation energy the F-center absorption band overlaps the intrinsic absorption band. With different ratios of the intensity of the two bands,

Half-width in eV

Temperature in °C	Crystals						
	AgBr						AgCl
	№ 1	№ 2	№ 3	№ 4	№ 5	№ 6	
90	0.22	0.42	0.24	0.46	0.23	0.34	0.22
350	—	0.60	0.44	0.57	0.35	0.57	0.35
408	0.47	0.76	—	0.87	0.42	—	—

the apparent maximum of the F-center absorption band may be displaced to some extent. Some investigators fail to take this circumstance into account and hence place an erroneous interpretation on the relative shift of the F-center absorption band for different silver halide crystals, as contrasted with the invariable position of the F-center peak for alkali metal halides, although it is known that for the latter the F-center band is well separated from the intrinsic absorption band.

It is shown in Grenishin's article that the F-center absorption increases with the ripening time of the emulsion. This was also shown in my communication [3].

Translated by E. Rosen
44

* P. S. Shimanskii has kindly supplied the listed data.

[1] S. G. Grenishin, J. Exper. Theoret. Phys. USSR **26**, 736 (1954)

[2] E. K. Putseiko and P. V. Meikliar, J. Exper. Theoret. Phys. USSR **21**, 341 (1951)

[3] P. V. Meikliar, Doklady Akad. Nauk SSSR **77**, 391 (1951)

[4] P. V. Meikliar, Proceedings of the Meeting dedicated to the memory of Academician S. I. Vavilov, Moscow, 1953, p. 214.

[5] P. V. Meikliar and R. S. Shimanskii, J. Exper. Theoret. Phys. USSR **27**, 156 (1954)

[6] N. Mott and R. Gurney, *Electronic Processes in Ionic Crystals*, p. 138

On the Resonance-Fluorescence of Atoms

M. N. Alentsev, V. V. Antonov-Romanovskii, B. I. Stepanov and M. V. Fok
P. N. Lebedev Physical Institute, Academy of Sciences USSR
Physical Institute of the Academy of Sciences, Byelorussian SSR

(Submitted to JETP editor November 25, 1954)
J. Exper. Theoret. Phys. USSR **28**, 253-254 (February, 1955)

ONE of the present authors[1] recently investigated the statistical relation of the radiation absorbed and the radiation emitted by a system, consisting of atoms with two energy levels. It was shown that the radiation output of such a system may vary, depending on the density of the exciting radiation. This deduction applies to the total output, i.e., to the ratio of the total energy emitted to the total energy absorbed.

In the present communication we propose to apply the suggested method to calculating the luminescence output of such a system, for example, to the resonance fluorescence of atoms.

According to the definition given by Vavilov [2], luminescence is understood to mean the excess of the radiation over temperature radiation, having a finite duration which exceeds the period of light oscillations. This definition corresponds to the experimental conditions under which luminescence output is normally measured. It will be recalled that any radiation detector does not register the background of "black body" radiation, corresponding to its temperature (since it is in equilibrium with this background), and reacts only to the excess radiation over and above this background. It follows that in determining the exciting light-energy absorbed by the body as well as the light energy radiated by the luminescent body, we measure only the excess above the heat radiation.

Taking this factor into account we obtain the following expression for the output of photoluminescence in place of Eq. (15) of reference 1:

$$q = \frac{(A + Bu_0)\, n_2 - Bu_0 n_1}{Bs\,(n_1 - n_2)}. \qquad (1)$$

The symbols are as given by Stepanov[1]: s is the energy density of the exciting light, An_2 is the number of spontaneous transitions, accompanied by radiation, from the upper level per unit time, $Bu_0 n_2$ is the number of transitions from this level, forced by heat radiation, the density of which, for the frequency $\nu = (E_2 - E_1)/h$, equals u_0. The resultant forced radiation is characterized by a certain duration, since it continues after the cessation of excitation until the number of molecules in the higher excited state drops to the number consistent with thermodynamic equilibrium. Hence the $(A + Bu_0)n_2$ term represents the total number of quanta released per unit time. A certain number of these quanta is not recorded by the detector since it serves to compensate the number of quanta of black-body radiation absorbed by the system. This number per unit time is $Bu_0 n_2$. Hence in determining the luminescence energy this term must be substracted from the numerator.

In the denominator of Eq. (1) we also have only the excess of radiation (absorbed in this case) over the black-body radiation background. As in reference 1, the forced emission under the influence of the exciting radiation is regarded here as equivalent to a reduction of the absorption.

In reference 1 it was shown that with constant excitation

$$\frac{n_1}{n_2} = \frac{A + B(u_0 + s) + d_0}{B(u_0 + s) + d_0 \exp\{h\nu/kT\}}. \qquad (2)$$

Substituting (2) in (1), we find that the quantum output of fluorescence is

$$q = \frac{1}{1 + (d_0/A)[1 - \exp\{-h\nu/kT\}}. \quad (3)$$

The principal deduction to be drawn from the above is that q is independent of the density s of the exciting light, in which respect it differs from the quantum output of the total radiation. The latter is a monotonic function of s, tending to unity as $s \to 0$ and to the magnitude of q when $s \to \infty$[1].

For $d_0=0$, i.e. in the absence of radiationless transitions, we obtain the trivial result $q=1$. The output q also equals unity when the temperature is so high (flame temperatures) or the transition frequency ν so low (radio frequency region) that $\exp\{-h\nu/kT\}$ virtually equals unity. In physical terms, this means that under such conditions the presence of external radiation does not disturb the energy distribution between the levels, and consequently the number of quenchings equals the number of excitations, i.e., no heat is lost (radiated).

Under the conditions commonly obtained in luminescence experiments the value of $\exp\{-h\nu/kT\}$ is approximately zero and, therefore, according to (3),

$$q = A/(A + d_0). \quad (4)$$

Translated by M. Rosen
45

[1] B. I. Stepanov, Doklady Akad. Nauk SSSR 99, 971 (1954)

[2] S. I. Vavilov, Introduction to the Russian translation of *"Fluorescence and Phosphorescence"* by P. Pringsheim.

Self-Neutralizing Light Meter with Adjustable Red Boundary

M. S. KHAIKIN AND E. I. ABAULINA
Institute for Physical Problems, Academy of Sciences, USSR

(Submitted to JETP editor June 29, 1954)
J. Exper. Theoret. Phys. USSR 28, 254-256
(February, 1955)

THE photoelectric meter is the most sensitive instrument for measuring the luminous flux[1]; therefore, work on its perfection or the extension of its application presents practical interest. This article is devoted to experiments on the design of a photometer with controllable spectral characteristics. Such an instrument could combine the functions of a light receiver and spectrometer. The first experiment in this direction was carried out by Kudriavtseva[2].

In order to control the red boundary of spectral sensitivity of the photometer, an additional electrode, a screen, was installed near the photocathode of the meter. The retarding field, created between the screen and the photocathode permitted the selection of the photoelectrons, passing through the screen into a sensitive zone of the meter, according to their speeds. In order that such a separation of photoelectrons be effective, it is necessary that the electrons not lose the speeds obtained under the photoelectric effect on the path from the photocathode to the screen (in absence of the restraining field), i.e., that the distance between the screen and photocathode shall be of the order of the free path length of the electrons in the gas in the meter. For this purpose the distance from the screen to photocathode should be made very small, or about 50 μ, and the argon gas should be used to fill the meter; in argon the mean free path is a maximum for electrons with velocity 0.3 - 1.5 V[3]. As the neutralizing component of the mixture methylal was used in 10% strength; the pressure of the mixture in the meter was 80 mm of mercury.

The meter had a cylindrical shape. A thin wall tube, 15 mm in diameter, of non-corrosive steel served as the cathode. The slits (12 × 8 mm) were cut on the opposite sides of the tube. One slit was used for illumination, and another was covered by a screen, behind which the cylindrical aluminum photo-cathode was attached to the insulation support. The aluminum was of a type having a red boundary for the photoelectric effect of about 3500 Å (3.6 ev). The screen was made of 20 micron tungsten foil by means of anodic etching under a thin rolled copper screen, pressed to the foil surface. In such a manner a copy of the copper screen was impressed on the tungsten foil, the cells of which were 0.33 × 0.25 mm and the transparency about 60%. The tungsten metal was selected for preparation of the screen on account of its high energy yield. It served the purpose of lowering the uncontrollable photoeffect from the screen surface under illumination by the light under investigation. A steel cathode tube was subjected to chlorinization for the same purpose.

The complete meter represented a separate apparatus suitable for long work[1]. The anode and cathode of the meter were connected in the usual manner in a standard measuring system. The voltage given between the photocathode and screen (connected with the cathode of the meter) was supplied from a potentiometer, fed by dry cells.

A quartz lamp served as the light source for an examination of the meter during experiments. For the separation of required spectral bands Shott's light filters Wg 1, 3, 6 and 7 were used, and therefore the spectral characteristics of the meter, given below, are only approximate.

The meter has an energy plateau of about 100v (near 1050 v), while the dark background amounts to 100 impulses per minute – (independently of the voltage between the photcathode and screen).

During the operation of the meter with initial illumination, the general background, interfering with the measurements, is composed of dark background and uncontrollable photoeffect from the screen and inner surface of the cathode. Therefore the region of the meter operation from the short wavelength side is determined by the red boundary of the photo-effect of the screen and cathode materials. On the long wavelength side it is determined by the red boundary of the photocathode. The light of a quartz lamp passing through the filter Wg 7 (boundary of the transparency 2600 Å or 4.9 ev) created a background apparently equal to the photocathode effect; consequently, the measurements of spectral characteristics of the meter were made mainly with the filters Wg 7 and the more "red" Wg 6 (with boundary of transparency at 2800 Å or 4.5 ev).

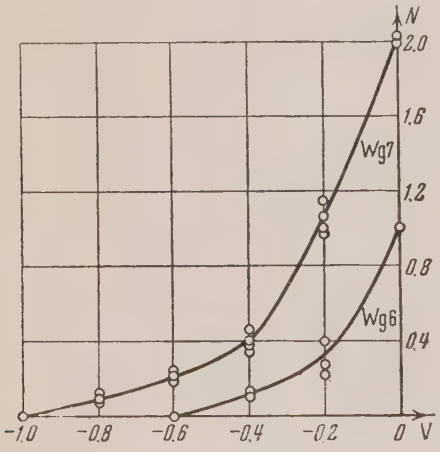

Fig. 1

On Figure 1 is shown the number of meter impulses, reduced by general background (in relative units) and the voltage added between the photocathode and screen affected by the light which passed through the filters Wg 7 (upper curve) and Wg 6 (lower curve). The experimental points were obtained during a few tests with the illumination varying from three to four times. Figure 1 also shows that the photoelectrons, excited by the light passing through the filter Wg 7, were slowed down by the retarding field of 1.0 v and by the light passing through the filter Wg 6 by a field of 0.6 v. The Figures, and also the boundary of transparency of the filters (see above), lead one to the conclusion that the amount of the energy yield from the photocathode (3.9 ev) exceeds the amount of the energy yield of the aluminum sample, used for preparation of the photocathode by 0.3 ev. This difference should be related to the difference of potentials at contacts (between aluminum photocathode and tungsten screen), which creates an additional retarding field of 0.3 v.

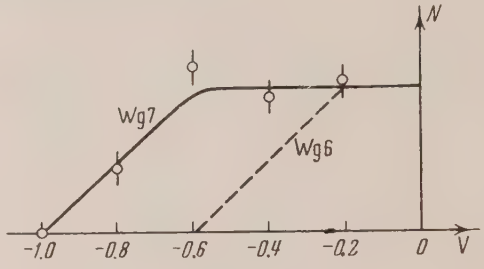

Fig. 2

From Figure 1 it is also seen that the retarding field changes the spectral characteristics of the meter. This is still better illustrated in Fig. 2, where the points of a solid line were obtained from the curve for Wg 7 (Figure 1) by means of recomputation with the approximate consideration of the spectral characteristics of the light filter Wg 7. The dotted line on Figure 2 was obtained in the same manner for the filter Wg 6. Gradual lowering of the spectral sensitivity of the meter seems to be explained by non-uniformity of the retarding field.

Figure 3 illustrates the construction of the orientating relation (solid line) of the red boundary of light sensitivity of the meter to the magnitude of the restraining field (without account of the potential difference at contacts). The light passing filter Wg 7 is conditionally related to the wave length 2650 Å and that passing Wg 6 to 2900 Å. (At this wavelength the transparency of the filters is about 20 %.) The dotted straight lines were drawn through the pair of experimental points (ordinates corresponding to the impulse numbers without background) related to each retarding field and were extended to their intersection with the abscissa. The intersection points are used as the orientating values of the red boundary of the meter for the given value of retarding field for construction of the solid line. The ordinate of this curve is the value of retarding field (right scale). The point (3500 Å + 0.3 v) char-

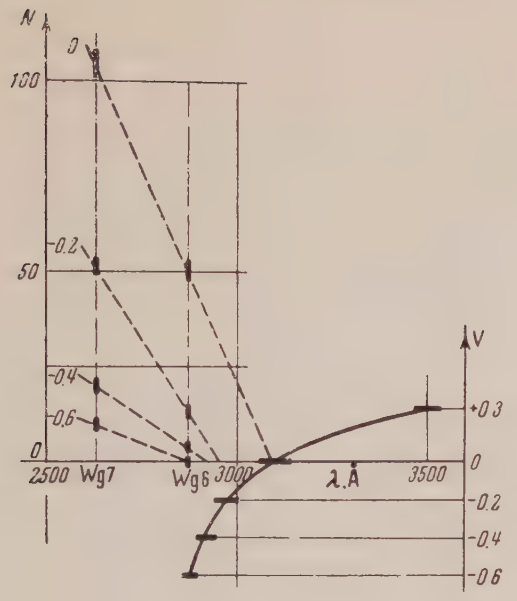

Fig. 3

acterizes the aluminum photocathode in the absence of the screen and the difference of potentials at contact appearing under this condition.

It is necessary to note that the sensitivity of the meter with the screen is substantially smaller (by more than an order of magnitude) than the sensitivity of the conventional photometer with open photocathode. The reason for this seems to be due to the dispersion of considerable amounts of the photoelectrons on the path from the photocathode to the screen.

According to available published data only one attempt was made to create a meter with a controllable screen[2] However the results of this work are uncertain, inasmuch as the observed effect of the screen action lay within the limits of precision of measurements. Moreover, this meter generally could not serve as a stable measuring instrument, because it was operated exclusively in a vacuum installation. The present work proves the experimental possibility of construction of a self-neutralizing light meter with regulated red boundary and possessing all the operating characteristics of the contemporary photometer[1].

The authors express their gratitude to Professor A. I. Shal'nikov for his valuable advice and attention to the work.

Translated by N. P. Setchkin
46

[1] S. F. Rodionov, M. S. Khaikin and A. I. Shal'nikov, J. Exper. Theoret. Phys. USSR 28, 223 (1955); Sov. Phys. 1 64 (1955)

[2] V. M Kudriavtseva, J. Exper. Theoret. Phys. USSR 5, 557 (1939)

[3] K. Ramsauer and R. Kollat, Usp. Fiz. Nauk 15, 128 (1935)

Translator's note: General principles of the light meter are also given by Radionov in J. Exper. Theoret. Phys. USSR 10, 294 (1940).

CONTENTS

JOURNAL OF TECHNICAL PHYSICS, USSR VOLUME 25, NO. 3 MARCH, 1955

JOURNAL OF TECHNICAL PHYSICS, USSR VOLUME 25, NO. 4 APRIL, 1955

JOURNAL OF TECHNICAL PHYSICS, USSR VOLUME 25, NO. 5 MAY, 1955

25th ANNIVERSARY CELEBRATION
of the
AMERICAN INSTITUTE OF PHYSICS

Features

Meetings and special sessions by each of the Member Societies
Special Institute session and banquet
Instrument and apparatus exhibit
Book and magazine displays
Placement Register

JANUARY 30–FEBRUARY 4, 1956
NEW YORK CITY

MARK YOUR CALENDAR NOW

CONTENTS—*continued*

SOVIET PHYSICS JETP VOLUME 1, NUMBER 1 JULY, 1955

CONTENTS